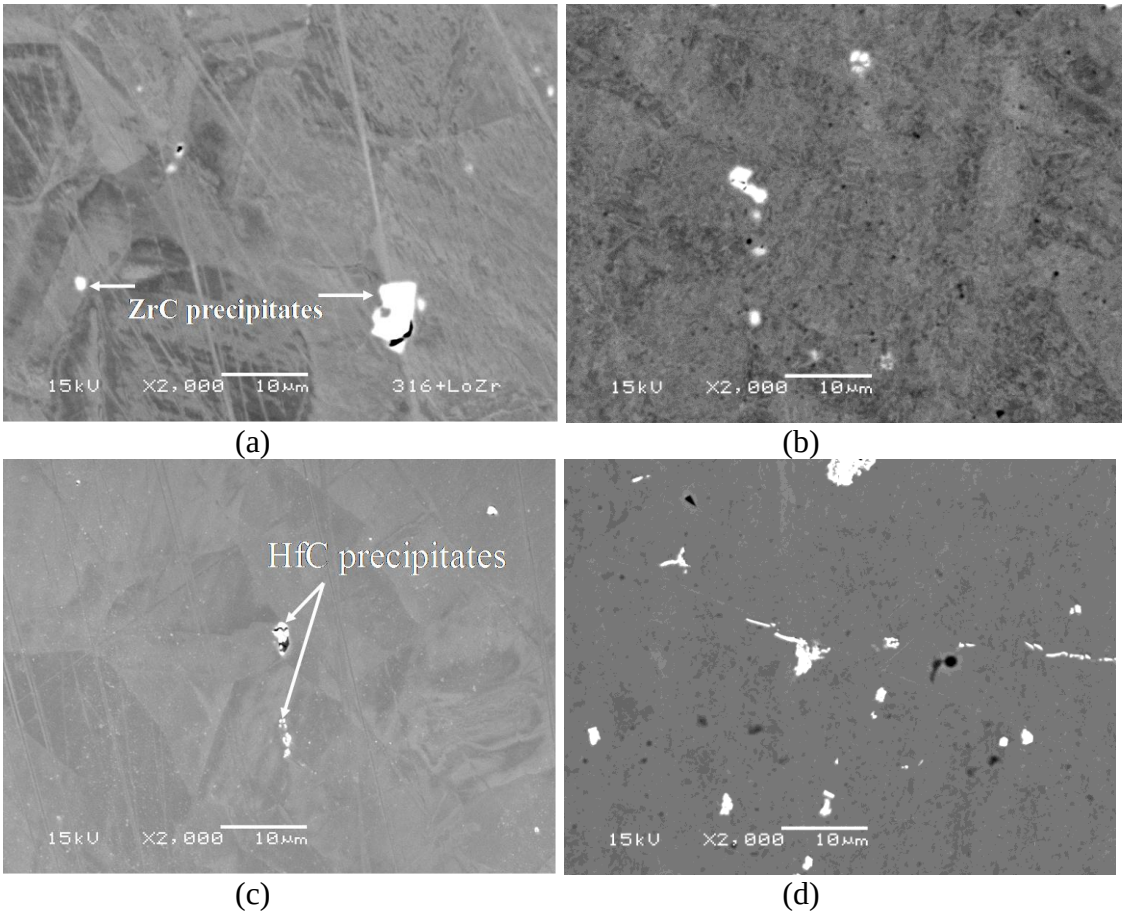

(a) (b)

(c) (d)

Figure 5.28 SEM-BSE images showing high-contrast precipitates for (a) LoZr, (b) HiZr, (c) LoHf, and (d) HiHf alloys. These precipitates are highlighted in (a) for LoZr.

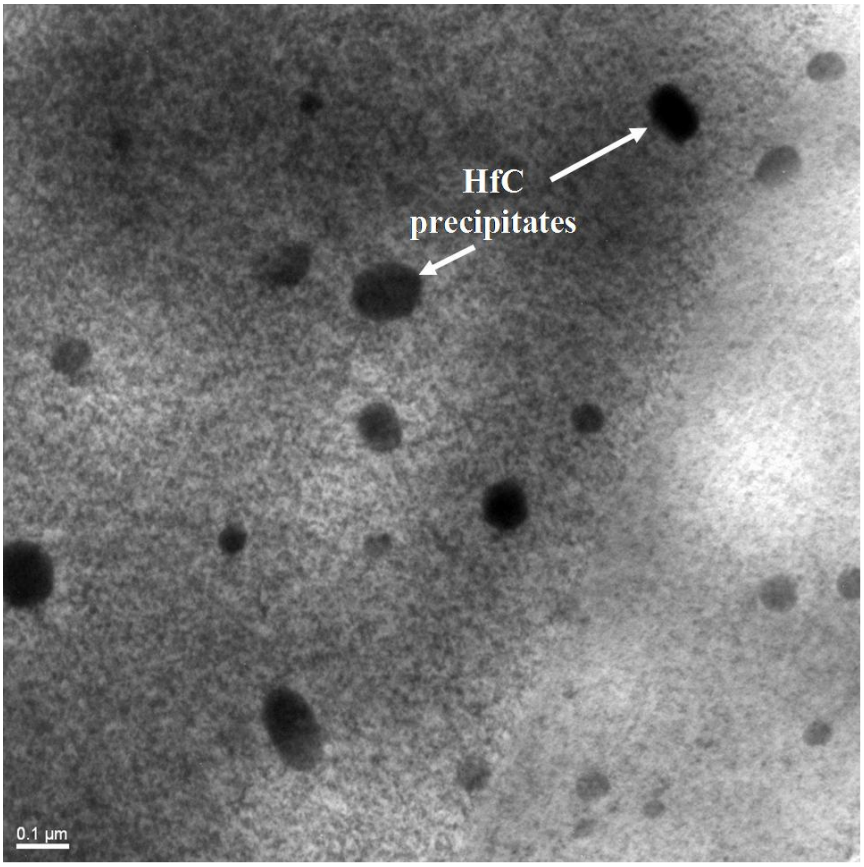

Figure 5.29 TEM image of the HfC precipitate microstructure in HiHf in the unirradiated condition.

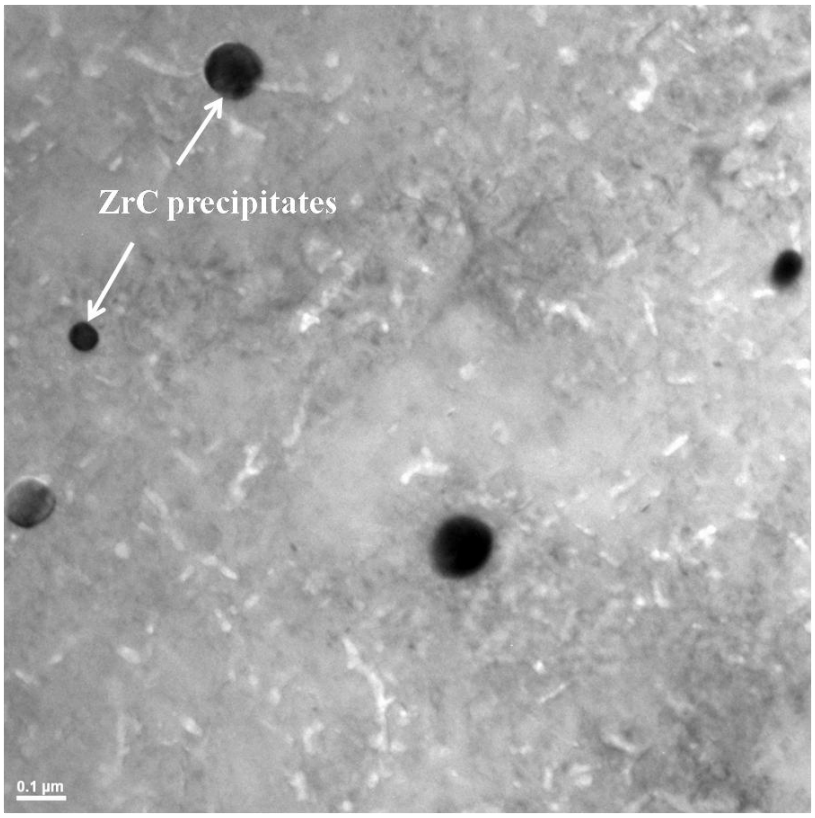

Figure 5.30 TEM image of the ZrC precipitate microstructure in HiZr in the unirradiated condition.

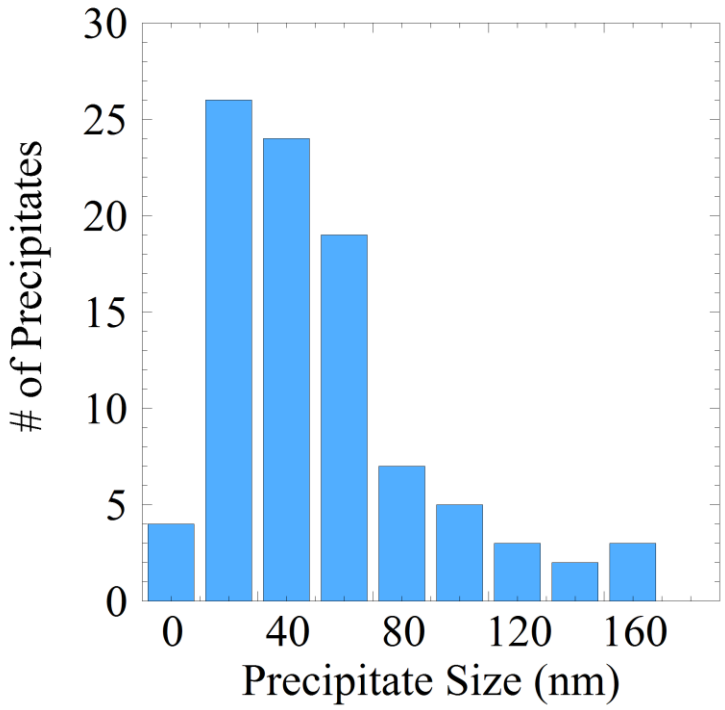

Figure 5.31 Size distribution of HfC precipitates in unirradiated HiHf.

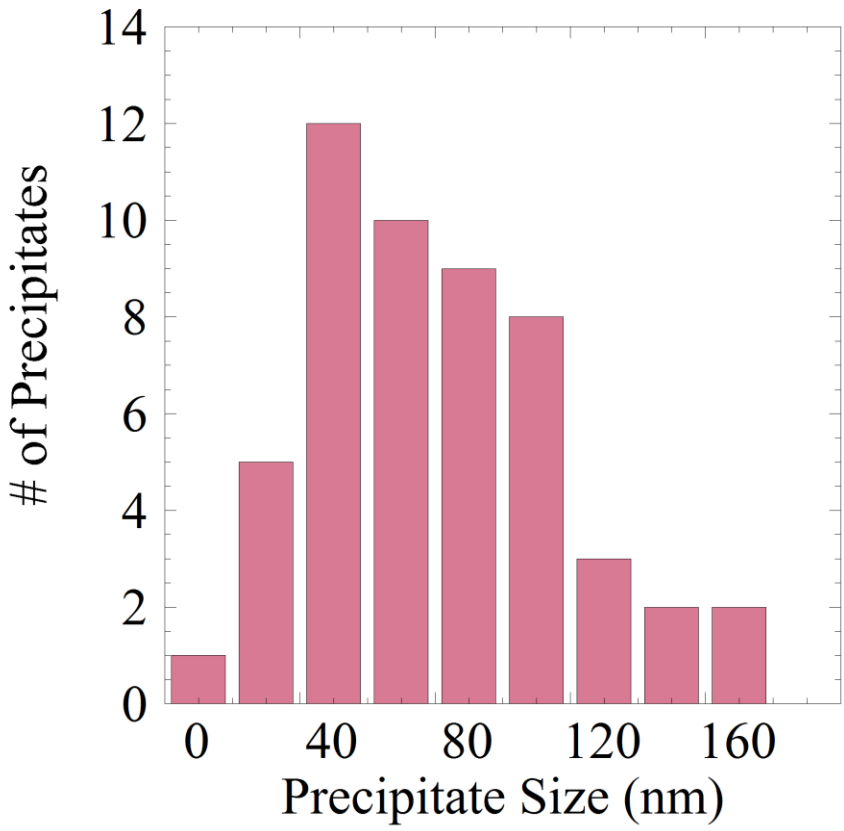

Figure 5.32 Size distribution of ZrC precipitates in unirradiated HiZr.

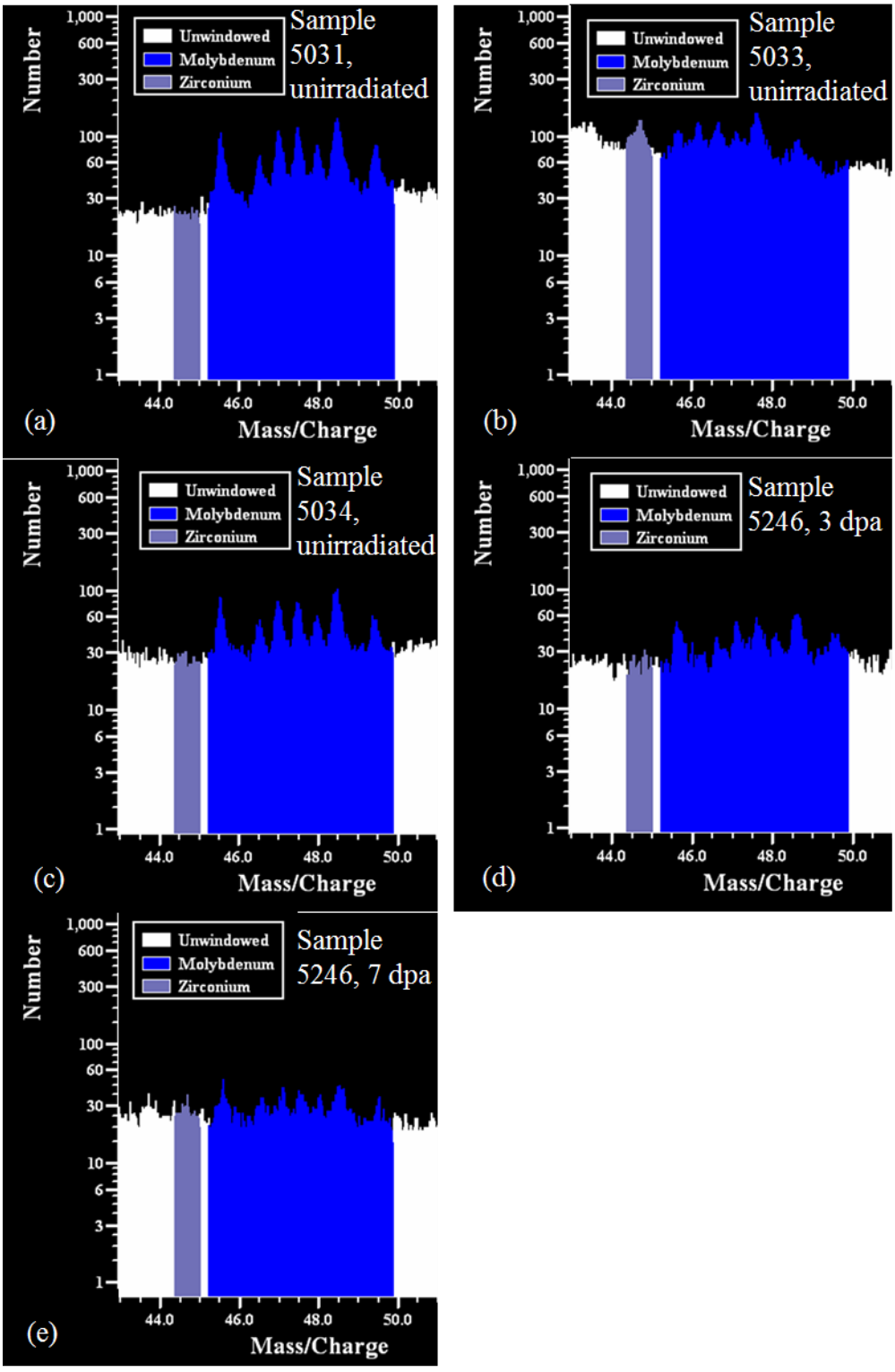

Figure 5.33 Mass/charge ratio for LoZr: (a), (b), and (c) in the unirradiated condition, (d) at 3 dpa, and (e) at 7 dpa. Zr intensity peaks are shown with Mo peaks to demonstrate the presence of the 2+ Zr^{90} peak and the overlap of subsequent 2+ Zr peaks with Mo 2+ peaks. The presence of Zr is detected for the unirradiated condition in (b).

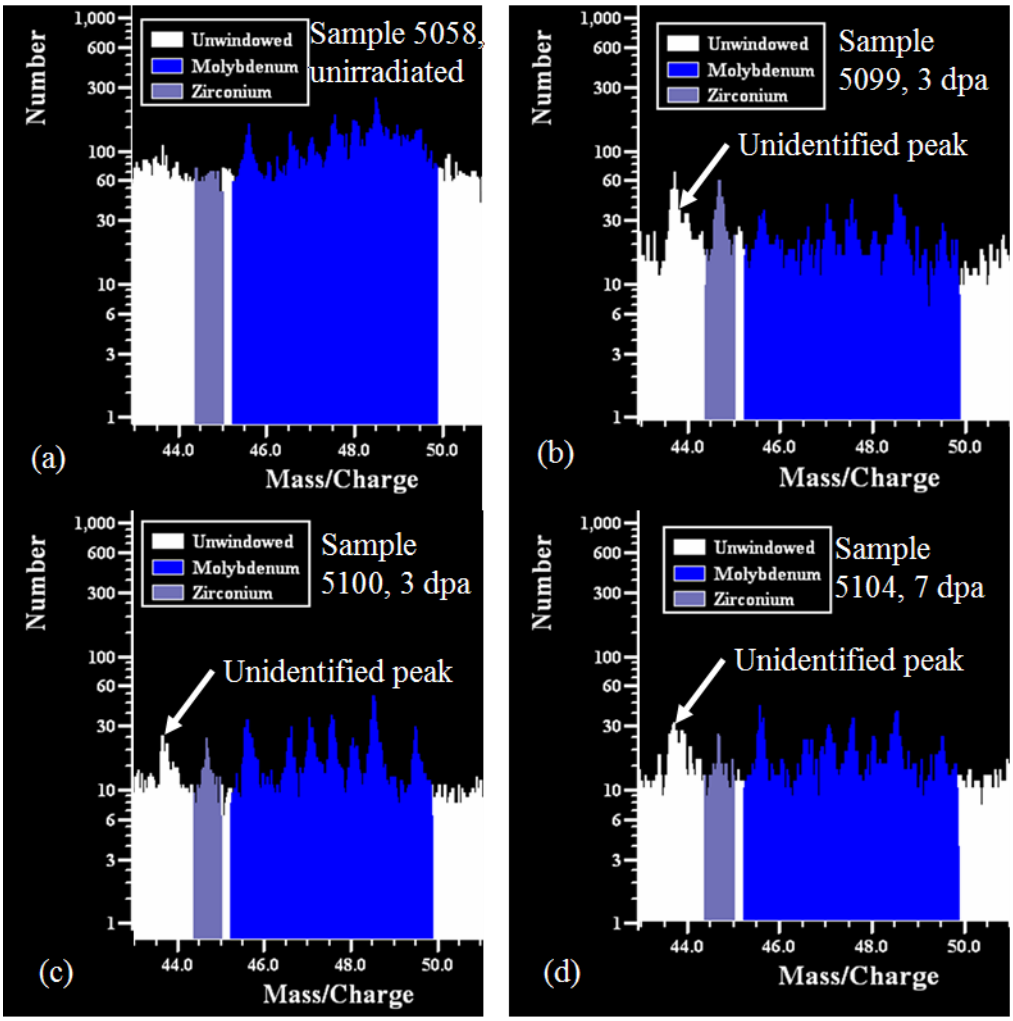

Figure 5.34 Mass/charge ratio for HiZr: (a) in the unirradiated condition, (b) and (c) at 3 dpa, and (d) at 7 dpa. Zr intensity peaks are shown with Mo peaks to demonstrate the presence of the 2+ Zr^{90} peak and the overlap of subsequent 2+ Zr peaks with Mo 2+ peaks. The presence of Zr is detected in the unirradiated condition and at 3 and 7 dpa, shown in (b), (c) and (d). Unidentified peaks occur (b), (c) and (d) which cannot be attributed to any particular element.

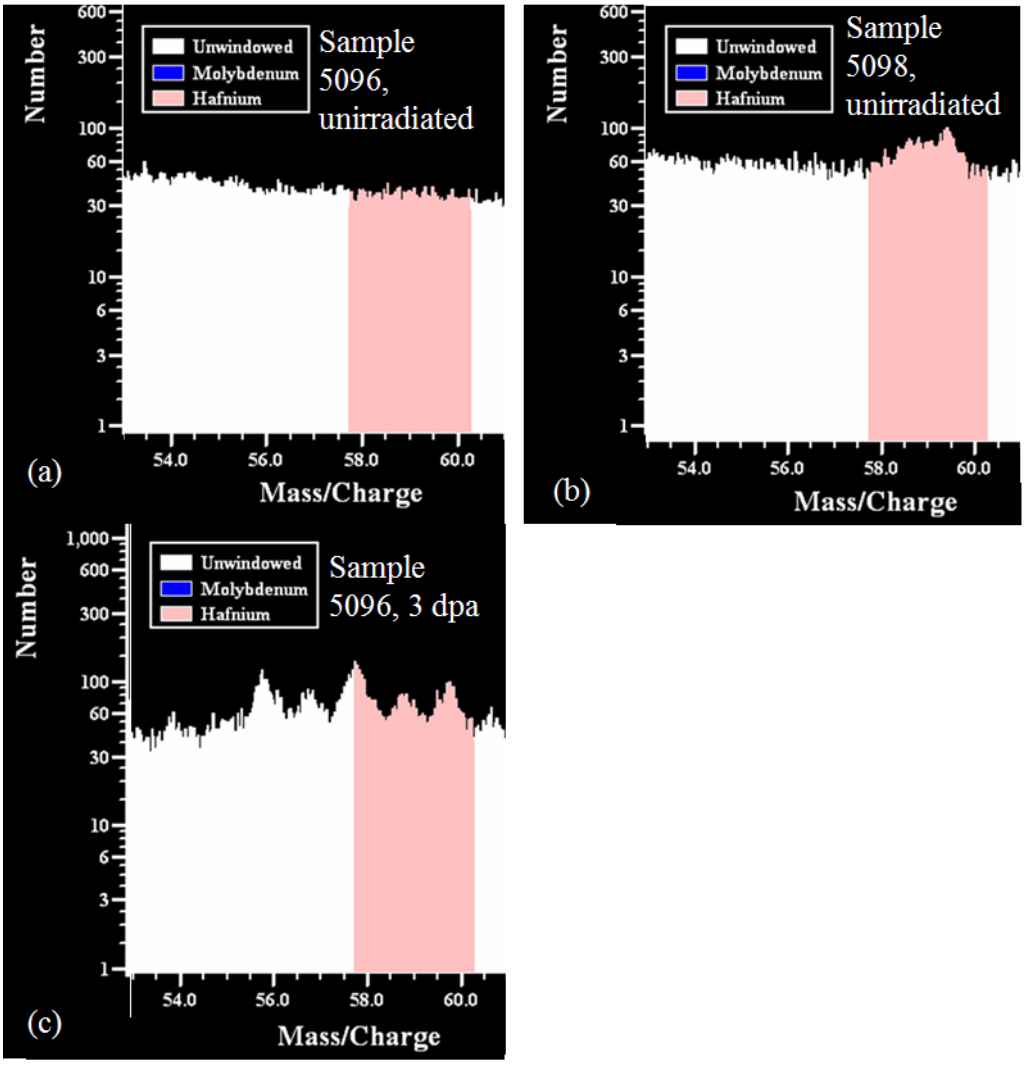

Figure 5.35 Mass/charge ratio for (a) unirradiated LoHf, (b) unirradiated HiHf, and (c) HiHf at 3 dpa. Hf intensity peaks are shown for the HiHf alloy only. The absence of Hf peaks for LoHf indicates that the Hf in solution is below the detectable limit. The presence of Hf is detected in the unirradiated condition in (b) but uncertain in (c), due to additional peaks with a lower mass/charge ratio than Hf which cannot be identified. Notice that any Hf in solution in LoHf is below the detection limit and cannot be seen in the mass/charge ratio spectrum.

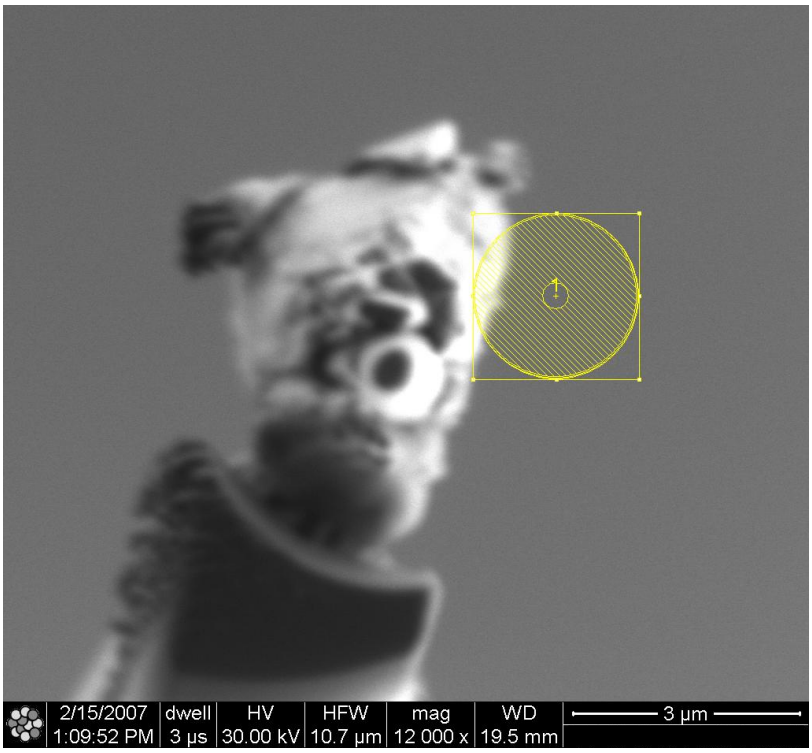

Figure 5.36 The final image taken in FIB prior to last annular milling process. Although the image is blurry and may require additional focusing, more scans for the purpose of focusing mean more Ga^{+} ion implantation into the sample tip.

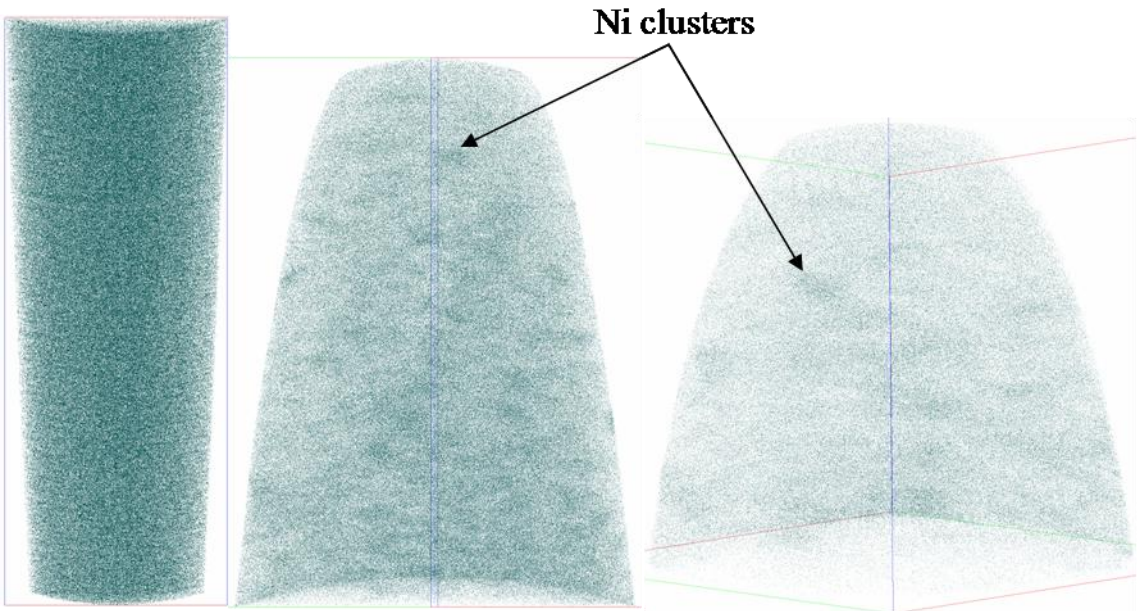

Figure 5.37 Atom maps of Ni for (a) unirradiated HiZr, (b) LoZr at 3 dpa, and (c) HiZr at 7 dpa. No precipitation of Ni is observed until after irradiation of the alloys.

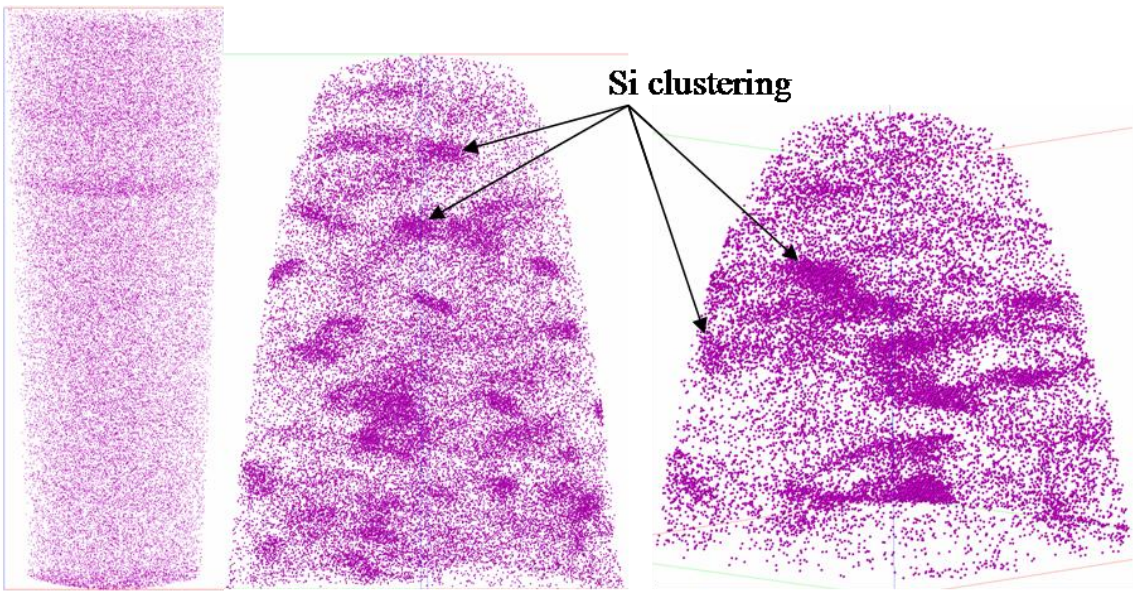

Figure 5.38 Atom maps of Si for (a) unirradiated HiZr, (b) LoZr at 3 dpa, and (c) HiZr at 7 dpa. No clustering of Si is observed until after irradiation of the alloys.

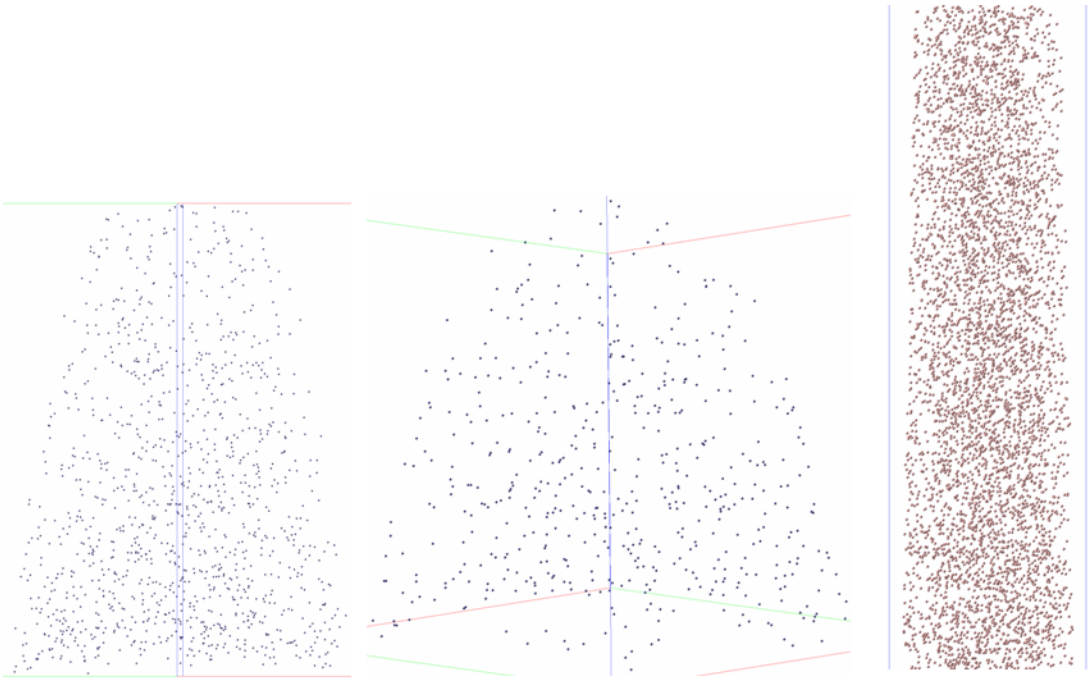

(a) (b) (c)

Figure 5.39 Atom maps of oversized solute for (a) unirradiated LoZr (b) HiZr at 7 dpa, and (c) unirradiated HiHf. The distribution of oversized solute does not appear to be clustered nor is there any change in distribution due to irradiation dose.

CHAPTER 6

MODELING OF OVERSIZED SOLUTE EFECTS ON RIS

This chapter consists of three principal parts: 1) the use of the MIK model to calculate RIS for Fe-Cr-Ni alloys, and the incorporation of the process by which oversized solute atoms are believed to affect RIS, 2) determination of the solute-vacancy binding energies for Zr and Hf in a pure fcc Fe system, using a first-principles method, and 3) assessment of the effect of oversized solutes on RIS using the calculated binding energies.

6.1 RIS Modeling

This section describes the use of the MIK model, a rate-theory model, to determine the amount of radiation-induced segregation. The MIK model is modified to incorporate a process for the trapping of point defects by oversized solute atoms in stainless steel. The MIK model is first benchmarked to match past results in the literature. The trapping process is then incorporated into the MIK model, and the resulting model, MIK-T, is exercised over the various parameters controlling the trapping process, followed by variations in temperature, dose, dose rate and oversized soluteconcentration. Finally, the section concludes with a sensitivity analysis and the significance of the results to the MIK-T model predictions.

6.1.1 The MIK Model

The MIK model is a rate-theory model that determines RIS for a binary or ternary alloy [33]. The model has been presented in detail in section 2.1. This model is used as

the basis for the modeling of oversized solutes because of the good agreement between model calculations and experimental values. The MIK model is based on the "Perk's" model developed by Perks et al. [60]. The Perks model is also a rate-theory model for calculating RIS, which assumes that segregation occurs through differences in the vacancy diffusivities for the alloy elements. Allen et al. [33] extended the Perk's model to include composition-dependent vacancy diffusivities for Fe, Cr and Ni. The MIK model is the foundation for testing the process of vacancy trapping with oversized solute atoms.

The input parameters to the MIK model have been described in detail by Allen et al. [33]. These input parameters formed the basis of the MIK model and resulted in good agreement in segregation results between model and experiment. Since alloy and irradiation conditions in this study are very similar to those used by Allen et al., this study will continue to use the MIK model parameters. The values of the parameters are listed in table 6.1 and include the references from which the values were taken.

6.1.2 The MIK Model with Trapping

Oversized solutes are believed to affect RIS by altering the concentrations of vacancies and interstitials in the matrix by acting as traps for vacancies, thus promoting enhanced recombination with migrating interstitials. The processes by which oversized solutes affect RIS are: 1) trapping, whereby freely migrating vacancies are captured by the oversized solute atom, forming a solute-vacancy complex, 2) recombination, in which freely migrating interstitials are able to recombine with the bound vacancy when the interstitial enters the recombination volume of the solute-vacancy complex, and 3) release, where bound vacancies are able to dissociate from the solute-vacancy complex before recombination occurs. The ratio of recombination to release determines the effectiveness of the oversized solute in altering RIS.

Using the MIK model as a foundation, a trapping process is included to simulate the effects of oversized solute additions in the ternary alloy. The approach is more productive than changing the ternary alloy to a quaternary alloy to treat the oversized solute explicitly because thermodynamic data for Zr or Hf in an austenitic stainless steel are lacking. Similar work by Mansur et al. [6, 80] and Sakaguchi et al. [21] was

described in section 2.4.2. The key reaction rate equations are presented again for reference.

The first three rate equations are for the ternary alloy elements, Fe, Cr and Ni:

$$\frac{\partial C_{Fe}}{\partial t} = -\nabla \cdot J_{Fe}, \tag{6.1}$$

$$\frac{\partial C_{Cr}}{\partial t} = -\nabla \cdot J_{Cr}, \tag{6.2}$$

$$\frac{\partial C_{Ni}}{\partial t} = -\nabla \cdot J_{Ni}. \tag{6.3}$$

These rate equations describe the time rate of change of the concentrations of Fe, Cr and Ni, in terms of $-\nabla \cdot J_x$, the divergence of the elemental flux, where *x* represents Fe, Cr or Ni.

The next two rate equations for the free vacancy and interstitial concentrations, C_v and C_i, are:

$$\frac{\partial C_v}{\partial t} = -\nabla \cdot J_v + G_{dpa} - K_{iv} C_v C_i - S_v D_v \left(C_v - C_v^{eq}\right) - K_v C^s C_v + \tau_v C_v^s, \tag{6.4}$$

$$\frac{\partial C_i}{\partial t} = -\nabla \cdot J_i + G_{dpa} - K_{iv} C_v C_i - S_i D_i C_i - R_v C_v^s C_i. \tag{6.5}$$

In these equations, $-\nabla \cdot J_x$ is the divergence of the defect flux, G_{dpa} is the defect production rate, $K_{iv} C_v C_i$ is the recombination rate of vacancies and interstitials, and $S_v D_v \left(C_v - C_v^{eq}\right)$ and $S_i D_i C_i$ are the loss rates of vacancies and interstitials to sinks, respectively. The remaining terms of equations 6.4 and 6.5 represent the trapping process, where $K_v C^s C_v$ is the trapping rate of freely-migrating vacancies, $R_v C_v^s C_i$ is the recombination rate of trapped vacancies with freely migrating interstitials, and $\tau_v C_v^s$ is the release rate of vacancies from trapping sites. As for the individual variables in the equations, K_{iv} is the recombination coefficient, C_v^{eq} is the thermal equilibrium concentration for vacancies, and D_x is the diffusion coefficient, C_x is the concentration, and S_x is the sink density, where, *x* represents the defect type, either vacancies or interstitials.

The trapping process terms require additional detail. Starting with the capture term, $K_v C^s C_v$, K_v is the capture coefficient and C^s is the concentration of oversized solute in solution in the alloy. K_v is defined as:

$$K_v = 4\pi \cdot r_v' D_v N_D, \tag{6.6}$$

where D_v is the vacancy diffusion coefficient, r_v' is the capture radius for vacancy defects, and N_D is the alloy number density [52].

In the recombination term, $R_v C_v^s C_i$, R_v is the recombination coefficient, defined as:

$$R_v = 4\pi \cdot r_i' D_i N_D, \tag{6.7}$$

where D_i is the interstitial diffusion coefficient and r_i' is the recombination radius [52].

The last term of equation 6.4 is the vacancy release rate, $\tau_v C_v^s$, where τ_v is the dissociation coefficient and describes the rate at which trapped vacancies are released from the oversized solute atom [52]:

$$\tau_v = \frac{D_v}{a_0^2} \exp\left[-\frac{E_v^b}{k_B T} \right]. \tag{6.8}$$

Here, a_0 is the lattice spacing, k_B is Boltzmann's constant, T is the irradiation temperature, and E_v^b is the binding energy of the solute-vacancy complex.

Finally, the MIK-T model has two additional rate equations for the concentrations of solute-vacancy complexes and unbound solute atoms, respectively:

$$\frac{\partial C_v^s}{\partial t} = K_v C^s C_v - \tau_v C_v^s - R_v C_v^s C_i, \tag{6.9}$$

$$\frac{\partial C^s}{\partial t} = -K_v C^s C_v + \tau_v C_v^s + R_v C_v^s C_i. \tag{6.10}$$

Note that equation 6.10 does not need to be solved because it is not an independent equation. The concentration of unbound solute atoms can be found by:

$$C^s = C_0^s - C_v^s, \tag{6.11}$$

where C_0^s is the initial unbound solute concentration. Note that this model assumes only one trapped vacancy per solute atom. Furthermore, both free oversized solute and trapped solute-vacancy complexes are immobile and do not diffuse to sinks. Also, it is assumed that solute atoms are neither created nor destroyed and that the amount of oversized solute in solution is constant.

The mechanism of solute trapping and recombination with diffusing interstitials requires interactions between trapped vacancies and interstitials. Since a trapped vacancy relieves stress from an oversized solute, it may be a weaker sink for an interstitial than a free vacancy. However, trapped vacancies do not need to be as strong of sinks as free vacancies to enhance recombination because their concentration is significantly higher. For example, for HiZr with a binding energy of 1.08 eV at 400°C and dose rate of $1x10^{-6}$ dpa/s, the trapped vacancy fraction is 1.1×10^{-3} compared to 6.8×10^{-10} for the free vacancy concentration, a difference more than six orders of magnitude. The result is a much higher probability for interaction between trapped vacancies and interstitials as compared to interactions with free vacancies that overwhelms the difference in sink strength and results in a substantial increase in the recombination of point defects.

6.1.3 Model Results

To solve for the differential equations in section 6.1.2, the MIK model uses GEAR, a software package that solves initial value problems for a system of differential equations [102-104]. The system of differential equations is solved by GEAR, with appropriate initial conditions and boundary conditions, using finite differences to solve spatial derivatives with a continuous time variable [105]. A driver subroutine calculates initial values for the current time step based on the values from the previous time step until the solution reaches the final time step desired. Considering symmetry at the grain boundary surface, only half of the thin-foil problem needs to be solved, with the other side of the boundary reflecting the same concentration profile.

6.1.4 Model Benchmarking

The MIK model is used to calculate Cr depletion and Ni enrichment for a Fe-20Cr-24Ni alloy to a dose of 0.5 dpa using a dose rate of 7×10^{-6} dpa/s to match the

results shown from Allen et al. [33]. Calculations are performed with temperatures ranging from 200 – 600°C. Figure 6.1 gives the calculated grain boundary Cr concentration as a function of temperature shown previously by Allen et al. [33] and the MIK and MIK-T model results for the same input data, where the trapping process is turned off by setting input parameters equal to zero in the MIK-T model. The MIK and MIK-T model results in this study are identical, which shows that the trapping process has not modified the RIS behavior of the MIK model when the trapping process is turned off. The MIK and MIK-T model results have a small difference from the results of Allen et al. [33] at less than 0.3 at% at any temperature. The difference from the MIK and MIK-T model results from the results by Allen et al. [33] is likely due to differences in convergence criteria used for the calculations.

Figure 6.2 gives MIK results from Allen et al. [33] compared to MIK-T results, this time for grain boundary Ni concentration as a function of temperature. The results for the MIK and MIK-T model results are again identical, showing that the trapping process does not modify RIS behavior in the MIK model. Again, a small difference exists from the results by Allen et al. [33], and the difference is attributed to differences in convergence criteria used to solve the calculations.

6.1.5 MIK Model Results

The MIK model is exercised as a function of temperature, dose and dose rate. The purpose is to identify trends in segregation behavior in the MIK model so that future comparisons with the MIK-T model can reveal the predicted effects of oversized solute alloys on segregation. The calculations are based on a Fe-16Cr-13Ni alloy using the input values listed in table 6.1.

6.1.5.1 Irradiation Temperature Dependence

The MIK model results for grain boundary concentrations of Cr and Ni as a function of temperature from 200 – 600°C using a constant dose rate of 10^{-6} dpa/s are shown in figure 6.3. Cr is distinguished by a green line and Ni by an orange line. The figure also shows horizontal lines across the figure to denote the bulk, or matrix, Cr and Ni concentrations. The figure shows that RIS peaks at intermediate temperatures of 400

– 500°C. At low temperature, point defect diffusivity is low, so recombination dominates and few defects migrate to the grain boundary to cause segregation. At high temperature, point defect diffusivity is so high that large concentration gradients at the grain boundary cannot be established. Maximum segregation occurs around 450°C, as shown previously for the MIK model [33]. This temperature represents the point at which point defect diffusivity is high enough that diffusion to the grain boundary dominates over recombination, but low enough that a large concentration gradient at the boundary can be maintained without substantial back-diffusion.

6.1.5.2 Dose Dependence

Grain boundary concentrations for Ni and Cr as a function of dose at 400°C are shown in figure 6.4. Horizontal lines on the figure denote the matrix Cr and Ni concentrations. Concentrations for both Cr and Ni change quickly at low dose, with most of the change in concentration occurring by 1 dpa. After 3 dpa, RIS has saturated and changes in grain boundary concentrations are small.

6.1.5.3 Dose Rate Dependence

The MIK model results for grain boundary concentrations of Cr and Ni as a function of dose rate from 10^{-3} – 10^{-8} dpa/s using a constant temperature of 400°C are shown in figure 6.5. The figure shows horizontal lines across the figure to denote the matrix Cr and Ni concentrations. At the highest dose rate of 10^{-3} dpa/s, point defect diffusivity is low enough that, given the high production rate, recombination will dominate as there is less time for point defects to diffuse to sinks. At 10^{-8} dpa/s, the production rate is low enough, and the temperature high enough, that back diffusion at the grain boundary will limit the amount of segregation that will develop. Maximum segregation occurs around 10^{-7} dpa/s where low recombination and limited back diffusion at the boundary balance with the rate of defect diffusion to the grain boundary to cause the maximum segregation.

6.1.6 MIK-T Model

To determine the expected effects of oversized solute additions on RIS, the MIK-T model must be exercised as a function of the same variables as the MIK model, temperature, dose and dose rate. However, before doing so, values must be established for the three additional input parameters required for the MIK-T model. These parameters include the solute-vacancy binding energy, trapping radius, and recombination radius. Values for these parameters, however, are not known. Others have examined the values for binding energy, even back-calculating its value based on experimental data [6, 21, 23, 80]. But no experiments exist that have directly measured these parameters. Therefore, it is important to test the MIK-T model to determine variations in grain boundary concentrations as a function of these input parameters.

The input parameters have reference values of 0.5 eV for the binding energy and 0.5 nm for the trapping and recombination radii. Sakaguchi et al. [21] inferred a larger binding energy than 0.5 eV when measuring segregation of Zr and Hf additions to 316SS. However, the lower value of 0.5 eV is chosen so that more variation in segregation can be seen for the trapping and recombination radii. A large binding energy (1.0 eV) would diminish the effect of any variation seen in these radii. The trapping and recombination radii represent the distance to a 4^{th} nearest-neighbor position in a face-centered cubic (fcc) unit cell for a Fe-Cr-Ni alloy. This value is a reasonable approximation of the interaction distance of oversized solute atoms. Further justification for the trapping and recombination radius will be addressed in section 6.2.4. Values for the MIK-T model input parameters used here are the same that will be used in the sensitivity analysis of section 6.1.8.

The following analyses are of the MIK-T model input parameters is conducted for a Fe-16Cr-13Ni alloy with the experimental variables set to a temperature of 400°C with a dose rate of 1×10^{-6} dpa/s, a dose a 1 dpa, and a solute concentration of 0.5 at%.

6.1.6.1 Binding Energy

The binding energy describes the strength of the solute-vacancy trap. Increasing the binding energy decreases the probability that the vacancy will escape the solute atom, which increases the probability for recombination with an interstitial. Consequently,

large binding energies will have a significant impact on the MIK-T model by reducing the defect population, and hence the flux of defects to grain boundary sinks through enhanced recombination.

To quantify the effect of binding energy on RIS, the binding energy is varied from 0 to 1.0 eV, and the changes in grain boundary Cr and Ni concentration are shown in figure 6.6, with Cr in green and Ni in orange. The reference value of 0.5 eV is also shown on the figure with a vertical line. With a binding energy of 0 eV, such that no trapping exists, the Cr concentration at the grain boundary is nearly 10 at%, while Ni is around 22 at%. This represents the same values seen for the MIK model given the same irradiation and alloy conditions as shown in figure 6.3 (at 400°C). At low binding energies, the changes in segregation are small. Increasing the binding energy further has an increasing impact on RIS, such that by 1.0 eV, both Cr and Ni concentrations have a difference from the matrix concentrations of less than 1 at%, so RIS is mostly eliminated by 400°C with a binding energy of 1.0 eV.

6.1.6.2 Trapping Radius

The trapping radius controls the rate at which vacancies are trapped by oversized solute atoms. No known experimental measurements exist on which to base a trapping radius for Hf or Zr in oversized solute alloys. Therefore, this input parameter is exercised to determine its effect on segregation behavior.

Figure 6.7 shows the grain boundary concentrations for Ni and Cr as a function of trapping radius. The trapping radius is varied from 0 to 1 nm, with 1 nm representing about 3 times the lattice parameter. The reference value of 0.5 nm is shown by a vertical line on the figure. The trapping radius of 0 nm represents the system without trapping. The result at this point is the same as the value for the MIK model without trapping, shown in figure 4.3 (at 400°C). The next data point occurs at 0.3 nm, which is approximately the distance to the first nearest neighbor position. A distance less than the first nearest neighbor position for the recombination radius would not be physically meaningful, so the region is shaded in grey to denote that values less than 0.3 nm are not considered.

Most of the change in concentration occurs with a trapping radius of 0 – 0.3 nm. By 0.3 nm, the grain boundary Cr concentration has increased from 10 at % to nearly 15 at%, and little change in grain boundary concentration occurs with a larger trapping radius. The significance here is that small, realistic values for the trapping radius are all that is required for reductions in RIS.

The reason why a large value for the trapping radius does little to change RIS is due to the interaction volume. The trapping radius defines an interaction volume around the oversized solute atom, so a radius of 1.0 nm has an interaction volume of 4.19 nm^3, compared to an atomic volume of roughly 0.012 nm^3. The interaction volume encompasses over 300 lattice sites, so if the solute concentration is 0.5 at%, then 1 in 200 lattice sites contain an oversized solute, and the solute interaction volumes are overlapping. This illustrates that the interaction volume is a function of both the trapping radius and the solute concentration. When interaction volumes overlap, further increases in the trapping radius will have little additional impact on RIS.

6.1.6.3 Recombination Radius

The recombination radius controls the rate at which migrating interstitials recombine with vacancies trapped in a solute-vacancy complex. Like the trapping radius, there is no experimental basis for the recombination radius of Hf or Zr in oversized solute alloys. Again, this input parameter must be exercised to determine its effect on segregation behavior.

The results for the variation of the recombination radius, shown in figure 6.8, are nearly the same as figure 6.7. Figure 6.8 shows the grain boundary Cr and Ni concentrations as a function of the recombination radius, which is varied from 0 – 1 nm. Again, the reference value of 0.5 nm is noted by a vertical line on the figure. A radius of 0 nm is the same as the value for the MIK model without trapping, shown in figure 6.3 (at 400°C). The next data point occurs at 0.3 nm, which, as explained in section 6.1.6.2, is approximately the distance to the first nearest neighbor position. The region from 0 – 0.3 nm is again shaded grey as this represents a radius less than the distance to the 1st nearest neighbor.

Like the trapping radius, most RIS reduction occurs by 0.3 nm for the recombination radius. Increasing the value beyond this does little to increase the effectiveness of the MIK-T model due to overlapping interaction volumes.

6.1.7 Variation of Experimental Variables

The MIK-T model is exercised to explore the variations in segregation behavior as a function of irradiation and alloy variables such as temperature, dose, dose rate and oversized solute concentration. The purpose is to understand segregation behavior as a function of these variables to establish what effect they have on segregation when comparing the reference alloys to the oversized solute alloys. For variations in temperature, dose and dose rate, the MIK and MIK-T model results are compared. This explains in what temperature and dose rate regime oversized solutes are expected to have the most effect in reducing grain boundary segregation.

All model calculations are for a Fe-16Cr-13Ni alloy, with results shown at 1 dpa. The MIK-T model uses the same input parameter values as section 6.1.6 for the trapping and recombination radii at 0.5 nm. The exception is the binding energy, which is now 1.0 eV and represents an approximate value of the binding energies determined by Sakaguchi et al. [21] when measuring segregation of Zr and Hf additions to 316SS.

6.1.7.1 Irradiation Temperature

RIS is calculated as a function of irradiation temperature to determine where the MIK-T model is most sensitive to temperature and, therefore, most effective at reducing segregation as compared to the MIK model.

Figure 6.9 shows grain boundary Cr concentrations for both the MIK and MIK-T models as a function of irradiation temperature at 1 dpa with a constant dose rate of 10^{-6} dpa/s. MIK results are in black while MIK-T results are in green. For the MIK model, maximum segregation occurs around 450°C, and segregation is substantially less at the temperature extremes of 200°C or 600°C, as discussed in section 6.1.5.1. Results for MIK-T are somewhat different, with a maximum segregation at 350°C, and virtually no segregation occurring at temperatures of 500°C or higher.

Temperature results at either end of the spectrum in figure 6.9 show little segregation for the MIK model, so it is no surprise that the MIK-T model also shows little to no segregation at these temperatures. Seen another way, the percent difference between the MIK and MIK-T models, which is shown in figure 6.10, reveals that with increasing temperature, the percent difference between the two models increases. The difference reaches a maximum at 450°C, whereupon at higher temperatures, differences between the models begin to decrease.

At low temperature, point defect diffusivity is very low, so RIS for the MIK model is also low. Consequently, the difference between the MIK and MIK-T models is small. The difference between models is also small at high temperatures, except that here, point defect diffusivity is large enough that a concentration gradient at the grain boundary does not develop. Again, RIS for the MIK model will be small at high temperature, so its difference from MIK-T is small.

For results around 450°C, where the MIK model shows a maximum in segregation behavior, the MIK-T model is most effective. This is due to the fact that segregation in the MIK model has reached a maximum, so the MIK-T model is able to make the greatest difference at 450°C and therefore exhibits the highest degree of effectiveness.

The MIK model has about the same amount of Cr depletion at both 400°C and 500°C, as shown in figure 6.9, but the MIK-T model shows less segregation at 500°C than 400°C. The reason for a more effective trapping process at the higher temperature requires a more detailed explanation.

Examining the dissociation coefficient in equation 6.8, the temperature is in the denominator of the exponential. Figure 6.11 shows the value of the exponential as a function of temperature. Increasing the temperature makes the dissociation coefficient larger, so the rate of solute-vacancy dissociation (or vacancy release) increases. As a higher fraction of trapped vacancies are released, it follows that a lower fraction of trapped vacancies recombine. These ratios are shown in figure 6.12, where the release and recombination rates divided by the trapping rate are plotted as a function of temperature, with release rate in blue and recombination rate in red. With increasing temperature, relative to the trapping rate, as the release rate increases, the recombination

rate must decline. Although the trapping process appears to be less effective with increasing temperature, this is not necessarily the case, as explained next.

Increasing the temperature increases the magnitudes of the trapping, recombination and release coefficients in the MIK-T model. The capture and recombination coefficients in equations 6.6 and 6.7 contain the temperature-dependent variables of vacancy diffusivity (in the trapping coefficient) or interstitial diffusivity (in the recombination coefficient). Increasing the temperature means that the diffusivities, and hence the coefficients for trapping and recombination, will increase with temperature. The same is also true for the release rate, which includes the exponential and the vacancy diffusivity.

The values for the recombination rate as a function of temperature are shown in figure 6.13, where the ratio is relative to the rate at 200°C where recombination was highest. From 200 – 450°C, the recombination rate decreases due to competition from the release term, as explained by figure 6.12. By 450°C, the release coefficient is increasing less rapidly (the magnitude of the slope decreases) than at low temperatures, as explained by figure 6.11. From 450 – 600°C, the magnitudes of trapping and recombination coefficients increase faster than the magnitude of the release coefficient, with the result that the relative recombination rate increases again after 450°C. The effect is for MIK-T to show less segregation at 500°C than at 400°C because of the higher recombination rate.

The results shown in figure 6.11 through 6.13 illustrate that at temperatures of 450°C and above, the relative recombination rate increases, making the trapping process more effective. The result is that the MIK-T model calculates less segregation at 500°C than at 400°C and indicates that oversized solute alloys should show less RIS at the higher temperature.

6.1.7.2 Dose

Grain boundary Cr depletion for the MIK and MIK-T models are plotted as a function of dose up to 3 dpa at 400°C in figure 6.14. MIK values are the same as the values shown in figure 6.4. Both MIK and MIK-T change at similar rates after ~ 0.5 dpa. However, the MIK model changes quickly at low dose, such that the differences between

models are substantial by 0.5 dpa. The percent difference between the MIK and MIK-T models can be seen in figure 6.15, where the difference between models increases quickly at low dose, and at less than 0.5 dpa the difference between the models is close the maximum. By 1 dpa, neither model shows any significant change in Cr concentration, indicating that segregation is mostly saturated, and the difference between the models is nearly constant.

6.1.7.3 Dose Rate

Although proton irradiations are performed with a relatively fixed dose rate, knowing how the MIK-T model varies as a function of dose rate might help in understanding results between irradiations with different particle types, where dose rates can vary considerably.

Variations of the dose rate are shown in figure 6.16, where the MIK model is again shown in black and MIK-T model shown in green. The MIK model shows increasing grain boundary Cr concentration with increasing dose rate up to 10^{-7} dpa/s, after which the Cr concentration decreases, as mentioned in section 6.1.5.3. The MIK-T model shows the opposite trend, with the lowest grain boundary concentration occurring at 10^{-3} dpa/s and increasing Cr concentration with decreasing dose rate.

For a 400°C irradiation, at the highest dose rate of 10^{-3} dpa/s, the MIK model shows the least segregation. Although recombination is enhanced in the MIK-T model, increased recombination is insignificant compared to the number of point defects diffusing to the grain boundary. The traps are overwhelmed by the high production rate. Figure 6.17 shows the trapped vacancy concentration and the ratio of the trapped vacancy concentration to the defect production rate (dose rate) as functions of dose rate. Although the trapped vacancy concentration is larger at 10^{-3} dpa/s than at 10^{-8} dpa/s, the dose rate of 10^{-8} dpa/s has a much higher ratio of trapped vacancies to production rate. This means that, relative to the number of vacancies being created per unit time, the number of trapped vacancies is much higher at 10^{-8} dpa/s, and more trapped vacancies are available for recombination, with fewer vacancies migrating to the grain boundary to cause RIS.

Figure 6.18 plots the concentrations of freely migrating vacancies and trapped vacancies relative to their maximum values at 10^{-3} dpa/s. The figure shows that, as the

dose rate decreases, the freely migrating vacancy concentration decreases dramatically while the trapped vacancy concentration decreases only slightly, leaving a higher fraction of vacancies trapped with solute atoms and available for recombination, and consequently less RIS.

6.1.7.4 Oversized Solute Concentration

Sensitivity of the MIK-T model to oversized solute concentration provides an understanding of segregation in alloys with varying solute levels. Figure 6.19 shows the grain boundary Cr and Ni concentrations, but now as a function of the oversized solute concentration from 0 to 1.0 at%. The reference value is shown by a vertical line in the figure at 0.5 at%. Binding energy is 0.5 eV and the trapping and recombination radii are 0.5 nm. The solute concentration will dictate the number of trapping sites available for the trapping of vacancies.

Even by the highest concentration of 1.0 at%, grain boundary Cr is still substantially less than that seen in figure 6.6 with a binding energy of 1.0 eV. In fact, there is little change in grain boundary concentrations after about 0.1 at% of solute. Looking at the Ni concentration, for example, the grain boundary value drops from 22 at% with no solute to just below 19 at% Ni with 0.1 at% solute. By 0.3 at% solute, the amount of Ni is down to 18 at%, and even with 1.0 at% oversized solute in the alloy, the grain boundary value is still above 17 at%. So the majority of the change in grain boundary concentrations occurs with less than 0.1 at% oversized solute. Increasing the solute concentration may increase the number of vacancy trapping sites available, but the effect is incremental because the solute concentration is already substantially higher than the vacancy concentration in the alloy at this dose rate. So relatively little solute in solution is required to cause a substantial change in RIS.

6.1.8 Sensitivity Analysis

A sensitivity analysis reveals the input parameters to which the grain boundary Cr concentrations in the MIK-T model are most sensitive. Allen et al. [33] performed a sensitivity analysis for the MIK model previously. Therefore, only the input parameters

introduced to the MIK-T model will be studied here, which are the binding energy, trapping radius and recombination radius.

Model sensitivity is determined by the derivative, $\partial X/\partial P$, of the grain boundary concentration as a function of an input parameter, where ∂X is the change in grain boundary concentration and ∂P is the change in the input parameter [33]. Calculation of the sensitivity uses the ratio of the difference in grain boundary concentration and input parameter, $\delta X/\delta P$, where each input parameter is varied by a factor of 10^{-4} about the reference value to find the difference in grain boundary concentration. The variation of $\partial C/\partial P$ is approximated by the following:

$$\frac{\partial C}{\partial P} \approx \frac{\delta C}{\delta P} = \frac{C' - C_{reference}}{P' - P_{reference}}, \tag{6.12}$$

where C' is the model-calculated grain boundary concentration, with $C' = C_{reference} + \delta C$, and P' is for the input parameter, with $P' = P_{reference} + \delta P$. To make it easier to interpret the results from the sensitivity analysis, the sensitivities are expressed in the form of a significance, S_P^C, which is defined as the fractional change in calculated concentration relative to the fractional change in input parameter. The significance is expressed by,

$$S_C^P = \frac{C' - C_{reference}}{P' - P_{reference}} \cdot \frac{P_{reference}}{C_{reference}}. \tag{6.13}$$

The larger the significance of the input parameter, the more sensitive the model is to that parameter.

The sensitivity calculations are performed for a Fe-16Cr-13Ni ternary alloy irradiated at a dose rate of 10^{-6} dpa/s at 400°C or 500°C to a dose of 1 dpa with an oversized solute concentration of 0.5 at%. The three input parameters to the MIK-T model which are varied are the trapping radius, recombination radius, and binding energy. The standard value of each input parameter for the sensitivity study is given in table 6.2, with a binding energy of 0.5 eV, and trapping and recombination radii of 0.5 nm.

Results from the sensitivity study, consisting of the significance values for the input parameters, are given in table 6.3 for 400°C and table 6.4 for 500°C. According to

the analysis, the most sensitive of the three input parameters at either temperature is clearly the solute-vacancy binding energy. With a significance of 0.22 for Cr and -0.32 for Ni at 400°C and 0.24 and -0.25 for Cr and Ni at 500°C, this value is a factor of 4 to 5 times higher than the other input parameters. From 400°C – 500°C, the change in grain boundary Cr depletion increases slightly, hence the increase in significance. Meanwhile, the Ni enrichment decreases slightly from 400 – 500°C, so the Ni significance decreases slightly as a result.

Significance values for the trapping and recombination radii range from 0.02 to 0.03 at 400°C and 0.03 at 500°C for Cr, and range from -0.04 to -0.03 at 400°C and -0.03 at 500°C for Ni. Changing the reference value for the trapping and recombination radii would have little impact on the significance values. Since sensitivity is a reflection of the rate of change (slope) of the concentration, figures 6.7 and 6.8 show that the slope does not change for the entire range of these values from 0.3 – 1 nm.

The sensitivity analysis reveals that grain boundary segregation is not highly sensitive to any of the input parameters. Comparing the significance values of tables 6.3 and 6.4 to those calculated for the MIK model by Allen et al. [33], they found that vacancy migration energies for Cr and Ni had a significance of 57 and -52, respectively, at 400°C for a Ni-18Cr-9Fe alloy at 0.5 dpa. The vacancy migration energies have significance values that are two orders of magnitude higher relative to the input parameters of the MIK-T model.

The reason for the differences in magnitude lies in the importance of the input parameters to the vacancy migration energy. The MIK model was highly sensitive to vacancy migration energy [33]. Since the MIK Model has many variables that affect the composition-dependent vacancy migration energy directly, these input parameters also had a large significance. On the other hand, input parameters that have no effect on vacancy migration energy, like dislocation density or interstitial jump frequency, have very small significance values. Likewise, the inputs to the MIK-T model do not change the vacancy migration energies, so their significance is low. This simply means that very small changes to the inputs will have little or no effect on the model. It does not mean, however, that the trapping process is ineffective at changing grain boundary segregation, as seen in sections 6.1.6 and 6.1.7.

The importance of the MIK-T significance values is twofold. First, they have identified vacancy binding energy as the most important variable in the trapping process. Accurate values for this input parameter are critical. Second, even with the higher significance of the binding energy, the sensitivity of the input parameters is low enough that some uncertainty in the values will have minimal impact upon the RIS results.

6.2 Determination of Binding Energies

As shown in section 6.1.8, the most sensitive variable in the MIK-T model of the MIK model is the solute-vacancy binding energy. Solute-vacancy binding energies for Zr and Hf in stainless steel are not available experimentally. Therefore, the quantitative method of *ab initio* calculations is used to determine the magnitude of these energies. This section describes the details of the first-principles method using the Vienna *Ab initio* Simulation Package (VASP) and how it is used to calculate the binding energies. The calculations reveal that Zr has a significantly larger binding energy than Hf, 1.08 eV vs. 0.71 eV, and the reason for the difference will be discussed. Justification for the trapping and recombination radii is also provided through first principles. Finally, the section concludes with calculations of lattice parameters for Fe, Hf and Zr to show that Hf and Zr have similar size factors in a fcc Fe system, despite their difference in binding energy.

6.2.1 *Ab initio* Method

In order to determine the solute-vacancy binding energies, a first-principles approach based on Kohn-Sham density functional theory (DFT) [106] is selected for its ability to describe defect energies [79, 107-109]. Calculations are performed using the Vienna *Ab Initio* Simulation Package (VASP) [110-113]. The projector-augmented plane-wave (PAW) method [114] allows efficient calculations of transition elements like Fe, Zr and Hf. Calculations use the Perdew and Wang [115] parameterization of the generalized gradient approximation (GGA). All calculations are performed with an automatically generated Monkhorst-Pack 4x4x4 *k* point mesh [116] and energy cutoff of 500 eV. This ensures convergence with respect to energy and k point mesh to within 1 meV/atom. Defects are studied in a 108(-1) atom periodic 3x3x3 supercell of the fcc

conventional cell, where the cell shape and volume were fixed but ionic relaxations were allowed. The ternary Fe-Cr-Ni alloy is approximated by pure fcc Fe to avoid the configuration dependence of the less abundant Cr and Ni elements. For all defect calculations, the system is constrained to maintain a constant volume but permits relaxation of ions.

Both spin polarized (magnetic) and non-spin polarized (non-magnetic) calculations are performed to test the effects of magnetism on the defect properties. Spin-polarized calculations are initiated with ferromagnetic alignment [109]. Both spin-polarized and non-spin-polarized calculations use 8 valence electrons for Fe and 4 for Zr and Hf. A second set of non-spin-polarized calculations uses an extra *p*-shell of electrons in the valence band to treat more of the electrons explicitly to test the dependence on number of valence electrons. In this case, Fe includes 14 electrons, Zr and Hf have 12.

6.2.2 Binding Energy Determination

The solute-vacancy binding energy is calculated using two methods, direct and indirect [79, 107]. The direct method compares two energies, that of the solute and vacancy sitting on first nearest-neighbor sites and that of the solute and vacancy as far apart as possible in the cell considering the periodic boundary conditions. The farthest separation possible from a vacancy in a cubic 108 atom simulation cell is an 11^{th} nearest-neighbor (nn), which in the ideal lattice (no relaxation of the fcc positions) gives a separation of $a\sqrt{11/2}$, where a is the lattice constant. The direct method is an approximation of the binding energy since even at a separation distance to the 11^{th} nn, the solute and vacancy may still interact with each other.

The indirect method accounts for possible interactions beyond the 11^{th} nn by calculating the binding energy with four different VASP calculations. In this method the energy of the vacancy and solute atom are subtracted separately from the energy of the system where they interact as first nearest-neighbors, and the method is described in detail in Ref. 107. As the number of atoms in the simulation cell increases the binding energies of these two methods should converge. The binding energy determined for the direct and indirect methods are given as:

$$E_b^{direct}(OS-v) = E(^{106}Fe, OS, v, 1^{st}\,nn) - E(^{106}Fe, OS, v, 11^{th}\,nn), \qquad (6.14)$$

$$E_b^{indirect}(OS-v) = E(^{106}Fe, OS, v, 1^{st}\,nn) - E(^{107}Fe, OS) - E(^{107}Fe, v) + E(^{108}Fe)\,. \quad (6.15)$$

In these equations, *OS* represents the oversized solute atoms, Zr or Hf, and *v* represents a vacancy. In equation 6.14, $E_b^{direct}(OS-v)$ is the solute-vacancy binding energy by the direct method, $E(^{106}Fe, OS, v, 1^{st}\,nn)$ is the energy with 106 Fe atoms, 1 oversized solute, and a vacancy as a 1st nn, and $E(^{106}Fe, OS, v, 9^{th}\,nn)$ is the energy with 106 Fe atoms, 1 oversized solute, and a vacancy as a 11th nn. In equation 6.15, $E_b^{indirect}(OS-v)$ is the binding energy by the indirect method, $E(^{107}Fe, OS)$ is the energy for 107 Fe atoms and 1 oversized solute, $E(^{107}Fe, v)$ is the energy for 107 Fe atoms and 1 vacancy, and $E(^{108}Fe)$ is the energy for 108 Fe atoms.

The indirect method is generally considered the more accurate method for calculating solute-vacancy binding energy [107]. Binding energies based on the nn position are presented in table 6.5. These calculations assume non-spin-polarization. Table 6.5 includes the distance of the nn position from the origin. For the values shown in the table, a negative sign denotes repulsion and a negative binding energy for the solute-vacancy complex. Using the indirect method, binding energies are shown to be 1.08 eV for Zr and 0.71 eV for Hf when the vacancy is a 1st nn to the oversized solute. Binding energy as a function of nn position is shown in figure 6.20 for the 1st through 6th and at the 11th nn positions of both Hf, in blue, and Zr, in red. Included in figure 6.20 along the top x-axis is the distance, in nm, of each nn position from the origin. By the 11th nn position, the binding energy is close to zero, which represents weak interaction between the vacancy and the solute.

The direct method can also be used to determine the binding energy and verify the values calculated by the indirect method. Values for the direct method are also shown in table 6.5. Using the direct method, the solute-vacancy binding energy is 1.05 eV for Zr and 0.69 eV for Hf, which is essentially the same as the energies found using the indirect method. By definition, the 11th nn position has a binding energy of 0.0 eV as it is used for the reference for the direct method.

Calculations are also performed for Zr and Hf using an additional *p*-shell of electrons to test the sensitivity of the binding energy with respect to the number of

valence electrons. Using the direct method only to calculate binding energy, the values are shown in table 6.6 for just the 1st, 4th and 11th nn positions. These solute-vacancy binding energies are in good agreement with the calculations that neglected the extra *p*-shell electrons.

Finally, using the direct method, table 6.6 also shows binding energies for Zr in a spin-polarized Fe system. Calculations are repeated for spin-polarized Fe using the lattice parameter of 0.3638 nm. Values for just the 1st and 11th nn positions are shown. Again, the solute-vacancy binding energy of 1.12 eV for Zr is in good agreement with the binding energy of 1.05 eV without spin-polarization using the direct method and 1.08 eV calculated by the indirect method.

6.2.3 Differences between Zr and Hf

The reason for the difference in binding energy between Zr and Hf is due to the differences in the electronic effects with the surrounding Fe atoms. System relaxation permits the ions to find the most energetically stable configuration. When placed next to a vacancy defect, the relaxation of Zr toward the vacancy is substantial, as Zr finally rests close to midway between its lattice site and the vacant lattice site. The result is a substantial reduction in energy. The same relaxation occurs for Hf, but it is less substantial. The Hf ion still rests much closer to its original location on the fcc Fe lattice. The differences between these ions and their proximity to the vacant lattice site can be seen in figure 6.21. The Fe atoms are shown in green while the Hf and Zr atoms are shown in light blue and purple, respectively, with Hf on the left and Zr on the right. Notice that Zr is much closer to the vacant lattice site position than Hf. The center of the vacant lattice site is aligned with the tips of the arrows denoting the vacant lattice site position. The solutions for both sets of calculations converged to the same convergence criteria of 1 meV/atom, so the differences in relaxation are not a result of convergence.

6.2.4 Trapping and Recombination Radii

In section 6.1.8, for the sensitivity analysis used a value of 0.5 nm for the trapping and recombination radii. No experimental data exists that could be used to determine the true radius of trapping or recombination for Zr or Hf solute atoms in a Fe-Cr-Ni alloy.

However, the binding energy calculations discussed in section 6.2.2 offer some evidence for a reasonable value. As shown in figure 6.20, the solute-vacancy binding energy decreases dramatically when a vacancy moves from a 1st nn position to a position farther from the oversized solute atom. A vacancy in the 2nd nn position has a negative binding energy, indicating repulsion. A vacancy in the 4th nn position is more stable relative to the 2nd or 3rd nn positions, hence the higher binding energy.

A drawing of the nn positions relative to the oversized solute at the origin is shown in figure 6.22. The figure shows just the first (unit) cell of 27 cells that comprise the supercell for 108 lattice positions. Included in the figure are 1st, 2nd, 3rd, 4th and 6th nn positions; the 5th nn position is in the face of the neighboring cell, one lattice parameter distance (away from the origin) from the 1st nn position.

Notice in figure 6.22 that the 2nd, 3rd, and 4th nn positions are all nearest-neighbors to the 1st nn position. This means any one of them is a possible diffusion path to the 1st nn position. Since it is more favorable for a vacancy to diffuse directly from the 4th to the 1st nn position, the distance separating the origin and the 4th nn position, ~ 0.5 nm, makes a logical choice for the radius for trapping vacancies.

Interstitial configurations with a solute-vacancy complex are not examined to determine the recombination radius. However, using the same analysis as the preceding paragraph, it may be reasonable to assume that the recombination radius has a value similar to the radius for trapping.

6.2.5 Lattice Parameters

Calculations of the lattice parameters for Fe, Zr and Hf are performed in order to determine the atomic volumes of these elements in a fcc system. These atomic volumes could then be used to determine the size factors. An equation for calculating the linear size factor was given previously in equation 2.34, but the calculations have always used the atomic volumes based on body-centered cubic (bcc) Fe and hexagonal close-packed (HCP) Zr or HCP Hf. Yet, austenitic stainless steel is in the fcc structure with the oversized solute atoms on substitutional sites, so atomic volumes and hence a linear size factor would be more relevant for a fcc system. These can be determined using *ab initio*.

A primitive fcc unit cell with a single atom enables lattice parameter calculations, assuming full relaxation without a constrained volume. This is done for both spin-polarized (magnetic) and non-spin-polarized (non-magnetic) fcc Fe and the results for lattice parameters of Fe, Zr and Hf along with the size factors for Zr and Hf are shown in table 6.7. In either case the size factors for Hf and Zr are similar, and they are both close to those calculated based on experimental atomic volumes for bcc Fe and HCP Hf and Zr, also shown in table 6.8.

The similarity in size factors between Zr and Hf reveal that the solute-vacancy binding energy is not simply a function of the elastic strain around the solute atom, as has been proposed in the literature [13, 14, 21, 23, 25]. Calculations with *ab initio* show that electronic interactions play a large part in determining the binding energies for oversized solute atoms, shown by the large difference in binding energy between Zr and Hf of 1.08 eV vs. 0.71, respectively.

6.3 Model Results for the Alloys

The final section concludes with segregation results for the MIK-T model for the oversized solute alloys. The model uses the binding energy values for Zr and Hf calculated through *ab initio*.

6.3.1 MIK-T Model Results

Using the first-principles approach to binding energy not only provides a quantitative value on which to base the trapping mechanism, it also gives understanding of how RIS results between Zr and Hf solute additions should differ. The different binding energies reflect a very large difference in how effectively Zr or Hf may trap and bind vacancy defects. Figure 6.23 is similar to figure 6.11 and shows the value of the exponential in the solute-vacancy dissociation rate, now based on the binding energies for Zr and Hf of 1.08 and 0.71 eV, respectively. The exponential is temperature-dependent, and at 400°C, the difference in binding energy between Hf and Zr means a difference in the solute-vacancy dissociation rate of nearly three orders of magnitude.

6.3.2 Alloy Results

Starting with the +Zr alloys at 400°C, figure 6.24 shows the change in grain boundary Cr and Ni concentrations, respectively, at 3, 7 and 10 dpa. These doses are shown because they are the doses at which RIS measurements are made at 400°C for +Zr and +Hf alloys, as presented in chapter 5. In the figure the grey bars are for Ref-Zr while LoZr and HiZr are in shades of red. All model calculations are represented by cross-hatch bars in chapters 6 and 7. Both figures show that Cr depletion and Ni enrichment is kept to less than 2 at% at 3, 7 and 10 dpa for both LoZr and HiZr. Segregation values for Ref-Zr, on the other hand, are near 6 at% for Cr depletion and around 10 at% for Ni enrichment. Ni enrichment is more than Cr depletion for Ref-Zr because of the amount of Fe depletion. For LoZr and HiZr, Ni enrichment is only slightly greater because the MIK-T model reduces Fe depletion to a small value.

The magnitude of reduction in segregation is not the same for the +Hf alloys, where binding energy is only 0.69 eV. The segregation results are shown in figure 6.25 for changes in grain boundary Cr and Ni concentrations, with Ref-Hf in dark grey and LoHf and HiHf in shades of blue. Cr depletion at 3 dpa is 5 at% and 4 at% for LoHf and HiHf, respectively, compared to close to 8 at% for Ref-Hf. Similarly Ni enrichment exceeds 5 at% for LoHf and 4 at% for HiHf. There is still a large difference from Ref-Hf, however, which has 11 at% Ni enrichment. Meanwhile, segregation changes very little from 3 dpa to 7 and 10 dpa.

Figures 6.26 shows the amounts of Cr depletion and Ni enrichment for the +Zr alloys at 500°C using a binding energy of 1.08 eV. Based on the model results shown in figure 6.9 using a 1 eV binding energy, it is not surprising that with a binding energy of 1.08 eV, LoZr and HiZr show virtually no Cr depletion or Ni enrichment, less than 0.1 at% at 1 and 3 dpa. Ref-Zr shows more than 7 at% Cr depletion and almost 12 at% Ni enrichment at 1 dpa. At 3 dpa, Ref-Zr has more than 7.5 at% Cr depletion and more than 13.5 at% Ni enrichment. The doses of 1 and 3 dpa are shown because they are the doses at which RIS measurements were made at 500°C for +Zr and +Hf alloys.

Given the lower binding energy for Hf, figure 6.27 shows higher amounts of Cr depletion and Ni enrichment for the +Hf alloys as compared to the +Zr alloys. At 1 dpa, Ref-Hf has close to 9 at% Cr depletion and 13 at% Ni enrichment. By 3 dpa, these values

have increased slightly to 9.5 at% Cr depletion and about 15 at% Ni enrichment. For LoHf Cr depletion and Ni enrichment are around 3.5 at% at 1 and 3 dpa, while HiHf has less than 2 at% Cr depletion and Ni enrichment.

MIK-T model results predict a large reduction in RIS for the oversized solute alloys relative to the reference alloys. Zr is shown to be more effective at reducing RIS than Hf because of the large difference in solute-vacancy binding energy calculated by first-principles methods between Zr at 1.08 eV vs. Hf at 0.71 eV.

Table 6.1 MIK model input values. Adapted from [33].

Input Parameter	Value	Reference
Vacancy jump frequency for Fe	2.8×10^{13} s	[63]
Vacancy jump frequency for Cr	5.0×10^{13} s	[63]
Vacancy jump frequency for Ni	1.5×10^{13} s	[63]
Interstitial jump frequency	1.5×10^{12} s	[117]
Atom-interstitial correlation factor	0.44	[118]
Cohesive energy for pure Fe	-4.28 eV	[72]
Cohesive energy for pure Cr	-4.10 eV	[72]
Cohesive energy for pure Ni	-4.44 eV	[72]
Vacancy migration energy for pure Fe	1.28 eV	[119]
Vacancy migration energy for pure Cr	0.97 eV	[119]
Vacancy migration energy for pure Ni	1.04 eV	[119]
Vacancy formation energy for pure Fe	1.40 eV	[119]
Vacancy formation energy for pure Cr	1.60 eV	[119]
Vacancy formation energy for pure Ni	1.79 eV	[119]
Vacancy formation on grain boundary	1.4 eV	[120]
Ordering energy for NiCr pairs	0.005 eV	best fit
Ordering energy for NiFe pairs	-0.001 eV	best fit
Ordering energy for FeCr pairs	0.003 eV	best fit
Fe Free energy difference	0.01 eV	[72]
Cr free energy difference	-0.10 eV	[72]
Interstitial migration energy	0.9 eV	[121]
Dislocation density	1×10^{14} m^2	[122]
Coordination number	12	-

Table 6.2 Standard values of the MIK-T model input parameters used for the sensitivity study

Input Parameter	Symbol	Input Value
Trapping Radius	r_v'	5.0×10^{-10} m
Recombination Radius	r_i'	5.0×10^{-10} m
Binding Energy	E_v^b	0.5 eV

Table 6.3 Changes in grain boundary concentration and the significance of MIK-T model input parameters at 400°C and 1 dpa after changing the input values by a factor of 10^{-4}

Input	Reference Value	Change in Value	Dose (dpa)	$\Delta_{Conc.}$ at GB (at%)		Significance	
				Cr	Ni	Cr	Ni
E_v^b	0.5 eV	$5x10^{-6}$ eV	1	$2.5x10^{-4}$	$-6.1x10^{-4}$	**0.22**	**-0.32**
r_v'	$5x10^{-10}$ m	$5x10^{-15}$ m	1	$3.0x10^{-5}$	$-7.4x10^{-5}$	**0.03**	**-0.04**
r_i'	$5x10^{-10}$ m	$5x10^{-15}$ m	1	$3.1x10^{-5}$	$-7.6x10^{-5}$	**0.03**	**-0.04**

Table 6.4 Changes in grain boundary concentration and the significance of MIK-T model input parameters at 500°C and 1 dpa after changing the input values by a factor of 10^{-4}

Input	Reference Value	Change in Value	Dose (dpa)	$\Delta_{Conc.}$ at GB (at%)		Significance	
				Cr	Ni	Cr	Ni
E_v^b	0.5 ev	$5x10^{-7}$ ev	1	$2.8x10^{-4}$	$-4.6x10^{-4}$	**0.24**	**-0.25**
r_v'	$5x10^{-10}$ m	$5x10^{-15}$ m	1	$3.7x10^{-5}$	$-6.1x10^{-5}$	**0.03**	**-0.03**
r_i'	$5x10^{-10}$ m	$5x10^{-15}$ m	1	$3.7x10^{-5}$	$-6.0x10^{-5}$	**0.03**	**-0.03**

Table 6.5 Binding energy as a function of nearest neighbor distance for Zr or Hf in non-spin-polarized Fe using the indirect method

Vacancy Position	Distance from Solute (nm)	Indirect Method		Direct Method	
		Binding Energy (eV)			
		Zr	Hf	Zr	Hf
1st nn	0.244	1.08	0.71	1.05	0.69
2nd nn	0.345	-0.10	-0.06	-0.13	-0.07
3rd nn	0.422	0.09	0.11	0.07	0.09
4th nn	0.488	0.14	0.11	0.12	0.09
5th nn	0.545	0.04	0.08	0.02	0.07
6th nn	0.597	0.04	0.08	0.02	0.06
11th nn	0.809	0.02	0.02	0.00	0.00

Table 6.6 Binding energy as a function of nearest neighbor distance using the direct method, first for Zr or Hf in non-polarized Fe with an additional *p*-shell of electrons, and also Zr in spin-polarized Fe

Vacancy Position	Distance from Solute (nm)	Non-Spin-Polarized, extra *p*-shell Binding Energy (eV)		Distance from Solute (nm)	Spin-Polarized Binding Energy (eV)
		Zr	Hf		Zr
1^{st} nn	0.2438	0.98	0.70	0.257	1.12
4^{th} nn	0.4876	0.12	0.09	0.515	-
11^{th} nn	0.8085	0.00	0.00	0.853	0.00

Table 6.7 Calculated lattice parameters and linear size factors for Zr and Hf in fcc Fe plus experimental size factors [25]

Atom Species	Lattice Parameter (nm)	Size Factor (%)	Calculated		Experimental from hcp Zr and hcp Hf
			Fe – non-spin-polarized	Fe – spin-polarized	
Fe – non-spin-polarized	0.3447	Zr	31.42	24.53	26.87
Fe – spin-polarized	0.3638	Hf	29.58	22.79	25.04
Zr (fcc)	0.4531				
Hf (fcc)	0.4467				

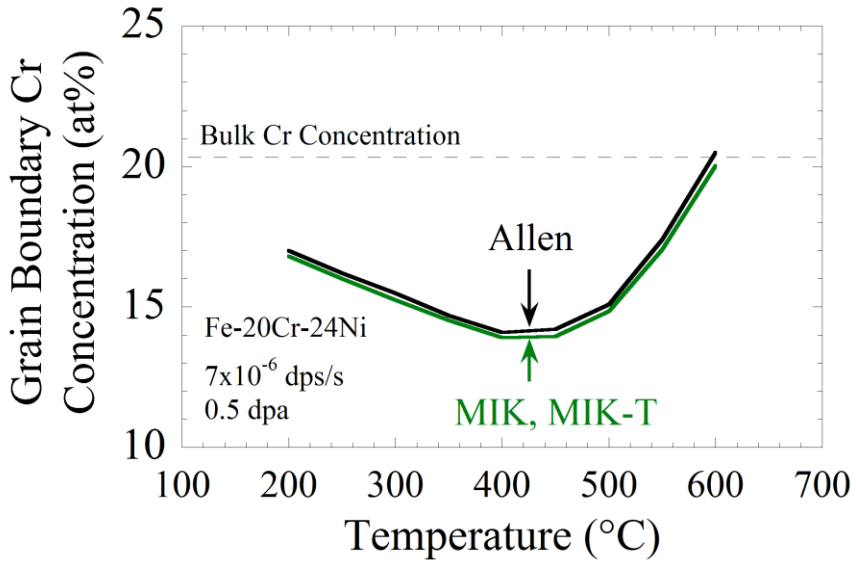

Figure 6.1 Benchmarking of the MIK model, showing grain boundary Cr concentration as a function of temperature for Fe-20Cr-24Ni alloy with a dose rate of $7x10^{-6}$ dpa/s at 0.5 dpa with MIK in black and MIK-T in green [33].

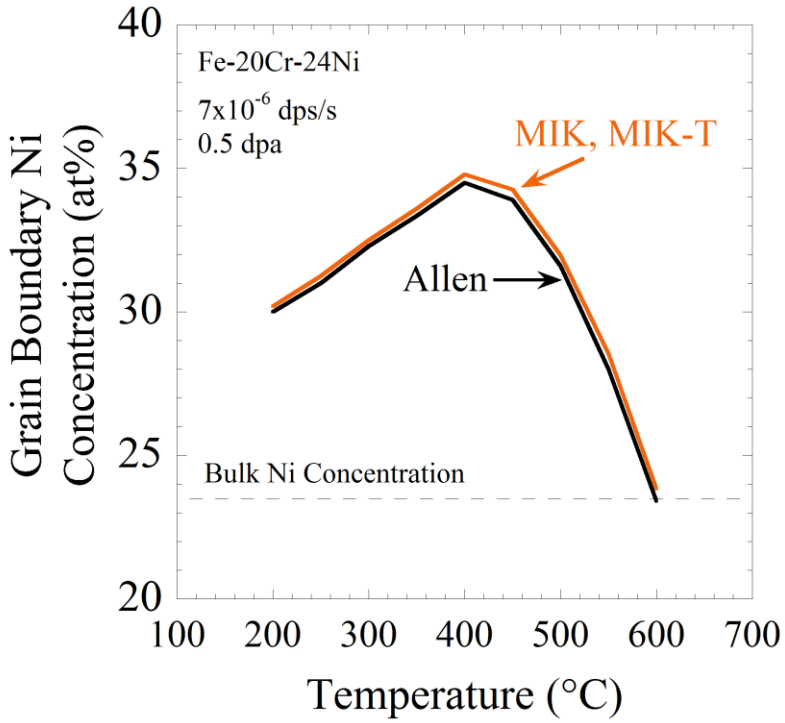

Figure 6.2 Benchmarking of the MIK model, showing grain boundary Ni concentration as a function of temperature for Fe-20Cr-24Ni alloy with a dose rate of $7x10^{-6}$ dpa/s at 0.5 dpa with MIK in black and MIK-T in orange [33].

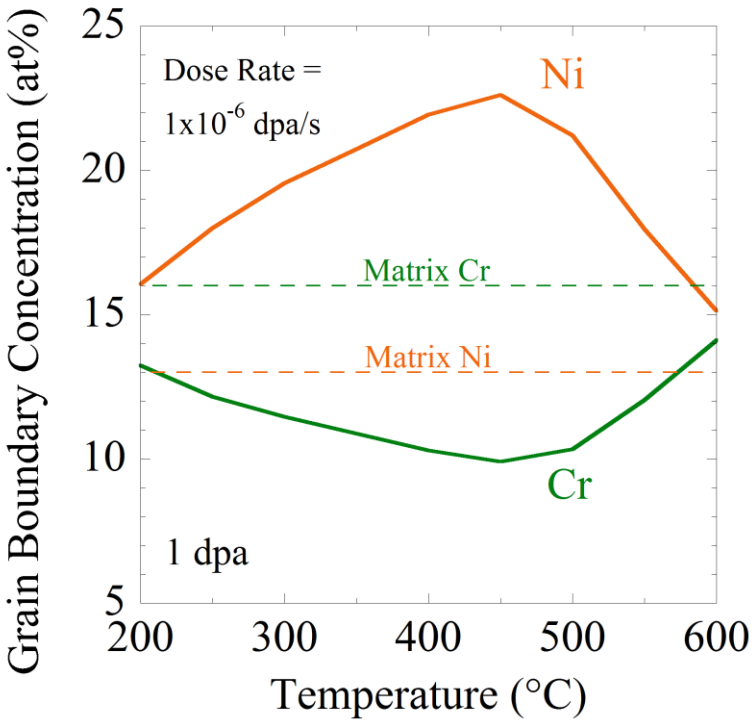

Figure 6.3 Variation of grain boundary Ni and Cr concentration as a function of temperature from 200 – 600°C for the MIK model at 1 dpa

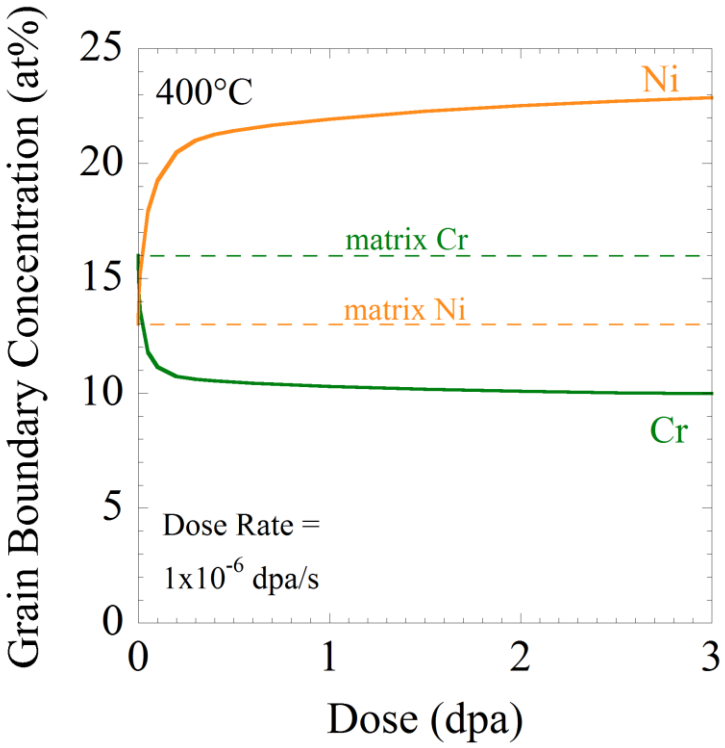

Figure 6.4 Grain boundary concentrations for Ni and Cr as a function of dose for the MIK model at 400°C.

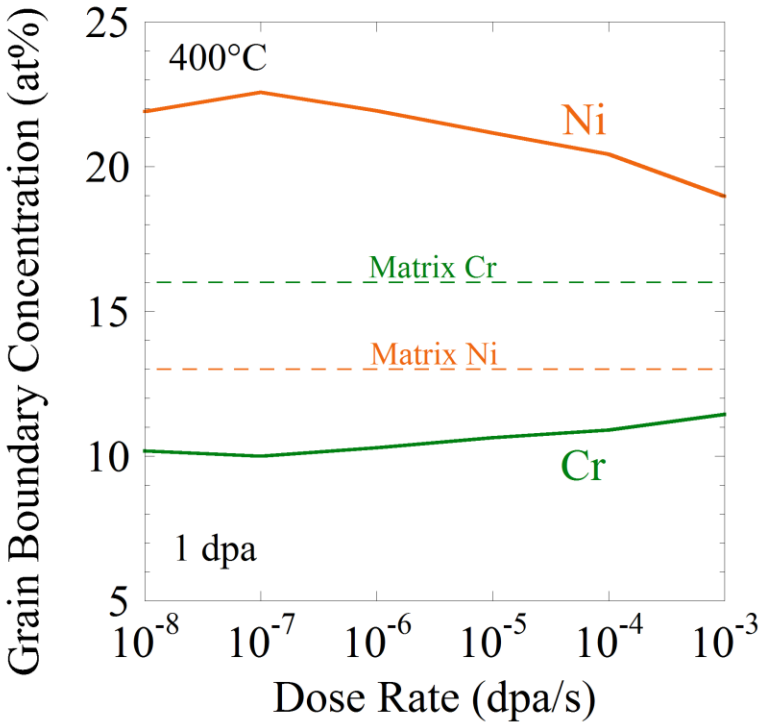

Figure 6.5 Variation of grain boundary Ni and Cr concentration as a function of dose rate from 10^{-8} – 10^{-3} dpa/s for the MIK model

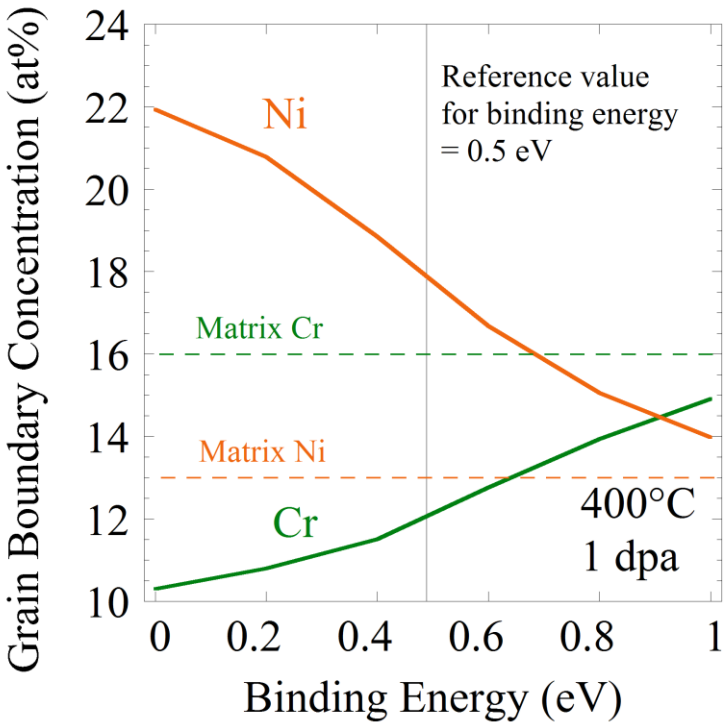

Figure 6.6 Grain boundary concentrations for Cr and Ni as a function of the binding energy from 0 to 1.0 eV at 400°C, 1 dpa, with a dose rate of 10^{-6} dpa/s and a solute concentration of 0.5 at%. The reference value for studying the variation of other MIK-T model input parameters is shown in the figure by a vertical line at 0.5 eV.

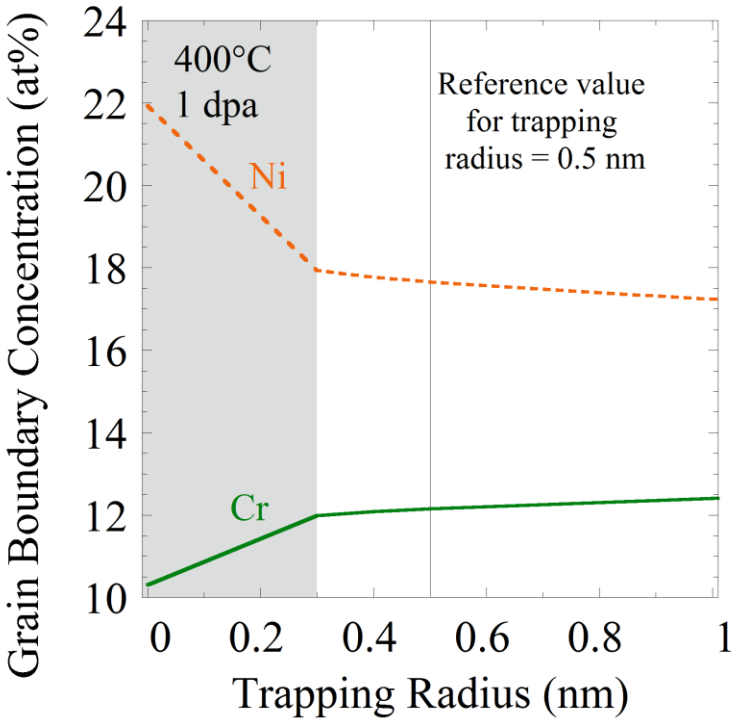

Figure 6.7 Grain boundary concentrations for Cr and Ni as a function of the oversized solute trapping radius from 0 – 1 nm at 400°C, 1 dpa, with a dose rate of 10^{-6} dpa/s, a binding energy of 0.5 eV, recombination radius of 0.5 nm, and solute concentration of 0.5 at%. The reference value for studying the variation of other MIK-T model input parameters is shown in the figure by a vertical line at 0.5 nm. The shaded region represents a radius less than the 1st nearest neighbor distance of 0.3 nm.

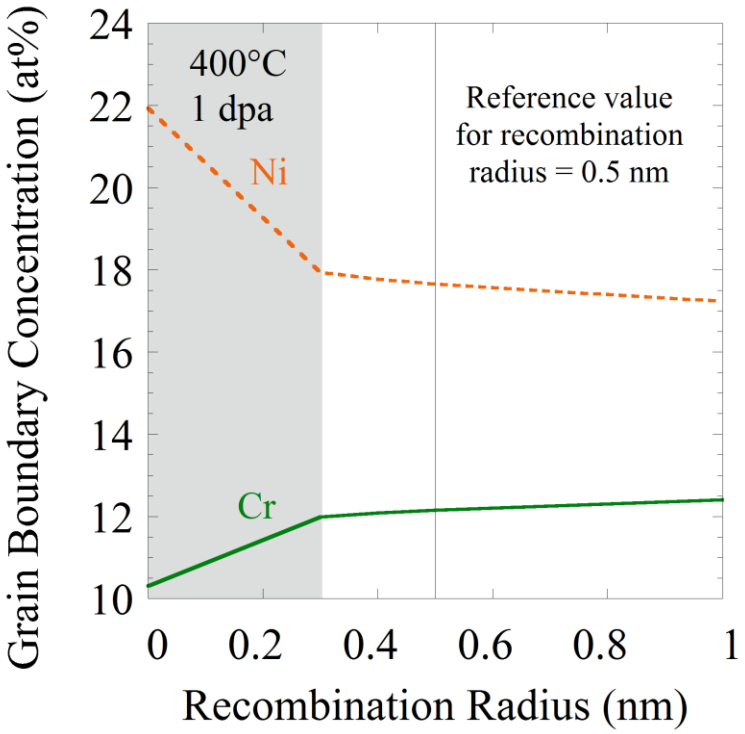

Figure 6.8 Grain boundary concentrations for Cr and Ni as a function of the solute-vacancy recombination radius from 0 – 1 nm at 400°C, 1 dpa, with a dose rate of 10^{-6} dpa/s, a binding energy of 0.5 eV, trapping radius of 0.5 nm, and solute concentration of 0.5 at%. The reference value for studying the variation of other MIK-T model input parameters is shown in the figure by a vertical line at 0.5 nm. The shaded region represents a radius less than the 1st nearest neighbor distance of 0.3 nm.

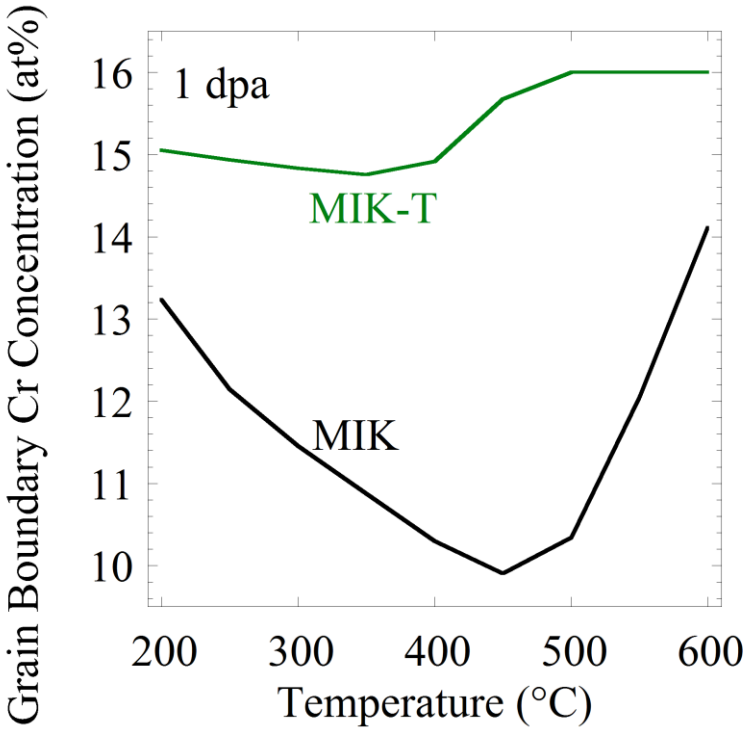

Figure 6.9 Grain boundary Cr concentrations as a function of temperature at 10^{-6} dpa/s and 1 dpa for the MIK and MIK-T models, with a binding energy of 1.0 eV and solute concentration of 0.5 at% for the MIK-T model.

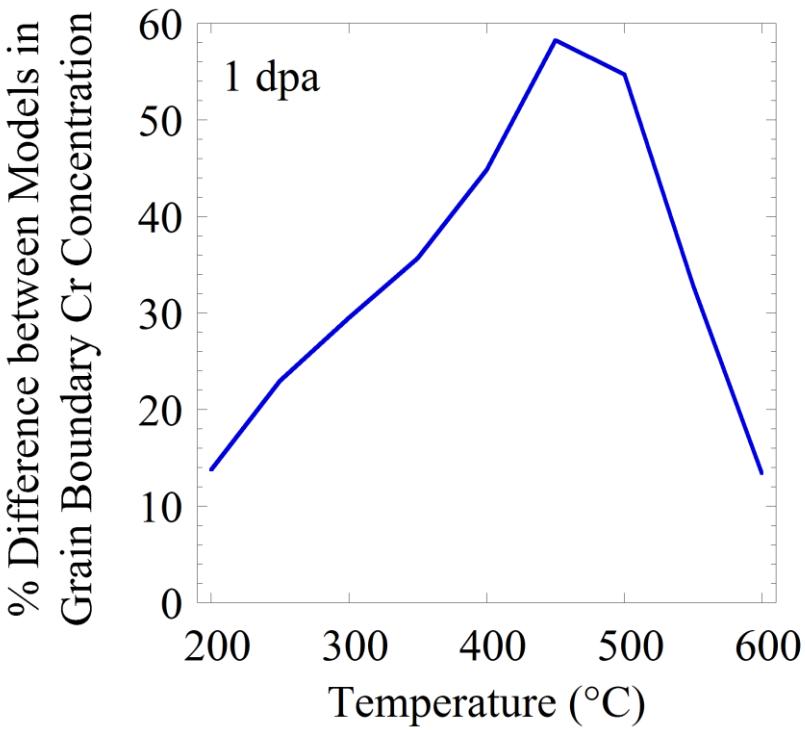

Figure 6.10 Percent difference in the grain boundary Cr concentration between the MIK and MIK-T models as a function of temperature at 10^{-6} dpa/s and 1 dpa.

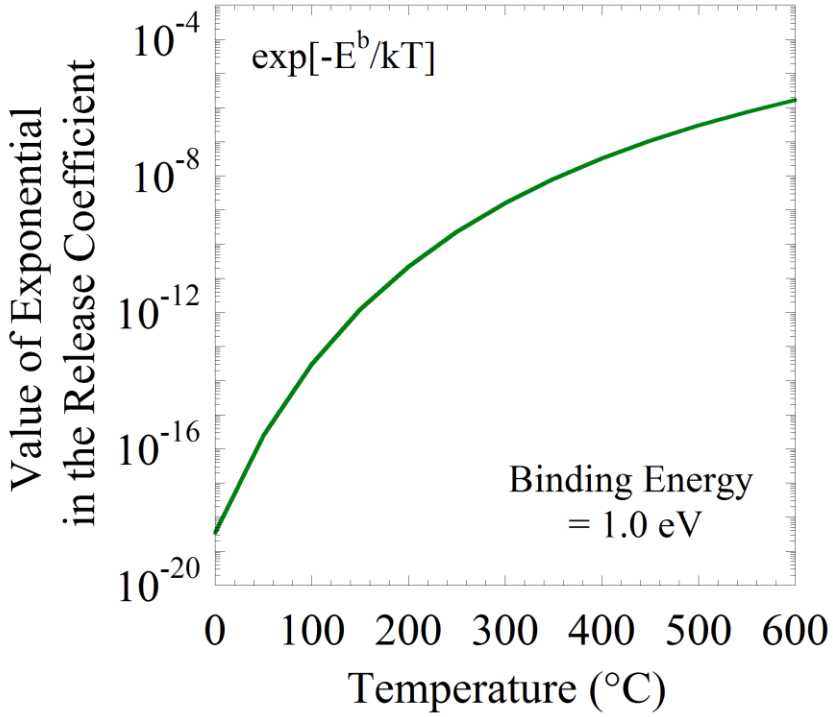

Figure 6.11 Value of the exponential in the solute-vacancy dissociation rate as a function of temperature with a binding energy of 1.0 eV

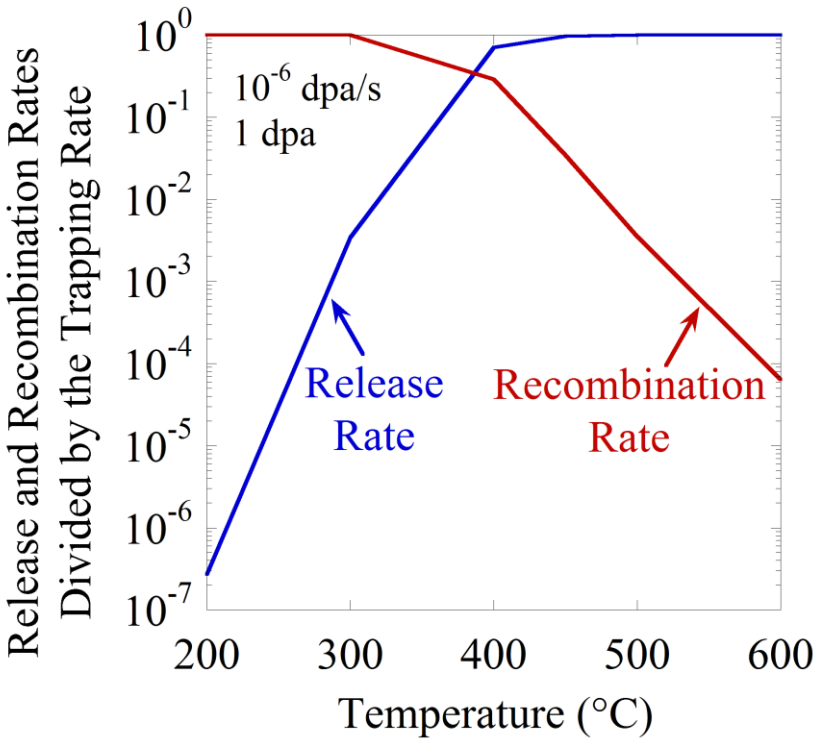

Figure 6.12 The release and recombination rates divided by the trapping rate as a function of temperature, at 10^{-6} dpa/s, 1 dpa.

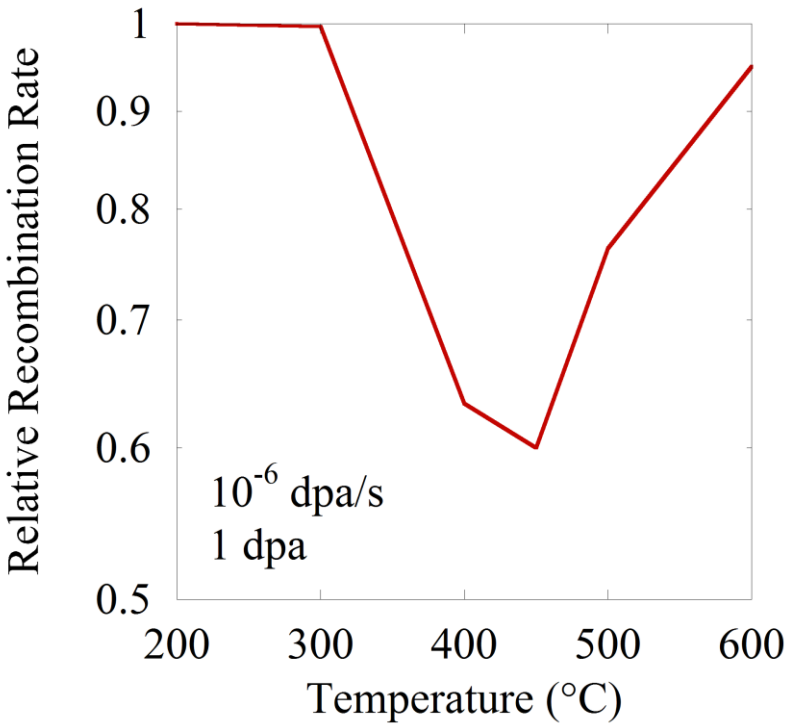

Figure 6.13 The recombination rate relative to its maximum value, at 200°C, as a function of temperature, at 10^{-6} dpa/s, 1 dpa.

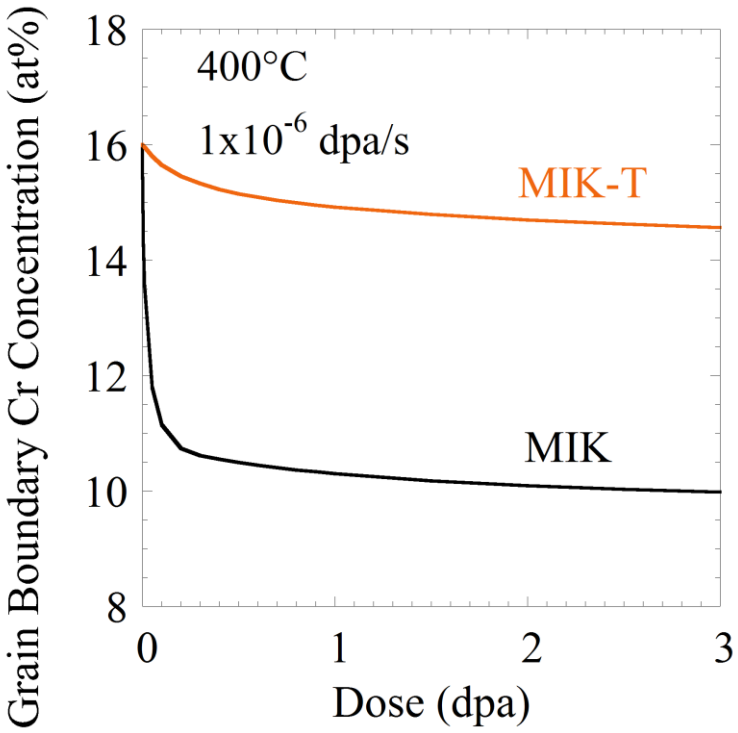

Figure 6.14 Grain boundary Cr concentrations as a function of dose for the MIK and MIK-T models at 400°C.

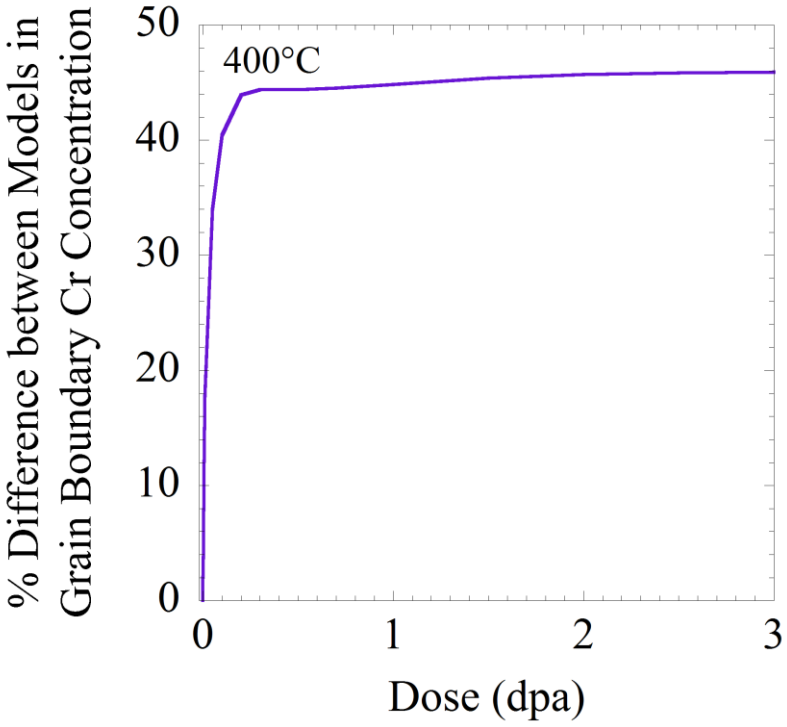

Figure 6.15 Percent difference in the grain boundary Cr concentration between the MIK and MIK-T models as a function of dose at 10^{-6} dpa/s and 400°C.

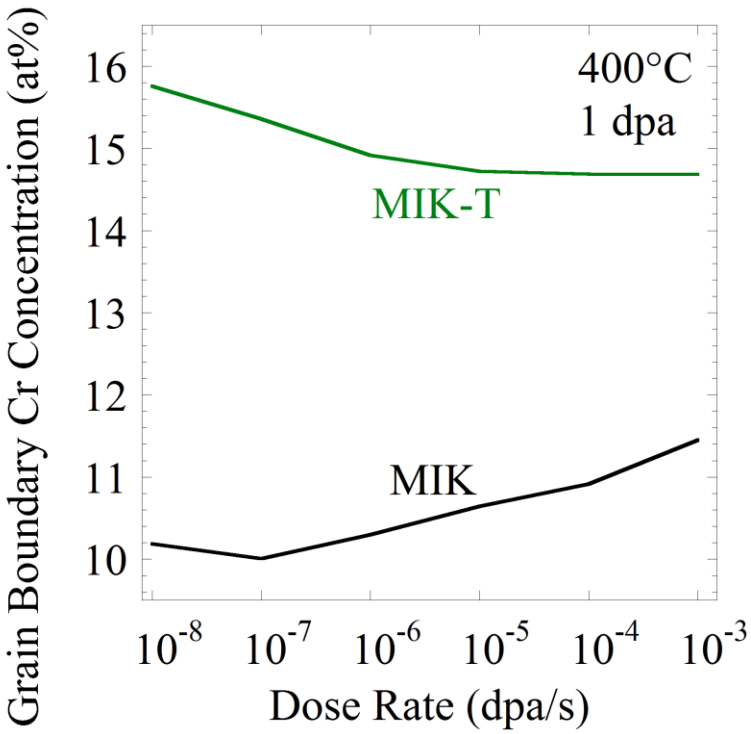

Figure 6.16 Grain boundary Cr concentrations as a function of dose rate at 400°C and 1 dpa.

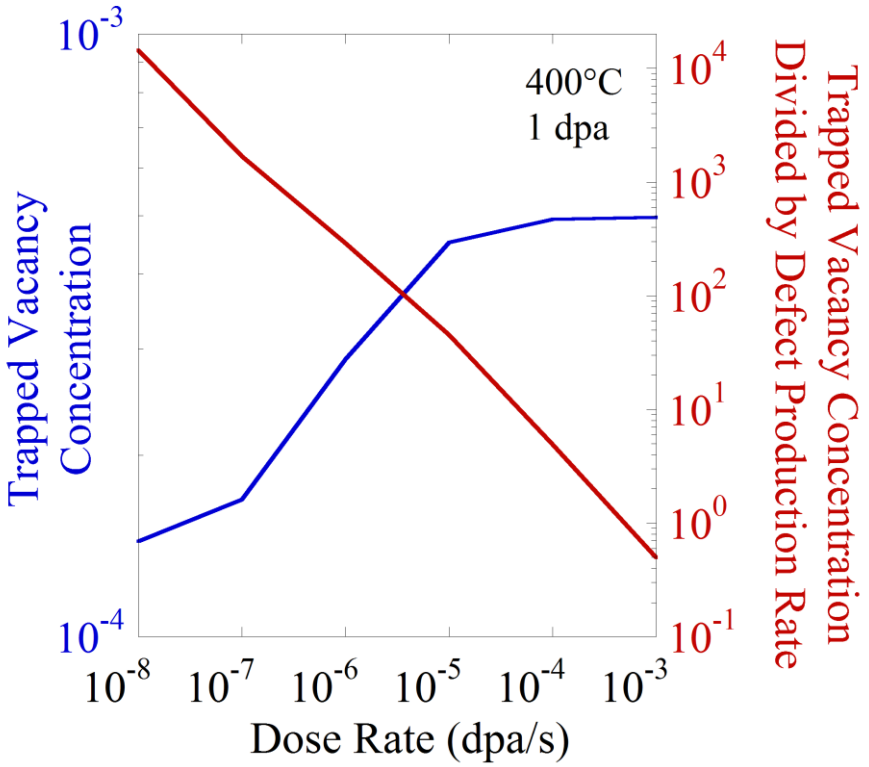

Figure 6.17 The trapped vacancy concentration as a function of dose rate on the left y-axis in blue, and the trapped vacancy concentration divided by the defect production rate as a function of dose on the right y-axis in red, at 400°C and 1 dpa.

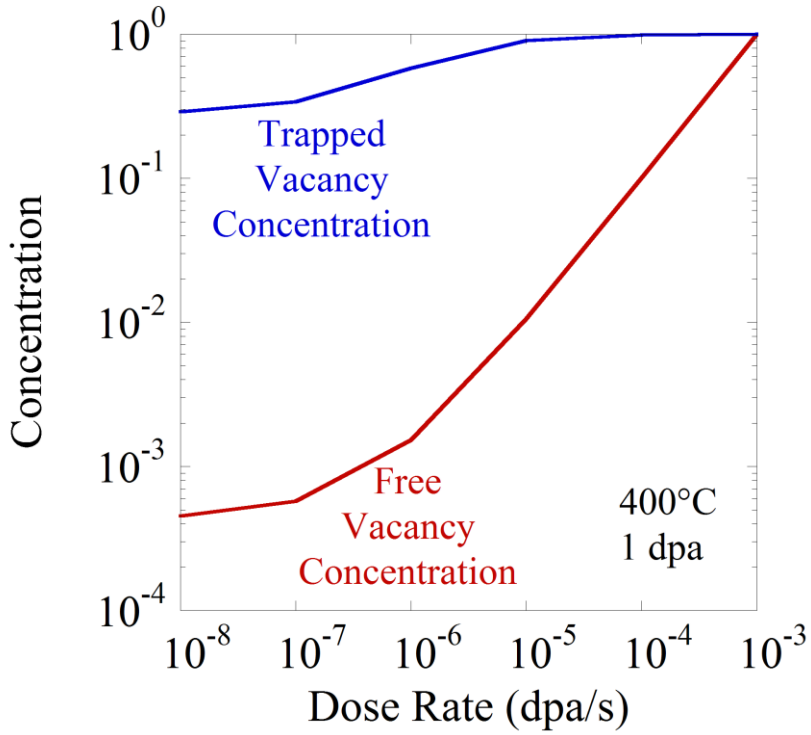

Figure 6.18 Concentrations for the freely migrating vacancies and the trapped vacancies as a function of dose rate at 400°C, 1 dpa.

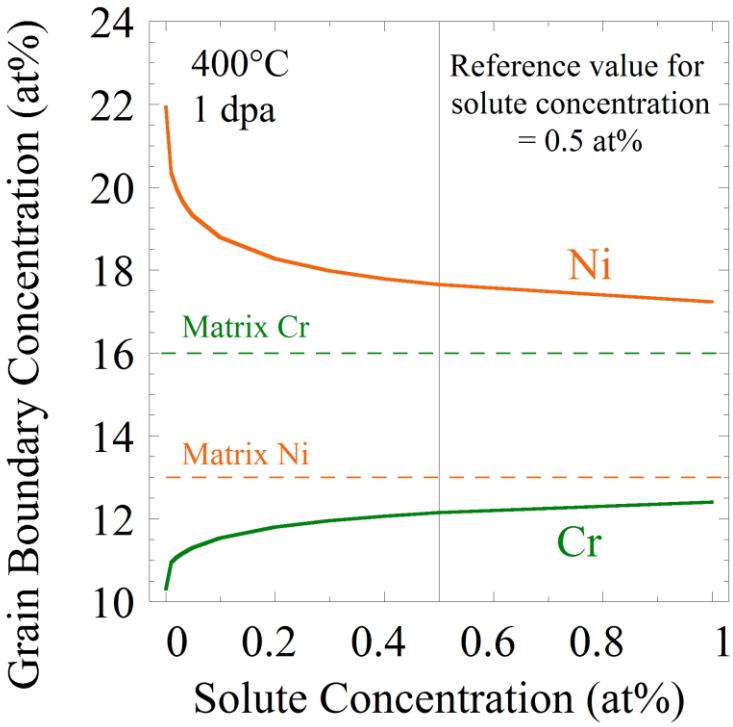

Figure 6.19 Grain boundary concentrations for Cr and Ni as a function of the oversized solute concentration from 0 to 1.0 at% at 400°C and 1 dpa, with a binding energy of 0.5 eV and trapping and recombination radii of 0.5 nm. The reference value for studying the variation of other MIK-T model input parameters is shown in the figure by a vertical line at 0.5 at%.

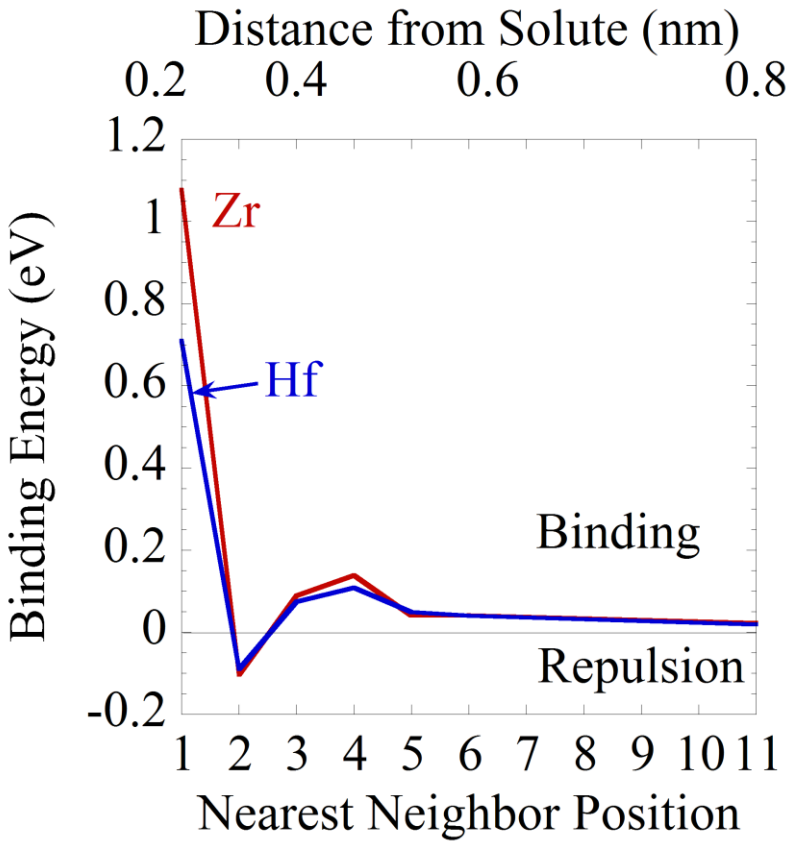

Figure 6.20 Binding energy as a function of nearest neighbor distance from the oversized solute assuming a non-spin-polarized (non-magnetic) system. The top x-axis also includes the distance from the origin, in nm.

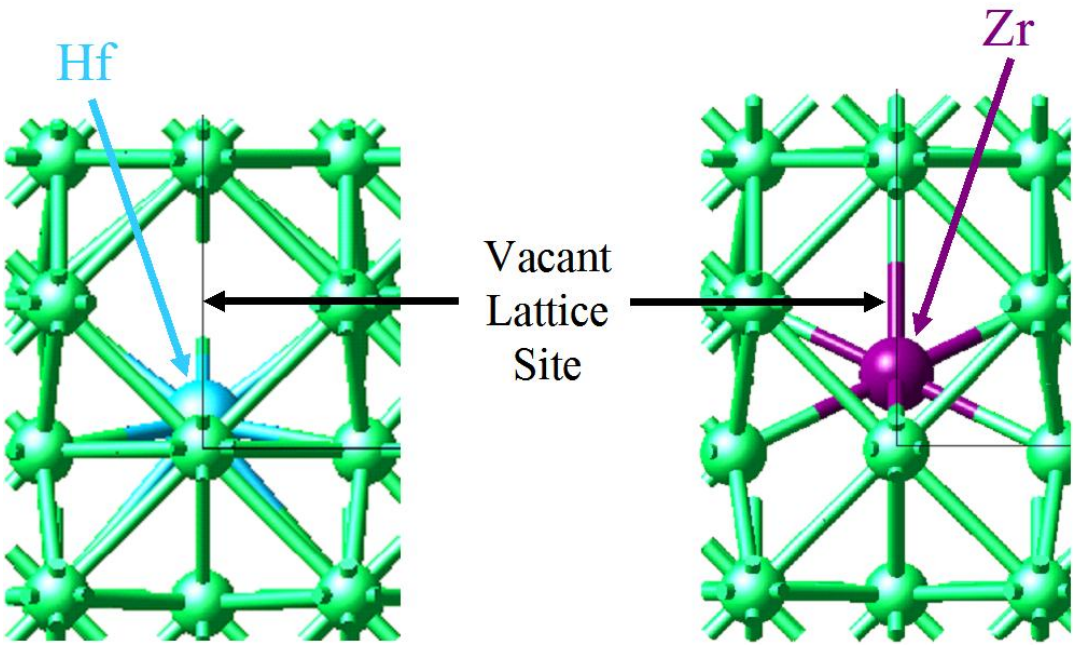

Figure 6.21 Relaxation of Hf and Zr ions with 1st nn vacancies. The vacancy lattice position is by the tip of the horizontal arrows. Relaxation of Zr ion toward the vacancy position is much greater than the relaxation of Hf, accounting for the larger binding energy for Zr compared to Hf.

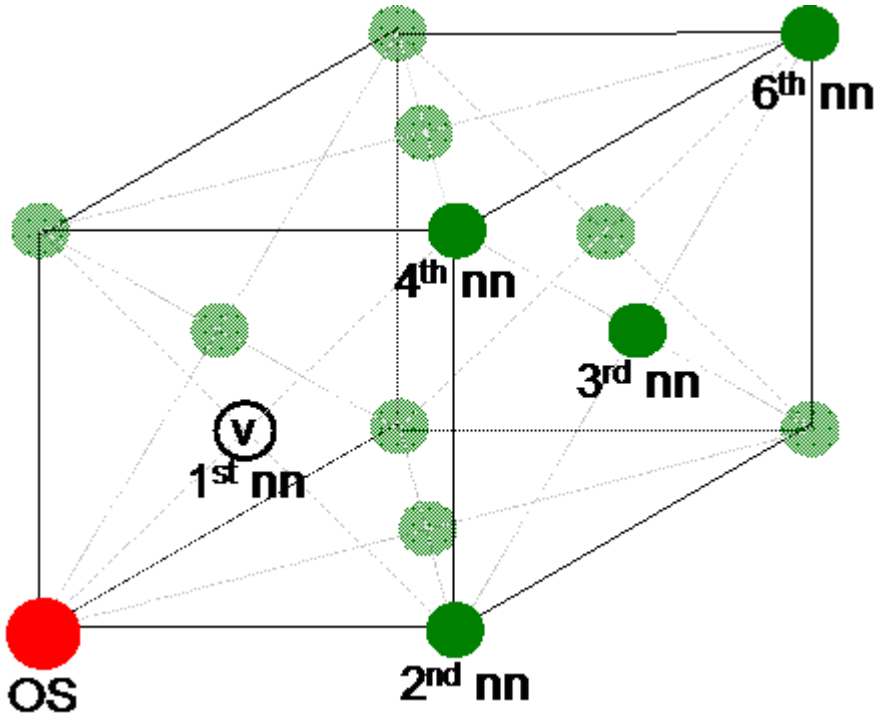

Figure 6.22 The nn positions relative to the oversized solute (OS) atom at the origin for a fcc cell. The 1st, 2nd, 3rd, 4th, and 6th nn positions are shown. The 5th nn position rests in the face of the adjacent cell away from the oversized solute, one lattice parameter distance from the 1st nn position.

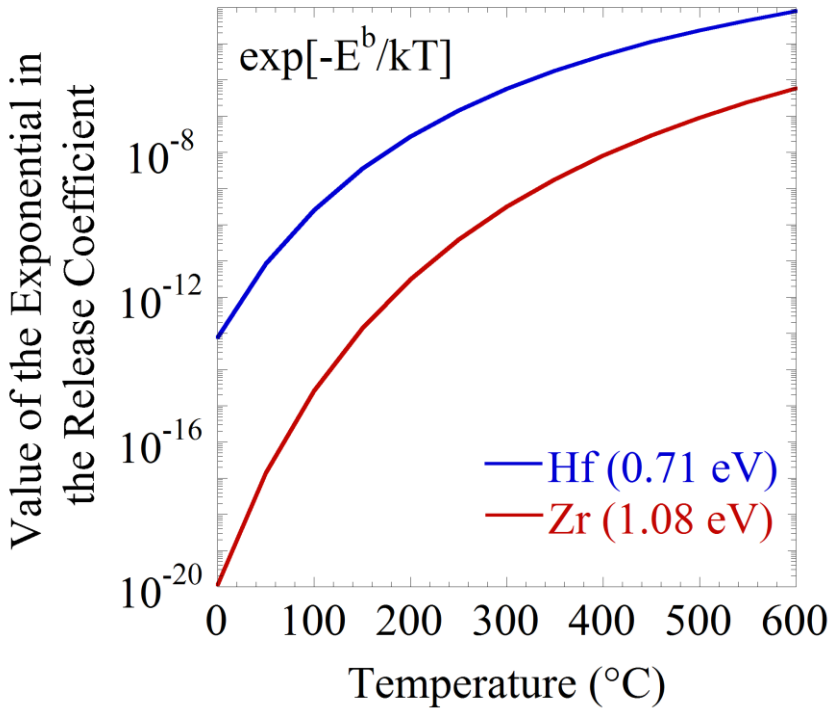

Figure 6.23 Effect of binding energy on the value of the exponential in the solute-vacancy dissociation rate

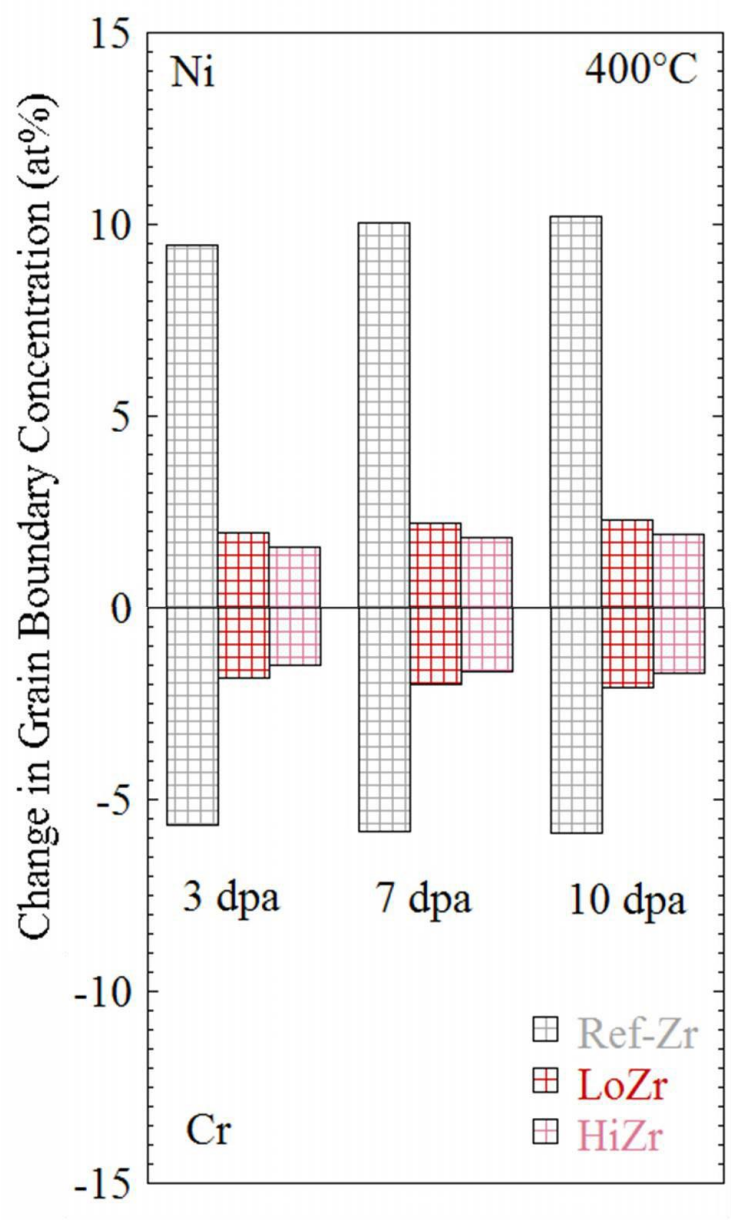

Figure 6.24 Calculate change in grain boundary concentrations for the +Zr alloys at doses of 3, 7 and 10 dpa at 400°C with a solute-vacancy binding energy of 1.08 eV

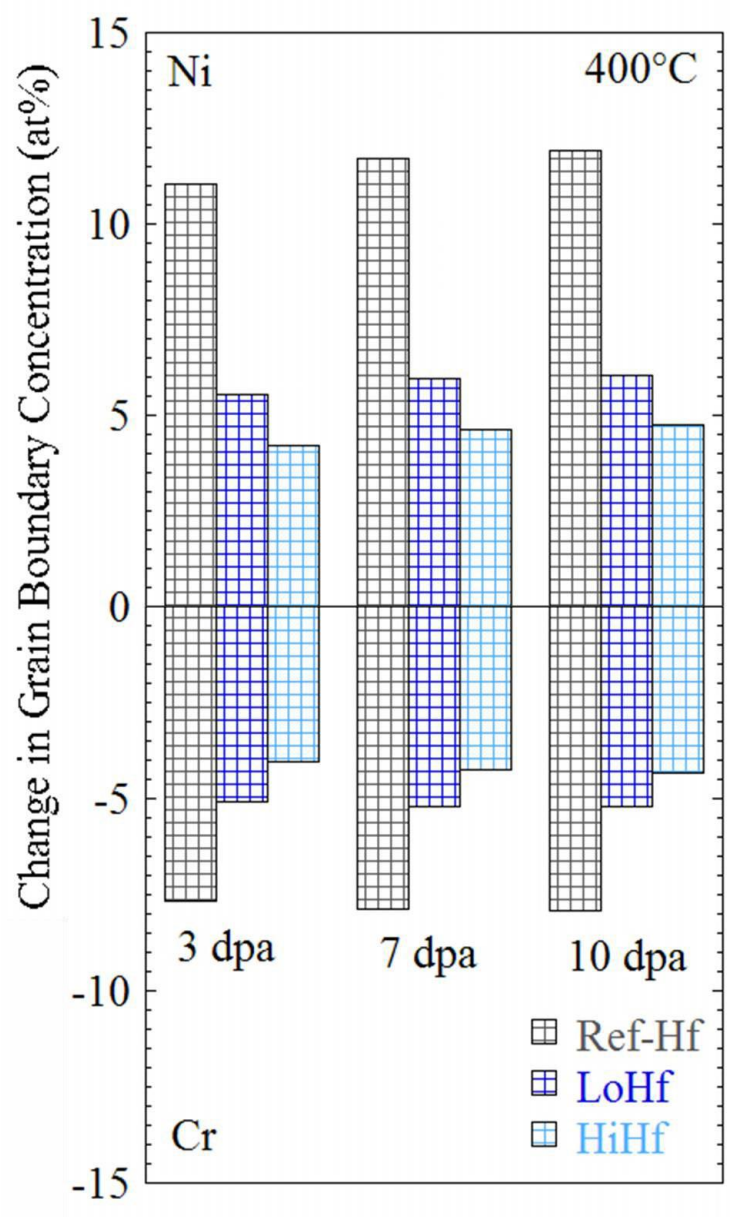

Figure 6.25 Calculate change in grain boundary concentrations for the +Hf alloys at doses of 3, 7 and 10 dpa at 400°C with a solute-vacancy binding energy of 0.71 eV

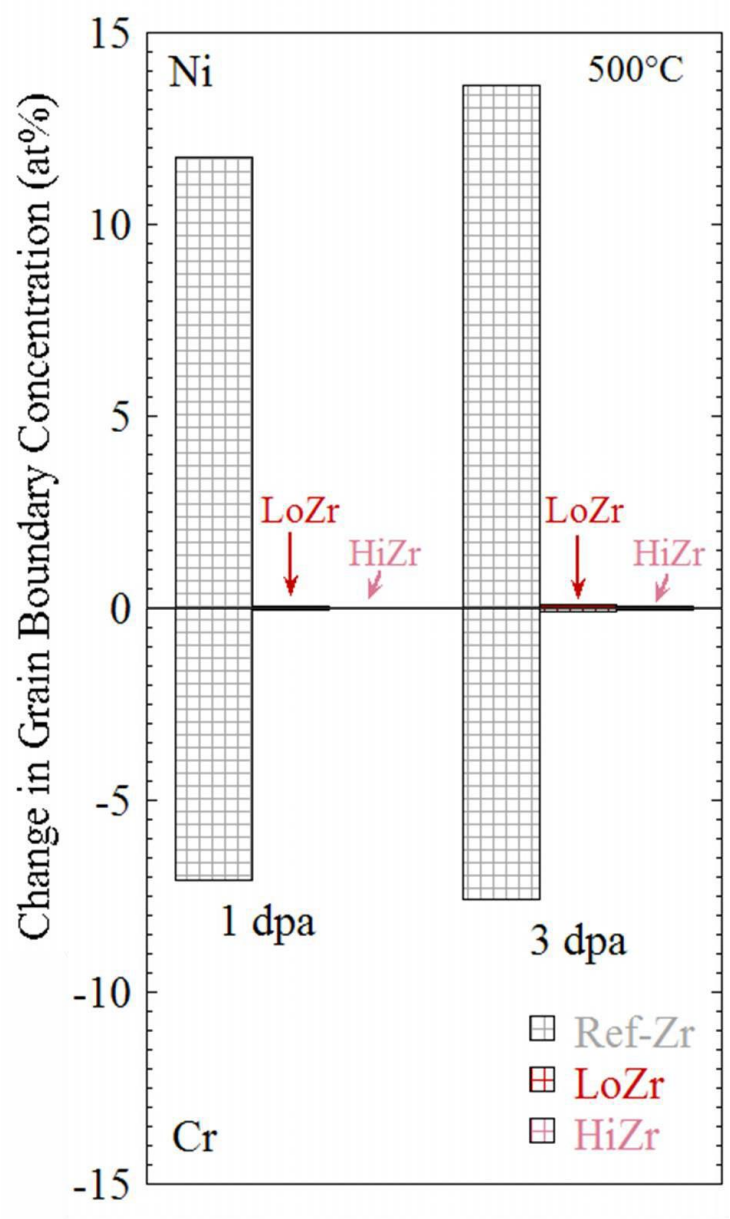

Figure 6.26 Calculated change in grain boundary concentrations for the +Zr alloys at doses of 1 and 3 dpa at 500°C with a solute-vacancy binding energy of 1.08 eV

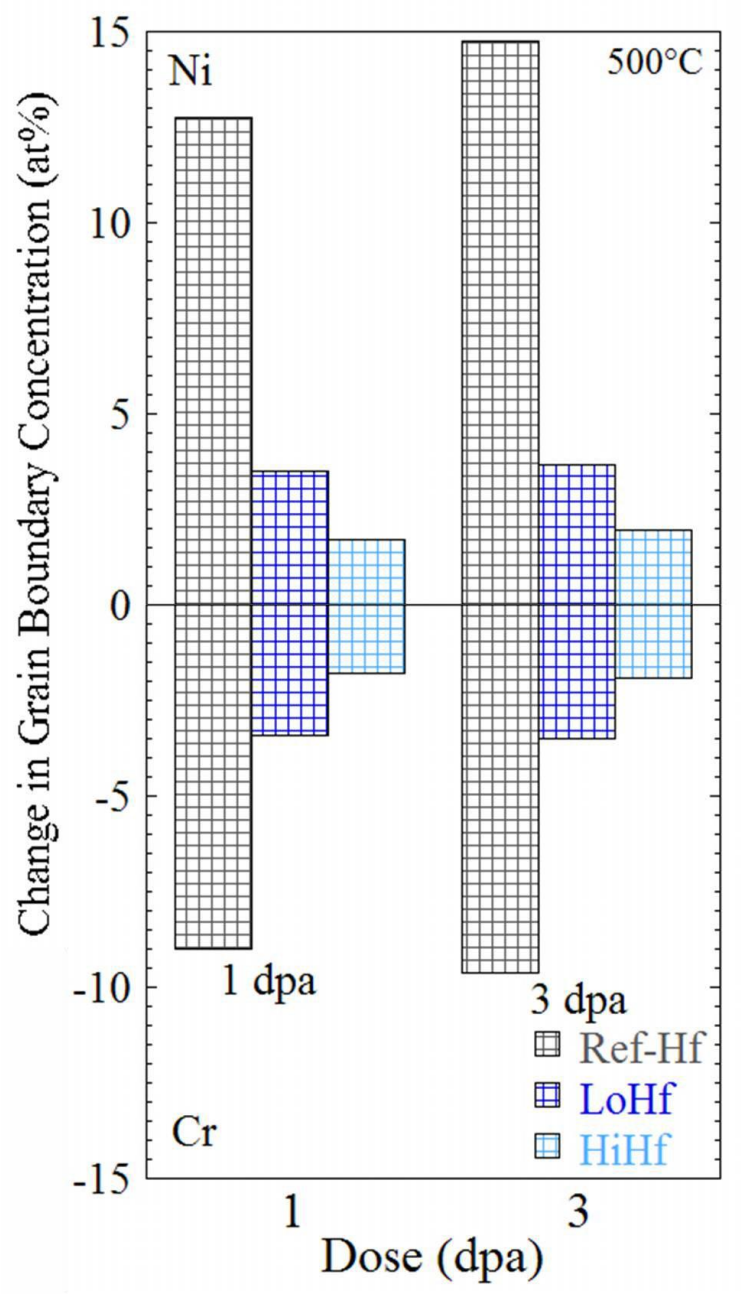

Figure 6.27 Calculated change in grain boundary concentrations for the +Hf alloys at doses of 1 and 3 dpa at 500°C with a solute-vacancy binding energy of 0.71 eV

CHAPTER 7

DISCUSSION

This chapter discusses the results of RIS and dislocation loop measurements and compares the trapping model results of RIS with experimental measurements in order to assess the validity of the vacancy trapping mechanism of oversized solute additions on RIS. The discussion consists of three parts: 1) validation of the RIS measurements, 2) assessment of the comparison between the MIK-T model calculations with RIS measurements that reveal a loss of solute effectiveness in reducing RIS, and 3) a discussion of possible reasons for the loss of solute effectiveness on RIS as a function of radiation dose.

7.1 Validity of RIS Results

This section validates reference alloy RIS measurements against literature data of similar alloys under similar irradiation conditions. Since the objective of this thesis is to understand the effect of oversized solutes on RIS behavior, the validity of the RIS data will be established by the following: 1) comparison of the reference alloy data with literature data, 2) comparison of the reference alloy data with model predictions, 3) validation of the loop microstructure data, and 4) validation of RIS behavior of the oversized solute alloys through the behavior of the irradiated microstructure. This section concludes with a comparison of RIS results following proton irradiations with 2 MeV and 3.2 MeV to show that protons in this energy range give the same grain boundary segregation results.

7.1.1 Comparison of Reference Alloy RIS to Literature Values

A comparison of the reference alloy RIS measurements to literature values is first made against other proton irradiation data for similar alloys under similar irradiation conditions. The objective is to first validate the measurements against other literature data for the same irradiation particle type before the comparison is extended to neutron data [17, 25, 26, 28, 33].

Comparison of Cr depletion resulting from proton irradiation in the range of 360 – 500°C is shown in figure 7.1. Cr depletion is plotted as the change from the bulk composition. The literature data is shown with grey symbols at 360°C, black symbols at 400°C, and green symbols at 500°C, while the data from this study is shown in shades of red for Ref-Zr and shades of blue for Ref-Hf at both 400°C and 500°C. At 400°C, the literature data shows that the amount of Cr depletion increases quickly at low dose, followed by a gradual increase and saturation after 3 dpa to around 6 – 8 at%. Cr depletion in this study at 400°C also falls in the range of 6 – 8 at% and follows the same trend with dose.

Much of the literature data at 400°C is for alloys with higher Ni content than the reference alloys in this study. Increasing the bulk Ni content increases the vacancy diffusivity in an alloy, with the result that segregation also increases [30]. Rothman et al. [63] performed tracer diffusion experiments in a series of austenitic alloys with increasing Ni content. Their measurements indicated that $D_{Cr} > D_{Fe} > D_{Ni}$. Since RIS is due to differences in the vacancy diffusivity ratios, then increasing Ni content increases the diffusivity ratios for Cr and Fe relative to Ni. As the vacancy diffusivity ratios increase, the concentration gradients at the grain boundary also increase, causing more RIS.

Damcott et al. [30] confirmed the effects of Ni on RIS using a series of alloys with a range of Ni contents irradiated with protons at 400°C and found that increasing bulk Ni increased the grain boundary Cr depletion. Busby et al. [18] showed similar behavior by comparing a Fe-18Cr-9Ni alloy with Fe-18Cr-24Ni after proton irradiation at 360°C to 5.5 dpa. The alloy with increased bulk Ni content caused an increase in grain boundary Cr depletion of 2.0 at% relative to the reference alloy. With the same irradiation conditions, Was et al. [92] used the MIK model to calculate 2 at% more Cr

depletion for Fe-18Cr-24Ni relative to Fe-18Cr-9Ni, which matched the measured increase in Cr depletion. Consequently, the literature data with higher Ni content than Ref-Zr and Ref-Hf may be expected to have more Cr depletion, and the alloys Fe-20Cr-24Ni, Fe-24Cr-24Ni, and Fe-24Cr-19Ni do measure more Cr depletion at 1 dpa than that in Ref-Zr or Ref-Hf at any dose at 400°C [26]. For a Fe-16Cr-13Ni alloy, where the alloy composition is similar to Ref-Zr and Ref-Hf, Allen et al. [28] measured 8.3 at% Cr depletion at 400°C, 1 dpa, which is similar to the amount of Cr depletion for Ref-Zr and Ref-Hf from 3 – 10 dpa at 400°C. Finally, for the same alloy heat as Ref-Hf in this study, Founier et al. [25] also measured similar levels of Cr depletion at 5 dpa, 400°C as Ref-Hf at 3 and 7 dpa, 400°C.

The 500°C data from this study has more Cr depletion than at 400°C by about 1.5 at% for Ref-Zr and 3.5 at% for Ref-Hf. The MIK model calculates peak segregation to occur between 400 – 500°C [33], while Damcott et al. [30] also measured slightly more Cr depletion at 500°C, shown in green, than at 400°C for Fe-20Cr-24Ni irradiated at 1 dpa. Results from this study are similar to data from Damcott et al. [30] by showing more segregation at 500°C than at 400°C.

Finally, RIS at 360°C is expected to be less than RIS at 400°C [29]. After 3 dpa, the 360°C literature data show Cr depletion ranging from 3 – 7 at%. The literature data at 360°C is consistent with the expected behavior by generally showing less Cr depletion than Ref-Zr and Ref-Hf at 400°C.

The results for Cr depletion are also compared against neutron irradiation data in figure 7.2 [45, 84, 123]. The figure contains the original proton irradiation data at 400°C and 500°C in grey, with neutron data from 275 – 288°C in black. Given the change in dose rate from protons to neutrons, the shift in temperature required to keep the number of defects lost to sinks invariant can be calculated by:

$$N_{Sj} = \int_0^{\tau} K_j C_j \, dt \tag{7.1}$$

where N_{Sj} is the number of defects lost to sinks per unit volume for a given time, τ, K_j is the sink strength for absorption of defects, C_j is the defect concentration, and *j* is the defect type [124]. At steady state, defect concentrations are given by:

$$C_v = \left(\frac{K_0}{K_{iv}} \frac{z_i D_i}{z_v D_v} \right)^{1/2} \quad \text{and} \quad C_i = \left(\frac{K_0}{K_{iv}} \frac{z_v D_v}{z_i D_i} \right)^{1/2}, \tag{7.2}$$

where K_0 is the defect production rate, K_{iv} is the recombination rate, D_v and D_i are the diffusion coefficients for vacancies and interstitials, respectively, and the ratio of z_v and z_i describes the sink bias for defects. Plugging Eq. 7.2 into Eq. 7.1 for vacancies gives:

$$N_{Sv} = \frac{K_v}{(K_0 K_{iv})^{1/2}} \left(\frac{z_i D_i}{z_v D_v} \right)^{1/2} \Phi, \tag{7.3}$$

where Φ is the dose. Using different dose rates to determine the shift in temperature assuming constant dose, then ${N_{Sv}}^1 = {N_{Sv}}^2$, and canceling terms, gives the equality:

$$\left(\frac{D_v}{K_0} \right)_1^{1/2} = \left(\frac{D_v}{K_0} \right)_2^{1/2}. \tag{7.4}$$

Since $D_v = D_0 \exp\left(- E_m^v / kT\right)$, Eq. 7.4 can be solved in terms of temperature, given by:

$$T_2 - T_1 = \frac{\frac{kT_1^2}{E_m^v} \ln\left(\frac{K_{0_2}}{K_{0_1}} \right)}{1 - \frac{kT_1}{E_m^v} \ln\left(\frac{K_{0_2}}{K_{0_1}} \right)}. \tag{7.5}$$

Assuming a dose rate of 7 x 10^{-6} for protons and 5 x 10^{-8} for neutrons, and vacancy migration energy of ~ 1.20 eV as calculated by the MIK model for a Fe-20Cr-24Ni alloy [33], RIS for 275°C neutron irradiations should be similar to proton irradiations at ~ 400°C. From figure 7.2, at doses of less than 3 dpa, the neutron irradiation data shows 2 – 6.5 at% Cr depletion. At doses of 3 dpa or above, the amount of Cr depletion for the commercial purity alloys from Was et al. [91] and Asano et al. [84] is 5 – 9 at%, which bounds the amount of Cr depletion measured for Ref-Zr and Ref-Hf at 400°C from 3 – 10 dpa. The comparison shows similar results between proton irradiations at 400°C and neutron irradiations at 275 - 288°C, which is consistent with the expected effects of proton and neutron irradiations at these temperatures.

A comparison is now made for the Ni enrichment data, where figure 7.3 compares Ref-Zr and Ref-Hf with proton-irradiated alloys over the temperature range of 360 – 500°C. Again, literature data is shown in grey for 360°C, black for 400°C, green for

500°C, and Ref-Zr and Ref-Hf are shown with shades of red and blue, respectively. Ni enrichment for the reference alloys exceeds 11 at% for all temperatures and doses. Ref-Zr also shows more Ni enrichment than Ref-Hf for all cases.

As mentioned, much of the 400°C literature data is for higher-Ni alloys, and increases in bulk Ni increase the vacancy diffusivity to cause more RIS. Damcott et al. [26, 30] found that a Fe-24Cr-24Ni alloy measured 9.5 at% more Ni enrichment than a Fe-24Cr-19Ni alloy. Busby et al. [18] observed a similar effect at 360°C, 5.5 dpa, where a Fe-18Cr-24Ni alloy measured 4.0 at% more Ni enrichment than a Fe-18Cr-9Ni alloy with the same irradiation conditions. As a result, the high-Ni alloys should have more Ni enrichment, which is true relative Ref-Hf Ni enrichment. At the same time, Allen et al. [28] observed similar amounts of Ni enrichment for Fe-16Cr-13Ni at 400°C, 1 dpa as Ref-Hf at 400°C. In addition, Fournier et al. [25] measured the same amount of Ni enrichment for 316L at 5 dpa, 400°C as Ref-Hf at 7 dpa, 400°C, and both of these alloys are from the same heat of material.

The Ni enrichment data for Ref-Zr at 400°C and 500°C generally shows higher levels of Ni enrichment than those observed in the literature. However, much of the literature data is for alloys with comparatively lower Si content. Both Kenik [125] and Busby et al. [18] have shown that increased bulk Si can increase the grain boundary RIS, as presented in section 2.1.3. Kenik [125] measured about 3 at% more Ni enrichment for an alloy with 1.1 at% bulk Si compared to his high purity reference alloy. Busby et al. [18] measured a 4 at% increase in Ni enrichment in an alloy with 1.05 wt% bulk Si relative to their high purity reference alloy.

Ref-Zr exhibits more Ni enrichment than Ref-Hf at both temperatures for all doses. Ref-Zr also contains more Si than Ref-Hf, with 0.75 at% Si compared to 0.24 at% Si in Ref-Hf. The higher amount of Ni enrichment for Ref-Zr is consistent with the trend of increased segregation from higher levels of Si. Also, the reference alloys consistently show similar amounts of Ni enrichment as a function of dose at both 400°C and 500°C. Finally, the higher levels of Si in the reference alloys compared to the high purity alloys in the literature may explain why Ni enrichment for the reference alloys in this study is higher than much of the literature data.

The amount of RIS for Ref-Zr and Ref-Hf matches the expected trend as a function of dose at both 400°C and 500°C. Cr depletion for the reference alloys is in good agreement with literature data, while Ni enrichment is generally higher than the literature data, which may be due to the higher Si concentrations in Ref-Zr and Ref-Hf compared to the high purity alloys in the literature. Finally, the amount of RIS for the reference alloys has been shown to be consistent with past literature results of similar alloys under similar irradiation conditions and provides a solid basis for comparison with the oversized solute alloys.

7.1.2 MIK Model Compared to Reference Alloy RIS

The reference alloy RIS measurements are compared to values calculated by the MIK model which has been shown to predict RIS in austenitic alloys rather well [29, 32, 33]. The purpose of this analysis is to provide further support for the validity of RIS measurements by comparing each measurement to its expected value for that particular temperature and dose.

Figure 7.4 shows the change in grain boundary concentrations for Cr and Ni for the Ref-Zr and Ref-Hf alloys at 400°C. Model calculations are shown with cross-hatch bars, and measurements are solid bars. These patterns for model and experiment will be used throughout this chapter. Ref-Zr is shown in light grey and Ref-Hf in dark grey, with the error bars representing one standard deviation of the measurement. Model values for Ref-Zr and Ref-Hf differ slightly because of their differences in composition. Note that Ref-Zr is not measured at 10 dpa.

In all cases but one, Cr depletion measurements match the MIK model calculations within the error of the measurements. The only exception is Ref-Zr at 3 dpa, where the measured Cr depletion is 1 at% greater than the calculated value. Generally, these results show good agreement between model and measurement for Cr depletion. Also, the measured results are relatively constant as a function of dose, which fits the expected trend for the model between 3 – 10 dpa.

For the change in Ni concentration, the MIK model under-predicts the amount of Ni enrichment for Ref-Zr. At 3 dpa, the measured Ni enrichment is twice the amount of the calculated value. For Ref-Hf, the calculated values and experimental measurements

compare well at all three doses of 3, 7 and 10 dpa, where calculated Ni enrichment is consistently within the error of the measured value. Ref-Zr has a higher content of Si than Ref-Hf, at 0.75 at% compared to 0.24 at%, respectively. Therefore, Ref-Zr may be expected to have more Ni enrichment than Ref-Hf. The higher Si content in Ref-Zr may also explain why the measured value for Ref-Zr is higher than the model prediction.

Figure 7.5 compares the change in grain boundary concentrations for Cr and Ni between the MIK model and measured values for the reference alloys at 500°C. Note that Ref-Hf is not measured at 1 dpa. Cr depletion for Ref-Zr shows that the measured segregation is about 2 at% greater than calculated by the model at 1 dpa. However, by 3 dpa, the model value is within the error of the measurement. Ref-Hf at 3 dpa also shows good agreement between model and experiment, where the model calculates Cr depletion within the error of the measurement.

Comparisons between model and experiment for Ni enrichment again show that the model consistently under-predicts the measured Ni enrichment, this time for Ref-Zr and Ref-Hf. Ni enrichment for Ref-Zr differs from the model by 5 at% at 1 dpa and by 7.5 at% at 3 dpa. Ref-Hf has less of a difference from the model than Ref-Zr, but still amounts to about 4.5 at% more Ni enrichment than the model at 3 dpa. Similar to the 400°C comparison, Ref-Zr has more Ni enrichment than model calculation at all doses, but the trend is consistent as a function of dose at 500°C. And although Ref-Hf exhibits more Ni enrichment than the model, it is less of a difference than for Ref-Zr due to the lower Si concentration in Ref-Hf.

Overall, the MIK model is consistent with the reference alloy RIS measurements by showing good agreement between model results and experimental measurements for Ref-Zr and Ref-Hf as a function of dose at temperatures of 400°C and 500°C. The model under-predicts measured Ni enrichment consistently for Ref-Zr at both temperatures and also for Ref-Hf at 500°C, but the differences may be attributed to the higher Si concentrations in the reference alloys. Moreover, the amounts of Cr depletion and Ni enrichment in Ref-Zr and Ref-Hf are similar between the alloys and with temperature and dose. Agreement of RIS in the reference alloys with both literature data of similar alloys irradiated under similar conditions and with MIK model predictions establishes the

reasonableness of the data measurements as a foundation for assessing the role of oversized solutes on RIS.

7.1.3 Comparison of Reference Alloy Loop Microstructure with Literature Values

The measured loop microstructure of the reference alloys is compared to literature data to assess the validity of the measurements in this study. Comparison to literature data is important because both the loop microstructure and grain boundary segregation result from the creation of point defects during irradiation, so the effect of oversized solutes on loop microstructure should be consistent with that on RIS.

A comparison of average dislocation loop diameter as a function of dose is first made with literature data for proton irradiations at 360°C and 400°C before extending the comparison to neutron irradiation data [43-45, 91, 126, 127]. Figure 7.6 shows the comparison between literature data and the reference alloys in this study at 400°C, with Ref-Zr shown in red and Ref-Hf shown in blue. All 400°C data is shown with closed symbols while 360°C data is shown with open symbols. Of the commercial purity alloys, Teysseyre et al. [126] measured a loop diameter of 6.9 nm for a commercial purity 316L irradiated with protons at 400°C to 7 dpa, which is close to the loop diameters for the reference alloys in this study measuring between 8.7 – 10.0 nm. The other 400°C data in the literature have larger loop diameters than Ref-Zr and Ref-Hf, but the literature data is for high purity alloys. Higher Si concentrations may be a factor in causing a decrease in loop diameter, and Si concentrations vary from 0.12 wt% for Ref-Hf to 0.38 wt% for Ref-Zr. Cookson et al. [128] reported a decrease in loop diameter for a Fe-20Cr-9Ni high purity alloy and the same heat with 0.46 wt% Si addition from 16 nm to 10 nm, respectively, after proton irradiation at 400°C to 1 dpa. However, Was et al. [92] did not measure a change in loop diameter between a high purity 304SS and 304SS with 1.05 wt% Si after proton irradiation at 360°C to 5.5 dpa. As a result, the role of Si on loop diameter is unclear. Nevertheless, the reference alloys have similar loop diameters as literature data for a commercial purity 316L irradiated at the same temperature.

Decreasing irradiation temperature to 360°C should decrease the average loop diameter relative to 400°C by less than a factor of two according to comparisons made by Gan et al. [43] for a high purity 304SS irradiated to the same dose at both temperatures.

For the commercial purity and high purity alloys irradiated at 360°C, loop diameters range from 4 – 10 nm and are generally smaller than the reference alloys in this study, with many of the loops at about half the diameter of the reference alloys at 400°C. The results are consistent with the effect of a lower temperature in decreasing the average loop size.

Figure 7.7 makes the comparison of average loop diameters for the reference alloys with neutron irradiation data in the temperature range of 275 – 400°C, where proton irradiation data is shown now in grey and neutron irradiation data in black [36, 129-131]. The relationship between dose rate and temperature for the microstructure can be derived in a similar fashion to Eq. 7.5 except that it does not require N_s to be invariant. Instead, the *net* flux of defects to a particular type of sink must remain invariant. In this case, the net flux of interstitials to interstitial-type dislocation loops must remain invariant, and the net flux of interstitials will be similar to the net flux of vacancies to vacancy-type sinks. From Ref. 124, the temperature shift is defined by:

$$T_2 - T_1 = \frac{\frac{kT_1^2}{E_m^v + 2E_f^v}\ln\left(\frac{K_{0_2}}{K_{0_1}}\right)}{1 - \frac{kT_1}{E_m^v + 2E_f^v}\ln\left(\frac{K_{0_2}}{K_{0_1}}\right)}, \tag{7.6}$$

where E_f^v is the interstitial formation energy. Assuming dose rates of 5 x 10^{-8} dpa/s for neutrons, 7 x 10^{-6} dpa/s for protons, and a vacancy migration energy of 1.2 eV and formation energy of 1.6 eV [33], then the effect of neutron irradiations at 340°C is similar to the effect of proton irradiation at ~ 380°C, and the reference alloy loop diameters compare well with neutron irradiation data from 320 - 340°C. However, the reference alloy data also compares well with neutron data at 275°C, where loop diameters range from 7 – 12 nm above 3 dpa, and assuming invariance, neutron irradiation at 275°C compares to proton irradiation at 300°C. Finally, loop diameters from Maziasz et al. [130] for 400°C neutron irradiation, which is comparable to 450°C proton irradiation, are much larger than the reference alloys, and the larger loop diameters are consistent with the effects of a higher temperature [130].

Average loop densities for Ref-Zr and Ref-Hf are compared against literature data, starting with proton irradiation data at 360°C and 400°C [43-45, 91, 126, 127].

Figure 7.8 shows the average loop densities as a function of dose, with 400°C proton irradiation data shown with closed symbols and 360°C data shown with open symbols. Ref-Zr has loop densities from 5.06 – 5.48 x 10^{22} m^{-3} for 3 – 7 dpa, and loop densities for Ref-Hf range from 2.29 – 2.32 x 10^{22} m^{-3} for 3 – 7 dpa.

The loop density for the commercial purity 316L irradiated with protons at 400°C by Teysseyre et al. [126] is similar to the value for Ref-Zr at 7 dpa, where both alloys have similar compositions. Loop densities for the reference alloys are also similar to the values reported by Gan et al. [43] for Fe-20Cr-24Ni irradiated with protons at 400°C. Otherwise, Ref-Zr and Ref-Hf generally have higher loop densities than the high purity alloy data at 400°C, but this is likely due to their relatively higher Si concentrations. Was et al. [92] reported a doubling of the loop density for 304SS with 1.05 wt% Si compared to the high purity reference alloy after 360°C proton irradiation to 5.5 dpa. Cookson et al. [128] measured nearly twice the loop density for a Fe-20Cr-9Ni alloy with 0.46 wt% Si addition compared to the reference alloy after 400°C proton irradiation to 1 dpa. Shigenaka et al. [132] measured more than twice the loop density for 316SS with 0.3 wt% Si compared to the reference alloy without Si after He^{+}-ion irradiation at 400°C to 0.1 dpa. These results indicate an increase in loop density with higher bulk Si concentration, which may explain the higher loop densities for the reference alloys relative to the high purity alloys in the literature. In addition, Ref-Zr has a loop density that is approximately twice the loop density of Ref-Hf, which is also consistent with the higher Si concentration for Ref-Zr at 0.38 wt% compared to 0.12 wt% for Ref-Hf.

Based on a relationship developed by Gan et al. [43] for loop density as a function of temperature, the effect of irradiation at 360°C relative to 400°C is to increase the loop density by roughly a factor of five. The loop densities for the literature data at 360°C are generally a factor of 2 – 5 higher than Ref-Zr and Ref-Hf for the same dose, which is consistent with the effect of a lower irradiation temperature in increasing the loop density. The reference alloy loop densities match the expected trend of lower loop densities than the 360°C literature data.

The final comparison with literature data for average loop density includes neutron irradiation data, as shown in figure 7.9 [36, 129-131]. Neutron irradiation data are shown in black while proton irradiation data are shown in grey, similar to figure 7.8.

The neutron irradiation data at 275°C has loop densities that are nearly an order of magnitude higher than Ref-Zr and Ref-Hf. Assuming invariance of the net flux of defects to a particular sink outlined by Eq. 7.6, neutrons at 275°C compare to protons at 300°C, so the higher loop densities for the neutron data are consistent with the effect of lower temperature on increasing loop density. Loop densities for neutron irradiation at 400°C, which are comparable to proton irradiation at 450°C, are more than an order of magnitude lower than for Ref-Zr and Ref-Hf and are consistent with the effect of higher temperature on decreasing loop density. Finally, the neutron irradiation data at 320 – 340°C, 7.4 dpa, most closely resembles the reference alloy data. The neutron data from 320 – 340°C, which compares to protons at 355 – 380°C, has a loop density that is twice that of Ref-Zr at 7 dpa. Irradiation temperatures and densities are similar, with the lower neutron irradiation temperature consistent with a higher loop density.

Loop diameters for Ref-Zr and Ref-Hf compare well with one another, and loop densities are higher for Ref-Zr compared to Ref-Hf due to the increase in Si concentration. The reference alloys have loop microstructures that are similar to 400°C proton irradiation data for commercial alloys and neutron irradiation data from 320 – 340°C. More importantly, the loop microstructure data for the reference alloys can be used in a comparative fashion to understand the effects of oversized solute additions on irradiated loop microstructure.

7.1.4 Relationship between Loop Microstructure and RIS

This section discusses the effects of oversized solute additions on loop microstructure and how those effects are consistent with the RIS measurements of oversized solute alloys. The effect of oversized solutes on the defect microstructure should be to decrease the bulk defect concentration and decrease the defect flux arriving at sinks by enhancing recombination. As a result, oversized solutes should exhibit some combination of either lower loop density or lower loop diameter due to the decrease in bulk defect concentration and defect flux to sinks.

In terms of the average loop diameter, the oversized solute alloys show no significant difference from the reference alloys. Figure 7.10 plots average loop diameter as a function of dose for all of the alloys in this study, with the reference alloys in shades

of grey, LoZr and HiZr shown in shades of red, and LoHf and HiHf shown in shades of blue. LoZr and HiZr loop diameters are similar to Ref-Zr at 3 dpa, and none of the +Zr alloys show any significant change in diameter from 3 to 7 dpa. The behavior is similar for LoHf and HiHf, with loop diameters slightly smaller than Ref-Hf by 2 nm at 3 dpa. By 7 dpa, average loop diameters for LoHf and HiHf are within 1 nm of Ref-Hf, and none of the alloys show much change in loop diameter from 3 to 7 dpa. There is no clear trend in loop size as a function of dose, with average diameters increasing for some alloys and decreasing for other alloys.

The oversized solute alloys do, however, show a significantly lower loop density compared to the reference alloys. Figure 7.11 uses a semi-log plot to show average loop density for all of the alloys as a function of dose, using the same color scheme as the previous figure. There are two things to notice from this figure. First, loop densities for the oversized solute alloys are significantly lower than the loop densities for the corresponding reference alloys at 3 dpa. This is true for LoZr and HiZr whose densities are 4 – 5 times lower than for Ref-Zr and again for LoHf and HiHf which are 2 – 4 times lower than that for Ref-Hf at 3 dpa. The second important point from this figure is that while loop densities remain constant for the reference alloys, all the oversized solute alloys exhibit significant increases in loop density by a factor or 1.5 or more between 3 and 7 dpa. In fact, by 7 dpa LoHf even measures a similar loop density as Ref-Hf.

The effects of oversized solute additions on loop microstructure are consistent with other loop microstructure studies of oversized solute alloys. Watanabe et al. [66] observed reductions in loop density with Ti and, to a lesser extent, Nb additions to austenitic stainless steel. Shigenaka et al. [20] found that Zr additions to 316L decreased both the loop size and density after electron irradiation to 0.85 dpa at 500°C. And Gan et al. [85] reported that after proton irradiation, Zr additions to 304SS caused a decrease in the loop density, while average diameters remained unchanged. These studies support the results found here, that oversized solute additions have a small effect on the average loop diameter but show a strong reduction in the loop density.

In the trapping mechanism, oversized solutes trap vacancies and enhance the recombination of point defects. Fewer point defects in the matrix mean that there are fewer defects diffusing to sinks, including both grain boundaries and dislocation loops.

The decrease in defect flux should affect both RIS and loop microstructure in a similar fashion, with less grain boundary segregation and a less developed loop microstructure.

A comparison is made between the amount of Cr depletion and the total loop line length, which is a product of the average loop circumference and density. The expectation is that less Cr depletion should correspond to a lower loop line length. Figure 7.12 shows loop line length as a function of grain boundary Cr depletion for the +Zr alloys. The figure shows a direct relationship between the amount of grain boundary Cr depletion and the loop line length. At 3 dpa, Ref-Zr has 3 times more Cr depletion and 5 times the total loop line length than for LoZr and HiZr. By 7 dpa, increases in the Cr depletion for LoZr and HiZr correspond to similar increases in the loop line length. The relationship between Cr depletion and loop line length is similar at 3 and 7 dpa, and illustrates how changes in the loop microstructure reflect changes in grain boundary RIS.

The comparison between Cr depletion and loop line length is made for the +Hf alloys in figure 7.13 at 3 dpa. The relationship between Cr depletion and loop line length again shows that lower amounts of Cr depletion correspond to a lower loop line length. HiHf shows the lowest amount of Cr depletion and the lowest loop line length. Meanwhile, the absence of oversized solute in the Ref-Hf alloy results in the highest amount of Cr depletion and loop line length. The correlation between Cr depletion and loop line length for the +Hf alloys is similar to the correlation for the +Zr alloys and again illustrates the connection between changes in microchemistry and microstructure.

The observations for loop line length and Cr depletion are consistent with a study by Gan et al. [44] who reported a substantial decrease in the loop line length compared to a reference 316SS after proton irradiation of the alloy heat as HiHf to 2.5 dpa at 400°C. And Fournier et al. [25], in measuring the same irradiated specimens from Gan et al. [44], found substantially less Cr depletion for the +Hf alloy compared to their reference alloy. The work combined showed a simultaneous decrease in Cr depletion and loop line length with Hf addition to 316SS.

The loop microstructures of the irradiated oversized solute alloys are consistent with the RIS measurements in two ways: 1) the suppression of loop nucleation and decrease in total loop line length at 400°C and 3 dpa corresponds to a decrease in RIS at the same temperature and dose, and 2) increases in loop line lengths for the oversized

solute alloys from 3 to 7 dpa are mirrored by similar increases in RIS. The loop microstructure data supports the vacancy trapping mechanism for oversized solutes by showing decreased defect concentrations through vacancy trapping and enhanced recombination.

7.1.5 Effect of Proton Energy on RIS

Proton irradiations are performed using either 2.0 MeV or 3.2 MeV, as mentioned in section 4.2.2, where the difference between 2.0 MeV and 3.2 MeV proton irradiations was discussed. The main difference between the two irradiations is in the displacement damage as a function of depth into the damaged layer. For a given ion current, at a fixed depth into the material, the dose rate for 2.0 MeV protons is greater than that for 3.2 MeV protons (within the 2.0 MeV damage region of ~ 20 μm). The same dose rate between the two proton energies can be achieved by lowering the current of 2.0 MeV proton irradiations relative to the currents used for 3.2 MeV proton irradiations. With the same dose rate, the effects on the irradiated microstructure should be the same.

Comparing segregation measurements between 2.0 MeV and 3.2 MeV irradiations, using the same alloy, temperature, and dose, confirms that proton energy does not affect RIS. In figure 7.14, changes in the grain boundary concentration for Ni and Cr are shown for 2.0 MeV and 3.2 MeV proton irradiations of HiZr, Ref-Hf, and HiHf at 3 dpa in shades of blue and 7 dpa in shades of red. The error bars represent one standard deviation of the measurements. All three alloys have RIS measurements made at both proton energies at 3 dpa, and HiZr and HiHf have measurements for both energies at 7 dpa. Measurements for HiZr at 3 dpa differ by slightly more than their errors. The difference between measurements for HiHf at 7 dpa is more substantial, but there is no reason to suspect the data because trends in segregation behavior are consistent for all alloys, temperatures and doses with the exception of HiHf at 7 dpa. The difference for HiHf at 7 dpa is discussed in greater detail in section 7.2. Otherwise, the measurements between 2.0 MeV and 3.2 MeV are similar to within the measurement error. Further, the results show no systematic trend in variation between 2.0 MeV and 3.2 MeV measurements. The results show that the difference in proton energy between 2.0 and 3.2 MeV has no measurable impact on measured grain boundary segregation.

7.2 Comparison of MIK-T Model Results with Experimental RIS Measurements

This section compares the MIK-T model with experimental segregation measurements for the +Zr and +Hf alloys. The comparison will provide an indication of whether the vacancy trapping mechanism can describe the observed behavior.

The solute-vacancy binding energies that were calculated using *ab initio* methods described in chapter 6 are used in model calculations. The binding energies are 1.08 eV for Zr and 0.71 eV for Hf. Section 6.2.4 defined the trapping radius and recombination radius as being the distance to the 4^{th} nn position at roughly 0.5 nm. Also, the oversized solute concentrations of the alloys are used as input with the assumption that all of the solute is in solution.

Comparisons between model and experiment at 400°C are made at 3 and 7 dpa for the +Zr alloys, representing a low dose and high dose for the alloys. To be consistent, the comparison for the +Hf alloys should also be made at 3 and 7 dpa. However, the measurements for HiHf at 7 dpa do not agree with one another, with a difference of 7 at% Ni enrichment and 3 at% Cr depletion between the two measurements. Figure 7.15 plots the changes in grain boundary Cr and Ni concentrations for all of the measurements at 400°C for the +Hf alloys.

Figure 7.15 shows a consistent trend in the data, where the reference alloy shows the most segregation while the alloy with highest solute concentration shows the least amount of segregation. The trend applies at 3 dpa, and again at 10 dpa, where Ref-Hf and LoHf have similar segregation within the errors of their measurements and HiHf has the lowest amount of segregation. The trend in segregation behavior is also consistent among the +Zr alloys at 400°C for all doses, and again at 500°C, 1 and 3 dpa for both +Hf and +Zr alloys. Only at 7 dpa for HiHf is the trend different, with HiHf having more segregation than Ref-Hf or LoHf.

A detailed review of the experiments showed no reason to suspect the data to be incorrect. Yet the measurements for HiHf at 7 dpa show different values for RIS from one another and are not consistent with the other data. As a result, comparisons between model and experiment for the +Hf alloys will not rely on this irradiation condition and will use segregation data at 3 and 10 dpa instead.

As the accurate prediction of Cr depletion is the most important aspect of RIS modeling, the comparison between model and experiment focuses on Cr depletion. This comparison is sufficient to understand the behavior of oversized solutes on RIS and to assess the results between the MIK-T model and experimental measurements.

Starting with comparisons at 400°C and 3 dpa, figure 7.16 shows the amount of Cr depletion between model and experiment. The left side of the figure is for the +Zr alloys and the right side of the figure is for the +Hf alloys. The most striking feature is that the model predicts a significant reduction in Cr depletion for LoZr and HiZr relative to Ref-Zr, and the RIS measurements are consistent with the model in showing a significant reduction in RIS. The MIK-T model predicts a reduction in Cr depletion for LoHf and HiHf compared to Ref-Hf, but not as significant as predicted for the +Zr alloys. Measurements for LoHf and HiHf also show a reduction in Cr depletion, and though it is not as much as predicted by the model, it is consistent with the trend of showing less of an effect on Cr depletion for the +Hf alloys as compared to the +Zr alloys.

Recall from chapter 6 that *ab initio* calculations determined that the solute-vacancy binding energy for Zr, at 1.08 eV, is larger than for Hf, at 0.71 eV. The results mean that Zr should be more effective in suppressing RIS than Hf. Thus, the MIK-T model predicts a larger reduction in RIS for Zr as compared to Hf. And segregation measurements confirm the calculated difference in solute-vacancy binding energies between Zr and Hf by showing a more significant reduction in Cr depletion for the +Zr alloys compared to the +Hf alloys at 400°C and 3 dpa.

Figure 7.17 shows the comparison between model and experiment at 400°C and 7 dpa for the +Zr alloys and 10 dpa for the +Hf alloys. The model still predicts significant reduction of Cr depletion for LoZr and HiZr compared to Ref-Zr, and again for LoHf and HiHf compared to Ref-Hf. The measured values, however, no longer show a reduction in Cr depletion for the oversized solute alloys. LoZr and HiZr now more closely resemble the amount of Cr depletion for Ref-Zr, where only HiZr has a statistically-significant difference in Cr depletion from Ref-Zr. Measurements for LoHf and HiHf have no statistically-significant difference from Ref-Hf, indicating no effect of Hf at the higher dose. One explanation for the lack of agreement between model and experiment is that oversized solutes lose the ability to reduce segregation at the higher dose.

The loss of solute effectiveness was observed by Fournier et al. [25] for 316SS with Hf, the same alloy heat as HiHf in this study, irradiated to doses of 2.5 and 5 dpa at 400°C. At 2.5 dpa, Cr depletion was suppressed for the +Hf alloy relative to the reference alloy, with a difference of more than 3 at%. By 5 dpa, Hf addition shows little benefit in reducing RIS, with a difference in Cr depletion of less than 1 at% from the reference, similar to the difference in this study between Ref-Hf and HiHf at 10 dpa.

Figure 7.18 makes a comparison between model and experiment for the +Zr and +Hf alloys at 500°C and 1 dpa. The model predicts almost complete suppression of Cr depletion for LoZr and HiZr and calculates a large reduction in Cr depletion for LoHf and HiHf compared to Ref-Hf. The experimental measurements do not agree quantitatively with the model, but all four oversized solute alloys are qualitatively consistent with the trend of the model in showing a reduction in Cr depletion. In addition, LoZr and HiZr show less Cr depletion than LoHf and HiHf, which is consistent with Zr being more effective than Hf in reducing RIS.

Finally, model and experiment are compared for the oversized solute alloys at 500°C and 3 dpa in figure 7.19. The model continues to show suppression of RIS for all of the oversized solute alloys. At 3 dpa, however, only HiZr still shows a reduction in Cr depletion relative to Ref-Zr, and the reduction is less than it was at 1 dpa. The measurements for LoZr, LoHf and HiHf show a similar amount of Cr depletion as their reference alloys, and the difference between model and experiment can again be explained by a loss of solute effectiveness on RIS at higher dose.

Segregation measurements confirm the calculated difference in solute-vacancy binding energies between Zr and Hf. At all temperatures (400°C and 500°C) and at all doses studied from 1 – 10 dpa, any reduction in Cr depletion is greater for the +Zr alloys than for the +Hf alloys. As a result, RIS measurements confirm the results of first-principles calculations in showing a greater effectiveness of Zr relative to Hf on reducing RIS due to the larger binding energy for Zr at 1.08 eV relative to Hf at 0.71 eV.

Measured reduction of Cr depletion disappears after 3 dpa at 400°C and after 1 dpa at 500°C for the +Zr and +Hf alloys, indicating that the effectiveness of oversized solute disappears more quickly as a function of dose at the higher temperature. Given that: 1) the behavior of reference alloy RIS was validated against literature data and also

against model calculations of RIS, and 2) the effect of oversized solute additions in suppressing Cr depletion is observed at low doses, then the disappearance of the effect of oversized solutes on RIS with increasing dose must be due to changes in the irradiated microstructure.

7.3 Mechanism Responsible for Loss of Effect from Oversized Solutes

The loss of effect on RIS from oversized solutes could come from two sources: 1) a loss of solute effectiveness in trapping vacancies and enhancing recombination due to solute poisoning, and 2) a loss of the oversized solute itself from the matrix. This section analyzes the role of these two sources for explaining the loss of effect on RIS.

7.3.1 Loss of Oversized Solute Effectiveness due to Solute Poisoning

Vacancy trapping causes enhanced recombination with freely migrating interstitials. Smaller substitutional atoms, like Si, migrating as interstitials, could recombine with the vacancy to become first nearest neighbors of the oversized solute atom. Alternatively, a small interstitial could bind with the vacancy and sit near the vacant lattice site without recombination. In either case, the effect would be a reduction in the strain field surrounding the oversized solute atom or a change in electronic effects with neighboring atoms. Such solute "poisoning" may decrease the oversized solute atom's ability to trap vacancy defects and enhance recombination. The effects of solute poisoning could take two forms: 1) a decrease in the trapping and recombination radii, and 2) a decrease in the solute-vacancy binding energy.

The trapping and recombination radius are based on the distance to the 4^{th} nearest neighbor (nn) atom and define the interaction volume around the solute atom. The *range* of the interaction does not depend on solute type or on electronic effects with neighboring atoms. The binding energy as a function of nn distance for both Zr, in red, and Hf, in blue, is shown in figure 7.20. The difference in binding energy at the 1^{st} nn position is attributed to electronic effects, but the ranges for Hf and Zr are similar and so are not attributed to electronic effects with neighboring atoms. Since the range of interaction is not likely to depend on the types of neighboring atoms, then solute poisoning should not

affect the trapping and recombination radii. Furthermore, the MIK-T model was shown in chapter 6 to be relatively insensitive to the trapping and recombination radii, so changing their values to a 1st or 2nd nn distance will have virtually no effect on segregation. For these reasons, decreases in the trapping or recombination radii are unlikely to be the cause for the loss of effect from oversized solutes on RIS.

Solute poisoning could also reduce the binding energy of oversized solute atoms by decreasing the elastic interaction energy between the vacancy and solute atom. No calculations have been performed to quantify this effect. Nevertheless, the fact that Zr and Hf differ so much in binding energy demonstrates that electronic effects with neighboring atoms are an important contribution to the binding energy. For this reason, solute poisoning could cause a substantial change in binding energy.

In figure 7.21, grain boundary Cr depletion for LoZr and HiZr irradiated to 7 dpa at 400°C is calculated in the MIK-T model for a binding energy of 0 to 1 eV. The figure also represents the measured Cr depletion values for the alloys with dashed lines. For LoZr, the measured value is greater than any of the calculated values and best matches the model at 0 eV. For HiZr agreement between model and experiment is at approximately 0.3 eV.

The binding energy is varied from 0 to 1 eV for the +Hf alloys and compared with the measured Cr depletion at 400°C and 10 dpa as shown in figure 7.22. Dashed lines are again used to represent the measured Cr depletion at 10 dpa for LoHf and HiHf. LoHf agrees with the model at 0 eV and HiHf agrees with the model at approximately 0.3 eV. Agreement between model experiment for the +Hf alloys is similar to the +Zr alloys.

The result of the binding energy analysis shows that solute poisoning would have to reduce the solute-vacancy binding energies to 0 – 0.3 eV for Zr and Hf. Kato et al. [23] estimated binding energies for Ti and Nb in 316L to be 0.14 and 0.18 eV, respectively. Sakaguchi et al. [21] fit a RIS model with vacancy trapping to measured segregation values for Ti and Nb in 316SS and estimated binding energies for the oversized solutes to be ~ 0.2 and 0.4 eV, respectively. The results shown here indicate that vacancy-trapping effectiveness for Zr and Hf would have to at least be reduced to the equivalent effectiveness of Ti or Nb for the MIK-T model to match measured segregation values at high dose. For LoZr and LoHf, almost a complete loss of solute-vacancy

binding is necessary to explain their experimental measurements of Cr depletion at high dose.

No experimental measurements or calculations exist which can be used to substantiate the reduction in binding energy for Zr or Hf. But in terms of atomic volume, Gan et al. [44] listed the 316SS atomic volume, 1Ω, as 6.86 cm^3/mol compared to ~ 1.6Ω for Ti and Nb and ~ 2Ω for Hf and Zr. A vacancy defect in fcc Ni has a calculated relaxation volume of ~ 0.4Ω [133], so to reduce lattice strain for Zr and Hf to be equivalent to Ti and Nb would require at least the capture of a vacancy defect. Discussion of the relaxation volume assumes that binding energy correlates with lattice strain, but the calculated solute-vacancy binding energies for Zr and Hf indicate that binding energy depends only in part on strain effects, and partly also on electronic interactions. As a result the strain-binding energy relationship is more complicated than the treatment given here. Nevertheless, the reduction in lattice strain for HiZr and HiHf would still be substantial, and for the LoZr and LoHf alloys, the lattice strain would likely need to be reduced even more than 0.4Ω in order to give a binding energy near zero. Such a large reduction in strain would include at least the reaxlation from a trapped vacancy defect. Since the reduction in binding energy requires the trapping of a vacancy, it contributes to the mechanism of enhanced recombination. The end result is that solute poisoning is not able to explain the loss of solute effectiveness on RIS.

7.3.2 Loss of Oversized Solute to Precipitation

Another possible explanation for the loss of solute effectiveness on RIS is that the solute is lost from solution due to a precipitation reaction. As seen in section 5.3, solute-rich precipitates exist prior to irradiation, so it is known that the actual concentrations of Zr or Hf in solution and available for vacancy trapping is less than the bulk alloy concentrations.

The oversized solute concentrations are varied from 0 – 0.1 at% for calculations in the MIK-T model for the +Zr alloys in figure 7.23 and the +Hf alloys in figure 7.24. The measured values of Cr depletion for the oversized solute alloys are shown by dashed lines. For HiZr and HiHf, solute concentrations would need to be about 0.01 at% at 7 dpa and 10 dpa, respectively, for the measurements to match the MIK-T model. LoZr and

LoHf would require a complete loss of solute concentration from solution for the measured Cr depletion to match the model.

The loss of oversized solute in solution would require radiation-induced precipitation or radiation-enhanced diffusion to existing precipitates. The solubility limit of Zr and Hf in Fe, Ni or Cr is negligible [134, 135], so Zr and Hf may be expected to come out of solution during irradiation since the diffusion kinetics are increased due to higher point defect concentrations. The loss of solute means a loss of vacancy trapping sites and therefore a loss of enhanced recombination of defects. The result is that grain boundary concentrations begin to more closely resemble the reference alloys.

Suzuki et al. [136] found growth of TiC precipitates in the matrix in austenitic stainless steel with fast neutron irradiation at 300°C. High purity 316SS with additions of 0.90 wt% Hf or 0.78 wt% Zr were neutron irradiated by Ohnuki et al. [86], and though no precipitates were observed prior to irradiation, a high density of fine ZrC or HfC precipitates developed after irradiation at temperatures of 500°C and 600°C, demonstrating that both Zr and Hf are susceptible to radiation-induced precipitation with carbon. Finally, Fournier et al. [25] observed Hf-rich precipitates in 316SS prior to irradiation with a density of 1×10^{19} m^{-3} for a 30-minute, 1100°C anneal or 8.6×10^{20} m^{-3} for a 20-minute, 900°C anneal, where the Hf-doped alloy is the same heat as HiHf in this study.

An existing oversized solute-rich precipitate microstructure prior to irradiation is supported by SEM observations of all four oversized solute alloys that show precipitates both before and after irradiation. TEM observations for the HiHf alloy resulted in a measured precipitate density of 7×10^{19} m^{-3} with an average size of 62 ± 36 nm after a 60-minute, 1000°C anneal. Similarly, the HiZr alloy had a measured precipitate density of 2.5×10^{19} m^{-3} with an average size of 81 ± 32 nm after a 60-minute, 1000°C anneal for HiZr. XRD analyses from section 5.3.1 confirm these precipitates as ZrC and HfC prior to irradiation, due to thermal aging [49]. This does not exclude the presence of other intermetallic-type precipitates; rather, their concentration could be below the detection limit in XRD. In addition, radiation-induced precipitation could form other types of phases apart from just carbides [49]. Given that Ohnuki et al. [86] did not observe precipitation below 500°C, an analysis of precipitation will consider only radiation-

enhanced diffusion of oversized solute to pre-existing precipitates to determine whether or not this can explain the loss of solute from the matrix.

Precipitate growth is used to explain the loss of solute from solution. However, precipitate growth cannot be confirmed by measuring a change in precipitate size. Assuming the precipitate density remains constant, a complete loss of 0.37 at% Hf in the HiHf alloy would require a mean precipitate size of 76 nm. The precipitates have a size distribution with a mean of 62 nm and a standard deviation of 36 nm, so the increase in size of the precipitates by absorption of all solute is less than the standard deviation. Similarly for the HiZr alloy, a complete loss of 0.28 at% Zr would lead to a mean precipitate size of 97 nm, and the difference from the measured average of 81 nm is less than the standard deviation of the measurement, 32 nm. Therefore, TEM imaging as a function of irradiation dose cannot be used to confirm precipitate growth from the loss of solute to precipitates.

Precipitation kinetics developed by Shewmon [137] considers the loss of oversized solute as a function of irradiation time. If the precipitates are homogenously distributed, then each precipitate can be defined in a unit cell where the remaining solute in solution will then diffuse to the precipitate as a function of irradiation time. The diffusion of solute to the precipitate can be described by:

$$\frac{4\pi r_e^3}{3}\frac{\partial \bar{c}}{\partial t} = J(\alpha)\cdot 4\pi\alpha^2. \qquad (7.7)$$

The term on the left is the loss rate of solute from the unit cell and the term on the right is the rate of gain for solute diffusing to the precipitate, where r_e is the radius of the unit cell, t is the irradiation time, $\bar{c}$ is the average solute concentration, α is the radius of the precipitate, and $J(\alpha)$ is the flux in the solid solution at the surface of the precipitate, $r = \alpha$. For clarity, an example of the solute concentration in a unit cell as a function of the radius of the unit cell is shown in figure 7.25, where c_0 is the initial solute concentration *outside* of the precipitate and c' is the matrix concentration in equilibrium with the precipitate.

The evaluation of $J(\alpha)$ is made using the steady-state solution of the concentration within the unit cell, at $r = r_e$, according to:

$$\frac{\partial^2 c}{\partial r^2} + \frac{2}{r}\frac{\partial c}{\partial r} = 0. \tag{7.8}$$

The solute is subject to the following boundary conditions:

$c = c_0$ for $r = r_e$,

$c = c'$ for $r = \alpha(t)$.

Solving for $c(r)$ from Eq. 7.8, assuming $r_e >> \alpha(t)$, gives:

$$c(r) = -\frac{(c_0 - c')}{\alpha(t)} + c_0. \tag{7.9}$$

The flux at the surface of the precipitate is given by:

$$J(\alpha) = -D\left(\frac{\partial c}{\partial r}\right)_{r=\alpha(t)} = -D\frac{(c_0 - c')}{\alpha(t)}, \tag{7.10}$$

where D is the diffusion coefficient. Substituting for the flux from Eq. 7.10 into Eq. 7.7, the resulting expression for the rate of change of $\bar{c}$ is given by:

$$\frac{\partial \bar{c}}{\partial t} = -\frac{3D}{r_e^3}\cdot(c_0 - c')\cdot\alpha(t). \tag{7.11}$$

An expression for $\alpha(t)$ is required based on the conservation of solute according to the equation:

$$\frac{4}{3}\pi c_p \alpha^3(t) = \frac{4}{3}\pi r_e^3\left[c_0 - \bar{c}(t)\right], \tag{7.12}$$

where c_p is defined as the atom fraction of the solute *in* the precipitate. Equation 7.12 also assumes that $\alpha = 0$ at $t = 0$. Solving for $\alpha(t)$ gives the following equation:

$$\alpha(t) = r_e\left[\frac{c_0 - \bar{c}(t)}{c_p}\right]^{\frac{1}{2}}. \tag{7.13}$$

After plugging the solution for $\alpha(t)$ into Eq. 7.11 and integrating, the final solution is:

$$\bar{c} = c_0 - \left(\frac{2D(c_0 - c')t}{c_p^{\frac{1}{3}} r_e^{\,2}}\right)^{\frac{3}{2}}. \tag{7.14}$$

Note that this solution is valid for short times, where $r_e >> \sqrt{Dt}$.

The diffusion coefficient, D, is described by:

$$D = D_0 e^{\left(\frac{-Q}{kT}\right)}, \quad (7.15)$$

where D_0 is the pre-exponential factor, Q is the activation energy, k is Boltzmann's constant and T is the irradiation temperature. Under irradiation, the activation energy is the migration energy, and the diffusion coefficient is described by:

$$D = D_x C_x, \quad (7.16)$$

which is the product of the defect diffusion coefficient, D_x, and the defect concentration, C_x, where x describes the defect type.

The analysis considers the loss of oversized solute through the vacancy flux only. The large size of Zr and Hf relative to the matrix atoms makes their diffusion as interstitials improbable. Vacancy migration energies for Zr or Hf in a Fe-Cr-Ni system are not known but can be bounded by the Cr migration energy calculated in the MIK model, since Cr represents the largest element in the ternary Fe-Cr-Ni alloy. The calculated diffusion coefficient for Fe-20Cr-9Ni in the MIK model [33] uses a migration energy of 1.18 eV and a pre-exponential factor of 4.08 x 10^{-6} m^2/s. The resulting Cr diffusion coefficient via vacancies is 5.93 x 10^{-15} m^2/s at 400°C and 8.25 x 10^{-14} m^2/s at 500°C.

Defect concentrations are the steady-state matrix concentrations taken from the MIK model, with vacancy atom fractions of ~ 1.3 x 10^{-6} at 400°C and 2.0 x 10^{-7} at 500°C. The initial concentration of solute in the matrix, $c_{0,}$ prior to irradiation was estimated at 0.16 at% for HiHf using an TEM imaging study described in section 5.3.3. Assuming that HfC precipitates are stoichiometric, then c_p is 0.5. For a precipitate density of 7 x 10^{19} m^{-3}, then r_e = 1.21 x 10^{-7} m. Recall that the solution in Eq. 7.14 is valid for short times, where $r_e >> \sqrt{Dt}$. Using the values for r_e and D, then r_e is not equal to $\sqrt{Dt}$ until doses of 18 dpa at 400°C and more than 8 dpa at 500°C. These irradiation doses are substantially higher than the doses used in this study, so the short-time solution is valid.

The results of the precipitation kinetics analysis are shown in figure 7.26, where the concentration of Hf in the matrix is plotted as a function of irradiation dose. The calculated vacancy diffusion coefficients are shown at 400°C, in blue, and 500°C. The result is a small loss of oversized solute to precipitates at both 400°C and 500°C on the

time scales of proton irradiations. At higher doses, a total loss of Hf to precipitates occurs at both temperatures, so faster diffusion rates or shorter diffusion distances could cause the total loss of solute on the time scales of proton irradiations.

The analysis is dependent on the migration energy because it has a large impact on the amount of solute remaining in solution. The analysis uses the Cr vacancy migration energy, but a lower migration energy for the oversized solutes may be a reasonable assumption based on first principles calculations by Krčmar et al. [16] and Janotti et al. [15], where large solute atoms in fcc Ni are shown to diffuse faster through the vacancy flux than small solute atoms. Janotti et al. specifically addressed the diffusion of 4d and 5d transition elements in Ni, and migration energies are the lowest for Zr and Hf at around 0.2 eV.

Figure 7.27 shows Hf concentration as a function of migration energy. The Cr migration energy of 1.18 eV is shown by a vertical line in the figure, and migration energies of approximately 1.03 and 1.06 eV would explain a loss of solute from the matrix at 500°C, 3 dpa and 400°C, 7 dpa, respectively. The shaded region marks the migration energy range from 1.03 – 1.06 eV that accounts for the estimated solute in solution from figures 7.23 and 7.24, between 0 – 0.01 at%. Based on diffusion rate trends from Krčmar and Janotti, Hf and Zr may be expected to have lower migration energies than Cr and therefore diffuse faster through the vacancy flux. And similar migration energies for Hf are able to explain the loss of solute at both 400°C and 500°C at the doses where a loss of solute effectiveness on RIS is observed.

The mobility of oversized solute to diffuse to precipitates through the vacancy flux is not fully consistent with the trapping mechanism, since solute diffusion through vacancies may prevent them from acting as recombination centers. However, the processes for diffusion and recombination occur on very different time scales, with a trapped vacancy-interstitial recombination event occurring on a much shorter time scale relative to the time scales required for precipitate growth. The trapping mechanism results in either the recombination of a trapped vacancy with a free interstitial or the release of the trapped vacancy. The inverse of the dissociation coefficient, τ, describes an average trapping time for a vacancy defect with a solute atom. For Zr with a binding energy of 1.08 eV, the average trapping time for a defect is 6×10^3 s at 400°C.

Considering a vacancy migration energy of 1.05 eV, the diffusion distance, described by $\sqrt{Dt}$, for the same time period is 3.5 nm, which is much less than the spacing between precipitates. For Hf with a binding energy of 0.71 eV, the average trapping time at 400°C is only 11 s, and the diffusion distance is ~ 0.2 nm. Given that diffusion to precipitates requires time scales on the order of 10^7 s, the mobility of solute atoms is small relative to the time scales of vacancy trapping, recombination and release events. The solute atoms remain as sites for trapping and recombination for most of their time in solution.

As solute is lost to precipitates, the trapped vacancies return to the matrix as part of the free vacancy concentration. The release of trapped vacancies, however, is not expected to have an impact on the interstitial loop microstructure. In the temperature regime of the proton irradiations, the defect concentrations are dominated by recombination, though loss to sinks is also significant. Based on defect fractions from the MIK-T model, for the HiZr alloy with 0.28 at% Zr at 400°C, the trapped vacancy fraction is 1.1×10^{-3}. Since solute is lost over the time scale of ~ 10^7 s, trapped vacancies released to the matrix amounts to ~ 1×10^{-10} s^{-1}, much less than the defect production rate of 1×10^{-6} s^{-1}. Moreover, the ratio of free vacancies to free interstitials is no different for an oversized solute alloy compared to an alloy without solute. For the HiZr alloy under the same irradiation conditions, the free vacancy fraction is 6.8×10^{-10} and free interstitial fraction is 1.6×10^{-10}, for a ratio of 4.35. For the same alloy without Zr, the free vacancy fraction is 1.3×10^{-6} and free interstitial fraction is 3.1×10^{-7}, for a ratio of 4.25. The point is that addition of oversized solutes does not change the ratio of vacancies to interstitials, so the loss of solute from solution will not affect the net flux of defects to sinks, like dislocation loops, and therefore will not affect the loop morphology.

The kinetics analysis is a good approximation for $\bar{c}/c_0 > 2/3$, but figures 7.26 and 7.27 plot the solution for $\bar{c}$ = zero. According to Refs. 137 and 138, when the concentration in the unit cell drops to less than two-thirds of the initial concentration, the driving force for solute diffusing to the precipitate decreases because of a smaller difference between $\bar{c}$ and c'. The rate of solute lost to the precipitate then becomes less than predicted by Eq. 7.6, meaning that the solution under-estimates the diffusion time and the migration energy. However, as shown in figure 7.27, lower migration energies

for the solute atoms will enhance the diffusion. Since the actual migration energy for Hf or Zr is not known, the analysis can still predict a loss of solute to precipitates given sufficiently low migration energy. Figure 7.27 shows that migration energies of ~ 1 eV show a complete loss of solute to precipitates, but Janotti et al. [15] calculated migration energies for Zr and Hf of 0.2 eV, which are sufficient to explain the loss of solute when $\bar{c}/c_0 < 2/3$.

This analysis was performed only for HiHf, but the conclusions would not depend on the alloy. The initial concentration for HiZr was 0.11 at% Zr in solution. The migration energies and times required for the loss of solute from solution are similar to the values shown for HiHf, with a complete loss of Zr at 400°C, 7 dpa and 500°C, 3 dpa occurring with migration energies from 1.02 – 1.05 eV. Similarly, although initial concentrations of solute remaining in solution for LoHf and LoZr would be different than HiHf or HiZr, conclusions from the analysis would be similar. Since the analysis is not strongly dependent on the value of the initial concentration, the error in the TEM estimate of solute in solution is not important.

The analysis assumes that the solubility limit of Hf or Zr in stainless steel at the irradiation temperatures is negligible. Work by Abraham et al. [139] has shown that for stainless steel with Zr, the solubility of Zr drops to zero at temperatures below 600°C. Phase diagram calculations using FactSage [140] with the SGTE database (applicable to metals and alloys) support the lack of solubility for Zr and Hf. The calculated phase diagrams show that for a Fe-Ni-C austenite system, at temperatures below 600°C, the solubility of Zr or Hf drops to zero. In simpler binary phase diagrams of Fe, Cr or Ni with either Zr or Hf, the solubility of solute again is negligible at irradiation temperatures. Drawing from both experimental work and calculations from databases, no Zr or Hf is expected to be in solution at 400°C or 500°C for proton irradiations.

Figures 7.16 to 7.19 make comparisons of measured RIS with the MIK-T model using the oversized solute concentration for the bulk alloy. However, TEM imaging from chapter 5 revealed that not all of the oversized solute remained in solution prior to irradiation. An estimate of the amount of solute remaining in solution prior to irradiation may be used in the MIK-T model to observe the effect on the calculated RIS results. Figure 7.28 uses the estimated solute concentration to re-calculate Cr depletion for the

HiZr and HiHf alloys at 400°C. For the HiZr alloy, the solute concentration is 0.11 at% Zr and for HiHf, the solute concentration is 0.16 at%. In figure 7.16, the MIK-T model values did not lie within the error of the measured values for HiZr or HiHf at 3 dpa. By using the estimated solute concentrations based on TEM imaging, figure 7.28 shows that the model values now lay within the errors of the measured values for HiZr and HiHf at 400°C and 3 dpa. The improved agreement between model and experiment confirms that an accurate value for the amount of solute in solution is important for understanding RIS behavior. In addition, figure 7.28 shows that at higher doses, the calculated and measured values for Cr depletion no longer agree. But if the model included a further loss of solute due to precipitate growth at the higher dose, the model values may again be consistent with experimental measurements at high dose, as has been shown by figures 7.23 and 7.24.

The significance of this analysis is that the removal of solute to precipitates by vacancy diffusion is possible under the conditions in these experiments. The loss of solute effectiveness observed in RIS at 500°C, 3 dpa and 400°C, 7 dpa can be explained by the precipitation kinetics analysis. The estimated migration energy required to explain the loss of solute by precipitate growth is less than the Cr vacancy migration, which is consistent with the results of Janotti et al. [15] in showing lower migration energies for elements with a larger atomic radius such as Zr and Hf relative to Cr. And account accounting for the loss of oversized solute from solution due to precipitation results in better agreement between model-calculated RIS and measured values. As a result, the loss of solute by precipitate growth is the most likely mechanism to explain the loss of solute effectiveness on RIS.

7.3.3 Atom Probe Analysis

A final technique to confirm the loss of oversized solute with irradiation dose is through atom probe analysis. Local electrode atom probe (LEAP) results were presented in section 5.3.3. Each of the four oversized solute alloys was analyzed in the unirradiated condition. Of these, LoZr, HiZr and HiHf showed solute remaining in solution, while LoHf did not. LEAP analyses were also conducted on specimens irradiated at 400°C.

For LoHf, there is no confirmed Hf above the detection limit in LEAP in the unirradiated condition. LoHf also shows no difference in Cr depletion from Ref-Hf beyond the error of the measurements for the two alloys at 400°C and 3 dpa. Since no Hf could be detected in LoHf in the unirradiated condition, analyses on the irradiated alloy were not performed.

The HiHf alloy also shows Hf present in the unirradiated condition. And HiHf does show a small reduction in Cr depletion from Ref-Hf at 400°C and 3 dpa. By 7 dpa, there is again no difference in Cr depletion between the Ref-Hf and HiHf alloys. LEAP analysis also could not confirm the presence of Hf in solution, though there is uncertainty in the analysis due to a number of unidentified peaks near the expected mass/charge ratios for Hf which complicated the analysis.

For LoZr, Zr is detected in the unirradiated alloy, but Zr cannot be confirmed in the mass/charge spectra at 3 or 7 dpa. Reductions in Cr depletion are observed at 3 dpa, 400°C, but this disappears by 7 dpa. The apparent loss of Zr based on RIS measurements is consistent with the LEAP analysis.

Finally, only the HiZr alloy shows a statistically significant reduction in Cr depletion from the reference alloy at 7 dpa. HiZr is also the only alloy to have confirmed oversized solute in solution at 3 and 7 dpa from LEAP analysis, showing that at least some measurable concentration of Zr has remained in solution.

The results of LEAP analysis and their correlation with RIS data is shown in figure 7.29. The figure answers the questions: 1) is any oversized solute remaining in solution according to LEAP, and 2) if so, does the alloy show a reduction in Cr depletion? For example, if oversized solute is confirmed by LEAP to be in solution at 0 dpa, then the oversized solute should suppress Cr depletion at 3 dpa. The figure shows that for every alloy condition measured in LEAP, there is consistency between the reduction in Cr depletion and the detection of solute in solution by LEAP.

The LEAP results indicate when the amount of oversized solute in solution has dropped below the detectability limit, but some solute may still remain in solution, and even a small amount of solute has a large effect in reducing RIS. For example, LEAP did not detect solute in solution for LoZr and HiHf at 3 dpa, 400°C. Since LoZr and HiHf still show a reduction in RIS, the solute in solution is below the detectability limit.

According to figure 7.30, which shows grain boundary Cr depletion as a function of oversized solute concentration from the MIK-T model, even low solute concentrations of 0.01 at% can still reduce RIS by several at%. The model result is consistent with the LEAP analysis in showing that, even as solute is lost to precipitates, the remaining solute continues to reduce RIS until the solute is lost from solution entirely. The reduction in RIS is consistent with the MIK-T model in showing a large reduction in RIS, even for a small amount of solute, and RIS is also consistent with LEAP results in showing that small concentrations below the detectability limit for these alloys conditions can still cause a large reduction in Cr depletion.

The loss of oversized solute atoms from solution due to precipitate growth is the most likely cause for the disappearance of solute effectiveness on RIS with increasing dose. Results from the literature indicate that both precipitate growth and radiation-induced precipitation have been observed for similar irradiated alloys. Experimental observations in this study have confirmed the presence of a ZrC or HfC precipitate microstructure prior to irradiation. The loss of oversized solute to precipitate growth during irradiation is consistent with LEAP analysis, where for every alloy condition measured, solute in solution corresponds to a measured reduction in RIS, and the loss of solute is accompanied by a loss of solute effectiveness on RIS.

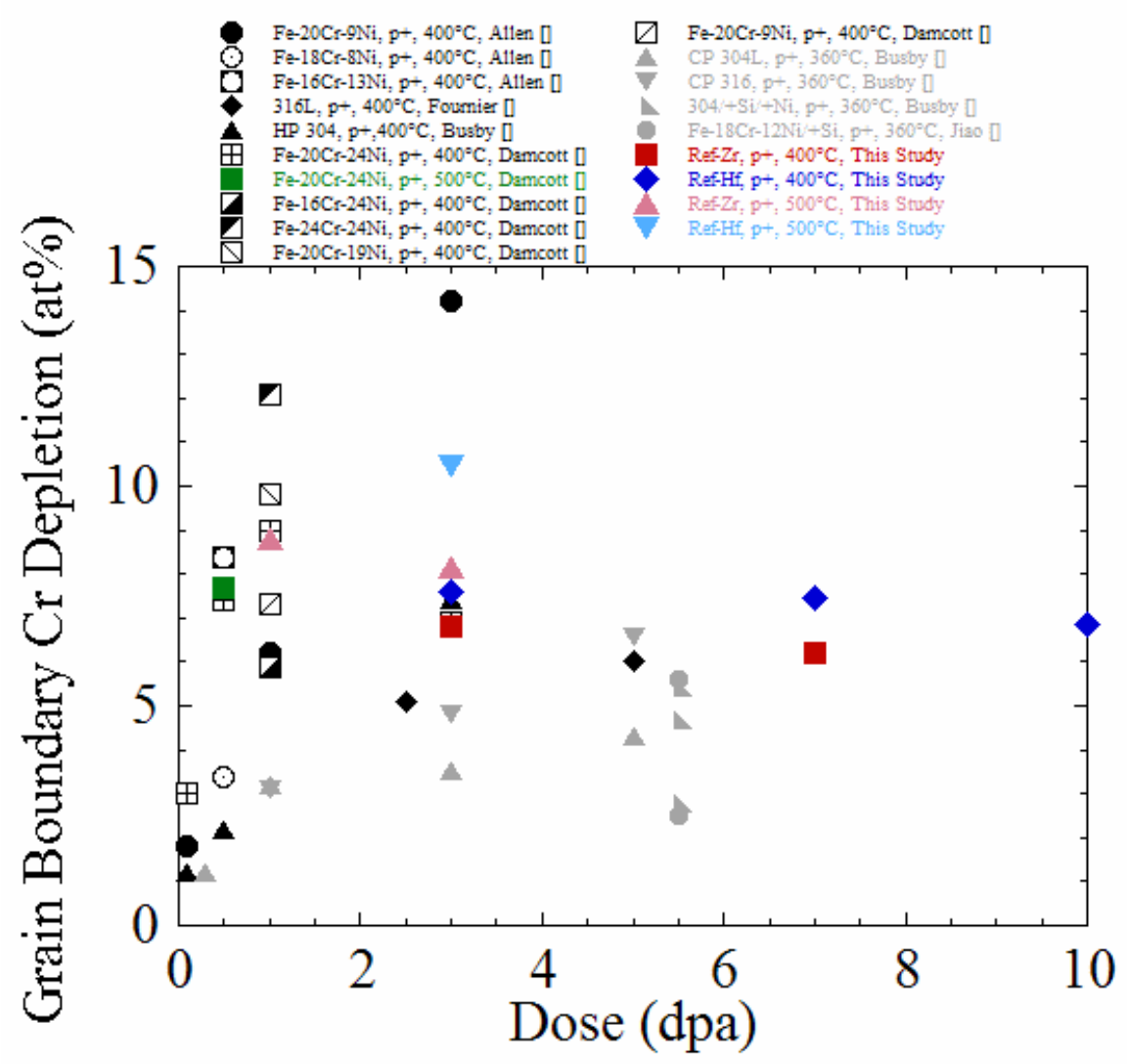

Figure 7.1 A comparison of Cr depletion between the reference alloys in this study and literature values for proton irradiation data, showing the amount of grain boundary (GB) Cr depletion as a function of dose for austenitic stainless steels at temperatures of 360 – 500°C [17, 25, 26, 28, 33].

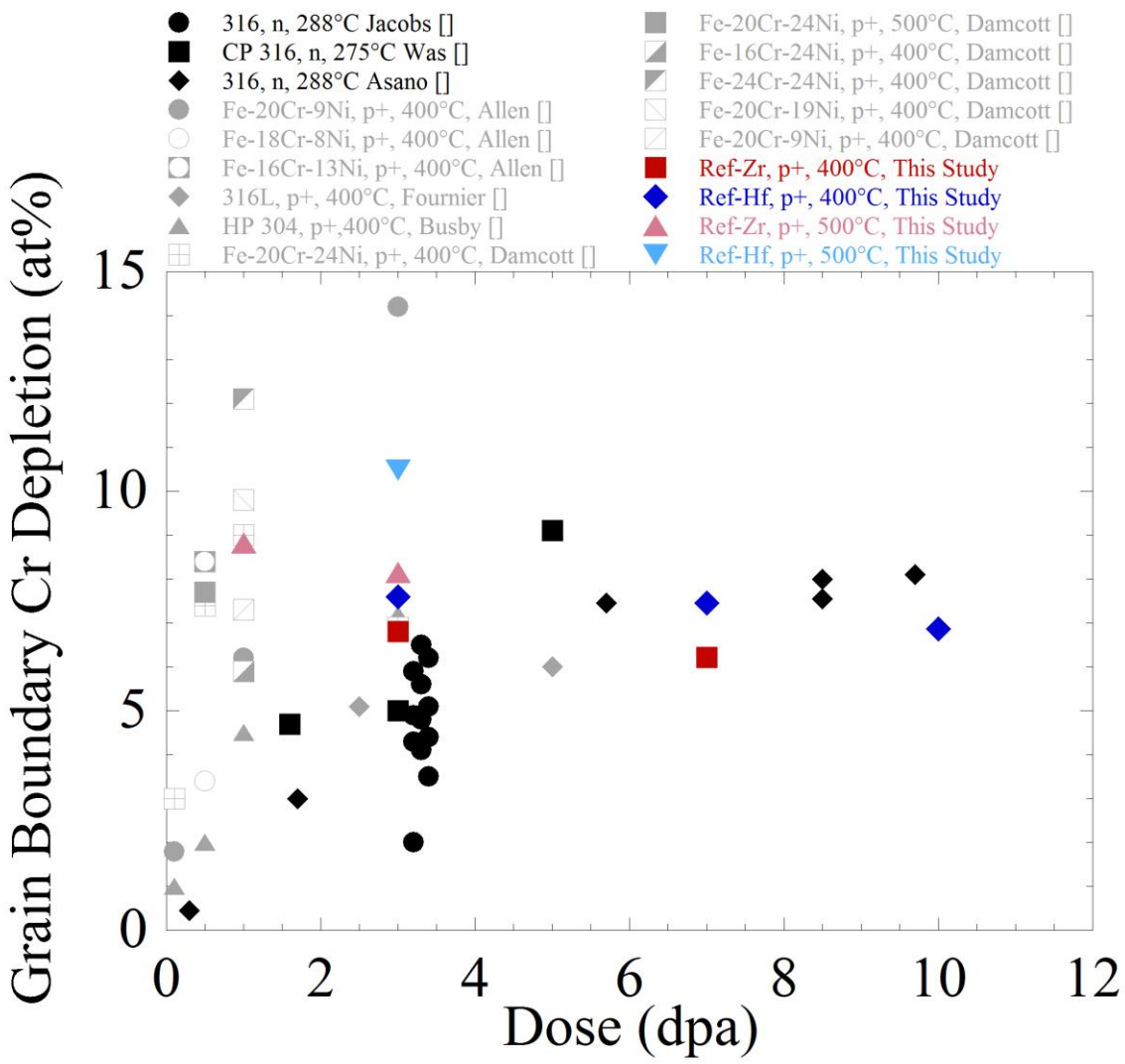

Figure 7.2 A comparison of Cr depletion between the reference alloys in this study and literature values for neutron irradiation data (black symbols) and proton irradiation data (grey symbols), showing the amount of grain boundary (GB) Cr depletion as a function of dose for austenitic stainless steels at temperatures of 275 – 500°C [17, 25, 26, 28, 33, 45, 84, 123].

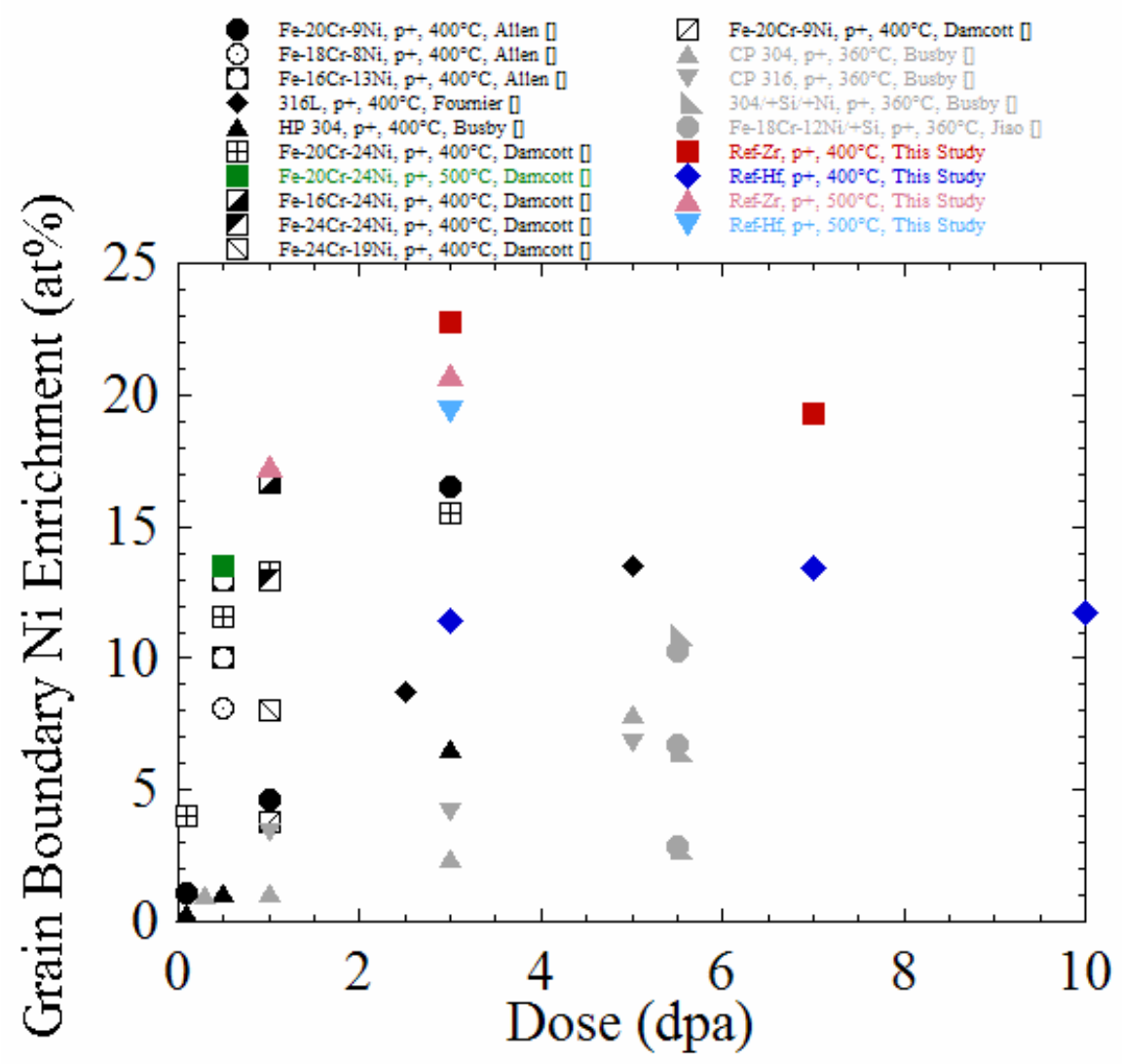

Figure 7.3 A comparison of Ni enrichment between the reference alloys in this study and literature values for proton irradiation data, showing the amount of grain boundary (GB) Ni enrichment as a function of dose for austenitic stainless steels at temperatures of 360 – 500°C [17, 25, 26, 28, 33].

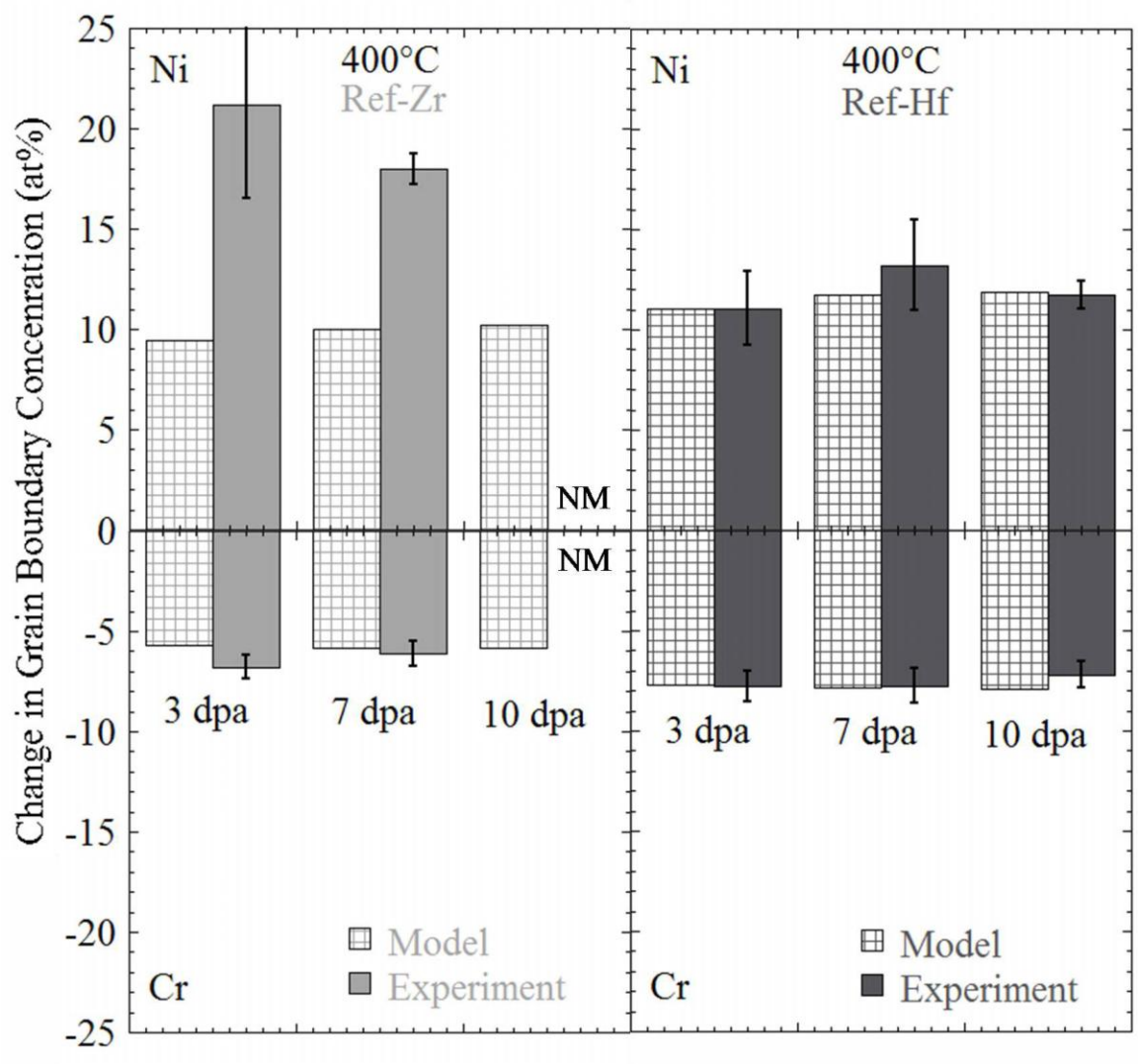

Figure 7.4 A comparison at 400°C of the MIK model and experimental measurements for the change in grain boundary Ni and Cr concentrations for Ref-Zr and Ref-Hf.

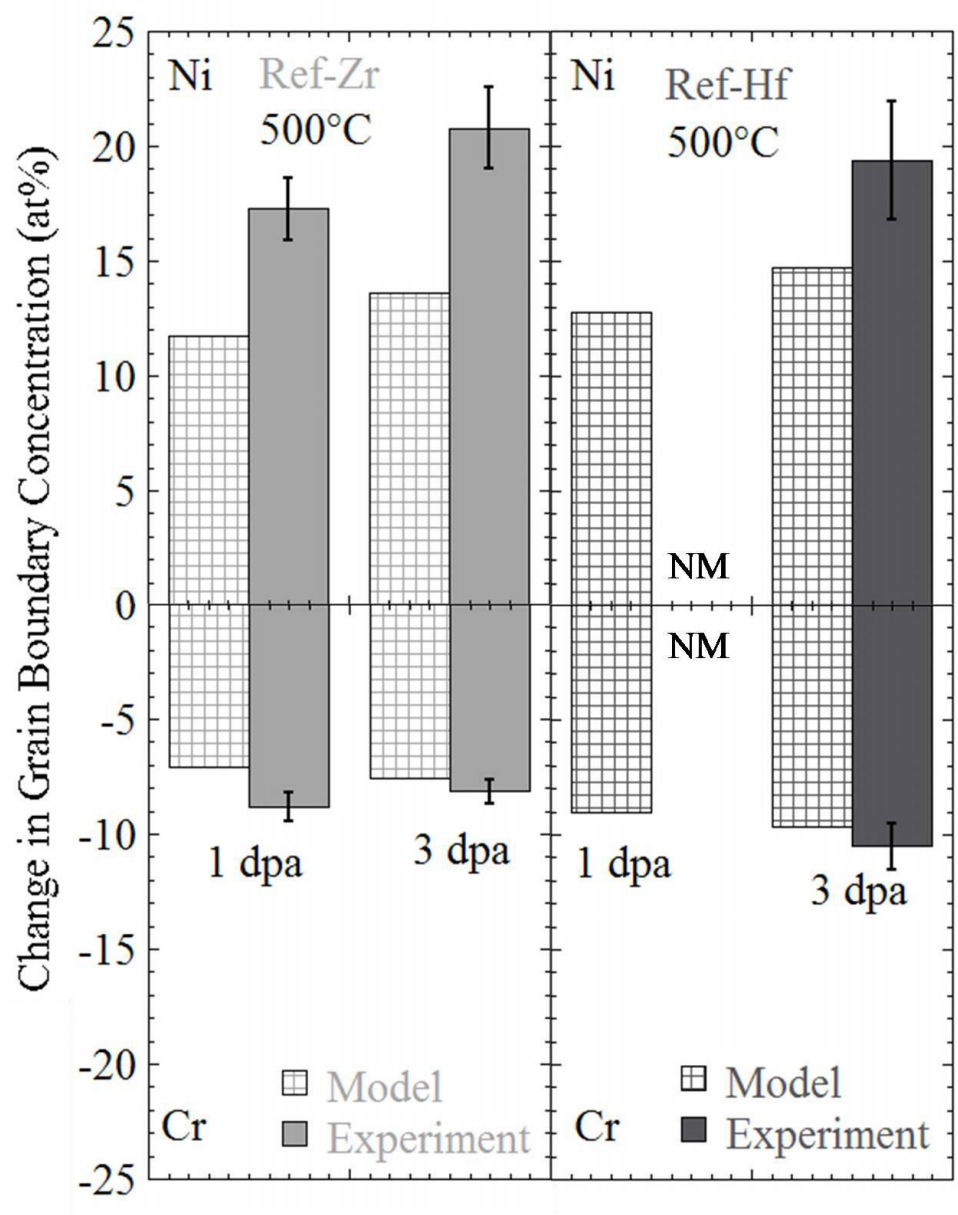

Figure 7.5 A comparison at 500°C of the MIK model and experimental measurements for the change in grain boundary Ni and Cr concentrations for Ref-Zr and Ref-Hf.

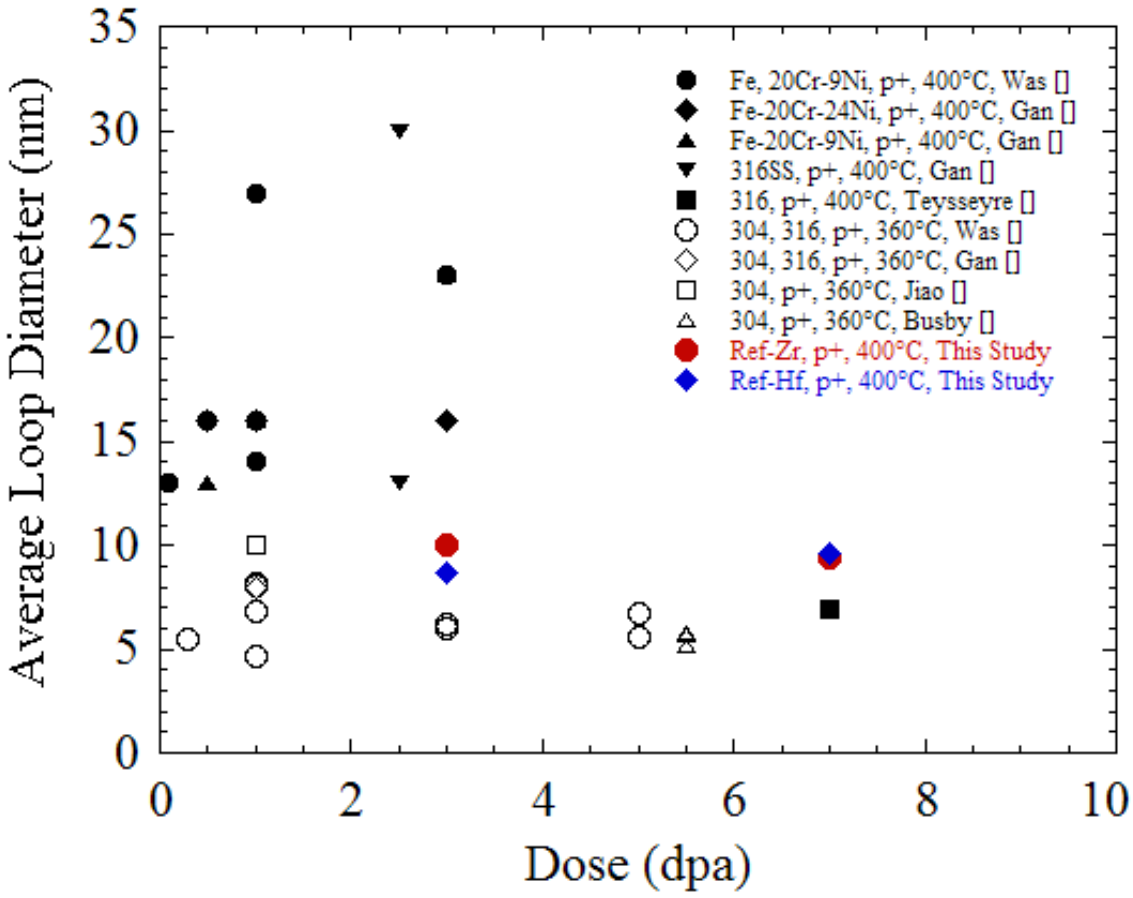

Figure 7.6 Average loop diameters for the reference alloys in this study compared to literature values for 316-type stainless steels irradiated with protons at temperatures of 360°C and 400°C [43-45, 91, 126, 127].

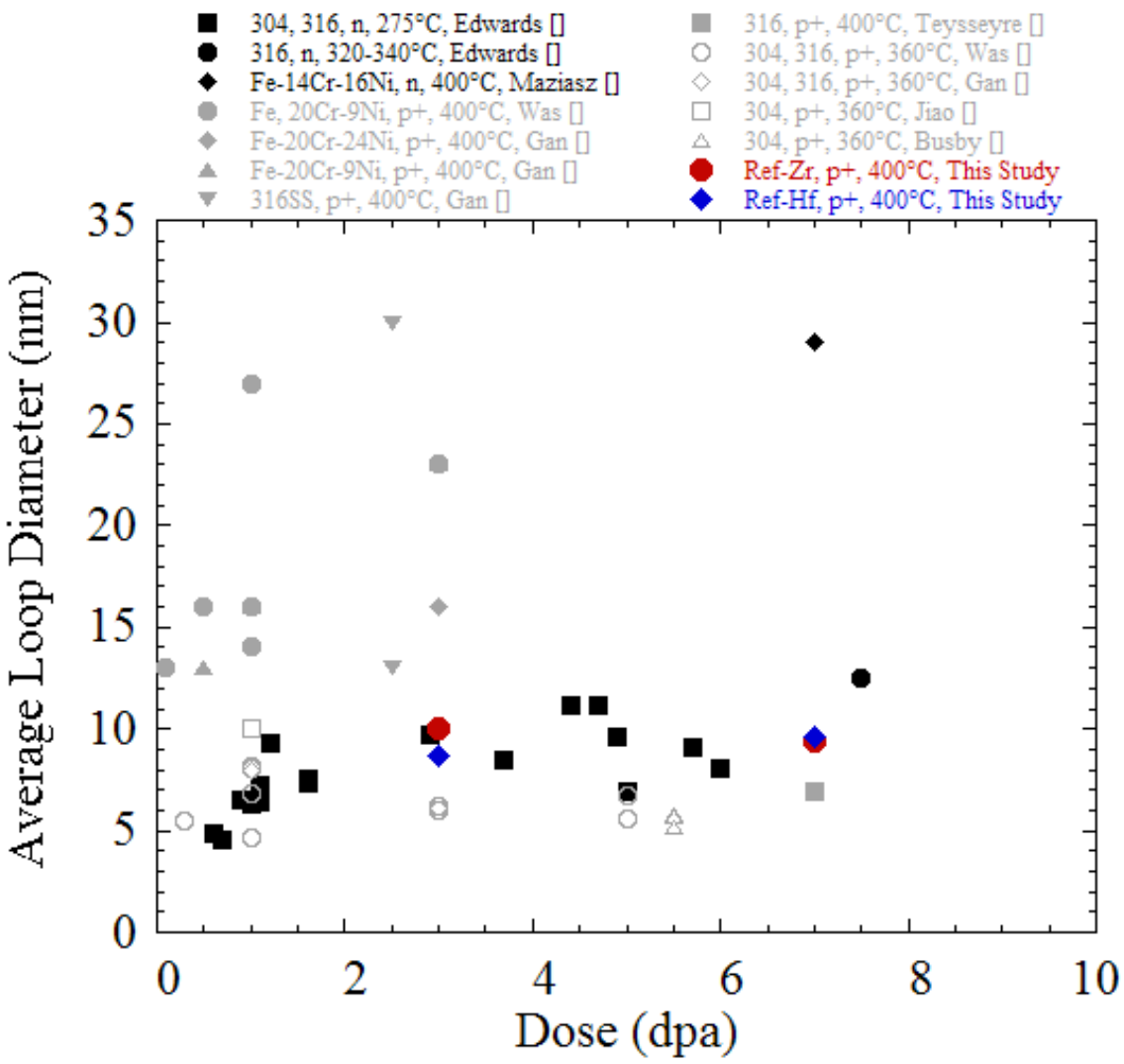

Figure 7.7 Average loop diameters for the reference alloys in this study compared to literature values for 316-type stainless steels irradiated with protons (grey symbols) and neutrons (black symbols) at temperatures of 275 – 400°C [36, 43-45, 91, 126, 127, 129-131].

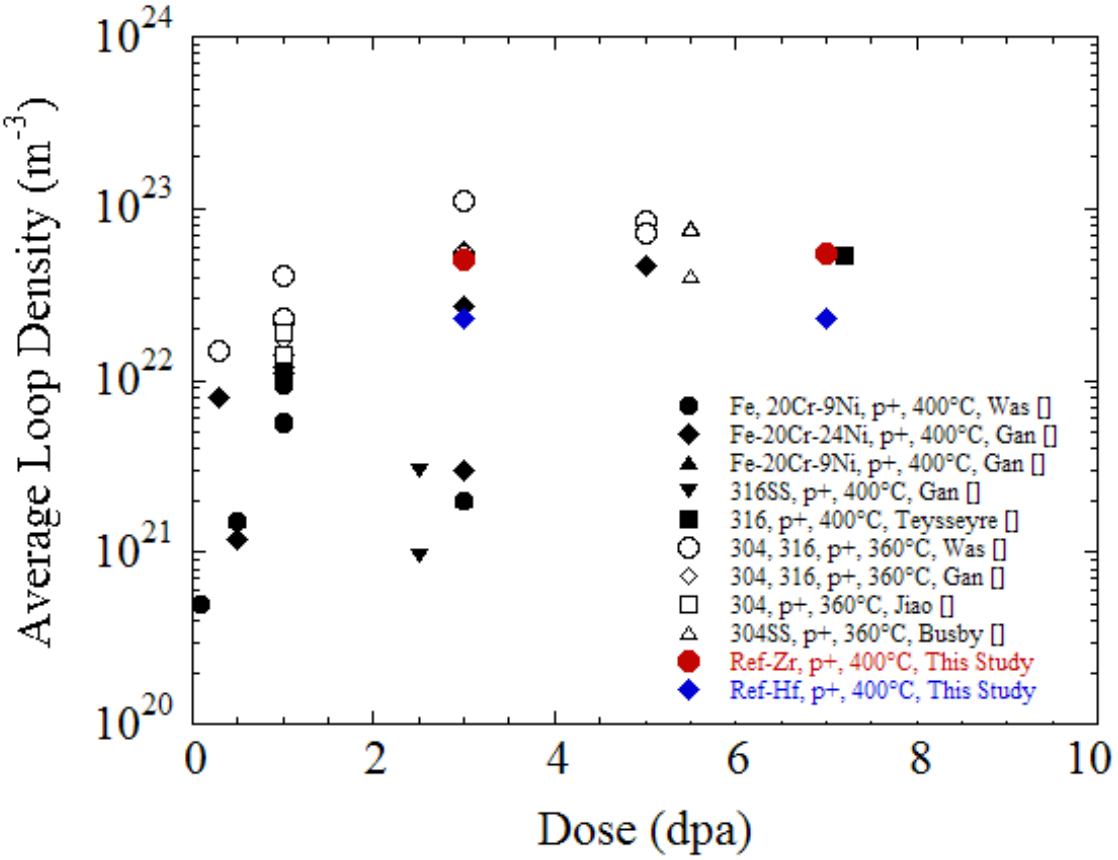

Figure 7.8 Average loop densities for the reference alloys in this study compared to literature values for 316-type stainless steels irradiated with protons at temperatures of 360°C and 400°C [43-45, 91, 126, 127].

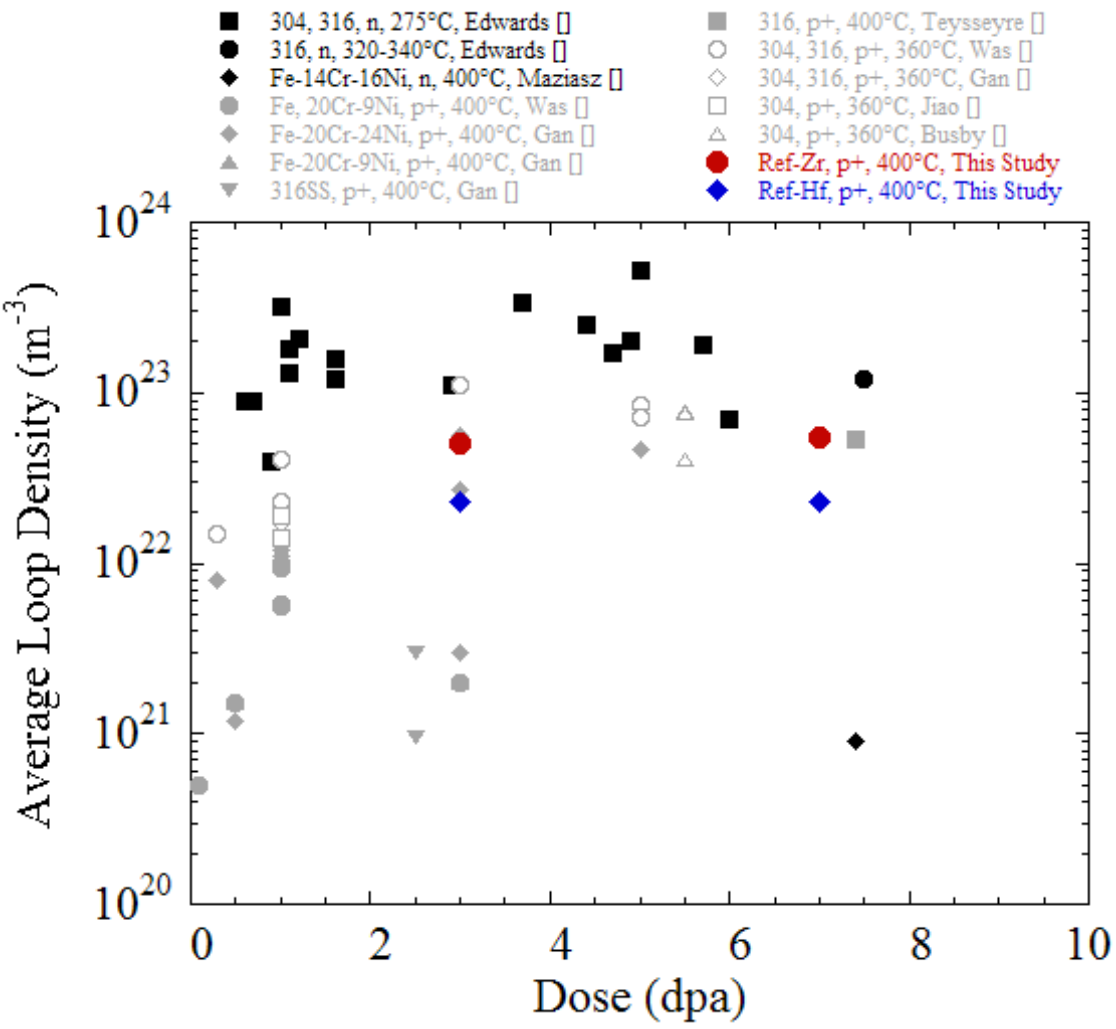

Figure 7.9 Average loop densities for the reference alloys in this study compared to literature values for 316-type stainless steels irradiated with protons (grey symbols) and neutrons (black symbols) at temperatures of 275 – 400°C [36, 43-45, 91, 126, 127, 129-131].

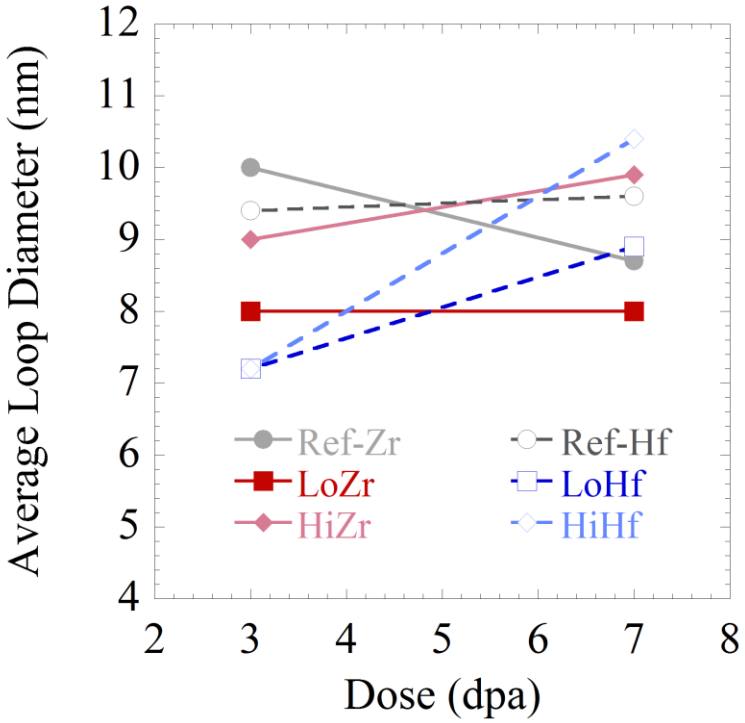

Figure 7.10 Average loop diameters for all alloys in this study, plotted vs. dose for 3 and 7 dpa at 400°C.

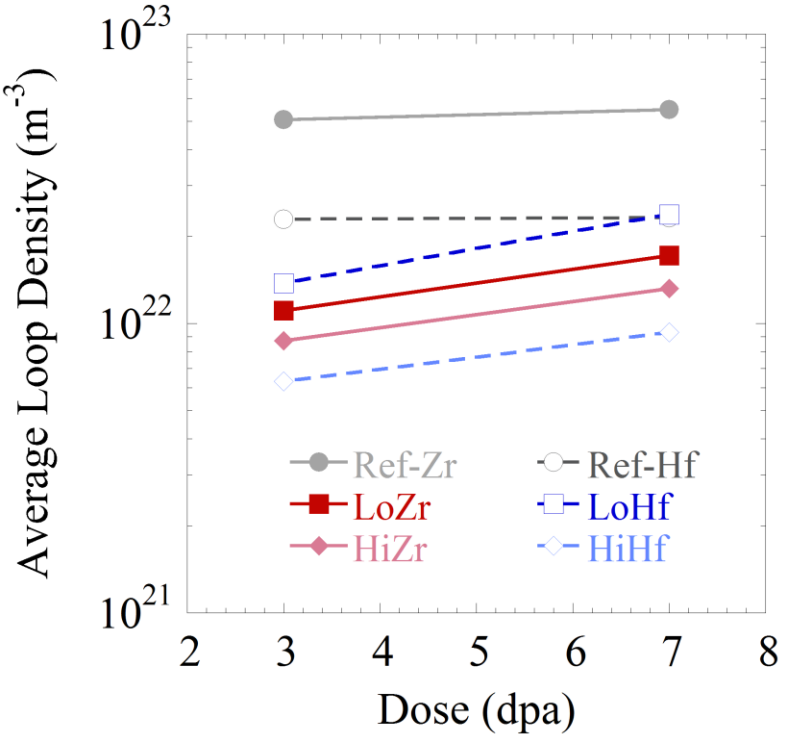

Figure 7.11 Average loop densities for all alloys in this study, plotted vs. dose for 3 and 7 dpa at 400°C.

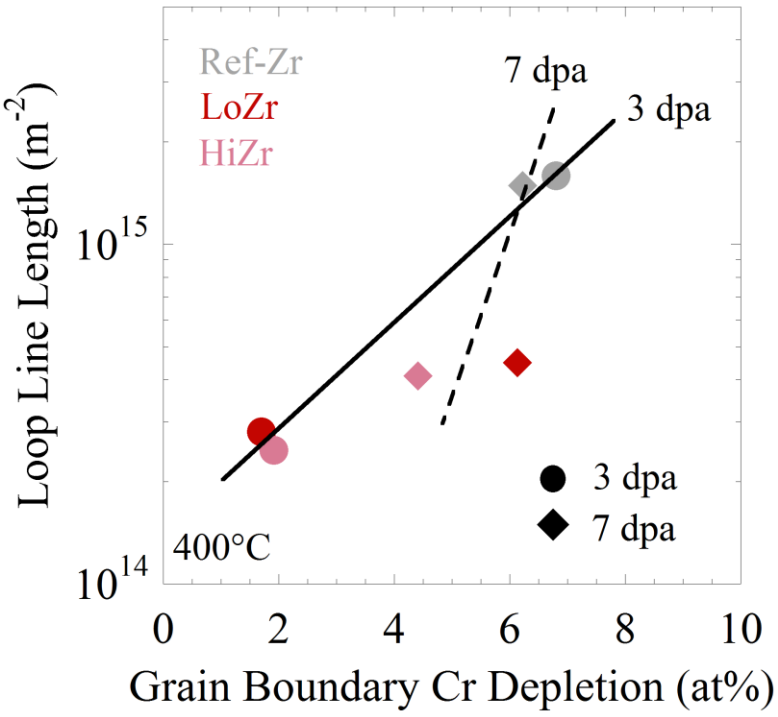

Figure 7.12 Loop line length as a function of grain boundary Cr depletion for the +Zr alloys at 3 and 7 dpa, 400°C.

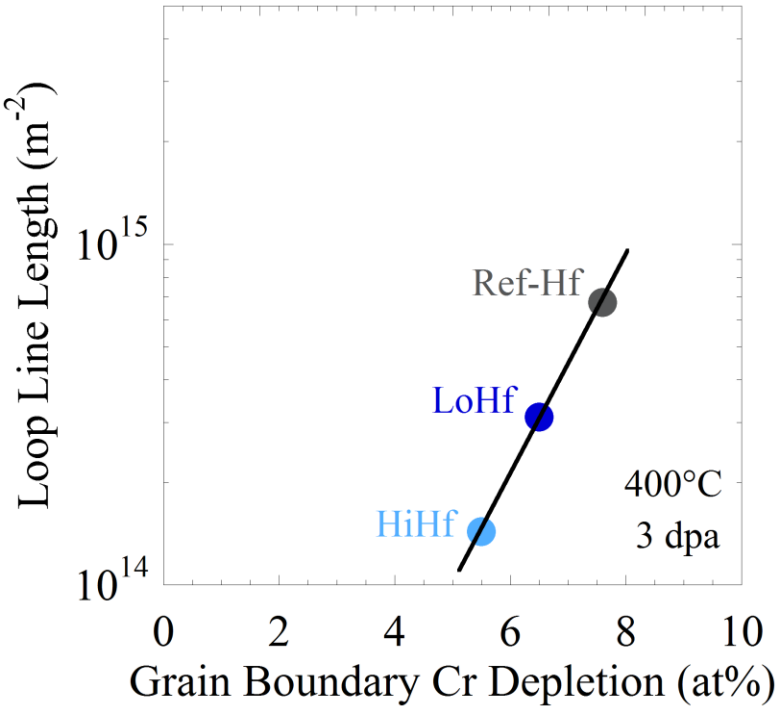

Figure 7.13 Loop line length as a function of grain boundary Cr depletion for the +Hf alloys at 3 and 7 dpa, 400°C.

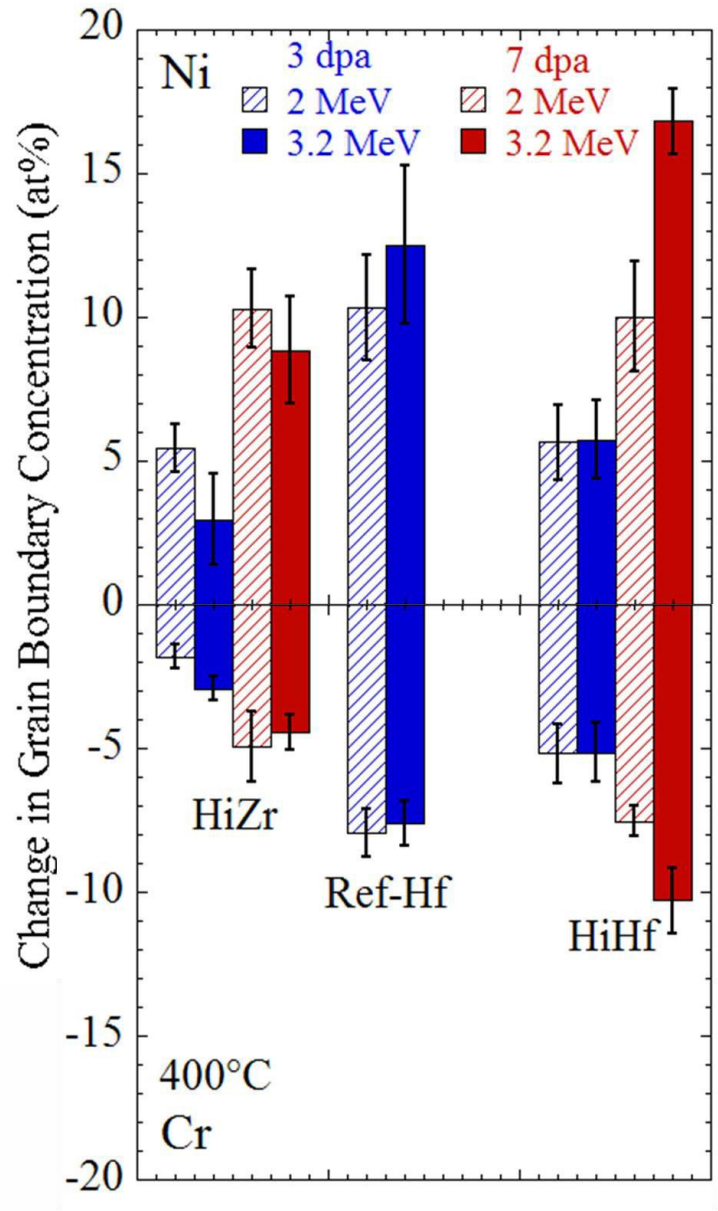

Figure 7.14 Measured changes in grain boundary Ni and Cr concentrations for the alloys HiZr, Ref-Hf, and HiHf at doses of 3 and 7 dpa, using either 2 MeV or 3.2 MeV protons. The comparison of Cr depletion between 2 MeV and 3.2 MeV irradiations shows that grain boundary segregation values are not affected by protons in this energy range.

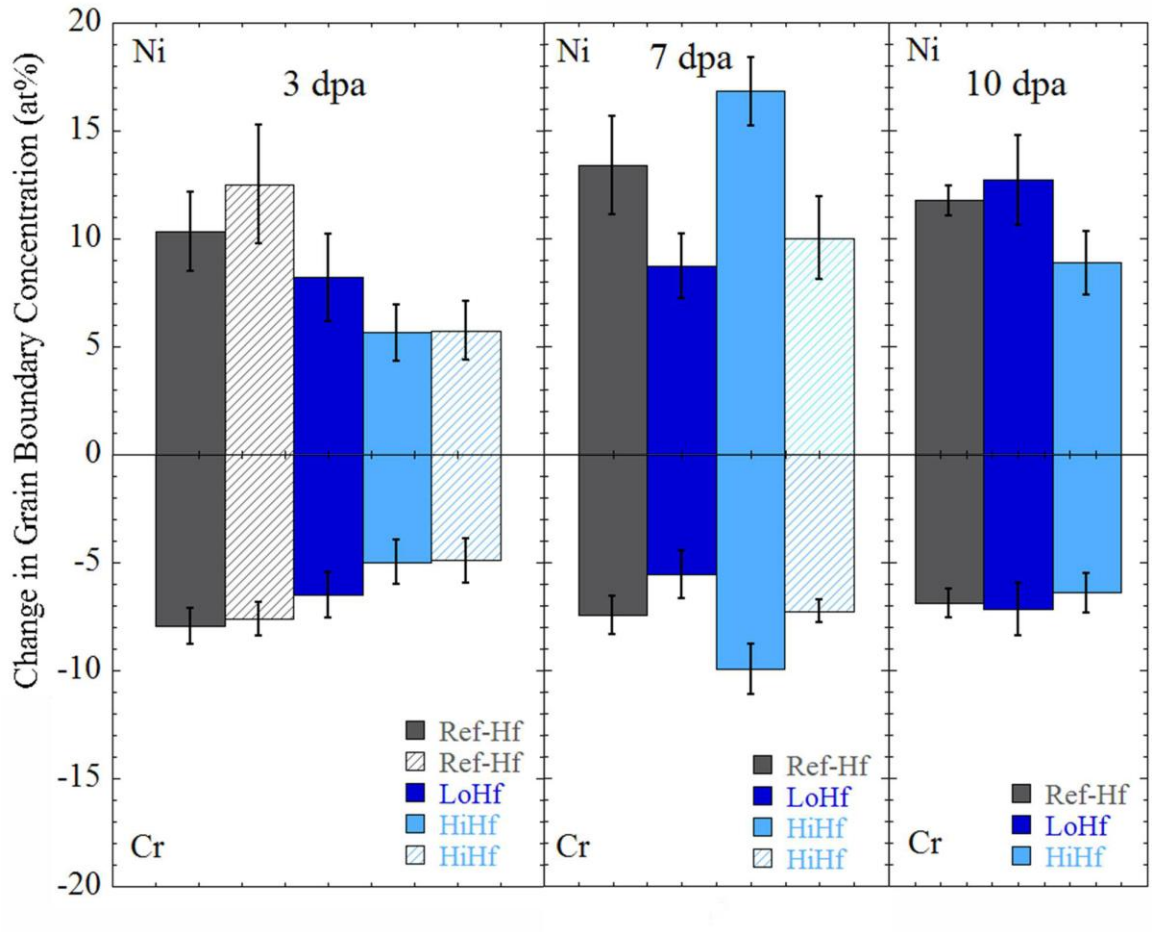

Figure 7.15 Change in grain boundary Cr and Ni concentration at 400°C to doses of 3, 7 and 10 dpa for all measurements for the +Hf alloys.

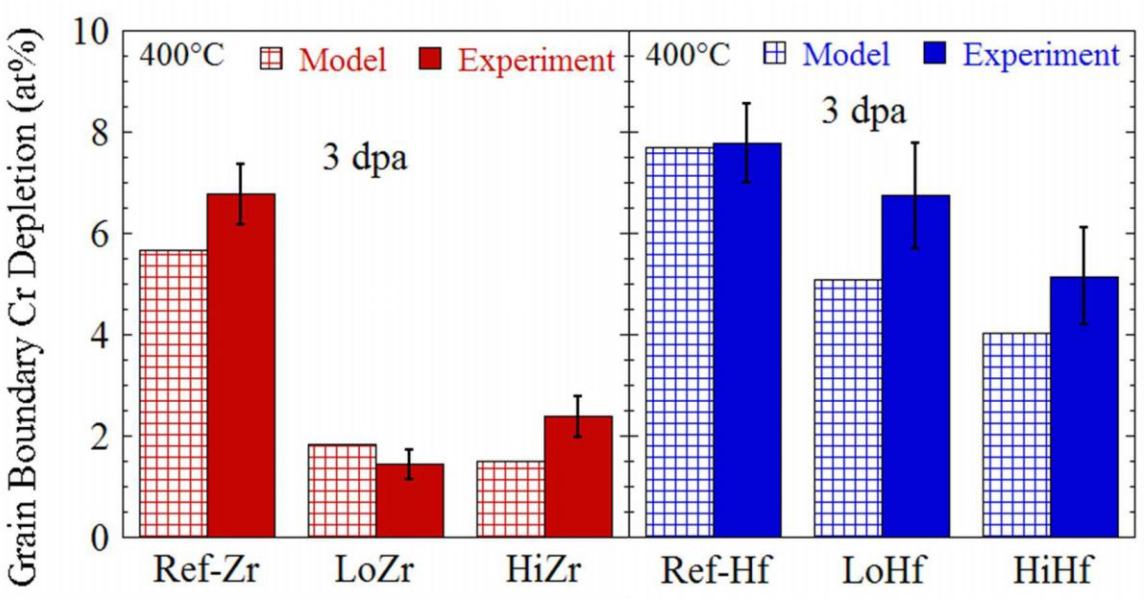

Figure 7.16 Comparison of MIK-T and measured values of GB Cr depletion for the +Zr and +Hf alloys irradiated at 400°C to 3 dpa.

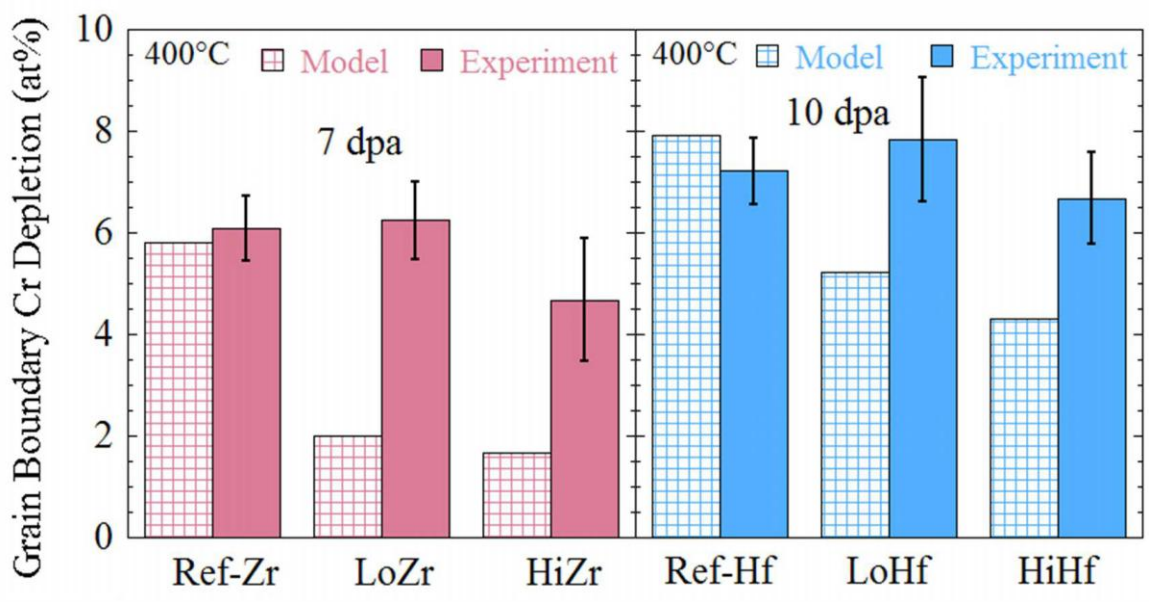

Figure 7.17 Comparison of MIK-T and measured values of GB Cr depletion for the +Zr and +Hf alloys irradiated at 400°C to 7 dpa.

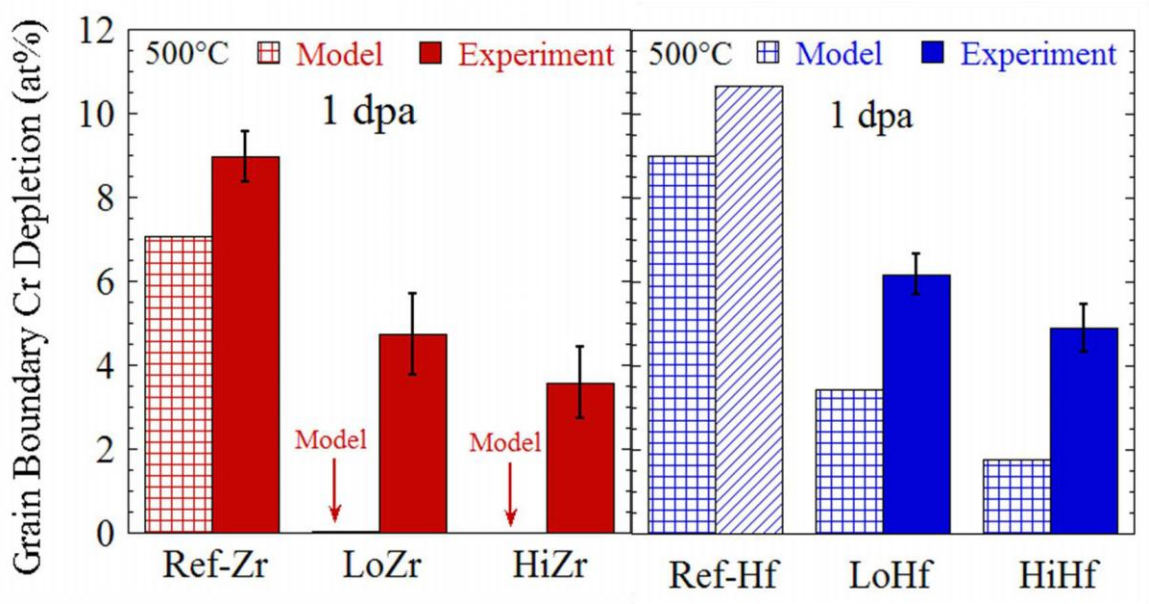

* Ref-Hf at 1 dpa was not measured. The value for Ref-Hf at 3 dpa serves as an estimate of the expected Cr depletion at 1 dpa.

Figure 7.18 Comparison of MIK-T and measured values of GB Cr depletion for the +Zr and +Hf alloys irradiated at 500°C to 1 dpa.

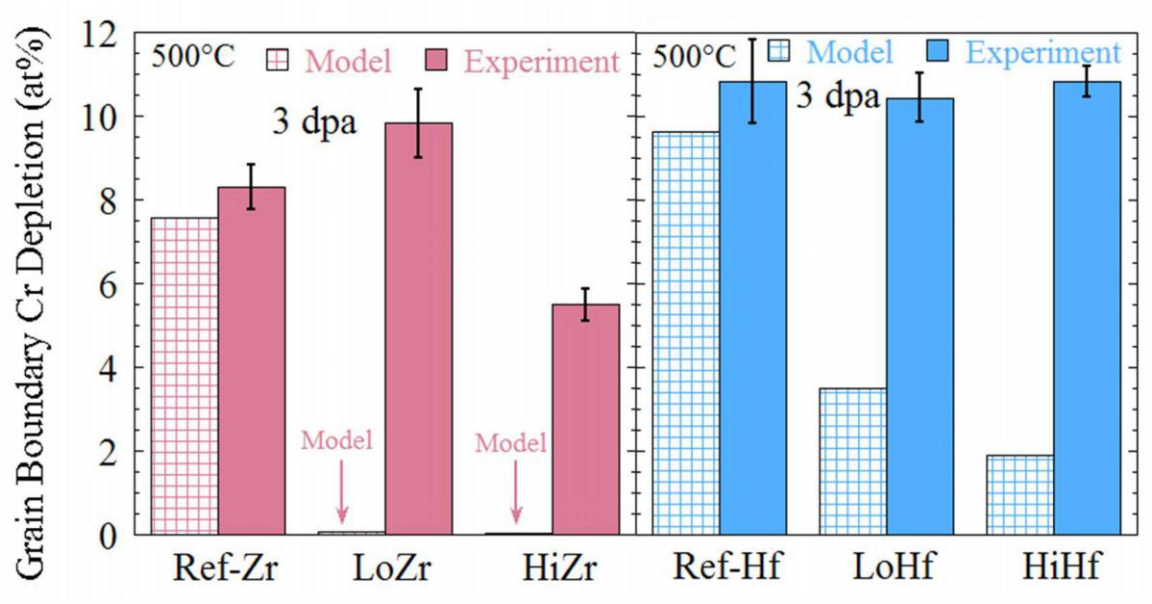

Figure 7.19 Comparison of MIK-T and measured values of GB Cr depletion for the +Zr and +Hf alloys irradiated at 500°C to 3 dpa.

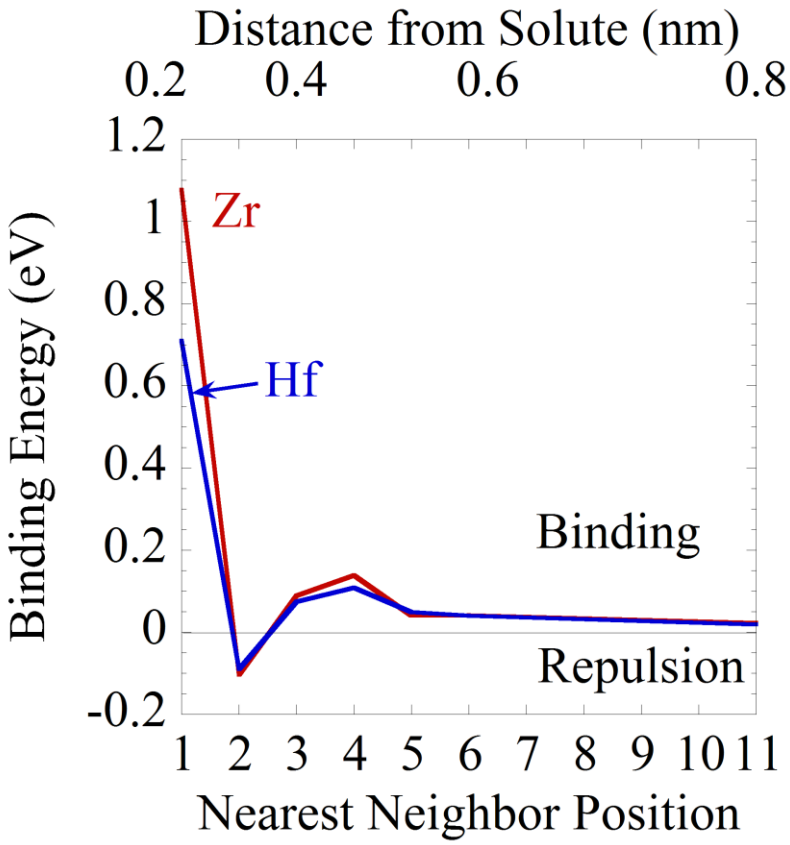

Figure 7.20 Binding energy as a function of nearest neighbor distance from the oversized solute. The top x-axis also includes the distance from the origin (oversized solute atom position), in nm.

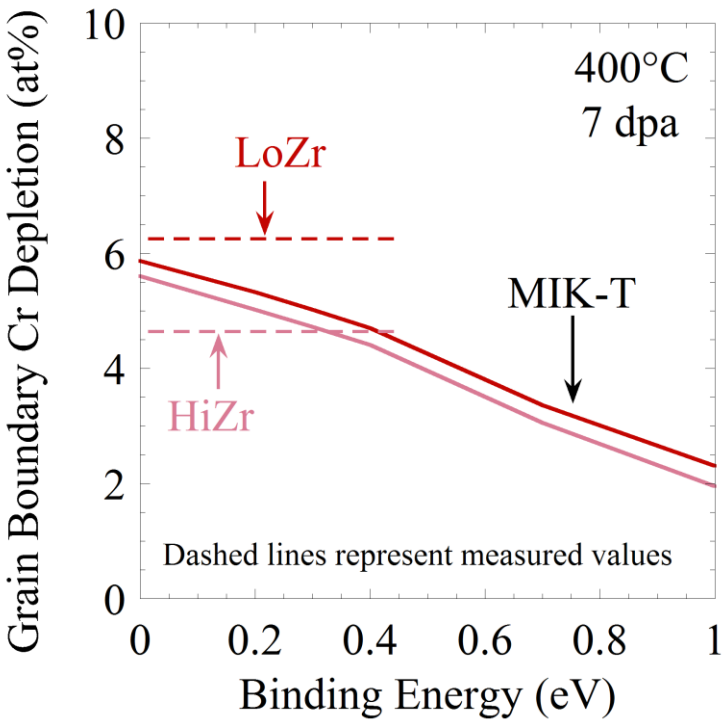

Figure 7.21 Amount of GB Cr depletion at 400°C for LoZr and HiZr at 7 dpa compared to the MIK-T model using a binding energy of 0 – 0.3 eV.

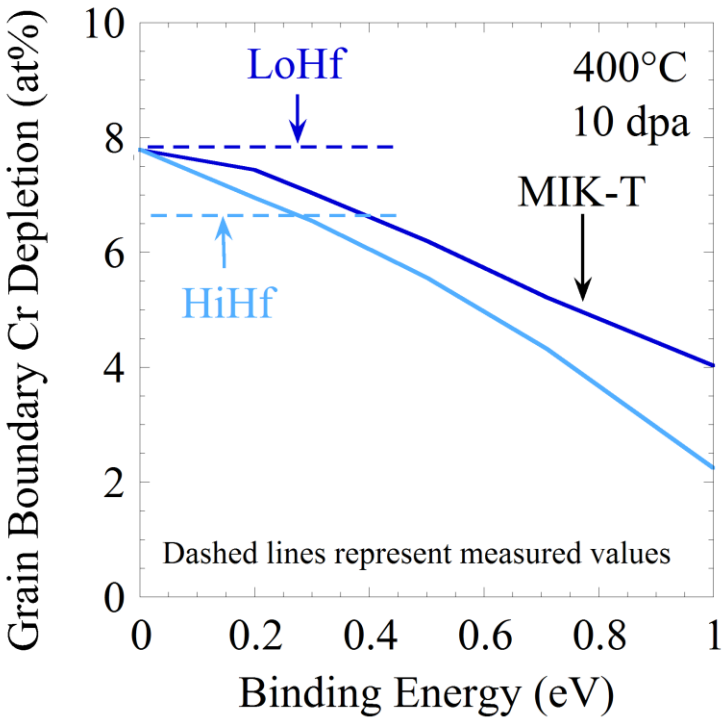

Figure 7.22 Amount of GB Cr depletion as a function of binding energy at 400°C for LoHf and HiHf at 10 dpa compared to the MIK-T model.

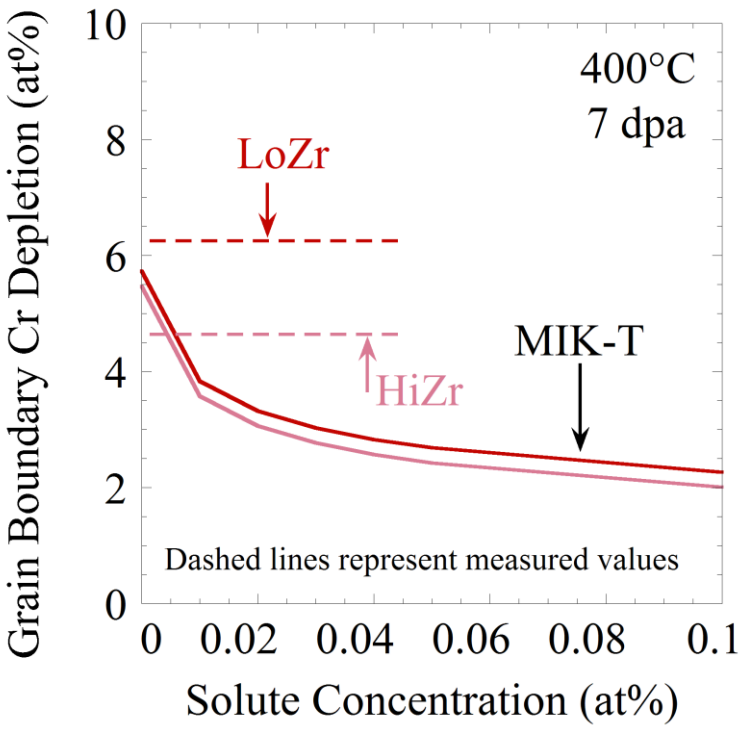

Figure 7.23 Amount of GB Cr depletion as a function of solute concentration in solution for LoZr and HiZr at 400°C, 7 dpa. Trapping and recombination radii are 0.5 nm, and binding energies are 1.08 eV for Zr and 0.71 eV for Hf.

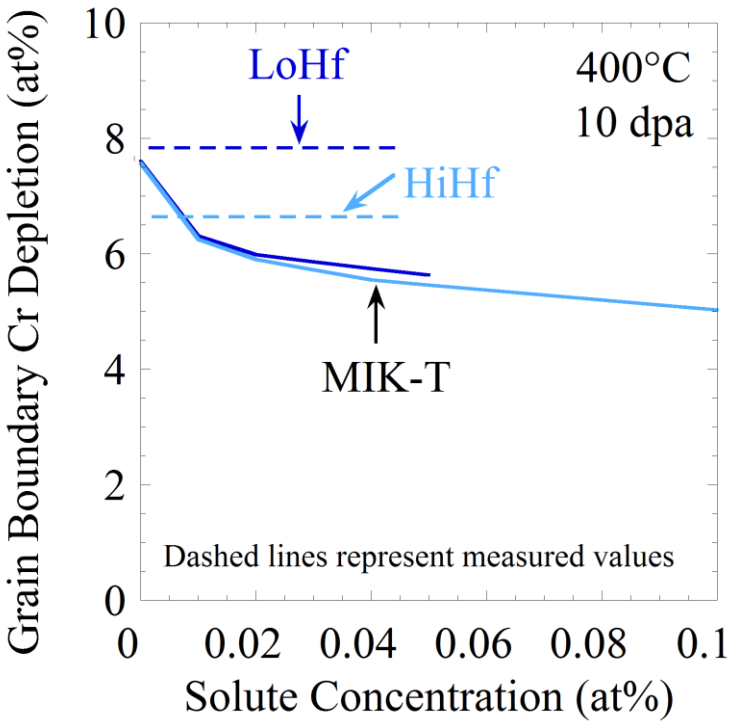

Figure 7.24 Amount of GB Cr depletion as a function of solute concentration in solution for LoHf and HiHf at 400°C, 10 dpa. Trapping and recombination radii are 0.5 nm, and binding energies are 1.08 eV for Zr and 0.71 eV for Hf.

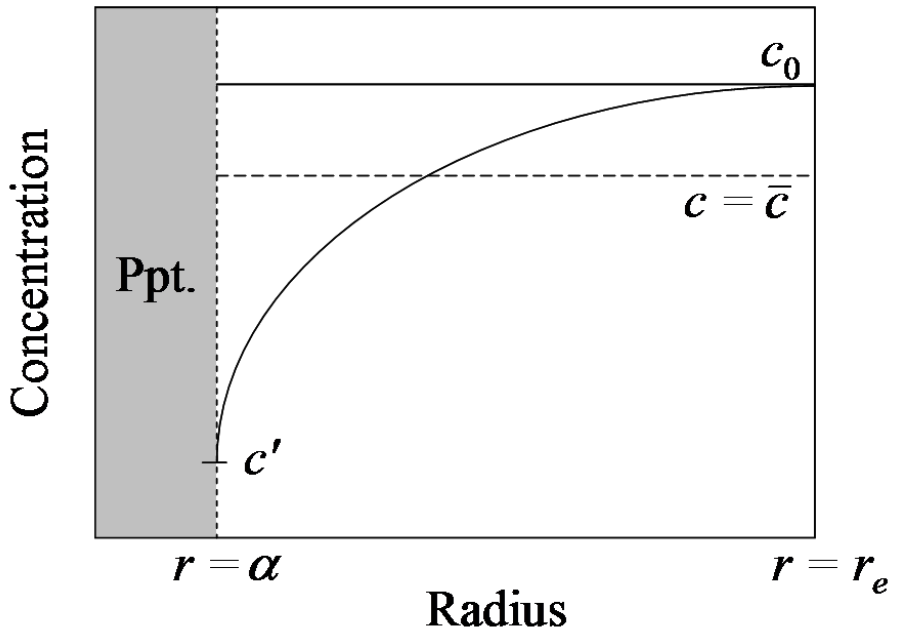

Figure 7.25 Drawing of the concentration of solute in a unit cell as a function of the radius of the unit cell, where $r = \alpha$ at the precipitate boundary and $r = r_e$ at the unit cell boundary, c_0 is the initial solute concentration in the unit cell, $\bar{c}$ is the average solute concentration as a function of irradiation time, and c' is the equilibrium solute concentration at the precipitate boundary.

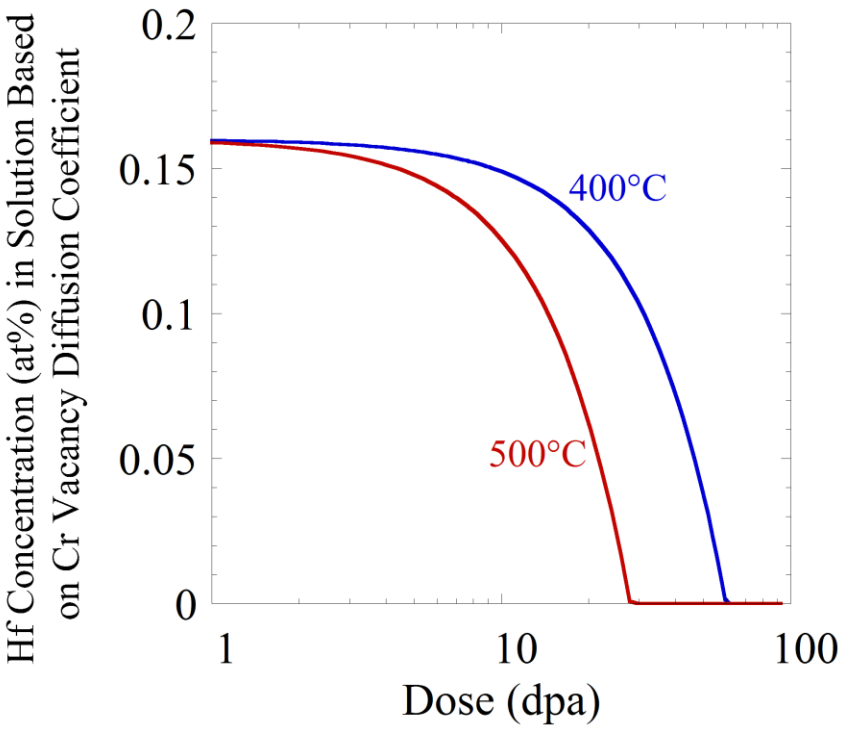

Figure 7.26 Hf concentrations remaining in the matrix as a function of irradiation dose at temperatures of 400°C and 500°C, based on the Cr vacancy diffusion coefficient, using a precipitation kinetics analysis developed by Shewmon [137].

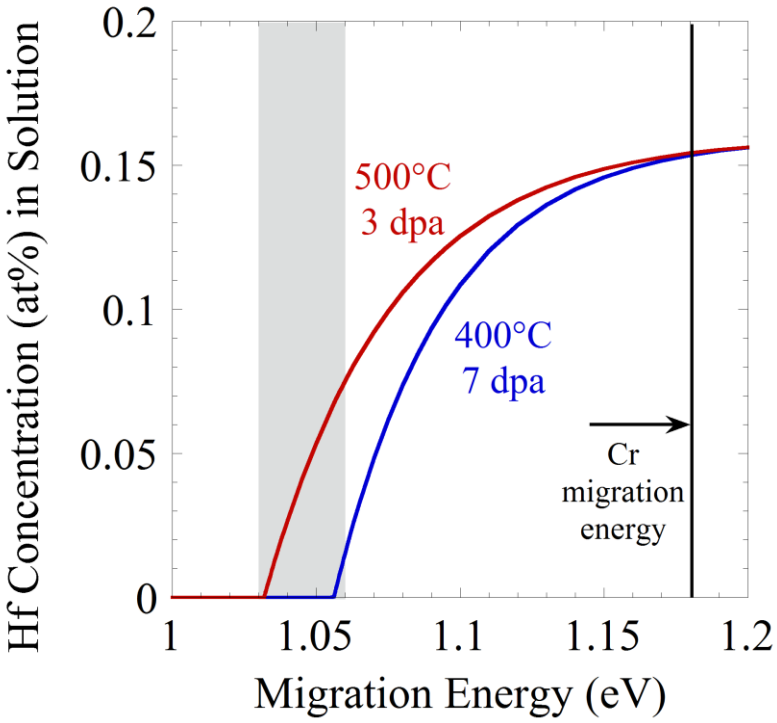

Figure 7.27 Hf concentration remaining in the matrix as a function of density at temperatures of 400°C and 500°C, based on the Cr vacancy diffusion coefficient, using a precipitation kinetics analysis developed by Shewmon [137]. The vertical line shows the reference value for the migration energy of 1.18 eV.

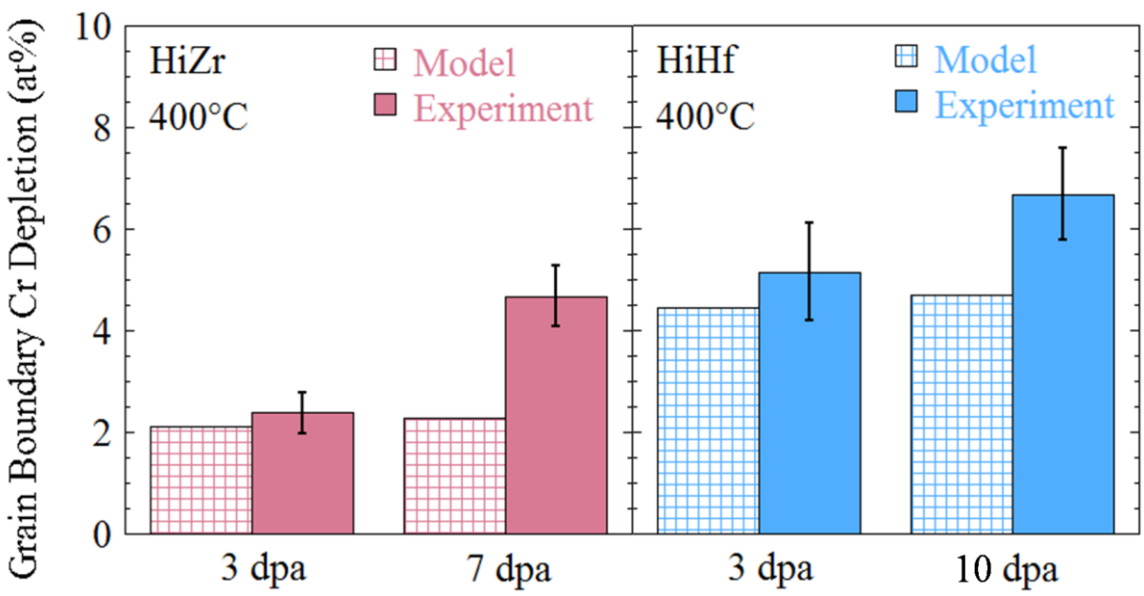

Figure 7.28 Comparison of MIK-T model and measured values of GB Cr depletion at 400°C for HiHZr and HiHf. Oversized solute concentrations for the MIK-T model are the estimated values prior to irradiation based on TEM imaging of ZrC and HfC precipitate microstructure, with 0.11 at% Zr for HiZr and 0.16 at% Hf for HiHf.

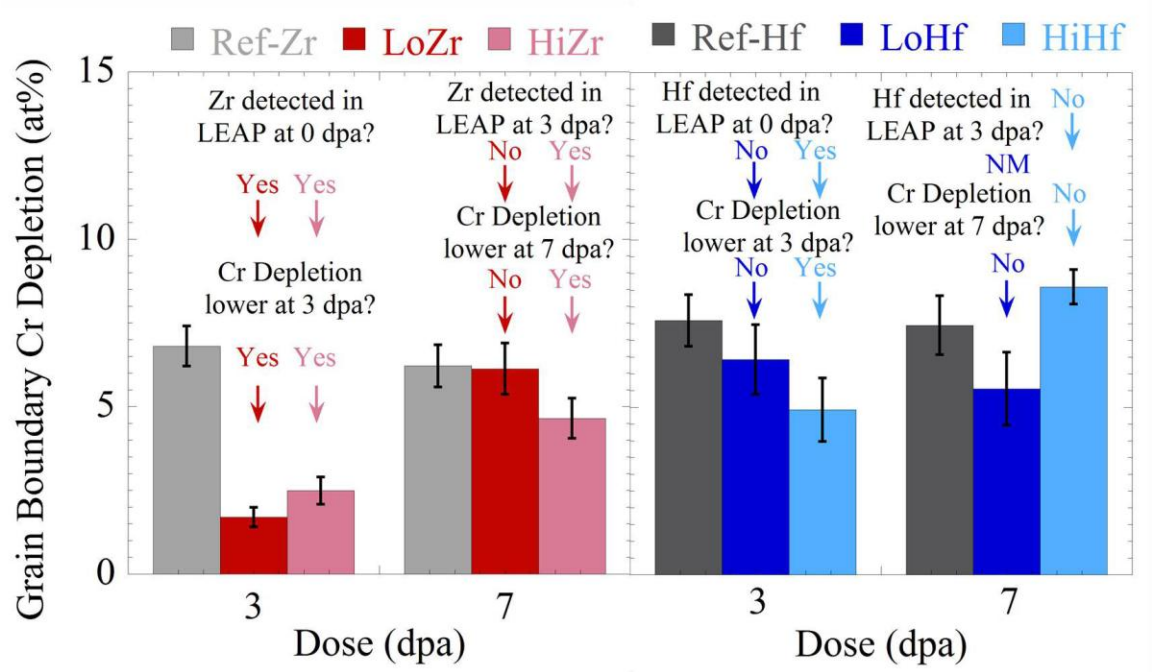

NM: Not Measured

Figure 7.29 Correlation of Cr depletion measurements and LEAP analysis, where for each irradiation condition, the detection of oversized solute in solution is consistent with the measured reduction of Cr depletion.

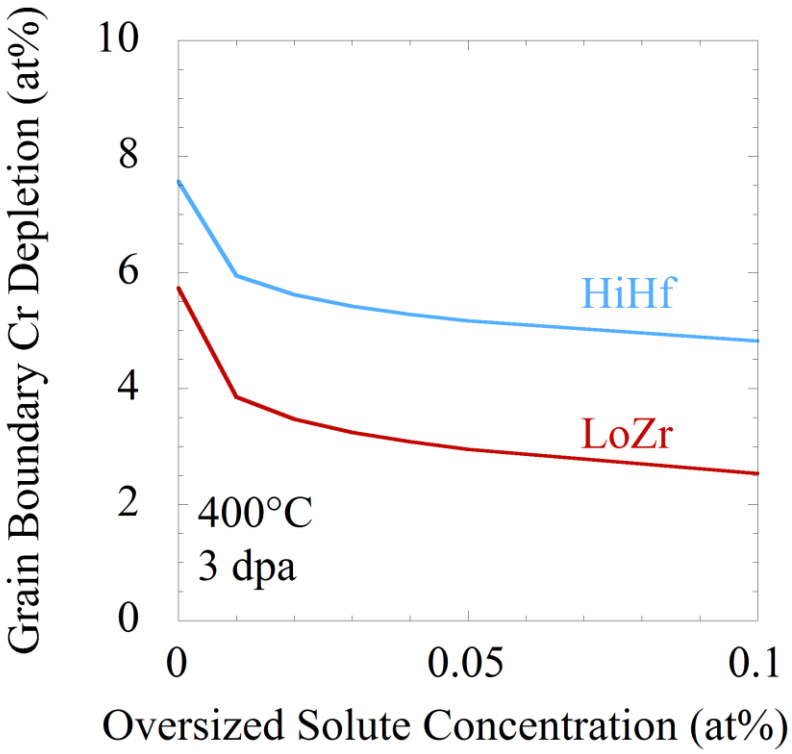

Figure 7.30 Grain boundary Cr depletion as a function of oversized solute concentration for LoZr and HiHf at 400°C, 3 dpa.

CHAPTER 8

CONCLUSIONS

The conclusions of this thesis are:

1. Enhanced point defect recombination, due to oversized solute atoms through a solute-vacancy trapping mechanism, is responsible for a reduction in grain boundary RIS of Cr and Ni. Model and measurements both show a significant reduction in Cr depletion after proton irradiation to temperatures of 400°C and 500°C.
2. Zr is observed to be more effective than Hf in reducing RIS because of the larger solute-vacancy binding energy for Zr. The measurements are consistent with first principle calculations of binding energy, and the MIK-T model agrees with RIS measurements in predicting greater effectiveness on RIS suppression by Zr compared to Hf.
3. Solute-vacancy binding energies for Zr and Hf are not just a function of the linear size factor, as proposed in the literature, but must include the electronic interactions with first nearest neighbor atoms.
4. The effect of oversized solutes in reducing RIS disappears by 7 dpa at 400°C and by 3 dpa at 500°C. Since the MIK-T model predicts continued suppression of RIS, the difference between model and experiment indicates a change in the irradiated microstructure as the cause for the loss of solute effectiveness on RIS.
5. Enhanced recombination through vacancy trapping is confirmed by the large differences in total loop line length between reference alloys and oversized solute alloys. Significant increases in loop line length with increasing dose in the

oversized solute alloys indicates a change in irradiated microstructure and also reveals a loss of solute effectiveness on loop microstructure.

6. Removal of solute from solution to precipitates is the most likely explanation for the loss of solute effectiveness on RIS. The mechanism is explained by solute diffusion through vacancies, resulting in precipitate growth. The MIK-T model shows that almost a complete loss of solute is necessary to explain the RIS results. LEAP measurements showing a loss of oversized solute in solution with increasing dose can explain the increases in grain boundary Cr depletion.

Future Work

Future work in this area may include some of the following approaches. First, to assess the mechanism for the loss oversized solute during irradiation, in situ TEM irradiation may be capable of observing the precipitate growth as it occurs with irradiation. However, other scientists [21, 23] have performed electron irradiation studies of oversized solute alloys without reporting a loss of solute effect on RIS, or the observation of precipitates in the microstructure. Therefore, one might use a combination of heavy ions and in situ TEM to simulate the large damage cascades of neutrons using Ar+ or Xe+ ions while still maintaining the capability of observing precipitate growth or other changes in the irradiated microstructure. Such work could be performed with a dual beam IVEM – tandem microscope.

One method for preventing the loss of solute effect on RIS would be to eliminate any formation of secondary phases with the oversized solute in order to keep as much of the solute in solution as possible. For Zr and Hf, this would mean the elimination of C in order to prevent the formation of carbides. Unfortunately, work by Ohnuki et al. [86] suggests that even with very low levels of C (<0.003 wt%), the formation of carbides still occurs. Perhaps the most important question to answer would be whether or not additional secondary phases, such as $ZrNi_5$ or $HfNi_5$ intermetallics would form in the

absence of C. With a low level of C, sufficient solute should remain in solution unless intermetallics also form. This could be assessed by the fabrication of very low C alloys and the post-irradiation examination of irradiated materials using XRD or other phase identification techniques in TEM.

Oversized solute elements include more than just Zr and Hf. A substantial body of work exists on Nb and Ti additions, and these solute additions do indeed seem to reduce the amount of void swelling and RIS. However, because of their low solute-vacancy binding energies, they may not have the same effect as solutes with much larger binding energies. Nevertheless, the issue is binding energy vs. solubility. Additions of Y and Sc, for example, may be expected to have even larger binding energies because of their larger size relative to Zr and Hf. Fabrication of alloys with these solute additions was done in a recent study [83], but the alloys showed high degrees of cracking, especially during cold-rolling. These alloys were discarded due to significant issues with fabrication which prevented them from being in a usable condition. Therefore, one must choose solute atoms with a large binding energy but also with sufficient solubility in the stainless steel. Since the MIK-T model predicts that only a small amount of solute will have a large effect on RIS, the addition of the solute may require only low concentrations in order to see a significant benefit in reducing radiation damage, so long as that solute remains in solution and does not form secondary phases like carbides or intermetallics.

Determining the types of solute atoms on which to focus might first start with the examination of their solute-vacancy binding energies using first principles methods. One may employ a more sophisticated technique at determining binding energy by using a more realistic system compared to the fcc Fe used in this study. The incorporation of Cr and Ni, or even the study of the change in binding energy with changes in nearest neighbor atoms (i.e. solute poisoning with Si), may give significant insight into more realistic calculations for the binding energy. Also, binding energy studies of other oversized solute atom types, including such exotic solutes such as Y, Sc, or Ta, may provide further guidance into the choice of the best solute type for mitigating radiation damage.

Finally, additional work on RIS modeling may improve the understanding of oversized solute effects on RIS. The MIK-T model does not account for the loss of

solute effectiveness on RIS, and this could be done by assuming that the solute concentration in solution decreases with increasing dose. The loss of solute could be some simple function of dose, or it could incorporate a more complex diffusion analysis that accounts for diffusivity based on alloy concentration, oversized solute concentration, solute type and temperature, to name a few of the important parameters. Also, some of the results from this study have suggested that Si may be affecting RIS behavior in the alloys, and there is plenty of room for expanding the MIK model to account for changes in diffusivity of the major elements (Fe, Cr, Ni) based on the minor element additions. Such changes to the MIK model would aid in understanding RIS not only for the oversized solute alloys but for standard stainless steels, also.

APPENDICES

APPENDIX A

ACTIVITY CALCULATIONS

The following appendix outlines the radioactivity that is created from the irradiation of a standard 316-type stainless steel. The radioactivity is created when a proton interacts with the nucleus of an atom and creates a new isotope. There are many different types of reactions that can take place with protons, but this document is going to focus on the most probable reaction that can occur, namely the (p^+,n) reaction. Since this reaction usually occurs with a certain minimum energy threshold, only those reactions occurring below the energy of the incoming proton will be considered. The (p^+, He) reaction was also considered, but for all of the naturally-occurring isotopes in this study, either the reaction energy threshold was above the proton energies in consideration, or there simply was no cross section data available at the relevant energies.

The standard 316SS being considered is, in atom percent, 66Fe-18Cr-13Ni-2Mo-1Mn. These radioactivity calculations should be viewed with some caution because there are many reaction types which are not being taken into account. Moreover, while impurity additions of Si, P, C or any other low-Z elements will not create any long-lived radioisotopes, other substantial impurity additions, such as Ti, V, Co, or Cu may need to be taken into account, as necessary. No assessments of those are made here, however. Nevertheless, considering the proton-induced reactions discussed below will give a general idea of the amount of radioactivity in a particular sample. The calculation of activity for a particular isotope can be described as follows:

$$RadioactiveAtoms(\#) = Irr.Depth(cm) \cdot Irr.Area\left(cm^2\right) \cdot Fluence\left(\frac{\#}{cm^2}\right) \cdot IsotopeAtomDensity\left(\frac{at}{cm^3}\right) \cdot CrossSection\left(cm^2\right) \quad \text{(A.1)}$$

The irradiation depth refers to the total depth to which the proton penetrates into the material. The fluence is the total number of protons to hit the target, while the irradiation area describes the total area exposed and the atom density gives a measure of how many atoms of a particular isotope exist within the volume of material that is exposed. The cross section provides a probability that a reaction between the parent isotope and proton will occur in order to produce new daughter isotope. All cross section data was obtained using the database for Experimental Nuclear Reaction Data [141].

Isotopes shown in table A.1 are considered in the radioactivity calculations for 2, 3 and 3.2 MeV protons. These five parent isotopes, listed in the first column, represent only a fraction of the naturally-occurring isotopes for Fe, Cr, Ni, Mn and Mo. Consideration of the other isotopes is not necessary because the half-life of the daughter isotope is very short (a few hours or less) or the daughter isotope is stable or the energy threshold is too high for a (p^+,n) reaction to occur. Be aware that dose calculations assume a minimum elapsed time of 100 hours from irradiation. When considering activity of less than 100 hours, the isotopes of Cu^{61} and Cu^{64} should be considered because they add considerable activity to the irradiated samples at short times. However, with half-lives of 3.35 and 12.7 hours, respectively, they will no longer exist in significant quantities after 100 hours from the irradiation and will therefore be ignored in this analysis.

It should be noted that the reaction cross sections in table A.1 were evaluated at the energy of the incoming proton. The cross section databases, however, showed a decreasing reaction cross section with decreasing energy. So when evaluating the reaction rate for a given volume based on the incoming ion energy and neglecting any decrease in reaction rate as the ion loses energy, it would be safe to assume that these calculations will over-estimate the amount of radioactivity produced.

By assuming an irradiation area of 0.2 cm^2 for each specimen, an average alloy atomic mass of 56 g/mol, and a density of 7.89 g/cm^3, the proton fluence for a 3 dpa

irradiation can be calculated by the following equation, which is shown with the average displacement rate for a 2-MeV irradiation:

$$Fluence = \frac{\frac{7.89\frac{g}{cm^3} * 6.022\times10^{23}\frac{at}{mol}}{56\frac{g}{mol}}}{8.0\times10^{-5}\frac{disp.}{\AA\cdot ion} * 10^{8}\frac{\AA}{cm}} * 3dpa \quad \text{(A.2)}$$

Irradiation parameters at the relevant proton energies are shown in table A.2. All displacement rates were calculated using the Stopping and Range of Ions in Matter [93] given a displacement energy average of 40 eV. The number of radioactive atoms for each isotope in a specimen is calculated according to equation A.1 and shown in table A.3. The calculation must account for the activation volume, including irradiation depth and area, the atom fraction in the alloy and the fraction of that isotope that is naturally occurring. Calculated values are shown for 2, 3, and 3.2 MeV irradiations.

The number of radioactive atoms is converted to activity using the equation,

$$A = \lambda N \quad \text{(A.3)}$$

where λ is the decay constant for the isotope and N is the number of radioactive atoms. In order to calculate the activity after a certain amount of elapsed time, Eq. (3) becomes,

$$A = \lambda N * e^{-\lambda t} \quad \text{(A.4)}$$

where t is the amount of time that has elapsed since the irradiation. The decay constant is given by λ and t represents the elapsed time since irradiation. For the purpose of these calculations, it is assumed that all activity was induced instantaneously rather than over the course of an irradiation, which can itself take many hours. Activity calculations, provided in μCi, are shown in table A.4 for all three proton energies. The activity is calculated after a decay time of both 100 hours and 100 days.

There are two measurements against which these calculations can be benchmarked. Irradiations have been performed for a standard 316SS at proton energies of 3.2 MeV, and measurements of beta and gamma radiation have been taken. The first benchmark is of gamma radiation, which is essentially equivalent to the total activity. Measurements of samples irradiated to 3 dpa detected the isotopes Mn-54, Co-57 and Co-58. The total initial activity was back-calculated to be about 2.5 μCi. Considering that a

3.2 MeV irradiation after 100 hours was calculated to have 2.69 μCi, there is little difference between calculated and measured, and the measured results provide an accurate benchmark of the calculations shown here. The larger value for the calculation reflects, as previously mentioned, the assumption that the cross section remains the same at any energy. Of course, the reaction cross section decreases with decreasing energy and ceases completely once the proton energy has dropped below the reaction energy threshold.

In summary, 3.2 MeV irradiations will generate the most activity, in large part because of the production of Co-58, which does not occur for the 2 or 3 MeV irradiations. Irradiations at 2 MeV will produce much less activity because neither Mn-54 nor Co-58 is produced, the proton fluence is lower due to a higher displacement rate at 2 MeV, and the total volume of material activated is less due to a shorter penetration depth of the protons. Table A.5 gives an overview of the calculated activity for a standard 316SS after a 3-dpa irradiation. These values represent an upper limit on the amount of activity created from irradiation and, especially in the case of 3.2 MeV irradiations, almost certainly overestimate the actual radioactivity.

Table A.1 Production of relevant isotopes in the (p^+,n) reaction

	Reaction			Cross Section (mb)		
Parent Isotope	(p,n) Energy Threshold (MeV)	Daughter	Half-life	2 MeV	3 MeV	3.2 MeV
Ni-61	2.49	Cu-61	3.35 h	N/A	9.5	15.5
Ni-64	2.52	Cu-64	12.7 h	N/A	13.9	27.3
Cr-53	1.39	Mn-53	3.7E6 y	5	42	57
Cr-54	2.21	Mn-54	312.1 d	N/A	30	43
Mn-55	1.03	Fe-55	2.73 y	4.5	60.5	62
Fe-57	1.65	Co-57	271.8 d	0.9	12.4	33
Fe-58	3.15	Co-58	70.88 d	N/A	N/A	15.8

Table A.2 Irradiation parameters in calculating activity

	Irradiation Depth (cm)	Displacement Rate (disp./Å/ion)	Proton Fluence (p^+/cm^2)
2 MeV	2.1E-03	8.0E-05	3.18E+19
3 MeV	3.8E-03	5.6E-05	4.55E+19
3.2 MeV	4.3E-03	5.3E-05	4.80E+19

Table A.3 Production of radioactivity through the (p^+,n) reaction after 3 dpa

Parent Isotope	Daughter Isotope	Atom Fraction	Alloy Atom Density (atoms/cm^3)	Isotope Fraction	Isotope Density (atoms/cm^3)	Radioactive Atoms per Sample		
						2 MeV	3 MeV	3.2 MeV
Ni-61	Cu-61	0.13	8.48E+22	0.011399	1.26E+20	0.00E+00	4.13E+10	8.04E+10
Ni-64	Cu-64	0.13	8.48E+22	0.009256	1.02E+20	0.00E+00	4.90E+10	1.15E+11
Cr-53	Mn-53	0.18	8.48E+22	0.09501	1.45E+21	9.68E+10	2.10E+12	3.41E+12
Cr-54	Mn-54	0.18	8.48E+22	0.02365	3.61E+20	0.00E+00	3.74E+11	6.41E+11
Mn-55	Fe-55	0.01	8.48E+22	1.0	8.48E+20	5.10E+10	1.77E+12	2.17E+12
Fe-57	Co-57	0.66	8.48E+22	0.02119	1.19E+21	1.43E+10	5.08E+11	1.62E+12
Fe-58	Co-58	0.66	8.48E+22	0.00282	1.58E+20	0.00E+00	0.00E+00	1.03E+11

Table A.4 Post-irradiation radioactivity for 2, 3, and 3.2 MeV protons after 3 dpa

		Activity (μCi)					
		2 MeV		3 MeV		3.2 MeV	
Isotope	Half-life	100 hours	100 days	100 hours	100 days	100 hours	100 days
Cu-61	3.35 h	0.00E+00	0.00E+00	6.62E-08	0.00E+00	1.29E-07	0.00E+00
Cu-64	12.7 h	0.00E+00	0.00E+00	8.55E-02	2.60E-56	2.01E-01	6.10E-56
Mn-53	3.7E6 y	1.55E-08	1.55E-08	3.38E-07	3.38E-07	5.48E-07	5.48E-07
Mn-54	312.1 d	0.00E+00	0.00E+00	2.57E-01	2.08E-01	4.41E-01	3.57E-01
Fe-55	2.73 y	1.11E-02	1.03E-02	3.84E-01	3.60E-01	4.71E-01	4.41E-01
Co-57	271.8 d	1.13E-02	8.81E-03	4.01E-01	3.14E-01	1.28E+00	9.99E-01
Co-58	70.88 d	0.00E+00	0.00E+00	0.00E+00	0.00E+00	3.02E-01	1.18E-01
Total		2.23E-02	1.92E-02	1.13E+00	8.81E-01	2.69E+00	1.91E+00

Table A.5 Summary of sample activity after 2, 3, and 3.2 MeV proton irradiation

	Activity (μCi)		
Decay Time	2 MeV	3 MeV	3.2 MeV
t = 100 h	0.02	1.13	2.68
t = 100 d	0.02	0.88	1.91

APPENDIX B

LEAP SAMPLE FABRICATION

The following document outlines the steps take to fabricate specimens suitable for analysis in the local electrode atom probe (LEAP) at Oak Ridge National Laboratory. The procedure goes step by step through the preparation of a single specimen from an irradiated TEM disc using a focused ion beam (FIB) employing the lift-out method. This procedure does not necessarily describe the optimum steps that should be used, nor does it a describe a process that always produced samples with a functional data set, where a functional data set is one that contains at least 1 million data points (atoms). But some specimens prepared according to the steps outlined here did yield useful data sets for analysis. For some steps, recommendations are given as to how the sample preparation could have been improved.

A FIB is a dual-beam electron microscope. The microscope couples an electron source with a secondary electron detector. In addition, there is typically a Ga^+ beam that is used for high-precision milling of the specimen for a wide variety of sample fabrication and preparation techniques. In the images shown below, some pictures were taken using the electron source while others used the Ga^+ beam for imaging. The primary drawback from imaging with the Ga^+ source is that each scan of the beam introduces some damage into the sample, so generally imaging must be limited and performed with as few scans as possible. Figure B.1 shows the first steps at preparing an area for the creation of a sample post. After performing the necessary microscope alignments and eucentric height adjustments for the specimen, the sample stage was tilted to +52° in preparation for milling work in the Ga^+ beam. In Figure B.1(a) a suitable area was selected in which analysis would be performed. This could be any area which is featureless or,

alternatively, contains a key feature for the desired analysis. In Figure B.1(b), a thin layer of Pt was deposited on the specimen surface using a 15 µm x 3 µm pattern with a layer depth of 1000 nm and a gun current of 0.3 nA.

Figure B.1(c) shows a saved pattern that was created specifically for this technique. The purpose of the pattern was to cut the edges and underneath the sample on 3 sides. The current was changed to 7 nA for this cutting pattern because a great deal of material must be milled away, and lower currents would take a prohibitively long time. The end result was a sample post, with rough edges, particularly on the top edge of the post as shown in Figure B.1(d).

At this point the sample stage was then tilted to –10° and a cutting pattern was prepared with dimensions of 15 µm x 750 nm with a depth of 7 µm using a cutting current of 7 nA. Figure B.1(e) shows the sample post after the cutting process. There are two critical things that should be observed after this cutting process. First, the surface on the top edge of the post should be smooth; this is an indication that the sample has been cut from underneath – not cutting at too great a depth so as to miss cutting out the post, and not starting too high so as to mill away the post. Second, the left edge of the post should have a clear line signifying that the post is completely free on three sides, like a cantilevered beam. Figure B.1(f) is the same view but zoomed out slightly to show the post in its entirety, including the milling damage on the sides from the cutting process.

The sample stage was then rotated counterclockwise 90° and tilted to a 0° position. A compucentric rotation of –90° is recommended as it keeps the post in roughly the same position relative to visible space. This was the start of a time-consuming process requiring patience. The Kleindieck probe was affixed with a tungsten wire that had been electropolished to a sharp tip. This wire was rotated into position directly above the sample post and slowly lowered onto the surface of the sample post. During the rotation process, the scan rate time on the e^- beam was lowered to 50 ns to enable quick scanning to view the tungsten wire as it was rotated into the beam path of the microscope. Once the tungsten wire was somewhat close to the sample stage, the stage was tilted to 30°. It is important to note here that if the tungsten wire was too close to the objective lens, the wire would hit the lens during the tilting process, which is damaging to the lens and microscope in general. So the wire had to be lowered

sufficiently that it wouldn't hit the lens while at the same time preventing the wire tip from hitting the stage, as this would have bent and destroyed the tungsten wire tip onto which the sample post was going to be affixed.

Figure B.2(a) shows an image in the Ga^+ beam of the tungsten wire as it was being lowered into position. The current was switched to 0.3 nA when viewing with the Ga^+ beam now; otherwise, the tungsten wire was liable to be milled away during the final process of lowering the wire onto the sample post, which could take considerable time. Also, in re-centering the image during this process, the beam shifts were used rather than moving the stage; otherwise, there was a risk of damaging the tip of the tungsten wire probe. Figure B.2(b) shows the wire just after it had touched the surface of the sample post. Note that the tip of the wire was resting on just a few μm's of the lower end of the sample post. Notice also that the point of contact between the sample post and the tungsten was signaled only by the faint shadow that appeared on the sample post on either side of the wire. In effect, the wire was "shadowing" the sample post from Ga^+ ions and therefore appeared a little darker. This step had to be done slowly and carefully as lowering the wire too quickly would have caused a sudden impact on the wire and bent the tip. If the tip were bent, it would have attached to the sample post at an improper angle and made the final milling steps difficult. Moreover, the specimen tip would not have been aligned properly relative to the local electrode in the LEAP, which means analysis would likely fail.

A pattern for Pt deposition was then used to deposit Pt onto the tungsten wire and sample post in order to bond them together. The outcome is shown in Figure B.2(c). Typical patterns used had a width of 2.4 μm and a height of 7.5 μm, although the height could vary, with the purpose of depositing Pt from the base of the post to a height several μm's above the end of the tungsten wire. The depth was 3 μm using a current of 0.3 nA. In retrospect, more uniform Pt deposition layers might have been possible using a lower current of, say, 0.1 nA. More uniform Pt layers would have provided a better bond between the post and tungsten wire and made dissection of the post from the wire less probable during the annular milling process.

The next step was to finish cutting out the sample post in order to release it from the sample. A pattern of 5 μm x 500 nm was commonly used, with a depth of 7 μm. The

cutting height had to be made large enough, e.g. > 500 nm, or else there was a risk of re-depositing milled sample material back into the cutting area and preventing release of the sample post. The final post had to be completely free from the sample, as shown in Figure B.2(d). The sample was then raised slightly using the Kleindieck probe to ensure it had been cut free. If successful, it would look similar to Figure B.2(e). Then the stage was lowered back to the starting position before tilting to 0°.

After appropriately affixing the tungsten wire into a sample holder and reloading into the FIB, the steps for tip preparation could begin. Figure B.3(a) shows the sample post after reloading of the tungsten wire. The cross-section of the post was now visible in the normal e^- beam. Notice the uneven layers of the Pt deposition layer, which might be mitigated by a lower deposition current, as mentioned previously. After tilting to +52° in the Ga^+ beam, the post was again viewed edge-on. The beam current was set to 0.3 nA to prevent excessive milling of the post surface while imaging. Figure B.3(b) shows the post after a quick milling of the sharp edge. This milling step eliminated the edge which would otherwise lie outside the large annular milling pattern to be performed in the next step. This milling step was a box pattern of appropriate size, as shown in the figure, to a depth of typically 3 µm.

Figure B.3(c) depicts the first annular milling process. A large annular milling pattern was created, with an outside diameter that just fit over the edge of the post. An inner diameter was set to 1 µm; the inner hole was also positioned so that it rested roughly in the middle of the sample post, away from the protective Pt layer on the top surface of the post. Care was taken not to have the milling pattern overlapping too much with the Pt layer that bonds the post to the tungsten wire. Sufficient milling would destroy this bond and dissect the post from the wire. The large annular milling pattern was performed to a depth of 750 nm – 1 µm at a current of 0.3 nA. Annular milling was always performed with an outer-to-inner milling direction.

Figure B.3(d) shows the next annular milling process, this time at a current of 0.1 nA. The outer milling diameter was 1.5 µm with an inner diameter of 300 nm and a total depth of 150 nm. In retrospect, it may have been better to perform both annular milling steps at the lower beam current of 0.1 nA for two reasons. First, milling at this lower current produces a better tip because the milling is done more slowly with greater

precision, although the milling process is then going to take roughly 3 times longer. This means the FIB must be stable without too much sample movement that would cause a shift in the position of the tip and result in the tip being destroyed during milling. This was always a danger. Second, when switching currents from 0.3 to 0.1 nA between the annular mills, the image had to be refocused and the brightness and contrast readjusted, which required several beam scans. Each beam scan damages the tip and introduces additional Ga^+ that are implanted into the tip surface. The fewer the beam scans required, the better, as it preserved a better tip for the second milling process. Also, as few beam scans as possible were performed after the second annular milling process.

The final tip is shown in figure B.3(e), although it is barely visible in the image. To better visualize the tip would have required refocusing and additional balancing of the brightness and contrast, which would have damaged or destroyed the tip.

Returning to the e^- beam, the tip can be imaged without damaging the tip. Figure B.4(a) shows the sharp tip in the foreground, but notice the secondary peak directly behind the primary peak. This was due to re-deposition of milled material during the annular milling process, which failed to remove this secondary peak. At this point, secondary tips had to be milled away one by one using box milling patterns that could eliminate the secondary tips. This required additional imaging with the Ga^+ beam, and that would inevitably damage the primary sample tip. Any extensive milling after annular milling likely led to failed specimens in the LEAP.

The challenge in making these tips was to create an annular milling pattern with sufficient outer diameter without destroying the Pt bond between the post and the tungsten wire. In addition, the milling pattern had to mill with sufficient depth, again without destroying the Pt bond and without removing too much of the post or damaging the tip. Figure B.4(b) shows a close up of the sample tip, which is indeed a very sharp tip suitable for LEAP analysis. Notice that at the end of the tip, the image become blurry because the specimen is so thin that it produces a poorly defined secondary electron image.

Figure B.4(c) shows a different specimen tip without any secondary peaks to interfere with the analysis. Figure B.4(d) provides a close-up image of the tip, with a line

measurement showing the thickness near the tip of the specimen. This sample is adequate for producing valuable LEAP results.

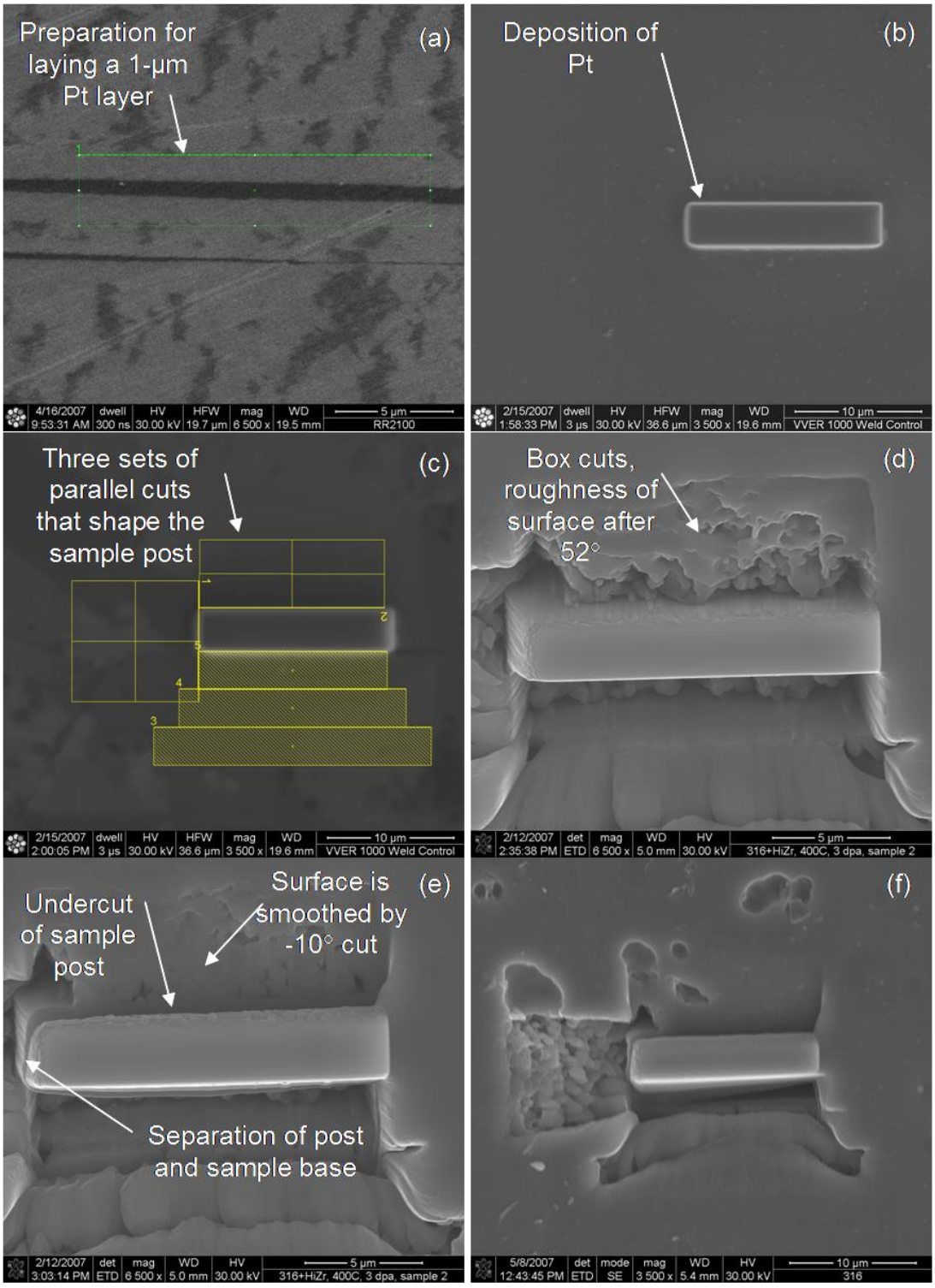

Figure B.1 (a) Selection of an area for Pt deposition to protect the sample during cutting; (b) after deposition of Pt; (c) arrangement of a series of box cuts to drill out a sample post; (d) after the first set of box cuts performed at +52°; (e) a second box cutting at -10° undercuts the sample, leaving a cantilevered sample post; (f) a full view of the post under a protective Pt layer, with surrounding ion beam drilling damage.

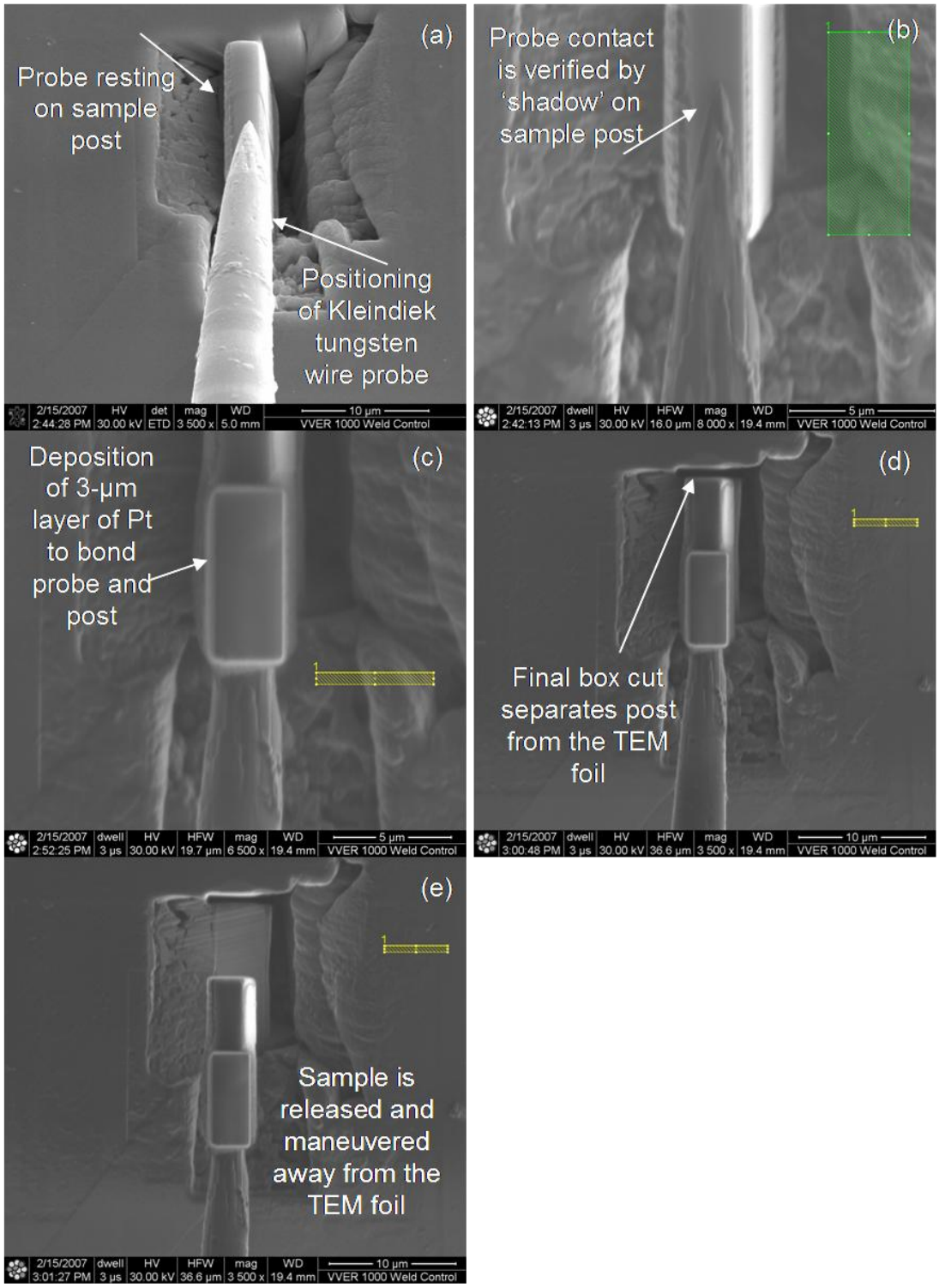

Figure B.2 (a) The Kleindiek tungsten probe is maneuvered and placed on top of the sample post; (b) a top-down view reveals a shadow on the post from the probe; (c) deposition of Pt connects the post to the probe; (d) a final cut releases the sample from the TEM foil; (e) and the probe plus sample post are removed and positioned for the next step in the fabrication process.

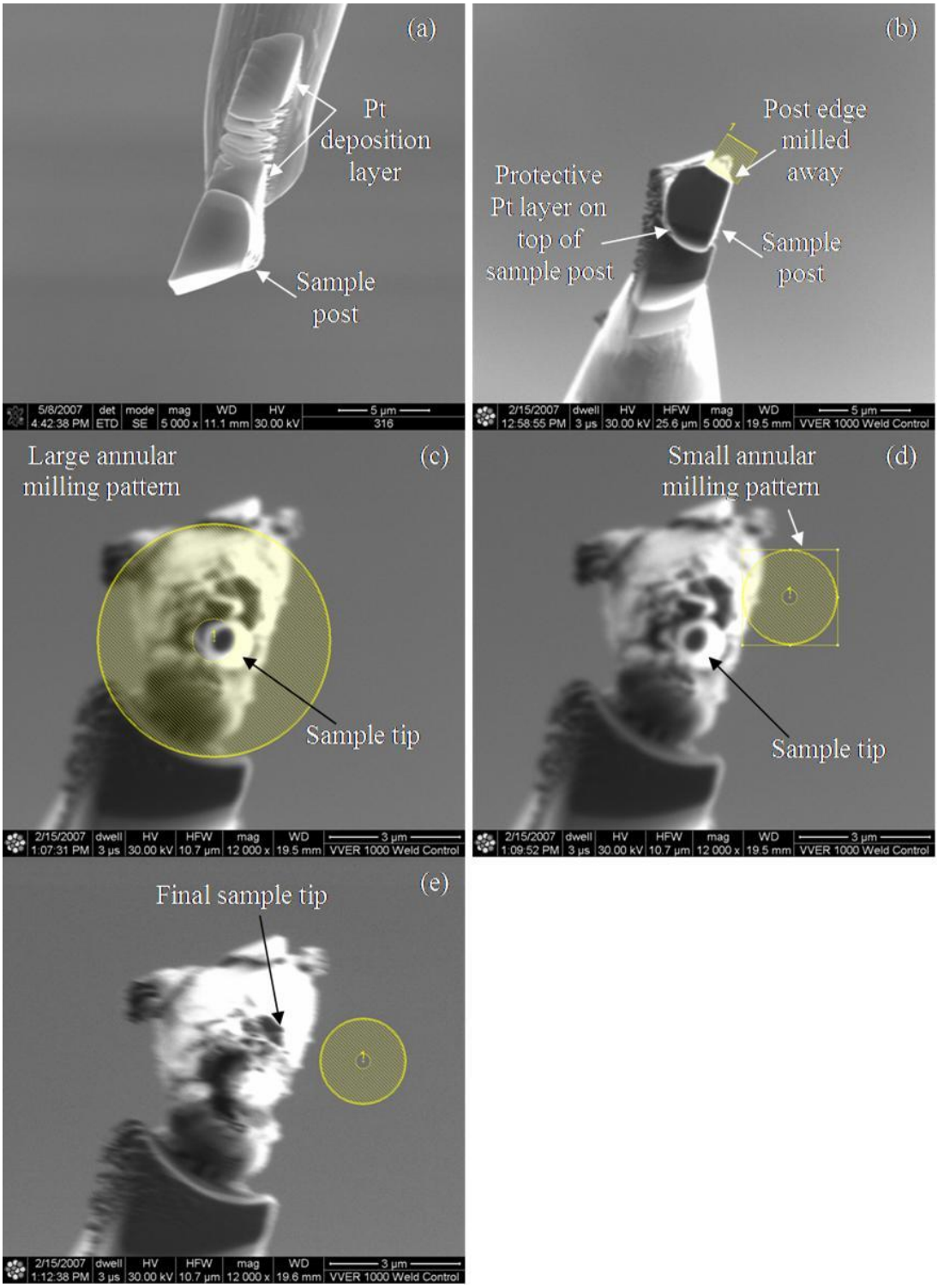

Figure B.3 (a) The sample attached to a tungsten wire is reloaded back into the FIB and imaged in the e^- beam; (b) box mill of the post edge, with imaging in the Ga^+ beam; (c) large annular milling pattern to establish the initial shape of the sample tip; (d) final annular milling pattern to shape and define the final sample tip; and (e) an image of the final specimen tip.

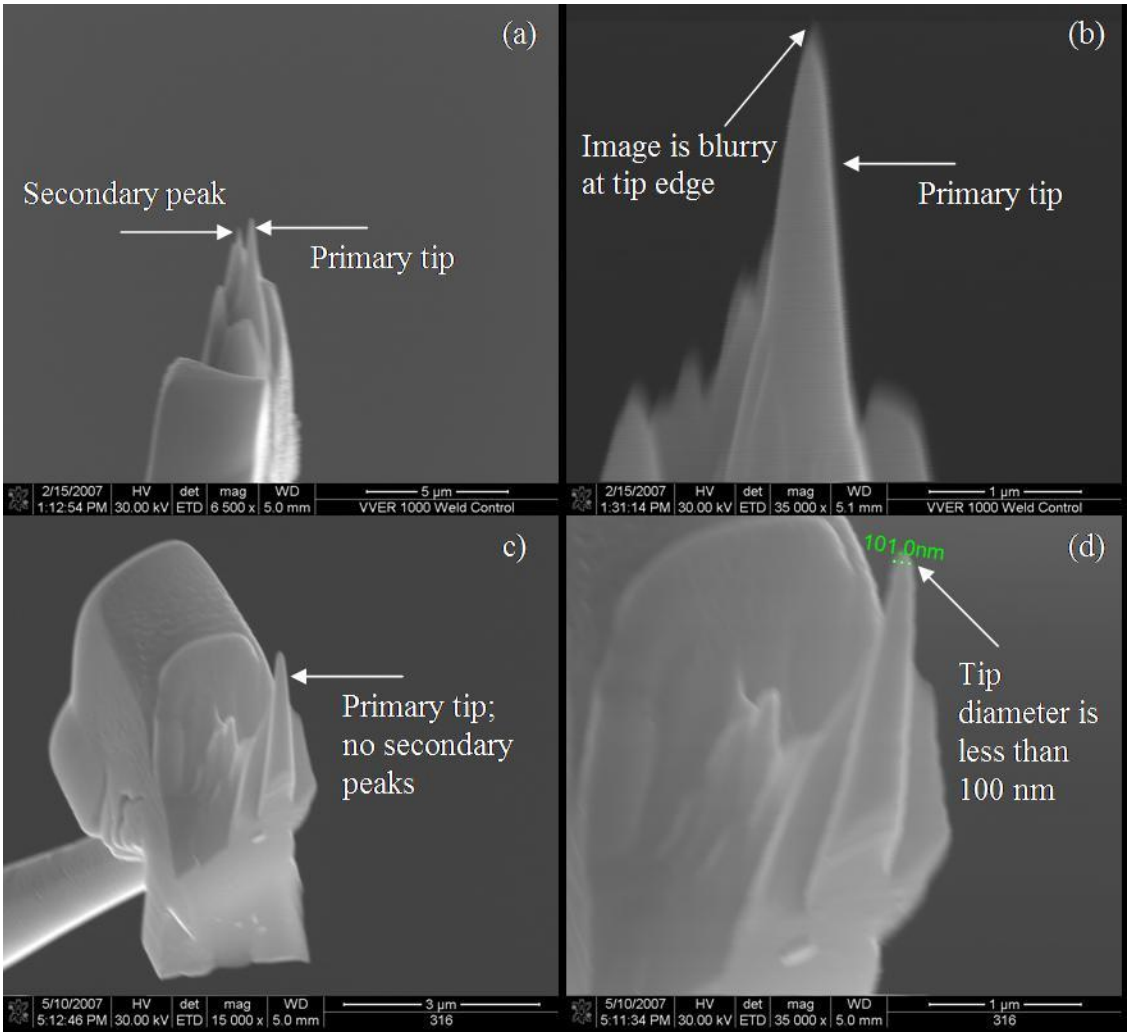

Figure B.4 (a) an image of a primary and secondary tip after the final milling process, imaged in the e^- beam; (b) close up view of the primary peak; (c) image of a primary tip without any secondary tips that might interfere with LEAP analysis; and (d) a close of the final specimen tip showing the final tip diameter of less than 100 nm.

APPENDIX C

MINIMUM DETECTABILITY LIMIT OF HF IN EDS

This appendix calculates the minimum detectable limit of Hf based on STEM-EDS measurements. In the ideal case, minimum detectability would be determined by using standards of Hf and some other measurable element in the oversized solute alloys (such as Ni) to determine their intensity ratios on the same instrument used for the RIS measurements. From the intensity ratio and the intensity of the other element in a RIS profile, the minimum Hf signal required for detection could be calculated.

The standards to make these measurements were not available, however, so an alternative method is used. First, an assumption is made that a Hf X-ray signal measuring twice the background signal is required for detection. The Hf X-ray peak is compared to a neighboring Ni X-ray peak to ignore changes in detector efficiency as a function of energy. Then, knowing the Ni concentration, the measured Ni peak intensity and minimum detectable Hf signal, and the estimated intensity ratios of two neighboring X-ray energies for Ni and Hf, the concentration of Hf can be determined.

The fluorescence yield for X-rays from electron interactions is approximated by the following equation [142]:

$$\omega = \frac{Z^4}{a + Z^4} \tag{C.1}$$

where ω is the fluorescence yield, Z is the atomic number and a is a constant with the value of approximately 10^6 for K-shell electrons. From the Table of Isotopes [143], fluorescence yields for the K-shell electrons for Ni and Hf are $\omega_K^{Ni} = 0.406$ and $\omega_K^{Hf} = 0.950$.

An EDS spectrum of measured intensity as a function of energy is given in figure C.1 and shows the positions of the peaks for the Ni and Hf X-rays used in this analysis. For Ni, $K_{\alpha 1}^{Ni}$ = 7.478 keV and $K_{\alpha 2}^{Ni}$ = 7.461 keV while $K_{\beta 1}^{Ni}$ = 8.265 keV. Meanwhile, $L_{\alpha 1}^{Hf}$ = 7.899 keV and $L_{\alpha 2}^{Hf}$ = 7.844 keV. Since the $L_{\alpha 1}^{Hf} + L_{\alpha 2}^{Hf}$ X-rays for Hf are close in energy to the Kβ X-ray for Ni, changes in detector efficiency will be ignored. The $\frac{K_{\alpha 1}^{Ni}}{K_{\beta 1}^{Ni}}$ ratio for Ni = 0.17, and the $\frac{K_{\alpha 1}^{Hf}}{\left(L_{\alpha 1}^{Hf} + L_{\alpha 2}^{Hf}\right)}$ ratio for Hf = 0.12 [143].

For $\left(L_{\alpha 1}^{Hf} + L_{\alpha 2}^{Hf}\right)$ to have the same signal as $K_{\beta 1}^{Ni}$, we have the relationship:

$$\omega_K^{Ni} * \frac{K_{\alpha 1}^{Ni}}{K_{\beta 1}^{Ni}} * X_{at\%}^{Ni} = \omega_K^{Hf} * \frac{K_{\alpha 1}^{Hf}}{\left(L_{\alpha 1}^{Hf} + L_{\alpha 2}^{Hf}\right)} * X_{at\%}^{Hf} \qquad \text{(C.2)}$$

$X_{at\%}^{Ni}$ = 14.0 at% in the matrix. For $K_{\beta 1}^{Ni}$ the peak intensity measures 600 counts, of which the background is 100 counts. The Hf X-ray peak intensity should double the background intensity, for a total of 200 counts. The resulting signals above background due to Ni and Hf are then 500 counts and 100 counts, respectively, for a Ni-to-Hf ratio of 0.2. This means that the detectable limit for $\left(L_{\alpha 1}^{Hf} + L_{\alpha 2}^{Hf}\right)$ peak intensity is 0.29 times the peak intensity of $K_{\beta 1}^{Ni}$.

Determining the minimum detectable concentration of Hf is found by the relationship:

$$X_{at\%}^{Hf} = 0.20 * X_{at\%}^{Ni} * \frac{\omega_K^{Ni}}{\omega_K^{Hf}} * \frac{K_{\alpha 1}^{Ni}}{K_{\beta 1}^{Ni}} * \frac{\left(L_{\alpha 1}^{Hf} + L_{\alpha 2}^{Hf}\right)}{K_{\alpha 1}^{Hf}} \qquad \text{(C.3)}$$

The result is that $X_{at\%}^{Hf}$ = 1.7 at% is the minimum detectable Hf concentration.

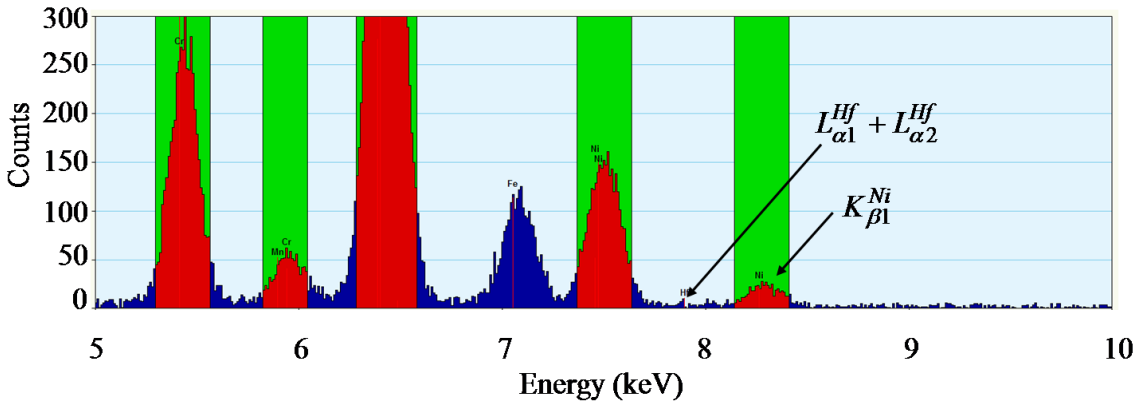

Figure C.1 EDS spectrum for a grain boundary RIS measurement showing the $K_{\beta 1}^{Ni}$ X-ray peak and the position of the $L_{\alpha 1}^{Hf} + L_{\alpha 2}^{Hf}$ X-ray peak.

APPENDIX D

RADIATION-INDUCED SEGREGATION MEASUREMENTS

Ref-Zr, 400C, 3 dpa

Meas.	Pos. (nm)	Fe	Cr	Ni	Mn	Si	Zr	Meas.	Fe	Cr	Ni	Mn	Si	Zr
1	0	70.49	16.00	11.46	1.36	0.70	0	2	70.25	14.08	13.92	1.08	0.68	0
	1.5	70.32	16.32	11.38	1.35	0.63	0		71.52	14.29	12.37	1.11	0.71	0
	3	70.44	16.26	11.39	1.37	0.53	0		70.09	14.56	13.49	1.09	0.77	0
	4.5	70.69	16.56	10.78	1.43	0.54	0		69.80	14.37	13.97	1.10	0.75	0
	6	71.03	16.34	11.07	1.06	0.50	0		69.45	13.92	14.57	1.39	0.67	0
	7.5	71.48	15.69	10.91	1.36	0.56	0		70.31	14.73	13.06	1.18	0.72	0
	9	72.58	14.37	11.56	0.87	0.62	0		71.05	15.81	11.43	1.00	0.71	0
	10.5	71.68	15.23	11.36	1.05	0.67	0		71.83	15.28	11.14	1.10	0.66	0
	12	67.32	11.67	18.84	0.81	1.37	0		72.36	13.93	11.92	1.00	0.79	0
	13.5	54.65	10.23	31.44	0.54	3.14	0		56.43	10.20	29.92	0.49	2.96	0
	15	62.40	11.46	23.61	0.46	2.08	0		54.00	9.66	32.97	0.37	2.99	0
	16.5	73.04	14.76	10.50	1.01	0.69	0		62.99	10.32	24.00	0.59	2.10	0
	18	72.79	15.44	10.05	1.00	0.72	0		74.11	14.07	9.98	1.11	0.73	0
	19.5	71.28	16.08	10.94	1.02	0.68	0		72.25	15.27	10.51	1.21	0.77	0
	21	70.35	16.74	10.93	1.24	0.73	0		72.56	15.80	9.98	0.98	0.69	0
	22.5	69.89	16.40	11.95	1.04	0.72	0		71.89	15.91	10.29	1.20	0.71	0
	24	70.64	16.27	11.26	1.30	0.52	0		70.66	16.45	10.75	1.37	0.77	0
	25.5	69.46	16.68	11.74	1.40	0.73	0		70.99	16.60	10.40	1.36	0.65	0
	27	69.75	15.76	12.18	1.64	0.67	0		70.89	16.28	10.82	1.33	0.68	0
	28.5	70.36	16.50	11.18	1.31	0.65	0		71.01	16.22	10.67	1.42	0.69	0
	30	70.12	16.40	11.26	1.56	0.65	0		69.94	15.64	12.23	1.24	0.96	0
3	0	70.25	14.08	13.92	1.08	0.68	0	4	68.47	15.28	14.06	1.25	0.94	0
	1.5	71.52	14.29	12.37	1.11	0.71	0		68.46	16.08	13.49	1.12	0.84	0
	3	70.09	14.56	13.49	1.09	0.77	0		70.60	15.94	11.66	1.17	0.62	0
	4.5	69.80	14.37	13.97	1.10	0.75	0		70.27	16.31	11.39	1.39	0.63	0
	6	69.45	13.92	14.57	1.39	0.67	0		69.95	16.43	11.40	1.62	0.60	0
	7.5	70.31	14.73	13.06	1.18	0.72	0		69.90	16.43	11.89	1.16	0.63	0
	9	71.05	15.81	11.43	1.00	0.71	0		70.02	16.29	11.75	1.28	0.65	0
	10.5	71.83	15.28	11.14	1.10	0.66	0		71.28	16.10	10.93	1.15	0.53	0
	12	72.36	13.93	11.92	1.00	0.79	0		72.36	14.58	11.44	0.91	0.71	0
	13.5	56.43	10.20	29.92	0.49	2.96	0		64.53	10.90	21.90	0.87	1.80	0
	15	54.00	9.66	32.97	0.37	2.99	0		56.10	10.60	30.06	0.46	2.79	0
	16.5	62.99	10.32	24.00	0.59	2.10	0		63.57	10.58	23.04	0.71	2.10	0
	18	74.11	14.07	9.98	1.11	0.73	0		70.66	13.36	14.37	0.59	1.02	0

Meas.	Pos. (nm)	Fe	Cr	Ni	Mn	Si	Zr	Meas.	Fe	Cr	Ni	Mn	Si	Zr
	19.5	72.25	15.27	10.51	1.21	0.77	0		71.40	14.03	12.75	1.01	0.81	0
	21	72.56	15.80	9.98	0.98	0.69	0		71.20	15.03	12.00	1.02	0.74	0
	22.5	71.89	15.91	10.29	1.20	0.71	0		71.07	15.57	11.56	1.05	0.76	0
	24	70.66	16.45	10.75	1.37	0.77	0		71.08	15.49	11.75	0.95	0.73	0
3	25.5	70.99	16.60	10.40	1.36	0.65	0	4	70.77	16.01	11.30	1.24	0.68	0
	27	70.89	16.28	10.82	1.33	0.68	0		69.90	16.13	12.10	1.24	0.63	0
	28.5	71.01	16.22	10.67	1.42	0.69	0		70.84	15.73	11.40	1.32	0.71	0
	30	69.94	15.64	12.23	1.24	0.96	0		70.29	15.50	12.41	1.17	0.63	0
5	0	69.62	15.90	12.43	1.37	0.67	0	6	69.83	16.00	12.17	1.27	0.72	0
	1.5	69.19	16.41	12.31	1.35	0.73	0		70.22	15.78	12.04	1.35	0.61	0
	3	69.22	16.21	12.43	1.43	0.71	0		69.97	15.94	12.06	1.37	0.66	0
	4.5	70.50	16.16	11.53	1.18	0.63	0		70.05	16.31	11.80	1.27	0.57	0
	6	69.84	16.58	11.75	1.12	0.71	0		71.44	15.97	10.61	1.34	0.63	0
	7.5	70.91	16.31	10.94	1.18	0.66	0		71.39	15.66	11.24	1.11	0.61	0
	9	69.89	16.44	11.54	1.50	0.63	0		72.26	13.82	12.04	1.12	0.76	0
	10.5	71.03	15.64	11.34	1.31	0.68	0		70.78	13.68	13.88	0.77	0.90	0
	12	72.94	14.57	10.89	0.88	0.72	0		58.77	9.81	28.08	0.64	2.71	0
	13.5	61.45	10.32	25.02	0.69	2.52	0		55.94	9.45	30.61	0.73	3.27	0
	15	60.86	10.50	25.49	0.54	2.61	0		71.98	12.11	14.07	0.65	1.19	0
	16.5	70.57	12.77	14.52	0.82	1.32	0		71.95	15.26	11.14	0.93	0.73	0
	18	71.91	15.46	10.61	1.11	0.91	0		72.53	14.53	11.25	0.96	0.73	0
	19.5	71.74	15.65	10.44	1.32	0.85	0		70.68	15.35	12.25	0.98	0.74	0
	21	71.59	15.96	10.64	1.10	0.71	0		70.20	15.29	12.84	0.79	0.87	0
	22.5	71.69	15.69	10.62	1.22	0.78	0		68.85	14.27	15.02	0.96	0.89	0
	24	70.27	15.91	11.42	1.67	0.74	0		68.15	13.60	16.14	1.09	1.02	0
	25.5	70.01	16.15	11.69	1.32	0.83	0		67.78	14.11	16.06	1.05	0.99	0
	27	70.25	16.16	11.61	1.23	0.74	0		68.75	14.55	14.60	1.11	1.00	0
	28.5	69.68	16.06	12.09	1.35	0.81	0		69.81	14.36	13.68	1.28	0.87	0
	30	69.45	16.40	12.20	1.16	0.79	0		70.38	14.65	12.88	1.31	0.79	0
7	0	69.17	17.21	11.56	1.35	0.71	0	8	67.88	14.85	15.38	1.08	0.81	0
	1.5	70.34	16.40	11.36	1.26	0.64	0		68.51	14.79	14.78	1.13	0.79	0
	3	70.28	16.01	11.70	1.33	0.68	0		69.38	15.01	13.88	1.09	0.65	0
	4.5	70.90	15.75	11.24	1.42	0.69	0		70.11	14.81	13.16	1.21	0.72	0
	6	70.14	16.43	11.65	1.19	0.59	0		69.63	15.86	12.92	1.03	0.57	0
	7.5	70.65	16.40	11.16	1.19	0.60	0		71.25	15.27	11.61	1.18	0.69	0
	9	71.46	15.82	10.98	1.09	0.64	0		71.99	14.89	11.12	1.34	0.67	0
	10.5	70.56	12.74	14.75	0.71	1.24	0		71.69	14.71	11.72	1.18	0.70	0
	12	71.89	13.09	13.03	0.97	1.01	0		73.13	14.41	10.74	1.04	0.68	0
	13.5	60.51	9.99	26.22	0.57	2.70	0		70.49	12.36	15.33	0.71	1.12	0
	15	54.42	9.27	32.40	0.43	3.47	0		61.97	11.11	24.35	0.54	2.03	0
	16.5	71.46	12.55	13.92	0.75	1.33	0		59.15	10.93	26.90	0.64	2.39	0
	18	73.29	14.71	10.15	1.04	0.81	0		64.71	11.74	21.04	0.69	1.82	0
	19.5	72.62	15.03	10.46	1.14	0.76	0		72.16	12.51	13.50	0.74	1.09	0
	21	71.73	15.99	10.37	1.14	0.78	0		72.03	14.71	11.52	0.92	0.82	0
	22.5	73.01	15.15	9.87	1.27	0.70	0		70.63	15.17	12.30	1.22	0.68	0
	24	70.77	16.48	10.69	1.37	0.70	0		70.65	15.23	12.05	1.32	0.75	0
	25.5	70.61	16.10	11.35	1.18	0.76	0		70.24	15.60	12.49	0.94	0.73	0

Meas.	Pos. (nm)	Fe	Cr	Ni	Mn	Si	Zr	Meas.	Fe	Cr	Ni	Mn	Si	Zr
	27	70.67	15.81	11.27	1.49	0.77	0		70.25	16.03	11.75	1.28	0.68	0
	28.5	70.38	16.06	11.49	1.27	0.80	0		69.80	17.17	10.96	1.36	0.71	0
	30	70.17	15.72	11.78	1.40	0.94	0		70.13	16.37	11.41	1.43	0.66	0
9	0	68.78	17.11	11.81	1.71	0.59	0	10	68.54	16.86	12.25	1.46	0.89	0
	1.5	69.35	16.44	11.95	1.71	0.56	0		68.23	17.22	12.75	1.15	0.65	0
	3	70.59	16.82	10.68	1.28	0.63	0		69.29	16.47	12.42	1.22	0.60	0
	4.5	68.91	16.97	12.15	1.46	0.51	0		68.80	16.65	12.49	1.47	0.58	0
	6	71.66	15.04	11.43	1.30	0.57	0		70.28	16.94	11.26	0.95	0.57	0
	7.5	71.68	15.96	10.80	1.04	0.52	0		70.86	16.52	11.04	1.02	0.56	0
	9	72.80	15.28	10.21	1.16	0.56	0		73.10	15.51	9.71	1.08	0.61	0
	10.5	73.02	13.63	11.84	0.93	0.58	0		73.96	14.16	10.29	0.81	0.78	0
	12	70.77	11.68	15.77	0.63	1.14	0		72.97	10.89	14.34	0.72	1.08	0
	13.5	60.32	8.16	28.11	0.80	2.61	0		59.49	9.09	28.22	0.63	2.56	0
	15	56.30	7.80	32.39	0.68	2.83	0		55.84	7.97	32.33	0.85	3.01	0
	16.5	73.06	11.41	14.09	0.41	1.04	0		70.60	11.01	16.26	0.80	1.32	0
	18	73.42	14.08	10.80	1.10	0.59	0		74.28	13.30	10.54	1.12	0.76	0
	19.5	72.75	14.79	10.62	1.20	0.64	0		71.12	13.59	13.56	0.97	0.77	0
	21	72.89	14.44	10.87	1.30	0.51	0		69.31	12.69	15.54	1.23	1.22	0
	22.5	71.68	14.54	11.89	1.26	0.64	0		66.43	12.12	19.37	0.77	1.31	0
	24	72.19	14.66	11.05	1.43	0.66	0		65.13	11.83	20.94	0.81	1.28	0
	25.5	70.62	15.41	12.11	1.34	0.52	0		67.04	12.18	18.60	0.94	1.24	0
	27	70.09	15.38	12.76	1.19	0.59	0		70.57	14.21	13.12	1.31	0.79	0
	28.5	69.99	14.85	13.25	1.35	0.56	0		71.52	15.28	11.07	1.09	1.04	0
	30								70.66	16.07	11.08	1.43	0.76	0
11	0	67.37	15.32	14.76	1.24	1.31	0	12	59.01	13.59	24.24	1.04	2.12	0
	1.5	69.78	14.91	13.43	0.94	0.94	0		60.68	12.69	23.44	0.97	2.22	0
	3	69.96	14.71	13.48	0.89	0.96	0		62.90	13.05	21.41	0.98	1.66	0
	4.5	70.54	14.98	12.31	1.39	0.78	0		66.64	13.20	18.00	1.10	1.07	0
	6	70.79	16.29	11.13	1.23	0.56	0		70.74	13.63	13.80	1.15	0.69	0
	7.5	71.14	16.45	10.75	1.11	0.54	0		71.19	14.17	12.70	1.19	0.75	0
	9	71.20	16.43	10.26	1.60	0.50	0		70.99	15.22	11.58	1.29	0.92	0
	10.5	71.70	15.94	10.71	1.04	0.60	0		72.42	14.84	10.77	1.06	0.92	0
	12	72.61	15.31	10.37	1.00	0.71	0		72.52	15.01	10.72	0.92	0.84	0
	13.5	73.20	12.62	12.35	0.85	0.98	0		68.25	11.01	17.89	0.90	1.95	0
	15	63.86	9.50	23.83	0.61	2.19	0		59.85	8.83	27.38	0.82	3.12	0
	16.5	51.99	7.77	35.99	0.58	3.67	0		53.69	7.75	33.98	0.65	3.93	0
	18	70.52	10.44	16.76	0.52	1.76	0		73.54	12.14	11.69	0.93	1.69	0
	19.5	75.64	12.21	10.08	1.02	1.05	0		74.77	13.97	8.86	1.22	1.17	0
	21	73.67	14.70	9.89	0.75	0.99	0		73.28	14.87	9.75	0.98	1.12	0
	22.5	73.34	13.78	10.61	1.20	1.06	0		71.55	15.49	10.64	1.41	0.91	0
	24	72.92	15.00	9.79	1.10	1.20	0		72.86	14.65	10.11	1.52	0.87	0
	25.5	70.92	15.44	11.33	1.28	1.03	0		72.88	14.90	10.47	1.07	0.68	0
	27	70.72	15.25	11.52	1.38	1.12	0		70.60	14.75	12.94	0.96	0.74	0
	28.5	70.14	15.53	12.14	1.37	0.81	0		69.50	15.50	13.25	0.98	0.77	0
	30	70.34	16.16	11.49	1.27	0.75	0		69.71	14.95	13.47	1.08	0.79	0
13	0	68.96	14.70	14.31	1.01	1.02	0	14	69.53	13.91	14.47	1.14	0.95	0

Meas.	Pos. (nm)	Fe	Cr	Ni	Mn	Si	Zr	Meas.	Fe	Cr	Ni	Mn	Si	Zr
	1.5	68.66	14.95	14.11	1.33	0.95	0		69.17	13.05	15.88	0.93	0.97	0
	3	69.67	15.49	12.90	1.21	0.74	0		67.48	13.34	16.89	1.19	1.09	0
	4.5	69.10	15.99	12.91	1.35	0.65	0		67.99	15.18	14.78	1.12	0.94	0
	6	69.86	16.04	12.04	1.39	0.67	0		70.21	15.44	12.31	1.32	0.72	0
13	7.5	71.46	15.45	11.00	1.40	0.70	0	14	70.88	15.73	11.41	1.38	0.59	0
	9	72.72	15.22	10.49	1.00	0.58	0		72.38	14.90	10.69	1.49	0.54	0
	10.5	73.14	13.52	11.75	0.82	0.76	0		72.70	14.36	11.11	1.02	0.81	0
	12	69.05	10.84	18.02	0.73	1.36	0		65.75	12.32	19.41	0.89	1.64	0
	13.5	54.87	8.51	33.20	0.53	2.89	0		46.62	7.31	40.96	0.67	4.44	0
	15	63.47	9.63	24.27	0.64	1.99	0		65.10	9.33	22.88	0.49	2.19	0
	16.5	72.83	12.42	13.00	0.80	0.94	0		75.20	11.76	11.61	0.65	0.78	0
	18	70.71	14.30	13.20	0.81	0.98	0		74.38	14.31	9.58	1.16	0.57	0
	19.5	69.90	14.18	13.94	0.89	1.08	0		73.86	14.94	9.58	1.07	0.56	0
	21	69.48	13.62	14.84	0.83	1.23	0		73.09	14.59	10.55	1.15	0.63	0
	22.5	70.40	13.52	13.65	1.30	1.13	0		71.76	15.43	11.01	1.16	0.65	0
	24	69.79	12.57	15.45	1.04	1.15	0		71.35	15.09	11.61	1.25	0.70	0
	25.5	68.56	11.84	17.36	0.72	1.52	0		71.17	14.72	12.00	1.42	0.69	0
	27	68.44	11.85	17.43	1.00	1.29	0		70.37	14.85	12.81	1.26	0.71	0
	28.5	69.71	13.07	15.49	0.87	0.86	0		70.34	14.23	13.47	1.28	0.68	0
	30	69.32	13.70	15.17	0.93	0.88	0							
15	0	66.49	13.23	18.10	0.82	1.36	0							
	1.5	63.24	12.35	21.49	1.15	1.77	0							
	3	63.90	13.34	20.04	1.05	1.67	0							
	4.5	67.86	14.13	16.05	0.78	1.19	0							
	6	71.03	14.68	12.50	1.14	0.64	0							
	7.5	71.96	14.76	11.37	1.34	0.57	0							
	9	72.23	15.60	10.56	1.09	0.53	0							
	10.5	73.28	14.33	10.63	1.11	0.64	0							
	12	71.53	13.54	13.17	0.90	0.86	0							
	13.5	58.84	8.78	28.89	0.67	2.82	0							
	15	47.22	7.23	40.79	0.59	4.18	0							
	16.5	57.80	8.00	30.72	0.58	2.90	0							
	18	75.85	13.03	9.86	0.62	0.64	0							
	19.5	74.76	13.98	10.03	0.71	0.53	0							
	21	74.44	13.86	10.07	1.09	0.53	0							
	22.5	72.76	15.27	10.39	1.05	0.53	0							
	24	71.71	14.88	11.82	1.04	0.54	0							
	25.5	71.21	15.01	11.99	1.25	0.54	0							
	27	70.67	15.26	12.29	1.14	0.64	0							
	28.5	70.33	14.80	13.12	1.19	0.55	0							
	30	70.03	15.30	12.61	1.35	0.71	0							

Ref-Zr, 400C, 7 dpa

Meas.	Pos. nm)	Fe	Cr	Ni	Mn	Si	Zr	Meas.	Fe	Cr	Ni	Mn	Si	Zr
1	0	69.56	16.04	12.39	1.08	0.93	0.00	2	68.50	15.68	13.52	1.52	0.78	0.00
	1.5	69.43	15.31	13.06	1.47	0.73	0.00		68.75	15.61	13.60	1.20	0.84	0.00
	3	69.23	15.74	13.16	1.24	0.64	0.00		68.82	15.03	13.99	1.27	0.89	0.00
	4.5	68.25	15.69	13.94	1.22	0.89	0.00		68.80	15.50	13.42	1.52	0.76	0.00
	6	69.22	16.37	12.50	1.14	0.78	0.00		69.89	15.33	13.19	0.93	0.67	0.00
	7.5	69.77	15.70	12.80	1.10	0.63	0.00		69.17	16.25	12.48	1.43	0.68	0.00
	9	70.30	15.23	12.41	1.30	0.76	0.00		70.83	16.23	11.51	0.76	0.67	0.00
	10.5	70.18	15.77	12.13	1.17	0.74	0.00		71.82	15.05	11.31	1.02	0.79	0.00
	12	69.95	16.26	11.96	1.23	0.61	0.00		71.00	14.87	12.19	1.13	0.82	0.00
	13.5	71.44	14.23	12.61	0.91	0.81	0.00		70.99	13.11	13.56	0.97	1.38	0.00
	15	71.28	13.59	13.08	1.19	0.86	0.00		63.36	10.17	23.04	0.55	2.88	0.00
	16.5	67.00	12.54	17.86	0.79	1.81	0.00		56.01	9.08	30.16	0.48	4.27	0.00
	18	55.13	9.07	31.04	0.55	4.21	0.00		72.36	14.43	11.49	0.79	0.93	0.00
	19.5	68.92	11.88	16.78	0.73	1.69	0.00		71.77	14.66	11.62	1.21	0.74	0.00
	21	71.86	13.73	12.74	0.71	0.97	0.00		70.64	14.33	12.99	1.23	0.81	0.00
	22.5	71.80	13.20	13.15	0.97	0.89	0.00		71.35	14.78	11.95	1.13	0.80	0.00
	24	71.15	13.90	12.84	1.14	0.96	0.00		71.41	14.94	12.00	0.95	0.69	0.00
	25.5	71.05	14.77	12.42	1.04	0.71	0.00		71.16	14.72	12.17	1.20	0.75	0.00
	27	70.50	14.81	12.70	1.28	0.71	0.00		69.69	14.17	13.95	1.29	0.90	0.00
	28.5	69.14	15.20	13.77	1.15	0.73	0.00		69.18	14.46	14.31	1.11	0.95	0.00
	30	68.67	15.15	14.15	1.27	0.75	0.00		69.38	14.58	14.14	1.02	0.89	0.00
3	0	68.93	16.51	12.67	1.22	0.66	0.00	4	69.99	15.12	12.80	1.17	0.92	0.00
	1.5	69.55	17.03	11.55	1.13	0.74	0.00		69.65	15.50	12.86	1.17	0.82	0.00
	3	70.03	15.11	12.64	1.55	0.66	0.00		70.12	15.40	12.50	1.28	0.70	0.00
	4.5	69.70	15.18	13.30	1.21	0.62	0.00		69.35	15.46	13.11	1.41	0.67	0.00
	6	69.49	15.21	13.39	1.09	0.82	0.00		69.32	15.06	13.59	1.27	0.76	0.00
	7.5	70.12	15.35	12.40	1.45	0.67	0.00		69.67	15.65	12.82	1.15	0.71	0.00
	9	69.99	15.54	12.44	1.26	0.77	0.00		70.50	14.36	13.15	1.09	0.90	0.00
	10.5	71.95	14.73	11.48	1.14	0.70	0.00		70.70	14.38	12.78	1.31	0.83	0.00
	12	72.84	14.32	10.93	1.07	0.84	0.00		70.32	15.08	12.79	1.06	0.74	0.00
	13.5	71.82	13.49	12.63	0.75	1.32	0.00		69.39	13.39	14.87	1.06	1.29	0.00
	15	64.38	11.00	21.40	0.71	2.50	0.00		63.25	11.11	22.15	0.64	2.84	0.00
	16.5	54.80	9.30	31.26	0.55	4.09	0.00		60.38	10.31	25.48	0.62	3.22	0.00
	18	71.90	14.11	12.39	0.65	0.94	0.00		62.06	10.41	24.11	0.48	2.94	0.00
	19.5	71.62	14.40	12.04	0.97	0.96	0.00		69.24	12.08	16.24	0.76	1.68	0.00
	21	71.20	14.49	12.27	0.95	1.09	0.00		70.72	13.58	13.68	0.83	1.18	0.00
	22.5	71.01	14.89	12.23	1.18	0.68	0.00		70.14	14.02	13.92	1.01	0.91	0.00
	24	70.43	14.99	12.66	1.17	0.74	0.00		69.58	13.98	14.36	1.20	0.89	0.00
	25.5	69.51	14.89	13.74	1.09	0.77	0.00		70.10	14.16	13.74	1.09	0.90	0.00
	27	69.68	15.65	12.84	0.99	0.83	0.00		69.88	14.55	13.56	1.10	0.91	0.00
	28.5	69.96	14.71	13.28	1.23	0.82	0.00		69.47	14.25	14.31	1.04	0.94	0.00
	30	68.34	14.88	14.72	1.18	0.88	0.00		68.95	14.40	14.70	1.04	0.90	0.00
5	0	69.65	14.96	13.27	1.30	0.82	0.00	6	69.69	15.17	13.21	1.22	0.71	0.00
	1.5	69.63	14.84	13.61	1.11	0.81	0.00		69.94	15.00	13.07	1.24	0.75	0.00
	3	69.63	14.94	13.37	1.29	0.76	0.00		69.13	14.88	14.00	1.13	0.86	0.00
	4.5	69.65	14.76	13.50	1.32	0.76	0.00		69.51	14.65	13.85	1.08	0.91	0.00

Meas.	Pos. nm)	Fe	Cr	Ni	Mn	Si	Zr	Meas.	Fe	Cr	Ni	Mn	Si	Zr
5	6	69.92	14.74	13.39	1.28	0.67	0.00	6	70.05	14.71	13.36	1.05	0.83	0.00
	7.5	69.56	15.26	13.06	1.42	0.70	0.00		70.69	14.76	12.59	1.17	0.78	0.00
	9	69.88	14.65	13.51	1.13	0.82	0.00		71.09	14.48	12.46	1.31	0.66	0.00
	10.5	70.89	14.27	12.75	1.26	0.83	0.00		71.07	15.12	11.95	1.03	0.83	0.00
	12	70.55	14.48	12.84	1.27	0.85	0.00		68.46	13.43	15.78	0.76	1.57	0.00
	13.5	71.28	13.74	12.87	0.96	1.15	0.00		67.72	12.91	16.53	0.93	1.90	0.00
	15	67.90	12.49	17.12	0.75	1.74	0.00		62.13	11.22	23.47	0.70	2.48	0.00
	16.5	61.39	10.43	24.54	0.64	2.99	0.00		65.76	11.85	19.52	0.83	2.04	0.00
	18	70.18	12.50	15.31	0.68	1.32	0.00		68.95	12.74	15.99	0.86	1.46	0.00
	19.5	71.38	13.87	12.84	0.95	0.96	0.00		72.01	13.62	12.62	0.81	0.93	0.00
	21	71.53	14.17	12.39	0.96	0.95	0.00		71.15	14.73	12.28	1.07	0.77	0.00
	22.5	71.14	13.88	13.17	0.96	0.85	0.00		71.43	14.54	12.38	1.07	0.58	0.00
	24	70.11	14.35	13.55	1.26	0.72	0.00		71.05	14.96	12.21	1.08	0.71	0.00
	25.5	70.35	14.80	13.13	0.98	0.74	0.00		69.91	14.97	13.12	1.27	0.73	0.00
	27	70.22	14.69	13.17	1.20	0.72	0.00		70.07	15.25	12.83	1.16	0.69	0.00
	28.5	69.14	15.23	13.62	1.24	0.78	0.00		70.30	15.09	12.72	1.22	0.67	0.00
	30	69.23	15.35	13.46	1.19	0.76	0.00		70.02	15.87	12.06	1.29	0.77	0.00
7	0	69.69	15.17	13.21	1.22	0.71	0.00							
	1.5	69.94	15.00	13.07	1.24	0.75	0.00							
	3	69.13	14.88	14.00	1.13	0.86	0.00							
	4.5	69.51	14.65	13.85	1.08	0.91	0.00							
	6	70.05	14.71	13.36	1.05	0.83	0.00							
	7.5	70.69	14.76	12.59	1.17	0.78	0.00							
	9	71.09	14.48	12.46	1.31	0.66	0.00							
	10.5	71.07	15.12	11.95	1.03	0.83	0.00							
	12	68.46	13.43	15.78	0.76	1.57	0.00							
	13.5	67.72	12.91	16.53	0.93	1.90	0.00							
	15	62.13	11.22	23.47	0.70	2.48	0.00							
	16.5	65.76	11.85	19.52	0.83	2.04	0.00							
	18	68.95	12.74	15.99	0.86	1.46	0.00							
	19.5	72.01	13.62	12.62	0.81	0.93	0.00							
	21	71.15	14.73	12.28	1.07	0.77	0.00							
	22.5	71.43	14.54	12.38	1.07	0.58	0.00							
	24	71.05	14.96	12.21	1.08	0.71	0.00							
	25.5	69.91	14.97	13.12	1.27	0.73	0.00							
	27	70.07	15.25	12.83	1.16	0.69	0.00							
	28.5	70.30	15.09	12.72	1.22	0.67	0.00							
	30	70.02	15.87	12.06	1.29	0.77	0.00							

LoZr, 400C, 3 dpa

Meas.	Pos. (nm)	Fe	Cr	Ni	Mn	Si	Zr	Meas.	Fe	Cr	Ni	Mn	Si	Zr
1	0	67.80	16.06	12.64	1.66	1.80	0.04	2	68.00	16.02	12.72	1.44	1.60	0.23
	1.5	67.62	15.72	12.57	2.18	1.61	0.30		67.78	15.74	12.74	1.62	1.91	0.21
	3	67.86	15.96	12.78	1.79	1.63	-0.02		67.56	15.37	13.12	1.92	1.92	0.11
	4.5	67.43	16.65	12.75	1.62	1.53	0.02		67.64	15.56	13.34	1.78	1.73	-0.04
	6	66.63	17.01	12.40	2.24	1.72	0.00		67.29	15.77	13.59	1.58	1.79	-0.02
	7.5	67.52	16.17	12.77	2.17	1.46	-0.09		67.55	16.07	12.75	1.97	1.61	0.05
	9	67.25	17.03	12.04	1.98	1.78	-0.06		67.28	16.69	12.73	1.70	1.76	-0.17
	10.5	68.73	15.18	11.78	2.41	1.81	0.10		67.38	16.63	12.01	2.24	1.64	0.10
	12	67.23	14.37	14.77	1.34	1.98	0.31		67.33	16.56	12.39	2.16	1.55	0.01
	13.5	66.57	13.39	16.00	1.34	2.60	0.10		68.23	15.14	12.94	1.85	1.83	0.01
	15	67.09	14.05	15.09	1.61	2.02	0.14		67.43	13.47	15.12	1.39	2.30	0.29
	16.5	67.74	15.74	12.79	2.12	1.45	0.17		66.58	13.54	15.70	1.71	2.34	0.13
	18	68.14	16.14	11.99	2.42	1.22	0.08		67.89	14.59	14.22	1.43	1.82	0.06
	19.5	69.10	15.33	11.77	1.84	1.63	0.33		68.38	15.09	12.75	1.99	1.65	0.14
	21	67.26	16.37	13.09	1.89	1.29	0.09		67.36	16.40	12.64	2.17	1.32	0.11
	22.5	66.95	16.42	13.15	1.64	1.45	0.39		67.54	15.94	12.79	2.16	1.45	0.12
	24	67.69	16.16	12.81	1.91	1.41	0.02		68.09	15.82	12.63	1.89	1.39	0.19
	25.5	67.15	15.16	13.59	2.08	1.71	0.32		67.58	15.82	12.97	2.17	1.29	0.18
	27	67.38	15.59	13.09	2.03	1.77	0.13		67.24	16.10	13.18	1.87	1.39	0.22
	28.5	68.25	14.99	13.18	1.80	1.67	0.11		68.01	15.85	12.44	2.15	1.40	0.14
	30	67.76	15.65	12.77	2.29	1.53	0.00		67.54	16.02	13.04	1.94	1.39	0.07
3	0	67.39	15.57	13.02	1.91	1.90	0.20	4	68.42	15.63	12.27	1.72	1.74	0.21
	1.5	68.02	15.04	13.13	1.91	1.85	0.05		68.25	15.44	12.37	2.04	1.80	0.10
	3	67.12	16.01	13.27	1.63	1.96	0.02		67.88	15.14	13.24	1.92	1.74	0.08
	4.5	67.46	15.82	12.89	1.68	1.93	0.22		67.31	15.81	13.20	1.86	1.75	0.06
	6	67.83	15.32	12.91	2.20	1.60	0.14		67.88	16.10	12.55	1.66	1.76	0.06
	7.5	67.57	15.89	12.76	1.99	1.66	0.14		67.54	16.06	12.78	1.98	1.65	-0.02
	9	66.90	16.01	13.23	1.99	1.75	0.12		67.11	16.27	12.62	2.13	1.80	0.07
	10.5	66.51	16.31	13.23	2.17	1.68	0.10		67.89	16.25	11.92	2.22	1.57	0.14
	12	67.71	16.07	12.38	2.12	1.54	0.19		67.27	16.19	12.37	2.32	1.60	0.25
	13.5	68.39	16.17	12.17	1.79	1.36	0.13		67.64	16.01	12.41	2.02	1.68	0.24
	15	68.12	15.62	12.26	2.12	1.78	0.09		66.59	14.06	14.66	1.91	2.48	0.29
	16.5	67.54	14.89	13.46	1.78	2.02	0.32		66.62	13.44	15.39	1.69	2.72	0.13
	18	67.11	13.39	15.43	1.60	2.36	0.12		66.63	14.69	14.90	1.28	2.20	0.29
	19.5	66.91	14.39	14.61	1.98	1.94	0.17		67.47	15.09	13.54	1.70	1.96	0.24
	21	68.02	15.34	13.10	1.58	1.89	0.06		68.13	16.14	12.45	1.74	1.41	0.13
	22.5	68.24	15.55	12.88	1.98	1.42	-0.07		67.83	15.92	12.58	2.09	1.45	0.13
	24	67.25	16.13	12.82	2.05	1.60	0.14		67.11	16.68	12.71	1.74	1.51	0.24
	25.5	67.69	15.88	12.74	2.10	1.47	0.13		66.72	16.22	13.08	2.08	1.59	0.31
	27	67.83	16.08	12.44	2.08	1.48	0.09		67.30	15.62	13.49	1.67	1.73	0.19
	28.5	68.01	15.70	12.75	1.57	1.67	0.30		66.74	15.96	13.39	2.20	1.65	0.05
	30	67.93	15.86	12.82	2.02	1.29	0.07		67.99	15.54	12.78	1.74	1.71	0.23
5	0	67.76	14.69	13.53	2.13	1.80	0.09		67.10	15.59	13.19	2.14	1.87	0.11
	1.5	67.55	15.46	13.33	1.78	1.78	0.10		67.31	14.98	13.83	2.10	1.62	0.16
	3	67.66	15.56	13.34	1.86	1.62	-0.04		67.21	15.71	12.97	2.13	1.87	0.10
	4.5	68.09	15.90	12.67	1.64	1.66	0.04		67.29	15.82	13.07	1.77	1.97	0.09

Meas.	Pos. (nm)	Fe	Cr	Ni	Mn	Si	Zr	Meas.	Fe	Cr	Ni	Mn	Si	Zr
5	6	68.33	15.24	12.75	1.99	1.68	0.01	6	66.70	16.00	13.19	2.14	1.77	0.19
	7.5	67.75	15.58	12.80	1.94	1.82	0.11		67.65	16.29	12.52	1.88	1.57	0.08
	9	66.64	16.13	13.29	2.24	1.57	0.13		67.61	15.93	12.48	2.06	1.70	0.22
	10.5	67.37	16.40	12.32	2.10	1.68	0.13		67.34	16.10	12.46	2.03	1.92	0.14
	12	68.28	16.10	11.99	1.81	1.59	0.23		67.37	15.33	13.33	1.80	1.95	0.22
	13.5	68.40	14.96	12.87	1.71	1.81	0.25		66.14	13.87	15.26	1.61	2.84	0.28
	15	66.93	14.61	14.79	1.58	2.04	0.06		66.64	14.25	15.20	1.38	2.33	0.20
	16.5	66.73	13.81	15.03	1.84	2.43	0.17		67.98	15.62	12.34	1.99	1.92	0.15
	18	67.85	14.48	14.26	1.09	1.92	0.40		67.53	16.19	12.18	1.95	2.04	0.11
	19.5	67.69	15.50	13.18	1.79	1.69	0.16		67.05	16.35	12.74	2.01	1.97	-0.12
	21	67.71	16.12	12.22	2.31	1.43	0.22		67.30	15.90	12.95	1.81	2.04	0.01
	22.5	67.11	16.50	12.64	2.06	1.42	0.27		67.48	16.10	12.89	1.70	1.84	-0.01
	24	67.38	16.70	12.59	1.76	1.21	0.35		66.61	16.00	13.41	1.65	2.30	0.02
	25.5	67.36	16.07	12.78	2.04	1.39	0.36		67.17	16.08	12.97	1.91	1.99	-0.11
	27								67.23	15.70	12.97	2.06	1.93	0.10
	28.5								67.67	16.03	12.70	2.00	1.66	-0.05
	30								67.48	15.81	12.95	1.83	1.86	0.07
7	0	68.20	15.41	12.95	1.62	1.71	0.11	8	67.64	15.68	12.78	1.99	1.65	0.26
	1.5	67.85	15.63	12.53	2.01	1.76	0.22		67.65	15.73	12.96	1.74	1.70	0.21
	3	66.63	16.35	13.26	1.92	1.78	0.05		66.65	15.81	13.52	1.84	1.79	0.38
	4.5	67.61	15.99	12.80	1.97	1.64	-0.01		66.85	15.78	13.62	1.99	1.79	-0.02
	6	67.51	16.05	12.60	2.08	1.66	0.10		67.60	15.66	12.75	1.98	1.88	0.13
	7.5	67.38	16.29	12.82	1.74	1.65	0.11		66.71	15.88	13.43	1.94	1.91	0.13
	9	67.47	16.09	12.74	1.90	1.73	0.08		67.82	15.64	12.74	2.05	1.72	0.04
	10.5	67.79	16.41	12.15	1.92	1.58	0.16		67.17	16.31	12.29	2.30	1.75	0.18
	12	68.00	15.64	12.52	2.13	1.65	0.07		68.32	15.49	12.46	1.71	1.82	0.20
	13.5	67.16	15.35	13.52	1.94	1.87	0.15		67.08	14.87	13.91	1.69	2.11	0.34
	15	66.87	13.68	15.25	1.66	2.41	0.13		66.22	14.11	15.32	1.46	2.55	0.33
	16.5	65.89	14.43	15.13	1.50	2.67	0.36		67.52	15.27	13.43	1.68	1.93	0.17
	18	67.05	15.57	13.25	1.61	2.34	0.18		68.19	16.08	12.37	1.58	1.92	-0.15
	19.5	68.04	15.50	12.25	2.14	1.97	0.11		67.39	16.54	12.53	1.83	1.78	-0.06
	21	67.25	16.53	12.67	1.83	1.90	-0.18		66.51	16.48	13.23	1.98	1.86	-0.07
	22.5	67.03	16.08	12.93	1.71	2.09	0.17		67.20	15.65	13.11	2.15	2.00	-0.11
	24	67.14	15.84	13.20	1.69	1.96	0.17		66.60	15.70	13.29	2.15	2.09	0.19
	25.5	67.01	15.43	13.11	2.03	2.22	0.19		68.18	14.76	12.90	2.16	1.89	0.10
	27	67.14	15.48	13.57	1.73	2.04	0.04		67.50	15.41	13.01	1.77	2.16	0.15
	28.5	67.56	16.07	12.64	1.92	1.87	-0.05		67.10	15.39	13.23	1.93	2.22	0.13
	30	67.01	16.66	12.77	1.92	1.88	-0.24		66.92	15.78	13.33	2.05	2.02	-0.11
9	0	67.66	15.36	13.37	1.59	1.85	0.17	10	68.07	15.60	12.69	1.83	1.80	0.01
	1.5	67.59	15.65	12.89	1.98	1.78	0.11		68.33	15.74	12.19	2.00	1.60	0.13
	3	67.63	16.05	12.96	1.52	1.65	0.18		68.03	15.47	12.82	1.76	1.73	0.19
	4.5	67.09	16.08	12.96	2.15	1.44	0.28		67.78	15.68	12.64	2.20	1.51	0.18
	6	67.68	15.65	12.73	2.29	1.58	0.07		67.38	16.34	12.68	1.78	1.58	0.24
	7.5	68.22	15.92	12.23	1.82	1.35	0.46		67.02	15.85	13.08	1.96	1.97	0.12
	9	68.36	15.65	12.31	1.91	1.46	0.31		67.02	16.70	12.62	1.64	1.78	0.24
	10.5	67.39	14.14	14.88	1.36	1.96	0.27		67.55	16.69	12.01	1.90	1.65	0.19
	12	67.37	13.45	15.29	1.35	2.44	0.11		67.77	15.33	13.11	1.85	1.79	0.15

Meas.	Pos. (nm)	Fe	Cr	Ni	Mn	Si	Zr	Meas.	Fe	Cr	Ni	Mn	Si	Zr
9	13.5	65.57	14.64	15.81	1.38	2.38	0.22	10	65.69	14.28	15.43	1.35	2.84	0.41
	15	66.89	15.92	13.50	1.59	2.04	0.07		66.91	15.29	13.97	1.65	2.19	-0.01
	16.5	67.29	16.05	12.83	1.88	1.65	0.29		67.16	16.30	12.79	1.60	1.92	0.24
	18	67.26	16.58	12.34	1.83	2.02	-0.02		67.78	15.96	12.45	1.98	1.83	0.00
	19.5	67.13	16.43	12.56	1.99	1.87	0.01		66.99	16.12	13.07	2.03	1.95	-0.16
	21	68.07	15.94	12.03	2.12	1.81	0.03		67.79	15.73	12.65	1.93	1.91	-0.01
	22.5	67.04	16.54	12.64	1.86	1.81	0.12		67.52	15.91	12.77	1.92	1.94	-0.07
	24	67.77	15.38	12.88	2.10	1.86	0.00		67.32	15.30	13.57	2.11	1.81	-0.11
	25.5	66.96	14.96	13.56	2.40	2.17	-0.04		68.06	15.12	13.09	1.68	2.07	-0.01
	27	67.00	15.64	13.43	1.58	2.08	0.27		67.90	15.31	12.91	1.88	1.99	0.00
	28.5	66.51	16.37	13.14	1.99	2.00	-0.02		67.71	15.45	13.04	1.89	1.91	0.00
	30	67.11	15.65	13.54	1.81	1.94	-0.05		67.91	14.93	12.78	2.11	2.10	0.17
11	0	68.75	15.09	12.84	1.91	1.41	0.02	12	67.30	15.83	12.92	2.12	1.67	0.15
	1.5	67.73	16.11	12.58	2.02	1.43	0.13		67.43	15.52	13.34	1.79	1.99	-0.08
	3	68.47	15.65	12.28	2.00	1.32	0.27		67.75	15.79	12.81	1.98	1.74	-0.08
	4.5	67.34	15.47	13.54	2.36	1.22	0.07		67.53	15.70	12.89	1.75	1.92	0.21
	6	67.66	16.32	12.70	1.78	1.35	0.19		67.76	15.64	12.95	1.88	1.67	0.10
	7.5	67.60	15.63	12.55	2.24	1.62	0.36		67.73	16.29	12.66	1.91	1.31	0.10
	9	68.05	14.24	13.50	2.20	1.74	0.27		68.17	16.14	11.68	2.10	1.80	0.12
	10.5	66.59	13.87	14.94	1.71	2.41	0.49		68.73	16.08	11.46	1.89	1.89	-0.05
	12	66.04	13.88	15.55	1.66	2.60	0.27		67.61	14.37	13.67	1.96	2.01	0.39
	13.5	66.19	14.51	14.51	2.05	2.48	0.26		66.38	14.10	15.10	1.57	2.47	0.37
	15	66.93	15.34	13.52	1.94	2.16	0.12		66.24	14.45	14.89	1.73	2.41	0.27
	16.5	66.41	16.77	13.02	1.72	1.98	0.10		67.10	15.62	13.16	2.03	1.92	0.16
	18	66.93	15.76	13.04	2.12	2.09	0.05		67.50	16.23	12.31	1.85	1.89	0.22
	19.5	66.38	16.07	13.10	2.37	2.09	-0.02		67.54	15.63	12.56	2.26	1.99	0.01
	21	67.26	16.35	12.46	1.78	1.99	0.17		67.02	16.81	12.17	1.80	2.07	0.13
	22.5	67.04	15.82	12.90	2.14	2.01	0.09		67.40	16.99	11.96	1.74	1.78	0.12
	24	67.78	15.79	12.65	1.78	2.03	-0.03		67.18	15.93	12.82	1.97	1.99	0.11
	25.5	67.17	16.62	12.90	1.76	1.61	-0.05		67.32	15.42	13.44	2.19	1.70	-0.08
	27	67.39	16.27	13.25	1.53	1.91	-0.35		67.48	15.87	12.82	1.87	1.91	0.05
	28.5	67.08	15.47	13.59	1.73	2.13	0.00		67.54	16.02	12.67	1.68	1.95	0.14
	30	67.30	15.01	13.36	2.15	2.23	-0.04		67.09	15.84	13.11	2.11	1.86	-0.01
13	0	67.35	15.87	13.15	1.77	1.64	0.22	14	67.73	15.64	13.08	1.92	1.42	0.21
	1.5	67.68	15.65	12.86	1.97	1.50	0.34		66.84	16.29	13.15	1.86	1.53	0.33
	3	68.11	15.01	12.98	2.05	1.45	0.41		65.84	16.62	13.54	2.12	1.68	0.21
	4.5	68.11	15.62	12.60	2.17	1.35	0.15		67.96	15.66	12.69	2.16	1.41	0.12
	6	66.67	16.37	13.27	2.28	1.33	0.09		67.67	16.35	12.06	1.93	1.66	0.33
	7.5	67.86	16.11	12.30	2.00	1.41	0.32		67.19	16.15	12.63	2.16	1.61	0.25
	9	67.41	15.06	13.58	2.13	1.87	-0.05		67.60	15.66	12.98	1.80	1.66	0.29
	10.5	66.70	14.04	14.98	1.77	2.22	0.29		66.54	14.08	14.90	1.79	2.31	0.38
	12	66.58	13.74	15.57	1.54	2.57	0.01		66.07	13.82	16.22	1.23	2.56	0.10
	13.5	66.76	14.54	14.53	1.78	2.18	0.21		67.41	14.51	14.30	1.39	2.24	0.14
	15	67.81	16.28	12.01	1.73	2.17	0.01		67.58	15.54	12.49	2.48	1.92	0.00
	16.5	67.58	16.22	12.43	1.93	1.85	-0.01		67.47	16.32	12.17	1.93	1.91	0.20
	18	67.56	16.21	12.40	2.13	1.83	-0.13		66.66	16.26	12.34	2.59	1.95	0.20
	19.5	67.83	15.89	12.48	1.97	1.81	0.02		66.96	16.62	12.57	1.82	2.11	-0.09

Meas.	Pos. (nm)	Fe	Cr	Ni	Mn	Si	Zr	Meas.	Fe	Cr	Ni	Mn	Si	Zr
	21	67.59	16.75	11.93	1.98	1.91	-0.16		66.70	16.27	12.98	1.98	1.90	0.17
	22.5	68.35	15.44	12.18	2.05	2.00	-0.02		66.00	16.37	13.58	2.34	1.89	-0.18
	24	66.74	16.26	13.18	1.71	2.15	-0.05		68.20	15.93	12.77	1.70	1.74	-0.33
	25.5	67.51	15.41	12.90	2.13	2.09	-0.03		66.77	16.44	12.66	1.87	2.16	0.10
	27	68.38	14.91	13.00	1.83	2.11	-0.23		68.13	15.37	12.47	2.10	2.00	-0.07
	28.5	67.64	15.08	13.10	2.08	2.02	0.08		67.99	15.83	12.27	2.15	1.80	-0.05
	30	68.37	14.96	12.64	2.07	2.10	-0.14		67.18	15.78	12.86	2.16	2.12	-0.11
15	0	68.31	15.64	12.99	1.73	1.21	0.12							
	1.5	67.84	15.96	12.63	1.76	1.52	0.28							
	3	67.69	15.89	12.82	1.99	1.30	0.32							
	4.5	66.99	16.03	13.18	1.99	1.55	0.26							
	6	66.99	16.10	13.41	2.17	1.30	0.03							
	7.5	66.59	16.44	12.74	2.09	1.88	0.26							
	9	68.25	16.12	11.75	2.10	1.55	0.24							
	10.5	68.61	15.66	11.84	2.07	1.48	0.33							
	12	68.40	15.28	12.74	1.84	1.71	0.03							
	13.5	67.37	14.29	14.32	1.67	2.14	0.21							
	15	66.46	13.45	15.91	1.24	2.70	0.25							
	16.5	65.96	14.58	15.00	1.65	2.55	0.25							
	18	68.29	15.49	12.22	2.01	2.02	-0.03							
	19.5	66.99	15.97	12.94	2.31	1.71	0.09							
	21	66.86	15.85	13.23	2.29	1.85	-0.07							
	22.5	67.82	15.93	12.35	2.09	1.81	0.01							
	24	67.90	15.82	12.54	1.74	1.91	0.11							
	25.5	67.03	15.74	13.31	1.98	1.83	0.11							
	27	67.12	15.85	13.24	1.84	1.99	-0.04							
	28.5	68.16	15.37	12.86	1.76	1.94	-0.10							
	30	67.83	16.01	12.62	1.26	2.15	0.13							

LoZr, 400C, 7 dpa

Meas.	Pos. (nm)	Fe	Cr	Ni	Mn	Si	Zr	Meas.	Fe	Cr	Ni	Mn	Si	Zr
1	0	68.22	15.55	14.25	1.10	0.70	0.18	2	70.37	15.71	11.70	1.36	0.67	0.19
	1.5	66.49	14.77	16.93	0.89	0.73	0.18		70.24	16.23	10.99	1.69	0.66	0.18
	3	65.37	13.56	19.17	0.98	0.77	0.15		70.15	16.85	10.67	1.54	0.62	0.18
	4.5	69.45	14.47	14.03	1.20	0.65	0.20		69.60	14.68	13.55	1.31	0.70	0.17
	6	71.87	13.50	12.76	1.01	0.66	0.20		68.58	13.73	15.65	1.09	0.78	0.16
	7.5	72.91	15.12	10.33	1.02	0.49	0.13		70.96	13.57	13.14	1.30	0.82	0.21
	9	70.49	16.15	11.31	1.31	0.56	0.17		70.71	15.39	11.34	1.75	0.59	0.21
	10.5	70.09	16.11	11.59	1.47	0.54	0.20		72.28	16.20	9.53	1.17	0.62	0.21
	12	69.73	14.66	13.94	0.90	0.60	0.18		72.43	12.39	13.31	0.73	0.96	0.19
	13.5	73.95	13.96	10.20	1.08	0.62	0.20		64.22	10.30	22.99	0.57	1.64	0.28
	15	60.44	8.13	28.61	0.69	1.89	0.24		65.11	12.48	19.52	1.13	1.50	0.26
	16.5	57.75	7.26	32.02	0.76	2.00	0.21		70.23	15.59	11.85	1.01	1.14	0.18
	18	70.24	13.77	13.78	1.23	0.85	0.14		69.33	15.39	12.72	1.37	1.01	0.18
	19.5	72.13	14.46	11.14	1.44	0.67	0.16		67.98	16.68	12.76	1.45	0.97	0.17
	21	67.99	16.60	12.88	1.69	0.68	0.15		70.43	15.77	11.60	1.14	0.87	0.19
	22.5	71.79	16.54	9.28	1.45	0.78	0.15		71.54	15.05	10.99	1.48	0.74	0.20
	24	69.60	17.90	10.59	1.13	0.59	0.20		70.15	15.36	11.84	1.64	0.84	0.18
	25.5	67.20	18.55	12.10	1.17	0.83	0.15		69.62	15.13	12.71	1.64	0.69	0.20
	27	69.44	15.05	13.13	1.44	0.76	0.18		70.25	15.48	11.88	1.59	0.64	0.16
	28.5	70.25	16.91	11.00	1.00	0.67	0.18		69.01	15.79	13.02	1.37	0.63	0.19
	30	70.58	16.10	11.54	0.91	0.70	0.17		69.86	16.29	11.88	1.01	0.79	0.16
3	0	64.89	14.68	17.78	1.52	0.92	0.20	4	64.89	14.68	17.78	1.52	0.92	0.20
	1.5	66.36	14.11	17.39	1.16	0.80	0.19		66.36	14.11	17.39	1.16	0.80	0.19
	3	66.06	16.15	15.50	1.32	0.81	0.17		66.06	16.15	15.50	1.32	0.81	0.17
	4.5	67.82	16.28	13.56	1.39	0.75	0.20		67.82	16.28	13.56	1.39	0.75	0.20
	6	69.54	16.46	11.73	1.39	0.69	0.19		69.54	16.46	11.73	1.39	0.69	0.19
	7.5	70.60	16.52	10.28	1.70	0.67	0.23		70.60	16.52	10.28	1.70	0.67	0.23
	9	71.44	16.63	9.62	1.49	0.64	0.19		71.44	16.63	9.62	1.49	0.64	0.19
	10.5	73.51	14.36	10.28	1.07	0.59	0.20		73.51	14.36	10.28	1.07	0.59	0.20
	12	67.65	10.58	19.71	0.46	1.36	0.24		67.65	10.58	19.71	0.46	1.36	0.24
	13.5	62.10	9.87	25.57	0.31	1.85	0.30		62.10	9.87	25.57	0.31	1.85	0.30
	15	70.00	14.36	13.76	0.79	0.91	0.19		70.00	14.36	13.76	0.79	0.91	0.19
	16.5	70.34	15.37	11.92	1.50	0.68	0.18		70.34	15.37	11.92	1.50	0.68	0.18
	18	68.14	17.03	12.01	1.80	0.82	0.19		68.14	17.03	12.01	1.80	0.82	0.19
	19.5	69.75	16.46	11.25	1.48	0.84	0.22		69.75	16.46	11.25	1.48	0.84	0.22
	21	69.65	16.96	11.34	1.14	0.73	0.18		69.65	16.96	11.34	1.14	0.73	0.18
	22.5	69.59	17.02	11.26	1.22	0.74	0.17		69.59	17.02	11.26	1.22	0.74	0.17
	24	70.22	16.36	11.21	1.28	0.77	0.17		70.22	16.36	11.21	1.28	0.77	0.17
	25.5	70.78	15.87	10.95	1.50	0.70	0.20		70.78	15.87	10.95	1.50	0.70	0.20
	27	70.87	15.79	10.98	1.45	0.70	0.21		70.87	15.79	10.98	1.45	0.70	0.21
	28.5	69.69	15.30	13.04	0.93	0.84	0.19		69.69	15.30	13.04	0.93	0.84	0.19
	30	69.00	14.01	14.68	1.12	1.00	0.19		69.00	14.01	14.68	1.12	1.00	0.19
5	0	69.13	16.56	12.35	1.10	0.61	0.24		68.34	15.45	13.43	1.66	0.92	0.20
	1.5	70.17	15.29	12.30	1.34	0.72	0.18		67.19	13.68	16.65	1.37	0.96	0.16
	3	68.35	13.77	15.76	1.10	0.84	0.18		67.85	15.53	13.91	1.61	0.89	0.21
	4.5	66.53	14.29	16.89	1.25	0.87	0.18		68.88	15.43	13.06	1.61	0.81	0.21

Meas.	Pos. (nm)	Fe	Cr	Ni	Mn	Si	Zr	Meas.	Fe	Cr	Ni	Mn	Si	Zr
5	6	69.02	13.03	15.40	1.57	0.77	0.21	6	68.74	15.19	13.73	1.40	0.71	0.23
	7.5	70.68	15.05	12.17	1.23	0.68	0.19		69.35	15.74	12.10	1.76	0.86	0.18
	9	71.17	15.05	11.55	1.39	0.65	0.20		70.15	15.28	12.31	1.33	0.74	0.20
	10.5	71.56	15.26	11.52	0.72	0.71	0.24		73.21	14.05	10.49	1.30	0.72	0.22
	12	66.89	12.00	18.92	0.53	1.43	0.22		62.03	8.93	25.93	0.84	2.01	0.26
	13.5	63.36	9.37	24.90	0.57	1.64	0.17		66.63	10.01	20.90	0.80	1.42	0.23
	15	71.24	13.33	13.58	0.81	0.84	0.21		69.62	12.19	16.21	1.00	0.81	0.18
	16.5	69.17	16.41	12.22	1.13	0.88	0.20		69.88	16.79	10.99	1.32	0.83	0.20
	18	70.68	16.44	10.54	1.46	0.69	0.18		70.24	14.83	12.66	1.37	0.71	0.20
	19.5	70.51	16.86	10.41	1.43	0.59	0.21		68.74	14.30	14.94	1.10	0.71	0.22
	21	67.67	17.07	12.70	1.70	0.67	0.19		69.00	13.90	15.15	1.14	0.62	0.19
	22.5	69.63	16.57	11.37	1.62	0.64	0.16		72.16	14.70	11.63	0.64	0.69	0.17
	24	70.74	15.60	11.10	1.70	0.65	0.20		73.46	12.44	12.20	1.24	0.47	0.18
	25.5	70.59	15.65	11.76	1.23	0.60	0.17		71.35	14.17	12.09	1.44	0.74	0.23
	27	71.44	14.81	11.69	1.18	0.70	0.18		71.79	15.34	11.25	0.83	0.63	0.16
	28.5	72.13	14.44	11.37	0.96	0.92	0.18		73.17	12.30	12.34	1.08	0.83	0.27
	30	69.17	15.52	12.82	1.40	0.90	0.19		72.20	13.07	12.83	0.92	0.73	0.24
7	0	66.30	14.03	17.32	1.24	0.86	0.25							
	1.5	68.15	14.54	15.10	1.14	0.85	0.22							
	3	70.36	12.82	14.15	1.56	0.90	0.22							
	4.5	68.12	14.56	14.95	1.16	0.97	0.23							
	6	68.40	14.16	15.25	1.09	0.79	0.30							
	7.5	68.57	16.82	12.57	1.08	0.73	0.22							
	9	69.21	16.68	12.20	0.91	0.78	0.22							
	10.5	72.88	12.07	12.78	1.04	1.04	0.20							
	12	62.43	8.21	26.60	0.59	1.95	0.22							
	13.5	68.94	10.47	18.56	0.68	1.15	0.20							
	15	72.18	13.02	12.83	0.90	0.85	0.22							
	16.5	70.25	15.04	12.47	1.26	0.77	0.22							
	18	70.21	14.83	12.78	1.35	0.65	0.18							
	19.5	72.49	13.68	12.02	1.00	0.60	0.21							
	21	71.25	14.96	11.96	1.02	0.61	0.20							
	22.5	73.05	14.89	10.09	1.08	0.70	0.18							
	24	73.07	13.10	12.03	0.72	0.85	0.23							
	25.5	70.10	14.90	12.77	1.12	0.88	0.23							
	27	72.51	12.92	12.71	0.79	0.80	0.26							
	28.5	68.83	15.77	12.79	1.43	0.90	0.28							
	30	68.46	15.20	13.83	1.39	0.91	0.21							

LoZr, 400C, 10 dpa

Meas.	Pos. (nm)	Fe	Cr	Ni	Mn	Si	Zr	Meas.	Fe	Cr	Ni	Mn	Si	Zr
1	0	69.05	16.20	11.86	1.27	0.23	1.39	2	69.05	16.2	11.86	1.271	0.233	1.385
	1.5	69.64	16.01	11.07	1.71	0.25	1.32		69.64	16.01	11.07	1.706	0.254	1.32
	3	68.08	16.45	12.25	1.42	0.32	1.49		68.08	16.45	12.25	1.419	0.315	1.49
	4.5	70.12	14.52	12.09	1.65	0.25	1.37		70.12	14.52	12.09	1.649	0.246	1.374
	6	66.67	13.84	16.29	0.88	0.30	2.02		66.67	13.84	16.29	0.879	0.304	2.015
	7.5	68.01	15.26	13.94	1.16	0.36	1.27		68.01	15.26	13.94	1.164	0.359	1.269
	9	67.52	12.46	16.17	1.05	0.41	2.39		67.52	12.46	16.17	1.048	0.408	2.391
	10.5	62.81	10.18	22.71	1.11	0.34	2.84		62.81	10.18	22.71	1.114	0.339	2.843
	12	66.13	11.00	19.57	0.96	0.31	2.02		66.13	11	19.57	0.958	0.315	2.024
	13.5	68.50	14.09	14.02	1.40	0.38	1.60		68.5	14.09	14.02	1.402	0.381	1.596
	15	69.45	13.23	14.26	1.39	0.26	1.41		69.45	13.23	14.26	1.392	0.255	1.409
	16.5	68.84	15.01	12.41	1.59	0.36	1.79		68.84	15.01	12.41	1.591	0.359	1.793
	18	68.81	15.65	12.28	1.38	0.35	1.54		68.81	15.65	12.28	1.377	0.351	1.536
	19.5	69.75	15.04	11.90	1.62	0.28	1.41		69.75	15.04	11.9	1.625	0.277	1.411
	21	68.16	15.86	12.84	1.72	0.29	1.12		68.16	15.86	12.84	1.723	0.292	1.123
	22.5	68.76	15.45	12.40	1.46	0.37	1.55		68.76	15.45	12.4	1.461	0.373	1.553
	24	68.01	15.56	13.18	1.50	0.29	1.46		68.01	15.56	13.18	1.503	0.289	1.457
	25.5	68.78	15.35	12.77	1.59	0.35	1.16		68.78	15.35	12.77	1.59	0.354	1.162
	27	67.84	15.28	13.54	1.45	0.38	1.51		67.84	15.28	13.54	1.448	0.383	1.508
	28.5	66.97	16.16	14.16	1.16	0.36	1.18		66.97	16.16	14.16	1.162	0.365	1.178
	30								67.53	13.95	14.84	1.662	0.33	1.688
3	0	67.86	14.91	14.66	1.46	0.22	0.89	4	67.86	14.91	14.66	1.462	0.217	0.89
	1.5	69.42	15.33	12.60	1.43	0.24	0.98		69.42	15.33	12.6	1.434	0.239	0.975
	3	69.70	15.38	12.37	1.28	0.20	1.06		69.7	15.38	12.37	1.279	0.201	1.064
	4.5	69.31	15.54	12.52	1.48	0.22	0.92		69.31	15.54	12.52	1.484	0.223	0.922
	6	69.49	15.89	11.95	1.48	0.23	0.96		69.49	15.89	11.95	1.48	0.23	0.96
	7.5	69.04	15.59	12.86	1.32	0.21	0.98		69.04	15.59	12.86	1.321	0.214	0.979
	9	68.59	16.00	12.84	1.53	0.21	0.83		68.59	16	12.84	1.53	0.208	0.831
	10.5	69.45	16.35	11.54	1.54	0.23	0.88		69.45	16.35	11.54	1.545	0.229	0.885
	12	70.62	15.66	11.23	1.26	0.21	1.02		70.62	15.66	11.23	1.258	0.21	1.024
	13.5	71.28	15.59	10.78	1.18	0.21	0.96		71.28	15.59	10.78	1.176	0.213	0.963
	15	70.96	13.16	13.51	0.98	0.22	1.18		70.96	13.16	13.51	0.979	0.215	1.184
	16.5	66.65	11.17	19.37	0.98	0.23	1.60		66.65	11.17	19.37	0.979	0.235	1.597
	18	65.31	10.83	21.03	0.83	0.24	1.76		65.31	10.83	21.03	0.833	0.238	1.758
	19.5	70.29	12.57	14.59	1.22	0.17	1.16		70.29	12.57	14.59	1.216	0.173	1.156
	21	70.66	15.55	11.30	1.35	0.18	0.96		70.66	15.55	11.3	1.349	0.176	0.962
	22.5	70.07	16.13	11.55	1.17	0.18	0.90		70.07	16.13	11.55	1.172	0.181	0.898
	24	70.57	16.01	11.15	1.33	0.17	0.78		70.57	16.01	11.15	1.328	0.169	0.779
	25.5	69.97	15.82	11.83	1.40	0.17	0.82		69.97	15.82	11.83	1.396	0.167	0.82
	27	69.44	15.63	12.70	1.31	0.17	0.75		69.44	15.63	12.7	1.308	0.166	0.753
	28.5	69.99	15.33	12.08	1.58	0.16	0.85		69.99	15.33	12.08	1.583	0.159	0.853
	30								69.71	16.18	11.87	1.29	0.18	0.78
5	0	69.04	14.41	14.70	1.05	0.11	0.69	6	69.04	14.41	14.7	1.051	0.107	0.691
	1.5	68.76	14.81	14.43	1.27	0.14	0.60		68.76	14.81	14.43	1.267	0.144	0.596
	3	70.07	15.34	12.64	1.29	0.12	0.54		70.07	15.34	12.64	1.292	0.12	0.542
	4.5	69.73	15.48	12.85	1.26	0.13	0.56		69.73	15.48	12.85	1.255	0.134	0.562

Meas.	Pos. (nm)	Fe	Cr	Ni	Mn	Si	Zr	Meas.	Fe	Cr	Ni	Mn	Si	Zr
5	6	69.52	14.99	13.61	1.19	0.15	0.54	6	69.52	14.99	13.61	1.188	0.153	0.54
	7.5	69.26	15.35	13.16	1.34	0.17	0.72		69.26	15.35	13.16	1.342	0.175	0.72
	9	68.64	15.52	13.57	1.50	0.14	0.63		68.64	15.52	13.57	1.505	0.138	0.627
	10.5	68.76	15.52	13.67	1.33	0.16	0.56		68.76	15.52	13.67	1.333	0.162	0.562
	12	69.27	15.63	12.86	1.44	0.16	0.65		69.27	15.63	12.86	1.443	0.156	0.647
	13.5	69.85	15.85	12.08	1.42	0.13	0.66		69.85	15.85	12.08	1.425	0.13	0.664
	15	70.40	16.88	10.50	1.45	0.14	0.64		70.4	16.88	10.5	1.447	0.139	0.637
	16.5	71.21	17.09	9.69	1.36	0.15	0.50		71.21	17.09	9.691	1.356	0.152	0.504
	18	71.11	16.83	9.97	1.39	0.16	0.54		71.11	16.83	9.967	1.389	0.158	0.544
	19.5	71.88	14.87	11.39	1.15	0.13	0.58		71.88	14.87	11.39	1.15	0.133	0.576
	21	70.73	13.10	14.22	1.09	0.17	0.69		70.73	13.1	14.22	1.087	0.169	0.693
	22.5	67.22	11.11	19.97	0.72	0.15	0.83		67.22	11.11	19.97	0.72	0.153	0.827
	24	65.70	11.91	20.54	0.72	0.15	0.99		65.7	11.91	20.54	0.718	0.148	0.992
	25.5	70.48	13.44	14.25	1.00	0.14	0.69		70.48	13.44	14.25	1.004	0.135	0.69
	27	70.85	15.16	12.23	1.15	0.10	0.51		70.85	15.16	12.23	1.151	0.102	0.507
	28.5	70.16	15.51	12.61	1.17	0.08	0.47		70.16	15.51	12.61	1.173	0.08	0.465
	30	70.33	14.63	12.91	1.47	0.12	0.54		70.33	14.63	12.91	1.474	0.115	0.536
7	0	69.49	14.90	13.62	1.28	0.15	0.55	8	69.49	14.9	13.62	1.283	0.152	0.547
	1.5	69.88	15.48	12.56	1.26	0.14	0.67		69.88	15.48	12.56	1.262	0.145	0.674
	3	70.14	15.33	12.52	1.24	0.12	0.65		70.14	15.33	12.52	1.236	0.118	0.651
	4.5	69.95	14.73	13.20	1.27	0.17	0.68		69.95	14.73	13.2	1.273	0.168	0.683
	6	70.16	14.99	12.79	1.25	0.14	0.66		70.16	14.99	12.79	1.251	0.142	0.663
	7.5	69.72	15.37	13.02	1.11	0.14	0.64		69.72	15.37	13.02	1.114	0.141	0.637
	9	70.67	15.27	12.00	1.37	0.16	0.53		70.67	15.27	12	1.371	0.163	0.535
	10.5	70.63	15.89	11.60	1.20	0.14	0.55		70.63	15.89	11.6	1.196	0.14	0.545
	12	70.17	15.70	12.19	1.09	0.15	0.70		70.17	15.7	12.19	1.086	0.152	0.705
	13.5	70.82	15.04	12.12	1.26	0.17	0.58		70.82	15.04	12.12	1.264	0.171	0.584
	15	69.88	15.71	12.31	1.27	0.17	0.67		69.88	15.71	12.31	1.267	0.168	0.667
	16.5	70.32	15.71	12.17	1.11	0.17	0.53		70.32	15.71	12.17	1.109	0.168	0.527
	18	69.87	16.05	12.27	1.08	0.13	0.59		69.87	16.05	12.27	1.084	0.134	0.588
	19.5	70.88	14.74	12.63	1.07	0.12	0.56		70.88	14.74	12.63	1.073	0.116	0.563
	21	70.43	13.95	13.55	1.19	0.14	0.74		70.43	13.95	13.55	1.194	0.137	0.737
	22.5	68.37	12.62	17.22	0.87	0.18	0.73		68.37	12.62	17.22	0.872	0.181	0.731
	24	65.72	10.24	21.74	1.00	0.18	1.12		65.72	10.24	21.74	0.998	0.184	1.119
	25.5	64.68	11.32	21.79	0.95	0.16	1.10		64.68	11.32	21.79	0.945	0.163	1.103
	27	70.78	13.28	14.03	1.09	0.15	0.68		70.78	13.28	14.03	1.086	0.147	0.683
	28.5	70.92	14.57	12.51	1.26	0.12	0.62		70.92	14.57	12.51	1.26	0.119	0.617
	30	70.89	15.44	11.74	1.30	0.12	0.52		70.89	15.44	11.74	1.296	0.115	0.518
9	0	69.34	15.07	13.35	1.38	0.13	0.72	10	69.34	15.07	13.35	1.382	0.133	0.722
	1.5	69.43	14.68	13.45	1.43	0.19	0.83		69.43	14.68	13.45	1.426	0.188	0.829
	3	68.76	15.02	13.78	1.27	0.20	0.98		68.76	15.02	13.78	1.268	0.197	0.978
	4.5	69.36	15.56	12.84	1.14	0.18	0.92		69.36	15.56	12.84	1.14	0.183	0.916
	6	69.29	15.46	12.94	1.19	0.18	0.95		69.29	15.46	12.94	1.189	0.176	0.952
	7.5	69.30	15.63	12.57	1.42	0.20	0.87		69.3	15.63	12.57	1.424	0.203	0.868
	9	69.09	15.74	12.73	1.36	0.22	0.86		69.09	15.74	12.73	1.357	0.224	0.864
	10.5	69.52	15.95	12.36	1.23	0.19	0.75		69.52	15.95	12.36	1.234	0.193	0.748
	12	69.76	16.16	11.68	1.42	0.19	0.80		69.76	16.16	11.68	1.424	0.189	0.795

Meas.	Pos. (nm)	Fe	Cr	Ni	Mn	Si	Zr	Meas.	Fe	Cr	Ni	Mn	Si	Zr
9	13.5	69.74	16.00	11.85	1.28	0.21	0.92	10	69.74	16	11.85	1.284	0.211	0.923
	15	70.62	14.91	12.25	1.07	0.18	0.98		70.62	14.91	12.25	1.065	0.178	0.98
	16.5	68.79	14.15	14.77	1.08	0.21	1.00		68.79	14.15	14.77	1.084	0.214	1.002
	18	66.07	11.58	19.88	1.03	0.15	1.28		66.07	11.58	19.88	1.026	0.15	1.284
	19.5	63.79	11.30	22.23	0.96	0.16	1.56		63.79	11.3	22.23	0.958	0.16	1.565
	21	67.52	12.50	17.80	0.97	0.16	1.05		67.52	12.5	17.8	0.967	0.159	1.046
	22.5	70.22	14.90	12.98	1.05	0.13	0.71		70.22	14.9	12.98	1.047	0.135	0.714
	24	70.33	15.31	12.32	1.26	0.15	0.64		70.33	15.31	12.32	1.259	0.149	0.639
	25.5	69.92	15.15	12.68	1.41	0.16	0.69		69.92	15.15	12.68	1.408	0.159	0.687
	27	70.23	15.22	12.50	1.20	0.16	0.68		70.23	15.22	12.5	1.197	0.16	0.682
	28.5	69.68	15.72	12.49	1.13	0.18	0.80		69.68	15.72	12.49	1.128	0.18	0.804
	30	68.56	16.16	13.15	1.11	0.14	0.88		68.56	16.16	13.15	1.105	0.144	0.884
11	0	68.75	14.35	14.29	1.21	0.34	1.06	12	68.75	14.35	14.29	1.209	0.339	1.061
	1.5	68.47	14.99	13.94	1.23	0.33	1.03		68.47	14.99	13.94	1.234	0.33	1.033
	3	68.98	14.24	14.09	1.21	0.36	1.13		68.98	14.24	14.09	1.21	0.359	1.125
	4.5	66.54	14.66	16.04	1.27	0.36	1.14		66.54	14.66	16.04	1.267	0.363	1.139
	6	66.87	14.17	16.15	1.20	0.39	1.23		66.87	14.17	16.15	1.196	0.393	1.231
	7.5	67.51	13.34	16.23	1.38	0.37	1.17		67.51	13.34	16.23	1.377	0.372	1.167
	9	68.96	14.53	13.98	1.24	0.31	0.98		68.96	14.53	13.98	1.244	0.312	0.978
	10.5	69.03	15.31	12.94	1.23	0.36	1.13		69.03	15.31	12.94	1.23	0.36	1.129
	12	70.63	14.63	11.98	1.37	0.34	1.06		70.63	14.63	11.98	1.367	0.339	1.062
	13.5	69.54	14.41	13.01	1.36	0.41	1.27		69.54	14.41	13.01	1.361	0.406	1.271
	15	69.65	12.53	14.97	1.04	0.44	1.37		69.65	12.53	14.97	1.04	0.439	1.375
	16.5	66.06	11.34	19.82	0.73	0.50	1.56		66.06	11.34	19.82	0.728	0.497	1.557
	18	64.83	10.60	21.46	0.79	0.56	1.76		64.83	10.6	21.46	0.785	0.562	1.762
	19.5	66.46	11.06	19.57	0.87	0.49	1.55		66.46	11.06	19.57	0.866	0.493	1.546
	21	69.29	13.32	15.00	1.02	0.33	1.04		69.29	13.32	15	1.017	0.332	1.04
	22.5	69.86	15.30	12.29	1.36	0.29	0.90		69.86	15.3	12.29	1.355	0.288	0.902
	24	70.46	15.77	11.67	1.07	0.25	0.78		70.46	15.77	11.67	1.074	0.25	0.784
	25.5	69.96	15.80	11.65	1.47	0.27	0.86		69.96	15.8	11.65	1.465	0.274	0.86
	27	69.24	15.96	12.31	1.46	0.25	0.78		69.24	15.96	12.31	1.456	0.25	0.784
	28.5	68.79	16.05	12.68	1.32	0.28	0.88		68.79	16.05	12.68	1.321	0.279	0.876
	30	69.63	15.32	12.75	1.29	0.25	0.77		69.63	15.32	12.75	1.287	0.245	0.769
13	0	69.21	15.89	12.73	1.17	0.34	0.66	14	69.21	15.89	12.73	1.174	0.337	0.662
	1.5	69.61	16.35	11.72	1.31	0.27	0.74		69.61	16.35	11.72	1.314	0.268	0.742
	3	70.26	15.58	11.48	1.54	0.32	0.82		70.26	15.58	11.48	1.544	0.323	0.816
	4.5	69.19	15.48	13.08	1.20	0.34	0.71		69.19	15.48	13.08	1.196	0.343	0.713
	6	70.08	15.43	11.88	1.52	0.32	0.77		70.08	15.43	11.88	1.516	0.325	0.773
	7.5	69.82	15.61	12.10	1.37	0.32	0.79		69.82	15.61	12.1	1.367	0.321	0.789
	9	69.12	15.67	12.92	1.25	0.30	0.74		69.12	15.67	12.92	1.253	0.303	0.737
	10.5	69.86	16.23	11.40	1.48	0.33	0.70		69.86	16.23	11.4	1.481	0.327	0.701
	12	70.26	16.09	11.34	1.32	0.35	0.65		70.26	16.09	11.34	1.321	0.347	0.646
	13.5	69.64	15.56	12.56	0.95	0.36	0.93		69.64	15.56	12.56	0.953	0.357	0.928
	15	68.11	12.64	16.96	0.94	0.47	0.88		68.11	12.64	16.96	0.941	0.466	0.883
	16.5	62.72	10.18	24.85	0.84	0.57	0.83		62.72	10.18	24.85	0.84	0.572	0.832
	18	64.76	10.69	22.25	0.90	0.56	0.85		64.76	10.69	22.25	0.896	0.556	0.845
	19.5	67.83	13.46	16.21	1.38	0.42	0.71		67.83	13.46	16.21	1.376	0.418	0.707

Meas.	Pos. (nm)	Fe	Cr	Ni	Mn	Si	Zr	Meas.	Fe	Cr	Ni	Mn	Si	Zr
13	21	70.16	15.67	12.39	0.96	0.28	0.53	14	70.16	15.67	12.39	0.964	0.284	0.533
	22.5	70.59	15.23	12.26	1.27	0.32	0.34		70.59	15.23	12.26	1.268	0.317	0.341
	24	69.78	16.06	11.77	1.57	0.28	0.54		69.78	16.06	11.77	1.57	0.285	0.535
	25.5	69.15	16.40	12.06	1.41	0.38	0.59		69.15	16.4	12.06	1.412	0.379	0.594
	27	69.03	15.81	12.82	1.38	0.34	0.63		69.03	15.81	12.82	1.385	0.336	0.629
	28.5	68.63	15.39	14.15	1.05	0.27	0.51		68.63	15.39	14.15	1.049	0.274	0.508
	30	67.77	15.38	14.95	1.08	0.33	0.49		67.77	15.38	14.95	1.083	0.329	0.49

HiZr, 400C, 3 dpa, 3.2 MeV p+

Meas.	Pos. (nm)	Fe	Cr	Ni	Mn	Zr	Si	Meas.	Fe	Cr	Ni	Mn	Zr	Si
1	0	70.01	15.13	12.41	1.22	0.38	0.87	2	69.10	14.64	13.11	1.46	0.76	0.93
	1.5	70.02	14.59	13.41	1.53	0.55	1.00		70.14	14.69	12.73	1.37	0.21	0.86
	3	69.97	14.94	12.72	1.26	0.12	0.99		69.94	14.73	12.53	1.58	0.36	0.85
	4.5	69.73	14.81	13.07	1.31	0.04	1.13		70.69	15.11	12.37	1.42	-0.46	0.87
	6	69.85	15.11	12.87	1.59	0.26	0.85		70.06	15.14	13.19	1.47	-0.74	0.88
	7.5	69.38	15.05	12.59	1.24	0.77	0.97		69.17	14.56	13.25	1.48	0.57	0.97
	9	69.36	15.31	12.77	1.55	0.01	1.02		69.48	14.98	13.03	1.46	0.02	1.02
	10.5	70.07	15.67	12.20	1.65	0.46	0.87		69.45	14.95	12.39	1.77	0.52	0.92
	12	70.98	15.17	12.04	1.49	0.67	1.00		69.38	15.34	12.56	1.23	0.58	0.91
	13.5	70.59	14.44	12.67	1.28	0.03	1.05		69.91	14.44	12.62	1.59	0.42	1.03
	15	68.16	12.53	15.32	1.11	1.47	1.40		69.94	14.60	13.38	1.25	-0.18	1.01
	16.5	68.98	13.32	14.09	1.25	0.93	1.43		68.65	13.21	14.82	1.10	0.85	1.37
	18	70.75	13.98	12.30	1.37	0.61	1.00		69.15	13.59	14.27	1.15	0.39	1.45
	19.5	69.67	15.37	12.31	1.53	0.22	0.90		69.98	14.91	12.71	1.45	0.04	0.91
	21	68.91	15.27	12.70	1.57	0.61	0.94		69.10	15.17	12.09	1.31	1.48	0.85
	22.5	68.95	15.20	12.65	1.44	0.76	1.01		70.06	15.03	12.20	1.34	0.37	0.99
	24	69.40	14.99	12.29	1.44	0.90	0.97		69.81	15.27	11.87	1.49	0.74	0.83
	25.5	69.47	14.63	12.31	1.26	1.34	1.00		69.43	15.24	12.12	1.44	0.82	0.95
	27	70.40	15.00	12.49	1.20	0.03	0.94		69.29	14.64	13.28	1.42	0.37	1.00
	28.5	68.93	14.76	13.13	1.40	0.74	1.05		69.69	14.65	12.88	1.25	0.60	0.93
	30	70.30	14.25	12.68	1.24	0.45	1.08		69.67	14.45	12.48	1.47	0.87	1.06
3	0	70.58	14.59	13.59	0.61	0.21	0.43	4	68.81	14.99	13.43	1.41	0.31	1.06
	1.5	70.69	15.01	12.43	0.91	0.45	0.51		68.88	14.79	13.09	1.46	0.85	0.93
	3	70.87	14.90	12.95	0.97	0.19	0.49		69.10	15.43	13.29	1.41	-0.23	1.01
	4.5	71.44	14.96	13.25	0.56	0.70	0.49		68.64	15.06	12.78	1.37	1.23	0.92
	6	69.80	14.83	13.05	0.82	1.03	0.47		69.70	14.93	12.42	1.38	0.59	0.98
	7.5	70.35	14.95	12.74	1.21	0.31	0.45		69.44	15.33	13.08	1.52	-0.18	0.82
	9	70.78	15.61	12.88	0.76	0.42	0.38		68.32	14.98	12.76	1.46	1.63	0.85
	10.5	71.20	15.38	11.90	0.90	0.29	0.32		70.47	15.10	12.42	1.46	-0.37	0.93
	12	70.46	16.05	12.40	0.87	0.18	0.40		70.46	15.38	12.17	1.37	-0.35	0.96
	13.5	71.56	14.92	13.13	0.75	0.82	0.46		69.19	14.36	13.51	1.30	0.59	1.05
	15	70.03	13.57	14.50	0.49	0.62	0.79		69.13	13.55	14.94	1.11	-0.17	1.44
	16.5	68.12	12.82	16.12	0.50	1.32	1.12		66.37	13.10	15.81	1.00	2.03	1.68
	18	70.09	14.29	13.63	0.63	0.70	0.66		69.95	13.77	13.07	1.26	0.72	1.23
	19.5	71.04	15.27	11.99	0.93	0.49	0.29		69.89	15.32	12.00	1.46	0.37	0.97
	21	70.50	14.90	12.97	0.90	0.31	0.42		68.83	15.21	12.08	1.35	1.62	0.92
	22.5	69.98	15.45	12.59	0.90	0.70	0.38		68.91	15.16	12.59	1.33	0.99	1.01
	24	70.63	15.00	12.55	0.89	0.48	0.45		68.74	15.07	13.53	1.45	0.14	1.08
	25.5	70.31	14.81	13.15	0.89	0.41	0.44		67.57	15.03	13.52	1.52	1.41	0.94
	27	69.59	14.04	13.53	0.94	1.46	0.44		68.35	14.92	13.36	1.22	1.17	0.96
	28.5	70.81	14.82	12.89	0.79	0.26	0.42		69.74	14.70	13.09	1.44	0.10	0.94
	30	70.45	14.83	12.84	0.58	0.84	0.46		68.42	15.07	13.05	1.47	0.99	0.99
5	0	69.24	15.32	12.55	1.36	0.54	1.00	6	69.91	14.34	13.07	1.43	0.08	1.17
	1.5	69.72	15.33	12.07	1.41	0.57	0.91		70.18	14.05	12.96	1.54	0.29	0.98
	3	70.17	15.37	12.88	1.27	0.55	0.85		69.85	15.03	12.95	1.12	0.01	1.04
	4.5	70.35	14.82	12.71	1.40	0.34	1.06		69.96	14.54	13.70	1.25	-0.52	1.07

Meas.	Pos. (nm)	Fe	Cr	Ni	Mn	Si	Zr	Meas.	Fe	Cr	Ni	Mn	Si	Zr
5	6	70.04	14.69	12.69	1.47	0.18	0.93	6	69.63	15.47	12.69	1.34	-0.16	1.04
	7.5	69.68	14.49	12.78	1.52	0.45	1.09		69.85	15.28	12.43	1.36	-0.04	1.11
	9	70.98	15.41	12.33	1.32	1.10	1.05		70.51	15.13	12.73	1.61	-0.89	0.91
	10.5	68.96	15.38	12.58	1.64	0.48	0.96		69.63	15.10	12.66	1.44	0.28	0.90
	12	69.54	15.40	12.78	1.53	0.13	0.88		69.49	15.15	12.44	1.46	0.54	0.91
	13.5	70.14	15.41	12.15	1.42	0.07	0.95		70.95	14.72	13.09	1.18	-1.15	1.20
	15	69.04	13.89	13.72	1.30	0.75	1.30		68.38	13.01	15.05	1.05	1.10	1.40
	16.5	67.75	13.02	15.32	1.03	1.36	1.51		68.33	12.86	15.40	1.04	0.63	1.74
	18	68.68	13.20	14.77	1.05	0.74	1.55		70.59	14.43	11.89	1.21	0.91	0.97
	19.5	69.03	14.45	12.73	1.36	1.34	1.09		69.41	15.24	12.47	1.38	0.58	0.92
	21	70.41	15.23	11.86	1.32	0.33	0.85		69.20	15.13	12.48	1.44	0.92	0.83
	22.5	70.24	14.80	12.68	1.42	0.18	1.04		68.63	15.33	12.42	1.36	1.31	0.95
	24	70.07	15.08	12.37	1.24	0.29	0.94		69.99	14.76	12.70	1.45	0.10	0.99
	25.5	69.49	15.17	12.53	1.54	0.29	0.98		68.93	14.30	13.32	1.43	1.03	1.00
	27	68.76	14.44	12.45	1.45	1.90	1.00		69.34	14.42	13.06	1.47	0.71	1.00
	28.5	69.47	15.09	13.13	1.27	0.05	1.00		68.39	14.69	13.67	1.43	0.58	1.25
	30	69.36	14.68	13.29	1.10	0.56	1.01		69.53	13.95	13.10	1.37	1.03	1.02
7	0	70.02	15.20	12.87	1.27	0.26	0.90							
	1.5	69.90	14.78	12.13	1.42	0.74	1.02							
	3	69.89	14.71	12.87	1.39	0.13	1.02							
	4.5	70.27	14.23	13.01	1.44	0.01	1.05							
	6	70.44	14.70	12.85	1.31	0.38	1.09							
	7.5	69.72	14.65	12.39	1.42	0.85	0.97							
	9	69.18	14.99	13.50	1.46	0.18	1.06							
	10.5	70.04	15.14	12.27	1.29	0.29	0.97							
	12	70.25	14.99	12.00	1.76	0.18	0.83							
	13.5	69.57	14.51	13.33	1.34	0.20	1.05							
	15	69.23	13.17	15.20	1.13	0.14	1.40							
	16.5	67.99	12.72	15.36	1.15	1.04	1.73							
	18	70.04	14.28	13.44	0.93	0.05	1.25							
	19.5	69.97	14.77	12.38	1.47	0.53	0.88							
	21	70.43	15.62	12.24	1.26	0.48	0.92							
	22.5	69.86	15.26	12.80	1.53	0.30	0.86							
	24	70.18	15.27	12.88	1.41	0.62	0.89							
	25.5	70.19	15.06	12.59	1.46	0.26	0.96							
	27	69.92	14.71	12.59	1.39	0.43	0.96							
	28.5	69.77	14.63	12.43	1.65	0.53	0.99							
	30	69.91	14.71	12.87	1.44	0.05	1.02							

HiZr, 400C, 3 dpa, 2 MeV protons

Meas.	Pos. (nm)	Fe	Cr	Ni	Mn	Si	Zr	Meas.	Fe	Cr	Ni	Mn	Si	Zr
1	0	69.16	15.27	13.23	1.21	0.32	0.82	2	71.24	14.98	11.55	1.27	0.27	0.69
	1.5	69.79	15.19	12.46	1.51	0.28	0.77		70.58	15.28	11.93	1.31	0.26	0.65
	3	70.46	15.77	11.31	1.52	0.26	0.68		70.19	15.56	11.98	1.33	0.29	0.65
	4.5	71.48	15.68	10.43	1.48	0.28	0.66		70.49	15.39	11.51	1.60	0.29	0.71
	6	70.58	16.06	10.80	1.60	0.29	0.67		69.98	15.95	11.65	1.44	0.25	0.73
	7.5	71.33	15.35	11.14	1.23	0.24	0.71		70.47	15.50	11.69	1.37	0.24	0.73
	9	71.31	15.47	10.67	1.58	0.32	0.65		71.55	14.66	11.66	1.23	0.25	0.66
	10.5	71.52	14.58	11.85	0.91	0.31	0.83		71.10	15.24	11.59	1.23	0.25	0.59
	12	67.69	11.91	17.68	0.71	0.40	1.60		70.84	14.17	12.69	1.13	0.30	0.86
	13.5	67.86	12.65	16.83	0.72	0.45	1.50		67.92	12.37	16.91	0.85	0.42	1.55
	15	71.20	14.96	11.61	1.11	0.30	0.81		71.20	14.18	12.30	1.16	0.35	0.82
	16.5	71.04	15.10	11.67	1.23	0.26	0.70		71.34	15.12	11.28	1.25	0.29	0.72
	18	70.62	15.20	11.89	1.39	0.31	0.59		70.99	15.56	11.34	1.11	0.30	0.71
	19.5	71.17	15.14	11.46	1.37	0.24	0.61		70.62	15.68	11.33	1.42	0.31	0.64
	21	70.47	14.98	12.15	1.40	0.28	0.72		69.89	16.21	11.75	1.26	0.31	0.58
	22.5	71.94	15.29	10.51	1.26	0.33	0.68		70.95	15.50	11.37	1.22	0.30	0.66
	24	70.99	14.88	11.82	1.24	0.34	0.73		70.77	15.43	11.57	1.33	0.28	0.62
	25.5	71.16	14.70	11.89	1.20	0.30	0.75		70.19	15.20	12.42	1.25	0.22	0.73
	27	70.49	15.22	12.16	0.99	0.28	0.86		69.61	15.43	12.51	1.34	0.33	0.78
	28.5	70.94	14.09	12.83	1.06	0.29	0.80		70.57	15.23	11.81	1.49	0.30	0.61
	30	70.37	14.10	13.13	1.31	0.28	0.81		69.87	16.07	11.63	1.38	0.28	0.77
3	0	70.63	14.68	12.42	1.37	0.25	0.66	4	70.11	15.22	12.50	1.21	0.27	0.70
	1.5	70.40	14.90	12.59	1.05	0.25	0.80		70.60	15.11	12.19	1.20	0.22	0.69
	3	69.80	15.09	12.73	1.34	0.23	0.81		70.05	15.13	12.34	1.49	0.29	0.71
	4.5	69.26	14.58	13.84	1.22	0.27	0.83		70.69	15.08	12.07	1.24	0.26	0.66
	6	68.94	15.11	13.47	1.24	0.27	0.96		70.53	14.97	12.21	1.29	0.20	0.81
	7.5	70.22	14.72	12.78	1.14	0.25	0.89		71.02	14.72	12.02	1.29	0.23	0.72
	9	71.16	14.68	11.92	1.20	0.29	0.75		70.71	15.19	11.95	1.16	0.27	0.72
	10.5	71.24	14.84	11.74	1.21	0.27	0.70		70.98	15.05	11.88	1.23	0.24	0.63
	12	70.64	15.51	11.64	1.16	0.28	0.76		71.30	14.46	11.86	1.25	0.28	0.85
	13.5	71.35	14.22	12.27	0.99	0.28	0.89		71.11	12.20	14.10	1.16	0.32	1.11
	15	68.62	12.71	15.86	0.88	0.38	1.55		66.73	11.87	18.35	0.97	0.45	1.63
	16.5	66.85	11.45	18.66	0.91	0.42	1.71		68.94	12.45	15.89	0.95	0.37	1.40
	18	71.74	14.55	11.40	1.21	0.29	0.81		71.32	14.97	11.24	1.30	0.33	0.83
	19.5	70.77	15.20	11.48	1.60	0.26	0.69		71.23	15.62	10.87	1.29	0.26	0.72
	21	70.02	16.02	11.57	1.44	0.30	0.66		70.86	15.77	11.18	1.15	0.32	0.72
	22.5	71.10	15.45	11.43	1.12	0.28	0.62		70.32	15.10	12.18	1.25	0.31	0.84
	24	70.32	15.77	11.73	1.27	0.26	0.65		70.33	14.88	12.53	1.21	0.26	0.80
	25.5	70.18	15.63	11.87	1.36	0.30	0.66		70.61	14.87	12.44	1.04	0.27	0.77
	27	70.99	15.19	11.53	1.40	0.27	0.61		69.76	14.65	13.35	1.05	0.31	0.89
	28.5	69.96	15.93	11.86	1.25	0.26	0.75		69.69	14.43	13.56	1.19	0.30	0.83
	30	70.07	15.45	12.19	1.13	0.32	0.84		70.60	14.27	12.84	1.22	0.31	0.76
5	0	69.98	15.35	12.49	1.14	0.26	0.77	6	70.92	15.14	11.69	1.33	0.29	0.63
	1.5	70.51	15.42	11.98	1.11	0.25	0.73		70.47	15.04	12.15	1.31	0.27	0.76
	3	70.72	15.00	12.04	1.30	0.25	0.69		70.95	14.81	12.17	1.17	0.24	0.65
	4.5	70.80	15.15	11.94	1.21	0.24	0.64		71.36	14.64	11.76	1.14	0.27	0.83

Meas.	Pos. (nm)	Fe	Cr	Ni	Mn	Si	Zr	Meas.	Fe	Cr	Ni	Mn	Si	Zr
5	6	70.33	15.22	12.39	1.11	0.29	0.66	6	70.11	14.92	12.95	0.95	0.24	0.83
	7.5	69.94	15.02	12.87	1.20	0.25	0.72		70.82	14.61	12.47	1.05	0.30	0.75
	9	70.77	15.30	11.66	1.23	0.24	0.79		71.24	14.73	11.90	1.13	0.25	0.76
	10.5	71.39	15.22	11.24	1.26	0.25	0.64		70.15	15.43	11.84	1.54	0.26	0.77
	12	71.54	15.23	11.07	1.26	0.24	0.66		70.48	15.23	11.95	1.32	0.28	0.74
	13.5	71.58	14.54	11.92	0.92	0.29	0.75		70.60	12.89	14.10	0.79	0.38	1.25
	15	70.64	12.29	14.55	0.89	0.40	1.22		66.90	11.92	18.54	0.54	0.43	1.66
	16.5	67.09	12.17	17.96	0.72	0.34	1.73		69.75	13.22	14.46	0.89	0.38	1.30
	18	71.52	14.63	11.67	0.97	0.32	0.89		71.16	14.87	11.69	1.17	0.30	0.81
	19.5	70.38	15.53	11.71	1.33	0.34	0.71		70.83	15.14	11.75	1.27	0.27	0.74
	21	70.79	15.11	11.76	1.26	0.34	0.74		71.49	15.08	11.28	1.15	0.29	0.71
	22.5	69.85	15.22	12.32	1.41	0.30	0.90		71.49	15.03	11.06	1.40	0.31	0.71
	24	69.69	15.24	12.77	1.20	0.31	0.79		71.09	15.26	11.32	1.34	0.27	0.72
	25.5	69.96	15.06	12.90	1.05	0.28	0.75		70.02	16.06	11.73	1.22	0.28	0.69
	27	70.19	14.78	12.61	1.42	0.25	0.75		69.68	14.92	13.07	1.15	0.27	0.91
	28.5	70.58	15.02	12.41	1.02	0.25	0.72		69.69	15.14	12.91	1.18	0.28	0.79
	30	70.58	14.77	12.52	1.13	0.29	0.72		70.24	14.98	12.39	1.28	0.27	0.84

HiZr, 400C, 7 dpa, 3.2 MeV p+

Meas.	Pos. (nm)	Fe	Cr	Ni	Mn	Si	Zr	Meas.	Fe	Cr	Ni	Mn	Si	Zr
1	0	69.59	14.99	12.89	1.21	0.43	0.88	2	70.55	14.57	12.41	1.29	0.42	0.76
	1.5	69.32	14.90	13.28	1.20	0.36	0.94		70.52	14.93	12.12	1.24	0.36	0.84
	3	69.95	15.27	12.22	1.29	0.42	0.85		69.72	15.27	12.59	1.20	0.38	0.84
	4.5	69.99	15.38	12.11	1.32	0.39	0.82		70.42	15.40	11.93	1.14	0.38	0.71
	6	70.28	15.49	11.74	1.31	0.45	0.74		69.82	15.36	12.09	1.45	0.44	0.83
	7.5	70.20	16.07	11.37	1.15	0.40	0.80		70.40	14.65	12.21	1.40	0.46	0.87
	9	70.44	15.27	11.68	1.40	0.39	0.82		70.76	14.80	12.21	0.94	0.44	0.84
	10.5	70.65	15.41	11.60	1.08	0.47	0.79		71.64	13.85	11.98	1.04	0.48	1.01
	12	70.88	14.57	12.10	1.10	0.44	0.91		69.05	11.59	16.69	0.75	0.52	1.40
	13.5	70.25	12.87	14.31	0.86	0.45	1.26		63.32	9.52	23.58	0.62	0.54	2.41
	15	67.35	11.21	18.49	0.86	0.44	1.66		65.94	10.10	20.50	0.85	0.53	2.07
	16.5	64.91	9.94	21.59	0.64	0.51	2.43		70.68	13.33	13.59	0.82	0.39	1.19
	18	64.39	10.30	22.05	0.70	0.49	2.07		70.90	14.52	11.97	1.19	0.46	0.96
	19.5	69.09	12.77	15.28	0.95	0.46	1.45		70.51	15.03	11.86	1.33	0.39	0.87
	21	70.98	14.79	11.59	1.20	0.45	0.99		70.42	14.99	11.94	1.34	0.41	0.91
	22.5	70.56	15.02	11.93	1.18	0.42	0.89		70.01	14.59	12.92	1.16	0.46	0.85
	24	69.69	15.46	12.29	1.31	0.37	0.89		70.07	14.68	12.72	1.27	0.43	0.84
	25.5	69.54	15.38	12.30	1.47	0.35	0.97		69.09	15.07	13.48	1.14	0.43	0.79
	27	70.37	14.71	12.46	1.34	0.34	0.78		69.61	14.30	13.66	1.06	0.42	0.95
	28.5	69.65	15.52	12.33	1.34	0.36	0.81		69.71	14.12	13.83	0.93	0.44	0.98
	30	70.17	15.01	12.14	1.47	0.39	0.82		68.87	14.74	13.61	1.38	0.40	1.00
3	0	69.73	14.90	13.01	0.99	0.46	0.92	4	69.49	15.16	12.83	1.22	0.45	0.84
	1.5	69.86	14.70	13.09	1.07	0.38	0.90		70.10	15.02	12.28	1.27	0.52	0.81
	3	69.69	14.00	13.78	1.13	0.41	0.99		69.59	15.52	12.41	1.18	0.43	0.88
	4.5	68.99	14.59	13.92	1.09	0.45	0.98		69.97	15.29	12.16	1.23	0.41	0.95
	6	68.89	14.85	13.42	1.34	0.47	1.03		69.67	14.66	12.76	1.36	0.50	1.04
	7.5	69.71	14.85	12.97	1.14	0.42	0.91		70.44	14.96	12.44	0.97	0.45	0.75
	9	70.96	15.03	11.66	1.11	0.41	0.83		70.50	15.09	11.93	1.16	0.47	0.87
	10.5	71.19	14.90	11.64	1.11	0.36	0.79		70.77	14.14	12.28	1.39	0.49	0.93
	12	71.40	14.07	12.05	1.05	0.48	0.95		70.44	12.97	13.80	1.01	0.53	1.25
	13.5	70.57	11.95	14.91	0.83	0.44	1.31		66.25	10.90	19.59	0.67	0.54	2.06
	15	67.33	11.02	18.55	0.77	0.49	1.84		63.20	10.13	23.31	0.60	0.54	2.21
	16.5	62.71	10.10	23.63	0.64	0.56	2.36		67.41	11.01	18.67	0.59	0.52	1.79
	18	67.26	11.51	18.19	0.60	0.49	1.95		70.95	13.36	13.18	1.03	0.39	1.10
	19.5	70.89	13.77	12.76	1.09	0.39	1.10		70.55	14.77	12.20	1.20	0.39	0.88
	21	70.57	15.54	11.47	1.14	0.42	0.86		69.55	15.04	12.58	1.48	0.44	0.90
	22.5	70.48	15.40	11.55	1.30	0.43	0.85		69.02	15.55	13.12	1.10	0.37	0.85
	24	70.18	15.47	12.02	1.11	0.42	0.80		69.87	14.78	12.73	1.29	0.43	0.90
	25.5	69.93	15.08	12.57	1.21	0.38	0.84		70.22	14.46	12.82	1.05	0.46	1.00
	27	69.35	14.97	13.31	1.16	0.42	0.79		70.16	14.24	13.00	1.14	0.47	0.99
	28.5	70.47	14.17	12.85	1.21	0.36	0.94		70.03	14.20	13.08	1.24	0.47	0.98
	30	70.08	14.81	12.41	1.50	0.35	0.85		68.89	14.98	13.72	1.00	0.38	1.03
5	0	70.11	14.63	12.88	1.16	0.38	0.84	6	69.32	14.75	13.33	1.17	0.40	1.03
	1.5	69.91	14.81	12.62	1.29	0.39	0.97		69.06	14.59	13.69	1.16	0.43	1.07
	3	69.99	14.98	12.62	1.07	0.47	0.86		69.47	14.40	13.36	1.28	0.47	1.02
	4.5	69.79	14.82	12.67	1.30	0.52	0.89		69.76	14.82	12.59	1.42	0.43	0.99

Meas.	Pos. (nm)	Fe	Cr	Ni	Mn	Si	Zr	Meas.	Fe	Cr	Ni	Mn	Si	Zr
5	6	69.40	15.78	12.13	1.33	0.45	0.92	6	69.78	15.39	12.06	1.33	0.49	0.94
	7.5	70.06	15.12	12.21	1.19	0.44	0.98		70.09	15.65	11.82	1.10	0.49	0.85
	9	70.87	14.65	11.77	1.48	0.37	0.86		70.88	14.88	11.48	1.42	0.52	0.82
	10.5	71.14	14.37	12.13	0.98	0.45	0.94		71.44	14.21	11.72	1.10	0.48	1.04
	12	70.79	13.00	13.56	0.87	0.48	1.29		71.15	13.11	13.20	0.87	0.48	1.20
	13.5	68.13	10.56	18.26	0.83	0.48	1.75		66.44	10.65	20.02	0.57	0.56	1.77
	15	63.27	10.41	22.82	0.55	0.54	2.42		64.66	10.79	21.22	0.60	0.50	2.24
	16.5	68.26	11.79	16.85	0.84	0.51	1.75		68.01	12.04	17.03	0.69	0.50	1.72
	18	71.75	14.40	11.30	1.21	0.38	0.95		70.70	14.22	12.67	0.96	0.36	1.10
	19.5	70.91	15.30	11.26	1.31	0.42	0.80		71.03	15.58	10.82	1.20	0.42	0.95
	21	70.54	15.43	11.54	1.29	0.41	0.80		71.10	15.52	10.92	1.30	0.38	0.79
	22.5	70.01	15.33	12.26	1.14	0.40	0.85		69.43	15.33	12.62	1.28	0.38	0.96
	24	69.11	15.58	12.64	1.19	0.48	0.99		69.24	14.94	13.31	1.18	0.37	0.95
	25.5	68.69	15.00	13.72	1.20	0.38	1.01		68.64	14.74	13.98	1.25	0.37	1.03
	27	69.49	14.55	13.35	1.38	0.37	0.85		69.24	15.11	13.18	1.23	0.36	0.89
	28.5	69.58	14.60	13.18	1.28	0.39	0.97		70.19	14.08	13.01	1.34	0.43	0.95
	30	69.59	14.73	13.25	1.20	0.36	0.88		69.75	14.62	12.95	1.42	0.40	0.86
7	0	70.28	15.72	11.46	1.36	0.33	0.85	8	69.72	15.45	12.23	1.41	0.33	0.86
	1.5	69.98	15.32	12.14	1.35	0.35	0.85		69.29	15.75	12.44	1.35	0.31	0.85
	3	69.75	15.18	12.72	1.14	0.35	0.87		70.02	15.81	11.57	1.35	0.35	0.89
	4.5	70.21	14.78	12.45	1.30	0.37	0.89		70.22	15.71	11.59	1.30	0.35	0.83
	6	70.44	14.79	12.33	1.12	0.35	0.98		69.99	15.53	11.93	1.35	0.34	0.86
	7.5	70.52	14.37	12.84	0.93	0.35	0.99		69.94	15.15	12.40	1.29	0.30	0.93
	9	70.82	13.29	13.48	0.98	0.34	1.10		70.82	15.34	11.43	1.05	0.37	1.00
	10.5	68.62	11.71	16.98	0.87	0.38	1.43		71.19	14.11	12.26	1.06	0.33	1.06
	12	66.27	10.94	19.79	0.75	0.40	1.85		70.13	12.17	15.14	0.89	0.35	1.32
	13.5	68.53	11.70	17.10	0.78	0.41	1.48		67.48	10.94	18.80	0.75	0.42	1.61
	15	70.62	13.40	13.44	1.10	0.39	1.04		66.96	10.52	19.58	0.76	0.38	1.79
	16.5	71.03	14.70	12.08	1.03	0.34	0.82		68.03	11.34	17.91	0.85	0.41	1.46
	18	71.13	15.05	11.43	1.17	0.41	0.80		71.55	13.60	12.45	1.08	0.38	0.95
	19.5	70.64	15.18	11.87	1.22	0.35	0.72		71.27	14.87	11.42	1.28	0.40	0.76
	21	69.72	15.43	12.35	1.32	0.37	0.82		71.28	15.20	11.29	1.08	0.37	0.78
	22.5	69.59	15.15	12.98	1.20	0.36	0.72		70.78	15.88	10.99	1.13	0.42	0.80
	24	69.14	14.59	13.90	1.16	0.38	0.82		69.80	15.37	12.35	1.26	0.44	0.77
	25.5	69.35	14.43	13.76	1.21	0.37	0.87		69.80	15.51	12.20	1.24	0.39	0.86
	27	70.03	14.98	12.55	1.22	0.41	0.81		69.79	14.66	13.15	1.22	0.38	0.79
	28.5	70.24	15.15	12.29	1.18	0.40	0.75		69.52	15.14	12.84	1.29	0.33	0.89
	30	70.32	14.78	12.55	1.21	0.39	0.76		69.53	14.89	13.06	1.22	0.38	0.92
9	0	70.23	14.88	12.45	1.18	0.36	0.91	10	69.58	14.62	13.40	1.13	0.32	0.95
	1.5	69.80	15.33	12.33	1.31	0.33	0.89		69.21	15.10	13.29	1.08	0.34	0.98
	3	70.25	15.04	12.20	1.27	0.36	0.88		70.11	14.59	12.74	1.27	0.34	0.96
	4.5	70.19	15.45	11.89	1.29	0.35	0.83		70.13	14.77	12.71	1.18	0.32	0.89
	6	70.12	14.99	12.40	1.24	0.33	0.92		70.29	14.89	12.41	1.17	0.35	0.89
	7.5	71.02	14.18	12.39	1.07	0.31	1.03		70.55	15.27	11.75	1.14	0.35	0.95
	9	70.63	14.23	12.75	1.00	0.39	1.01		70.23	14.76	12.40	1.24	0.38	0.98
	10.5	67.68	11.20	18.29	0.76	0.35	1.72		71.11	13.79	12.71	1.04	0.35	1.00
	12	65.75	10.24	20.84	0.81	0.44	1.93		69.93	13.36	14.14	1.08	0.36	1.12

Meas.	Pos. (nm)	Fe	Cr	Ni	Mn	Si	Zr	Meas.	Fe	Cr	Ni	Mn	Si	Zr
9	13.5	66.41	10.42	20.05	0.84	0.41	1.87	10	67.55	12.19	17.60	0.85	0.34	1.48
	15	70.93	12.96	13.61	1.02	0.38	1.12		68.72	12.05	16.68	0.77	0.41	1.36
	16.5	71.80	13.91	12.17	0.87	0.37	0.88		70.02	13.11	14.37	1.10	0.36	1.04
	18	71.36	14.94	11.46	1.04	0.41	0.79		70.61	13.41	13.46	1.11	0.45	0.95
	19.5	71.09	15.44	11.13	1.21	0.38	0.76		69.82	14.05	13.59	1.15	0.39	1.00
	21	70.22	15.56	11.72	1.31	0.37	0.82		70.20	14.42	12.93	1.11	0.39	0.95
	22.5	69.49	15.55	12.35	1.47	0.37	0.78		69.53	14.57	13.37	1.26	0.34	0.94
	24	69.42	15.40	12.74	1.33	0.38	0.73		69.55	14.80	13.22	1.11	0.37	0.96
	25.5	69.62	15.53	12.42	1.27	0.41	0.75		68.64	14.76	13.99	1.27	0.45	0.88
	27	69.47	15.12	13.05	1.28	0.38	0.70		69.12	14.74	13.67	1.10	0.38	0.99
	28.5	68.95	15.15	13.51	1.25	0.36	0.78		69.27	14.62	13.49	1.18	0.42	1.01
	30	69.23	15.01	13.58	1.06	0.35	0.77		69.44	14.77	13.22	1.15	0.45	0.96
11	0	70.16	15.08	12.14	1.36	0.38	0.88	12	69.41	15.36	12.86	1.16	0.33	0.87
	1.5	69.92	15.03	12.29	1.47	0.38	0.90		70.27	15.06	11.94	1.46	0.36	0.91
	3	70.19	15.29	12.06	1.25	0.32	0.89		70.01	15.02	12.61	1.12	0.35	0.90
	4.5	70.92	15.04	11.68	1.17	0.30	0.89		69.93	14.56	13.08	1.19	0.32	0.92
	6	70.52	14.44	12.64	1.15	0.37	0.88		70.38	14.37	12.73	1.16	0.34	1.02
	7.5	70.78	14.01	12.69	1.19	0.33	1.00		70.42	14.53	12.64	1.07	0.35	1.01
	9	70.86	13.09	13.60	1.00	0.35	1.11		70.73	13.52	13.20	1.09	0.36	1.09
	10.5	69.50	11.67	16.24	0.87	0.35	1.37		69.19	12.57	15.76	0.79	0.37	1.32
	12	67.20	11.04	19.01	0.72	0.33	1.70		67.71	11.25	18.16	0.74	0.42	1.72
	13.5	67.04	10.62	19.12	0.90	0.40	1.91		67.08	11.18	18.90	0.77	0.41	1.65
	15	69.25	12.16	15.81	0.90	0.42	1.46		68.63	11.62	17.05	0.91	0.37	1.42
	16.5	71.52	14.26	11.77	1.18	0.42	0.86		71.10	14.92	11.68	1.14	0.39	0.78
	18	70.94	15.48	11.43	0.95	0.38	0.81		70.84	15.35	11.54	1.09	0.36	0.81
	19.5	70.19	15.53	11.80	1.30	0.42	0.76		70.58	15.37	11.61	1.28	0.40	0.77
	21	70.25	15.60	11.83	1.19	0.41	0.72		70.65	14.85	11.76	1.65	0.37	0.71
	22.5	70.31	14.85	12.24	1.37	0.42	0.81		69.74	15.13	12.78	1.18	0.36	0.81
	24	69.63	14.91	12.95	1.35	0.40	0.76		69.51	14.74	13.28	1.28	0.40	0.79
	25.5	70.31	14.74	12.49	1.21	0.45	0.79		69.63	14.76	13.11	1.22	0.40	0.89
	27	69.91	14.98	12.72	1.21	0.42	0.77		70.09	14.68	12.73	1.31	0.38	0.82
	28.5	70.40	14.79	12.54	1.12	0.41	0.74		70.22	14.71	12.55	1.33	0.36	0.83
	30	69.83	15.16	12.57	1.32	0.36	0.75		69.88	14.66	13.01	1.23	0.43	0.80
13	0	70.11	14.66	12.86	1.22	0.29	0.86							
	1.5	70.33	14.69	12.54	1.25	0.35	0.83							
	3	69.79	14.91	12.72	1.42	0.32	0.85							
	4.5	69.70	14.89	12.89	1.24	0.33	0.95							
	6	70.12	14.94	12.49	1.22	0.36	0.87							
	7.5	70.13	14.87	12.43	1.27	0.35	0.95							
	9	71.04	14.37	12.20	1.05	0.36	0.98							
	10.5	70.18	13.32	14.25	0.80	0.35	1.10							
	12	67.96	11.83	17.59	0.72	0.38	1.52							
	13.5	66.54	10.63	19.91	0.79	0.41	1.73							
	15	68.59	11.86	16.93	0.76	0.35	1.52							
	16.5	71.68	13.77	12.26	1.02	0.39	0.88							
	18	71.10	14.79	11.82	1.10	0.40	0.79							
	19.5	71.19	14.92	11.68	1.03	0.41	0.78							

Meas.	Pos. (nm)	Fe	Cr	Ni	Mn	Si	Zr	Meas.	Fe	Cr	Ni	Mn	Si	Zr
13	21	70.59	14.84	12.23	1.26	0.33	0.75							
	22.5	70.19	14.92	12.50	1.19	0.43	0.78							
	24	69.56	15.02	12.95	1.30	0.37	0.80							
	25.5	69.54	14.95	13.07	1.33	0.39	0.73							
	27	69.50	14.98	13.12	1.28	0.38	0.74							
	28.5	70.13	14.63	12.84	1.26	0.37	0.77							
	30	70.25	14.95	12.31	1.40	0.37	0.72							

HiZr, 400C, 7 dpa, 2 MeV p+

Meas.	Pos. (nm)	Fe	Cr	Ni	Mn	Si	Zr	Meas.	Fe	Cr	Ni	Mn	Si	Zr
1	0	71.22	15.07	11.75	1.07	0.23	0.66	2	70.55	14.57	12.41	1.29	0.42	0.76
	1.5	70.71	15.41	11.75	1.26	0.22	0.64		70.52	14.93	12.12	1.24	0.36	0.84
	3	71.10	15.01	11.79	1.22	0.26	0.60		69.72	15.27	12.59	1.20	0.38	0.84
	4.5	70.90	14.91	11.94	1.45	0.21	0.60		70.42	15.40	11.93	1.14	0.38	0.71
	6	70.42	14.55	12.80	1.28	0.24	0.71		69.82	15.36	12.09	1.45	0.44	0.83
	7.5	69.71	15.19	12.98	1.07	0.26	0.79		70.40	14.65	12.21	1.40	0.46	0.87
	9	70.21	15.01	12.40	1.46	0.22	0.70		70.76	14.80	12.21	0.94	0.44	0.84
	10.5	71.97	14.66	11.17	1.20	0.27	0.73		71.64	13.85	11.98	1.04	0.48	1.01
	12	73.18	12.91	11.70	1.16	0.26	0.78		69.05	11.59	16.69	0.75	0.52	1.40
	13.5	69.58	11.06	16.70	0.70	0.26	1.71		63.32	9.52	23.58	0.62	0.54	2.41
	15	65.62	10.38	20.85	0.70	0.29	2.16		65.94	10.10	20.50	0.85	0.53	2.07
	16.5	72.90	12.54	12.42	1.02	0.28	0.84		70.68	13.33	13.59	0.82	0.39	1.19
	18	73.01	15.26	9.96	0.97	0.25	0.55		70.90	14.52	11.97	1.19	0.46	0.96
	19.5	72.82	14.54	10.38	1.44	0.25	0.57		70.51	15.03	11.86	1.33	0.39	0.87
	21	71.63	15.03	11.35	1.18	0.23	0.58		70.42	14.99	11.94	1.34	0.41	0.91
	22.5	70.29	15.14	12.06	1.68	0.25	0.57		70.01	14.59	12.92	1.16	0.46	0.85
	24	70.40	15.78	11.51	1.43	0.29	0.59		70.07	14.68	12.72	1.27	0.43	0.84
	25.5	70.39	15.81	11.45	1.54	0.20	0.60		69.09	15.07	13.48	1.14	0.43	0.79
	27	70.77	15.90	11.06	1.42	0.24	0.61		69.61	14.30	13.66	1.06	0.42	0.95
	28.5	71.05	16.33	10.38	1.44	0.24	0.56		69.71	14.12	13.83	0.93	0.44	0.98
	30	70.57	15.80	11.38	1.43	0.25	0.57		68.87	14.74	13.61	1.38	0.40	1.00
3	0	70.46	14.83	12.41	1.21	0.24	0.86	4	69.49	15.16	12.83	1.22	0.45	0.84
	1.5	69.90	15.24	12.69	1.13	0.26	0.78		70.10	15.02	12.28	1.27	0.52	0.81
	3	70.95	14.49	12.43	1.14	0.24	0.74		69.59	15.52	12.41	1.18	0.43	0.88
	4.5	70.73	15.09	11.80	1.50	0.25	0.62		69.97	15.29	12.16	1.23	0.41	0.95
	6	71.28	15.06	11.67	1.15	0.27	0.57		69.67	14.66	12.76	1.36	0.50	1.04
	7.5	71.54	14.69	11.53	1.36	0.24	0.63		70.44	14.96	12.44	0.97	0.45	0.75
	9	71.72	15.44	10.78	1.21	0.21	0.64		70.50	15.09	11.93	1.16	0.47	0.87
	10.5	72.62	14.77	10.57	1.08	0.26	0.70		70.77	14.14	12.28	1.39	0.49	0.93
	12	72.45	11.78	13.42	0.96	0.27	1.13		70.44	12.97	13.80	1.01	0.53	1.25
	13.5	64.99	10.21	21.76	0.74	0.28	2.02		66.25	10.90	19.59	0.67	0.54	2.06
	15	68.64	11.37	17.50	0.79	0.27	1.43		63.20	10.13	23.31	0.60	0.54	2.21
	16.5	73.01	13.75	11.43	0.86	0.22	0.73		67.41	11.01	18.67	0.59	0.52	1.79
	18	71.70	16.20	10.26	1.15	0.22	0.47		70.95	13.36	13.18	1.03	0.39	1.10
	19.5	70.89	15.84	11.06	1.48	0.22	0.50		70.55	14.77	12.20	1.20	0.39	0.88
	21	71.08	15.76	10.92	1.46	0.24	0.54		69.55	15.04	12.58	1.48	0.44	0.90
	22.5	70.71	16.09	11.07	1.32	0.24	0.57		69.02	15.55	13.12	1.10	0.37	0.85
	24	70.84	14.82	12.24	1.32	0.23	0.55		69.87	14.78	12.73	1.29	0.43	0.90
	25.5	70.50	14.93	12.43	1.44	0.20	0.50		70.22	14.46	12.82	1.05	0.46	1.00
	27	71.23	15.54	11.16	1.26	0.26	0.56		70.16	14.24	13.00	1.14	0.47	0.99
	28.5	71.26	16.03	10.49	1.41	0.25	0.56		70.03	14.20	13.08	1.24	0.47	0.98
	30	72.02	15.66	10.49	1.07	0.21	0.55		68.89	14.98	13.72	1.00	0.38	1.03
5	0	71.47	14.68	11.66	1.27	0.28	0.64	6	69.32	14.75	13.33	1.17	0.40	1.03
	1.5	70.89	15.16	11.61	1.51	0.22	0.61		69.06	14.59	13.69	1.16	0.43	1.07
	3	71.21	15.08	11.29	1.48	0.29	0.65		69.47	14.40	13.36	1.28	0.47	1.02
	4.5	71.81	13.80	12.24	1.25	0.20	0.70		69.76	14.82	12.59	1.42	0.43	0.99

Meas.	Pos. (nm)	Fe	Cr	Ni	Mn	Si	Zr	Meas.	Fe	Cr	Ni	Mn	Si	Zr
5	6	69.40	15.78	12.13	1.33	0.45	0.92	6	71.02	14.62	12.12	1.19	0.26	0.79
	7.5	70.06	15.12	12.21	1.19	0.44	0.98		71.83	14.77	11.21	1.41	0.22	0.56
	9	70.87	14.65	11.77	1.48	0.37	0.86		72.71	15.22	9.92	1.25	0.24	0.66
	10.5	71.14	14.37	12.13	0.98	0.45	0.94		73.31	14.37	10.20	1.10	0.27	0.74
	12	70.79	13.00	13.56	0.87	0.48	1.29		71.50	11.71	14.32	0.99	0.25	1.23
	13.5	68.13	10.56	18.26	0.83	0.48	1.75		64.47	9.82	22.78	0.58	0.26	2.10
	15	63.27	10.41	22.82	0.55	0.54	2.42		71.41	11.26	15.13	0.98	0.24	0.98
	16.5	68.26	11.79	16.85	0.84	0.51	1.75		73.08	13.79	11.12	1.15	0.24	0.62
	18	71.75	14.40	11.30	1.21	0.38	0.95		72.57	15.49	10.00	1.20	0.23	0.51
	19.5	70.91	15.30	11.26	1.31	0.42	0.80		72.38	15.09	10.34	1.41	0.24	0.55
	21	70.54	15.43	11.54	1.29	0.41	0.80		71.47	15.67	10.85	1.21	0.23	0.57
	22.5	70.01	15.33	12.26	1.14	0.40	0.85		71.74	15.55	10.77	1.20	0.22	0.52
	24	69.11	15.58	12.64	1.19	0.48	0.99		71.21	15.55	11.07	1.41	0.19	0.56
	25.5	68.69	15.00	13.72	1.20	0.38	1.01		70.89	15.40	11.57	1.36	0.21	0.58
	27	69.49	14.55	13.35	1.38	0.37	0.85		70.15	15.33	12.47	1.26	0.19	0.60
	28.5	69.58	14.60	13.18	1.28	0.39	0.97		70.92	14.71	12.20	1.23	0.24	0.70
	30	69.59	14.73	13.25	1.20	0.36	0.88		70.89	15.06	11.96	1.29	0.24	0.56
7	0	70.45	15.87	11.60	1.25	0.25	0.59	8	71.23	15.12	11.69	1.07	0.26	0.62
	1.5	70.43	15.44	12.04	1.26	0.26	0.57		71.27	14.70	11.82	1.28	0.26	0.67
	3	70.81	15.25	11.85	1.23	0.24	0.61		70.73	14.42	12.46	1.43	0.26	0.68
	4.5	71.26	14.98	11.56	1.40	0.23	0.57		71.18	14.67	11.96	1.22	0.27	0.70
	6	70.57	14.72	12.62	1.26	0.21	0.62		71.53	15.25	11.12	1.24	0.25	0.61
	7.5	70.50	14.81	12.71	1.09	0.23	0.66		71.66	15.57	10.50	1.38	0.24	0.64
	9	72.43	14.86	10.71	1.14	0.24	0.62		73.03	14.83	10.16	1.17	0.21	0.60
	10.5	72.63	14.30	10.81	1.35	0.25	0.65		73.35	14.11	10.54	1.04	0.23	0.73
	12	72.39	13.57	11.87	1.10	0.22	0.85		69.88	12.11	15.64	0.84	0.27	1.26
	13.5	67.02	10.47	19.70	0.70	0.30	1.82		73.24	13.63	11.11	1.02	0.20	0.79
	15	69.25	12.42	15.84	0.89	0.28	1.32		72.95	14.79	10.42	1.11	0.23	0.50
	16.5	73.24	14.03	10.72	1.07	0.26	0.68		72.49	14.85	10.69	1.20	0.25	0.51
	18	72.48	15.42	10.15	1.15	0.22	0.57		71.22	16.04	10.61	1.33	0.26	0.54
	19.5	71.56	15.79	10.59	1.23	0.21	0.62		71.42	15.89	10.56	1.37	0.21	0.55
	21	71.33	15.82	10.81	1.25	0.21	0.58		70.51	15.12	12.17	1.36	0.25	0.58
	22.5	70.75	16.04	10.98	1.40	0.25	0.58		70.58	15.85	11.11	1.65	0.27	0.54
	24	70.88	15.29	11.40	1.54	0.22	0.67		70.41	15.64	11.68	1.44	0.21	0.63
	25.5	70.69	15.13	11.95	1.29	0.23	0.71		71.40	15.36	11.13	1.28	0.24	0.60
	27	69.40	14.83	13.50	1.26	0.22	0.78		70.80	15.65	11.25	1.47	0.26	0.57
	28.5	69.88	14.68	13.36	1.12	0.25	0.71		71.50	15.51	10.84	1.36	0.21	0.59
	30	70.58	14.53	12.70	1.28	0.25	0.66		70.91	15.81	11.03	1.54	0.20	0.51
9	0	69.51	15.32	13.05	0.98	0.22	0.92	10	71.42	15.93	10.47	1.13	0.21	0.83
	1.5	69.91	15.49	12.10	1.60	0.22	0.67		70.69	15.87	11.19	1.34	0.22	0.70
	3	70.16	15.46	12.29	1.20	0.25	0.64		71.48	15.43	10.92	1.21	0.27	0.69
	4.5	70.39	14.80	12.29	1.59	0.21	0.72		71.42	14.86	11.43	1.40	0.20	0.69
	6	69.22	15.10	13.64	1.06	0.19	0.80		70.98	14.37	12.35	1.31	0.23	0.76
	7.5	70.69	15.30	11.53	1.26	0.21	1.00		70.68	14.60	12.49	1.19	0.23	0.82
	9	71.00	15.90	10.64	1.11	0.25	1.09		70.78	15.01	12.24	0.97	0.25	0.76
	10.5	72.63	14.25	10.80	1.02	0.26	1.04		71.23	15.48	11.11	1.01	0.24	0.93
	12	61.16	9.13	25.10	0.81	0.53	3.27		68.97	13.05	14.91	1.11	0.31	1.64

Meas.	Pos. (nm)	Fe	Cr	Ni	Mn	Si	Zr	Meas.	Fe	Cr	Ni	Mn	Si	Zr
9	13.5	65.48	10.05	20.73	0.60	0.46	2.69	10	62.71	10.63	22.78	0.57	0.49	2.82
	15	72.35	12.84	12.30	0.97	0.43	1.10		71.13	13.13	12.99	1.00	0.38	1.37
	16.5	72.50	15.51	9.61	1.37	0.33	0.68		68.28	12.65	16.21	0.63	0.41	1.82
	18	73.10	15.55	8.97	1.28	0.37	0.73		72.82	15.07	9.89	1.10	0.34	0.79
	19.5	71.43	16.77	9.56	1.33	0.37	0.53		72.18	15.01	10.65	1.06	0.34	0.77
	21	71.15	16.53	9.83	1.35	0.39	0.76		71.08	15.43	11.27	1.11	0.31	0.80
	22.5	70.10	16.58	10.79	1.41	0.37	0.76		72.03	14.52	11.29	1.06	0.33	0.77
	24	70.50	16.81	10.40	1.31	0.35	0.63		70.76	15.16	12.00	0.86	0.29	0.93
	25.5	71.47	16.71	9.23	1.54	0.35	0.70		71.02	16.02	10.56	1.35	0.33	0.72
	27	71.66	15.68	10.34	1.29	0.37	0.66		70.50	15.89	11.07	1.48	0.36	0.70
	28.5	71.07	15.81	10.82	1.22	0.35	0.73		71.41	16.23	9.93	1.39	0.38	0.66
	30	24.98	22.55	24.26	15.43	6.63	6.15		70.57	15.34	11.64	1.37	0.32	0.75
11	0	70.58	16.85	10.20	1.35	0.24	0.77	12	71.04	15.32	11.31	1.29	0.28	0.75
	1.5	69.46	15.64	12.51	1.31	0.20	0.88		70.78	15.91	10.97	1.28	0.25	0.82
	3	67.69	16.14	13.81	1.18	0.25	0.93		71.22	15.66	11.05	1.09	0.24	0.75
	4.5	67.72	15.97	14.08	1.05	0.26	0.93		71.90	15.37	10.74	0.99	0.21	0.78
	6	69.59	15.33	12.57	1.33	0.26	0.91		71.68	15.08	11.20	0.97	0.28	0.79
	7.5	71.87	15.57	10.53	1.14	0.22	0.67		72.17	15.44	10.46	0.85	0.28	0.79
	9	71.13	16.00	10.99	0.87	0.20	0.80		74.15	14.33	9.54	1.02	0.22	0.75
	10.5	72.58	16.23	9.08	1.17	0.24	0.69		69.62	10.73	16.56	0.92	0.31	1.86
	12	74.09	14.11	9.63	1.00	0.28	0.90		60.93	9.05	26.04	0.86	0.49	2.63
	13.5	64.04	10.51	21.95	0.71	0.42	2.36		71.80	12.81	13.09	0.81	0.43	1.07
	15	62.63	9.42	23.72	0.85	0.56	2.83		72.47	15.45	9.93	1.12	0.34	0.69
	16.5	71.82	12.76	12.96	0.92	0.38	1.15		71.72	16.38	9.66	1.28	0.32	0.64
	18	72.15	14.50	11.40	0.80	0.37	0.79		71.28	16.62	9.79	1.42	0.31	0.56
	19.5	72.01	15.28	10.41	1.30	0.32	0.68		71.61	15.67	10.27	1.39	0.39	0.68
	21	71.40	15.20	11.11	1.28	0.34	0.67		70.49	15.14	12.09	1.28	0.30	0.71
	22.5	70.93	15.46	11.42	1.15	0.33	0.72		69.35	15.03	13.58	0.98	0.35	0.70
	24	70.64	15.73	11.56	1.17	0.38	0.52		70.30	14.29	13.06	1.18	0.33	0.84
	25.5	71.04	14.58	12.13	1.15	0.31	0.78		70.36	14.04	13.30	1.07	0.30	0.92
	27	70.15	14.69	12.89	1.08	0.33	0.86		69.79	13.88	13.79	1.35	0.36	0.83
	28.5	70.65	14.34	12.69	0.97	0.35	1.00		69.73	15.15	12.68	1.20	0.33	0.91
	30	70.32	14.58	12.74	1.07	0.38	0.90		69.91	14.88	12.92	1.23	0.38	0.67
13	0	69.42	14.61	13.80	1.03	0.20	0.95	14	70.44	16.47	10.88	1.38	0.19	0.64
	1.5	71.05	15.19	11.56	1.25	0.20	0.75		70.24	16.99	10.84	1.10	0.19	0.65
	3	72.00	15.94	9.90	1.29	0.25	0.61		69.96	15.67	12.18	1.19	0.22	0.78
	4.5	71.57	16.86	9.38	1.36	0.21	0.61		70.43	14.92	12.10	1.57	0.27	0.72
	6	70.02	17.68	9.84	1.60	0.24	0.63		69.21	15.68	13.06	1.16	0.24	0.65
	7.5	71.56	16.70	9.72	1.26	0.21	0.55		69.75	15.49	12.56	1.22	0.23	0.75
	9	70.81	17.21	9.90	1.27	0.23	0.58		70.52	15.03	12.30	1.24	0.26	0.66
	10.5	72.70	15.97	9.09	1.21	0.28	0.74		72.29	15.40	10.23	1.04	0.28	0.77
	12	73.18	14.04	10.86	0.79	0.23	0.90		73.61	12.52	11.42	1.16	0.26	1.03
	13.5	64.09	9.36	22.93	0.71	0.46	2.43		59.63	8.40	27.41	0.88	0.45	3.24
	15	65.98	10.07	20.62	0.76	0.48	2.10		69.84	9.92	17.14	0.85	0.40	1.86
	16.5	72.67	12.43	12.43	0.96	0.42	1.09		73.34	14.70	9.74	1.05	0.39	0.78
	18	72.89	13.14	11.86	0.96	0.36	0.80		73.10	15.50	9.43	0.82	0.36	0.79
	19.5	72.27	14.39	11.13	1.16	0.32	0.74		72.08	15.75	9.93	1.19	0.40	0.66

Meas.	Pos. (nm)	Fe	Cr	Ni	Mn	Si	Zr	Meas.	Fe	Cr	Ni	Mn	Si	Zr
13	21	71.67	15.26	11.10	0.97	0.31	0.70	14	71.63	15.30	10.60	1.44	0.37	0.66
	22.5	70.63	15.15	11.70	1.49	0.35	0.67		71.22	15.52	11.17	1.05	0.34	0.70
	24	70.24	16.03	11.29	1.47	0.29	0.68		70.12	15.29	12.45	0.98	0.35	0.82
	25.5	70.09	15.49	11.99	1.39	0.36	0.69		70.65	14.57	12.67	1.05	0.37	0.69
	27	70.69	15.31	11.73	1.18	0.37	0.72		69.74	13.89	13.96	1.08	0.35	0.98
	28.5	71.29	15.46	10.99	1.20	0.41	0.65		68.46	13.94	15.10	1.10	0.34	1.05
	30	70.88	15.79	10.80	1.41	0.34	0.77		69.27	13.93	14.31	1.02	0.38	1.08

HiZr, 400C, 10 dpa

Meas.	Pos. (nm)	Fe	Cr	Ni	Mn	Si	Zr	Meas.	Fe	Cr	Ni	Mn	Si	Zr
1	0	70.81	14.01	13.03	1.10	0.30	0.75	2	70.08	14.89	12.71	1.19	0.33	0.80
	1.5	70.32	14.40	12.82	1.40	0.27	0.79		69.40	14.74	13.66	1.09	0.28	0.83
	3	70.62	14.60	12.46	1.28	0.26	0.78		69.14	14.45	14.10	1.12	0.28	0.92
	4.5	70.66	14.63	12.40	1.28	0.27	0.75		70.21	14.44	12.91	1.19	0.31	0.93
	6	70.01	14.60	13.26	1.19	0.25	0.67		70.38	14.93	12.33	1.19	0.30	0.87
	7.5	70.46	14.69	12.59	1.24	0.27	0.75		70.54	14.54	12.66	1.24	0.29	0.74
	9	70.22	15.02	12.71	1.05	0.30	0.68		70.28	15.63	11.79	1.26	0.25	0.79
	10.5	70.84	15.03	12.00	1.11	0.29	0.73		69.93	15.93	11.70	1.43	0.29	0.73
	12	71.17	14.31	12.21	1.26	0.29	0.77		71.71	14.55	11.62	1.13	0.28	0.71
	13.5	70.42	14.09	13.22	1.13	0.25	0.89		69.66	11.96	15.85	0.99	0.33	1.21
	15	69.46	12.51	15.78	0.86	0.33	1.07		65.81	11.56	19.96	0.65	0.37	1.64
	16.5	70.18	12.93	14.37	1.22	0.29	1.01		70.32	14.09	13.37	0.96	0.32	0.93
	18	70.54	15.29	12.16	1.07	0.25	0.69		71.46	15.61	10.99	0.92	0.31	0.70
	19.5	71.53	15.01	11.26	1.26	0.25	0.69		69.84	16.06	11.93	1.25	0.27	0.66
	21	70.93	15.43	11.47	1.23	0.27	0.67		69.83	16.19	11.72	1.31	0.24	0.72
	22.5	71.24	14.47	12.30	1.12	0.23	0.64		70.09	16.04	11.65	1.26	0.24	0.72
	24	70.21	14.96	12.75	1.18	0.27	0.62		69.64	15.87	12.12	1.43	0.24	0.70
	25.5	70.75	14.53	12.50	1.26	0.27	0.68		70.25	15.43	12.08	1.29	0.25	0.70
	27	70.22	14.35	13.51	1.07	0.20	0.65		70.23	14.93	12.38	1.50	0.24	0.72
	28.5	70.69	14.15	13.07	1.27	0.22	0.60		70.50	14.99	12.36	1.15	0.26	0.74
	30	70.96	14.33	12.77	1.03	0.26	0.65		70.47	14.72	12.76	1.12	0.25	0.69
3	0	70.14	15.07	12.76	1.02	0.31	0.70	4	70.04	15.23	12.42	1.20	0.29	0.82
	1.5	70.94	14.43	12.33	1.22	0.29	0.79		71.06	14.89	11.90	1.14	0.29	0.73
	3	71.25	14.42	12.02	1.25	0.31	0.76		69.94	15.83	12.06	1.16	0.26	0.74
	4.5	70.60	14.26	12.82	1.24	0.30	0.78		69.30	15.04	13.29	1.19	0.35	0.83
	6	70.06	14.81	12.79	1.31	0.29	0.73		69.36	15.24	13.20	1.15	0.29	0.76
	7.5	70.41	15.21	11.99	1.42	0.30	0.68		69.77	16.10	11.78	1.27	0.29	0.79
	9	70.51	15.92	11.38	1.19	0.30	0.71		70.27	15.54	11.83	1.38	0.26	0.73
	10.5	70.68	15.50	11.36	1.42	0.33	0.71		71.12	15.84	10.62	1.28	0.29	0.85
	12	71.14	14.78	11.76	1.33	0.29	0.70		70.93	15.83	11.23	0.96	0.33	0.72
	13.5	70.15	13.38	14.32	0.96	0.30	0.90		71.25	13.12	13.51	0.84	0.29	0.98
	15	68.02	11.59	17.99	0.78	0.33	1.30		66.88	10.93	19.50	0.65	0.35	1.70
	16.5	69.52	13.04	15.12	0.90	0.32	1.10		69.31	12.80	15.36	0.93	0.30	1.30
	18	70.55	14.46	12.72	1.13	0.29	0.85		71.74	14.71	11.34	1.16	0.30	0.75
	19.5	72.03	14.90	11.04	1.15	0.29	0.58		70.73	15.50	11.55	1.29	0.27	0.65
	21	70.96	15.51	11.06	1.48	0.27	0.71		70.99	15.52	11.10	1.38	0.29	0.72
	22.5	70.57	15.14	11.94	1.44	0.30	0.62		70.33	15.76	11.54	1.41	0.26	0.70
	24	70.20	15.01	12.58	1.27	0.27	0.67		70.09	16.38	11.05	1.52	0.26	0.70
	25.5	70.14	14.88	12.98	1.04	0.27	0.69		69.76	15.71	12.44	1.11	0.30	0.69
	27	70.18	14.42	12.95	1.43	0.27	0.76		71.02	14.31	12.48	1.13	0.28	0.78
	28.5	70.33	14.61	12.77	1.35	0.28	0.66		70.05	14.59	13.19	1.08	0.26	0.83
	30	70.36	14.95	12.64	1.09	0.27	0.69		69.64	14.30	13.84	1.16	0.25	0.81
5	0	70.49	14.82	12.42	1.07	0.31	0.89	6	69.91	13.84	14.01	1.08	0.31	0.86
	1.5	70.42	15.21	12.23	1.10	0.27	0.77		70.40	14.39	12.88	1.13	0.29	0.90
	3	70.11	15.24	12.27	1.22	0.30	0.86		70.80	14.26	12.47	1.27	0.29	0.91
	4.5	69.87	15.57	12.23	1.17	0.30	0.85		70.28	14.91	12.33	1.31	0.30	0.86

Meas.	Pos. (nm)	Fe	Cr	Ni	Mn	Si	Zr	Meas.	Fe	Cr	Ni	Mn	Si	Zr
5	6	69.53	15.92	12.29	1.21	0.29	0.76	6	70.47	14.74	12.37	1.32	0.30	0.80
	7.5	69.82	15.76	12.09	1.20	0.29	0.85		70.73	14.39	12.35	1.40	0.29	0.84
	9	70.37	15.77	11.50	1.23	0.32	0.80		69.88	15.75	12.03	1.36	0.28	0.69
	10.5	70.56	15.33	11.98	1.05	0.31	0.77		70.24	16.12	11.27	1.25	0.31	0.81
	12	70.49	13.91	13.49	0.86	0.33	0.92		70.24	15.77	11.65	1.25	0.31	0.78
	13.5	67.46	12.81	17.27	0.76	0.32	1.37		71.60	14.06	12.04	1.18	0.32	0.81
	15	68.07	12.31	17.15	0.86	0.31	1.29		68.51	12.22	16.87	0.75	0.36	1.29
	16.5	70.53	14.91	12.56	0.94	0.27	0.79		65.78	12.16	19.66	0.53	0.34	1.53
	18	71.17	15.48	11.25	1.11	0.26	0.72		69.67	13.15	14.89	0.88	0.32	1.10
	19.5	70.43	15.89	11.33	1.29	0.29	0.76		70.55	15.18	12.01	1.18	0.30	0.77
	21	70.09	15.96	11.63	1.40	0.25	0.67		70.28	15.72	11.42	1.53	0.28	0.77
	22.5	70.40	15.79	11.55	1.33	0.28	0.65		69.99	16.31	11.26	1.44	0.31	0.69
	24	70.28	15.01	12.36	1.45	0.27	0.64		70.16	16.05	11.68	1.14	0.26	0.70
	25.5	70.45	15.09	12.44	1.08	0.26	0.67		69.73	15.74	12.50	1.06	0.26	0.71
	27	70.44	14.51	12.91	1.18	0.26	0.70		69.23	15.14	13.26	1.22	0.26	0.89
	28.5	70.52	14.62	12.91	0.91	0.30	0.74		69.37	15.01	13.55	1.11	0.26	0.70
	30	70.51	13.98	13.33	1.22	0.28	0.68		69.51	14.91	13.37	1.23	0.25	0.73
7	0	69.47	14.51	13.54	1.31	0.28	0.88	8	68.08	15.72	13.35	1.45	0.48	0.92
	1.5	70.30	15.19	12.10	1.27	0.34	0.81		67.69	16.23	13.49	1.13	0.43	1.03
	3	70.25	15.75	11.56	1.30	0.31	0.82		68.86	16.33	12.25	1.11	0.54	0.91
	4.5	70.08	15.57	12.14	1.07	0.31	0.83		68.17	17.09	11.87	1.48	0.49	0.90
	6	69.82	15.61	12.25	1.09	0.33	0.91		68.39	16.81	12.10	1.36	0.45	0.89
	7.5	69.69	15.39	12.35	1.40	0.34	0.82		68.61	16.60	12.26	1.14	0.50	0.89
	9	70.74	15.80	11.32	1.05	0.30	0.78		67.66	15.55	14.06	1.18	0.47	1.08
	10.5	70.64	16.52	10.65	1.10	0.31	0.78		68.50	13.79	14.74	1.11	0.52	1.35
	12	71.42	14.96	11.18	1.28	0.32	0.85		68.03	13.50	15.50	0.90	0.53	1.54
	13.5	70.21	13.07	14.40	0.80	0.39	1.12		66.92	13.46	16.47	0.95	0.48	1.71
	15	65.88	11.51	20.07	0.52	0.35	1.67		68.03	15.14	13.70	1.06	0.42	1.65
	16.5	67.10	11.99	18.64	0.53	0.32	1.42		69.21	15.80	11.86	1.38	0.38	1.37
	18	71.08	13.25	13.76	0.77	0.30	0.84		68.33	17.20	11.71	1.27	0.31	1.19
	19.5	70.05	15.97	11.54	1.45	0.29	0.71		69.16	16.68	11.33	1.40	0.39	1.05
	21	70.18	16.56	10.92	1.39	0.26	0.69		68.17	16.75	12.43	1.14	0.38	1.13
	22.5	69.97	15.96	11.83	1.34	0.25	0.66		68.94	16.09	12.32	1.20	0.34	1.10
	24	69.66	16.61	11.46	1.40	0.29	0.60		69.32	15.46	12.58	1.13	0.34	1.16
	25.5	70.24	15.20	12.33	1.26	0.30	0.68		69.05	15.93	12.25	1.25	0.39	1.14
	27	70.37	14.75	12.48	1.36	0.27	0.77		68.83	16.66	11.75	1.24	0.36	1.16
	28.5	70.05	15.64	12.04	1.17	0.31	0.79		68.29	16.79	12.45	1.16	0.32	0.98
	30	69.26	15.15	13.31	1.23	0.23	0.81		68.00	16.56	12.73	1.22	0.30	1.19
9	0	67.16	14.94	14.85	1.36	0.52	1.17	10	67.89	16.68	12.90	1.04	0.44	1.05
	1.5	67.15	15.45	14.64	1.13	0.53	1.11		67.54	15.94	13.67	1.34	0.45	1.07
	3	68.28	15.90	13.61	0.81	0.49	0.91		67.84	16.98	12.46	1.17	0.51	1.05
	4.5	67.69	16.61	12.90	1.28	0.44	1.09		68.58	17.22	11.67	1.24	0.42	0.88
	6	68.22	16.88	12.11	1.33	0.47	1.00		68.56	16.92	11.66	1.37	0.51	0.99
	7.5	68.72	17.31	11.27	1.37	0.51	0.83		67.99	16.28	12.85	1.44	0.46	0.98
	9	68.52	16.44	12.07	1.46	0.50	1.00		67.97	16.37	12.79	1.23	0.48	1.16
	10.5	68.74	15.23	13.18	1.21	0.58	1.06		67.86	16.03	13.43	1.25	0.45	0.97
	12	66.65	14.27	15.98	0.98	0.44	1.68		68.40	14.56	14.22	0.96	0.51	1.34

Meas.	Pos. (nm)	Fe	Cr	Ni	Mn	Si	Zr	Meas.	Fe	Cr	Ni	Mn	Si	Zr
9	13.5	66.11	13.39	17.41	0.80	0.46	1.82	10	67.51	13.33	16.02	0.84	0.50	1.80
	15	67.61	14.43	14.85	1.00	0.46	1.64		66.50	14.12	16.29	0.76	0.38	1.95
	16.5	69.49	15.93	11.83	1.14	0.37	1.25		68.47	15.30	13.17	1.16	0.39	1.51
	18	69.20	17.74	10.24	1.44	0.39	0.99		69.57	16.41	11.38	1.13	0.37	1.15
	19.5	68.14	17.19	11.78	1.52	0.31	1.06		68.73	16.86	11.59	1.27	0.38	1.16
	21	68.25	17.13	11.97	1.16	0.37	1.11		69.28	16.65	11.31	1.38	0.29	1.08
	22.5	68.18	17.29	11.92	1.17	0.35	1.08		68.87	16.21	12.04	1.51	0.30	1.07
	24	68.19	16.38	12.62	1.39	0.37	1.05		67.89	15.99	13.41	1.16	0.36	1.19
	25.5	68.46	15.92	12.87	1.24	0.35	1.16		68.61	15.06	13.74	1.06	0.36	1.17
	27								68.58	15.78	12.71	1.36	0.37	1.20
	28.5								68.45	16.10	12.79	1.15	0.35	1.16
	30								68.41	15.52	13.34	1.03	0.38	1.32
11	0	70.41	14.04	13.22	1.35	0.25	0.74	12	69.25	15.31	13.29	1.29	0.20	0.66
	1.5	70.48	13.90	13.41	1.22	0.28	0.69		68.90	15.57	13.13	1.26	0.31	0.82
	3	70.02	14.38	13.45	1.24	0.26	0.66		69.62	15.75	12.65	0.95	0.26	0.76
	4.5	69.62	15.45	12.56	1.40	0.24	0.73		69.00	15.97	12.39	1.68	0.21	0.75
	6	69.77	15.32	12.38	1.54	0.27	0.73		70.25	15.61	12.37	0.88	0.24	0.65
	7.5	70.12	16.07	11.42	1.50	0.29	0.59		71.39	15.01	11.27	1.26	0.29	0.78
	9	71.14	15.45	10.82	1.68	0.30	0.60		71.74	14.16	11.94	1.11	0.35	0.71
	10.5	68.80	13.35	15.39	1.08	0.42	0.96		68.52	11.97	17.10	1.00	0.30	1.12
	12	68.25	11.56	17.56	0.88	0.30	1.46		68.58	12.22	16.77	0.88	0.35	1.20
	13.5	68.23	12.30	17.00	1.00	0.36	1.10		69.71	12.45	15.27	1.06	0.37	1.15
	15	69.67	13.16	14.91	1.01	0.30	0.94		70.36	13.85	13.12	1.34	0.27	1.05
	16.5	70.03	14.46	12.99	1.61	0.24	0.67		70.70	14.86	11.90	1.37	0.32	0.85
	18	69.88	15.01	12.78	1.25	0.23	0.85		71.01	14.66	11.81	1.46	0.25	0.81
	19.5	70.35	14.34	12.98	1.29	0.27	0.77		71.02	16.20	10.91	0.89	0.21	0.78
	21	71.66	14.26	11.84	1.15	0.30	0.79		71.08	14.90	11.83	1.15	0.27	0.77
	22.5	72.19	14.17	10.88	1.62	0.32	0.82		69.30	15.02	13.37	1.12	0.25	0.94
	24	71.50	14.56	11.34	1.57	0.20	0.83		68.60	14.33	14.72	1.06	0.30	0.99
	25.5	71.50	14.44	11.74	1.31	0.19	0.82		68.36	13.94	15.62	0.89	0.26	0.93
	27	70.35	14.52	12.67	1.27	0.30	0.89		69.38	13.00	15.04	1.31	0.29	0.97
	28.5	69.97	13.73	14.20	1.02	0.24	0.85		68.61	13.08	16.14	1.00	0.22	0.96
	30													
13	0	68.29	15.66	13.19	1.22	0.52	1.11	14	69.24	15.03	13.48	1.17	0.32	0.76
	1.5	66.83	15.05	15.43	1.22	0.42	1.04		68.49	15.46	13.75	1.27	0.24	0.79
	3	65.94	15.39	15.70	1.15	0.47	1.35		69.83	15.60	12.52	1.06	0.31	0.68
	4.5	66.14	15.19	15.30	1.62	0.48	1.27		69.43	15.43	12.95	1.43	0.28	0.48
	6	67.78	15.32	13.97	1.20	0.44	1.29		70.14	16.15	11.21	1.50	0.25	0.75
	7.5	68.67	16.26	12.39	1.14	0.47	1.07		69.55	15.99	11.72	1.74	0.37	0.64
	9	69.17	16.70	11.42	1.24	0.52	0.95		70.14	15.57	11.86	1.44	0.28	0.70
	10.5	68.64	17.26	11.23	1.40	0.54	0.94		71.41	16.11	10.80	0.87	0.28	0.54
	12	67.88	17.28	12.12	1.10	0.49	1.14		70.74	15.15	11.78	1.61	0.26	0.46
	13.5	66.65	15.04	15.31	1.25	0.51	1.25		72.77	11.90	12.75	1.24	0.29	1.05
	15	66.86	13.79	16.53	0.69	0.45	1.69		64.48	10.76	21.98	0.63	0.41	1.74
	16.5	66.92	13.34	16.76	0.71	0.47	1.79		68.55	11.24	17.61	0.75	0.37	1.47
	18	67.83	14.42	14.88	0.99	0.40	1.48		71.99	13.27	12.10	1.44	0.37	0.84
	19.5	68.19	16.23	12.68	1.33	0.35	1.21		70.49	14.31	12.77	1.27	0.30	0.85

Meas.	Pos. (nm)	Fe	Cr	Ni	Mn	Si	Zr	Meas.	Fe	Cr	Ni	Mn	Si	Zr
13	21	68.52	16.58	11.81	1.49	0.37	1.24	14	70.50	15.64	11.54	1.47	0.31	0.54
	22.5	68.70	15.86	12.64	1.29	0.36	1.14		71.53	16.17	10.05	1.18	0.32	0.74
	24	67.64	17.05	12.48	1.35	0.39	1.09		69.56	15.15	13.01	1.35	0.28	0.66
	25.5	67.96	17.16	11.99	1.36	0.31	1.22		69.96	13.87	13.61	1.42	0.24	0.90
	27	68.31	16.21	12.65	1.35	0.36	1.12		71.47	14.50	11.86	1.02	0.24	0.91
	28.5	67.89	15.66	13.64	1.22	0.36	1.23		69.57	14.27	14.07	1.03	0.25	0.82
	30	68.46	16.21	12.34	1.43	0.45	1.12							
15	0	69.31	16.23	12.09	1.40	0.36	0.61	16	68.13	13.90	15.37	1.34	0.32	0.94
	1.5	70.15	16.35	11.41	1.20	0.24	0.66		68.75	13.38	15.50	1.10	0.29	0.98
	3	70.42	14.25	12.58	1.49	0.31	0.94		67.60	14.28	15.79	1.05	0.35	0.93
	4.5	69.04	15.20	13.40	1.31	0.27	0.78		69.26	14.74	13.75	1.16	0.29	0.80
	6	69.66	14.38	13.84	1.26	0.20	0.66		70.65	15.37	11.82	1.28	0.24	0.64
	7.5	69.29	14.12	14.13	1.54	0.24	0.67		70.49	16.08	11.12	1.44	0.27	0.60
	9	70.75	14.93	11.82	1.30	0.31	0.90		68.79	17.71	11.14	1.36	0.28	0.72
	10.5	71.67	14.68	11.66	1.02	0.29	0.68		69.47	16.71	11.37	1.39	0.30	0.76
	12	71.24	12.56	14.01	1.04	0.22	0.93		71.87	14.15	11.40	1.69	0.28	0.62
	13.5	65.15	10.97	21.24	0.59	0.45	1.61		68.54	12.56	16.38	1.02	0.33	1.17
	15	69.33	11.75	16.10	1.13	0.41	1.29		66.89	10.56	20.04	0.82	0.33	1.35
	16.5	71.89	14.12	11.58	1.31	0.23	0.87		69.72	12.39	15.46	1.08	0.39	0.97
	18	71.06	15.14	11.32	1.15	0.30	1.04		70.82	14.52	11.99	1.42	0.29	0.97
	19.5	70.94	14.58	11.87	1.45	0.29	0.86		69.41	16.64	11.71	1.24	0.25	0.75
	21	70.87	14.44	12.26	1.30	0.26	0.88		71.12	15.50	11.03	1.17	0.28	0.90
	22.5	70.86	14.47	12.35	1.28	0.21	0.83		70.17	14.31	13.12	1.27	0.31	0.81
	24	70.59	15.32	12.05	1.03	0.25	0.76		70.16	14.51	13.10	1.16	0.27	0.81
	25.5	70.58	14.05	13.07	1.21	0.25	0.83		70.89	13.27	13.60	1.25	0.28	0.71
	27	71.01	14.64	11.98	1.25	0.26	0.86		70.70	13.96	12.90	1.34	0.26	0.84
	28.5	71.17	14.71	11.70	1.28	0.29	0.84		69.37	13.48	14.81	1.08	0.32	0.95
	30								69.61	13.45	14.90	0.91	0.30	0.82
17	0	71.14	16.23	10.17	1.53	0.26	0.66	18	69.39	14.06	14.46	1.08	0.24	0.78
	1.5	70.46	16.01	11.30	1.32	0.26	0.65		69.52	13.90	14.37	1.12	0.29	0.80
	3	69.56	16.46	11.63	1.36	0.27	0.72		70.27	14.02	13.58	1.22	0.21	0.70
	4.5	69.78	15.59	12.40	1.26	0.25	0.71		70.80	15.61	11.58	1.24	0.22	0.54
	6	70.99	14.77	11.97	1.23	0.27	0.77		70.70	15.20	11.73	1.36	0.24	0.77
	7.5	69.28	14.90	13.41	1.48	0.25	0.67		69.91	15.61	12.59	1.06	0.27	0.57
	9	70.08	15.46	12.23	1.17	0.27	0.78		70.13	15.09	12.38	1.32	0.35	0.71
	10.5	71.19	14.22	12.39	1.15	0.35	0.71		67.71	12.63	17.16	0.81	0.37	1.32
	12	68.38	11.53	17.71	0.83	0.25	1.29		68.85	11.14	17.68	0.66	0.38	1.28
	13.5	68.87	10.31	18.55	0.56	0.36	1.36		69.77	12.32	15.65	0.87	0.36	1.02
	15	69.42	12.02	16.06	0.91	0.36	1.23		71.26	14.24	12.17	0.99	0.31	1.03
	16.5	70.65	14.12	13.00	1.12	0.30	0.80		70.00	14.97	12.17	1.59	0.34	0.92
	18	70.50	15.21	12.35	1.00	0.27	0.67		70.34	14.56	12.56	1.46	0.20	0.87
	19.5	70.56	15.11	12.05	1.20	0.29	0.79		69.48	14.96	12.93	1.37	0.27	0.99
	21	71.01	15.20	11.43	1.36	0.28	0.72		71.33	13.82	12.33	1.46	0.26	0.81
	22.5	71.70	14.76	11.41	1.21	0.27	0.65		69.59	13.87	13.98	1.27	0.27	1.01
	24	70.34	15.01	12.26	1.24	0.30	0.85		70.25	13.28	14.16	1.05	0.29	0.96
	25.5	69.99	15.60	12.44	1.08	0.21	0.67		70.13	13.39	14.25	1.04	0.25	0.95
	27	70.71	15.07	11.60	1.44	0.33	0.86		70.15	13.90	13.77	1.23	0.28	0.67
	28.5	71.79	14.07	11.92	1.24	0.29	0.70		70.26	14.30	13.15	1.23	0.30	0.74
	30													

Ref-Hf, 400C, 3 dpa, 3.2 MeV p+

Meas.	Pos. (nm)	Fe	Cr	Ni	Mn	Mo	Si	Meas.	Fe	Cr	Ni	Mn	Mo	Si
1	0	62.39	19.84	12.15	2.24	2.42	0.96	2	63.55	19.12	12.68	1.54	2.12	0.98
	1.5	62.97	19.79	12.15	1.85	2.32	0.92		64.32	18.69	12.67	1.54	1.95	0.83
	3	63.64	19.99	11.73	1.43	2.24	0.97		64.50	18.60	12.60	1.68	1.83	0.79
	4.5	62.64	19.57	12.95	1.76	2.05	1.03		65.89	19.06	11.44	1.25	1.54	0.81
	6	63.11	19.48	13.09	1.35	1.86	1.10		67.18	16.72	12.48	1.16	1.50	0.96
	7.5	63.16	19.23	13.20	1.45	1.87	1.09		65.51	13.22	18.08	0.67	1.17	1.34
	9	64.56	19.09	12.24	1.50	1.74	0.87		55.93	10.21	29.32	0.77	1.35	2.42
	10.5	65.42	19.08	11.58	1.33	1.74	0.86		66.26	17.40	12.52	1.12	1.64	1.06
	12	66.00	18.76	11.47	1.30	1.55	0.93		64.14	19.46	12.52	1.21	1.58	1.08
	13.5	67.58	16.90	12.17	0.92	1.44	0.99		64.10	18.75	12.77	1.57	1.74	1.06
	15	62.92	12.86	20.48	0.90	1.37	1.48		64.01	18.38	13.05	1.51	1.88	1.16
	16.5	58.32	10.54	27.04	0.69	1.27	2.15		62.43	19.83	13.33	1.50	1.93	0.97
	18	64.15	14.42	17.84	0.58	1.38	1.62		62.77	19.80	12.89	1.50	2.03	1.01
	19.5	65.98	18.40	11.92	1.11	1.64	0.95		62.03	20.35	12.55	1.49	2.37	1.21
	21	64.40	18.92	11.92	1.74	1.88	1.14		62.68	19.89	11.99	1.93	2.48	1.03
	22.5	62.70	20.55	12.19	1.59	1.94	1.04		62.87	19.44	12.40	1.77	2.31	1.21
	24	62.49	20.15	12.30	1.62	2.31	1.14							
	25.5	61.85	20.60	12.39	1.71	2.32	1.13							
	27	61.97	20.16	12.41	1.85	2.46	1.16							
	28.5	62.59	20.14	12.21	1.69	2.25	1.11							
	30	62.59	19.83	12.66	1.45	2.41	1.06							
3	0	63.74	19.61	11.92	1.80	2.04	0.90	4	62.31	20.52	12.40	1.58	2.28	0.90
	1.5	63.32	19.58	12.49	1.79	1.85	0.97		62.34	20.81	12.29	1.51	2.18	0.87
	3	63.14	20.21	12.30	1.36	2.03	0.95		62.72	20.24	12.73	1.24	2.09	0.98
	4.5	63.15	19.84	12.68	1.37	2.02	0.94		63.55	18.78	13.51	1.17	1.94	1.05
	6	63.57	19.41	12.48	1.46	2.05	1.03		63.10	18.96	13.65	1.41	1.89	0.98
	7.5	64.13	19.33	12.45	1.54	1.80	0.76		62.51	18.82	14.62	1.26	1.78	1.01
	9	64.28	19.67	11.98	1.56	1.67	0.85		63.89	17.96	13.94	1.57	1.60	1.04
	10.5	65.03	19.43	11.73	1.30	1.63	0.88		64.18	18.16	13.63	1.36	1.63	1.03
	12	67.24	17.49	11.88	0.83	1.63	0.93		66.09	17.89	12.61	0.94	1.46	1.02
	13.5	64.82	12.97	18.66	0.78	1.49	1.28		67.17	16.21	13.42	0.68	1.46	1.05
	15	58.28	11.59	26.03	0.57	1.49	2.03		56.48	10.88	28.52	0.74	1.33	2.06
	16.5	65.73	17.25	13.28	0.98	1.51	1.24		65.46	15.08	15.92	0.75	1.42	1.37
	18	65.30	19.29	11.53	1.12	1.73	1.02		66.06	18.59	11.57	1.06	1.48	1.24
	19.5	64.32	19.32	11.97	1.42	1.91	1.06		64.67	18.84	12.53	1.29	1.71	0.96
	21	63.74	19.56	12.37	1.33	1.95	1.06		62.95	18.95	13.74	1.45	1.91	1.00
	22.5	62.77	19.83	12.61	1.72	1.99	1.09		62.79	18.79	13.89	1.49	1.80	1.25
	24	62.54	19.64	13.18	1.54	2.00	1.10		62.51	19.11	13.79	1.45	1.97	1.17
	25.5	62.30	19.20	13.43	1.75	2.17	1.15		62.20	19.54	13.31	1.59	2.17	1.19
	27	63.55	19.11	12.71	1.37	2.07	1.18		62.02	19.61	13.50	1.63	2.18	1.06
	28.5	63.58	18.72	13.30	1.31	1.91	1.17		61.92	19.82	13.44	1.51	2.33	0.96
	30	62.87	18.83	13.56	1.80	1.89	1.05		62.01	20.17	12.66	1.62	2.44	1.10
5	0	62.61	20.28	11.88	1.87	2.40	0.96	6	62.28	20.20	12.49	1.64	2.43	0.97
	1.5	62.73	19.91	12.51	1.58	2.30	0.96		61.98	20.31	12.92	1.47	2.20	1.12
	3	62.70	19.91	12.52	1.58	2.33	0.97		63.00	19.43	13.10	1.37	2.08	1.01
	4.5	62.59	20.31	12.68	1.40	2.18	0.85		62.55	19.38	13.60	1.61	1.91	0.95

Meas.	Pos. (nm)	Fe	Cr	Ni	Mn	Mo	Si	Meas.	Fe	Cr	Ni	Mn	Mo	Si
5	6	65.40	18.58	13.99	0.79	1.02	0.21	6	62.95	19.52	13.01	1.60	1.94	0.98
	7.5	67.06	18.24	12.82	0.68	0.96	0.23		63.66	19.78	12.57	1.22	1.79	0.98
	9	67.66	17.50	13.11	0.62	0.90	0.20		63.78	18.99	13.26	1.23	1.81	0.94
	10.5	69.37	15.21	13.63	0.63	0.93	0.22		64.25	18.83	13.16	0.88	1.86	1.02
	12	63.37	11.70	23.11	0.57	0.82	0.43		66.11	18.13	12.26	1.06	1.51	0.94
	13.5	62.58	11.07	24.11	0.72	1.08	0.43		66.57	16.47	13.61	0.99	1.33	1.02
	15	68.24	15.82	14.18	0.57	0.91	0.28		61.81	12.06	22.30	0.64	1.47	1.72
	16.5	67.31	18.01	12.38	0.97	1.06	0.27		60.90	11.51	23.51	0.78	1.31	1.98
	18	66.97	18.72	12.13	0.71	1.22	0.24		66.85	17.28	12.11	0.89	1.57	1.30
	19.5	65.38	19.29	12.84	1.00	1.25	0.25		64.60	19.31	12.21	1.12	1.61	1.15
	21	65.13	19.12	13.29	1.00	1.23	0.23		64.21	19.17	12.19	1.39	1.92	1.10
	22.5	64.86	19.20	13.55	1.00	1.15	0.24		63.32	19.78	12.68	1.15	1.92	1.16
	24	64.56	19.28	13.69	1.13	1.09	0.25		63.28	19.72	12.66	1.26	2.04	1.04
	25.5	65.31	18.39	13.90	0.84	1.32	0.24		62.67	19.10	13.15	1.65	2.29	1.14
	27	65.31	18.82	13.17	0.97	1.46	0.26		62.74	19.75	12.85	1.56	2.01	1.09
	28.5	64.93	19.58	12.52	1.17	1.54	0.27		63.11	19.98	12.28	1.56	1.99	1.08
	30	65.69	19.32	12.42	1.03	1.32	0.22		63.33	19.28	12.51	1.60	2.20	1.08
7	0	61.71	19.49	13.60	1.80	2.23	1.17	8	64.53	19.45	12.23	1.43	1.61	0.76
	1.5	62.22	20.13	12.77	1.58	2.27	1.04		64.60	19.78	11.69	1.42	1.64	0.87
	3	61.52	20.39	12.81	1.92	2.42	0.94		64.99	19.53	11.68	1.46	1.50	0.83
	4.5	61.95	20.21	12.73	1.73	2.46	0.92		64.97	19.13	11.81	1.45	1.70	0.93
	6	62.70	19.81	12.72	1.53	2.30	0.93		64.77	18.75	12.67	1.34	1.67	0.80
	7.5	63.06	19.38	12.86	1.36	2.27	1.07		65.89	17.58	12.81	1.08	1.67	0.97
	9	63.81	19.72	12.46	1.10	2.02	0.89		66.77	17.15	12.63	1.07	1.46	0.93
	10.5	64.32	18.71	13.18	1.17	1.75	0.86		66.22	16.65	14.06	0.65	1.55	0.88
	12	65.62	17.35	13.32	1.19	1.57	0.96		66.68	14.53	15.44	0.77	1.48	1.10
	13.5	66.25	16.04	14.11	1.04	1.54	1.01		64.57	14.12	17.92	0.87	1.29	1.23
	15	62.15	12.53	21.19	0.84	1.65	1.65		61.54	12.48	22.19	0.80	1.40	1.59
	16.5	61.94	12.56	21.33	0.88	1.35	1.94		62.32	11.54	22.62	0.50	1.60	1.43
	18	66.61	17.02	12.92	0.97	1.42	1.07		64.64	11.59	20.20	0.89	1.34	1.35
	19.5	64.89	18.38	12.57	1.26	1.76	1.14		65.80	13.93	16.72	0.83	1.60	1.11
	21	63.38	19.09	13.29	1.55	1.60	1.08		66.78	15.33	14.40	0.93	1.44	1.12
	22.5	63.25	18.83	13.55	1.42	1.73	1.22		67.12	16.68	12.65	0.84	1.72	1.00
	24	63.15	18.83	13.09	1.83	1.93	1.16		67.22	17.35	11.90	0.95	1.60	0.98
	25.5	63.14	19.08	12.78	1.67	2.20	1.13		65.16	18.51	12.07	1.46	1.79	1.01
	27	62.49	19.38	13.33	1.51	2.09	1.19		65.05	18.69	11.96	1.46	1.70	1.15
	28.5	62.96	19.31	12.94	1.52	2.10	1.17		65.22	18.60	11.96	1.42	1.83	0.97
	30	63.29	19.47	12.63	1.49	2.08	1.04		64.07	19.25	12.34	1.44	1.82	1.08
9	0	62.34	20.35	12.33	1.56	2.46	0.96	10	64.53	19.45	12.23	1.43	1.61	0.76
	1.5	62.44	20.04	12.58	1.91	2.18	0.85		64.60	19.78	11.69	1.42	1.64	0.87
	3	61.49	20.96	12.51	1.71	2.31	1.02		64.99	19.53	11.68	1.46	1.50	0.83
	4.5	61.86	20.52	12.49	1.59	2.56	0.98		64.97	19.13	11.81	1.45	1.70	0.93
	6	61.91	20.47	12.73	1.87	2.09	0.93		64.77	18.75	12.67	1.34	1.67	0.80
	7.5	63.32	19.17	13.07	1.62	1.85	0.97		65.89	17.58	12.81	1.08	1.67	0.97
	9	63.29	18.77	13.80	1.27	1.94	0.93		66.77	17.15	12.63	1.07	1.46	0.93
	10.5	64.52	18.14	13.44	1.21	1.69	1.00		66.22	16.65	14.06	0.65	1.55	0.88
	12	66.02	17.52	12.51	1.29	1.58	1.08		66.68	14.53	15.44	0.77	1.48	1.10

Meas.	Pos. (nm)	Fe	Cr	Ni	Mn	Mo	Si	Meas.	Fe	Cr	Ni	Mn	Mo	Si
9	13.5	65.75	14.97	15.26	0.90	1.58	1.54	10	64.57	14.12	17.92	0.87	1.29	1.23
	15	59.22	11.59	25.01	0.73	1.43	2.02		61.54	12.48	22.19	0.80	1.40	1.59
	16.5	63.19	14.65	18.27	0.71	1.66	1.51		62.32	11.54	22.62	0.50	1.60	1.43
	18	65.25	18.07	12.88	1.17	1.39	1.24		64.64	11.59	20.20	0.89	1.34	1.35
	19.5	64.99	18.62	12.51	1.04	1.63	1.21		65.80	13.93	16.72	0.83	1.60	1.11
	21	63.87	18.19	13.55	1.35	1.72	1.33		66.78	15.33	14.40	0.93	1.44	1.12
	22.5	62.90	18.69	14.01	1.18	1.94	1.28		67.12	16.68	12.65	0.84	1.72	1.00
	24	62.95	19.63	13.22	1.11	2.02	1.07		67.22	17.35	11.90	0.95	1.60	0.98
	25.5	62.53	19.50	13.10	1.47	2.09	1.32		65.16	18.51	12.07	1.46	1.79	1.01
	27	61.96	19.46	13.55	1.40	2.24	1.40		65.05	18.69	11.96	1.46	1.70	1.15
	28.5	62.48	19.97	12.63	1.58	2.19	1.15		65.22	18.60	11.96	1.42	1.83	0.97
	30	63.26	19.69	12.57	1.40	2.13	0.96		64.07	19.25	12.34	1.44	1.82	1.08
11	0	65.75	19.29	12.54	0.79	1.26	0.37	12	63.39	20.01	13.12	1.63	1.38	0.48
	1.5	65.43	18.78	12.66	1.25	1.40	0.48		64.82	19.98	12.90	1.13	1.06	0.11
	3	65.36	19.19	12.72	1.05	1.20	0.47		64.78	18.67	13.65	1.46	1.29	0.15
	4.5	66.37	18.35	12.52	0.92	1.13	0.72		64.54	19.69	13.59	0.98	0.93	0.28
	6	66.06	18.67	12.93	0.98	1.06	0.31		64.96	18.95	13.67	1.18	1.13	0.10
	7.5	66.46	18.91	12.12	0.93	1.06	0.52		65.86	19.14	13.13	1.10	0.75	0.02
	9	66.76	18.73	12.12	0.91	1.14	0.34		66.44	18.18	12.71	1.06	1.36	0.25
	10.5	66.60	19.34	11.49	0.56	1.22	0.79		67.78	18.15	12.08	0.83	0.94	0.23
	12	67.68	19.12	11.64	0.53	0.81	0.23		68.87	17.55	11.90	0.91	0.64	0.13
	13.5	69.63	16.88	12.18	0.48	0.54	0.29		70.01	15.29	13.07	0.45	0.76	0.43
	15	68.49	14.32	15.26	0.66	0.65	0.63		64.69	12.12	20.65	0.75	0.76	1.03
	16.5	61.81	12.39	22.86	-0.02	1.17	1.80		61.74	12.04	23.60	0.54	1.00	1.08
	18	60.31	12.46	24.53	-0.03	0.91	1.81		67.69	14.38	15.94	0.73	0.57	0.68
	19.5	69.01	16.47	12.86	0.35	0.90	0.40		67.31	17.48	12.74	0.72	1.25	0.49
	21	67.70	17.54	11.98	0.99	1.22	0.57		66.85	18.17	12.25	1.36	1.17	0.21
	22.5	66.74	18.11	12.83	0.42	1.25	0.65		66.70	18.50	12.22	1.03	1.50	0.05
	24	65.13	18.92	13.22	1.00	1.07	0.66		64.65	19.42	12.90	1.42	1.41	0.20
	25.5	65.90	18.54	12.60	0.87	1.47	0.61		65.09	18.65	12.97	1.28	1.81	0.20
	27	64.74	18.38	13.96	0.80	1.66	0.46		64.52	19.24	12.81	1.36	1.69	0.39
	28.5	64.50	19.09	13.67	0.82	1.32	0.60		65.42	19.04	12.77	0.98	1.51	0.27
	30	65.22	18.40	13.80	0.96	1.26	0.36		64.77	19.25	12.86	1.31	1.56	0.26
13	0	65.45	19.71	12.50	0.44	1.44	0.45	14	64.43	19.00	13.82	1.46	1.12	0.17
	1.5	65.94	18.73	12.87	0.90	1.20	0.36		63.55	20.16	13.41	1.45	1.25	0.17
	3	66.42	18.19	13.01	0.87	1.10	0.42		63.95	19.21	13.98	1.27	1.32	0.28
	4.5	65.38	19.90	12.90	0.39	0.97	0.46		64.64	19.16	13.39	1.21	1.40	0.20
	6	66.23	18.54	12.95	1.07	0.56	0.65		64.76	19.41	13.07	1.53	1.22	0.00
	7.5	66.07	18.84	13.24	0.34	0.96	0.54		65.26	18.93	13.21	1.17	1.19	0.24
	9	67.83	17.43	12.41	1.00	0.89	0.45		65.99	19.17	12.58	1.21	0.92	0.12
	10.5	67.43	17.73	12.54	0.94	1.00	0.37		66.24	19.11	12.20	0.88	1.16	0.40
	12	67.96	17.77	12.67	0.45	0.70	0.45		67.74	17.73	12.65	1.14	0.60	0.15
	13.5	69.39	14.90	14.02	0.26	0.68	0.75		68.75	13.91	15.53	0.52	0.76	0.53
	15	65.14	11.28	20.58	0.25	1.15	1.60		63.43	12.39	21.71	0.45	0.64	1.37
	16.5	63.14	11.88	21.92	0.29	1.01	1.76		64.03	13.49	20.41	0.19	0.92	0.96
	18	66.92	14.01	16.39	0.70	0.94	1.04		66.78	16.50	14.76	0.51	0.99	0.46
	19.5	67.37	17.26	12.62	0.89	1.34	0.52		67.29	17.46	12.44	1.11	1.31	0.39

Meas.	Pos. (nm)	Fe	Cr	Ni	Mn	Mo	Si	Meas.	Fe	Cr	Ni	Mn	Mo	Si
13	21	66.45	19.57	11.92	0.36	1.34	0.36	14	65.20	18.89	13.45	0.97	1.27	0.22
	22.5	66.85	18.06	12.50	0.85	1.27	0.48		63.96	19.51	13.26	1.07	1.66	0.54
	24	65.21	18.67	13.29	0.67	1.55	0.62		64.43	19.27	13.57	0.97	1.56	0.19
	25.5	66.31	18.07	12.34	1.27	1.58	0.44		63.85	19.04	13.79	1.30	1.63	0.39
	27	65.00	19.26	13.02	0.62	1.73	0.37		63.88	19.53	13.35	1.48	1.52	0.24
	28.5	64.06	19.22	13.54	1.20	1.51	0.47		64.23	19.38	13.08	1.23	1.67	0.41
	30	64.94	18.88	13.32	0.87	1.71	0.29		65.10	19.18	12.76	1.05	1.45	0.46
15	0	64.24	19.28	13.64	1.27	1.18	0.39	16						
	1.5	63.75	19.30	13.74	1.43	1.44	0.33							
	3	64.05	19.37	13.36	1.52	1.27	0.43							
	4.5	65.42	19.56	13.02	0.80	1.04	0.17							
	6	63.54	20.04	13.56	1.45	1.13	0.27							
	7.5	64.66	20.55	12.46	1.23	1.13	-0.02							
	9	65.95	19.59	12.26	1.18	0.87	0.15							
	10.5	67.42	18.39	12.10	1.07	0.80	0.21							
	12	67.10	17.58	13.24	0.97	0.74	0.36							
	13.5	67.93	14.79	15.72	0.61	0.58	0.37							
	15	59.18	11.93	26.40	0.25	0.85	1.39							
	16.5	64.98	15.02	17.61	0.48	0.88	1.03							
	18	67.70	16.55	13.61	0.61	1.05	0.50							
	19.5	66.33	18.32	13.16	0.72	1.09	0.39							
	21	65.77	17.59	14.76	0.75	0.80	0.32							
	22.5	65.60	17.05	15.36	0.73	0.85	0.41							
	24	65.10	17.13	15.27	1.02	1.16	0.31							
	25.5	64.45	16.88	15.93	0.89	1.31	0.55							
	27	65.27	17.93	13.67	1.08	1.56	0.49							
	28.5	65.10	18.88	13.76	0.65	1.27	0.34							
	30	65.04	19.01	13.27	1.01	1.34	0.33							

Ref-Hf, 400C, 3 dpa, 2 MeV p+

Meas.	Pos. (nm)	Fe	Cr	Ni	Mn	Mo	Si	Meas.	Fe	Cr	Ni	Mn	Mo	Si
1	0	65.56	18.26	14.09	0.87	0.96	0.26	2	65.46	18.00	14.40	0.78	1.13	0.23
	1.5	65.75	17.87	14.01	1.11	1.02	0.23		63.52	17.66	16.61	0.87	1.06	0.28
	3	65.97	18.20	13.59	0.95	1.05	0.23		64.90	17.66	15.11	1.05	1.01	0.27
	4.5	64.72	17.64	15.30	1.02	1.12	0.21		65.73	17.84	14.11	0.99	1.12	0.21
	6	66.07	17.93	13.64	1.12	1.01	0.23		66.03	18.36	13.35	0.89	1.17	0.21
	7.5	65.43	18.23	14.25	0.88	0.99	0.23		64.88	19.13	13.71	0.92	1.14	0.22
	9	65.37	18.96	13.38	0.92	1.15	0.22		66.02	19.08	12.74	0.91	1.03	0.23
	10.5	67.74	17.57	12.68	0.81	0.97	0.23		69.10	16.59	12.53	0.55	0.98	0.26
	12	67.05	15.87	15.24	0.75	0.82	0.27		66.27	12.79	19.21	0.45	0.92	0.36
	13.5	60.14	11.69	25.99	0.66	1.06	0.46		63.46	12.20	22.46	0.48	1.03	0.37
	15	67.56	14.02	16.80	0.41	0.87	0.34		65.47	13.35	19.32	0.46	0.98	0.43
	16.5	68.81	16.32	13.06	0.75	0.79	0.28		68.90	16.14	12.82	0.95	0.94	0.25
	18	68.49	17.49	12.07	0.81	0.94	0.20		67.83	18.27	11.95	0.68	1.02	0.25
	19.5	66.68	18.80	12.37	0.85	1.07	0.23		66.56	18.85	12.49	0.69	1.18	0.24
	21	65.35	19.76	12.31	1.16	1.17	0.25		65.59	19.30	12.57	0.99	1.35	0.20
	22.5	65.16	19.74	12.51	1.09	1.25	0.24		65.25	19.23	12.90	1.05	1.33	0.24
	24	64.06	20.41	12.96	1.02	1.31	0.24		65.27	18.61	13.08	1.46	1.36	0.21
	25.5	64.51	20.04	12.56	1.18	1.42	0.28		64.55	18.44	14.23	1.31	1.17	0.29
	27	65.47	19.49	12.21	1.26	1.34	0.23		64.26	19.54	13.51	1.17	1.27	0.26
	28.5	64.08	19.78	13.50	0.95	1.42	0.26		65.30	19.27	12.72	1.10	1.34	0.26
	30	63.94	19.70	13.23	1.25	1.64	0.24		64.21	19.68	13.02	1.27	1.56	0.25
3	0	65.16	19.11	13.45	0.79	1.28	0.20	4	65.79	18.45	13.32	1.07	1.16	0.19
	1.5	65.07	19.21	13.21	1.01	1.32	0.18		64.62	19.70	13.23	1.05	1.17	0.23
	3	65.37	18.77	13.08	1.26	1.30	0.22		64.77	19.42	13.42	0.90	1.29	0.20
	4.5	66.27	17.62	13.64	1.05	1.22	0.22		65.45	19.11	13.00	1.03	1.24	0.17
	6	66.40	18.62	12.65	1.01	1.11	0.22		65.74	19.50	12.46	1.01	1.08	0.20
	7.5	66.73	18.31	12.70	0.91	1.13	0.21		66.27	19.08	12.63	0.74	1.09	0.19
	9	67.72	17.95	12.20	0.81	1.10	0.21		67.89	17.51	12.49	0.96	0.95	0.20
	10.5	69.38	16.35	12.52	0.62	0.94	0.19		66.40	14.35	17.42	0.65	0.90	0.28
	12	64.60	12.05	21.45	0.70	0.82	0.38		62.83	12.08	22.95	0.65	1.05	0.44
	13.5	66.34	18.49	12.77	1.03	1.10	0.28		68.52	16.41	13.17	0.64	1.05	0.22
	15	65.30	18.78	13.60	0.86	1.22	0.24		67.09	18.79	12.02	0.83	1.01	0.25
	16.5	64.85	19.33	13.46	1.04	1.06	0.26		65.21	19.76	12.47	1.25	1.10	0.22
	18	65.63	19.00	12.89	1.02	1.16	0.31		65.79	19.46	12.10	1.10	1.31	0.23
	19.5	65.54	18.87	12.77	1.18	1.36	0.28		64.30	19.78	13.25	1.03	1.38	0.25
	21	64.50	19.49	13.32	0.98	1.42	0.29		65.07	19.37	12.54	1.26	1.50	0.25
	22.5	65.02	18.93	13.27	1.18	1.33	0.27		63.90	20.23	13.14	1.05	1.43	0.26
	24	63.62	20.21	13.42	1.00	1.52	0.23		64.27	19.66	13.11	1.22	1.51	0.23
	25.5	64.35	19.10	13.63	1.23	1.44	0.25		64.34	20.48	12.16	1.13	1.63	0.27
	27	65.13	19.04	13.26	0.96	1.39	0.22		63.63	19.70	13.49	1.23	1.69	0.27
	28.5	65.62	19.14	12.78	0.80	1.34	0.31		64.33	19.98	12.41	1.35	1.67	0.26
	30	65.04	19.74	12.22	1.23	1.47	0.30		64.47	19.67	13.08	0.93	1.59	0.27
5	0	64.77	18.91	13.67	1.11	1.31	0.24	6	64.68	19.64	12.87	1.15	1.44	0.21
	1.5	64.95	19.27	13.45	0.93	1.18	0.22		64.99	19.51	12.67	1.19	1.44	0.21
	3	65.05	18.73	13.80	0.96	1.24	0.23		64.26	19.73	13.30	1.18	1.30	0.22
	4.5	65.76	18.44	13.67	0.92	0.98	0.22		65.39	18.73	13.37	1.01	1.26	0.24

Meas.	Pos. (nm)	Fe	Cr	Ni	Mn	Mo	Si	Meas.	Fe	Cr	Ni	Mn	Mo	Si
5	6	65.40	18.58	13.99	0.79	1.02	0.21	6	65.65	19.24	12.75	1.05	1.12	0.20
	7.5	67.06	18.24	12.82	0.68	0.96	0.23		65.50	19.17	12.92	1.01	1.19	0.21
	9	67.66	17.50	13.11	0.62	0.90	0.20		65.96	19.11	12.95	0.80	0.95	0.22
	10.5	69.37	15.21	13.63	0.63	0.93	0.22		68.37	17.43	12.31	0.76	0.91	0.22
	12	63.37	11.70	23.11	0.57	0.82	0.43		68.13	16.26	13.70	0.80	0.92	0.19
	13.5	62.58	11.07	24.11	0.72	1.08	0.43		68.30	15.25	14.41	0.86	0.94	0.24
	15	68.24	15.82	14.18	0.57	0.91	0.28		62.21	11.49	24.44	0.41	0.99	0.46
	16.5	67.31	18.01	12.38	0.97	1.06	0.27		66.00	13.87	18.47	0.47	0.84	0.35
	18	66.97	18.72	12.13	0.71	1.22	0.24		69.15	16.78	12.26	0.59	0.93	0.28
	19.5	65.38	19.29	12.84	1.00	1.25	0.25		67.60	17.94	12.38	0.82	1.00	0.26
	21	65.13	19.12	13.29	1.00	1.23	0.23		66.06	18.68	13.05	0.95	1.02	0.24
	22.5	64.86	19.20	13.55	1.00	1.15	0.24		65.74	19.37	12.52	0.94	1.19	0.24
	24	64.56	19.28	13.69	1.13	1.09	0.25		65.66	19.38	12.48	0.92	1.32	0.23
	25.5	65.31	18.39	13.90	0.84	1.32	0.24		64.86	19.67	12.75	1.06	1.39	0.26
	27	65.31	18.82	13.17	0.97	1.46	0.26		64.67	19.96	12.46	1.07	1.59	0.25
	28.5	64.93	19.58	12.52	1.17	1.54	0.27		64.26	20.12	12.67	1.23	1.47	0.25
	30	65.69	19.32	12.42	1.03	1.32	0.22		64.72	19.48	13.26	0.91	1.37	0.27

LoHf, 400C, 3 dpa

Meas.	Pos. (nm)	Fe	Cr	Ni	Mn	Mo	Si	Meas.	Fe	Cr	Ni	Mn	Mo	Si
1	0	65.65	18.05	14.06	0.94	1.03	0.27	2	66.09	18.05	13.37	1.11	1.08	0.29
	1.5	65.87	18.01	13.95	0.70	1.18	0.29		65.98	17.94	13.74	1.00	1.03	0.31
	3	66.48	18.17	13.27	0.80	1.03	0.25		66.39	18.00	13.20	0.98	1.14	0.29
	4.5	65.55	19.44	12.88	0.78	1.08	0.28		65.88	18.77	12.86	1.01	1.21	0.28
	6	66.57	18.63	12.20	1.33	1.04	0.23		65.28	19.72	12.44	1.01	1.31	0.24
	7.5	66.62	18.68	12.33	1.02	1.12	0.24		65.69	19.03	12.51	1.13	1.40	0.24
	9	67.52	17.58	12.35	1.17	1.15	0.23		65.98	19.20	12.39	0.83	1.34	0.26
	10.5	67.79	17.98	12.40	0.67	0.86	0.30		65.72	19.03	12.30	1.13	1.51	0.32
	12	67.39	17.00	13.73	0.61	0.97	0.30		66.49	18.68	12.17	1.02	1.34	0.30
	13.5	67.18	13.25	17.75	0.64	0.75	0.43		67.77	17.33	12.60	0.93	1.05	0.32
	15	65.12	12.31	20.90	0.50	0.74	0.43		68.34	16.38	13.17	0.75	1.08	0.29
	16.5	69.45	13.81	14.99	0.46	0.90	0.39		67.07	14.11	16.84	0.61	1.02	0.36
	18	70.69	15.06	12.30	0.74	0.87	0.33		66.17	13.13	18.96	0.41	0.86	0.47
	19.5	69.04	16.88	11.84	0.97	0.91	0.36		67.13	15.00	16.09	0.56	0.85	0.37
	21	68.32	18.56	11.33	0.64	0.88	0.27		68.90	16.96	12.16	0.69	0.95	0.34
	22.5	66.90	18.94	11.99	0.76	1.07	0.34		67.04	19.16	11.44	1.05	1.02	0.28
	24	66.12	19.31	11.92	0.94	1.44	0.28		67.13	19.41	10.98	1.04	1.15	0.30
	25.5	67.16	19.54	11.11	0.68	1.27	0.25		66.34	19.62	11.55	1.05	1.12	0.31
	27	65.92	18.52	12.97	0.95	1.42	0.24		66.73	19.00	11.47	1.13	1.35	0.32
	28.5	65.28	19.66	12.53	1.01	1.24	0.28		67.46	18.22	11.42	1.22	1.37	0.31
	30	65.31	19.32	12.52	1.16	1.40	0.29		67.43	18.18	11.69	1.01	1.35	0.33
3	0	67.46	17.30	13.11	0.93	0.94	0.25	4	65.87	19.41	12.47	0.78	1.20	0.27
	1.5	65.23	18.86	13.45	1.11	1.10	0.24		65.79	18.45	13.05	1.01	1.41	0.28
	3	65.75	18.35	13.59	0.89	1.13	0.29		65.87	18.70	12.89	1.04	1.21	0.29
	4.5	66.32	18.50	12.66	1.08	1.16	0.28		66.31	18.56	12.49	1.04	1.34	0.26
	6	65.52	19.01	13.04	1.00	1.15	0.28		65.31	19.43	12.29	1.16	1.55	0.26
	7.5	66.56	18.32	12.45	1.13	1.26	0.28		65.81	19.62	11.56	1.29	1.43	0.29
	9	65.68	19.63	11.95	1.27	1.21	0.25		66.23	18.86	12.32	1.02	1.25	0.31
	10.5	65.81	19.28	12.22	1.22	1.20	0.26		67.31	18.99	11.42	0.92	1.06	0.30
	12	66.05	19.23	11.96	1.24	1.23	0.28		68.33	17.53	12.11	0.66	1.06	0.31
	13.5	67.12	19.02	11.66	0.93	1.05	0.23		67.62	15.67	14.66	0.72	0.99	0.34
	15	67.98	18.12	11.67	1.05	0.87	0.30		67.54	13.46	17.30	0.36	0.91	0.43
	16.5	67.95	16.61	13.34	0.85	0.92	0.32		67.92	12.51	17.78	0.58	0.78	0.42
	18	65.15	12.58	20.75	0.38	0.68	0.46		68.06	14.32	15.90	0.39	0.95	0.38
	19.5	65.06	11.86	21.43	0.44	0.71	0.49		69.73	16.35	11.95	0.69	0.95	0.32
	21	66.52	12.77	19.03	0.36	0.85	0.47		68.13	17.79	12.00	0.74	1.05	0.28
	22.5	70.17	17.40	10.59	0.70	0.85	0.29		66.41	19.29	11.61	1.16	1.23	0.30
	24	68.83	17.46	11.53	1.02	0.89	0.26		66.10	18.95	12.28	1.09	1.29	0.30
	25.5	68.46	17.72	11.51	1.08	0.95	0.28		67.20	18.20	11.88	1.20	1.18	0.34
	27	66.88	18.74	11.83	1.03	1.23	0.30		66.49	17.75	13.00	1.17	1.29	0.30
	28.5	67.19	18.35	11.92	1.11	1.14	0.29		66.33	17.63	13.47	1.12	1.15	0.30
	30	67.15	18.32	12.06	0.94	1.20	0.33		65.40	17.38	14.72	0.92	1.25	0.33
5	0	65.30	19.22	12.54	1.35	1.33	0.27	6	66.43	19.03	12.01	1.15	1.13	0.25
	1.5	65.19	19.62	12.51	1.04	1.38	0.27		66.15	18.50	12.90	1.06	1.11	0.29
	3	64.92	19.86	12.63	1.04	1.30	0.25		66.16	19.18	12.06	1.02	1.27	0.30
	4.5	65.72	19.32	12.35	1.08	1.25	0.28		65.90	19.25	12.13	1.25	1.18	0.28

Meas.	Pos. (nm)	Fe	Cr	Ni	Mn	Mo	Si	Meas.	Fe	Cr	Ni	Mn	Mo	Si
5	6	66.06	18.89	12.26	1.24	1.32	0.23	6	66.56	19.12	11.88	0.97	1.17	0.30
	7.5	65.98	19.23	11.95	1.32	1.27	0.25		66.30	19.37	12.01	0.99	1.08	0.26
	9	66.49	19.19	11.79	1.04	1.24	0.25		66.85	18.73	12.33	0.86	0.94	0.29
	10.5	66.77	19.25	11.57	1.06	1.11	0.24		66.59	18.12	13.06	1.00	0.91	0.32
	12	67.37	18.55	11.82	0.87	1.14	0.26		67.66	16.47	13.96	0.82	0.81	0.28
	13.5	68.61	17.56	11.81	0.75	1.00	0.26		67.12	13.58	17.39	0.70	0.82	0.39
	15	68.92	15.68	13.60	0.61	0.88	0.32		65.35	12.64	20.30	0.47	0.76	0.49
	16.5	67.78	14.11	16.27	0.73	0.74	0.37		65.80	13.68	18.65	0.66	0.81	0.40
	18	66.30	12.58	19.51	0.36	0.80	0.45		68.03	17.01	13.16	0.63	0.86	0.32
	19.5	65.32	12.37	20.55	0.55	0.72	0.48		67.84	18.03	12.10	0.75	1.00	0.29
	21	68.92	13.38	15.79	0.80	0.75	0.36		67.31	18.40	11.93	0.96	1.07	0.33
	22.5	69.96	16.61	11.48	0.68	0.97	0.31		65.76	19.86	12.09	0.87	1.13	0.28
	24	67.96	17.99	11.95	0.76	1.02	0.31		66.83	18.38	12.41	1.05	1.05	0.28
	25.5	68.48	18.26	11.05	0.87	1.08	0.26		66.87	18.31	12.64	0.84	1.05	0.29
	27	67.52	18.21	11.66	1.04	1.28	0.28		66.66	17.82	13.34	0.94	0.92	0.32
	28.5	67.18	18.15	12.32	1.01	1.03	0.30		67.18	17.31	13.54	0.79	0.85	0.33
	30	66.28	18.41	12.85	0.86	1.25	0.36							
7	0	65.57	19.05	12.65	0.98	1.44	0.31	8	64.59	18.71	14.07	1.07	1.23	0.33
	1.5	66.35	18.69	12.29	1.11	1.29	0.28		64.46	18.70	14.05	1.14	1.38	0.28
	3	65.83	19.02	12.01	1.16	1.69	0.29		65.39	18.89	13.46	0.82	1.19	0.25
	4.5	65.39	19.15	12.50	1.07	1.59	0.30		64.42	18.93	14.24	0.98	1.17	0.26
	6	66.32	18.81	11.89	1.16	1.53	0.29		64.89	19.02	13.42	1.12	1.27	0.28
	7.5	66.42	19.33	11.64	0.96	1.33	0.33		66.32	19.15	11.95	1.08	1.21	0.29
	9	66.51	19.29	11.55	1.13	1.24	0.29		65.58	20.30	11.79	0.86	1.21	0.25
	10.5	67.39	18.68	11.64	0.76	1.26	0.27		67.38	18.23	12.00	0.90	1.26	0.25
	12	68.38	16.19	13.17	0.92	1.02	0.33		68.46	16.63	12.78	0.75	1.12	0.26
	13.5	67.93	13.52	16.55	0.61	0.97	0.41		69.04	12.68	16.34	0.59	0.94	0.41
	15	66.22	13.27	18.89	0.39	0.81	0.42		62.36	10.89	24.86	0.49	0.87	0.53
	16.5	67.07	14.20	16.82	0.61	0.89	0.41		68.67	13.43	15.99	0.66	0.91	0.35
	18	68.77	17.04	12.06	0.63	1.14	0.36		69.10	17.29	11.76	0.57	1.00	0.27
	19.5	68.09	18.11	11.53	0.81	1.18	0.29		67.55	18.12	12.02	0.84	1.19	0.28
	21	66.85	18.59	12.09	0.90	1.28	0.30		66.37	18.52	12.70	0.96	1.19	0.26
	22.5	66.35	19.19	11.72	1.00	1.47	0.28		64.92	19.45	12.89	1.10	1.33	0.31
	24	66.44	18.91	12.03	0.96	1.37	0.28		66.07	19.30	12.14	0.97	1.24	0.27
	25.5	66.58	18.55	11.93	1.27	1.37	0.30		65.45	19.32	12.41	1.04	1.47	0.31
	27	66.84	18.77	11.57	1.08	1.43	0.31		65.12	18.84	13.29	0.98	1.50	0.27
	28.5	65.80	18.73	12.56	1.13	1.50	0.29		65.00	19.07	13.29	1.03	1.36	0.25
	30	65.80	19.85	11.57	0.92	1.54	0.32		66.13	18.34	12.77	1.23	1.28	0.25
9	0	65.55	17.79	14.35	0.84	1.19	0.28	10	64.56	20.43	12.08	1.11	1.56	0.26
	1.5	64.95	18.34	14.20	1.00	1.24	0.27		62.97	21.18	13.01	1.07	1.52	0.25
	3	65.84	17.06	14.70	0.99	1.15	0.26		64.16	20.02	12.97	1.13	1.50	0.22
	4.5	65.08	18.01	14.72	0.80	1.14	0.26		64.83	20.16	12.26	1.18	1.28	0.29
	6	65.36	18.14	13.77	1.13	1.34	0.27		64.94	19.71	12.67	1.04	1.36	0.27
	7.5	66.19	19.28	12.18	0.90	1.21	0.25		66.08	19.09	12.32	1.08	1.19	0.26
	9	66.10	19.22	12.16	0.89	1.37	0.26		66.88	18.90	11.90	0.96	1.14	0.22
	10.5	66.39	19.69	11.60	0.79	1.22	0.30		67.99	18.33	11.94	0.43	1.06	0.25
	12	67.57	18.55	11.78	0.75	1.06	0.29		69.01	15.14	14.01	0.59	0.95	0.30

Meas.	Pos. (nm)	Fe	Cr	Ni	Mn	Mo	Si	Meas.	Fe	Cr	Ni	Mn	Mo	Si
9	13.5	69.19	16.33	12.55	0.62	1.02	0.30	10	64.91	12.69	20.51	0.52	0.89	0.48
	15	64.77	12.12	21.24	0.49	0.91	0.47		65.54	10.99	21.63	0.52	0.79	0.53
	16.5	66.29	12.65	19.24	0.50	0.93	0.39		68.67	15.91	13.45	0.64	1.03	0.30
	18	69.21	16.48	12.43	0.74	0.88	0.26		68.09	17.42	12.30	0.91	0.99	0.29
	19.5	67.79	17.62	12.41	0.78	1.13	0.28		67.45	17.98	12.24	0.91	1.15	0.27
	21	67.63	17.79	12.56	0.72	1.03	0.28		66.75	18.52	12.40	0.79	1.24	0.29
	22.5	65.92	17.70	14.19	0.91	1.01	0.28		65.41	18.86	12.90	1.24	1.32	0.26
	24	66.58	17.07	13.90	0.96	1.19	0.31		65.70	18.86	13.09	0.78	1.27	0.30
	25.5	66.33	17.43	14.03	0.90	1.02	0.28		65.80	18.89	12.71	1.04	1.29	0.28
	27	67.18	17.27	13.34	0.84	1.10	0.27		65.09	19.38	13.09	0.88	1.29	0.27
	28.5	66.99	17.62	12.85	1.04	1.25	0.25		66.12	18.75	12.61	0.94	1.26	0.32
	30	66.63	17.33	13.61	1.07	1.10	0.26		65.92	18.63	12.87	1.09	1.18	0.31
11	0	64.50	17.44	15.17	1.01	1.41	0.47	12	66.21	18.28	12.80	1.07	1.33	0.31
	1.5	65.80	18.09	13.51	0.91	1.36	0.34		65.57	19.35	12.23	1.20	1.34	0.31
	3	66.57	18.37	12.67	0.89	1.24	0.26		65.87	18.98	12.21	1.19	1.48	0.27
	4.5	66.12	18.68	12.65	1.00	1.26	0.28		65.30	19.77	12.14	1.10	1.42	0.28
	6	65.90	19.12	12.49	0.92	1.29	0.29		65.55	19.92	11.91	0.87	1.49	0.26
	7.5	65.69	19.30	12.41	0.95	1.35	0.29		65.30	20.13	11.92	0.99	1.39	0.26
	9	65.64	19.64	11.99	1.09	1.37	0.26		64.89	20.71	11.72	1.08	1.31	0.29
	10.5	66.50	19.15	11.99	0.82	1.24	0.30		65.79	19.36	11.96	1.16	1.49	0.25
	12	67.72	17.76	12.27	0.81	1.14	0.30		66.97	18.89	11.75	1.01	1.11	0.27
	13.5	66.80	13.47	17.65	0.77	0.91	0.41		68.61	17.99	11.50	0.55	1.05	0.30
	15	62.66	11.73	23.63	0.53	0.90	0.55		66.76	14.32	17.24	0.48	0.85	0.35
	16.5	69.56	14.30	14.39	0.58	0.83	0.34		62.31	12.11	23.72	0.41	0.90	0.55
	18	69.26	16.93	11.67	0.78	1.09	0.27		68.57	14.42	15.23	0.59	0.87	0.32
	19.5	67.16	18.73	11.91	0.88	1.08	0.25		68.78	17.00	12.22	0.76	0.99	0.26
	21	66.48	18.54	12.38	1.11	1.22	0.27		67.25	17.89	12.53	0.93	1.16	0.25
	22.5	66.78	18.91	11.64	1.10	1.28	0.30		66.08	19.16	12.47	0.91	1.15	0.23
	24	65.34	19.41	12.66	1.08	1.26	0.25		65.95	19.37	12.32	0.87	1.24	0.25
	25.5	65.77	19.26	11.97	1.40	1.34	0.26		66.21	18.81	12.41	1.08	1.21	0.28
	27	64.47	19.55	13.13	1.14	1.41	0.29		64.27	20.03	12.79	1.35	1.29	0.28
	28.5	65.61	18.59	13.27	0.97	1.31	0.26		65.49	18.59	13.17	1.10	1.41	0.25
	30	65.50	18.22	13.36	1.21	1.43	0.27		65.11	19.47	12.82	0.95	1.38	0.27
13	0	65.33	19.69	12.44	1.01	1.28	0.24	14	65.43	19.19	12.72	1.10	1.26	0.29
	1.5	65.13	19.00	12.98	1.11	1.49	0.29		65.68	19.14	12.60	0.96	1.32	0.29
	3	65.41	19.13	12.71	1.14	1.33	0.28		65.30	19.33	12.47	1.21	1.46	0.24
	4.5	65.07	18.97	13.10	1.14	1.45	0.28		65.35	19.00	12.73	1.26	1.38	0.29
	6	64.36	19.80	13.33	1.00	1.27	0.24		65.24	19.74	12.22	1.15	1.40	0.26
	7.5	65.26	19.40	12.44	1.26	1.37	0.27		65.43	20.11	11.82	1.00	1.39	0.25
	9	65.87	19.26	12.06	1.17	1.36	0.27		65.41	19.38	12.42	1.05	1.48	0.26
	10.5	66.10	19.39	12.12	1.05	1.09	0.26		66.15	18.93	12.17	1.13	1.37	0.25
	12	67.15	18.45	12.25	0.76	1.14	0.25		66.96	19.30	11.29	0.98	1.20	0.27
	13.5	68.01	16.09	14.00	0.59	1.02	0.28		67.24	17.82	12.92	0.68	1.07	0.27
	15	64.84	11.91	21.20	0.64	0.93	0.50		66.00	14.09	18.19	0.44	0.91	0.38
	16.5	65.79	13.42	19.14	0.34	0.89	0.42		64.11	12.88	21.16	0.47	0.94	0.44
	18	68.90	15.77	13.36	0.76	0.95	0.27		68.03	15.13	15.14	0.51	0.90	0.29
	19.5	67.45	18.05	12.33	0.91	1.01	0.26		68.12	16.98	12.82	0.87	0.97	0.25

Meas.	Pos. (nm)	Fe	Cr	Ni	Mn	Mo	Si	Meas.	Fe	Cr	Ni	Mn	Mo	Si
13	21	66.77	18.36	12.54	1.02	1.08	0.22	14	67.41	18.65	11.60	0.91	1.17	0.26
	22.5	66.58	18.81	12.12	0.99	1.25	0.25		66.61	19.10	11.95	0.92	1.17	0.25
	24	65.46	18.94	13.06	0.94	1.33	0.27		65.27	19.48	12.73	1.05	1.25	0.23
	25.5	65.28	19.08	13.02	1.05	1.32	0.24		65.59	19.44	12.14	1.16	1.42	0.24
	27	64.72	19.35	13.13	1.21	1.33	0.26		65.85	19.16	12.04	1.31	1.37	0.28
	28.5	65.39	18.52	13.29	1.12	1.43	0.25		65.05	19.41	12.62	1.23	1.45	0.24
	30	65.43	18.77	13.03	1.18	1.33	0.26		65.92	19.14	12.25	1.09	1.36	0.24
15	0	66.15	18.57	12.75	0.98	1.28	0.27							
	1.5	65.19	19.33	12.85	0.89	1.45	0.29							
	3	65.41	19.00	12.97	0.93	1.43	0.26							
	4.5	65.61	19.22	12.54	1.02	1.33	0.27							
	6	65.28	18.99	13.01	1.10	1.35	0.27							
	7.5	65.37	20.03	12.20	0.86	1.30	0.24							
	9	65.39	19.95	12.20	1.00	1.20	0.26							
	10.5	65.79	19.48	12.39	0.82	1.26	0.27							
	12	66.91	18.84	11.82	1.09	1.08	0.26							
	13.5	67.59	16.74	13.50	0.94	0.97	0.27							
	15	66.94	14.51	16.73	0.57	0.92	0.34							
	16.5	65.18	12.97	20.09	0.49	0.87	0.40							
	18	68.39	16.28	13.29	0.73	1.05	0.27							
	19.5	67.05	17.99	12.67	0.91	1.10	0.27							
	21	65.92	18.99	12.47	1.04	1.31	0.27							
	22.5	65.99	19.40	12.37	0.79	1.19	0.26							
	24	65.91	18.36	13.18	1.08	1.25	0.21							
	25.5	64.95	19.31	13.00	1.11	1.37	0.26							
	27	65.84	18.09	13.19	1.18	1.44	0.26							
	28.5	64.88	19.67	13.03	0.92	1.27	0.23							
	30	66.01	18.76	12.42	1.15	1.40	0.26							

Ref-Hf, 400C, 7 dpa

Meas.	Pos. (nm)	Fe	Cr	Ni	Mn	Mo	Si	Meas.	Fe	Cr	Ni	Mn	Mo	Si
1	0	65.65	18.86	12.81	1.01	1.45	0.24	2	63.64	19.89	13.43	1.01	1.77	0.27
	1.5	65.71	19.34	12.62	0.91	1.32	0.11		64.30	19.41	13.48	1.03	1.51	0.27
	3	66.68	18.69	12.25	0.83	1.33	0.22		65.18	18.92	13.28	0.86	1.43	0.34
	4.5	66.87	17.20	13.91	0.52	1.14	0.36		66.75	17.83	13.04	0.94	1.16	0.27
	6	66.02	16.01	15.80	0.64	1.11	0.42		66.80	17.99	12.96	0.59	1.43	0.24
	7.5	61.33	13.03	23.47	0.48	0.72	0.96		66.61	16.80	14.22	0.62	1.40	0.35
	9	57.55	12.31	27.45	0.27	0.89	1.54		65.29	15.38	17.05	0.49	1.26	0.52
	10.5	58.87	12.23	26.65	0.29	0.73	1.24		61.63	13.14	22.64	0.50	1.09	0.99
	12	61.94	13.70	21.97	0.62	0.79	0.97		58.80	12.53	26.06	0.42	0.95	1.25
	13.5	66.69	16.18	14.85	0.62	1.10	0.55		59.82	12.66	25.20	0.31	0.78	1.23
	15	66.75	17.14	13.54	0.62	1.36	0.60		63.01	13.57	21.66	0.32	0.72	0.74
	16.5	67.49	17.94	12.36	0.71	1.21	0.30		65.16	15.81	16.98	0.52	0.90	0.62
	18	66.02	18.85	12.40	0.94	1.47	0.32		66.81	17.29	13.43	0.84	1.21	0.42
	19.5	65.82	19.43	11.89	0.90	1.53	0.43		66.24	18.62	12.58	0.88	1.32	0.36
	21	65.10	19.47	12.65	0.95	1.63	0.21		65.83	19.53	12.03	1.02	1.21	0.38
	22.5	65.32	19.81	12.01	1.06	1.41	0.38		65.64	19.53	12.00	1.25	1.24	0.35
	24	64.01	19.76	13.14	1.33	1.40	0.37		64.65	20.01	12.22	1.12	1.72	0.28
	25.5	64.38	18.83	13.94	0.87	1.60	0.39		63.28	20.82	12.56	1.13	1.89	0.32
	27	64.39	19.38	13.65	0.81	1.40	0.37		63.53	20.37	12.73	1.40	1.58	0.39
	28.5	63.91	19.32	13.63	1.21	1.68	0.26		64.09	19.87	12.58	1.20	1.83	0.42
	30	64.52	18.69	13.88	1.08	1.49	0.34		63.83	20.06	12.76	1.09	1.95	0.32
3	0	65.42	18.17	14.33	0.87	0.90	0.30	4	66.68	19.15	11.76	1.12	1.06	0.23
	1.5	64.89	18.69	14.14	1.05	1.06	0.17		66.29	19.39	11.92	0.94	1.23	0.23
	3	64.53	18.89	14.06	0.99	1.18	0.35		67.18	17.95	12.12	1.37	1.15	0.23
	4.5	65.17	18.78	13.81	0.74	1.32	0.18		67.09	16.97	13.42	1.14	1.21	0.18
	6	65.35	18.47	13.58	1.05	1.24	0.30		66.60	16.22	14.83	0.80	1.12	0.43
	7.5	64.93	19.11	13.44	1.06	1.30	0.17		64.19	14.04	19.50	0.77	0.97	0.53
	9	65.31	18.71	13.15	1.28	1.32	0.23		61.18	12.95	23.88	0.52	0.67	0.80
	10.5	65.50	18.76	12.91	1.42	1.14	0.27		59.79	12.55	25.39	0.44	0.85	0.98
	12	65.81	18.87	13.15	0.80	1.10	0.28		62.67	14.27	20.77	0.56	0.81	0.92
	13.5	65.40	18.62	13.24	1.25	1.17	0.32		65.83	16.21	15.54	0.86	0.98	0.58
	15	66.50	18.69	12.44	1.11	1.04	0.22		66.76	17.59	13.26	0.80	1.23	0.36
	16.5	66.62	18.28	12.76	1.23	0.89	0.23		66.57	18.99	12.01	0.79	1.29	0.36
	18	67.04	17.43	13.46	1.07	0.78	0.23		66.65	19.04	12.07	1.01	1.14	0.09
	19.5	68.29	15.54	14.23	0.86	0.70	0.38		64.82	20.20	11.85	1.35	1.58	0.20
	21	64.84	12.86	20.87	0.50	0.41	0.52		64.59	20.05	12.41	1.12	1.64	0.19
	22.5	56.89	10.71	30.08	0.58	0.69	1.05		64.18	19.99	12.62	1.26	1.67	0.28
	24	60.85	11.92	25.67	0.24	0.63	0.68		63.56	20.32	12.96	1.25	1.66	0.25
	25.5	67.32	14.93	15.99	0.58	0.83	0.34		64.12	20.40	12.57	1.09	1.62	0.20
	27	68.11	17.01	12.57	0.85	1.13	0.33		63.70	20.26	12.94	1.12	1.82	0.17
	28.5	67.64	17.77	12.39	0.86	1.08	0.26		63.48	20.46	12.71	1.18	1.84	0.33
	30	67.01	18.31	12.05	1.25	1.11	0.28		63.87	20.29	12.64	1.24	1.74	0.22
5	0	64.35	18.35	14.74	1.11	1.09	0.36	6	66.87	18.59	12.35	0.76	1.19	0.23
	1.5	64.83	18.44	14.47	0.90	1.07	0.29		67.49	17.52	12.89	1.08	0.91	0.12
	3	64.76	18.52	14.65	1.03	0.72	0.32		67.32	17.14	13.52	0.90	0.92	0.21
	4.5	64.91	18.37	14.53	0.92	1.07	0.21		65.98	16.42	15.84	0.57	0.89	0.29

Meas.	Pos. (nm)	Fe	Cr	Ni	Mn	Mo	Si	Meas.	Fe	Cr	Ni	Mn	Mo	Si
5	6	64.80	18.70	13.92	1.20	1.14	0.24	6	63.74	13.93	20.20	0.78	0.83	0.52
	7.5	65.13	19.31	13.10	1.14	1.05	0.27		61.38	13.70	22.91	0.45	0.78	0.78
	9	65.69	18.75	13.29	1.28	0.88	0.11		60.08	12.64	24.97	0.63	0.79	0.89
	10.5	66.08	18.98	12.43	1.19	0.98	0.33		59.10	12.54	25.81	0.68	0.86	1.02
	12	65.93	18.98	12.70	0.96	1.10	0.33		61.42	14.02	22.30	0.71	0.81	0.74
	13.5	66.38	18.80	12.31	1.03	1.13	0.35		63.94	15.68	18.30	0.86	0.89	0.33
	15	67.30	17.69	12.88	0.98	0.96	0.20		66.36	18.38	12.64	1.24	1.07	0.32
	16.5	66.94	16.99	14.54	0.53	0.65	0.34		65.93	16.60	15.27	0.85	0.98	0.37
	18	64.17	13.75	20.37	0.55	0.59	0.57		65.91	19.10	12.50	0.99	1.36	0.14
	19.5	61.12	11.88	25.20	0.36	0.66	0.78		66.09	19.52	11.67	0.95	1.43	0.34
	21	60.78	11.29	25.87	0.41	0.72	0.93		65.42	19.56	12.15	1.32	1.47	0.08
	22.5	65.19	12.85	19.98	0.63	0.83	0.52		64.44	19.82	12.69	1.20	1.66	0.20
	24	68.14	15.05	15.57	0.39	0.58	0.28		64.05	20.24	12.59	1.39	1.36	0.37
	25.5	68.14	16.69	13.07	0.90	1.03	0.17		64.67	19.40	12.97	1.29	1.40	0.26
	27	67.08	18.05	12.76	0.89	1.00	0.23		63.82	20.12	12.67	1.24	1.65	0.49
	28.5	66.12	18.55	12.77	0.89	1.42	0.24		63.52	19.89	13.28	1.22	1.86	0.23
	30	65.97	18.68	13.03	0.90	1.27	0.14		64.15	19.67	12.89	1.38	1.43	0.48
7	0	64.93	18.30	14.38	1.06	1.06	0.26	8	65.68	19.09	12.79	0.81	1.35	0.28
	1.5	64.76	18.75	14.31	0.91	0.94	0.34		66.48	18.85	12.02	0.92	1.32	0.40
	3	64.83	18.52	14.33	1.18	0.84	0.30		67.18	18.19	12.46	0.68	1.17	0.31
	4.5	65.18	18.11	14.51	1.00	1.06	0.15		67.00	16.98	13.48	0.92	1.34	0.29
	6	65.48	18.12	14.09	1.07	0.96	0.28		67.08	17.32	13.22	0.68	1.37	0.33
	7.5	65.81	18.05	13.58	1.23	1.10	0.22		66.05	14.77	17.18	0.43	0.99	0.58
	9	66.01	18.59	13.27	0.95	0.91	0.26		61.78	12.94	22.60	0.69	0.93	1.07
	10.5	66.21	18.54	13.21	0.93	0.98	0.14		59.39	12.95	25.24	0.32	0.80	1.29
	12	66.37	19.06	12.60	1.00	0.79	0.17		59.85	12.66	25.23	0.44	0.66	1.15
	13.5	65.90	19.02	12.81	1.14	0.92	0.21		61.31	14.15	22.03	0.49	0.98	1.04
	15	67.31	17.83	12.89	0.81	0.96	0.21		62.61	14.87	20.17	0.51	1.02	0.83
	16.5	67.04	17.51	13.51	0.81	0.82	0.31		63.24	15.43	19.20	0.40	0.87	0.85
	18	67.22	15.80	15.24	0.75	0.77	0.22		65.61	16.29	15.32	1.12	1.00	0.65
	19.5	65.17	14.29	18.63	0.65	0.71	0.54		66.09	17.90	13.32	0.91	1.40	0.39
	21	62.33	12.28	23.66	0.67	0.48	0.58		66.09	18.87	12.34	0.99	1.37	0.33
	22.5	62.56	12.23	23.60	0.21	0.65	0.75		65.42	19.22	12.48	1.05	1.47	0.35
	24	63.43	12.37	22.64	0.40	0.57	0.59		65.49	19.62	12.02	1.13	1.45	0.28
	25.5	67.06	15.65	15.38	0.44	0.99	0.49		64.52	19.91	12.80	0.95	1.53	0.29
	27	67.95	17.16	12.81	1.10	0.87	0.12		64.21	20.17	12.46	1.19	1.69	0.28
	28.5	67.11	18.03	12.77	0.94	0.91	0.23		64.19	19.97	12.37	1.36	1.74	0.36
	30	66.83	18.25	12.55	1.11	1.08	0.17		64.48	19.81	12.86	1.13	1.47	0.25
9	0	64.86	17.47	15.35	1.18	0.97	0.17	10	65.40	19.07	12.83	1.05	1.42	0.23
	1.5	64.22	18.15	15.71	1.19	0.74	0.00		65.60	19.65	12.03	0.87	1.59	0.26
	3	64.67	18.05	15.20	1.04	0.86	0.18		65.78	19.21	12.13	0.86	1.67	0.34
	4.5	65.34	18.07	14.66	1.09	0.71	0.13		66.53	18.27	12.64	0.75	1.54	0.26
	6	65.04	17.94	14.74	1.10	0.96	0.22		66.78	16.91	14.21	0.53	1.17	0.40
	7.5	64.87	18.51	14.52	1.22	0.79	0.09		66.32	15.75	15.40	0.92	1.19	0.42
	9	64.64	19.10	13.89	1.27	0.86	0.24		60.53	13.21	24.16	0.38	0.65	1.07
	10.5	65.11	18.82	13.50	1.27	1.10	0.19		59.18	12.52	25.99	0.30	0.71	1.30
	12	65.48	18.57	13.74	1.01	1.02	0.17		60.61	12.94	24.06	0.31	0.94	1.14

Meas.	Pos. (nm)	Fe	Cr	Ni	Mn	Mo	Si	Meas.	Fe	Cr	Ni	Mn	Mo	Si
9	13.5	66.54	18.72	12.88	1.02	0.75	0.08	10	65.58	15.19	17.01	0.49	0.98	0.74
	15	66.33	18.59	12.71	1.12	1.02	0.23		66.66	15.31	15.84	0.50	1.04	0.64
	16.5	67.59	17.20	13.37	0.89	0.73	0.22		67.24	17.75	12.61	0.80	1.15	0.44
	18	67.68	16.27	14.17	0.82	0.81	0.25		67.38	17.86	12.55	0.72	1.17	0.32
	19.5	64.78	14.39	19.20	0.64	0.58	0.40		66.04	18.90	11.99	1.20	1.61	0.26
	21	61.20	12.85	24.05	0.57	0.49	0.84		66.30	18.98	11.85	0.92	1.66	0.29
	22.5	60.92	12.14	24.77	0.71	0.75	0.71		64.90	19.37	13.12	0.97	1.46	0.18
	24	63.44	13.53	21.20	0.46	0.90	0.47		64.96	18.72	13.23	1.13	1.67	0.28
	25.5	66.13	15.64	16.49	0.51	0.77	0.45		64.65	19.13	13.18	0.99	1.75	0.30
	27	67.02	16.81	14.01	0.86	1.01	0.29		64.88	18.94	13.48	0.97	1.50	0.23
	28.5	67.00	17.87	12.71	1.00	1.17	0.25		64.51	19.35	13.36	0.56	1.89	0.33
	30	66.73	18.13	12.74	1.06	1.20	0.16		64.04	19.42	13.61	1.04	1.57	0.32
11	0	64.60	18.97	14.02	1.30	0.97	0.14	12	65.19	18.68	13.91	1.00	1.01	0.22
	1.5	65.02	19.29	13.23	1.18	1.08	0.19		65.55	18.89	13.41	0.88	1.03	0.25
	3	65.62	18.69	13.15	1.27	1.10	0.17		65.25	18.79	13.39	1.21	1.11	0.24
	4.5	65.84	18.87	12.74	1.24	1.21	0.10		65.68	18.63	13.34	1.27	0.86	0.22
	6	65.22	19.44	12.71	1.25	1.24	0.14		65.94	18.70	13.16	1.05	0.95	0.20
	7.5	65.78	19.03	12.57	1.32	0.98	0.32		66.00	18.90	13.03	0.88	0.99	0.20
	9	65.58	18.83	13.02	1.32	1.09	0.15		66.58	18.17	13.25	0.86	0.89	0.25
	10.5	66.10	19.16	12.71	1.18	0.80	0.05		67.34	17.05	13.44	0.93	0.92	0.32
	12	66.53	18.60	12.59	1.27	0.85	0.14		66.32	15.63	16.35	0.74	0.63	0.33
	13.5	67.28	18.11	12.99	0.84	0.69	0.08		61.87	13.35	23.07	0.34	0.59	0.77
	15	67.90	16.89	13.42	0.87	0.70	0.22		61.12	12.11	25.13	0.22	0.64	0.78
	16.5	66.81	15.57	16.11	0.78	0.50	0.23		63.81	13.35	21.34	0.23	0.68	0.59
	18	62.63	13.05	22.81	0.47	0.51	0.53		67.20	14.80	16.14	0.69	0.81	0.35
	19.5	59.10	11.98	26.99	0.61	0.50	0.82		67.99	16.76	13.16	1.02	0.87	0.19
	21	62.11	12.39	23.56	0.72	0.59	0.62		67.94	17.38	12.49	1.06	0.92	0.22
	22.5	66.89	14.92	16.42	0.60	0.78	0.38		67.39	17.82	12.61	0.96	1.04	0.18
	24	67.88	16.38	13.75	0.83	0.99	0.18		66.36	18.50	12.75	1.10	1.12	0.18
	25.5	67.08	18.06	12.60	1.07	1.02	0.16		65.69	18.48	13.15	1.24	1.19	0.25
	27	67.07	17.97	12.56	1.08	1.23	0.08		65.74	18.93	13.01	0.81	1.26	0.25
	28.5	66.50	18.02	13.12	1.07	1.08	0.22		65.75	18.49	13.47	1.06	1.14	0.09
	30	65.58	18.52	13.20	1.40	1.11	0.19		65.51	18.34	13.50	1.08	1.27	0.29

Ref-Hf, 400C, 10 dpa

Meas.	Pos. (nm)	Fe	Cr	Ni	Mn	Mo	Si	Meas.	Fe	Cr	Ni	Mn	Mo	Si
1	0	66.81	19.28	11.72	0.90	0.87	0.42	2	65.07	19.42	12.60	1.62	1.02	0.27
	1.5	66.60	18.29	12.67	1.69	0.51	0.24		65.54	18.98	12.81	1.43	0.94	0.30
	3	66.77	18.84	12.61	0.91	0.67	0.21		65.51	19.11	12.72	1.47	0.91	0.29
	4.5	67.22	18.30	12.33	1.13	0.73	0.29		66.42	18.62	12.57	1.18	0.97	0.23
	6	68.46	17.66	12.65	0.54	0.54	0.16		67.26	18.98	12.14	0.86	0.53	0.23
	7.5	67.50	17.02	13.28	1.10	0.65	0.46		67.82	17.74	12.51	0.96	0.65	0.32
	9	67.52	15.06	15.90	0.83	0.40	0.30		67.49	16.86	13.80	0.62	0.78	0.46
	10.5	65.80	14.11	18.59	0.61	0.51	0.38		66.70	15.67	16.43	0.44	0.49	0.28
	12	63.38	13.26	21.84	0.43	0.70	0.39		63.76	13.40	21.25	0.59	0.53	0.47
	13.5	62.95	13.39	22.66	0.14	0.34	0.53		60.91	12.32	25.36	0.33	0.45	0.63
	15	61.56	13.96	22.96	0.42	0.56	0.55		61.96	13.52	22.96	0.42	0.56	0.59
	16.5	64.02	15.94	18.25	0.94	0.52	0.32		67.28	15.03	16.01	0.60	0.72	0.36
	18	66.64	16.73	14.44	1.04	0.90	0.26		69.03	17.98	11.30	0.75	0.79	0.16
	19.5	67.45	18.96	11.91	0.60	0.96	0.11		67.37	19.25	11.43	0.84	0.89	0.22
	21	67.35	18.55	11.77	1.13	1.16	0.03		67.33	19.20	11.50	0.94	0.88	0.15
	22.5	66.21	19.60	11.78	1.09	1.24	0.09		65.31	19.84	12.32	1.29	1.14	0.10
	24	64.92	20.24	12.20	1.03	1.37	0.24		65.95	18.82	12.81	1.10	1.17	0.15
	25.5	65.72	19.24	12.44	1.19	1.14	0.27		65.31	19.71	12.26	1.32	1.29	0.10
	27	64.72	18.99	13.27	1.28	1.52	0.21		65.09	19.29	12.79	1.34	1.33	0.16
	28.5	64.52	19.32	13.95	0.90	1.20	0.12		65.42	18.91	13.01	1.29	1.17	0.19
	30	64.74	18.21	14.28	1.39	1.22	0.17		64.74	18.90	13.69	1.35	1.08	0.24
3	0	65.07	19.42	12.60	1.62	1.02	0.27	4	65.92	18.99	12.41	1.28	1.10	0.31
	1.5	65.54	18.98	12.81	1.43	0.94	0.30		65.75	19.14	12.22	1.48	1.17	0.24
	3	65.51	19.11	12.72	1.47	0.91	0.29		67.10	18.04	12.97	1.01	0.71	0.17
	4.5	66.42	18.62	12.57	1.18	0.97	0.23		67.15	18.68	12.37	0.81	0.75	0.24
	6	67.26	18.98	12.14	0.86	0.53	0.23		67.27	18.29	12.59	1.01	0.53	0.31
	7.5	67.82	17.74	12.51	0.96	0.65	0.32		68.32	16.94	12.93	0.79	0.74	0.28
	9	67.49	16.86	13.80	0.62	0.78	0.46		67.60	14.73	15.87	0.77	0.73	0.30
	10.5	66.70	15.67	16.43	0.44	0.49	0.28		65.09	12.97	20.31	0.49	0.67	0.47
	12	63.76	13.40	21.25	0.59	0.53	0.47		61.77	12.10	24.39	0.65	0.45	0.64
	13.5	60.91	12.32	25.36	0.33	0.45	0.63		61.30	13.65	23.13	0.56	0.64	0.71
	15	61.96	13.52	22.96	0.42	0.56	0.59		66.33	15.56	16.57	0.43	0.68	0.42
	16.5	67.28	15.03	16.01	0.60	0.72	0.36		68.35	18.31	11.62	0.73	0.76	0.22
	18	69.03	17.98	11.30	0.75	0.79	0.16		68.04	18.97	10.97	1.11	0.75	0.16
	19.5	67.37	19.25	11.43	0.84	0.89	0.22		67.07	19.33	11.41	0.98	1.07	0.13
	21	67.33	19.20	11.50	0.94	0.88	0.15		65.93	19.92	11.92	0.93	1.08	0.22
	22.5	65.31	19.84	12.32	1.29	1.14	0.10		66.43	19.17	12.20	1.02	0.97	0.22
	24	65.95	18.82	12.81	1.10	1.17	0.15		65.45	19.26	12.81	1.45	0.90	0.12
	25.5	65.31	19.71	12.26	1.32	1.29	0.10		64.85	18.86	13.85	0.93	1.24	0.27
	27	65.09	19.29	12.79	1.34	1.33	0.16		65.23	18.73	13.81	1.10	1.03	0.09
	28.5	65.42	18.91	13.01	1.29	1.17	0.19		64.46	18.64	14.34	1.21	1.13	0.21
	30	64.74	18.90	13.69	1.35	1.08	0.24		64.53	18.91	13.83	1.20	1.43	0.09

LoHf, 400C, 3 dpa

Meas.	Pos. (nm)	Fe	Cr	Ni	Mn	Mo	Si	Meas.	Fe	Cr	Ni	Mn	Mo	Si
1	0	65.65	18.05	14.06	0.94	1.03	0.27	2	66.09	18.05	13.37	1.11	1.08	0.29
	1.5	65.87	18.01	13.95	0.70	1.18	0.29		65.98	17.94	13.74	1.00	1.03	0.31
	3	66.48	18.17	13.27	0.80	1.03	0.25		66.39	18.00	13.20	0.98	1.14	0.29
	4.5	65.55	19.44	12.88	0.78	1.08	0.28		65.88	18.77	12.86	1.01	1.21	0.28
	6	66.57	18.63	12.20	1.33	1.04	0.23		65.28	19.72	12.44	1.01	1.31	0.24
	7.5	66.62	18.68	12.33	1.02	1.12	0.24		65.69	19.03	12.51	1.13	1.40	0.24
	9	67.52	17.58	12.35	1.17	1.15	0.23		65.98	19.20	12.39	0.83	1.34	0.26
	10.5	67.79	17.98	12.40	0.67	0.86	0.30		65.72	19.03	12.30	1.13	1.51	0.32
	12	67.39	17.00	13.73	0.61	0.97	0.30		66.49	18.68	12.17	1.02	1.34	0.30
	13.5	67.18	13.25	17.75	0.64	0.75	0.43		67.77	17.33	12.60	0.93	1.05	0.32
	15	65.12	12.31	20.90	0.50	0.74	0.43		68.34	16.38	13.17	0.75	1.08	0.29
	16.5	69.45	13.81	14.99	0.46	0.90	0.39		67.07	14.11	16.84	0.61	1.02	0.36
	18	70.69	15.06	12.30	0.74	0.87	0.33		66.17	13.13	18.96	0.41	0.86	0.47
	19.5	69.04	16.88	11.84	0.97	0.91	0.36		67.13	15.00	16.09	0.56	0.85	0.37
	21	68.32	18.56	11.33	0.64	0.88	0.27		68.90	16.96	12.16	0.69	0.95	0.34
	22.5	66.90	18.94	11.99	0.76	1.07	0.34		67.04	19.16	11.44	1.05	1.02	0.28
	24	66.12	19.31	11.92	0.94	1.44	0.28		67.13	19.41	10.98	1.04	1.15	0.30
	25.5	67.16	19.54	11.11	0.68	1.27	0.25		66.34	19.62	11.55	1.05	1.12	0.31
	27	65.92	18.52	12.97	0.95	1.42	0.24		66.73	19.00	11.47	1.13	1.35	0.32
	28.5	65.28	19.66	12.53	1.01	1.24	0.28		67.46	18.22	11.42	1.22	1.37	0.31
	30	65.31	19.32	12.52	1.16	1.40	0.29		67.43	18.18	11.69	1.01	1.35	0.33
3	0	67.46	17.30	13.11	0.93	0.94	0.25	4	65.87	19.41	12.47	0.78	1.20	0.27
	1.5	65.23	18.86	13.45	1.11	1.10	0.24		65.79	18.45	13.05	1.01	1.41	0.28
	3	65.75	18.35	13.59	0.89	1.13	0.29		65.87	18.70	12.89	1.04	1.21	0.29
	4.5	66.32	18.50	12.66	1.08	1.16	0.28		66.31	18.56	12.49	1.04	1.34	0.26
	6	65.52	19.01	13.04	1.00	1.15	0.28		65.31	19.43	12.29	1.16	1.55	0.26
	7.5	66.56	18.32	12.45	1.13	1.26	0.28		65.81	19.62	11.56	1.29	1.43	0.29
	9	65.68	19.63	11.95	1.27	1.21	0.25		66.23	18.86	12.32	1.02	1.25	0.31
	10.5	65.81	19.28	12.22	1.22	1.20	0.26		67.31	18.99	11.42	0.92	1.06	0.30
	12	66.05	19.23	11.96	1.24	1.23	0.28		68.33	17.53	12.11	0.66	1.06	0.31
	13.5	67.12	19.02	11.66	0.93	1.05	0.23		67.62	15.67	14.66	0.72	0.99	0.34
	15	67.98	18.12	11.67	1.05	0.87	0.30		67.54	13.46	17.30	0.36	0.91	0.43
	16.5	67.95	16.61	13.34	0.85	0.92	0.32		67.92	12.51	17.78	0.58	0.78	0.42
	18	65.15	12.58	20.75	0.38	0.68	0.46		68.06	14.32	15.90	0.39	0.95	0.38
	19.5	65.06	11.86	21.43	0.44	0.71	0.49		69.73	16.35	11.95	0.69	0.95	0.32
	21	66.52	12.77	19.03	0.36	0.85	0.47		68.13	17.79	12.00	0.74	1.05	0.28
	22.5	70.17	17.40	10.59	0.70	0.85	0.29		66.41	19.29	11.61	1.16	1.23	0.30
	24	68.83	17.46	11.53	1.02	0.89	0.26		66.10	18.95	12.28	1.09	1.29	0.30
	25.5	68.46	17.72	11.51	1.08	0.95	0.28		67.20	18.20	11.88	1.20	1.18	0.34
	27	66.88	18.74	11.83	1.03	1.23	0.30		66.49	17.75	13.00	1.17	1.29	0.30
	28.5	67.19	18.35	11.92	1.11	1.14	0.29		66.33	17.63	13.47	1.12	1.15	0.30
	30	67.15	18.32	12.06	0.94	1.20	0.33		65.40	17.38	14.72	0.92	1.25	0.33
5	0	65.30	19.22	12.54	1.35	1.33	0.27	6	66.43	19.03	12.01	1.15	1.13	0.25
	1.5	65.19	19.62	12.51	1.04	1.38	0.27		66.15	18.50	12.90	1.06	1.11	0.29
	3	64.92	19.86	12.63	1.04	1.30	0.25		66.16	19.18	12.06	1.02	1.27	0.30
	4.5	65.72	19.32	12.35	1.08	1.25	0.28		65.90	19.25	12.13	1.25	1.18	0.28

Meas.	Pos. (nm)	Fe	Cr	Ni	Mn	Mo	Si	Meas.	Fe	Cr	Ni	Mn	Mo	Si
5	6	66.06	18.89	12.26	1.24	1.32	0.23	6	66.56	19.12	11.88	0.97	1.17	0.30
	7.5	65.98	19.23	11.95	1.32	1.27	0.25		66.30	19.37	12.01	0.99	1.08	0.26
	9	66.49	19.19	11.79	1.04	1.24	0.25		66.85	18.73	12.33	0.86	0.94	0.29
	10.5	66.77	19.25	11.57	1.06	1.11	0.24		66.59	18.12	13.06	1.00	0.91	0.32
	12	67.37	18.55	11.82	0.87	1.14	0.26		67.66	16.47	13.96	0.82	0.81	0.28
	13.5	68.61	17.56	11.81	0.75	1.00	0.26		67.12	13.58	17.39	0.70	0.82	0.39
	15	68.92	15.68	13.60	0.61	0.88	0.32		65.35	12.64	20.30	0.47	0.76	0.49
	16.5	67.78	14.11	16.27	0.73	0.74	0.37		65.80	13.68	18.65	0.66	0.81	0.40
	18	66.30	12.58	19.51	0.36	0.80	0.45		68.03	17.01	13.16	0.63	0.86	0.32
	19.5	65.32	12.37	20.55	0.55	0.72	0.48		67.84	18.03	12.10	0.75	1.00	0.29
	21	68.92	13.38	15.79	0.80	0.75	0.36		67.31	18.40	11.93	0.96	1.07	0.33
	22.5	69.96	16.61	11.48	0.68	0.97	0.31		65.76	19.86	12.09	0.87	1.13	0.28
	24	67.96	17.99	11.95	0.76	1.02	0.31		66.83	18.38	12.41	1.05	1.05	0.28
	25.5	68.48	18.26	11.05	0.87	1.08	0.26		66.87	18.31	12.64	0.84	1.05	0.29
	27	67.52	18.21	11.66	1.04	1.28	0.28		66.66	17.82	13.34	0.94	0.92	0.32
	28.5	67.18	18.15	12.32	1.01	1.03	0.30		67.18	17.31	13.54	0.79	0.85	0.33
	30	66.28	18.41	12.85	0.86	1.25	0.36							
7	0	65.57	19.05	12.65	0.98	1.44	0.31	8	64.59	18.71	14.07	1.07	1.23	0.33
	1.5	66.35	18.69	12.29	1.11	1.29	0.28		64.46	18.70	14.05	1.14	1.38	0.28
	3	65.83	19.02	12.01	1.16	1.69	0.29		65.39	18.89	13.46	0.82	1.19	0.25
	4.5	65.39	19.15	12.50	1.07	1.59	0.30		64.42	18.93	14.24	0.98	1.17	0.26
	6	66.32	18.81	11.89	1.16	1.53	0.29		64.89	19.02	13.42	1.12	1.27	0.28
	7.5	66.42	19.33	11.64	0.96	1.33	0.33		66.32	19.15	11.95	1.08	1.21	0.29
	9	66.51	19.29	11.55	1.13	1.24	0.29		65.58	20.30	11.79	0.86	1.21	0.25
	10.5	67.39	18.68	11.64	0.76	1.26	0.27		67.38	18.23	12.00	0.90	1.26	0.25
	12	68.38	16.19	13.17	0.92	1.02	0.33		68.46	16.63	12.78	0.75	1.12	0.26
	13.5	67.93	13.52	16.55	0.61	0.97	0.41		69.04	12.68	16.34	0.59	0.94	0.41
	15	66.22	13.27	18.89	0.39	0.81	0.42		62.36	10.89	24.86	0.49	0.87	0.53
	16.5	67.07	14.20	16.82	0.61	0.89	0.41		68.67	13.43	15.99	0.66	0.91	0.35
	18	68.77	17.04	12.06	0.63	1.14	0.36		69.10	17.29	11.76	0.57	1.00	0.27
	19.5	68.09	18.11	11.53	0.81	1.18	0.29		67.55	18.12	12.02	0.84	1.19	0.28
	21	66.85	18.59	12.09	0.90	1.28	0.30		66.37	18.52	12.70	0.96	1.19	0.26
	22.5	66.35	19.19	11.72	1.00	1.47	0.28		64.92	19.45	12.89	1.10	1.33	0.31
	24	66.44	18.91	12.03	0.96	1.37	0.28		66.07	19.30	12.14	0.97	1.24	0.27
	25.5	66.58	18.55	11.93	1.27	1.37	0.30		65.45	19.32	12.41	1.04	1.47	0.31
	27	66.84	18.77	11.57	1.08	1.43	0.31		65.12	18.84	13.29	0.98	1.50	0.27
	28.5	65.80	18.73	12.56	1.13	1.50	0.29		65.00	19.07	13.29	1.03	1.36	0.25
	30	65.80	19.85	11.57	0.92	1.54	0.32		66.13	18.34	12.77	1.23	1.28	0.25
9	0	65.55	17.79	14.35	0.84	1.19	0.28	10	64.56	20.43	12.08	1.11	1.56	0.26
	1.5	64.95	18.34	14.20	1.00	1.24	0.27		62.97	21.18	13.01	1.07	1.52	0.25
	3	65.84	17.06	14.70	0.99	1.15	0.26		64.16	20.02	12.97	1.13	1.50	0.22
	4.5	65.08	18.01	14.72	0.80	1.14	0.26		64.83	20.16	12.26	1.18	1.28	0.29
	6	65.36	18.14	13.77	1.13	1.34	0.27		64.94	19.71	12.67	1.04	1.36	0.27
	7.5	66.19	19.28	12.18	0.90	1.21	0.25		66.08	19.09	12.32	1.08	1.19	0.26
	9	66.10	19.22	12.16	0.89	1.37	0.26		66.88	18.90	11.90	0.96	1.14	0.22
	10.5	66.39	19.69	11.60	0.79	1.22	0.30		67.99	18.33	11.94	0.43	1.06	0.25
	12	67.57	18.55	11.78	0.75	1.06	0.29		69.01	15.14	14.01	0.59	0.95	0.30

Meas.	Pos. (nm)	Fe	Cr	Ni	Mn	Mo	Si	Meas.	Fe	Cr	Ni	Mn	Mo	Si
9	13.5	69.19	16.33	12.55	0.62	1.02	0.30	10	64.91	12.69	20.51	0.52	0.89	0.48
	15	64.77	12.12	21.24	0.49	0.91	0.47		65.54	10.99	21.63	0.52	0.79	0.53
	16.5	66.29	12.65	19.24	0.50	0.93	0.39		68.67	15.91	13.45	0.64	1.03	0.30
	18	69.21	16.48	12.43	0.74	0.88	0.26		68.09	17.42	12.30	0.91	0.99	0.29
	19.5	67.79	17.62	12.41	0.78	1.13	0.28		67.45	17.98	12.24	0.91	1.15	0.27
	21	67.63	17.79	12.56	0.72	1.03	0.28		66.75	18.52	12.40	0.79	1.24	0.29
	22.5	65.92	17.70	14.19	0.91	1.01	0.28		65.41	18.86	12.90	1.24	1.32	0.26
	24	66.58	17.07	13.90	0.96	1.19	0.31		65.70	18.86	13.09	0.78	1.27	0.30
	25.5	66.33	17.43	14.03	0.90	1.02	0.28		65.80	18.89	12.71	1.04	1.29	0.28
	27	67.18	17.27	13.34	0.84	1.10	0.27		65.09	19.38	13.09	0.88	1.29	0.27
	28.5	66.99	17.62	12.85	1.04	1.25	0.25		66.12	18.75	12.61	0.94	1.26	0.32
	30	66.63	17.33	13.61	1.07	1.10	0.26		65.92	18.63	12.87	1.09	1.18	0.31
11	0	64.50	17.44	15.17	1.01	1.41	0.47	12	66.21	18.28	12.80	1.07	1.33	0.31
	1.5	65.80	18.09	13.51	0.91	1.36	0.34		65.57	19.35	12.23	1.20	1.34	0.31
	3	66.57	18.37	12.67	0.89	1.24	0.26		65.87	18.98	12.21	1.19	1.48	0.27
	4.5	66.12	18.68	12.65	1.00	1.26	0.28		65.30	19.77	12.14	1.10	1.42	0.28
	6	65.90	19.12	12.49	0.92	1.29	0.29		65.55	19.92	11.91	0.87	1.49	0.26
	7.5	65.69	19.30	12.41	0.95	1.35	0.29		65.30	20.13	11.92	0.99	1.39	0.26
	9	65.64	19.64	11.99	1.09	1.37	0.26		64.89	20.71	11.72	1.08	1.31	0.29
	10.5	66.50	19.15	11.99	0.82	1.24	0.30		65.79	19.36	11.96	1.16	1.49	0.25
	12	67.72	17.76	12.27	0.81	1.14	0.30		66.97	18.89	11.75	1.01	1.11	0.27
	13.5	66.80	13.47	17.65	0.77	0.91	0.41		68.61	17.99	11.50	0.55	1.05	0.30
	15	62.66	11.73	23.63	0.53	0.90	0.55		66.76	14.32	17.24	0.48	0.85	0.35
	16.5	69.56	14.30	14.39	0.58	0.83	0.34		62.31	12.11	23.72	0.41	0.90	0.55
	18	69.26	16.93	11.67	0.78	1.09	0.27		68.57	14.42	15.23	0.59	0.87	0.32
	19.5	67.16	18.73	11.91	0.88	1.08	0.25		68.78	17.00	12.22	0.76	0.99	0.26
	21	66.48	18.54	12.38	1.11	1.22	0.27		67.25	17.89	12.53	0.93	1.16	0.25
	22.5	66.78	18.91	11.64	1.10	1.28	0.30		66.08	19.16	12.47	0.91	1.15	0.23
	24	65.34	19.41	12.66	1.08	1.26	0.25		65.95	19.37	12.32	0.87	1.24	0.25
	25.5	65.77	19.26	11.97	1.40	1.34	0.26		66.21	18.81	12.41	1.08	1.21	0.28
	27	64.47	19.55	13.13	1.14	1.41	0.29		64.27	20.03	12.79	1.35	1.29	0.28
	28.5	65.61	18.59	13.27	0.97	1.31	0.26		65.49	18.59	13.17	1.10	1.41	0.25
	30	65.50	18.22	13.36	1.21	1.43	0.27		65.11	19.47	12.82	0.95	1.38	0.27
13	0	65.33	19.69	12.44	1.01	1.28	0.24	14	65.43	19.19	12.72	1.10	1.26	0.29
	1.5	65.13	19.00	12.98	1.11	1.49	0.29		65.68	19.14	12.60	0.96	1.32	0.29
	3	65.41	19.13	12.71	1.14	1.33	0.28		65.30	19.33	12.47	1.21	1.46	0.24
	4.5	65.07	18.97	13.10	1.14	1.45	0.28		65.35	19.00	12.73	1.26	1.38	0.29
	6	64.36	19.80	13.33	1.00	1.27	0.24		65.24	19.74	12.22	1.15	1.40	0.26
	7.5	65.26	19.40	12.44	1.26	1.37	0.27		65.43	20.11	11.82	1.00	1.39	0.25
	9	65.87	19.26	12.06	1.17	1.36	0.27		65.41	19.38	12.42	1.05	1.48	0.26
	10.5	66.10	19.39	12.12	1.05	1.09	0.26		66.15	18.93	12.17	1.13	1.37	0.25
	12	67.15	18.45	12.25	0.76	1.14	0.25		66.96	19.30	11.29	0.98	1.20	0.27
	13.5	68.01	16.09	14.00	0.59	1.02	0.28		67.24	17.82	12.92	0.68	1.07	0.27
	15	64.84	11.91	21.20	0.64	0.93	0.50		66.00	14.09	18.19	0.44	0.91	0.38
	16.5	65.79	13.42	19.14	0.34	0.89	0.42		64.11	12.88	21.16	0.47	0.94	0.44
	18	68.90	15.77	13.36	0.76	0.95	0.27		68.03	15.13	15.14	0.51	0.90	0.29
	19.5	67.45	18.05	12.33	0.91	1.01	0.26		68.12	16.98	12.82	0.87	0.97	0.25

Meas.	Pos. (nm)	Fe	Cr	Ni	Mn	Mo	Si	Meas.	Fe	Cr	Ni	Mn	Mo	Si
13	21	66.77	18.36	12.54	1.02	1.08	0.22	14	67.41	18.65	11.60	0.91	1.17	0.26
	22.5	66.58	18.81	12.12	0.99	1.25	0.25		66.61	19.10	11.95	0.92	1.17	0.25
	24	65.46	18.94	13.06	0.94	1.33	0.27		65.27	19.48	12.73	1.05	1.25	0.23
	25.5	65.28	19.08	13.02	1.05	1.32	0.24		65.59	19.44	12.14	1.16	1.42	0.24
	27	64.72	19.35	13.13	1.21	1.33	0.26		65.85	19.16	12.04	1.31	1.37	0.28
	28.5	65.39	18.52	13.29	1.12	1.43	0.25		65.05	19.41	12.62	1.23	1.45	0.24
	30	65.43	18.77	13.03	1.18	1.33	0.26		65.92	19.14	12.25	1.09	1.36	0.24
15	0	66.15	18.57	12.75	0.98	1.28	0.27							
	1.5	65.19	19.33	12.85	0.89	1.45	0.29							
	3	65.41	19.00	12.97	0.93	1.43	0.26							
	4.5	65.61	19.22	12.54	1.02	1.33	0.27							
	6	65.28	18.99	13.01	1.10	1.35	0.27							
	7.5	65.37	20.03	12.20	0.86	1.30	0.24							
	9	65.39	19.95	12.20	1.00	1.20	0.26							
	10.5	65.79	19.48	12.39	0.82	1.26	0.27							
	12	66.91	18.84	11.82	1.09	1.08	0.26							
	13.5	67.59	16.74	13.50	0.94	0.97	0.27							
	15	66.94	14.51	16.73	0.57	0.92	0.34							
	16.5	65.18	12.97	20.09	0.49	0.87	0.40							
	18	68.39	16.28	13.29	0.73	1.05	0.27							
	19.5	67.05	17.99	12.67	0.91	1.10	0.27							
	21	65.92	18.99	12.47	1.04	1.31	0.27							
	22.5	65.99	19.40	12.37	0.79	1.19	0.26							
	24	65.91	18.36	13.18	1.08	1.25	0.21							
	25.5	64.95	19.31	13.00	1.11	1.37	0.26							
	27	65.84	18.09	13.19	1.18	1.44	0.26							
	28.5	64.88	19.67	13.03	0.92	1.27	0.23							
	30	66.01	18.76	12.42	1.15	1.40	0.26							

LoHf, 400C, 7 dpa

Meas.	Pos. (nm)	Fe	Cr	Ni	Mn	Mo	Si	Meas.	Fe	Cr	Ni	Mn	Mo	Si
1	0	66.33	17.61	13.65	1.03	1.12	0.26	2	66.61	18.42	12.50	1.07	1.14	0.27
	1.5	65.52	19.35	12.83	0.73	1.31	0.26		65.44	18.56	13.26	1.15	1.29	0.30
	3	65.23	19.26	12.80	1.16	1.28	0.27		66.01	18.13	13.26	0.87	1.46	0.27
	4.5	64.56	19.15	13.87	0.82	1.31	0.29		65.29	19.66	12.40	1.13	1.20	0.31
	6	65.67	18.40	13.33	0.83	1.54	0.23		65.42	18.82	13.21	0.84	1.43	0.28
	7.5	66.21	18.22	13.05	0.92	1.33	0.27		65.94	18.71	12.68	0.87	1.48	0.32
	9	66.49	18.78	12.06	1.11	1.28	0.27		64.94	17.89	14.36	1.06	1.41	0.34
	10.5	66.97	18.38	12.32	0.84	1.20	0.30		66.28	17.77	13.63	0.69	1.30	0.32
	12	67.09	17.41	13.05	1.05	1.07	0.33		67.51	17.22	13.00	0.81	1.12	0.34
	13.5	64.66	14.29	19.01	0.55	1.01	0.46		65.54	16.08	16.48	0.48	1.01	0.41
	15	64.38	13.44	20.36	0.55	0.88	0.40		63.76	13.93	20.18	0.57	1.01	0.55
	16.5	65.78	15.38	16.66	0.69	1.06	0.43		65.90	16.21	15.75	0.67	1.08	0.38
	18	65.85	17.98	14.06	0.55	1.26	0.31		67.37	17.04	13.26	0.90	1.07	0.35
	19.5	66.20	17.22	14.24	0.72	1.31	0.32		66.22	18.96	12.34	0.91	1.30	0.27
	21	65.79	18.45	13.09	1.15	1.29	0.24		65.55	19.50	12.28	0.97	1.41	0.30
	22.5	65.57	18.78	12.82	0.95	1.59	0.30		63.88	19.60	13.60	1.19	1.43	0.31
	24	65.57	18.09	13.63	1.29	1.20	0.22		64.68	19.26	13.40	1.07	1.34	0.26
	25.5	66.12	18.00	13.26	1.04	1.27	0.30		64.61	19.03	13.37	1.20	1.48	0.31
	27	67.73	17.15	12.72	0.91	1.16	0.33		65.59	18.72	12.96	0.85	1.51	0.37
	28.5	66.60	17.36	13.55	0.95	1.23	0.31		66.30	18.41	12.69	0.97	1.33	0.30
	30	64.85	18.01	14.37	1.02	1.43	0.33		66.75	19.04	11.49	0.95	1.47	0.31
3	0	66.26	18.31	12.92	0.94	1.27	0.31	4	65.77	18.36	13.23	1.06	1.25	0.32
	1.5	65.34	18.10	14.06	0.94	1.28	0.27		66.24	18.20	12.98	1.04	1.29	0.25
	3	64.93	18.71	13.94	0.78	1.35	0.30		65.64	18.59	13.11	0.93	1.45	0.27
	4.5	65.03	18.59	13.63	1.05	1.39	0.32		65.36	18.96	12.79	1.23	1.38	0.29
	6	64.87	19.71	12.67	1.04	1.36	0.34		65.96	18.81	12.50	0.98	1.45	0.30
	7.5	65.94	19.00	11.80	1.33	1.57	0.36		66.48	18.47	12.53	1.01	1.22	0.29
	9	66.21	19.19	11.89	0.89	1.53	0.30		66.17	18.85	12.61	0.89	1.23	0.25
	10.5	66.76	19.06	11.34	0.96	1.57	0.30		66.76	17.53	13.33	0.88	1.21	0.30
	12	66.75	17.16	13.43	1.07	1.27	0.32		64.64	15.36	17.58	0.81	1.22	0.40
	13.5	65.66	13.94	18.50	0.59	0.90	0.42		62.85	13.83	21.20	0.66	0.92	0.54
	15	63.31	13.32	21.43	0.41	1.02	0.50		65.04	17.09	15.80	0.72	0.98	0.38
	16.5	65.92	15.21	16.69	0.56	1.22	0.41		66.82	18.64	12.21	0.75	1.26	0.33
	18	66.46	19.06	12.34	0.74	1.08	0.33		65.79	19.55	12.25	0.86	1.28	0.28
	19.5	66.43	19.22	11.92	0.87	1.29	0.27		65.09	18.24	13.59	1.24	1.50	0.33
	21	64.89	19.61	12.69	1.00	1.51	0.30		65.61	18.49	13.36	0.91	1.34	0.28
	22.5	65.85	19.02	12.49	0.96	1.43	0.26		65.15	19.01	13.28	0.99	1.30	0.26
	24	64.92	19.45	12.83	1.02	1.45	0.34		65.98	17.78	13.86	0.88	1.20	0.30
	25.5	65.23	18.49	13.31	1.21	1.45	0.31		65.72	17.67	13.94	1.08	1.27	0.31
	27	65.26	17.99	14.00	1.21	1.23	0.32		64.74	18.35	14.54	0.77	1.31	0.28
	28.5	64.65	16.97	16.03	0.84	1.18	0.33		63.65	19.27	14.58	0.75	1.38	0.37
	30	64.96	17.02	15.59	0.84	1.27	0.32		64.95	17.96	14.64	0.83	1.30	0.31
5	0	66.38	18.21	12.75	1.16	1.24	0.26	6	65.92	17.99	13.52	1.03	1.26	0.28
	1.5	65.63	18.45	13.33	1.08	1.17	0.34		65.91	18.85	12.49	1.10	1.39	0.27
	3	65.37	18.48	13.45	1.10	1.29	0.32		66.03	18.84	12.21	1.22	1.37	0.32
	4.5	65.45	17.71	14.26	0.91	1.35	0.31		66.62	18.40	12.21	1.06	1.46	0.25

Meas.	Pos. (nm)	Fe	Cr	Ni	Mn	Mo	Si	Meas.	Fe	Cr	Ni	Mn	Mo	Si
5	6	64.29	18.77	14.45	0.88	1.30	0.31	6	65.44	18.88	12.81	1.10	1.47	0.30
	7.5	64.90	18.36	14.37	0.81	1.26	0.29		67.05	18.03	12.07	1.15	1.41	0.29
	9	66.31	17.96	13.40	0.81	1.18	0.34		66.90	17.90	12.64	1.08	1.21	0.27
	10.5	67.53	16.54	13.82	0.69	1.12	0.30		67.71	16.94	12.95	0.84	1.23	0.33
	12	66.57	14.86	16.66	0.55	0.98	0.38		66.75	15.89	15.10	0.77	1.10	0.40
	13.5	64.86	14.72	18.17	0.75	1.03	0.47		63.39	14.60	20.14	0.36	1.02	0.49
	15	65.22	14.74	17.72	0.72	1.10	0.50		65.69	15.64	16.53	0.66	1.05	0.43
	16.5	66.09	16.82	14.83	0.87	1.00	0.40		67.17	17.30	13.36	0.74	1.12	0.32
	18	67.11	17.45	13.15	0.86	1.15	0.28		66.73	18.43	12.79	0.77	1.03	0.26
	19.5	65.71	19.00	13.18	0.67	1.15	0.29		67.17	18.10	12.16	1.04	1.28	0.25
	21	65.99	17.78	13.76	0.93	1.26	0.28		65.43	19.05	12.79	1.03	1.35	0.34
	22.5	66.15	18.39	13.01	0.90	1.25	0.30		65.98	18.94	12.60	0.91	1.28	0.30
	24	65.80	18.83	12.73	0.97	1.41	0.26		67.17	18.05	12.00	1.02	1.43	0.32
	25.5	66.47	17.77	13.16	1.05	1.29	0.27		66.60	18.96	11.64	1.14	1.35	0.32
	27	65.57	18.70	13.23	1.05	1.19	0.27		67.25	17.94	12.13	1.02	1.36	0.31
	28.5	66.16	18.43	12.89	0.94	1.32	0.26		66.47	18.96	11.83	1.11	1.31	0.32
	30	66.09	18.49	12.70	1.00	1.42	0.29		65.32	19.81	12.13	1.11	1.34	0.29
7	0	65.60	15.37	16.88	0.84	1.00	0.31	8	65.91	18.47	13.53	0.81	0.97	0.32
	1.5	64.17	15.96	17.66	0.64	1.19	0.38		67.67	16.87	13.34	0.80	1.03	0.30
	3	63.88	15.91	17.87	1.13	0.90	0.31		65.56	16.68	15.63	0.49	1.26	0.38
	4.5	65.95	17.24	14.37	0.89	1.20	0.35		65.05	15.34	17.39	0.68	1.21	0.34
	6	67.79	15.51	14.06	0.94	1.42	0.29		66.47	17.32	13.71	0.96	1.21	0.33
	7.5	65.27	19.78	12.82	0.77	1.10	0.26		66.28	17.82	13.38	1.03	1.15	0.34
	9	66.10	19.14	12.46	1.03	0.96	0.31		65.73	18.91	12.66	1.07	1.26	0.36
	10.5	67.05	15.64	15.47	0.60	0.90	0.35		66.60	18.03	13.16	0.64	1.19	0.37
	12	63.24	13.54	21.75	0.20	0.80	0.46		65.25	15.51	17.16	0.71	1.00	0.37
	13.5	62.53	12.81	22.96	0.39	0.87	0.44		63.76	13.92	20.29	0.64	1.01	0.38
	15	62.88	12.27	23.08	0.60	0.59	0.57		62.38	13.81	21.47	0.89	0.85	0.60
	16.5	65.75	15.43	17.05	0.57	0.74	0.48		64.10	14.63	19.20	0.71	0.81	0.54
	18	67.27	17.16	13.23	0.94	0.91	0.49		65.05	15.35	17.70	0.65	0.78	0.48
	19.5	65.37	15.64	16.59	0.85	1.12	0.44		66.36	16.00	15.44	0.68	1.10	0.42
	21	63.19	17.02	17.20	1.24	0.95	0.40		66.59	16.71	14.58	0.81	0.88	0.43
	22.5	64.23	17.01	16.38	0.77	1.24	0.37		65.58	17.68	14.59	0.86	0.86	0.42
	24	64.58	19.79	13.77	0.56	0.96	0.33		65.71	16.15	15.60	1.08	1.08	0.37
	25.5	63.05	18.81	15.53	1.18	1.06	0.36		64.66	17.90	14.99	0.94	1.09	0.42
	27	64.78	17.55	15.08	0.93	1.18	0.48		64.37	17.97	14.89	1.13	1.20	0.43
	28.5	66.95	16.34	14.20	1.14	0.90	0.47		63.99	19.22	14.42	0.83	1.14	0.40
	30	63.02	19.92	14.54	0.91	1.21	0.40		64.09	18.83	13.94	1.56	1.25	0.33

LoHf, 400C, 10 dpa

Meas.	Pos. (nm)	Fe	Cr	Ni	Mn	Mo	Si	Meas.	Fe	Cr	Ni	Mn	Mo	Si
1	0	65.37	21.03	11.34	1.05	1.21	0.36	2	66.29	19.16	11.79	1.47	1.07	0.23
	1.5	64.50	21.04	12.18	1.05	1.23	0.33		64.83	18.48	13.24	1.59	1.35	0.51
	3	67.48	17.46	12.66	1.06	1.34	0.28		67.10	18.81	11.87	0.80	0.96	0.47
	4.5	65.29	18.95	13.33	1.15	1.28	0.36		64.08	19.99	12.97	1.34	1.71	-0.09
	6	66.79	18.24	12.59	1.18	1.20	0.27		65.29	20.02	11.53	1.38	1.28	0.50
	7.5	67.45	18.24	11.98	1.13	1.19	0.35		65.47	20.31	11.62	0.98	1.13	0.49
	9	67.89	17.87	11.88	1.21	1.15	0.29		67.32	19.07	10.88	0.89	1.65	0.19
	10.5	68.28	17.97	11.76	0.89	1.10	0.27		66.04	20.17	11.53	1.03	1.12	0.12
	12	67.92	16.26	13.81	0.94	1.07	0.28		67.62	18.30	12.04	0.67	0.98	0.40
	13.5	61.47	12.99	24.26	0.50	0.78	0.44		70.12	16.62	11.14	1.12	0.87	0.13
	15	64.94	13.12	20.12	0.78	1.04	0.44		67.29	11.51	19.09	0.50	0.66	0.95
	16.5	66.99	18.61	12.31	0.89	1.20	0.35		59.44	10.34	27.43	0.50	0.39	1.91
	18	66.12	19.57	11.57	1.26	1.49	0.23		69.95	15.86	12.29	1.21	0.54	0.14
	19.5	65.45	20.73	11.77	0.65	1.39	0.28		67.61	19.84	10.29	1.18	0.83	0.25
	21	66.66	19.06	11.66	1.05	1.58	0.28		67.67	19.76	10.01	1.52	0.67	0.36
	22.5	64.45	19.85	12.93	1.20	1.57	0.29		67.70	18.72	11.61	1.05	0.86	0.06
	24	65.67	19.45	12.39	0.94	1.56	0.28		67.01	18.91	11.68	1.13	1.07	0.19
	25.5	64.97	19.27	13.07	1.30	1.39	0.30		66.13	19.49	12.49	0.88	0.64	0.37
	27	65.42	19.55	12.83	0.80	1.40	0.28		65.85	17.82	14.05	0.65	1.03	0.60
	28.5	65.98	18.70	12.71	1.44	1.16	0.29		67.54	16.72	13.72	1.42	0.62	-0.01
	30	66.79	18.93	12.27	0.94	1.07	0.32		65.84	20.15	12.20	1.28	0.65	-0.13
3	0	64.89	20.47	12.23	1.29	1.12	0.26	4	63.96	20.45	12.58	1.56	1.19	0.26
	1.5	64.58	20.63	12.33	1.09	1.36	0.25		63.49	20.56	12.54	1.43	1.52	0.47
	3	65.84	19.01	12.77	1.08	1.30	0.28		64.25	19.90	12.62	1.34	1.41	0.48
	4.5	65.26	18.87	13.63	1.07	1.17	0.25		64.00	19.62	12.82	1.48	1.80	0.27
	6	66.33	18.52	12.84	1.08	1.23	0.23		64.51	19.80	12.29	1.29	1.65	0.45
	7.5	65.73	19.26	12.67	1.15	1.19	0.29		64.78	21.26	10.43	1.57	1.61	0.35
	9	67.28	19.16	11.52	0.94	1.09	0.24		67.09	18.60	10.60	1.23	2.30	0.18
	10.5	68.65	18.72	10.75	0.84	1.04	0.25		67.65	19.67	10.14	1.10	1.49	-0.05
	12	69.42	16.83	11.93	1.02	0.80	0.29		68.59	19.18	9.84	1.29	1.13	-0.02
	13.5	63.49	13.29	21.81	0.62	0.79	0.46		69.81	15.32	12.19	0.64	1.35	0.68
	15	63.93	13.44	20.95	0.88	0.81	0.47		62.35	10.23	23.69	0.79	1.04	1.90
	16.5	67.61	17.38	13.23	0.79	0.99	0.29		62.28	11.81	23.07	0.65	0.88	1.31
	18	67.15	18.62	12.57	0.60	1.06	0.27		68.75	16.31	13.38	0.75	0.84	-0.03
	19.5	66.61	19.19	12.17	0.84	1.19	0.24		66.36	19.30	12.28	0.91	0.98	0.18
	21	65.94	18.68	13.26	1.06	1.06	0.30		65.61	19.84	11.49	1.52	1.17	0.36
	22.5	66.98	18.31	12.48	0.98	1.25	0.28		67.50	18.44	11.94	0.67	1.05	0.39
	24	65.91	18.82	13.31	0.71	1.25	0.28		66.64	17.63	13.43	1.12	1.03	0.15
	25.5	66.14	19.52	12.32	0.86	1.16	0.30		64.54	18.51	14.15	0.71	1.44	0.65
	27	65.48	18.73	13.72	0.86	1.20	0.26		62.79	17.85	15.95	0.64	2.41	0.36
	28.5	65.35	18.23	14.22	1.00	1.21	0.31		61.32	20.27	14.90	0.65	2.65	0.20
	30	66.19	17.34	14.24	1.03	1.19	0.30		63.89	18.58	14.54	0.91	1.46	0.62
5	0	66.28	19.60	12.10	0.82	1.19	0.20	6	66.00	17.69	13.46	1.12	1.28	0.44
	1.5	66.03	19.00	12.51	1.18	1.28	0.20		65.31	19.60	12.93	0.60	1.05	0.51
	3	65.13	19.31	13.21	1.05	1.29	0.25		67.06	18.54	11.78	1.12	1.21	0.28
	4.5	65.90	18.87	12.75	1.23	1.25	0.21		67.85	17.59	11.70	1.16	1.46	0.24

Meas.	Pos. (nm)	Fe	Cr	Ni	Mn	Mo	Si	Meas.	Fe	Cr	Ni	Mn	Mo	Si
5	6	67.12	19.05	11.88	0.84	1.10	0.22	6	67.55	18.17	11.44	1.23	1.31	0.30
	7.5	67.64	17.71	12.33	1.06	1.26	0.21		64.83	18.26	13.69	1.09	1.47	0.66
	9	68.22	19.03	10.98	0.84	0.93	0.24		64.88	16.88	14.69	1.00	1.80	0.75
	10.5	70.19	16.01	12.02	0.82	0.95	0.23		66.33	19.94	10.77	1.22	1.48	0.27
	12	67.74	12.99	17.67	0.78	0.82	0.29		67.60	20.11	9.46	1.42	1.06	0.36
	13.5	60.49	11.73	26.38	0.52	0.87	0.54		69.13	17.66	10.40	1.07	1.31	0.43
	15	65.96	16.23	16.07	0.80	0.94	0.38		66.72	13.62	17.06	0.40	1.15	1.05
	16.5	68.49	18.14	11.41	0.87	1.09	0.25		61.50	12.32	22.98	0.45	0.60	2.15
	18	66.90	19.78	11.23	1.00	1.09	0.23		68.76	16.02	13.94	0.54	0.84	-0.09
	19.5	66.58	19.26	12.03	1.03	1.09	0.25		68.63	17.01	12.87	1.03	0.64	-0.19
	21	66.40	20.01	11.63	0.76	1.20	0.29		66.52	18.93	12.35	1.25	0.70	0.24
	22.5	66.34	19.33	11.74	1.27	1.32	0.28		65.86	17.96	13.66	1.27	1.22	0.04
	24	65.31	19.47	12.91	1.03	1.29	0.27		64.64	19.13	13.52	0.90	1.63	0.18
	25.5	65.52	18.39	13.97	0.86	1.26	0.30		65.23	19.13	13.04	0.96	1.55	0.09
	27	65.97	18.69	13.04	1.00	1.30	0.27		65.52	18.47	12.49	1.10	1.69	0.74
	28.5	66.90	18.03	12.61	1.17	1.28	0.28		65.41	16.94	14.50	0.98	1.63	0.55
	30	66.31	18.37	13.09	0.99	1.25	0.26		65.51	18.87	12.91	0.99	1.54	0.19
7	0	65.90	18.40	13.49	0.93	1.29	0.30	8	66.41	19.60	11.32	1.26	1.14	0.27
	1.5	66.16	18.96	12.37	1.15	1.36	0.30		64.72	18.99	13.54	0.99	1.14	0.62
	3	66.83	17.96	12.48	1.43	1.30	0.30		65.94	17.05	14.49	0.81	1.19	0.52
	4.5	67.27	19.30	10.83	1.16	1.44	0.32		65.77	18.90	12.75	1.01	1.29	0.29
	6	65.69	19.34	11.69	1.56	1.72	0.29		64.66	19.30	13.21	1.35	1.25	0.22
	7.5	67.56	20.53	9.56	0.87	1.48	0.26		64.74	18.71	12.88	1.71	1.66	0.31
	9	68.00	18.84	10.94	0.81	1.41	0.28		66.34	17.77	12.98	1.12	1.51	0.26
	10.5	68.69	18.06	11.03	0.93	1.29	0.31		67.07	18.86	11.34	1.22	1.29	0.21
	12	68.33	17.77	11.93	0.80	1.18	0.26		68.62	18.55	10.71	0.92	0.93	0.26
	13.5	67.54	14.66	15.65	1.00	1.15	0.36		65.20	11.32	20.13	0.70	0.78	1.87
	15	61.04	11.61	25.55	0.73	1.07	0.47		65.17	10.46	22.23	0.31	0.50	1.33
	16.5	66.74	16.52	14.78	0.79	1.17	0.39		69.50	13.25	15.51	0.71	0.41	0.61
	18	68.61	17.15	12.06	0.95	1.23	0.34		69.68	16.99	11.56	0.57	0.76	0.44
	19.5	69.37	17.09	11.63	0.63	1.28	0.30		69.19	17.33	11.01	0.94	0.82	0.70
	21	67.01	18.02	12.96	0.70	1.31	0.32		69.11	17.57	11.22	0.83	0.96	0.31
	22.5	67.90	17.28	12.18	1.03	1.61	0.33		68.22	16.89	12.93	0.77	0.77	0.42
	24	66.88	17.62	12.61	1.25	1.63	0.34		66.69	17.89	13.78	0.97	0.63	0.04
	25.5	66.68	17.20	13.64	1.03	1.44	0.29		68.07	17.15	12.40	1.18	1.03	0.16
	27	65.96	18.01	13.69	1.05	1.29	0.32		66.80	18.13	12.71	0.92	1.14	0.29
	28.5	65.95	16.49	15.41	0.73	1.42	0.27		65.31	20.57	11.33	1.54	1.24	0.01
	30	65.68	16.27	16.14	0.74	1.18	0.29		65.46	20.06	10.77	1.60	1.70	0.40
9	0	64.55	19.14	12.88	1.44	1.68	0.32	10	63.92	20.32	13.06	1.24	1.00	0.46
	1.5	65.23	18.87	12.64	1.15	1.77	0.34		63.46	21.23	12.56	1.28	1.21	0.26
	3	66.43	18.40	11.67	1.18	2.08	0.24		64.29	19.05	14.15	0.83	1.22	0.46
	4.5	66.25	18.19	11.60	1.43	2.52	0.02		63.92	19.02	14.37	1.14	1.20	0.34
	6	67.23	18.21	11.16	1.21	1.85	0.34		64.22	20.43	13.13	0.89	1.23	0.10
	7.5	66.57	18.96	11.40	1.04	1.69	0.34		65.08	19.32	12.63	1.25	1.61	0.11
	9	67.31	18.28	11.28	1.06	1.73	0.33		66.64	19.10	11.38	1.04	1.54	0.29
	10.5	67.94	17.45	12.08	1.09	1.26	0.17		68.58	17.19	12.08	1.02	0.93	0.20
	12	67.84	17.58	12.34	0.75	1.24	0.25		68.98	16.65	12.31	0.82	0.88	0.36

Meas.	Pos. (nm)	Fe	Cr	Ni	Mn	Mo	Si	Meas.	Fe	Cr	Ni	Mn	Mo	Si
9	13.5	64.09	10.71	22.15	0.86	1.05	1.14	10	67.30	13.24	17.44	0.71	0.52	0.78
	15	63.01	10.38	23.32	0.78	1.03	1.47		61.58	10.01	24.94	0.83	0.79	1.85
	16.5	66.49	15.12	15.68	1.13	1.06	0.53		65.67	15.13	17.20	0.85	0.44	0.71
	18	65.26	15.81	15.59	1.37	1.37	0.59		66.76	17.36	13.69	1.21	0.69	0.29
	19.5	66.82	18.98	11.84	1.15	1.24	-0.02		68.28	18.82	10.55	1.05	1.10	0.20
	21	65.81	19.68	11.74	1.14	1.60	0.03		67.90	17.91	11.13	1.40	1.36	0.32
	22.5	66.95	15.47	13.81	1.41	2.06	0.30		68.27	16.81	11.93	1.67	1.37	-0.06
	24	66.39	18.96	12.30	0.97	1.30	0.09		67.39	17.80	12.71	0.74	1.09	0.27
	25.5	65.29	19.63	12.12	1.00	1.74	0.21		65.82	17.28	13.61	1.36	1.17	0.75
	27	66.77	17.49	12.42	0.55	2.11	0.67		66.96	17.53	12.68	1.02	1.67	0.14
	28.5	66.53	16.45	14.49	0.62	1.62	0.29		65.50	18.94	12.45	1.51	1.54	0.05
	30	63.55	17.05	16.83	0.79	1.57	0.21		66.71	18.10	12.34	1.12	1.26	0.47

HiHf, 400C, 3 dpa, 3.2 MeV p+

Meas.	Pos. (nm)	Fe	Cr	Ni	Mn	Mo	Si	Meas.	Fe	Cr	Ni	Mn	Mo	Si
1	0	66.22	20.01	12.26	0.73	0.58	0.20	2	64.32	20.26	12.82	0.85	1.56	0.19
	1.5	66.69	18.78	12.62	1.09	0.61	0.21		65.07	18.89	13.16	1.22	1.41	0.24
	3	64.97	19.68	13.71	0.81	0.61	0.21		65.38	19.08	12.60	1.31	1.41	0.22
	4.5	65.67	19.34	13.12	1.07	0.59	0.20		65.36	18.80	12.91	1.22	1.50	0.21
	6	65.89	19.22	13.17	0.88	0.63	0.22		65.05	19.61	12.56	1.09	1.46	0.22
	7.5	65.46	20.30	12.31	0.96	0.72	0.25		65.77	18.91	12.34	1.26	1.49	0.23
	9	66.39	18.80	12.98	0.96	0.64	0.22		66.83	18.52	11.69	1.35	1.39	0.23
	10.5	66.62	18.95	12.49	1.03	0.67	0.23		66.33	18.88	12.01	1.18	1.35	0.24
	12	67.56	17.54	13.13	0.69	0.80	0.28		66.43	18.21	12.90	0.95	1.24	0.27
	13.5	67.32	15.78	14.95	0.75	0.89	0.31		65.83	17.41	14.31	0.90	1.28	0.27
	15	65.46	13.79	18.45	0.49	1.34	0.47		67.88	14.27	15.75	0.64	1.09	0.37
	16.5	67.11	15.45	15.51	0.56	1.01	0.35		67.58	13.38	16.92	0.83	0.86	0.43
	18	65.99	18.06	13.77	0.67	1.12	0.39		66.86	15.45	15.49	0.81	0.96	0.42
	19.5	66.39	18.37	13.27	0.73	0.92	0.32		67.24	17.30	12.91	1.05	1.21	0.28
	21	65.49	19.20	13.39	0.59	0.99	0.35		65.63	18.63	12.75	1.45	1.29	0.26
	22.5	64.92	19.65	13.24	0.98	0.90	0.31		66.21	18.60	12.46	1.17	1.32	0.24
	24	66.02	19.11	12.86	0.64	1.01	0.35		65.87	19.54	11.90	1.15	1.23	0.31
	25.5	64.90	18.73	14.01	1.02	1.00	0.35		66.09	18.30	12.69	1.24	1.40	0.28
	27	64.78	18.19	15.01	0.68	1.00	0.35		66.29	19.05	12.11	0.97	1.32	0.26
	28.5	65.12	18.79	14.03	0.62	1.07	0.37		65.12	19.67	12.60	0.91	1.44	0.27
	30	66.69	18.18	12.93	0.89	0.98	0.34		65.44	19.03	12.64	1.17	1.42	0.31
3	0	65.58	19.40	12.24	1.09	1.46	0.22	4	64.15	16.74	16.31	1.07	1.46	0.27
	1.5	65.18	19.10	12.92	1.04	1.51	0.25		65.26	17.44	14.77	1.03	1.27	0.23
	3	65.60	18.54	13.16	1.12	1.38	0.21		65.57	17.78	13.93	1.09	1.40	0.23
	4.5	65.06	19.10	12.59	1.47	1.57	0.22		65.02	18.29	14.25	0.90	1.31	0.23
	6	65.17	19.41	12.52	1.21	1.47	0.22		65.79	18.25	13.27	1.13	1.36	0.20
	7.5	65.26	19.05	12.77	1.19	1.51	0.24		65.22	18.94	13.31	1.06	1.25	0.22
	9	65.14	19.27	12.62	1.33	1.43	0.21		64.77	20.13	12.62	0.96	1.29	0.22
	10.5	65.23	19.67	12.21	1.21	1.46	0.21		66.42	17.73	13.20	1.05	1.39	0.21
	12	66.70	19.06	11.94	0.94	1.13	0.24		68.97	15.74	13.09	0.74	1.22	0.24
	13.5	67.00	17.21	13.31	1.01	1.18	0.30		65.18	12.50	20.30	0.58	0.97	0.47
	15	66.48	14.83	16.60	0.67	0.96	0.45		66.79	12.22	19.19	0.56	0.81	0.43
	16.5	65.31	14.41	18.04	0.85	0.98	0.42		67.38	16.24	14.16	0.81	1.06	0.36
	18	65.06	15.64	16.63	1.11	1.13	0.43		67.99	16.43	13.32	0.89	1.04	0.34
	19.5	66.61	18.40	12.51	1.05	1.15	0.27		67.24	17.86	12.55	0.83	1.25	0.26
	21	65.80	18.63	12.74	1.28	1.24	0.30		67.01	17.76	12.33	1.21	1.43	0.25
	22.5	66.11	18.67	12.42	1.22	1.31	0.26		66.35	18.97	12.26	0.98	1.17	0.26
	24	64.76	19.55	12.94	1.18	1.27	0.30		67.29	17.81	12.34	1.00	1.31	0.26
	25.5	66.45	17.98	13.17	1.06	1.04	0.29		67.02	17.86	12.38	0.98	1.47	0.30
	27	66.83	17.27	13.57	1.01	1.01	0.30		65.25	19.06	12.80	1.18	1.48	0.24
	28.5	66.72	16.00	14.74	1.15	1.10	0.29		65.53	18.74	12.60	1.27	1.58	0.28
	30	66.02	16.79	14.99	0.86	1.03	0.31		66.28	19.09	11.81	1.21	1.36	0.25
5	0	65.86	18.68	12.78	1.03	1.44	0.21	6	65.07	19.88	12.17	1.09	1.58	0.21
	1.5	65.27	18.24	13.65	1.29	1.32	0.23		64.31	19.43	13.20	1.22	1.62	0.22
	3	66.00	18.43	13.12	0.90	1.30	0.25		63.89	18.88	14.16	1.21	1.66	0.21
	4.5	65.80	17.78	13.89	1.04	1.24	0.24		64.42	20.15	12.34	1.39	1.51	0.19

Meas.	Pos. (nm)	Fe	Cr	Ni	Mn	Mo	Si	Meas.	Fe	Cr	Ni	Mn	Mo	Si
5	6	65.39	18.06	14.00	0.99	1.33	0.23	6	65.39	19.28	12.39	1.31	1.37	0.25
	7.5	65.40	18.36	13.76	1.11	1.14	0.22		64.90	19.24	12.85	1.24	1.53	0.24
	9	66.15	18.61	12.33	1.27	1.38	0.26		65.23	18.88	12.77	1.45	1.43	0.24
	10.5	66.26	18.71	12.48	1.03	1.28	0.24		65.72	19.31	12.62	1.02	1.08	0.25
	12	66.08	18.68	13.08	0.70	1.17	0.28		67.38	17.86	12.28	0.96	1.30	0.22
	13.5	66.02	16.53	15.12	0.84	1.16	0.32		68.59	16.49	12.67	0.88	1.11	0.25
	15	67.42	13.92	16.37	0.93	0.94	0.42		65.11	13.50	19.16	0.60	1.13	0.50
	16.5	66.36	13.52	17.87	0.76	1.05	0.43		67.14	12.44	18.37	0.69	0.93	0.43
	18	68.27	15.45	14.12	0.81	0.96	0.37		69.02	16.32	12.70	0.73	0.91	0.32
	19.5	66.72	18.17	12.67	1.07	1.04	0.33		68.03	18.27	11.60	0.89	0.98	0.24
	21	65.60	19.30	12.26	1.19	1.35	0.30		66.49	18.23	12.51	1.22	1.27	0.27
	22.5	66.08	19.47	11.76	1.19	1.26	0.25		66.92	18.08	12.15	1.20	1.40	0.24
	24	64.71	19.98	12.56	1.18	1.27	0.31		66.10	18.94	12.31	1.05	1.31	0.29
	25.5	66.11	18.58	12.60	1.21	1.27	0.23		66.34	18.55	12.31	1.15	1.41	0.25
	27	66.21	17.87	13.39	0.91	1.30	0.32		66.98	17.86	12.56	1.04	1.29	0.26
	28.5	65.24	18.58	13.83	0.82	1.20	0.33		65.19	17.81	14.50	1.04	1.17	0.29
	30	64.58	19.29	13.40	1.03	1.39	0.32		66.10	18.65	12.85	0.88	1.24	0.29
7	0	64.68	19.22	13.36	1.06	1.47	0.21	8	65.89	18.42	12.99	1.25	1.18	0.27
	1.5	65.80	17.93	13.18	1.40	1.49	0.21		65.94	17.51	13.72	1.23	1.39	0.21
	3	64.74	19.61	12.77	1.14	1.51	0.23		65.81	18.52	12.96	1.04	1.47	0.20
	4.5	64.35	19.40	13.01	1.41	1.65	0.19		64.89	19.40	12.82	1.10	1.57	0.22
	6	64.67	18.84	13.32	1.32	1.59	0.25		64.87	19.57	12.39	1.31	1.64	0.21
	7.5	65.12	18.49	13.30	1.27	1.59	0.23		64.84	19.36	12.71	1.36	1.53	0.19
	9	65.27	18.39	13.43	1.31	1.35	0.25		64.36	19.91	12.70	1.26	1.56	0.21
	10.5	65.72	19.05	12.50	1.19	1.33	0.21		65.09	19.03	13.17	1.14	1.35	0.23
	12	65.54	19.61	12.27	0.90	1.43	0.24		66.00	18.35	12.82	1.11	1.49	0.23
	13.5	66.52	18.10	12.56	1.23	1.36	0.23		66.81	18.38	12.18	1.01	1.38	0.23
	15	68.47	16.41	12.99	0.59	1.29	0.26		68.85	15.86	12.96	0.81	1.24	0.27
	16.5	66.11	13.58	18.26	0.59	1.05	0.42		66.41	12.37	19.32	0.59	0.94	0.38
	18	66.94	12.52	18.19	0.86	1.03	0.45		68.17	12.98	16.86	0.66	0.94	0.39
	19.5	69.28	15.61	12.90	0.95	0.96	0.30		68.45	15.90	13.70	0.58	1.06	0.31
	21	67.68	17.44	12.25	1.24	1.10	0.29		66.75	18.26	12.72	1.04	0.98	0.25
	22.5	66.66	18.34	12.40	1.03	1.30	0.27		66.83	18.20	12.58	0.99	1.12	0.28
	24	66.26	18.30	12.83	1.18	1.17	0.26		65.41	19.29	12.58	1.23	1.21	0.27
	25.5	65.78	17.56	13.84	1.25	1.31	0.25		64.46	19.50	13.17	1.24	1.38	0.25
	27	66.13	18.55	12.43	1.23	1.41	0.25		66.08	18.85	12.06	1.29	1.44	0.28
	28.5	66.21	17.70	13.06	1.19	1.58	0.27		65.46	19.12	12.47	1.28	1.41	0.26
	30	65.53	17.92	13.36	1.31	1.63	0.26		66.36	17.98	12.40	1.38	1.59	0.28
9	0	65.76	18.16	13.45	1.16	1.24	0.23	10	64.87	18.82	13.45	1.17	1.43	0.26
	1.5	65.93	18.11	13.43	1.03	1.28	0.22		64.65	19.56	12.92	1.16	1.47	0.25
	3	65.58	17.95	13.58	1.22	1.47	0.21		65.66	18.59	12.74	1.36	1.40	0.25
	4.5	65.09	18.87	13.10	1.27	1.49	0.19		64.40	19.92	12.71	0.98	1.71	0.28
	6	65.05	19.08	13.17	0.98	1.49	0.23		65.02	18.46	12.97	1.44	1.86	0.25
	7.5	64.54	19.70	13.10	1.07	1.41	0.19		65.06	18.02	13.32	1.32	2.01	0.26
	9	65.93	18.83	12.40	1.08	1.55	0.21		67.55	17.05	12.49	1.09	1.60	0.22
	10.5	65.23	19.33	12.73	1.03	1.46	0.22		67.42	17.36	12.67	0.95	1.34	0.26
	12	65.74	18.90	12.64	1.07	1.43	0.21		67.71	16.57	13.12	0.86	1.46	0.28

Meas.	Pos. (nm)	Fe	Cr	Ni	Mn	Mo	Si	Meas.	Fe	Cr	Ni	Mn	Mo	Si
9	13.5	67.45	17.36	12.70	1.01	1.26	0.22	10	70.34	14.30	12.70	1.06	1.31	0.28
	15	67.27	13.59	16.78	0.76	1.28	0.33		69.00	12.99	15.81	0.56	1.29	0.35
	16.5	65.82	12.34	19.59	0.82	0.98	0.45		67.28	13.63	16.79	0.61	1.30	0.39
	18	68.76	13.97	15.17	0.74	0.95	0.40		68.50	15.16	13.82	0.76	1.39	0.36
	19.5	67.73	16.89	13.30	0.74	1.04	0.31		67.32	17.94	12.17	0.87	1.43	0.27
	21	66.56	18.20	12.80	0.93	1.23	0.27		66.39	18.69	11.94	1.15	1.52	0.31
	22.5	66.13	17.99	13.48	0.76	1.37	0.27		65.95	18.90	12.14	1.04	1.68	0.29
	24	66.84	18.37	12.18	0.96	1.37	0.27		67.03	17.72	12.39	0.97	1.62	0.27
	25.5	65.40	18.67	13.11	1.11	1.49	0.22		65.58	17.97	13.08	1.22	1.87	0.27
	27	66.48	18.04	12.49	1.04	1.66	0.29		66.44	18.10	12.26	1.11	1.81	0.28
	28.5	66.14	18.08	12.86	1.16	1.51	0.25		65.88	17.57	13.31	1.06	1.90	0.28
	30	66.56	17.97	12.63	1.22	1.35	0.27		66.05	17.97	13.11	0.83	1.73	0.31
11	0	65.82	18.51	12.68	1.20	1.55	0.25	12	65.46	19.68	12.11	1.00	1.52	0.24
	1.5	65.70	18.02	13.43	0.92	1.72	0.22		65.20	19.16	12.39	1.39	1.64	0.21
	3	64.69	18.81	13.26	1.27	1.72	0.26		65.09	19.00	12.68	1.10	1.89	0.24
	4.5	65.35	18.82	12.96	0.94	1.66	0.28		65.61	18.95	12.32	1.17	1.71	0.25
	6	65.07	19.01	12.90	1.15	1.64	0.23		65.47	19.47	12.22	0.99	1.61	0.23
	7.5	65.88	18.67	12.36	1.13	1.71	0.24		65.86	18.82	12.16	1.29	1.64	0.23
	9	65.73	18.42	12.60	1.27	1.72	0.27		65.46	19.08	12.46	1.14	1.59	0.26
	10.5	66.01	18.58	12.24	1.11	1.79	0.27		67.20	18.02	11.87	1.13	1.49	0.30
	12	68.02	17.38	11.83	1.07	1.46	0.25		68.97	16.36	11.90	1.16	1.32	0.29
	13.5	68.63	15.23	13.76	0.77	1.31	0.30		68.69	15.49	13.42	0.90	1.20	0.31
	15	67.01	12.65	18.15	0.56	1.22	0.41		68.87	12.84	16.10	0.57	1.23	0.38
	16.5	67.57	13.93	16.15	0.93	0.99	0.43		68.27	13.28	16.36	0.54	1.09	0.46
	18	67.89	15.63	14.02	0.93	1.17	0.36		69.23	13.92	14.51	0.81	1.10	0.43
	19.5	67.31	17.84	11.86	1.28	1.46	0.26		67.27	17.72	12.48	0.91	1.35	0.27
	21	67.04	17.12	12.78	1.05	1.71	0.30		66.65	18.20	12.22	1.14	1.49	0.30
	22.5	66.27	17.80	13.52	0.67	1.46	0.28		66.72	18.84	11.43	1.24	1.48	0.29
	24	67.24	17.02	13.13	0.90	1.41	0.30		65.45	19.00	12.82	1.01	1.49	0.23
	25.5	67.46	16.98	12.89	0.78	1.62	0.27		64.53	19.63	13.12	0.90	1.53	0.29
	27	66.14	18.59	12.64	0.88	1.47	0.27		64.05	19.78	13.28	0.85	1.73	0.30
	28.5	66.72	18.21	11.75	1.26	1.80	0.26		63.90	19.47	13.79	1.04	1.48	0.32
	30	65.81	18.72	12.36	1.16	1.63	0.31		63.92	18.39	14.66	1.31	1.41	0.32
13	0	67.33	17.50	12.88	0.77	1.26	0.26	14	65.35	18.63	13.40	1.01	1.36	0.25
	1.5	65.11	18.77	13.29	1.03	1.56	0.24		66.50	17.09	13.86	0.94	1.40	0.21
	3	65.25	19.45	12.52	0.94	1.62	0.22		65.71	17.92	14.08	0.70	1.39	0.21
	4.5	65.31	18.39	12.50	1.61	1.91	0.28		65.38	17.99	14.01	1.07	1.28	0.27
	6	65.51	17.95	13.13	1.33	1.84	0.24		64.28	19.02	13.99	1.02	1.44	0.24
	7.5	65.62	19.07	12.04	1.13	1.88	0.24		65.07	18.71	13.35	1.09	1.53	0.26
	9	66.05	18.75	12.05	1.25	1.66	0.25		65.89	18.22	12.91	1.27	1.47	0.24
	10.5	66.64	18.42	12.31	0.90	1.51	0.21		66.62	18.59	12.09	1.08	1.39	0.23
	12	67.48	17.21	12.61	0.94	1.49	0.27		67.44	17.49	12.75	0.74	1.30	0.27
	13.5	68.13	16.48	12.88	0.85	1.36	0.31		66.83	15.17	15.70	0.73	1.21	0.36
	15	67.35	12.78	17.33	0.93	1.23	0.37		66.21	13.69	17.92	0.63	1.14	0.42
	16.5	66.40	12.43	18.99	0.65	1.14	0.39		67.36	13.84	16.55	0.57	1.23	0.45
	18	66.92	13.59	17.25	0.67	1.14	0.42		68.75	14.93	13.88	0.85	1.24	0.35
	19.5	67.67	17.07	12.45	1.14	1.31	0.36		68.12	17.15	12.36	0.89	1.22	0.26

Meas.	Pos. (nm)	Fe	Cr	Ni	Mn	Mo	Si	Meas.	Fe	Cr	Ni	Mn	Mo	Si
13	21	67.00	17.77	12.40	1.24	1.30	0.29	14	66.80	17.66	13.16	0.91	1.16	0.30
	22.5	67.06	17.56	12.44	1.04	1.62	0.29		66.20	17.03	14.12	1.10	1.22	0.32
	24	66.62	17.53	13.12	1.02	1.45	0.26		65.24	18.11	13.75	1.16	1.41	0.33
	25.5	65.90	17.88	13.12	1.24	1.60	0.25		65.61	18.53	12.86	1.21	1.50	0.28
	27	66.25	16.94	13.90	1.23	1.37	0.31		66.36	17.70	13.07	0.90	1.71	0.26
	28.5	65.48	18.21	13.65	0.95	1.42	0.30		64.57	19.66	12.50	1.31	1.66	0.31
	30	66.06	17.82	13.32	1.20	1.29	0.31		64.63	19.42	12.56	1.30	1.82	0.28
15	0	66.75	18.55	11.61	1.24	1.60	0.25							
	1.5	65.51	18.95	12.57	1.18	1.53	0.26							
	3	64.01	19.40	13.37	1.27	1.70	0.24							
	4.5	64.43	19.83	12.94	0.92	1.64	0.25							
	6	65.00	19.32	12.81	0.96	1.66	0.24							
	7.5	64.81	19.90	11.84	1.50	1.70	0.25							
	9	66.15	19.07	11.60	1.17	1.76	0.25							
	10.5	65.50	19.01	12.16	1.23	1.83	0.26							
	12	67.26	18.44	11.66	0.89	1.45	0.29							
	13.5	67.54	16.64	13.22	0.87	1.50	0.23							
	15	67.10	14.01	16.61	0.71	1.20	0.36							
	16.5	67.35	14.21	16.14	0.71	1.10	0.50							
	18	66.72	16.34	14.72	0.56	1.18	0.48							
	19.5	66.92	18.57	11.94	0.98	1.27	0.31							
	21	65.35	19.06	12.75	1.21	1.38	0.26							
	22.5	66.66	17.22	13.13	1.10	1.60	0.29							
	24	65.86	17.47	13.77	1.21	1.41	0.28							
	25.5	66.60	17.75	13.17	0.80	1.43	0.25							
	27	65.91	17.34	14.06	0.90	1.52	0.28							
	28.5	67.95	17.17	12.21	1.12	1.31	0.24							
	30	66.57	18.03	12.63	0.91	1.58	0.29							

HiHf, 400C, 3 dpa, 2 MeV protons

Meas.	Pos. (nm)	Fe	Cr	Ni	Mn	Mo	Si	Meas.	Fe	Cr	Ni	Mn	Mo	Si
1	0	65.92	20.41	10.82	1.30	1.30	0.25	2	65.41	19.90	11.78	1.24	1.43	0.25
	1.5	64.95	20.42	11.89	1.25	1.19	0.30		65.59	19.69	11.48	1.45	1.54	0.26
	3	64.68	20.61	11.82	1.37	1.28	0.25		65.08	20.00	11.89	1.22	1.54	0.27
	4.5	65.84	19.36	11.60	1.52	1.45	0.23		65.30	19.92	11.86	1.30	1.40	0.23
	6	65.13	20.71	11.63	1.07	1.23	0.23		65.18	20.43	11.61	1.15	1.39	0.24
	7.5	65.61	20.47	11.12	1.17	1.36	0.27		65.96	19.59	11.67	1.18	1.35	0.26
	9	67.33	19.63	10.55	1.14	1.09	0.26		67.05	19.32	11.14	1.19	1.08	0.22
	10.5	68.66	16.51	12.64	0.90	1.05	0.25		68.65	18.71	10.57	0.86	0.99	0.22
	12	67.01	12.93	18.30	0.48	0.93	0.37		67.59	13.83	16.80	0.68	0.75	0.35
	13.5	67.85	13.45	16.62	0.81	1.02	0.24		66.99	13.46	17.65	0.54	1.05	0.31
	15	67.95	16.91	13.11	0.60	1.24	0.19		67.54	18.69	10.94	1.32	1.33	0.18
	16.5	65.83	19.35	12.25	1.08	1.30	0.19		66.27	20.25	10.72	1.05	1.57	0.14
	18	67.27	18.86	11.47	0.85	1.39	0.16		64.71	20.81	11.47	1.36	1.45	0.20
	19.5	66.41	19.48	11.60	0.96	1.39	0.16		66.75	18.31	12.02	1.16	1.61	0.15
	21	65.25	19.42	12.56	1.12	1.44	0.20		65.42	19.64	11.97	1.09	1.68	0.19
	22.5	66.10	19.13	12.41	0.81	1.39	0.15		64.55	19.45	12.70	1.28	1.84	0.18
	24	65.91	18.71	12.13	1.28	1.77	0.20		65.42	19.33	12.15	1.25	1.68	0.17
	25.5	65.68	19.25	12.37	0.86	1.67	0.16		64.77	20.89	11.35	1.16	1.64	0.19
	27	65.45	18.90	12.90	0.91	1.65	0.18		64.79	20.50	11.74	1.04	1.76	0.17
	28.5	65.59	18.43	13.14	1.05	1.59	0.20		65.26	19.76	11.89	1.15	1.75	0.18
	30	66.18	18.59	12.30	1.01	1.72	0.20		63.91	20.19	12.90	1.17	1.67	0.17
3	0	65.75	19.70	11.56	1.32	1.40	0.28	4	65.36	19.90	11.69	1.30	1.46	0.28
	1.5	66.07	19.35	11.71	1.25	1.36	0.26		65.30	19.88	11.97	1.24	1.36	0.23
	3	65.28	20.36	11.67	1.18	1.29	0.22		65.41	18.83	12.68	1.61	1.22	0.25
	4.5	65.36	19.95	11.68	1.29	1.48	0.25		65.56	18.76	12.91	1.46	1.06	0.25
	6	66.58	19.66	11.25	0.99	1.28	0.23		65.82	18.85	12.54	1.27	1.26	0.26
	7.5	66.65	19.09	11.77	1.10	1.18	0.22		66.20	17.89	13.28	1.19	1.17	0.27
	9	66.86	19.02	11.62	1.20	1.08	0.23		66.74	18.19	12.75	0.94	1.13	0.24
	10.5	66.79	19.52	11.65	0.89	0.92	0.23		67.62	18.56	11.33	1.20	1.04	0.24
	12	68.57	17.48	11.85	0.87	1.00	0.24		68.12	16.32	13.64	0.79	0.83	0.30
	13.5	68.55	16.38	13.24	0.58	0.98	0.27		65.55	11.77	20.95	0.46	0.89	0.38
	15	66.28	13.43	18.35	0.54	1.09	0.31		67.68	16.76	13.71	0.53	1.11	0.21
	16.5	68.43	17.25	11.90	1.02	1.23	0.17		66.44	19.51	11.34	1.25	1.31	0.15
	18	66.54	19.52	11.30	1.02	1.45	0.18		66.05	20.25	10.96	1.11	1.49	0.15
	19.5	65.97	20.17	11.14	1.15	1.41	0.15		65.67	19.81	11.68	1.17	1.51	0.16
	21	65.70	20.26	11.45	0.89	1.54	0.17		64.70	19.69	12.33	1.42	1.70	0.16
	22.5	65.27	19.54	12.15	1.22	1.64	0.18		65.59	19.67	11.87	0.96	1.74	0.17
	24	65.65	19.10	12.30	1.07	1.67	0.21		65.14	19.46	12.35	1.17	1.73	0.15
	25.5	65.79	17.70	13.88	0.97	1.49	0.16		65.70	19.78	11.50	1.18	1.66	0.17
	27	66.59	18.19	12.93	0.84	1.26	0.19		65.02	20.07	12.16	1.05	1.55	0.15
	28.5	67.29	17.36	12.78	1.10	1.28	0.18		66.04	19.76	11.18	1.20	1.67	0.16
	30	65.09	20.22	11.63	1.36	1.54	0.16		65.78	19.56	11.37	1.34	1.78	0.17
5	0	65.62	19.74	12.01	1.07	1.27	0.28	6	64.88	20.57	11.73	1.17	1.40	0.24
	1.5	66.55	18.72	11.87	1.40	1.23	0.23		65.07	20.75	11.44	1.16	1.32	0.27
	3	66.36	19.14	12.08	1.11	1.08	0.22		65.24	20.39	11.78	1.03	1.30	0.26
	4.5	66.69	18.82	12.16	1.06	1.03	0.24		65.13	19.46	12.44	1.31	1.38	0.28

Meas.	Pos. (nm)	Fe	Cr	Ni	Mn	Mo	Si	Meas.	Fe	Cr	Ni	Mn	Mo	Si
5	6	67.01	17.98	12.49	1.10	1.16	0.25	6	65.11	19.90	11.97	1.34	1.41	0.27
	7.5	64.36	18.78	14.23	0.99	1.31	0.33		64.95	20.88	10.84	1.50	1.63	0.21
	9	66.24	20.13	11.14	1.11	1.11	0.27		66.28	20.18	11.00	0.90	1.41	0.24
	10.5	66.62	20.59	10.49	0.96	1.09	0.25		67.19	19.61	11.04	0.88	1.04	0.24
	12	68.28	16.48	13.21	0.86	0.89	0.29		68.59	14.72	15.02	0.50	0.83	0.34
	13.5	64.56	12.76	20.78	0.50	1.01	0.39		66.84	13.00	18.39	0.60	0.88	0.30
	15	68.15	17.60	11.99	0.78	1.32	0.17		67.77	19.20	10.70	1.04	1.12	0.17
	16.5	67.88	18.92	10.56	1.08	1.38	0.18		66.25	19.84	11.23	0.99	1.51	0.18
	18	65.92	20.02	11.13	1.26	1.51	0.14		65.98	19.69	11.65	1.06	1.45	0.17
	19.5	65.14	20.30	11.64	1.20	1.57	0.14		65.64	19.75	11.84	1.10	1.51	0.15
	21	65.69	19.30	12.31	1.08	1.47	0.15		65.37	20.33	11.15	1.16	1.80	0.18
	22.5	65.09	19.87	11.94	1.27	1.67	0.16		64.73	20.80	11.43	1.04	1.82	0.18
	24	65.57	20.31	11.34	1.15	1.48	0.15		64.80	19.86	12.13	1.29	1.75	0.16
	25.5	66.63	18.16	11.83	1.55	1.64	0.19		64.98	20.00	11.83	1.29	1.72	0.18
	27	66.17	19.03	11.85	1.29	1.47	0.19		64.46	20.39	12.19	1.04	1.74	0.18
	28.5	65.57	19.50	11.95	1.17	1.65	0.16		65.42	19.14	12.22	1.32	1.71	0.19
	30	65.87	19.31	11.60	1.39	1.67	0.17		65.34	18.27	13.52	1.18	1.52	0.18
7	0	64.85	20.50	11.19	1.75	1.44	0.27	8	65.48	20.36	11.09	1.46	1.31	0.29
	1.5	64.19	21.13	11.57	1.31	1.50	0.30		64.45	20.51	12.19	1.13	1.45	0.27
	3	64.37	20.81	11.49	1.54	1.53	0.26		65.09	20.58	11.57	1.11	1.37	0.28
	4.5	64.39	21.60	11.36	1.15	1.22	0.28		65.06	20.72	11.41	1.29	1.28	0.25
	6	64.97	20.46	11.65	1.38	1.29	0.26		65.23	19.87	12.22	1.16	1.25	0.27
	7.5	65.83	20.38	11.37	0.86	1.28	0.28		64.99	20.09	12.30	1.19	1.14	0.29
	9	65.49	19.91	12.10	1.10	1.11	0.29		66.35	18.91	12.18	1.24	1.06	0.27
	10.5	66.66	19.11	11.83	0.87	1.25	0.28		66.16	19.99	11.39	1.06	1.10	0.30
	12	65.99	15.03	16.73	0.74	1.04	0.47		67.17	16.88	13.91	0.87	0.83	0.34
	13.5	65.16	15.46	17.14	0.71	1.14	0.40		66.04	15.05	16.81	0.71	0.99	0.39
	15	67.31	18.90	11.21	1.27	1.02	0.29		67.06	14.52	16.58	0.45	1.04	0.36
	16.5	66.32	19.89	11.22	1.12	1.12	0.32		67.39	16.29	14.32	0.72	0.94	0.34
	18	66.15	19.70	11.65	1.04	1.17	0.29		67.99	18.45	11.07	1.12	1.09	0.29
	19.5	65.52	20.10	11.72	1.25	1.16	0.25		66.92	19.64	11.17	1.02	0.97	0.29
	21	65.76	19.82	11.62	1.34	1.18	0.27		65.22	20.74	11.56	1.08	1.09	0.31
	22.5	65.72	19.33	12.16	1.31	1.19	0.28		64.83	20.84	11.68	1.22	1.14	0.29
	24	65.71	20.08	11.71	1.09	1.17	0.24		65.13	19.55	12.96	0.99	1.10	0.26
	25.5	66.31	19.07	11.88	1.21	1.27	0.26		65.42	19.12	12.95	0.98	1.25	0.29
	27	64.73	19.47	12.92	1.32	1.29	0.27		65.60	19.13	12.82	1.02	1.20	0.23
	28.5	65.56	19.31	12.37	1.21	1.27	0.28		65.96	19.36	12.36	0.98	1.08	0.24
	30	65.43	20.11	11.94	1.00	1.25	0.27		66.06	18.82	12.27	1.42	1.14	0.30
9	0	65.61	19.73	11.68	1.54	1.15	0.29	10	64.43	21.65	10.79	1.49	1.40	0.25
	1.5	65.41	19.59	12.51	0.88	1.29	0.33		64.43	21.38	11.24	1.17	1.53	0.25
	3	65.03	19.83	12.61	1.08	1.18	0.27		64.28	21.27	11.03	1.68	1.52	0.22
	4.5	65.07	20.07	12.27	1.12	1.21	0.26		63.97	21.67	11.78	1.05	1.26	0.27
	6	65.38	20.19	11.81	1.16	1.19	0.27		65.09	20.95	11.30	1.04	1.39	0.24
	7.5	65.27	20.59	11.49	1.16	1.24	0.24		65.35	20.24	11.54	1.26	1.32	0.28
	9	65.81	20.40	10.95	1.16	1.38	0.29		64.88	20.83	11.49	1.31	1.28	0.22
	10.5	65.42	21.15	10.94	1.09	1.14	0.26		66.97	19.41	11.17	1.17	1.04	0.23
	12	67.40	19.18	11.18	0.84	1.11	0.28		67.10	19.10	11.68	0.87	0.96	0.28

Meas.	Pos. (nm)	Fe	Cr	Ni	Mn	Mo	Si	Meas.	Fe	Cr	Ni	Mn	Mo	Si
9	13.5	66.01	15.52	16.25	0.86	0.95	0.41	10	66.11	16.15	15.88	0.64	0.85	0.37
	15	66.17	13.89	17.90	0.84	0.78	0.42		66.30	14.73	16.79	0.90	0.88	0.40
	16.5	67.38	20.01	10.63	0.66	1.03	0.28		66.37	15.22	16.32	0.71	0.99	0.39
	18	66.61	19.76	11.19	1.06	1.12	0.28		65.99	19.87	11.83	1.01	1.04	0.27
	19.5	67.18	18.71	11.68	0.97	1.19	0.27		65.89	20.30	11.53	0.93	1.08	0.28
	21	66.49	19.38	11.58	1.14	1.17	0.24		64.77	20.90	11.50	1.24	1.32	0.27
	22.5	65.69	19.52	11.91	1.34	1.27	0.26		65.00	20.49	11.91	1.17	1.15	0.27
	24	65.37	20.55	11.23	1.24	1.33	0.28		65.11	20.26	11.82	1.26	1.28	0.27
	25.5	65.68	19.71	11.53	1.48	1.35	0.25		64.82	20.35	12.28	1.02	1.28	0.24
	27	64.70	21.06	11.41	1.20	1.35	0.28		65.53	20.47	11.33	1.19	1.23	0.26
	28.5	65.00	20.41	11.59	1.47	1.26	0.27		64.94	20.57	11.67	1.23	1.32	0.26
	30	65.10	20.69	11.13	1.39	1.38	0.31		64.55	20.59	11.92	1.21	1.48	0.25
11	0	64.78	20.74	11.40	1.43	1.34	0.30	12	65.68	20.27	11.68	1.01	1.12	0.24
	1.5	64.93	20.51	11.68	1.20	1.41	0.27		66.51	19.93	11.00	1.16	1.12	0.26
	3	65.43	20.58	11.23	1.18	1.32	0.25		67.83	18.40	11.73	0.91	0.85	0.28
	4.5	65.67	20.50	11.22	1.16	1.19	0.27		65.06	13.85	19.06	0.90	0.73	0.41
	6	66.13	20.50	10.92	1.06	1.13	0.27		68.30	18.32	11.26	0.82	0.99	0.31
	7.5	66.69	20.34	10.48	1.02	1.22	0.25		66.99	19.11	11.59	1.07	1.01	0.23
	9	67.87	19.34	10.65	0.94	0.91	0.29		65.69	20.43	11.38	0.96	1.27	0.27
	10.5	68.88	18.13	11.19	0.68	0.84	0.28		65.27	19.71	12.41	1.14	1.21	0.27
	12	65.20	13.34	19.44	0.76	0.83	0.42		65.06	19.36	12.99	1.04	1.31	0.25
	13.5	65.26	15.08	17.51	0.87	0.92	0.36							
	15	67.14	18.48	12.36	0.79	0.97	0.25							
	16.5	65.97	20.12	11.25	1.20	1.20	0.28							
	18	66.34	19.92	11.03	1.28	1.18	0.26							
	19.5	65.64	19.96	11.48	1.40	1.26	0.26							
	21	65.37	20.25	11.72	1.08	1.34	0.25							
	22.5	65.68	19.91	11.70	1.19	1.25	0.28							
	24	65.93	19.86	11.12	1.58	1.25	0.25							
	25.5	65.03	20.08	12.24	1.07	1.35	0.23							
	27	65.83	18.94	12.75	1.15	1.09	0.24							
	28.5	65.26	19.09	13.04	1.17	1.17	0.27							
	30	64.53	19.01	14.40	0.82	0.94	0.29							
13	0	65.97	21.11	10.76	0.91	0.99	0.26							
	1.5	68.76	18.00	11.23	0.79	0.95	0.28							
	3	67.25	20.06	10.38	1.05	0.99	0.27							
	4.5	68.41	17.25	12.34	0.80	0.89	0.30							
	6	66.76	14.19	17.26	0.50	0.89	0.40							
	7.5	68.43	16.32	13.06	0.94	0.91	0.35							
	9	68.01	17.27	12.66	0.94	0.85	0.27							
	10.5	65.11	20.68	11.27	1.38	1.30	0.26							
	12	65.43	20.74	11.03	1.31	1.22	0.28							

HiHf, 400C, 7 dpa, 3.2 MeV p+

Meas.	Pos. (nm)	Fe	Cr	Ni	Mn	Mo	Si	Meas.	Fe	Cr	Ni	Mn	Mo	Si
1	0	65.03	19.98	12.17	1.01	1.54	0.27	2	64.96	20.10	12.20	1.02	1.53	0.20
	1.5	65.88	18.87	12.67	1.20	1.14	0.24		66.60	17.97	12.25	1.55	1.42	0.22
	3	66.76	19.13	11.53	1.09	1.23	0.26		65.55	18.98	13.10	1.13	1.07	0.17
	4.5	68.49	17.44	11.27	1.25	1.34	0.21		65.39	19.09	12.58	1.29	1.40	0.25
	6	67.49	18.20	11.76	1.08	1.23	0.24		66.75	17.67	13.07	1.16	1.13	0.23
	7.5	70.19	17.09	10.66	0.86	0.97	0.21		65.76	18.12	13.65	0.87	1.35	0.25
	9	68.55	17.61	11.86	0.72	1.06	0.20		67.20	17.83	12.58	0.91	1.25	0.22
	10.5	72.13	13.83	12.32	0.66	0.81	0.25		70.10	16.69	11.22	0.65	1.11	0.23
	12	59.87	8.15	30.31	0.60	0.59	0.48		71.89	15.40	10.78	0.86	0.84	0.24
	13.5	61.44	8.15	28.85	0.50	0.67	0.39		73.06	11.64	13.71	0.74	0.58	0.26
	15	71.21	13.79	13.24	0.68	0.82	0.27		59.60	7.79	30.92	0.49	0.74	0.46
	16.5	69.11	17.30	11.28	1.01	1.05	0.26		65.77	11.24	21.39	0.60	0.72	0.28
	18	66.18	19.95	11.67	0.83	1.18	0.19		69.86	13.84	14.37	0.91	0.80	0.22
	19.5	66.43	18.93	11.69	1.33	1.39	0.22		68.22	17.74	12.04	0.76	1.01	0.23
	21	66.85	18.68	11.42	1.22	1.57	0.26		68.30	16.61	13.06	0.72	1.10	0.22
	22.5	66.39	18.84	11.63	1.07	1.84	0.22		68.56	15.63	13.78	0.69	1.13	0.21
	24	66.28	19.21	11.31	1.17	1.80	0.22		65.59	17.74	14.30	0.94	1.21	0.22
	25.5	65.58	18.89	12.72	1.15	1.44	0.23		67.68	16.72	13.21	0.93	1.19	0.27
	27	65.79	18.21	12.75	1.38	1.65	0.23		66.70	16.92	13.57	1.22	1.35	0.24
	28.5	64.38	19.50	13.07	1.11	1.72	0.23		65.86	17.28	14.21	1.14	1.29	0.22
	30	63.93	19.34	14.02	1.04	1.41	0.27		65.61	17.48	14.10	1.34	1.20	0.27
3	0	66.49	18.56	12.35	1.05	1.30	0.25	4	65.03	18.87	13.66	0.99	1.16	0.29
	1.5	65.80	19.46	12.12	1.08	1.35	0.18		64.90	19.37	13.09	1.25	1.13	0.26
	3	64.82	19.78	12.57	1.04	1.55	0.24		65.84	18.20	13.30	1.06	1.35	0.26
	4.5	66.22	18.68	12.32	0.96	1.61	0.21		65.57	18.83	13.27	0.90	1.20	0.22
	6	65.50	19.73	12.47	0.83	1.25	0.23		65.92	19.21	12.37	1.14	1.10	0.26
	7.5	64.88	19.10	13.40	1.02	1.36	0.24		67.29	18.30	12.11	0.82	1.22	0.27
	9	66.01	18.74	12.49	1.27	1.29	0.20		66.71	18.30	12.84	0.80	1.15	0.19
	10.5	66.32	18.05	13.40	1.02	0.96	0.25		67.74	18.04	12.24	0.86	0.93	0.19
	12	68.89	16.49	12.96	0.68	0.77	0.21		70.60	16.03	11.69	0.69	0.77	0.21
	13.5	68.17	10.60	19.66	0.53	0.68	0.35		71.83	12.74	13.62	0.86	0.72	0.23
	15	54.87	7.47	35.87	0.58	0.65	0.56		59.66	8.22	30.30	0.74	0.58	0.50
	16.5	69.34	12.16	17.06	0.49	0.70	0.25		63.65	10.66	24.33	0.40	0.63	0.33
	18	69.89	14.90	13.05	0.87	1.02	0.27		67.70	13.39	17.20	0.76	0.73	0.21
	19.5	68.96	16.96	11.80	0.98	1.11	0.19		68.24	16.48	13.12	0.98	0.91	0.26
	21	67.73	19.52	10.61	0.89	1.05	0.20		67.91	16.50	13.46	0.94	0.96	0.22
	22.5	68.93	17.34	10.70	1.34	1.47	0.22		67.20	17.00	13.86	0.49	1.25	0.20
	24	65.51	19.76	12.44	0.77	1.31	0.20		66.43	18.72	12.63	0.99	1.06	0.17
	25.5	64.15	19.42	13.69	0.89	1.61	0.24		65.89	18.39	13.34	0.95	1.22	0.21
	27	65.67	17.85	13.41	1.34	1.51	0.22		65.01	19.00	13.23	1.07	1.46	0.23
	28.5	65.88	19.06	12.34	1.17	1.36	0.20		65.64	18.80	13.00	0.83	1.48	0.25
	30	65.42	18.43	13.25	1.11	1.53	0.26		65.07	18.61	13.10	1.36	1.60	0.25
5	0	64.02	19.35	13.41	1.60	1.41	0.22	6	65.31	17.02	15.11	1.22	1.11	0.24
	1.5	63.81	19.63	13.60	1.04	1.69	0.24		65.41	18.08	14.01	0.96	1.26	0.28
	3	65.08	18.07	14.17	1.04	1.41	0.24		65.55	18.22	13.85	0.99	1.19	0.20
	4.5	64.19	18.25	14.76	1.07	1.50	0.22		64.97	18.04	14.51	0.94	1.36	0.18

Meas.	Pos. (nm)	Fe	Cr	Ni	Mn	Mo	Si	Meas.	Fe	Cr	Ni	Mn	Mo	Si
5	6	67.76	17.61	12.00	1.03	1.36	0.23	6	64.77	19.30	13.52	0.84	1.40	0.18
	7.5	68.13	17.71	11.75	1.00	1.17	0.24		66.32	19.46	11.73	1.21	1.12	0.17
	9	70.26	16.03	11.51	0.91	1.04	0.25		67.44	18.57	11.74	0.96	1.08	0.22
	10.5	71.42	15.81	10.67	1.00	0.85	0.24		67.53	18.33	12.21	0.86	0.88	0.19
	12	71.70	11.57	15.28	0.61	0.61	0.23		70.24	14.00	14.13	0.66	0.70	0.27
	13.5	59.46	7.96	30.99	0.43	0.74	0.42		65.47	11.41	21.87	0.39	0.49	0.37
	15	64.33	10.58	23.42	0.72	0.66	0.30		61.54	9.22	27.64	0.53	0.66	0.42
	16.5	68.44	15.64	13.69	1.09	0.90	0.24		67.34	13.34	17.85	0.56	0.65	0.26
	18	70.32	17.83	10.10	0.76	0.76	0.23		67.50	16.87	13.94	0.45	1.03	0.21
	19.5	68.96	17.20	11.87	0.81	0.96	0.19		66.72	19.06	12.07	1.02	0.90	0.24
	21	67.66	17.02	12.86	1.25	0.97	0.25		67.44	18.29	12.05	0.94	1.07	0.21
	22.5	66.60	18.91	12.17	1.00	1.06	0.26		65.25	19.37	12.80	1.07	1.28	0.23
	24	67.07	18.98	11.26	1.04	1.42	0.23		64.32	20.73	12.50	0.93	1.30	0.21
	25.5	68.36	17.45	11.64	0.86	1.46	0.23		64.23	19.62	13.54	0.92	1.45	0.24
	27	67.58	16.92	12.89	0.90	1.47	0.25		64.41	19.47	13.45	0.86	1.58	0.23
	28.5	67.51	17.55	11.73	1.36	1.61	0.23		63.31	20.62	13.58	0.92	1.34	0.23
	30	66.08	18.83	12.14	1.31	1.40	0.23		64.09	19.51	13.43	1.42	1.30	0.25
7	0	63.91	20.22	13.10	1.07	1.50	0.19	8	65.22	18.64	13.72	0.96	1.25	0.21
	1.5	64.60	18.49	13.55	1.07	2.01	0.28		65.96	19.07	12.51	0.81	1.44	0.22
	3	64.00	20.29	12.98	0.89	1.63	0.21		66.34	18.13	12.71	1.13	1.44	0.25
	4.5	66.45	18.92	11.64	1.03	1.74	0.22		65.89	18.54	12.45	1.62	1.29	0.20
	6	65.63	19.61	12.22	0.82	1.49	0.23		65.95	18.68	12.75	1.14	1.27	0.21
	7.5	66.64	18.30	12.45	0.82	1.59	0.20		66.91	17.68	12.67	1.28	1.26	0.21
	9	67.01	18.57	11.62	1.04	1.52	0.23		67.19	18.33	11.81	1.15	1.31	0.21
	10.5	67.37	17.65	12.22	0.92	1.65	0.19		67.42	17.94	12.24	1.08	1.11	0.20
	12	68.57	18.21	10.83	0.98	1.15	0.25		68.71	15.96	13.06	0.99	1.03	0.24
	13.5	70.74	15.10	12.15	0.80	1.02	0.19		68.67	12.49	17.20	0.47	0.93	0.25
	15	58.86	9.01	30.30	0.54	0.81	0.49		60.46	9.70	28.21	0.59	0.62	0.42
	16.5	67.75	11.07	19.76	0.47	0.70	0.26		60.15	8.67	29.54	0.54	0.65	0.44
	18	70.71	14.46	13.16	0.59	0.83	0.25		70.60	17.05	10.30	0.91	0.89	0.25
	19.5	68.91	16.40	12.29	0.87	1.32	0.21		68.20	17.17	12.42	1.01	1.01	0.19
	21	66.21	17.54	14.03	0.72	1.29	0.21		67.84	17.09	12.57	1.21	1.09	0.19
	22.5	66.50	17.09	13.73	1.22	1.20	0.25		68.31	16.43	12.44	1.03	1.53	0.26
	24	66.65	16.83	14.20	0.96	1.17	0.20		66.74	18.80	11.54	0.96	1.73	0.23
	25.5	66.82	17.28	13.62	0.86	1.21	0.22		64.83	19.29	12.49	1.41	1.74	0.24
	27	66.25	17.48	13.71	1.02	1.36	0.17		65.35	19.44	12.01	1.20	1.80	0.20
	28.5	65.51	18.14	13.90	1.07	1.18	0.18		66.02	18.81	11.95	1.12	1.89	0.22
	30	66.71	17.25	13.42	1.41	1.02	0.19		65.66	19.96	11.39	1.06	1.73	0.20
9	0	66.42	18.23	13.67	0.76	0.68	0.24	10	65.17	17.81	14.73	0.85	1.15	0.29
	1.5	66.62	18.69	12.50	0.92	1.08	0.19		65.55	18.24	13.62	1.06	1.31	0.21
	3	66.80	19.00	11.82	0.80	1.36	0.21		65.52	18.04	13.60	1.21	1.37	0.26
	4.5	66.93	19.27	11.44	0.51	1.61	0.24		65.58	19.09	12.33	1.19	1.58	0.23
	6	66.91	17.68	12.79	0.73	1.65	0.23		66.59	18.17	12.85	0.87	1.30	0.22
	7.5	67.35	18.83	11.25	0.88	1.44	0.25		67.43	17.04	12.90	1.01	1.42	0.21
	9	68.29	19.48	9.94	0.91	1.17	0.21		68.00	17.44	11.88	1.05	1.41	0.21
	10.5	67.00	20.07	11.11	0.54	1.07	0.21		67.50	18.26	11.77	0.88	1.35	0.24
	12	68.49	18.00	11.63	0.78	0.87	0.23		68.53	17.18	12.08	0.72	1.26	0.22

Meas.	Pos. (nm)	Fe	Cr	Ni	Mn	Mo	Si	Meas.	Fe	Cr	Ni	Mn	Mo	Si
9	13.5	69.23	17.81	11.30	0.70	0.75	0.21	10	69.65	16.56	11.41	0.78	1.37	0.23
	15	71.25	14.13	13.35	0.65	0.41	0.22		66.37	11.30	20.44	0.50	1.08	0.30
	16.5	61.58	9.60	28.01	0.15	0.24	0.42		61.45	8.58	28.17	0.56	0.80	0.44
	18	66.39	11.64	21.00	0.39	0.26	0.31		71.27	12.87	14.36	0.49	0.78	0.25
	19.5	70.78	17.48	10.61	0.50	0.40	0.22		69.67	16.38	12.00	0.79	0.97	0.19
	21	69.11	18.29	11.21	0.68	0.49	0.22		68.31	18.24	11.01	0.97	1.27	0.20
	22.5	67.84	18.38	11.93	1.01	0.64	0.20		68.19	18.09	11.00	1.03	1.48	0.22
	24	66.40	19.92	11.45	0.96	1.04	0.23		66.24	19.18	11.56	1.21	1.57	0.24
	25.5	66.55	19.40	11.94	0.83	1.07	0.21		66.04	18.61	12.26	1.25	1.60	0.24
	27	66.56	19.20	12.24	0.84	0.96	0.20		66.13	18.50	11.85	1.21	2.09	0.22
	28.5	65.52	19.77	12.44	0.79	1.27	0.21		66.27	18.04	12.31	1.37	1.78	0.23
	30	65.37	19.74	12.69	0.92	1.06	0.21		65.82	18.52	13.01	0.78	1.63	0.24
11	0	64.65	19.30	13.48	1.19	1.16	0.22	12	65.11	17.51	14.71	1.07	1.33	0.26
	1.5	66.39	17.14	14.11	0.82	1.33	0.21		65.56	18.84	13.30	0.88	1.22	0.19
	3	66.83	16.82	13.85	1.01	1.24	0.25		66.57	17.44	13.09	1.06	1.64	0.20
	4.5	67.02	17.29	13.43	0.84	1.18	0.23		65.85	18.96	12.76	0.96	1.25	0.22
	6	66.91	17.92	12.84	0.96	1.15	0.21		65.70	19.32	12.34	1.09	1.34	0.21
	7.5	66.64	18.12	12.84	0.90	1.32	0.19		66.08	18.46	12.81	0.91	1.49	0.25
	9	68.19	16.65	12.38	1.26	1.32	0.21		66.33	18.53	12.58	0.76	1.61	0.20
	10.5	67.43	17.11	12.79	1.14	1.31	0.22		67.26	17.28	12.88	0.97	1.38	0.22
	12	68.93	17.29	11.39	0.96	1.18	0.25		68.90	16.42	12.14	0.95	1.34	0.25
	13.5	71.21	15.50	10.94	1.03	1.10	0.22		69.27	13.46	15.07	0.80	1.17	0.23
	15	69.14	13.31	15.74	0.66	0.88	0.26		60.79	8.92	28.11	0.78	1.02	0.38
	16.5	61.60	9.04	27.71	0.52	0.80	0.33		69.34	11.89	17.24	0.55	0.75	0.23
	18	67.79	11.39	19.35	0.46	0.76	0.25		69.31	16.06	12.30	0.98	1.11	0.25
	19.5	69.72	16.16	11.85	1.01	1.05	0.21		69.14	17.19	11.46	0.78	1.20	0.23
	21	67.15	19.24	11.37	0.91	1.11	0.21		67.98	18.24	11.27	1.02	1.30	0.21
	22.5	66.77	19.35	11.14	1.01	1.52	0.21		68.48	17.47	11.44	0.74	1.63	0.24
	24	66.04	18.74	12.27	1.11	1.63	0.20		66.97	17.42	12.88	1.08	1.42	0.23
	25.5	65.11	19.71	12.05	1.10	1.80	0.23		67.56	18.00	11.73	1.01	1.50	0.21
	27	65.08	19.72	11.50	1.48	2.00	0.23		68.30	17.37	11.61	0.91	1.60	0.21
	28.5	64.86	19.32	12.67	1.01	1.92	0.22		67.58	17.41	12.48	0.86	1.41	0.26
	30	65.03	19.20	12.51	1.10	1.94	0.21		66.00	17.63	13.28	1.23	1.66	0.20

HiHf, 400C, 7 dpa, 2 MeV p+

Meas.	Pos. (nm)	Fe	Cr	Ni	Mn	Mo	Si	Meas.	Fe	Cr	Ni	Mn	Mo	Si
1	0	66.08	19.39	11.80	1.18	1.37	0.18	2	65.03	19.47	12.77	1.02	1.51	0.21
	1.5	66.07	19.58	11.74	1.07	1.38	0.16		64.63	19.25	13.23	1.13	1.56	0.20
	3	66.26	19.49	11.69	1.11	1.27	0.19		65.05	19.79	12.24	1.13	1.56	0.22
	4.5	66.65	19.87	10.89	1.18	1.21	0.20		65.52	20.93	10.66	1.24	1.43	0.22
	6	67.37	19.51	10.71	0.96	1.27	0.18		66.60	20.07	10.62	1.07	1.46	0.17
	7.5	67.76	19.08	10.65	1.02	1.28	0.20		67.20	19.92	10.23	1.09	1.38	0.19
	9	70.08	18.03	9.70	0.73	1.25	0.21		68.12	19.21	10.01	1.12	1.34	0.19
	10.5	69.79	17.58	10.37	0.97	1.05	0.23		68.79	19.12	9.71	0.93	1.25	0.19
	12	66.96	12.87	18.18	0.73	0.88	0.38		68.58	14.49	15.23	0.58	0.86	0.25
	13.5	64.11	11.08	23.12	0.58	0.74	0.37		62.28	10.74	25.14	0.62	0.80	0.42
	15	67.19	13.29	17.80	0.70	0.71	0.31		61.33	10.59	26.25	0.59	0.78	0.45
	16.5	68.63	18.99	10.10	1.01	1.07	0.20		62.70	11.40	24.14	0.66	0.72	0.38
	18	68.02	19.41	10.18	1.02	1.16	0.21		69.53	17.10	11.47	0.62	1.00	0.26
	19.5	65.51	20.20	11.65	1.20	1.24	0.20		68.37	19.04	10.61	0.72	1.03	0.22
	21	66.00	19.34	11.97	1.19	1.29	0.21		68.24	19.32	10.25	0.97	1.03	0.19
	22.5	65.33	19.55	12.38	1.22	1.31	0.20		66.89	19.09	11.70	0.87	1.26	0.20
	24	65.41	19.95	11.93	1.21	1.31	0.19		64.99	19.41	13.20	0.79	1.39	0.22
	25.5	64.98	19.68	12.91	0.96	1.27	0.20		65.87	19.82	11.99	0.95	1.18	0.19
	27	65.31	19.46	12.60	0.96	1.46	0.20		64.39	20.62	12.42	0.95	1.39	0.22
	28.5	65.51	19.47	12.06	1.41	1.35	0.19		65.77	20.46	11.20	1.12	1.25	0.20
	30	65.27	20.06	12.17	1.01	1.27	0.22		64.58	19.23	13.46	0.98	1.49	0.26
3	0	65.35	20.07	11.60	1.11	1.71	0.15	4	64.98	19.68	12.52	1.08	1.52	0.22
	1.5	65.50	20.44	11.31	1.14	1.42	0.18		65.71	19.31	11.88	1.28	1.58	0.24
	3	65.84	20.28	10.98	1.15	1.58	0.17		64.98	20.15	11.86	1.19	1.59	0.24
	4.5	65.31	21.00	11.09	0.91	1.49	0.21		65.30	19.85	11.82	1.24	1.55	0.25
	6	66.37	19.88	10.71	1.48	1.37	0.19		64.84	18.82	13.24	1.35	1.51	0.23
	7.5	66.64	20.34	10.68	1.00	1.16	0.18		64.97	19.66	12.66	0.96	1.50	0.25
	9	67.62	18.98	10.95	0.99	1.28	0.18		64.31	19.57	13.37	1.13	1.42	0.19
	10.5	68.47	18.93	10.33	0.97	1.12	0.18		66.87	18.17	12.16	1.26	1.29	0.25
	12	70.59	17.81	9.54	0.79	1.08	0.19		67.58	19.30	10.45	1.05	1.41	0.21
	13.5	68.93	14.22	14.88	0.80	0.91	0.25		68.50	18.63	10.35	0.92	1.43	0.18
	15	65.14	12.56	20.45	0.71	0.82	0.33		68.53	18.64	10.32	1.03	1.26	0.23
	16.5	64.45	11.30	22.35	0.76	0.80	0.34		68.63	15.22	14.14	0.78	0.99	0.25
	18	69.52	15.22	13.13	0.91	1.00	0.22		65.81	13.02	19.54	0.44	0.81	0.38
	19.5	68.89	18.10	10.68	1.02	1.10	0.21		67.11	17.52	12.73	1.19	1.27	0.18
	21	67.72	18.92	11.00	0.93	1.24	0.20		67.03	18.74	11.87	0.78	1.36	0.22
	22.5	67.11	19.10	11.16	1.13	1.29	0.21		65.11	18.26	14.15	0.80	1.50	0.17
	24	66.45	19.59	11.72	0.84	1.20	0.21		66.06	18.25	13.24	0.81	1.38	0.26
	25.5	65.18	20.25	11.99	1.14	1.25	0.19		65.26	19.43	13.03	0.77	1.32	0.18
	27	65.29	20.06	11.74	1.36	1.35	0.21		65.79	19.76	11.70	1.14	1.39	0.22
	28.5	65.28	19.88	12.13	1.18	1.35	0.18		66.64	18.80	12.08	0.99	1.31	0.17
	30	66.97	18.49	11.79	1.23	1.31	0.21		65.62	19.41	12.30	1.00	1.47	0.21
5	0	63.44	21.23	12.47	1.07	1.56	0.22	6	66.07	20.26	11.00	1.01	1.48	0.18
	1.5	64.22	20.53	12.11	1.27	1.63	0.24		65.11	20.46	11.58	1.17	1.50	0.19
	3	62.85	21.88	12.46	1.00	1.59	0.21		65.85	20.00	11.30	1.06	1.58	0.21
	4.5	66.16	19.41	11.76	1.12	1.36	0.19		64.75	20.43	11.83	1.20	1.58	0.21

Meas.	Pos. (nm)	Fe	Cr	Ni	Mn	Mo	Si	Meas.	Fe	Cr	Ni	Mn	Mo	Si
5	6	64.93	21.04	11.19	1.03	1.59	0.23	6	65.29	20.33	11.65	1.05	1.47	0.21
	7.5	64.27	21.18	11.77	1.06	1.47	0.26		66.31	19.86	11.13	1.07	1.46	0.18
	9	65.22	20.81	11.47	0.82	1.47	0.21		67.37	19.43	10.63	1.04	1.35	0.18
	10.5	66.77	19.22	11.58	0.87	1.33	0.24		68.35	18.35	10.45	1.24	1.40	0.21
	12	68.10	19.89	9.64	1.12	1.03	0.21		69.13	18.54	10.17	0.79	1.19	0.18
	13.5	68.22	15.93	13.84	0.84	0.89	0.28		69.93	14.42	13.56	0.80	1.05	0.24
	15	65.72	14.19	18.06	0.79	0.86	0.38		65.84	11.93	20.48	0.62	0.80	0.33
	16.5	64.14	11.51	22.21	0.77	0.95	0.42		67.95	13.51	16.58	0.83	0.83	0.31
	18	69.59	17.04	11.44	0.68	1.03	0.22		69.29	17.44	11.07	0.78	1.16	0.25
	19.5	66.79	19.61	11.47	0.85	1.11	0.17		67.96	18.71	10.85	1.01	1.26	0.21
	21	66.26	20.02	11.02	1.29	1.22	0.19		66.32	19.84	11.43	0.96	1.24	0.21
	22.5	65.06	21.04	11.01	1.21	1.41	0.27		66.43	19.42	11.74	1.06	1.16	0.19
	24	65.66	19.98	11.96	0.95	1.22	0.23		66.34	19.40	11.64	1.05	1.33	0.24
	25.5	65.25	19.86	12.13	0.89	1.65	0.21		66.66	19.46	11.64	0.78	1.24	0.22
	27	65.07	19.77	13.07	0.60	1.28	0.21		65.13	18.93	13.29	1.09	1.32	0.23
	28.5	65.00	19.90	12.82	0.86	1.27	0.16		66.16	18.49	12.76	1.21	1.16	0.21
	30	66.38	18.55	12.85	0.75	1.31	0.17		65.86	18.37	13.20	0.89	1.46	0.21
7	0	65.74	19.55	11.88	1.28	1.37	0.17	8	64.61	18.68	14.23	0.80	1.49	0.19
	1.5	65.50	19.86	12.03	1.08	1.34	0.20		65.69	19.05	12.39	1.21	1.47	0.19
	3	65.38	19.87	12.08	1.15	1.31	0.20		66.25	19.22	11.86	1.02	1.45	0.21
	4.5	66.94	20.18	10.42	0.88	1.36	0.21		65.86	19.04	12.24	1.16	1.50	0.20
	6	67.06	19.31	11.03	1.11	1.34	0.15		65.60	19.52	12.25	1.16	1.23	0.24
	7.5	67.90	19.17	10.29	1.17	1.28	0.19		65.02	20.03	12.14	1.22	1.39	0.20
	9	68.05	19.11	10.51	1.06	1.10	0.17		65.83	19.97	11.66	0.91	1.41	0.22
	10.5	69.44	18.23	9.94	0.96	1.23	0.21		66.07	20.07	11.27	1.00	1.36	0.23
	12	70.22	16.24	11.48	0.89	0.96	0.21		66.33	19.55	11.53	1.10	1.27	0.21
	13.5	69.11	13.38	15.51	0.79	0.96	0.25		67.05	19.60	10.88	0.91	1.38	0.20
	15	62.54	10.91	24.72	0.64	0.79	0.40		68.13	19.03	10.45	0.91	1.27	0.20
	16.5	65.73	13.43	18.85	0.79	0.90	0.29		68.94	17.53	11.23	0.89	1.21	0.19
	18	68.89	17.68	11.14	0.97	1.11	0.21		69.20	13.99	14.81	0.67	1.06	0.26
	19.5	67.41	18.91	11.12	1.09	1.30	0.17		67.01	12.62	18.51	0.68	0.84	0.33
	21	66.99	19.22	11.52	0.73	1.35	0.19		64.32	11.71	22.21	0.57	0.83	0.36
	22.5	65.51	20.41	11.66	0.98	1.25	0.19		64.25	12.68	21.18	0.68	0.88	0.32
	24	65.49	20.05	11.56	1.34	1.36	0.20		69.41	16.63	12.20	0.63	0.93	0.20
	25.5	65.71	19.90	11.95	0.93	1.27	0.22		65.96	13.19	18.82	0.81	0.88	0.34
	27	65.64	19.95	11.87	1.02	1.33	0.19		68.52	18.85	10.42	0.94	1.13	0.15
	28.5	64.86	19.89	12.43	1.13	1.49	0.20		67.84	18.99	10.48	1.16	1.33	0.19
	30	64.64	18.87	13.64	1.10	1.53	0.22		66.61	20.10	10.66	1.11	1.32	0.19

HiHf, 400C, 10 dpa

Meas.	Pos. (nm)	Fe	Cr	Ni	Mn	Mo	Si	Meas.	Fe	Cr	Ni	Mn	Mo	Si
1	0	65.66	18.03	13.40	1.19	1.50	0.21	2	65.41	19.29	12.70	0.82	1.52	0.26
	1.5	65.70	18.21	13.39	0.97	1.49	0.23		65.37	18.33	13.73	0.93	1.44	0.20
	3	64.33	19.17	13.64	1.02	1.58	0.26		65.70	17.55	13.98	0.99	1.50	0.27
	4.5	65.17	18.06	13.99	1.08	1.49	0.21		65.24	18.26	14.16	0.74	1.34	0.27
	6	65.31	19.11	12.97	0.98	1.40	0.23		66.83	17.62	13.07	0.92	1.35	0.22
	7.5	65.69	19.73	11.82	1.07	1.48	0.21		68.90	15.53	13.34	0.79	1.18	0.26
	9	66.41	19.48	11.62	0.79	1.48	0.22		66.62	12.72	18.78	0.58	0.96	0.34
	10.5	68.05	18.16	11.47	0.74	1.35	0.22		64.38	11.87	21.91	0.53	0.93	0.38
	12	68.58	14.82	14.55	0.67	1.09	0.29		68.23	13.93	15.61	0.93	0.96	0.33
	13.5	64.10	10.71	23.47	0.51	0.84	0.37		69.06	17.14	11.69	0.80	1.05	0.26
	15	64.55	12.40	21.37	0.47	0.81	0.40		68.28	17.71	11.42	1.14	1.21	0.25
	16.5	69.52	15.45	13.26	0.60	0.89	0.28		67.32	19.21	11.28	0.86	1.11	0.22
	18	69.47	17.53	10.86	0.89	0.99	0.25		66.82	18.42	12.27	0.98	1.27	0.24
	19.5	67.55	18.40	11.36	1.23	1.19	0.26		66.48	18.42	12.45	1.16	1.25	0.24
	21	66.11	19.45	12.13	0.93	1.11	0.25		65.96	18.05	13.31	1.06	1.34	0.29
	22.5	66.36	18.66	12.34	1.12	1.29	0.23		65.00	18.72	13.66	0.98	1.39	0.25
	24	65.66	19.05	12.85	0.96	1.24	0.25		65.79	17.83	13.64	1.14	1.32	0.28
	25.5	65.55	18.72	12.95	1.29	1.25	0.24		65.20	18.85	13.27	1.00	1.40	0.28
	27	65.88	18.86	12.82	0.91	1.24	0.29		66.32	18.21	12.87	1.04	1.27	0.29
	28.5	65.96	18.65	13.06	0.94	1.19	0.20		66.42	18.63	12.40	0.93	1.38	0.23
	30	65.23	18.60	13.51	1.09	1.32	0.24		65.46	18.31	13.40	1.33	1.26	0.24
3	0	65.41	18.43	13.24	1.20	1.47	0.25	4	64.99	17.79	14.26	1.06	1.65	0.25
	1.5	65.04	18.49	13.76	1.03	1.44	0.24		64.17	18.46	14.39	1.08	1.65	0.25
	3	65.45	18.56	13.27	1.00	1.51	0.21		64.54	18.53	14.05	1.08	1.56	0.23
	4.5	65.79	18.78	12.68	1.03	1.51	0.21		65.05	18.95	13.15	1.15	1.47	0.22
	6	65.02	19.49	12.53	1.20	1.53	0.23		65.36	19.05	12.66	1.12	1.57	0.25
	7.5	66.51	19.31	11.62	0.93	1.39	0.24		65.76	18.61	12.80	1.15	1.43	0.24
	9	66.07	19.26	11.88	1.15	1.40	0.24		65.95	18.67	12.54	1.16	1.45	0.22
	10.5	67.14	18.79	11.40	1.17	1.28	0.23		66.57	18.88	11.76	1.20	1.41	0.19
	12	67.11	14.59	16.21	0.60	1.20	0.29		67.12	18.26	12.17	0.89	1.31	0.26
	13.5	64.58	12.40	21.08	0.63	0.94	0.37		67.51	14.92	15.27	0.88	1.14	0.28
	15	65.00	12.83	20.57	0.46	0.78	0.36		63.17	11.78	23.39	0.46	0.81	0.40
	16.5	68.35	13.73	15.97	0.73	0.91	0.30		66.10	12.23	20.07	0.42	0.84	0.34
	18	68.56	17.49	11.65	0.94	1.15	0.21		69.92	15.97	12.23	0.71	0.92	0.25
	19.5	67.62	17.89	11.89	1.27	1.09	0.24		68.60	17.57	11.60	0.90	1.07	0.25
	21	66.91	19.04	11.72	0.91	1.21	0.21		67.93	18.25	11.44	1.01	1.16	0.21
	22.5	65.90	19.08	12.64	0.91	1.21	0.25		66.95	18.58	11.89	1.11	1.24	0.22
	24	65.51	18.78	12.92	1.17	1.32	0.30		67.11	17.94	12.44	0.93	1.32	0.27
	25.5	65.77	18.79	12.69	1.08	1.42	0.25		66.50	18.36	12.33	1.33	1.22	0.26
	27	65.62	18.61	13.12	1.16	1.23	0.26		65.44	19.44	12.52	0.97	1.37	0.26
	28.5	65.22	18.88	13.27	1.10	1.26	0.26		65.60	18.72	12.69	1.33	1.41	0.26
	30	65.90	18.08	13.43	0.93	1.39	0.27		65.66	18.88	12.82	1.08	1.33	0.24
5	0	65.30	19.22	12.74	0.88	1.62	0.23	6	65.63	17.86	13.55	1.11	1.63	0.23
	1.5	65.17	18.91	12.99	1.11	1.60	0.22		65.20	17.78	14.09	1.15	1.53	0.25
	3	65.42	19.23	12.65	1.04	1.41	0.25		65.37	18.34	13.38	1.12	1.54	0.25
	4.5	65.36	19.25	12.14	1.37	1.65	0.21		65.50	19.00	12.78	0.98	1.50	0.23

Meas.	Pos. (nm)	Fe	Cr	Ni	Mn	Mo	Si	Meas.	Fe	Cr	Ni	Mn	Mo	Si
5	6	65.47	19.11	12.41	1.32	1.48	0.21	6	66.25	18.82	11.79	1.40	1.50	0.24
	7.5	65.83	19.62	11.80	1.03	1.49	0.23		66.02	18.85	12.25	0.97	1.66	0.25
	9	67.52	19.11	10.82	0.83	1.49	0.23		66.71	18.58	12.02	1.07	1.41	0.22
	10.5	67.59	17.40	12.51	0.88	1.36	0.26		67.07	18.80	11.36	1.06	1.47	0.24
	12	65.78	13.50	18.64	0.66	1.09	0.33		67.65	17.65	12.31	0.89	1.28	0.22
	13.5	63.55	11.75	23.26	0.27	0.80	0.38		66.87	14.13	16.93	0.66	1.08	0.33
	15	67.13	14.40	16.75	0.53	0.90	0.28		63.55	11.65	23.22	0.43	0.71	0.43
	16.5	69.10	17.19	11.41	0.90	1.17	0.23		67.54	13.07	17.59	0.71	0.77	0.32
	18	67.64	18.42	11.68	0.90	1.12	0.24		69.12	16.90	11.79	0.85	1.06	0.28
	19.5	67.09	18.77	11.76	0.81	1.30	0.27		68.27	17.08	12.20	1.10	1.08	0.27
	21	65.96	18.69	12.66	1.10	1.35	0.24		67.17	18.53	11.92	0.93	1.21	0.24
	22.5	65.32	18.88	13.05	1.10	1.39	0.26		66.69	18.24	12.34	1.21	1.23	0.29
	24	66.52	18.08	12.67	1.12	1.34	0.28		66.49	18.44	12.36	1.14	1.33	0.24
	25.5	65.78	18.90	13.16	0.74	1.18	0.24		65.79	18.91	12.70	1.02	1.34	0.24
	27	65.67	18.61	13.11	1.07	1.31	0.23		66.49	18.23	12.55	1.21	1.30	0.22
	28.5	66.18	18.36	12.89	1.12	1.21	0.24		65.99	18.62	12.64	1.16	1.33	0.27
	30	64.57	18.60	13.95	1.06	1.55	0.26		66.81	17.87	12.39	1.26	1.38	0.28
7	0	65.47	18.61	13.23	1.09	1.41	0.19	8	65.73	19.26	12.30	1.17	1.33	0.22
	1.5	65.75	18.61	12.95	1.12	1.37	0.20		65.71	19.18	12.34	1.12	1.44	0.20
	3	65.64	19.09	12.56	1.17	1.35	0.20		65.52	19.30	12.50	1.12	1.34	0.22
	4.5	66.60	18.26	12.51	1.04	1.40	0.20		66.64	18.93	11.66	1.19	1.37	0.21
	6	66.25	18.82	12.26	1.10	1.40	0.18		66.27	18.64	12.29	1.16	1.44	0.20
	7.5	66.71	18.52	12.37	1.04	1.16	0.21		67.18	18.67	11.77	0.88	1.31	0.20
	9	67.47	18.00	12.12	0.94	1.24	0.23		67.42	18.48	11.68	0.97	1.21	0.23
	10.5	68.02	17.21	12.69	0.68	1.16	0.23		68.04	16.70	13.09	0.78	1.14	0.25
	12	67.62	15.43	14.87	0.77	1.04	0.27		66.64	13.71	17.81	0.68	0.86	0.30
	13.5	64.40	12.99	20.94	0.44	0.83	0.40		65.22	12.95	19.90	0.73	0.84	0.36
	15	65.90	13.75	18.57	0.60	0.86	0.32		67.00	15.73	15.16	0.92	0.89	0.30
	16.5	67.80	16.07	13.82	1.01	1.06	0.25		67.63	17.02	13.21	0.96	0.94	0.24
	18	67.87	17.34	12.42	1.11	1.03	0.23		67.01	18.04	12.39	1.23	1.10	0.23
	19.5	66.43	18.27	12.81	1.10	1.15	0.24		66.48	18.89	11.95	1.19	1.25	0.24
	21	66.10	18.61	12.97	0.86	1.24	0.22		65.76	18.92	12.85	1.04	1.20	0.23
	22.5	65.75	18.67	13.05	0.93	1.37	0.23		66.29	18.77	12.48	0.89	1.34	0.23
	24	65.63	18.40	13.33	1.24	1.20	0.20		65.36	18.82	13.26	0.99	1.36	0.22
	25.5	66.30	18.68	12.53	0.99	1.25	0.25		65.25	18.29	13.77	1.05	1.40	0.24
	27	65.87	18.37	13.28	1.04	1.21	0.23		65.78	18.04	13.72	1.03	1.17	0.25
	28.5	65.70	18.71	12.96	1.10	1.31	0.23		65.35	18.81	13.38	1.03	1.20	0.23
	30	65.40	18.80	13.21	1.17	1.22	0.21		65.76	17.71	13.93	1.08	1.30	0.22
9	0	66.11	17.81	13.46	1.12	1.29	0.22	10	65.63	18.26	13.33	1.21	1.37	0.21
	1.5	65.52	18.54	13.22	1.10	1.39	0.23		64.84	19.13	13.14	1.27	1.41	0.21
	3	65.46	18.46	13.45	1.02	1.38	0.21		65.74	18.88	12.63	1.14	1.42	0.19
	4.5	65.98	18.72	12.92	0.81	1.36	0.21		65.86	18.81	12.58	1.18	1.35	0.22
	6	65.79	18.82	12.79	1.00	1.40	0.19		66.07	19.05	12.10	1.19	1.38	0.21
	7.5	66.32	18.69	12.45	0.94	1.40	0.20		66.77	18.48	12.11	1.14	1.28	0.21
	9	66.57	19.08	11.70	1.13	1.31	0.20		67.32	18.39	11.85	1.05	1.18	0.22
	10.5	67.18	18.41	11.77	1.15	1.29	0.21		68.08	17.59	12.19	0.79	1.13	0.22
	12	67.73	17.47	12.38	1.09	1.13	0.21		67.66	15.18	15.19	0.79	0.91	0.26

Meas.	Pos. (nm)	Fe	Cr	Ni	Mn	Mo	Si	Meas.	Fe	Cr	Ni	Mn	Mo	Si
9	13.5	67.58	16.53	13.80	0.77	1.06	0.27	10	64.72	12.88	20.58	0.62	0.83	0.37
	15	65.22	13.45	19.58	0.48	0.91	0.35		66.36	14.05	17.74	0.64	0.90	0.32
	16.5	64.98	13.14	20.05	0.64	0.86	0.33		67.88	16.47	13.32	0.99	1.08	0.26
	18	66.09	14.07	17.80	0.83	0.89	0.32		66.52	18.25	12.80	1.00	1.22	0.21
	19.5	67.75	16.50	13.43	0.95	1.12	0.25		66.97	18.67	11.82	1.06	1.25	0.24
	21	67.36	17.66	12.52	1.11	1.11	0.25		66.28	18.97	12.17	1.10	1.26	0.22
	22.5	66.48	18.77	12.16	1.08	1.28	0.23		65.62	18.98	12.75	1.14	1.26	0.24
	24	66.57	18.69	12.27	1.05	1.20	0.22		65.84	18.40	13.13	1.17	1.23	0.23
	25.5	65.90	19.03	12.46	1.17	1.21	0.22		65.83	18.64	12.95	1.10	1.23	0.24
	27	65.78	18.74	12.79	1.21	1.26	0.22		65.70	18.33	13.55	0.91	1.27	0.23
	28.5	65.71	19.15	12.79	0.87	1.26	0.21		65.14	19.44	13.04	0.90	1.23	0.23
	30								65.68	18.18	13.59	1.10	1.21	0.24
11	0	65.90	18.92	12.52	1.11	1.34	0.20	12	65.92	18.29	13.21	1.02	1.35	0.21
	1.5	65.70	18.79	13.02	1.06	1.23	0.19		65.80	18.25	13.33	0.99	1.43	0.21
	3	65.84	19.07	12.74	0.89	1.26	0.19		65.46	18.15	13.85	0.97	1.35	0.22
	4.5	66.44	18.66	12.29	1.23	1.15	0.23		65.35	18.31	13.65	1.20	1.26	0.23
	6	66.05	18.45	12.78	1.20	1.32	0.20		65.91	18.23	13.31	1.01	1.31	0.24
	7.5	66.80	18.63	12.26	0.87	1.24	0.21		65.96	18.02	13.38	1.14	1.29	0.20
	9	67.33	18.04	12.18	1.03	1.19	0.23		67.13	18.31	12.19	0.99	1.16	0.22
	10.5	68.14	16.79	12.76	0.98	1.08	0.24		67.57	17.41	13.10	0.70	0.97	0.25
	12	66.87	14.72	16.39	0.72	0.98	0.31		66.84	15.68	15.49	0.68	1.04	0.27
	13.5	65.03	13.63	19.45	0.66	0.88	0.36		65.16	13.69	19.35	0.62	0.86	0.33
	15	66.50	15.57	15.98	0.84	0.85	0.27		65.81	14.50	17.71	0.76	0.91	0.31
	16.5	67.53	18.08	12.05	1.02	1.09	0.24		67.54	17.02	13.36	0.81	1.02	0.24
	18	66.19	18.90	12.41	1.00	1.26	0.23		67.47	17.54	12.75	0.87	1.10	0.27
	19.5	65.81	19.29	12.34	1.11	1.21	0.24		66.83	18.51	12.33	0.95	1.16	0.22
	21	65.90	18.70	12.67	1.25	1.23	0.25		66.34	18.54	12.73	1.02	1.17	0.21
	22.5	66.13	18.57	12.82	1.07	1.19	0.21		65.81	18.79	12.89	1.03	1.21	0.26
	24	66.39	18.62	12.28	1.22	1.27	0.22		66.02	18.28	13.15	1.14	1.19	0.22
	25.5	66.13	18.46	12.84	1.11	1.24	0.21		63.90	19.16	14.24	1.09	1.36	0.25
	27	65.78	18.61	13.05	1.02	1.26	0.27		65.02	18.02	14.39	1.06	1.27	0.24
	28.5	66.35	18.29	12.81	1.07	1.25	0.23		65.01	18.13	14.11	1.08	1.42	0.25
	30	65.31	18.64	13.48	1.03	1.30	0.24		65.56	18.52	13.15	1.18	1.36	0.23

Ref-Zr, 500C, 1 dpa

Meas.	Pos. (nm)	Fe	Cr	Ni	Mn	Si	Zr	Meas.	Fe	Cr	Ni	Mn	Si	Zr
1	0	73.20	12.23	12.78	0.88	0.91	0.00	2	73.88	11.39	12.56	1.12	1.05	0.00
	1.5	74.27	11.06	12.87	0.88	0.93	0.00		73.46	11.60	12.71	1.23	1.00	0.00
	3	74.96	9.71	13.55	0.91	0.87	0.00		73.36	11.47	13.50	0.63	1.05	0.00
	4.5	73.25	9.64	15.64	0.74	0.72	0.00		73.72	9.96	14.53	0.88	0.90	0.00
	6	70.93	8.09	19.63	0.60	0.75	0.00		72.86	9.48	16.07	0.61	0.97	0.00
	7.5	67.68	7.31	23.38	0.86	0.77	0.00		72.27	8.95	17.15	0.72	0.91	0.00
	9	64.15	7.44	26.52	0.95	0.93	0.00		66.47	7.52	24.28	0.69	1.05	0.00
	10.5	61.51	7.06	29.72	0.77	0.94	0.00		64.22	7.12	26.49	0.86	1.31	0.00
	12	62.79	6.70	28.75	0.69	1.08	0.00		61.43	6.42	29.26	0.66	2.23	0.00
	13.5	63.82	7.24	27.00	0.58	1.37	0.00		60.88	6.60	29.06	0.90	2.57	0.00
	15	68.90	9.40	18.48	0.87	2.35	0.00		65.25	7.29	24.28	0.58	2.59	0.00
	16.5	71.91	11.25	14.38	0.72	1.75	0.00		69.14	8.48	20.41	0.56	1.40	0.00
	18	72.19	11.91	13.89	1.13	0.89	0.00		73.86	10.66	13.58	1.04	0.87	0.00
	19.5	72.31	13.62	12.39	0.99	0.68	0.00		73.01	13.42	11.97	0.88	0.73	0.00
	21	71.12	14.60	12.35	1.34	0.59	0.00		72.32	13.34	12.70	0.88	0.76	0.00
	22.5	71.12	14.86	12.21	1.25	0.56	0.00		71.08	14.76	12.17	1.23	0.75	0.00
	24	70.26	15.59	12.45	1.07	0.63	0.00		71.37	14.65	12.20	1.16	0.63	0.00
	25.5	69.99	15.68	12.30	1.45	0.59	0.00		70.47	14.96	12.63	1.10	0.84	0.00
	27	69.18	16.55	12.29	1.33	0.66	0.00		70.34	15.83	12.07	1.12	0.64	0.00
	28.5	69.08	15.95	13.11	1.25	0.61	0.00		69.47	16.09	12.45	1.31	0.68	0.00
	30	69.50	15.01	13.27	1.62	0.59	0.00		68.69	16.04	12.84	1.60	0.83	0.00
3	0	73.06	12.56	12.40	0.93	1.05	0.00	4	71.51	12.98	13.83	0.72	0.97	0.00
	1.5	73.33	11.20	13.59	0.82	1.06	0.00		72.21	12.44	13.58	0.74	1.03	0.00
	3	74.48	10.10	13.48	0.79	1.15	0.00		74.46	11.45	12.32	0.81	0.95	0.00
	4.5	73.65	9.22	15.01	0.96	1.15	0.00		73.52	10.44	14.35	0.73	0.97	0.00
	6	71.43	9.30	17.31	0.93	1.03	0.00		72.27	10.03	15.97	0.92	0.81	0.00
	7.5	68.61	7.66	21.57	1.01	1.15	0.00		72.55	9.34	16.45	0.76	0.90	0.00
	9	66.52	7.50	24.01	0.89	1.07	0.00		70.31	7.77	20.18	0.71	1.03	0.00
	10.5	62.68	6.90	28.24	0.93	1.24	0.00		66.03	7.95	24.50	0.60	0.92	0.00
	12	61.58	6.63	28.94	0.65	2.21	0.00		63.63	7.16	27.27	0.73	1.20	0.00
	13.5	65.14	7.63	24.89	0.79	1.54	0.00		60.09	6.68	30.46	0.83	1.94	0.00
	15	69.11	9.12	18.54	0.62	2.61	0.00		61.36	6.77	28.46	0.76	2.64	0.00
	16.5	72.60	10.80	13.31	0.91	2.38	0.00		66.74	7.15	23.80	0.57	1.75	0.00
	18	72.43	12.74	12.41	1.15	1.27	0.00		72.79	9.43	15.82	0.91	1.05	0.00
	19.5	70.91	14.37	12.56	1.23	0.92	0.00		72.92	11.10	14.31	0.88	0.80	0.00
	21	69.72	15.85	12.28	1.23	0.92	0.00		72.60	12.96	12.61	1.01	0.82	0.00
	22.5	70.32	14.96	12.45	1.29	0.98	0.00		71.86	13.77	12.81	0.83	0.74	0.00
	24	69.33	14.81	13.33	1.55	0.98	0.00		71.61	13.78	12.66	1.12	0.83	0.00
	25.5	70.03	15.01	12.66	1.27	1.04	0.00		70.16	14.61	13.10	1.32	0.81	0.00
	27	69.51	16.06	12.36	1.09	0.98	0.00		70.16	15.20	12.84	1.10	0.71	0.00
	28.5	69.42	15.84	12.23	1.53	0.99	0.00		69.20	16.20	12.63	1.28	0.69	0.00
	30	68.21	16.37	12.99	1.62	0.80	0.00		68.85	16.38	12.81	1.28	0.68	0.00
5	0	73.26	11.85	12.99	0.84	1.05	0.00	6	73.87	12.15	12.08	0.95	0.96	0.00
	1.5	73.77	12.00	12.50	0.74	0.99	0.00		73.65	12.04	12.40	0.97	0.95	0.00
	3	73.80	10.65	13.71	0.95	0.88	0.00		74.60	10.88	13.14	0.58	0.80	0.00
	4.5	74.82	9.64	13.78	0.82	0.94	0.00		74.34	9.24	14.57	0.96	0.90	0.00

Meas.	Pos. (nm)	Fe	Cr	Ni	Mn	Si	Zr	Meas.	Fe	Cr	Ni	Mn	Si	Zr
5	6	72.89	9.00	16.30	0.77	1.04	0.00	6	73.04	9.11	16.14	0.89	0.82	0.00
	7.5	70.51	7.97	19.51	0.87	1.14	0.00		70.32	8.94	19.17	0.68	0.90	0.00
	9	66.58	7.69	23.86	0.87	1.00	0.00		67.44	7.57	23.50	0.63	0.86	0.00
	10.5	62.31	7.06	28.67	0.90	1.07	0.00		63.37	6.97	28.01	0.80	0.85	0.00
	12	61.05	6.38	30.55	0.77	1.25	0.00		59.45	6.37	32.48	0.72	0.98	0.00
	13.5	63.87	7.52	25.74	0.69	2.17	0.00		64.60	7.14	25.83	0.88	1.55	0.00
	15	68.00	9.06	19.72	0.63	2.59	0.00		67.81	8.22	20.82	0.73	2.42	0.00
	16.5	70.49	9.88	17.02	0.93	1.68	0.00		70.00	10.17	16.73	0.67	2.42	0.00
	18	72.85	11.72	13.46	0.89	1.07	0.00		72.27	12.34	13.17	1.01	1.22	0.00
	19.5	72.32	13.72	12.21	0.87	0.88	0.00		71.58	14.84	12.07	0.65	0.87	0.00
	21	71.39	14.94	12.01	0.91	0.75	0.00		72.04	13.99	12.13	1.26	0.58	0.00
	22.5	69.46	15.70	12.78	1.31	0.75	0.00		70.11	15.56	12.22	1.33	0.78	0.00
	24	69.58	15.67	12.65	1.22	0.88	0.00		69.61	16.10	12.54	1.02	0.72	0.00
	25.5	69.08	16.07	12.90	1.23	0.72	0.00		69.24	15.65	13.09	1.35	0.67	0.00
	27	69.30	16.30	12.17	1.47	0.76	0.00		69.01	16.62	12.26	1.35	0.76	0.00
	28.5	69.57	16.71	11.79	1.09	0.84	0.00		68.70	16.52	12.81	1.22	0.75	0.00
	30	68.03	16.85	12.91	1.30	0.91	0.00		68.90	15.86	12.64	1.78	0.82	0.00
7	0	72.39	11.49	13.63	0.69	1.80	0.00							
	1.5	72.99	11.05	13.34	1.09	1.54	0.00							
	3	72.41	10.71	14.63	0.74	1.51	0.00							
	4.5	71.75	9.65	16.29	0.97	1.34	0.00							
	6	71.19	8.74	18.13	0.67	1.28	0.00							
	7.5	69.02	8.30	20.62	0.89	1.18	0.00							
	9	65.61	7.16	24.56	0.88	1.78	0.00							
	10.5	63.39	6.92	26.83	0.62	2.24	0.00							
	12	58.78	6.60	30.04	0.78	3.80	0.00							
	13.5	62.73	7.38	26.91	0.66	2.32	0.00							
	15	66.56	7.88	23.35	0.77	1.44	0.00							
	16.5	70.56	9.18	18.36	0.64	1.26	0.00							
	18	72.87	11.61	13.17	1.13	1.22	0.00							
	19.5	71.87	13.78	11.95	1.11	1.29	0.00							
	21	72.12	13.23	12.21	1.09	1.34	0.00							
	22.5	70.69	14.56	12.04	1.23	1.48	0.00							
	24	70.51	14.29	12.61	1.01	1.58	0.00							
	25.5	69.06	15.12	13.33	0.99	1.50	0.00							
	27	70.38	14.98	12.12	1.14	1.38	0.00							
	28.5	68.61	15.64	13.02	1.17	1.56	0.00							
	30	69.85	15.85	12.90	1.33	0.06	0.00							

Ref-Zr, 500C, 3 dpa

Meas.	Pos. (nm)	Fe	Cr	Ni	Mn	Si	Zr	Meas.	Fe	Cr	Ni	Mn	Si	Zr
1	0	71.16	14.13	13.00	1.11	0.61	0.00	2	70.66	15.24	12.12	1.32	0.65	0.00
	1.5	71.60	14.30	12.53	0.99	0.59	0.00		70.96	15.45	12.00	0.96	0.63	0.00
	3	72.30	13.49	12.47	1.17	0.57	0.00		71.35	14.26	12.36	1.31	0.72	0.00
	4.5	73.87	12.40	12.32	0.77	0.64	0.00		71.32	14.82	12.12	1.07	0.67	0.00
	6	73.11	12.52	12.96	0.85	0.55	0.00		73.66	13.16	11.67	0.84	0.67	0.00
	7.5	71.89	10.52	16.38	0.57	0.64	0.00		73.76	12.50	12.36	0.65	0.73	0.00
	9	68.89	9.05	20.52	0.73	0.81	0.00		71.86	9.26	17.46	0.70	0.72	0.00
	10.5	58.34	7.82	31.74	0.82	1.27	0.00		69.71	8.95	19.89	0.72	0.72	0.00
	12	56.73	7.72	33.70	0.50	1.35	0.00		58.44	8.23	31.48	0.63	1.22	0.00
	13.5	60.29	9.10	27.90	0.82	1.90	0.00		59.32	7.43	31.20	0.75	1.30	0.00
	15	64.08	9.57	23.90	0.89	1.55	0.00		55.51	7.82	33.89	0.55	2.22	0.00
	16.5	72.02	11.77	14.29	0.95	0.97	0.00		66.21	9.80	21.82	0.67	1.49	0.00
	18	73.06	12.55	12.59	0.99	0.81	0.00		72.42	12.42	13.45	0.83	0.88	0.00
	19.5	71.18	14.74	12.59	0.75	0.75	0.00		71.24	13.43	13.69	0.80	0.85	0.00
	21	70.67	14.79	12.73	0.98	0.83	0.00		71.15	14.20	12.77	0.99	0.89	0.00
	22.5	70.32	15.02	12.80	1.10	0.76	0.00		71.39	14.56	12.24	0.90	0.91	0.00
	24	70.23	14.26	13.28	1.34	0.89	0.00		70.03	15.77	12.45	0.94	0.81	0.00
	25.5	70.56	15.45	12.00	1.21	0.78	0.00		70.43	15.34	12.27	1.19	0.77	0.00
	27	69.29	15.54	13.27	1.04	0.87	0.00		68.95	15.85	13.18	1.24	0.78	0.00
	28.5	69.20	15.36	13.60	1.10	0.73	0.00		69.09	15.77	13.02	1.32	0.80	0.00
	30	68.53	16.04	13.38	1.31	0.74	0.00		68.71	15.93	13.30	1.32	0.74	0.00
3	0	70.65	14.57	13.23	0.94	0.61	0.00	4	70.35	14.62	13.20	1.23	0.61	0.00
	1.5	71.11	14.22	12.99	1.06	0.62	0.00		70.18	14.84	13.04	1.27	0.67	0.00
	3	72.39	12.47	13.68	0.80	0.66	0.00		70.92	14.71	12.38	1.27	0.71	0.00
	4.5	73.13	11.49	13.74	0.94	0.70	0.00		71.74	14.55	12.10	0.93	0.68	0.00
	6	73.42	11.51	13.44	0.96	0.67	0.00		72.64	13.56	12.34	0.87	0.58	0.00
	7.5	70.50	10.06	18.22	0.47	0.74	0.00		72.03	13.78	12.50	1.04	0.64	0.00
	9	65.75	8.71	24.12	0.56	0.85	0.00		74.46	11.76	12.23	0.87	0.68	0.00
	10.5	63.06	8.25	27.07	0.66	0.96	0.00		74.51	11.03	13.04	0.66	0.77	0.00
	12	57.87	7.57	32.68	0.72	1.16	0.00		72.71	9.46	16.35	0.58	0.90	0.00
	13.5	56.14	7.49	34.28	0.49	1.59	0.00		58.50	7.58	31.73	0.70	1.49	0.00
	15	56.41	8.05	32.99	0.63	1.91	0.00		56.01	7.63	33.70	0.61	2.05	0.00
	16.5	68.51	12.03	17.81	0.58	1.07	0.00		58.39	8.32	30.62	0.74	1.92	0.00
	18	71.72	13.54	12.69	1.28	0.78	0.00		58.08	7.87	31.21	0.62	2.21	0.00
	19.5	72.40	13.51	12.30	1.01	0.78	0.00		67.13	9.81	20.88	0.70	1.48	0.00
	21	71.30	15.05	11.91	0.95	0.77	0.00		72.34	14.03	11.85	0.94	0.83	0.00
	22.5	70.78	14.72	12.52	1.17	0.81	0.00		71.60	14.58	11.86	1.12	0.85	0.00
	24	70.26	15.01	12.79	1.06	0.89	0.00		70.69	15.18	12.16	1.13	0.84	0.00
	25.5	70.03	15.38	12.62	1.09	0.87	0.00		70.85	15.46	11.65	1.26	0.78	0.00
	27	70.20	15.00	12.90	1.09	0.80	0.00		70.46	15.24	12.37	1.10	0.83	0.00
	28.5	70.34	15.39	12.28	1.25	0.75	0.00		69.70	16.20	12.35	0.89	0.86	0.00
	30	69.55	15.02	13.00	1.55	0.88	0.00		69.46	15.83	12.49	1.36	0.86	0.00
5	0	70.64	14.26	13.15	1.33	0.62	0.00	6	71.05	14.82	12.08	1.39	0.66	0.00
	1.5	70.12	15.19	13.05	0.98	0.66	0.00		70.87	14.80	12.22	1.46	0.66	0.00
	3	71.13	15.06	12.11	1.07	0.63	0.00		71.84	14.19	12.17	1.16	0.65	0.00
	4.5	70.84	14.51	13.00	1.06	0.59	0.00		72.43	14.01	11.74	1.13	0.69	0.00

Meas.	Pos. (nm)	Fe	Cr	Ni	Mn	Si	Zr	Meas.	Fe	Cr	Ni	Mn	Si	Zr
5	6	72.62	13.72	12.03	1.01	0.62	0.00	6	73.71	12.84	11.88	0.94	0.63	0.00
	7.5	74.76	10.89	12.93	0.72	0.70	0.00		74.27	12.69	11.62	0.79	0.63	0.00
	9	71.88	10.08	16.49	0.80	0.75	0.00		73.83	12.62	11.86	0.95	0.73	0.00
	10.5	62.42	7.91	28.13	0.60	0.94	0.00		75.43	11.16	12.04	0.71	0.66	0.00
	12	60.88	7.82	29.54	0.68	1.08	0.00		67.22	8.29	22.96	0.74	0.79	0.00
	13.5	55.39	7.04	34.91	0.78	1.89	0.00		59.20	7.66	31.14	0.71	1.29	0.00
	15	72.23	12.82	13.02	0.95	0.98	0.00		56.81	6.95	34.01	0.73	1.50	0.00
	16.5	68.54	10.77	18.80	0.57	1.32	0.00		59.93	8.45	28.95	0.71	1.97	0.00
	18	71.51	12.08	14.73	0.68	0.99	0.00		72.25	13.09	13.04	0.74	0.88	0.00
	19.5	69.30	10.43	18.08	0.91	1.28	0.00		72.30	13.50	12.60	0.86	0.75	0.00
	21	70.68	14.99	12.48	0.98	0.88	0.00		71.98	13.80	12.46	0.77	0.98	0.00
	22.5	70.49	14.45	13.03	1.14	0.89	0.00		72.41	13.70	11.94	1.06	0.89	0.00
	24	70.95	14.80	12.22	1.21	0.82	0.00		70.36	15.01	12.46	1.27	0.90	0.00
	25.5	69.95	15.40	12.73	1.16	0.75	0.00		70.20	15.07	12.60	1.29	0.84	0.00
	27	69.47	15.31	13.09	1.27	0.87	0.00		69.65	15.70	12.57	1.24	0.85	0.00
	28.5	70.44	14.84	12.46	1.39	0.88	0.00		70.36	15.83	11.95	1.00	0.87	0.00
	30	70.56	14.99	12.25	1.33	0.87	0.00		69.00	15.55	13.18	1.45	0.82	0.00

LoZr, 500C, 1 dpa

Meas.	Pos. (nm)	Fe	Cr	Ni	Mn	Si	Zr	Meas.	Fe	Cr	Ni	Mn	Si	Zr
1	0	71.25	16.16	9.91	1.82	0.19	0.67	2	66.80	18.93	10.88	2.30	0.27	0.82
	1.5	70.96	16.36	9.93	1.95	0.15	0.66		68.95	15.38	12.51	2.05	0.32	0.80
	3	69.85	16.06	11.47	1.59	0.19	0.84		66.80	17.13	12.73	2.20	0.29	0.86
	4.5	69.50	15.39	12.33	1.87	0.16	0.76		68.16	15.58	13.14	1.80	0.22	1.12
	6	68.99	13.60	14.85	1.48	0.17	0.91		68.32	14.36	14.43	1.64	0.29	0.96
	7.5	65.24	14.13	18.30	1.15	0.18	1.00		65.77	14.02	17.65	1.09	0.32	1.15
	9	57.83	12.26	26.96	1.30	0.20	1.45		60.85	12.39	24.26	1.12	0.20	1.17
	10.5	55.36	12.00	29.02	1.71	0.28	1.63		60.03	11.13	26.00	1.04	0.31	1.49
	12	56.09	12.53	28.05	1.48	0.30	1.55		58.48	11.95	26.25	1.55	0.28	1.50
	13.5	56.27	12.42	27.76	1.80	0.28	1.48		56.47	10.11	29.81	1.57	0.30	1.73
	15	58.22	12.52	26.15	1.57	0.29	1.25		60.11	11.09	25.27	1.97	0.21	1.34
	16.5	59.92	13.36	23.72	1.66	0.20	1.15		59.50	12.66	24.91	1.40	0.23	1.29
	18	62.03	14.52	20.86	1.40	0.16	1.02		63.14	12.94	21.07	1.60	0.22	1.04
	19.5	65.27	14.63	17.62	1.34	0.18	0.97		63.32	12.06	21.71	1.45	0.18	1.28
	21	68.00	14.98	14.77	1.22	0.20	0.82		63.48	13.52	20.04	1.80	0.20	0.96
	22.5	68.31	15.63	13.27	1.74	0.18	0.87		65.09	12.32	19.53	1.88	0.19	0.98
	24	69.60	16.43	11.59	1.41	0.18	0.78		66.03	13.79	17.91	1.26	0.21	0.80
	25.5	69.63	16.92	10.91	1.60	0.16	0.77		67.83	13.04	15.77	2.49	0.26	0.60
	27	68.43	18.94	9.99	1.80	0.16	0.67		68.03	14.38	15.00	1.80	0.17	0.62
	28.5	68.02	19.12	10.35	1.74	0.17	0.60		69.00	14.45	14.46	1.12	0.18	0.79
	30								68.45	15.13	14.19	1.40	0.22	0.61
3	0	65.94	18.53	11.67	2.72	0.31	0.83	4	68.17	17.50	11.43	2.01	0.20	0.69
	1.5	67.00	17.62	11.66	2.59	0.31	0.82		70.16	16.00	11.60	1.21	0.25	0.78
	3	66.79	19.12	11.11	1.64	0.42	0.92		70.04	15.11	12.00	1.76	0.28	0.81
	4.5	68.43	17.23	11.10	2.04	0.27	0.93		68.25	13.45	15.62	1.53	0.24	0.91
	6	69.13	16.35	11.90	1.27	0.32	1.03		64.48	12.97	19.89	1.40	0.21	1.05
	7.5	69.21	14.89	12.98	1.61	0.31	1.00		61.91	11.87	23.11	1.59	0.29	1.23
	9	67.93	14.85	14.35	1.50	0.34	1.02		60.35	11.40	25.13	1.52	0.23	1.37
	10.5	66.70	14.62	16.00	1.03	0.34	1.31		58.90	10.76	26.56	2.04	0.27	1.48
	12	63.52	11.89	21.70	1.20	0.30	1.40		60.54	10.84	25.72	1.54	0.20	1.17
	13.5	63.01	11.12	22.91	1.28	0.34	1.34		60.06	11.43	26.22	0.92	0.21	1.15
	15	60.44	10.34	25.54	1.74	0.37	1.58		60.44	11.17	25.02	2.14	0.16	1.06
	16.5	56.43	10.41	29.34	1.83	0.40	1.58		61.58	12.55	23.33	1.35	0.18	1.01
	18	55.55	11.29	29.22	1.86	0.37	1.71		63.11	12.78	21.55	1.42	0.19	0.95
	19.5	68.35	14.13	14.03	2.14	0.30	1.06		63.39	13.15	21.07	1.40	0.17	0.82
	21	68.86	14.54	12.99	2.00	0.37	1.23		63.82	12.95	20.65	1.54	0.17	0.86
	22.5	67.39	14.49	15.13	1.43	0.26	1.30		65.27	13.13	18.73	1.82	0.18	0.87
	24	66.02	13.19	17.99	1.39	0.27	1.14		64.25	13.36	19.73	1.56	0.22	0.88
	25.5	65.39	12.00	19.34	1.85	0.36	1.06		65.43	14.15	17.80	1.71	0.20	0.72
	27	62.69	11.66	22.12	1.95	0.26	1.32		66.37	12.72	18.19	1.75	0.18	0.80
	28.5	64.85	11.35	20.37	1.81	0.31	1.31		66.06	15.12	16.48	1.37	0.19	0.77
	30	64.44	12.29	20.42	1.24	0.31	1.30		67.00	15.13	15.44	1.59	0.18	0.67
5	0	69.53	16.02	11.75	1.22	0.25	1.23	6	69.11	17.64	10.58	1.81	0.15	0.71
	1.5	69.53	15.13	13.48	0.66	0.27	0.93		69.52	16.80	11.18	1.59	0.18	0.74
	3	67.79	14.38	15.11	1.48	0.24	1.00		69.47	15.95	12.05	1.66	0.13	0.74
	4.5	65.17	12.41	18.91	2.31	0.29	0.90		69.90	16.57	11.21	1.40	0.20	0.72

Meas.	Pos. (nm)	Fe	Cr	Ni	Mn	Si	Zr	Meas.	Fe	Cr	Ni	Mn	Si	Zr
5	6	60.97	12.17	22.33	3.32	0.32	0.88	6	69.25	15.59	12.67	1.54	0.15	0.80
	7.5	57.17	11.06	26.22	4.31	0.36	0.88		68.65	14.76	14.16	1.53	0.18	0.71
	9	56.19	10.94	27.66	4.03	0.30	0.88		65.29	12.39	19.43	1.50	0.18	1.21
	10.5	57.58	11.22	26.62	3.55	0.22	0.81		62.91	11.80	22.77	1.23	0.18	1.12
	12	58.79	12.00	25.35	2.80	0.27	0.79		61.58	10.23	25.62	1.17	0.20	1.20
	13.5	58.57	11.08	26.30	2.97	0.22	0.86		59.94	11.11	26.03	1.21	0.22	1.49
	15	60.81	12.58	23.52	2.06	0.27	0.77		60.73	11.07	25.46	1.34	0.21	1.18
	16.5	62.31	11.60	22.19	2.75	0.23	0.92		62.63	11.43	23.26	1.44	0.17	1.07
	18	62.61	13.61	20.99	1.67	0.19	0.93		66.18	12.19	19.47	1.01	0.19	0.96
	19.5	63.35	13.06	20.84	1.59	0.23	0.93		67.92	13.46	16.24	1.40	0.15	0.83
	21	64.14	13.61	19.71	1.33	0.19	1.02		71.07	12.44	14.03	1.51	0.17	0.77
	22.5	65.29	13.25	19.39	0.98	0.23	0.86		71.66	13.03	12.73	1.72	0.17	0.70
	24	65.97	13.83	17.75	1.26	0.22	0.97		71.67	14.28	11.93	1.37	0.17	0.59
	25.5	65.99	13.81	18.19	0.95	0.20	0.86		71.80	15.04	10.96	1.39	0.16	0.66
	27	65.09	14.81	18.02	0.91	0.22	0.96		70.73	16.29	10.60	1.59	0.14	0.64
	28.5	66.72	14.59	16.25	1.25	0.18	1.02		71.15	16.02	10.53	1.60	0.13	0.58
	30	66.04	15.42	16.92	0.38	0.20	1.04		70.96	16.45	10.09	1.84	0.14	0.53
7	0	71.53	15.52	10.43	1.59	0.16	0.77							
	1.5	71.00	15.22	10.96	1.93	0.17	0.73							
	3	70.40	15.12	11.94	1.59	0.19	0.76							
	4.5	70.13	15.25	12.13	1.52	0.18	0.78							
	6	69.94	13.80	13.69	1.50	0.19	0.87							
	7.5	68.16	12.76	16.09	1.78	0.20	1.01							
	9	66.63	11.85	18.51	1.74	0.23	1.03							
	10.5	63.68	11.89	21.78	1.30	0.21	1.12							
	12	61.87	11.36	23.78	1.46	0.20	1.34							
	13.5	58.50	10.94	27.26	1.56	0.23	1.51							
	15	59.47	10.05	27.49	1.16	0.24	1.59							
	16.5	61.07	11.33	25.01	0.85	0.23	1.51							
	18	62.95	11.73	22.31	1.59	0.22	1.20							
	19.5	66.11	11.74	19.24	1.59	0.20	1.12							
	21	68.20	13.23	16.33	1.12	0.17	0.96							
	22.5	69.61	12.74	15.16	1.36	0.16	0.97							
	24	71.04	13.49	12.90	1.45	0.18	0.94							
	25.5	71.44	14.24	11.64	1.74	0.18	0.77							
	27	71.74	15.80	10.33	1.20	0.17	0.76							
	28.5	71.45	16.14	10.10	1.42	0.17	0.72							
	30	70.21	16.59	10.65	1.60	0.18	0.78							

LoZr, 500C, 3 dpa

Meas.	Pos. (nm)	Fe	Cr	Ni	Mn	Si	Zr	Meas.	Fe	Cr	Ni	Mn	Si	Zr
1	0	69.55	16.77	11.42	1.50	0.16	0.59	2	72.53	16.88	8.71	0.93	0.17	0.78
	1.5	69.69	16.60	11.03	1.75	0.19	0.73		73.12	15.64	9.17	1.23	0.20	0.63
	3	70.24	17.71	9.82	1.38	0.11	0.75		73.95	15.21	8.93	1.04	0.17	0.70
	4.5	72.71	16.78	8.51	1.26	0.17	0.57		75.55	12.78	9.80	0.81	0.17	0.90
	6	72.88	15.88	8.76	1.73	0.16	0.58		69.78	8.58	19.25	0.64	0.25	1.49
	7.5	74.34	14.80	8.83	1.26	0.18	0.59		54.33	5.61	36.02	0.71	0.37	2.96
	9	74.52	14.79	9.11	0.75	0.20	0.63		69.64	7.92	19.55	0.70	0.26	1.92
	10.5	76.56	13.58	8.39	0.79	0.15	0.53		76.60	11.08	10.36	0.72	0.22	1.02
	12	72.04	9.35	16.54	0.55	0.15	1.37		76.51	12.30	9.37	0.88	0.17	0.78
	13.5	56.99	5.65	33.76	0.62	0.33	2.65		73.82	15.03	9.26	0.95	0.22	0.72
	15	52.03	5.93	37.86	0.51	0.41	3.27		73.57	15.72	8.79	1.11	0.20	0.62
	16.5	72.05	8.02	17.53	0.72	0.21	1.46							
	18	76.35	11.19	10.80	0.72	0.20	0.74							
	19.5	75.19	14.59	8.77	0.54	0.22	0.68							
	21	73.44	15.08	9.46	1.13	0.20	0.69							
	22.5	73.45	16.52	8.15	0.97	0.18	0.72							
	24	73.30	16.26	8.45	1.09	0.14	0.77							
	25.5	72.10	16.41	9.32	1.17	0.21	0.80							
	27	70.23	17.63	9.93	1.33	0.21	0.67							
	28.5	70.85	16.08	10.75	1.55	0.21	0.57							
	30	70.45	16.79	10.27	1.67	0.19	0.64							
3	0	73.26	15.51	9.33	1.00	0.17	0.72	4	72.73	15.72	9.65	1.10	0.19	0.61
	1.5	74.59	14.93	8.77	0.88	0.19	0.65		73.54	15.04	9.57	0.99	0.16	0.69
	3	74.66	14.57	9.06	0.92	0.17	0.62		75.01	14.21	9.06	0.82	0.21	0.68
	4.5	75.35	12.19	10.64	0.74	0.24	0.85		74.53	10.06	13.71	0.50	0.19	1.02
	6	73.34	10.15	14.41	0.65	0.17	1.27		68.02	8.17	21.39	0.67	0.21	1.54
	7.5	69.39	8.49	19.60	0.74	0.20	1.58		57.56	6.16	32.81	0.59	0.28	2.60
	9	59.16	6.34	31.17	0.59	0.33	2.42		51.42	5.21	39.06	0.65	0.44	3.21
	10.5	70.33	8.45	18.93	0.58	0.22	1.49		63.15	6.55	27.09	0.62	0.30	2.28
	12	74.14	10.56	13.29	0.65	0.22	1.14		73.33	8.78	15.73	0.69	0.20	1.27
	13.5	73.91	14.54	9.68	0.96	0.18	0.73		74.71	14.03	9.47	0.87	0.20	0.73
	15	74.35	13.95	9.73	1.06	0.19	0.72		73.42	15.19	9.58	0.82	0.18	0.81

HiZr, 500C, 1 dpa

Meas.	Pos. (nm)	Fe	Cr	Ni	Mn	Si	Zr	Meas.	Fe	Cr	Ni	Mn	Si	Zr
1	0	70.08	15.12	11.36	1.08	1.56	0.80	2	69.94	14.53	11.99	1.15	1.61	0.77
	1.5	69.66	14.50	12.50	1.09	1.55	0.70		69.34	14.80	11.91	1.46	1.69	0.80
	3	70.32	15.00	11.70	0.91	1.37	0.70		69.46	15.00	11.96	1.19	1.72	0.68
	4.5	70.44	14.12	12.20	0.98	1.42	0.85		68.76	15.47	11.90	1.39	1.72	0.75
	6	69.76	14.46	12.62	0.93	1.48	0.76		69.63	14.73	11.80	1.45	1.67	0.71
	7.5	70.57	13.54	12.21	1.30	1.53	0.85		68.85	15.02	12.08	1.42	1.80	0.83
	9	70.33	13.46	12.84	1.30	1.39	0.68		70.12	14.47	11.77	1.21	1.66	0.77
	10.5	69.86	13.39	13.63	0.85	1.60	0.67		69.84	14.60	12.18	1.24	1.54	0.59
	12	69.16	12.88	14.60	1.07	1.49	0.80		69.84	14.56	11.91	1.18	1.64	0.87
	13.5	67.49	12.52	16.13	1.32	1.73	0.79		69.36	14.14	12.69	1.29	1.79	0.74
	15	66.90	11.82	17.68	1.11	1.74	0.75		68.86	13.47	14.08	1.09	1.65	0.85
	16.5	65.79	11.59	19.06	0.99	1.81	0.76		68.21	13.05	15.17	0.99	1.88	0.71
	18	63.35	11.84	20.67	1.22	2.09	0.83		67.15	12.30	16.51	1.12	2.03	0.89
	19.5	62.14	11.22	22.32	1.21	2.04	1.07		66.46	11.99	17.54	1.25	1.98	0.78
	21	60.75	10.71	22.77	1.05	2.96	1.75		66.96	12.70	16.62	1.16	1.85	0.72
	22.5	63.10	11.73	20.40	1.07	2.20	1.50		67.49	12.33	16.35	1.16	1.90	0.77
	24	65.18	11.84	18.79	1.12	1.84	1.23		67.75	13.29	15.59	1.06	1.62	0.69
	25.5	66.15	12.06	17.53	1.10	2.06	1.10		68.40	13.40	14.59	1.08	1.71	0.81
	27	67.41	11.90	16.44	1.15	1.93	1.17		69.43	14.15	13.10	1.11	1.46	0.75
	28.5	68.18	12.51	15.16	1.17	1.72	1.27		70.89	14.17	11.71	1.12	1.42	0.69
	30	67.60	12.82	15.44	1.23	1.91	1.01		70.13	14.96	11.84	1.09	1.32	0.67
3	0	70.45	14.26	11.75	1.16	1.53	0.85	4	68.15	15.13	12.59	1.53	1.67	0.93
	1.5	70.15	14.67	11.91	1.17	1.41	0.69		66.90	16.98	12.07	1.12	1.83	1.09
	3	70.74	14.21	11.47	1.42	1.42	0.74		68.09	15.74	12.20	1.32	1.96	0.70
	4.5	70.57	13.55	12.40	1.45	1.28	0.75		68.82	15.13	12.43	1.11	1.75	0.77
	6	69.72	13.79	13.18	1.00	1.54	0.77		68.92	15.51	12.22	0.83	1.66	0.85
	7.5	69.53	13.70	13.37	1.17	1.45	0.77		69.53	13.98	12.52	1.40	1.96	0.61
	9	70.30	13.18	13.41	0.98	1.52	0.61		70.24	13.74	12.02	1.13	2.02	0.85
	10.5	69.63	13.10	13.92	1.14	1.53	0.69		70.73	13.11	12.17	1.27	1.93	0.79
	12	69.17	12.43	14.82	1.12	1.69	0.77		69.06	12.93	14.29	1.04	1.94	0.74
	13.5	66.67	12.57	17.15	0.99	1.82	0.81		67.01	10.83	17.84	0.89	2.43	1.02
	15	66.22	11.87	18.38	0.93	1.85	0.73		65.84	10.27	19.18	1.01	2.55	1.15
	16.5	64.18	12.60	19.55	0.76	1.92	0.99		65.03	10.54	19.87	1.06	2.41	1.09
	18	61.30	11.03	23.01	1.06	2.66	0.95		66.06	10.45	19.49	0.88	2.16	0.96
	19.5	59.96	10.98	23.74	1.10	2.81	1.42		68.45	10.64	17.11	0.88	1.97	0.96
	21	62.21	11.33	21.86	0.91	2.39	1.29		67.70	11.23	17.44	0.72	2.00	0.91
	22.5	65.66	11.86	18.51	0.87	2.05	1.05		69.47	11.58	15.32	1.07	1.85	0.71
	24	66.53	11.77	17.61	0.93	1.86	1.31		68.60	12.33	15.52	0.92	1.84	0.79
	25.5	66.94	12.93	16.09	1.04	1.92	1.07		68.83	12.98	14.88	0.91	1.57	0.84
	27	68.38	12.90	14.38	1.19	1.90	1.24		69.02	13.60	14.00	0.84	1.76	0.79
	28.5	67.78	13.80	14.21	0.91	2.04	1.25		69.21	12.68	14.03	1.26	1.80	1.01
	30	69.41	13.31	13.44	1.03	1.91	0.90		69.26	13.60	13.91	0.91	1.56	0.75
5	0	69.98	14.71	11.57	1.30	1.52	0.92	6	69.25	14.09	12.86	1.06	1.66	1.07
	1.5	70.34	14.88	11.67	0.99	1.48	0.65		69.44	13.95	12.85	1.14	1.54	1.08
	3	69.45	14.99	12.36	1.07	1.34	0.79		69.14	13.55	13.50	1.27	1.63	0.91
	4.5	70.40	14.62	11.85	1.18	1.31	0.63		68.74	13.03	14.17	1.13	1.86	1.07

Meas.	Pos. (nm)	Fe	Cr	Ni	Mn	Si	Zr	Meas.	Fe	Cr	Ni	Mn	Si	Zr
5	6	69.80	14.19	12.45	1.31	1.53	0.73	6	68.17	12.48	15.55	1.27	1.40	1.13
	7.5	69.72	13.83	12.84	1.20	1.53	0.88		67.29	12.59	16.04	1.30	1.75	1.04
	9	70.38	13.52	12.82	0.97	1.53	0.79		67.14	11.66	17.16	1.21	1.82	1.01
	10.5	69.83	12.62	14.02	1.19	1.58	0.76		66.49	12.24	17.58	0.91	1.84	0.95
	12	69.57	12.81	14.09	1.07	1.63	0.82		64.67	11.99	18.96	1.02	2.25	1.11
	13.5	68.27	12.79	15.26	1.13	1.62	0.94		61.97	10.71	22.57	1.18	2.39	1.18
	15	66.46	12.80	17.20	0.98	1.66	0.90		60.58	11.09	22.73	1.19	2.97	1.44
	16.5	67.31	12.92	16.68	0.69	1.67	0.73		63.47	11.32	20.32	1.21	2.20	1.48
	18	65.69	11.73	19.33	0.72	1.75	0.78		66.35	12.11	16.77	1.12	2.14	1.51
	19.5	62.66	11.74	21.02	1.24	2.25	1.09		67.61	12.76	15.04	1.07	2.19	1.33
	21	60.81	11.51	22.50	1.19	2.69	1.30		68.29	13.25	14.24	0.99	1.90	1.33
	22.5	60.86	11.54	22.78	1.07	2.59	1.17		70.00	12.84	12.76	1.12	1.88	1.40
	24	65.31	11.88	18.87	0.71	2.08	1.15		69.14	13.76	12.77	1.29	1.69	1.35
	25.5	65.60	12.27	18.15	0.85	1.92	1.21		68.70	14.08	13.13	1.19	1.58	1.31
	27	66.28	12.20	17.35	0.91	2.03	1.22		69.27	13.94	12.40	1.23	1.64	1.52
	28.5	68.23	12.81	15.20	0.76	1.92	1.08		69.06	14.27	12.00	1.51	1.76	1.40
	30	69.17	12.99	14.22	0.88	1.82	0.93		69.92	14.05	12.08	1.02	1.64	1.29
7	0	66.97	15.03	14.42	1.14	1.77	0.67	8	66.88	15.73	13.42	1.30	1.82	0.85
	1.5	66.81	14.86	14.30	1.54	1.64	0.86		65.98	16.12	14.30	1.02	1.79	0.80
	3	66.47	13.80	15.96	1.63	1.48	0.66		66.54	15.05	14.86	1.11	1.65	0.79
	4.5	65.84	13.95	16.43	1.00	1.79	0.98		57.62	13.43	25.32	1.43	1.57	0.63
	6	65.65	14.01	16.29	1.29	1.90	0.86		48.32	12.17	35.51	1.12	1.76	1.11
	7.5	66.07	12.82	17.32	1.32	1.64	0.84		45.97	10.91	38.36	1.42	2.35	0.99
	9	62.63	12.94	20.87	1.29	1.52	0.75		59.83	14.13	22.07	1.29	1.88	0.81
	10.5	58.74	12.37	25.13	1.20	1.69	0.87		63.62	14.24	18.70	0.91	1.73	0.80
	12	60.32	12.48	23.22	1.24	1.75	0.98		66.70	13.88	15.98	1.31	1.48	0.65
	13.5	66.59	13.57	16.26	1.18	1.64	0.75		66.84	14.86	15.02	1.16	1.33	0.79
	15	69.86	13.74	13.22	1.05	1.46	0.67		66.98	14.98	14.49	1.22	1.62	0.71
	16.5	69.65	14.37	12.69	1.00	1.53	0.76		68.12	14.59	13.77	1.19	1.45	0.88
	18	69.41	14.57	12.55	1.02	1.63	0.82		68.39	14.51	14.13	0.98	1.36	0.63
	19.5	69.73	14.53	12.04	1.49	1.40	0.81		67.02	16.70	13.05	1.24	1.47	0.51
	21	68.70	15.67	11.64	1.39	1.70	0.89		68.46	14.95	12.95	1.14	1.68	0.82
	22.5	68.99	15.11	12.19	1.48	1.59	0.64		68.23	15.25	13.32	1.05	1.50	0.64
	24	68.90	15.09	12.35	1.52	1.41	0.72		67.63	15.61	13.22	1.34	1.44	0.76
	25.5	68.83	15.49	12.04	1.57	1.49	0.59		68.37	15.57	12.92	1.21	1.27	0.66
	27	68.51	15.92	12.07	1.38	1.44	0.69		66.78	15.85	13.53	1.44	1.78	0.62
	28.5	68.52	15.15	12.64	1.50	1.32	0.86		67.50	15.30	13.26	1.51	1.60	0.84
	30	68.64	15.31	12.40	1.54	1.41	0.70		67.50	15.20	13.85	1.01	1.68	0.77
9	0	67.56	16.06	12.78	1.13	1.52	0.94	10	65.67	14.76	15.34	1.29	1.92	1.02
	1.5	68.05	15.46	13.10	1.17	1.39	0.83		52.05	11.98	31.55	1.49	1.90	1.03
	3	65.91	15.35	14.68	1.51	1.55	1.01		51.50	12.03	32.87	0.82	1.93	0.85
	4.5	64.88	16.48	14.80	1.01	1.68	1.16		54.83	11.52	30.08	0.91	1.92	0.75
	6	64.47	15.69	15.61	1.20	1.94	1.09		63.37	14.29	18.42	1.40	1.67	0.84
	7.5	63.64	14.94	17.55	0.83	1.99	1.04		64.82	15.81	15.71	1.21	1.64	0.82
	9	65.42	14.53	16.00	1.20	1.66	1.19		65.76	16.15	14.79	1.21	1.41	0.69
	10.5	63.97	14.00	18.22	1.20	1.64	0.96		66.83	15.33	14.55	1.00	1.63	0.65
	12	61.27	13.60	21.48	0.88	1.98	0.79		66.83	15.66	13.28	1.73	1.64	0.87

Meas.	Pos. (nm)	Fe	Cr	Ni	Mn	Si	Zr	Meas.	Fe	Cr	Ni	Mn	Si	Zr
9	13.5	57.64	12.40	25.87	1.10	1.82	1.16	10	68.39	15.30	12.87	1.16	1.56	0.73
	15	63.03	13.86	19.70	0.84	1.83	0.74		68.20	15.45	12.71	1.47	1.41	0.76
	16.5	67.01	13.43	15.62	0.89	2.20	0.85		68.10	15.58	12.91	1.23	1.60	0.59
	18	67.19	13.48	15.10	1.58	1.77	0.88		67.59	16.83	11.89	1.36	1.62	0.71
	19.5	68.49	13.32	13.77	1.48	2.21	0.73		66.86	16.20	13.65	1.11	1.50	0.68
	21	68.46	12.68	14.63	1.51	1.81	0.92		66.81	16.31	13.61	1.03	1.39	0.85
	22.5	68.90	14.37	12.60	1.49	1.92	0.72		67.83	15.52	12.85	1.53	1.46	0.80
	24	69.24	13.73	13.58	1.31	1.47	0.67		66.69	16.85	13.16	1.00	1.67	0.64
	25.5	68.51	14.25	13.72	1.31	1.42	0.79		67.37	15.44	13.71	1.06	1.58	0.84
	27	68.18	14.57	13.14	1.44	1.83	0.85		66.88	14.98	14.66	1.37	1.54	0.58
	28.5	68.65	15.01	12.77	1.37	1.28	0.92		66.90	14.85	14.78	1.22	1.41	0.84
	30	68.05	15.13	12.97	0.95	2.06	0.85		66.61	15.19	14.38	1.53	1.62	0.67
11	0	68.84	15.78	11.91	1.08	1.52	0.86	12	70.05	14.46	12.25	0.99	1.49	0.76
	1.5	69.50	14.94	12.15	1.27	1.34	0.79		70.04	14.82	11.81	1.18	1.38	0.77
	3	70.23	14.23	12.13	1.17	1.53	0.71		69.46	14.89	12.30	1.21	1.32	0.82
	4.5	70.05	14.50	12.11	1.13	1.52	0.71		70.51	13.17	12.94	1.06	1.55	0.78
	6	70.12	13.88	12.84	1.07	1.32	0.77		69.79	13.19	13.78	1.06	1.56	0.62
	7.5	69.47	13.54	13.71	0.97	1.66	0.65		69.02	13.01	14.23	1.18	1.90	0.67
	9	69.10	13.65	14.00	1.05	1.59	0.61		68.55	12.90	14.82	1.23	1.80	0.70
	10.5	68.21	12.79	15.45	1.22	1.59	0.75		67.17	12.08	17.15	1.19	1.69	0.73
	12	67.89	12.27	16.17	1.10	1.84	0.75		67.16	11.73	17.91	1.01	1.50	0.69
	13.5	66.90	12.28	16.99	1.26	1.88	0.69		64.63	11.01	20.20	1.21	2.20	0.75
	15	66.05	11.47	18.54	1.13	1.92	0.89		61.30	11.30	22.63	1.16	2.48	1.14
	16.5	64.15	11.69	19.86	0.94	2.30	1.06		59.83	11.22	24.22	0.73	2.84	1.15
	18	60.06	10.91	22.96	1.04	2.55	2.48		62.00	10.77	22.54	1.04	2.45	1.21
	19.5	57.88	10.69	23.36	0.97	3.11	3.99		63.76	11.37	20.28	1.08	2.27	1.25
	21	59.83	11.48	21.66	0.87	2.82	3.34		65.40	11.65	18.96	0.95	1.91	1.14
	22.5	63.70	11.40	20.35	0.90	2.21	1.45		66.61	12.51	16.71	1.20	1.90	1.07
	24	64.97	12.21	18.46	1.08	2.30	0.99		67.37	12.93	15.84	0.89	1.97	1.00
	25.5	65.03	11.95	18.84	1.05	2.03	1.10		69.17	12.80	13.95	1.22	1.75	1.10
	27	65.89	12.91	17.22	0.91	1.96	1.11		68.08	13.84	14.11	1.15	1.74	1.09
	28.5	67.88	12.33	15.71	0.99	2.02	1.07		69.34	13.65	12.97	1.18	1.89	0.97
	30	66.96	12.78	16.01	1.08	1.81	1.35		69.82	13.62	12.59	1.06	1.81	1.09
13	0	69.85	14.63	11.98	1.30	1.53	0.70							
	1.5	70.27	14.26	11.98	1.18	1.49	0.83							
	3	70.46	14.30	12.04	1.13	1.46	0.62							
	4.5	70.75	13.95	12.01	1.08	1.54	0.67							
	6	69.38	14.42	12.86	0.94	1.55	0.85							
	7.5	70.00	13.57	12.69	1.30	1.67	0.78							
	9	69.47	13.22	14.11	0.96	1.57	0.66							
	10.5	68.62	13.02	14.36	1.30	1.85	0.86							
	12	68.01	12.81	15.37	1.32	1.59	0.90							
	13.5	67.79	12.56	16.27	0.95	1.59	0.84							
	15	66.85	12.29	17.57	0.90	1.61	0.78							
	16.5	65.35	12.01	18.98	0.94	1.83	0.90							
	18	62.56	11.51	20.89	1.15	2.49	1.39							
	19.5	60.96	11.06	22.48	0.98	2.50	2.02							

Meas.	Pos. (nm)	Fe	Cr	Ni	Mn	Si	Zr	Meas.	Fe	Cr	Ni	Mn	Si	Zr
13	21	61.07	10.92	22.45	1.02	2.81	1.73							
	22.5	64.41	12.11	18.96	1.28	2.09	1.15							
	24	66.11	12.20	17.37	0.86	2.21	1.24							
	25.5	66.44	13.10	16.31	1.15	1.87	1.13							
	27	68.76	13.07	14.18	0.98	1.76	1.24							
	28.5	69.18	13.18	13.76	0.98	1.84	1.06							
	30	69.43	13.25	13.22	1.19	1.79	1.11							

HiZr, 500C, 3 dpa

Meas.	Pos. (nm)	Fe	Cr	Ni	Mn	Si	Zr	Meas.	Fe	Cr	Ni	Mn	Si	Zr
1	0	71.15	15.29	11.38	1.25	0.28	0.65	2	70.74	14.62	12.44	1.14	0.26	0.81
	1.5	71.62	14.88	11.35	1.26	0.28	0.63		71.80	14.40	12.01	1.02	0.21	0.56
	3	71.90	14.86	11.01	1.36	0.26	0.60		71.20	14.87	11.87	1.18	0.24	0.64
	4.5	72.52	14.05	11.47	1.00	0.29	0.67		71.07	14.81	11.94	1.23	0.27	0.68
	6	73.33	12.97	11.63	1.02	0.31	0.74		71.51	14.54	12.13	0.98	0.24	0.61
	7.5	72.81	11.33	13.67	0.72	0.27	1.20		71.06	14.46	12.45	1.03	0.28	0.72
	9	72.87	13.90	11.34	1.01	0.21	0.66		72.18	13.98	11.87	1.07	0.22	0.68
	10.5	73.45	12.93	11.64	0.78	0.24	0.95		72.14	14.19	11.69	0.87	0.23	0.87
	12	69.82	10.41	17.14	0.79	0.29	1.55		72.87	12.74	12.42	0.87	0.26	0.83
	13.5	63.40	9.14	24.17	0.66	0.41	2.22		69.99	10.94	16.65	0.67	0.29	1.47
	15	64.77	9.97	22.19	0.54	0.38	2.15		64.65	9.32	22.82	0.70	0.36	2.14
	16.5	71.34	12.19	14.37	0.66	0.30	1.14		65.29	9.76	21.94	0.70	0.30	2.01
	18	72.20	13.65	12.39	0.73	0.25	0.79		72.27	11.78	14.02	0.70	0.29	0.94
	19.5	71.47	14.08	12.43	0.98	0.27	0.76		72.95	12.83	12.36	0.82	0.29	0.74
	21	70.71	14.63	12.74	1.02	0.20	0.70		71.99	13.79	12.11	1.04	0.29	0.78
	22.5	71.65	14.40	11.98	1.04	0.24	0.69		71.88	14.29	11.95	0.98	0.23	0.67
	24	71.58	14.82	11.55	1.06	0.24	0.75		71.32	14.63	12.09	0.97	0.30	0.70
	25.5	71.07	14.95	12.02	0.99	0.25	0.72		71.40	14.51	12.13	1.12	0.22	0.64
	27	70.97	14.75	12.31	0.99	0.23	0.75		70.27	15.03	12.46	1.38	0.29	0.56
	28.5	71.41	14.67	11.61	1.32	0.32	0.68		70.99	14.89	11.96	1.29	0.24	0.62
	30	70.60	14.69	12.53	1.07	0.26	0.85		70.56	15.38	11.92	1.25	0.23	0.66
3	0	70.20	14.82	12.80	1.14	0.38	0.66	4	70.91	15.10	12.07	1.08	0.22	0.62
	1.5	70.94	14.78	12.27	1.03	0.34	0.65		70.93	15.00	11.94	1.19	0.26	0.68
	3	70.92	15.21	11.80	0.98	0.32	0.77		70.86	15.02	12.03	1.18	0.24	0.66
	4.5	70.94	15.08	11.94	1.01	0.31	0.72		70.86	14.91	12.28	1.05	0.23	0.67
	6	71.37	14.70	11.83	1.09	0.32	0.70		71.60	14.61	11.83	1.08	0.26	0.62
	7.5	71.38	14.91	11.43	1.11	0.35	0.82		71.83	14.75	11.39	1.01	0.25	0.77
	9	71.94	14.44	11.54	0.93	0.36	0.78		71.96	14.23	11.83	0.95	0.27	0.75
	10.5	72.05	14.41	11.71	0.82	0.33	0.69		73.19	12.95	11.87	0.96	0.25	0.78
	12	72.94	13.94	11.16	0.95	0.37	0.63		72.58	11.85	13.52	0.82	0.25	0.98
	13.5	69.76	9.96	17.94	0.72	0.90	0.72		64.73	9.69	22.47	0.63	0.40	2.08
	15	62.69	9.04	25.50	0.60	1.33	0.84		65.94	10.14	21.03	0.73	0.33	1.83
	16.5	65.90	9.62	21.98	0.61	1.03	0.86		70.47	11.10	16.11	0.71	0.28	1.33
	18	72.45	13.25	12.18	0.95	0.44	0.73		72.35	13.55	12.19	0.89	0.27	0.75
	19.5	71.90	14.16	11.88	0.95	0.39	0.72		71.94	14.24	11.86	0.93	0.27	0.76
	21	71.63	14.64	11.63	0.98	0.37	0.75		72.32	14.24	11.45	1.09	0.25	0.65
	22.5	71.53	14.68	11.80	0.84	0.38	0.77		71.54	14.77	11.77	1.01	0.29	0.63
	24	70.76	14.76	12.18	1.16	0.37	0.77		71.22	14.99	11.90	0.93	0.31	0.65
	25.5	70.45	15.06	12.24	1.02	0.36	0.88		71.54	14.76	11.79	1.04	0.25	0.61
	27	70.63	15.68	11.49	1.13	0.31	0.76		71.50	14.43	11.99	1.16	0.26	0.66
	28.5	70.85	15.32	11.71	1.07	0.28	0.77		71.00	15.23	11.49	1.31	0.28	0.69
	30	70.84	15.21	11.70	1.12	0.35	0.78		70.88	14.92	12.17	1.17	0.26	0.61
5	0	70.83	14.91	12.19	1.13	0.25	0.68	6	71.59	14.95	11.51	1.10	0.25	0.59
	1.5	70.61	15.11	12.22	1.16	0.24	0.67		70.92	15.35	11.58	1.21	0.23	0.71
	3	70.47	14.95	12.49	1.19	0.23	0.67		70.76	15.42	11.86	1.02	0.27	0.67
	4.5	71.13	14.40	12.27	1.26	0.24	0.70		71.10	15.09	11.73	1.17	0.26	0.66

Meas.	Pos. (nm)	Fe	Cr	Ni	Mn	Si	Zr	Meas.	Fe	Cr	Ni	Mn	Si	Zr
5	6	71.06	15.13	11.81	1.10	0.29	0.61	6	71.04	14.81	12.19	1.08	0.24	0.65
	7.5	71.91	15.15	11.01	0.89	0.25	0.79		71.05	14.61	12.44	1.00	0.26	0.65
	9	72.61	13.95	11.60	0.82	0.26	0.75		71.96	14.26	11.79	1.16	0.23	0.61
	10.5	72.90	12.62	12.50	0.78	0.28	0.92		70.95	14.77	12.29	1.12	0.21	0.67
	12	70.16	10.67	16.73	0.69	0.30	1.44		71.18	15.05	11.73	1.03	0.25	0.76
	13.5	62.55	9.08	25.05	0.46	0.46	2.39		72.01	14.20	11.92	0.99	0.25	0.64
	15	67.13	10.18	19.86	0.73	0.35	1.76		72.62	13.96	11.74	0.83	0.18	0.67
	16.5	71.64	12.12	14.21	0.70	0.32	1.01		73.48	12.79	11.72	0.97	0.23	0.82
	18	73.08	13.24	11.78	0.89	0.25	0.75		67.49	9.72	19.99	0.72	0.30	1.78
	19.5	72.31	14.33	11.50	0.87	0.24	0.75		63.54	8.93	24.14	0.66	0.39	2.35
	21	71.59	14.49	11.82	1.15	0.30	0.65		67.02	10.00	20.20	0.74	0.31	1.73
	22.5	70.75	14.87	12.51	0.89	0.28	0.71		72.08	12.47	13.66	0.67	0.26	0.86
	24	70.46	14.66	12.73	1.18	0.27	0.69		72.42	13.46	12.03	0.94	0.26	0.90
	25.5	70.95	14.07	12.88	1.19	0.24	0.67		72.49	13.74	11.85	0.89	0.27	0.76
	27	70.89	15.28	11.86	0.99	0.27	0.70		71.48	14.64	11.91	1.08	0.25	0.64
	28.5	70.23	15.64	12.17	1.05	0.22	0.69		71.08	14.68	12.05	1.20	0.32	0.68
	30	69.43	15.68	12.55	1.36	0.26	0.72		70.70	14.68	12.68	1.05	0.29	0.60
7	0	70.12	15.40	12.11	1.24	0.26	0.87	8	69.30	14.50	14.02	0.78	0.29	1.10
	1.5	69.85	15.53	12.06	1.36	0.30	0.89		69.81	14.33	13.51	1.01	0.33	1.01
	3	70.31	15.44	11.84	1.15	0.28	0.98		70.57	14.90	12.14	1.14	0.33	0.91
	4.5	71.07	15.19	11.38	1.14	0.31	0.91		70.22	14.82	12.35	1.33	0.30	0.97
	6	71.02	14.67	11.73	1.21	0.34	1.03		70.90	15.06	11.67	1.05	0.33	0.99
	7.5	70.43	14.37	12.72	1.00	0.33	1.15		70.24	15.73	11.62	1.16	0.30	0.95
	9	69.69	13.72	13.78	0.86	0.32	1.63		70.44	14.81	12.28	1.15	0.33	1.00
	10.5	68.84	12.46	15.48	0.81	0.37	2.03		70.88	14.30	12.49	1.02	0.29	1.02
	12	66.39	10.80	18.94	0.73	0.39	2.74		70.77	13.75	12.92	0.91	0.32	1.34
	13.5	71.39	12.29	13.38	0.78	0.34	1.81		70.49	12.77	13.96	0.73	0.34	1.71
	15	70.74	14.97	11.72	1.09	0.30	1.18		67.76	11.34	17.38	0.71	0.37	2.43
	16.5	70.07	14.92	12.39	1.22	0.29	1.10		62.76	9.40	23.08	0.71	0.45	3.60
	18	69.44	14.99	12.79	1.25	0.34	1.19		66.75	9.90	19.29	0.83	0.33	2.91
	19.5	69.10	15.24	13.02	1.21	0.31	1.12		71.51	11.83	13.69	0.82	0.33	1.84
	21	69.20	14.41	13.47	1.34	0.25	1.33		71.31	14.45	11.79	0.93	0.29	1.23
	22.5	68.21	14.62	14.25	1.16	0.29	1.47		71.79	13.98	11.81	0.85	0.26	1.32
	24	69.79	13.97	13.43	1.20	0.30	1.31		71.31	14.19	11.82	1.16	0.29	1.23
	25.5	69.35	14.37	13.63	1.06	0.26	1.33		71.57	14.37	11.75	0.92	0.28	1.11
	27	70.20	14.17	12.96	1.10	0.25	1.32		70.02	14.26	13.12	0.94	0.29	1.37
	28.5	69.89	15.03	12.47	1.14	0.28	1.18		69.80	14.27	13.31	1.14	0.27	1.20
	30	22.68	19.86	23.71	11.87	7.51	14.37		69.63	13.76	13.86	1.29	0.28	1.18
9	0	70.31	15.29	11.73	1.40	0.29	0.98	10	69.78	14.20	13.34	1.19	0.28	1.21
	1.5	69.72	15.80	11.97	1.26	0.31	0.95		70.56	14.12	12.80	1.24	0.31	0.97
	3	70.49	15.24	11.92	1.21	0.31	0.82		71.01	14.65	11.92	1.09	0.27	1.06
	4.5	70.57	15.32	11.71	1.18	0.34	0.87		71.10	14.56	11.82	1.24	0.31	0.96
	6	70.72	14.74	12.09	1.15	0.31	0.98		71.58	14.29	11.75	1.04	0.32	1.03
	7.5	70.89	14.63	12.19	1.11	0.28	0.89		70.50	14.74	12.40	1.14	0.28	0.95
	9	70.43	14.42	12.53	1.10	0.32	1.20		71.63	14.11	12.06	0.86	0.31	1.04
	10.5	70.49	13.46	13.12	0.80	0.37	1.76		70.78	13.71	13.06	0.91	0.34	1.20
	12	70.78	12.38	13.92	0.84	0.32	1.75		70.91	12.49	13.79	0.75	0.31	1.74

Meas.	Pos. (nm)	Fe	Cr	Ni	Mn	Si	Zr	Meas.	Fe	Cr	Ni	Mn	Si	Zr
9	13.5	68.74	11.69	16.24	0.70	0.41	2.22	10	71.59	11.90	13.71	0.78	0.33	1.69
	15	67.40	11.14	17.97	0.70	0.35	2.44		68.40	9.80	18.42	0.72	0.36	2.31
	16.5	65.43	9.35	20.92	0.81	0.41	3.08		71.71	11.34	14.10	0.69	0.35	1.82
	18	70.88	11.97	14.28	0.79	0.32	1.77		71.76	13.35	12.34	0.87	0.31	1.37
	19.5	72.26	13.06	12.18	0.84	0.30	1.34		71.71	14.14	11.58	0.97	0.31	1.30
	21	72.60	13.04	11.90	0.92	0.29	1.25		70.71	14.51	12.20	1.04	0.26	1.28
	22.5	70.85	14.33	12.29	1.00	0.29	1.24		70.15	14.89	12.33	1.02	0.29	1.32
	24	70.40	14.07	13.03	1.00	0.35	1.16		69.98	14.87	12.41	1.15	0.31	1.28
	25.5	70.63	14.07	12.79	1.05	0.28	1.18		69.61	14.77	13.03	1.03	0.28	1.28
	27	69.89	14.83	12.84	0.85	0.27	1.32		69.54	14.80	13.07	1.09	0.28	1.23
	28.5	69.97	14.74	12.57	1.20	0.30	1.21		69.44	14.18	13.44	1.19	0.29	1.46
	30	69.78	15.06	12.47	1.26	0.31	1.12		69.38	14.17	13.69	1.09	0.30	1.37
11	0	68.17	13.97	15.25	1.11	0.30	1.20	12	71.46	14.40	11.82	1.05	0.31	0.96
	1.5	67.80	13.84	15.82	0.96	0.30	1.27		71.28	14.36	11.88	1.26	0.28	0.94
	3	70.44	13.85	13.45	1.00	0.32	0.93		70.62	15.20	11.92	1.08	0.30	0.88
	4.5	70.16	13.88	13.59	1.03	0.31	1.02		71.42	14.41	11.90	1.03	0.30	0.94
	6	70.34	14.37	13.15	0.96	0.29	0.90		70.99	15.01	11.76	1.12	0.30	0.81
	7.5	70.75	14.25	12.58	1.04	0.30	1.07		70.88	13.92	12.76	1.17	0.31	0.96
	9	70.90	14.12	12.68	0.87	0.32	1.12		71.37	13.67	12.58	1.10	0.28	1.01
	10.5	71.16	13.26	13.36	0.90	0.29	1.04		70.98	13.51	13.28	0.74	0.31	1.19
	12	70.89	13.32	13.39	0.72	0.33	1.34		71.99	13.24	12.59	0.80	0.28	1.10
	13.5	67.39	10.05	18.81	0.86	0.39	2.49		69.73	11.16	16.27	0.74	0.32	1.77
	15	68.67	10.24	17.68	0.57	0.39	2.45		70.59	11.14	15.52	0.71	0.34	1.71
	16.5	71.05	11.82	14.18	0.78	0.31	1.86		66.69	9.68	20.08	0.60	0.45	2.51
	18	71.44	12.75	13.15	0.72	0.32	1.61		65.92	9.64	20.84	0.61	0.41	2.58
	19.5	70.07	14.80	12.19	1.28	0.30	1.35		68.17	9.84	18.45	0.74	0.34	2.46
	21	70.54	14.87	12.20	0.96	0.27	1.15		70.17	15.14	12.02	1.11	0.30	1.25
	22.5	70.48	14.68	12.21	1.14	0.29	1.20		69.70	15.01	12.61	1.11	0.30	1.26
	24	70.04	15.14	12.07	1.14	0.35	1.26		69.37	15.21	12.73	1.10	0.31	1.29
	25.5	69.17	15.33	12.91	1.11	0.27	1.23		70.19	14.96	12.18	1.04	0.32	1.30
	27	69.60	14.71	12.91	1.22	0.30	1.26		69.79	15.41	12.09	1.19	0.27	1.25
	28.5	69.29	15.42	12.67	1.03	0.27	1.32		69.79	14.84	12.70	1.03	0.28	1.36
	30	69.59	14.70	13.15	1.00	0.28	1.28		70.28	14.16	12.96	1.00	0.26	1.34

Ref-Hf, 500C, 1 dpa

Meas.	Pos. (nm)	Fe	Cr	Ni	Mn	Mo	Si	Meas.	Fe	Cr	Ni	Mn	Mo	Si
1	0	65.33	19.11	12.87	1.14	1.33	0.24	2	63.58	19.26	13.86	0.66	2.37	0.27
	1.5	65.13	19.16	13.13	0.96	1.38	0.25		62.52	19.93	13.66	1.00	2.64	0.26
	3	64.58	19.18	13.41	1.15	1.45	0.24		63.74	18.41	13.94	0.86	2.75	0.29
	4.5	65.02	19.36	12.63	0.98	1.75	0.27		64.79	17.82	13.98	0.80	2.36	0.24
	6	64.53	18.41	14.42	0.97	1.39	0.28		63.51	17.89	14.68	1.23	2.35	0.34
	7.5	64.64	19.05	13.70	0.99	1.33	0.29		63.89	18.10	14.08	0.86	2.82	0.25
	9	64.38	19.15	13.54	1.05	1.64	0.24		63.81	18.57	13.77	1.15	2.42	0.28
	10.5	63.89	20.83	12.38	0.96	1.72	0.22		63.16	19.02	13.44	1.20	2.87	0.30
	12	65.46	19.61	12.03	1.06	1.63	0.21		63.63	17.84	14.42	1.06	2.76	0.29
	13.5	63.68	18.35	15.41	0.84	1.32	0.40		63.42	20.51	12.36	0.81	2.66	0.24
	15	62.70	17.79	16.68	0.82	1.58	0.43		63.42	20.23	12.47	1.13	2.50	0.25
	16.5	65.63	18.36	13.33	0.90	1.51	0.27		64.33	18.93	12.72	1.01	2.75	0.26
	18	64.99	19.45	12.76	0.96	1.60	0.26		62.59	16.91	16.89	0.61	2.50	0.50
	19.5	65.13	19.40	12.57	1.14	1.54	0.23		64.47	16.92	14.48	0.88	2.89	0.35
	21	64.73	19.52	13.08	1.01	1.44	0.21		62.97	20.17	12.94	0.77	2.92	0.23
	22.5	65.58	19.23	12.28	1.06	1.65	0.21		63.81	18.63	13.40	0.95	2.93	0.29
	24	65.28	19.29	12.41	1.24	1.58	0.20		64.48	18.69	13.28	0.90	2.37	0.26
	25.5	64.93	19.58	12.52	1.13	1.61	0.22		64.32	18.97	13.30	0.81	2.38	0.21
	27	64.38	18.71	14.14	1.08	1.40	0.29		64.77	18.50	12.43	1.21	2.87	0.22
	28.5	64.02	18.39	14.63	1.11	1.58	0.28		64.20	19.07	12.77	1.12	2.57	0.27
	30	64.07	18.83	14.41	0.81	1.59	0.29		64.07	18.74	13.61	1.20	2.17	0.22
3	0	64.65	18.96	13.63	1.02	1.48	0.26	4	64.72	18.96	13.43	1.23	1.42	0.24
	1.5	64.75	19.10	14.02	0.70	1.22	0.22		64.91	19.34	13.05	1.00	1.46	0.24
	3	64.27	19.11	13.97	0.98	1.39	0.27		65.12	19.46	12.79	1.04	1.37	0.22
	4.5	64.29	18.61	14.41	0.97	1.45	0.27		65.31	18.94	12.91	1.21	1.43	0.20
	6	63.60	19.21	14.68	1.01	1.16	0.34		64.39	19.79	13.02	1.15	1.44	0.21
	7.5	64.83	18.76	13.71	1.04	1.37	0.29		64.37	19.68	13.21	1.17	1.34	0.22
	9	64.57	19.21	13.55	1.05	1.39	0.23		65.06	20.05	12.16	0.97	1.54	0.22
	10.5	65.26	18.90	12.83	1.23	1.55	0.24		65.65	19.72	11.89	1.17	1.39	0.18
	12	64.38	20.32	12.39	1.15	1.54	0.23		65.43	19.74	12.17	0.91	1.50	0.25
	13.5	65.59	19.43	12.23	1.03	1.48	0.24		65.47	19.02	12.84	0.98	1.44	0.26
	15	65.50	18.55	13.40	0.80	1.45	0.30		62.49	17.65	17.24	0.82	1.36	0.45
	16.5	63.54	17.55	16.55	0.61	1.32	0.44		64.21	17.73	15.33	0.91	1.45	0.37
	18	64.11	17.99	15.12	0.94	1.51	0.34		65.18	18.47	13.47	1.16	1.46	0.26
	19.5	64.67	19.85	12.50	1.18	1.59	0.21		65.24	19.45	12.27	1.14	1.68	0.22
	21	66.42	19.16	11.57	1.23	1.38	0.23		65.16	19.72	12.27	1.12	1.56	0.17
	22.5	65.12	19.93	12.22	1.09	1.42	0.22		64.85	19.55	12.37	1.41	1.63	0.18
	24	64.41	19.84	12.87	1.06	1.60	0.22		65.32	20.06	12.30	0.84	1.29	0.19
	25.5	64.36	19.78	12.90	1.24	1.51	0.21		65.81	18.64	12.86	1.12	1.37	0.21
	27	64.95	18.86	13.42	1.19	1.35	0.23		65.26	19.57	12.44	1.06	1.44	0.22
	28.5	65.24	18.82	12.97	1.25	1.46	0.26		65.01	19.35	12.77	1.11	1.55	0.22
	30	65.63	18.60	13.01	0.97	1.57	0.23		64.86	19.29	13.29	0.95	1.40	0.21
5	0	65.18	19.55	13.29	0.90	0.85	0.23	6						
	1.5	65.37	19.41	13.38	1.00	0.61	0.23							
	3	64.70	19.25	13.94	1.03	0.83	0.24							
	4.5	66.10	19.26	12.63	1.14	0.63	0.24							

Meas.	Pos. (nm)	Fe	Cr	Ni	Mn	Mo	Si	Meas.	Fe	Cr	Ni	Mn	Mo	Si
5	6	65.82	19.53	12.59	1.07	0.78	0.20							
	7.5	65.42	19.62	12.89	1.20	0.65	0.21							
	9	66.37	19.39	12.18	1.13	0.70	0.23							
	10.5	64.76	20.13	12.91	1.21	0.77	0.22							
	12	66.30	19.31	12.23	1.20	0.76	0.20							
	13.5	66.20	19.68	12.32	0.98	0.58	0.23							
	15	64.62	17.99	15.30	0.87	0.87	0.36							
	16.5	65.02	16.53	16.43	0.88	0.74	0.41							
	18	65.79	18.08	14.05	0.92	0.83	0.34							
	19.5	66.05	19.04	12.87	1.07	0.77	0.20							
	21	65.57	19.58	12.90	1.06	0.70	0.20							
	22.5	65.75	19.73	12.60	1.02	0.66	0.24							
	24	65.53	19.79	12.49	1.17	0.79	0.22							
	25.5	65.53	19.61	12.72	1.10	0.85	0.20							
	27	65.07	19.84	12.89	1.22	0.74	0.24							
	28.5	65.48	18.83	13.55	1.07	0.80	0.28							
	30	66.00	18.57	13.17	1.13	0.88	0.25							

Ref-Hf, 500C, 3 dpa

Meas.	Pos. (nm)	Fe	Cr	Ni	Mn	Mo	Si	Meas.	Fe	Cr	Ni	Mn	Mo	Si
1	0	63.72	18.90	14.79	1.18	1.19	0.22	2	66.59	16.88	14.17	1.01	1.14	0.21
	1.5	63.45	19.25	14.60	1.16	1.32	0.22		65.69	17.66	14.36	0.96	1.11	0.22
	3	65.28	18.46	13.85	0.98	1.16	0.26		66.04	17.06	14.41	1.09	1.14	0.26
	4.5	65.32	18.71	13.49	1.07	1.15	0.26		65.82	18.20	14.23	0.53	1.00	0.23
	6	66.33	18.64	12.77	0.86	1.15	0.26		66.71	16.85	14.36	0.95	0.87	0.27
	7.5	65.34	19.13	13.11	0.90	1.31	0.20		67.80	16.64	13.38	0.97	0.98	0.23
	9	66.66	18.02	12.96	0.93	1.21	0.22		67.96	16.79	13.09	0.98	0.92	0.27
	10.5	68.03	17.60	12.56	0.70	0.90	0.21		70.29	15.54	12.42	0.67	0.81	0.26
	12	67.85	16.23	14.02	0.78	0.82	0.30		70.94	13.05	14.18	0.81	0.77	0.25
	13.5	63.81	12.11	22.18	0.61	0.75	0.54		64.34	11.12	22.80	0.58	0.78	0.38
	15	50.71	8.15	39.36	0.38	0.63	0.76		58.38	9.77	30.05	0.60	0.70	0.49
	16.5	55.91	7.91	34.43	0.65	0.67	0.42		63.99	13.34	20.93	0.73	0.66	0.34
	18	63.58	10.64	24.33	0.59	0.61	0.25		68.31	16.83	13.20	0.71	0.69	0.26
	19.5	69.26	13.31	15.82	0.72	0.67	0.23		67.60	17.78	12.62	0.77	0.98	0.25
	21	69.01	15.16	13.85	0.83	0.91	0.24		65.94	18.05	13.46	1.24	1.06	0.25
	22.5	67.38	17.57	12.72	0.92	1.19	0.23		64.92	19.71	12.94	0.91	1.27	0.25
	24	65.99	17.98	13.68	0.92	1.18	0.25		64.43	19.67	13.08	1.15	1.40	0.27
	25.5	65.33	18.04	14.13	0.95	1.33	0.22		64.26	19.96	13.39	0.84	1.26	0.29
	27	64.88	17.45	14.84	1.28	1.25	0.30		65.80	19.23	12.58	0.92	1.28	0.19
	28.5	64.72	18.15	14.67	1.14	1.09	0.23		64.28	19.69	13.51	1.01	1.26	0.25
	30	64.12	18.08	15.44	0.86	1.28	0.23		63.52	20.38	13.77	0.85	1.21	0.27
3	0	65.36	19.27	12.86	0.96	1.30	0.24	4	65.53	18.44	13.74	0.78	1.25	0.26
	1.5	63.84	20.24	12.99	1.20	1.51	0.22		65.75	18.82	12.98	1.13	1.08	0.24
	3	65.63	19.16	12.35	1.21	1.43	0.22		66.00	17.42	14.26	0.95	1.16	0.22
	4.5	65.11	19.67	12.64	1.11	1.24	0.23		67.19	17.29	13.42	0.75	1.13	0.23
	6	65.66	19.32	12.50	0.98	1.31	0.23		67.07	17.58	13.30	0.73	1.05	0.27
	7.5	65.27	19.81	12.47	1.01	1.21	0.23		68.33	16.62	13.11	0.74	0.97	0.22
	9	65.84	19.21	12.74	0.88	1.08	0.26		69.52	15.67	12.94	0.82	0.80	0.25
	10.5	67.69	17.25	13.14	0.72	0.90	0.30		70.69	15.30	12.18	0.67	0.91	0.26
	12	59.82	12.22	26.29	0.35	0.78	0.54		70.53	12.58	15.03	0.76	0.80	0.31
	13.5	51.32	9.55	37.17	0.60	0.70	0.65		67.65	10.90	19.81	0.57	0.68	0.38
	15	53.12	7.40	37.71	0.69	0.62	0.47		57.99	8.69	31.51	0.68	0.63	0.50
	16.5	65.55	9.55	23.38	0.57	0.67	0.28		63.43	12.33	22.54	0.64	0.70	0.36
	18	65.48	10.58	22.52	0.43	0.71	0.27		67.82	13.96	16.33	0.77	0.78	0.34
	19.5	70.48	13.39	14.56	0.61	0.72	0.23		68.45	16.66	12.98	0.66	0.97	0.28
	21	68.79	16.29	13.00	0.90	0.82	0.19		67.04	17.71	12.94	0.96	1.05	0.29
	22.5	67.86	17.48	12.50	0.86	1.07	0.23		68.14	17.44	12.40	0.80	0.96	0.26
	24	66.58	18.39	12.92	0.91	0.96	0.25		66.24	16.90	14.84	0.84	0.94	0.23
	25.5	65.93	18.26	13.29	1.07	1.20	0.26		64.81	16.68	16.36	0.98	0.88	0.28
	27	65.41	17.84	14.20	1.13	1.17	0.24		64.57	17.26	16.29	0.65	0.89	0.32
	28.5	65.12	18.57	14.07	0.78	1.23	0.23		65.43	16.30	15.81	1.07	1.04	0.36
	30	65.23	18.39	14.05	0.85	1.21	0.26		65.76	16.75	15.26	1.02	0.87	0.34
5	0	65.24	18.73	13.20	1.16	1.42	0.24	6	66.02	17.72	13.60	1.35	1.07	0.24
	1.5	64.65	19.56	13.11	1.05	1.40	0.23		65.97	17.84	13.74	0.90	1.30	0.26
	3	65.72	18.95	12.76	1.06	1.28	0.23		66.22	18.01	13.42	0.85	1.27	0.24
	4.5	65.42	19.45	12.49	0.95	1.46	0.24		67.53	16.98	13.38	0.72	1.12	0.27

Meas.	Pos. (nm)	Fe	Cr	Ni	Mn	Mo	Si	Meas.	Fe	Cr	Ni	Mn	Mo	Si
5	6	65.75	19.32	12.46	0.94	1.27	0.25	6	67.09	17.60	13.16	0.76	1.10	0.29
	7.5	66.14	19.65	12.05	0.93	1.00	0.24		67.48	17.04	13.38	0.81	1.04	0.25
	9	67.47	18.75	11.57	0.86	1.07	0.27		69.06	16.05	12.65	1.05	0.94	0.26
	10.5	68.51	17.39	12.10	0.85	0.91	0.24		70.72	15.20	12.40	0.49	0.93	0.26
	12	68.60	13.93	15.70	0.58	0.84	0.35		71.12	14.79	12.49	0.54	0.80	0.26
	13.5	54.79	8.33	35.17	0.60	0.63	0.49		70.51	12.30	15.57	0.59	0.77	0.27
	15	66.02	11.48	21.01	0.44	0.76	0.29		56.55	9.27	32.50	0.50	0.67	0.50
	16.5	69.02	14.99	14.33	0.75	0.69	0.22		60.07	10.81	27.61	0.36	0.70	0.44
	18	66.30	12.34	19.66	0.80	0.67	0.23		68.03	16.35	13.71	0.78	0.84	0.29
	19.5	69.62	15.14	13.51	0.70	0.80	0.24		67.48	17.35	13.23	0.80	0.90	0.25
	21	68.87	16.00	12.99	1.01	0.91	0.22		66.72	17.14	14.05	1.00	0.84	0.26
	22.5	67.58	17.21	13.27	0.81	0.92	0.22		66.83	17.03	14.40	0.65	0.83	0.26
	24	66.12	18.16	13.46	1.00	1.04	0.22		66.15	16.69	15.06	0.86	0.97	0.27
	25.5	66.06	18.29	13.41	0.87	1.11	0.27		65.99	16.95	14.88	1.04	0.87	0.27
	27	65.07	18.24	14.31	0.97	1.16	0.25		65.59	17.19	14.96	1.08	0.93	0.25
	28.5	65.32	17.46	14.76	1.06	1.16	0.23		65.73	17.67	14.37	0.94	0.97	0.32
	30	64.75	18.30	14.56	1.09	1.03	0.27		66.40	17.59	13.69	1.00	1.00	0.33
7	0	63.91	20.60	12.62	1.12	1.51	0.25	8	65.92	18.16	13.55	0.94	1.25	0.19
	1.5	65.31	19.64	12.38	1.02	1.41	0.25		66.14	18.00	13.49	1.08	1.03	0.25
	3	64.96	19.94	12.56	0.90	1.40	0.24		66.81	17.61	13.45	0.84	1.03	0.26
	4.5	64.87	19.93	12.65	1.06	1.28	0.21		67.07	16.98	13.87	0.87	1.01	0.21
	6	66.69	19.34	11.58	0.98	1.17	0.23		67.67	16.54	13.60	0.96	1.01	0.22
	7.5	66.49	18.58	12.85	0.80	1.04	0.25		68.91	16.75	12.65	0.63	0.85	0.22
	9	66.79	18.46	12.47	0.92	1.13	0.23		70.48	14.85	12.83	0.67	0.98	0.18
	10.5	67.34	16.85	13.88	0.79	0.91	0.24		70.11	13.20	15.30	0.47	0.69	0.23
	12	68.83	14.84	14.44	0.79	0.83	0.27		69.59	11.38	17.35	0.63	0.72	0.33
	13.5	56.46	9.16	32.42	0.58	0.68	0.70		58.11	9.11	31.33	0.43	0.59	0.43
	15	61.08	9.24	27.80	0.66	0.76	0.46		68.27	12.59	17.54	0.63	0.69	0.28
	16.5	69.52	12.52	16.24	0.68	0.72	0.32		69.49	14.69	14.33	0.51	0.72	0.26
	18	70.15	14.65	13.60	0.60	0.76	0.24		67.96	17.56	12.61	0.84	0.82	0.21
	19.5	68.38	16.57	13.02	0.77	1.00	0.25		66.67	18.23	13.13	0.86	0.91	0.20
	21	67.82	16.47	13.51	0.93	1.02	0.23		66.17	18.38	13.18	0.97	1.09	0.21
	22.5	66.59	17.19	14.09	0.85	1.09	0.19		65.30	18.63	13.87	0.91	1.07	0.23
	24	65.79	18.01	14.10	0.84	1.02	0.24		65.83	19.23	12.67	0.90	1.11	0.25
	25.5	66.05	17.62	13.90	1.02	1.17	0.24		65.59	18.76	13.04	1.14	1.20	0.26
	27	65.54	18.30	13.65	1.05	1.22	0.24		65.78	18.72	12.94	1.09	1.26	0.22
	28.5	65.42	18.61	13.28	1.12	1.32	0.25		65.19	18.94	13.10	1.23	1.30	0.23
	30	65.08	19.55	13.21	0.70	1.17	0.29		65.22	18.62	13.29	1.17	1.48	0.22
9	0	64.73	19.56	13.14	0.90	1.45	0.22	10	65.89	17.73	13.99	0.93	1.22	0.24
	1.5	64.93	19.16	13.24	1.13	1.30	0.25		65.99	17.21	14.33	1.10	1.14	0.24
	3	65.12	19.80	12.26	1.21	1.40	0.22		66.40	17.59	13.24	1.26	1.23	0.29
	4.5	65.36	19.48	12.36	1.11	1.45	0.24		67.12	18.05	12.52	0.89	1.12	0.30
	6	65.42	19.64	12.38	0.88	1.46	0.22		68.28	16.97	12.40	0.88	1.16	0.31
	7.5	65.97	19.18	12.51	0.89	1.19	0.26		68.24	16.90	12.90	0.70	0.98	0.28
	9	67.19	18.35	12.24	0.84	1.13	0.25		72.05	14.15	12.22	0.58	0.73	0.27
	10.5	67.57	17.17	13.20	0.85	0.96	0.26		71.19	14.44	12.70	0.61	0.75	0.31
	12	68.06	14.70	15.54	0.58	0.82	0.30		72.12	14.35	11.96	0.64	0.68	0.26

Meas.	Pos. (nm)	Fe	Cr	Ni	Mn	Mo	Si	Meas.	Fe	Cr	Ni	Mn	Mo	Si
9	13.5	64.48	13.50	20.38	0.46	0.81	0.37	10	69.76	11.39	17.15	0.61	0.78	0.32
	15	56.65	8.87	32.45	0.61	0.77	0.66		58.46	9.67	30.42	0.43	0.54	0.48
	16.5	60.87	9.07	28.45	0.56	0.62	0.44		62.05	11.16	25.04	0.62	0.71	0.43
	18	69.54	16.59	12.06	0.68	0.88	0.25		67.90	15.18	15.11	0.82	0.68	0.31
	19.5	68.45	16.81	12.38	1.02	1.11	0.22		68.55	16.15	13.28	0.87	0.84	0.32
	21	66.39	18.18	13.10	0.93	1.14	0.26		66.22	18.88	13.01	0.73	0.88	0.28
	22.5	66.03	18.42	13.05	1.07	1.17	0.26		65.51	18.93	13.43	0.80	1.05	0.28
	24	65.41	18.93	13.10	0.98	1.37	0.21		65.99	18.27	13.45	0.96	1.08	0.25
	25.5	64.82	20.20	12.63	0.79	1.34	0.22		65.57	18.45	13.55	1.06	1.11	0.26
	27	64.87	20.61	11.91	0.90	1.45	0.26		64.27	19.44	13.62	0.97	1.40	0.29
	28.5	64.53	20.55	12.17	0.98	1.54	0.23		65.19	18.71	13.47	1.17	1.14	0.33
	30	64.86	19.85	12.53	1.13	1.38	0.25		65.67	18.64	13.18	1.10	1.07	0.34
11	0	64.56	19.87	12.73	1.14	1.44	0.27	12	65.58	18.34	13.58	1.05	1.19	0.26
	1.5	65.09	19.55	12.76	1.05	1.33	0.22		66.36	17.96	13.14	1.11	1.19	0.24
	3	64.66	19.74	12.90	1.21	1.28	0.20		67.22	16.66	13.91	0.92	1.06	0.23
	4.5	65.33	19.55	12.59	1.05	1.24	0.24		67.74	16.43	14.03	0.68	0.89	0.24
	6	65.25	19.66	12.77	0.84	1.24	0.24		68.40	16.41	13.37	0.68	0.90	0.24
	7.5	67.09	18.27	12.57	0.73	1.10	0.24		69.17	15.84	13.13	0.69	0.93	0.24
	9	67.79	18.15	11.81	0.92	1.10	0.23		70.15	15.28	12.78	0.75	0.83	0.22
	10.5	68.79	16.81	12.33	0.81	1.00	0.27		71.03	14.45	12.65	0.95	0.68	0.25
	12	66.59	14.68	16.95	0.57	0.91	0.31		58.81	9.07	30.66	0.39	0.64	0.43
	13.5	59.57	9.53	29.16	0.37	0.77	0.59		69.92	14.09	14.35	0.70	0.67	0.27
	15	60.55	8.52	29.12	0.65	0.64	0.52		70.35	13.52	14.59	0.54	0.72	0.28
	16.5	68.36	11.25	18.94	0.57	0.61	0.27		68.03	17.73	12.78	0.51	0.77	0.19
	18	70.82	14.51	12.97	0.62	0.83	0.25		68.20	17.52	12.54	0.65	0.84	0.26
	19.5	69.24	16.76	12.00	0.90	0.90	0.21		66.62	18.15	13.22	0.80	0.94	0.26
	21	67.92	17.61	12.74	0.61	0.93	0.19		66.34	18.13	13.07	1.13	1.04	0.28
	22.5	66.85	18.48	12.21	1.05	1.16	0.25		66.16	18.22	12.99	1.07	1.29	0.26
	24	65.59	18.53	13.11	1.31	1.22	0.24		65.25	18.83	13.40	1.05	1.24	0.22
	25.5	65.92	18.91	12.76	0.95	1.28	0.19		65.70	18.46	13.27	1.08	1.26	0.23
	27	63.92	20.63	12.87	0.89	1.45	0.24		65.00	18.66	13.61	1.18	1.31	0.25
	28.5	65.97	18.99	12.37	1.03	1.42	0.24		64.67	19.36	13.32	0.97	1.44	0.24
	30	64.52	20.08	12.66	1.15	1.36	0.22		65.20	18.95	13.21	1.07	1.33	0.25
13	0	64.82	18.70	14.07	1.00	1.19	0.22	14						
	1.5	67.08	17.77	12.57	1.08	1.26	0.24							
	3	66.36	17.89	12.93	1.35	1.20	0.26							
	4.5	66.15	17.58	13.99	0.98	1.08	0.24							
	6	67.23	16.93	13.74	0.82	1.08	0.20							
	7.5	67.76	16.83	13.42	0.69	1.07	0.23							
	9	67.49	16.37	14.07	0.89	0.95	0.22							
	10.5	68.83	15.66	13.82	0.64	0.83	0.23							
	12	70.06	14.52	13.42	0.86	0.88	0.26							
	13.5	61.88	9.64	26.92	0.49	0.68	0.40							
	15	61.59	10.53	26.39	0.43	0.62	0.44							
	16.5	69.56	14.63	14.29	0.57	0.69	0.26							
	18	69.05	15.02	14.30	0.60	0.73	0.30							
	19.5	70.12	15.08	13.19	0.69	0.70	0.21							

Meas.	Pos. (nm)	Fe	Cr	Ni	Mn	Mo	Si	Meas.	Fe	Cr	Ni	Mn	Mo	Si
13	21	66.69	18.23	13.02	0.82	0.99	0.25	14						
	22.5	67.17	18.27	12.71	0.64	0.98	0.24							
	24	65.44	18.85	13.17	1.19	1.12	0.23							
	25.5	66.65	18.24	12.77	0.87	1.21	0.26							
	27	65.65	18.93	12.94	1.02	1.25	0.21							
	28.5	65.63	18.87	12.99	1.02	1.25	0.25							
	30	64.67	19.53	13.27	1.01	1.29	0.23							

LoHf, 500C, 1 dpa

Meas.	Pos. (nm)	Fe	Cr	Ni	Mn	Mo	Si	Meas.	Fe	Cr	Ni	Mn	Mo	Si
1	0	65.16	18.72	13.36	1.18	1.33	0.26	2	65.29	18.74	13.27	1.08	1.34	0.28
	1.5	63.67	19.69	13.79	1.14	1.42	0.29		65.59	18.74	13.09	0.96	1.37	0.25
	3	65.52	18.41	13.10	1.36	1.33	0.27		66.19	18.35	12.90	0.91	1.40	0.24
	4.5	65.33	18.98	12.75	1.34	1.33	0.27		66.99	17.65	13.35	0.65	1.10	0.26
	6	64.61	19.50	13.32	1.19	1.09	0.29		67.70	16.01	13.87	0.82	1.30	0.30
	7.5	65.81	18.61	13.14	1.03	1.11	0.29		66.70	15.37	16.00	0.65	0.98	0.31
	9	65.75	18.93	12.80	1.16	1.07	0.29		63.20	14.12	20.75	0.53	1.09	0.30
	10.5	66.66	17.66	13.49	0.84	0.98	0.38		64.65	13.50	19.86	0.70	1.02	0.27
	12	64.68	15.58	17.53	0.79	0.94	0.48		67.64	14.37	15.84	0.79	0.98	0.38
	13.5	64.75	15.31	17.80	0.76	1.06	0.33		67.45	14.25	16.16	0.75	0.99	0.41
	15	62.03	13.96	22.03	0.62	1.00	0.36		67.87	15.48	14.43	0.87	0.91	0.44
	16.5	60.59	12.67	24.63	0.67	1.08	0.36		67.73	16.13	14.02	0.75	0.95	0.42
	18	62.83	13.08	21.96	0.68	1.17	0.28		68.16	16.48	13.35	0.72	0.95	0.34
	19.5	63.07	12.87	21.91	0.76	1.12	0.27		68.00	16.95	12.82	0.99	0.93	0.30
	21	63.21	13.48	21.07	0.69	1.28	0.28		67.42	17.60	12.76	0.85	1.07	0.29
	22.5	64.46	13.44	19.90	0.85	1.08	0.27		66.98	17.74	12.93	1.00	1.08	0.28
	24	64.89	13.94	18.88	0.81	1.21	0.27		66.55	18.27	12.87	0.86	1.16	0.28
	25.5	66.40	14.32	17.08	0.68	1.26	0.26		66.10	18.38	13.12	0.97	1.14	0.30
	27	68.03	15.84	13.71	0.91	1.25	0.26		66.82	18.22	12.30	1.17	1.20	0.29
	28.5	67.49	16.50	13.47	0.93	1.33	0.28		65.65	18.42	13.30	1.26	1.10	0.26
	30	67.04	16.68	13.75	0.90	1.36	0.26		66.25	18.14	12.90	1.19	1.22	0.30
3	0	65.00	19.23	13.08	1.01	1.40	0.28	4	64.91	18.93	13.32	1.26	1.33	0.26
	1.5	65.24	18.92	12.94	1.17	1.47	0.26		64.76	19.03	13.62	0.99	1.34	0.26
	3	65.22	18.81	13.09	1.07	1.55	0.26		65.18	18.69	13.54	0.97	1.32	0.30
	4.5	66.06	18.54	12.66	1.13	1.30	0.31		64.99	18.94	13.56	0.99	1.24	0.29
	6	65.87	18.88	12.74	0.99	1.25	0.27		65.71	18.62	13.25	0.99	1.19	0.24
	7.5	66.09	18.61	12.88	0.90	1.26	0.27		66.21	18.39	12.90	1.00	1.21	0.30
	9	66.56	18.02	12.91	0.97	1.24	0.30		66.07	17.93	13.49	1.02	1.23	0.27
	10.5	66.39	18.11	13.04	1.12	1.05	0.29		67.64	17.34	12.86	0.73	1.15	0.29
	12	67.23	17.15	13.43	0.78	1.07	0.35		66.83	16.88	14.08	0.86	1.06	0.29
	13.5	65.14	15.31	17.41	0.75	1.02	0.37		65.94	15.88	16.21	0.71	0.96	0.30
	15	62.20	14.57	21.01	0.79	0.99	0.44		63.82	14.50	19.64	0.74	0.94	0.36
	16.5	60.46	12.65	24.74	0.68	1.00	0.47		61.29	13.09	23.34	0.71	1.06	0.51
	18	64.71	13.19	20.08	0.78	0.93	0.30		64.14	13.34	20.57	0.70	0.85	0.39
	19.5	65.76	14.23	17.96	0.64	1.15	0.26		66.11	13.39	18.52	0.73	0.96	0.28
	21	67.46	14.53	15.98	0.66	1.10	0.27		67.55	14.58	15.71	0.73	1.14	0.30
	22.5	68.21	15.33	14.25	0.82	1.14	0.26		67.29	15.91	14.59	0.86	1.07	0.28
	24	68.28	16.08	13.41	0.80	1.15	0.28		68.88	16.03	13.04	0.66	1.12	0.27
	25.5	68.84	15.95	13.02	0.76	1.17	0.25		68.05	16.26	13.23	1.03	1.18	0.26
	27	66.84	17.37	13.25	1.05	1.22	0.27		67.84	16.13	13.62	0.94	1.19	0.29
	28.5	66.92	18.14	12.54	0.91	1.23	0.27		67.27	17.32	13.16	0.79	1.15	0.30
	30	66.89	17.45	13.11	1.00	1.29	0.27		67.76	17.23	12.77	0.80	1.14	0.31
5	0	64.96	18.88	13.50	1.16	1.23	0.27	6	66.02	18.49	12.88	1.18	1.16	0.26
	1.5	65.47	18.65	13.11	1.13	1.37	0.27		65.49	18.90	13.08	1.04	1.19	0.31
	3	65.33	18.67	13.42	0.96	1.32	0.31		65.64	18.67	13.06	1.17	1.15	0.31
	4.5	65.70	18.31	13.25	1.10	1.37	0.27		65.99	18.65	12.86	0.99	1.21	0.30

Meas.	Pos. (nm)	Fe	Cr	Ni	Mn	Mo	Si	Meas.	Fe	Cr	Ni	Mn	Mo	Si
5	6	65.93	18.26	13.18	0.91	1.45	0.27	6	66.55	17.85	13.03	1.18	1.08	0.31
	7.5	67.00	17.77	12.71	0.99	1.24	0.29		66.57	18.42	12.52	1.09	1.08	0.31
	9	67.40	16.83	13.45	0.90	1.16	0.27		67.09	17.07	13.59	0.83	1.10	0.31
	10.5	66.49	15.78	15.52	0.74	1.21	0.25		66.41	16.23	15.25	0.78	1.03	0.31
	12	63.31	14.72	19.89	0.69	1.09	0.30		64.91	14.99	18.22	0.58	1.02	0.28
	13.5	62.27	14.24	21.44	0.77	0.91	0.36		63.45	14.46	20.18	0.66	0.97	0.29
	15	63.49	13.73	20.75	0.68	0.91	0.45		63.90	13.64	20.56	0.66	0.91	0.33
	16.5	66.68	14.41	16.82	0.75	0.94	0.40		64.90	13.55	19.61	0.75	0.83	0.37
	18	68.01	15.26	14.67	0.80	0.88	0.38		66.78	14.07	17.25	0.67	0.78	0.45
	19.5	67.84	15.85	14.32	0.79	0.89	0.32		67.79	14.54	15.60	0.89	0.79	0.38
	21	68.09	16.52	13.33	0.76	1.03	0.28		68.40	15.29	14.46	0.65	0.93	0.28
	22.5	67.78	16.74	13.35	0.84	1.02	0.27		68.41	16.35	13.26	0.74	0.97	0.27
	24	67.31	17.31	13.14	0.86	1.12	0.25		67.25	16.69	13.76	0.99	1.05	0.27
	25.5	67.19	17.85	12.79	0.73	1.15	0.27		67.96	16.65	12.93	0.81	1.36	0.30
	27	67.75	17.58	12.56	0.64	1.17	0.30		67.29	16.77	13.29	1.12	1.27	0.25
	28.5	67.47	17.66	12.51	0.92	1.15	0.29		67.16	17.50	12.81	1.02	1.24	0.27
	30	66.99	17.71	12.64	1.07	1.27	0.32		66.79	18.24	12.61	0.81	1.30	0.25

LoHf, 500C, 3 dpa

Meas.	Pos. (nm)	Fe	Cr	Ni	Mn	Mo	Si	Meas.	Fe	Cr	Ni	Mn	Mo	Si
1	0	65.62	20.38	11.68	1.09	1.08	0.15	2	65.15	20.41	12.07	1.13	1.10	0.14
	1.5	66.25	20.27	11.31	1.06	1.00	0.12		65.65	21.07	11.15	0.93	1.06	0.14
	3	65.62	20.41	11.88	0.95	0.98	0.15		65.72	20.45	11.60	1.07	1.04	0.12
	4.5	65.96	20.13	11.86	1.04	0.90	0.12		66.43	20.17	11.49	0.88	0.92	0.12
	6	67.04	20.00	11.10	0.99	0.73	0.13		65.93	20.67	11.38	1.09	0.80	0.13
	7.5	66.42	20.22	11.77	0.70	0.77	0.12		67.37	19.50	11.38	0.82	0.80	0.12
	9	67.33	19.49	11.55	0.82	0.69	0.13		67.34	20.04	11.21	0.58	0.71	0.13
	10.5	66.84	19.52	12.06	0.78	0.66	0.14		68.33	18.38	11.82	0.71	0.60	0.16
	12	68.11	17.03	13.57	0.61	0.53	0.15		68.84	15.48	14.21	0.76	0.51	0.20
	13.5	66.71	13.90	18.13	0.44	0.63	0.19		67.98	15.65	15.13	0.46	0.63	0.16
	15	57.62	9.48	31.66	0.45	0.55	0.24		54.41	9.24	34.98	0.43	0.61	0.34
	16.5	57.55	8.52	32.84	0.32	0.59	0.18		53.37	8.21	37.15	0.43	0.62	0.22
	18	65.07	8.66	25.30	0.32	0.53	0.13		64.49	9.09	25.41	0.33	0.53	0.14
	19.5	69.28	9.60	19.97	0.53	0.51	0.11		69.34	10.50	19.24	0.33	0.49	0.09
	21	70.45	9.74	18.94	0.25	0.51	0.11		71.33	11.63	15.98	0.39	0.55	0.12
	22.5	72.98	11.64	14.26	0.46	0.56	0.09		71.80	12.26	14.93	0.38	0.53	0.11
	24	72.87	13.40	12.24	0.68	0.72	0.11		72.66	13.07	13.04	0.54	0.58	0.11
	25.5	72.39	14.92	11.32	0.49	0.75	0.12		72.70	14.11	11.63	0.67	0.78	0.12
	27	71.92	15.63	11.11	0.58	0.65	0.11		70.69	15.79	11.99	0.66	0.78	0.10
	28.5	70.92	15.78	11.57	0.85	0.76	0.12		71.20	16.33	10.68	0.81	0.86	0.12
	30								70.61	16.91	11.02	0.57	0.78	0.10
3	0	65.71	20.37	11.46	1.11	1.21	0.13	4	65.63	20.39	11.96	0.94	0.94	0.13
	1.5	65.63	20.21	11.73	1.15	1.13	0.15		66.33	20.00	11.43	1.03	1.08	0.13
	3	65.92	20.18	11.59	1.12	1.06	0.13		66.33	20.24	11.27	0.97	1.04	0.15
	4.5	66.52	20.19	11.40	0.95	0.81	0.13		66.10	20.36	11.64	0.81	0.94	0.15
	6	66.34	20.32	11.39	1.00	0.82	0.14		65.98	20.33	11.49	1.04	1.03	0.14
	7.5	66.34	20.23	11.40	1.08	0.82	0.13		66.93	19.52	11.79	0.95	0.68	0.13
	9	67.34	19.70	11.16	0.81	0.86	0.13		66.70	19.71	12.02	0.65	0.78	0.14
	10.5	68.49	18.43	11.51	0.75	0.68	0.14		67.34	19.37	11.57	0.94	0.64	0.14
	12	68.79	16.08	13.79	0.63	0.55	0.16		68.97	16.55	13.28	0.48	0.56	0.16
	13.5	65.81	14.19	18.65	0.64	0.53	0.18		64.86	13.58	20.40	0.39	0.56	0.22
	15	55.35	8.86	34.50	0.53	0.49	0.28		51.71	8.31	38.70	0.41	0.56	0.31
	16.5	56.91	8.30	33.73	0.32	0.56	0.17		58.28	8.32	32.29	0.29	0.64	0.17
	18	58.90	8.41	31.50	0.51	0.52	0.16		65.96	9.52	23.45	0.41	0.54	0.12
	19.5	67.66	9.14	22.03	0.46	0.58	0.12		70.56	10.33	17.86	0.61	0.52	0.13
	21	71.78	11.62	15.54	0.40	0.52	0.14		71.84	11.37	15.54	0.49	0.65	0.11
	22.5	72.87	12.67	13.18	0.50	0.66	0.11		71.61	11.83	15.47	0.40	0.59	0.10
	24	72.58	13.96	12.16	0.57	0.61	0.13		72.11	12.99	13.55	0.54	0.67	0.14
	25.5	72.82	13.69	12.14	0.57	0.67	0.11		73.03	13.97	11.55	0.60	0.74	0.11
	27	71.90	15.26	11.16	0.81	0.76	0.10		72.33	15.30	10.94	0.63	0.71	0.10
	28.5	71.70	15.85	11.02	0.56	0.75	0.11		71.26	15.52	11.46	0.85	0.81	0.10
	30	71.93	15.46	11.18	0.56	0.77	0.10		70.01	16.71	11.43	0.87	0.86	0.12
5	0	65.65	20.28	11.77	1.01	1.14	0.16	6	65.37	20.92	11.58	0.94	1.09	0.11
	1.5	66.21	20.16	11.25	1.20	1.06	0.12		66.23	20.22	11.23	1.09	1.09	0.13
	3	66.01	19.92	11.79	1.06	1.08	0.14		66.66	20.11	11.04	1.03	1.05	0.12
	4.5	66.06	20.29	11.69	0.94	0.92	0.11		66.34	20.42	11.04	1.15	0.92	0.13

Meas.	Pos. (nm)	Fe	Cr	Ni	Mn	Mo	Si	Meas.	Fe	Cr	Ni	Mn	Mo	Si
5	6	66.98	19.98	11.09	0.92	0.89	0.14	6	66.28	20.02	11.56	1.13	0.90	0.11
	7.5	67.15	20.25	11.03	0.70	0.73	0.14		67.13	20.47	10.82	0.73	0.75	0.11
	9	67.70	19.40	11.40	0.70	0.66	0.14		69.06	18.38	11.24	0.66	0.55	0.11
	10.5	68.47	18.04	12.11	0.61	0.65	0.13		66.51	14.15	18.18	0.52	0.47	0.17
	12	69.14	15.78	13.89	0.40	0.60	0.18		59.92	10.19	28.69	0.48	0.49	0.23
	13.5	67.36	13.90	17.34	0.61	0.60	0.18		61.20	10.77	26.82	0.47	0.53	0.20
	15	50.87	8.06	39.71	0.46	0.61	0.29		53.09	7.66	37.88	0.52	0.60	0.25
	16.5	58.33	8.24	32.35	0.37	0.54	0.16		63.49	8.86	26.57	0.45	0.47	0.16
	18	62.52	8.53	27.80	0.42	0.59	0.14		69.38	9.58	19.97	0.39	0.58	0.11
	19.5	68.84	9.95	20.12	0.50	0.48	0.11		72.21	12.02	14.85	0.31	0.51	0.10
	21	70.48	11.20	17.31	0.37	0.53	0.11		72.89	12.97	12.62	0.77	0.63	0.11
	22.5	71.89	11.94	15.09	0.38	0.60	0.11		72.81	13.48	12.02	0.86	0.71	0.13
	24	72.86	12.84	12.94	0.57	0.66	0.12		71.97	14.75	11.85	0.73	0.60	0.11
	25.5	72.93	14.22	11.49	0.47	0.77	0.12		71.09	15.55	11.64	0.81	0.80	0.11
	27	72.53	14.40	11.53	0.73	0.70	0.12		71.25	16.07	11.12	0.63	0.81	0.12
	28.5	70.80	16.07	11.42	0.86	0.73	0.13		70.39	17.39	10.43	0.72	0.96	0.11
	30	70.68	16.44	11.20	0.70	0.86	0.12		69.01	17.34	12.02	0.63	0.88	0.12
7	0	64.76	20.05	12.53	1.18	1.31	0.18	8	64.41	20.22	12.71	1.22	1.27	0.17
	1.5	63.42	21.18	12.88	1.12	1.19	0.21		65.03	19.90	12.46	1.13	1.29	0.18
	3	65.05	20.75	11.99	0.96	1.07	0.18		64.67	21.07	11.87	1.12	1.10	0.17
	4.5	64.76	20.85	12.51	0.81	0.93	0.14		64.55	20.60	12.39	1.26	1.02	0.19
	6	65.77	20.12	12.01	1.18	0.79	0.14		65.57	20.17	12.16	0.81	1.10	0.18
	7.5	66.02	20.25	11.60	1.11	0.88	0.14		64.65	20.56	12.90	0.87	0.86	0.17
	9	65.93	19.10	13.05	1.06	0.65	0.22		64.24	21.06	12.67	0.99	0.88	0.16
	10.5	55.97	13.42	29.08	0.54	0.49	0.50		63.89	17.35	17.14	0.76	0.61	0.25
	12	46.30	8.85	43.50	0.38	0.53	0.44		54.69	13.64	30.01	0.59	0.59	0.48
	13.5	47.29	8.86	42.39	0.34	0.63	0.49		47.66	8.35	42.64	0.48	0.46	0.41
	15	49.76	8.27	40.87	0.39	0.43	0.28		50.09	7.61	40.96	0.52	0.51	0.31
	16.5	55.66	8.12	34.71	0.67	0.56	0.28		55.23	8.19	35.42	0.40	0.51	0.25
	18	60.35	8.59	29.86	0.41	0.52	0.27		59.82	8.13	30.82	0.48	0.53	0.23
	19.5	66.54	8.88	23.60	0.27	0.45	0.26		59.94	8.66	30.26	0.44	0.46	0.25
	21	69.61	9.73	19.39	0.46	0.59	0.21		66.12	8.54	24.15	0.51	0.46	0.21
	22.5	71.29	10.11	17.23	0.57	0.51	0.29		71.92	10.60	16.35	0.39	0.53	0.21
	24	72.85	10.73	14.99	0.65	0.55	0.23		72.99	10.85	14.78	0.54	0.62	0.21
	25.5	73.50	12.33	12.82	0.47	0.66	0.21		73.16	12.91	12.76	0.29	0.63	0.24
	27	73.56	13.55	11.45	0.65	0.54	0.25		72.88	13.42	12.09	0.65	0.72	0.24
	28.5	72.58	14.17	11.67	0.57	0.73	0.27		72.27	13.98	12.22	0.60	0.68	0.25
	30	71.17	15.80	11.57	0.55	0.69	0.23		71.42	15.76	11.13	0.59	0.89	0.21
9	0	63.57	20.82	13.22	0.89	1.32	0.17	10	64.41	20.42	12.41	1.25	1.31	0.20
	1.5	64.99	20.78	11.79	1.04	1.25	0.14		64.33	20.97	12.16	1.18	1.17	0.19
	3	64.22	20.76	12.40	1.27	1.18	0.17		64.81	20.66	11.86	1.36	1.13	0.17
	4.5	65.49	20.53	11.71	0.94	1.17	0.16		64.64	20.45	12.46	1.01	1.23	0.21
	6	66.07	19.18	12.27	1.21	1.12	0.16		66.14	19.23	12.22	1.09	1.19	0.14
	7.5	64.82	20.98	12.01	1.08	0.94	0.16		64.66	21.14	11.98	1.05	0.99	0.17
	9	65.49	20.49	11.87	1.09	0.87	0.20		65.68	20.73	11.55	0.93	0.96	0.16
	10.5	65.58	19.28	13.50	0.79	0.68	0.16		66.01	19.92	11.79	1.15	0.96	0.16
	12	61.63	15.68	21.12	0.68	0.51	0.37		65.46	20.18	12.25	1.07	0.86	0.17

Meas.	Pos. (nm)	Fe	Cr	Ni	Mn	Mo	Si	Meas.	Fe	Cr	Ni	Mn	Mo	Si
9	13.5	47.81	8.16	42.42	0.65	0.47	0.49	10	65.70	19.57	12.91	0.93	0.72	0.18
	15	49.56	7.81	41.48	0.39	0.45	0.32		65.73	20.18	12.26	0.91	0.72	0.20
	16.5	52.38	8.36	38.22	0.25	0.50	0.29		65.30	17.24	16.02	0.62	0.56	0.26
	18	55.41	8.38	35.16	0.38	0.48	0.19		57.09	13.71	27.67	0.60	0.49	0.44
	19.5	58.46	7.86	32.53	0.44	0.46	0.25		47.87	8.54	42.17	0.49	0.51	0.43
	21	62.61	8.51	27.97	0.25	0.43	0.24		52.59	8.39	37.80	0.42	0.51	0.28
	22.5	58.65	7.77	32.31	0.49	0.53	0.24		56.46	8.46	33.88	0.41	0.55	0.22
	24	58.58	8.25	32.05	0.50	0.39	0.22		60.99	8.63	29.01	0.57	0.55	0.25
	25.5	67.86	8.93	21.95	0.46	0.54	0.26		67.42	9.12	22.29	0.38	0.54	0.24
	27	71.52	10.41	16.98	0.38	0.48	0.23		67.20	8.75	22.96	0.44	0.43	0.21
	28.5	73.48	13.06	12.20	0.45	0.58	0.24		71.37	9.75	17.68	0.51	0.48	0.22
	30	72.38	13.65	12.38	0.75	0.60	0.25		73.15	10.97	14.59	0.55	0.50	0.24
11	0	64.93	20.51	11.94	1.28	1.19	0.14	12	65.03	20.23	12.34	0.80	1.43	0.18
	1.5	64.46	21.00	11.85	1.22	1.28	0.18		64.50	20.36	12.50	1.03	1.44	0.17
	3	64.62	20.87	12.08	1.10	1.16	0.17		65.88	19.58	12.25	0.79	1.33	0.16
	4.5	65.19	20.84	11.76	1.11	0.96	0.14		63.30	21.53	12.48	0.99	1.52	0.18
	6	65.10	20.49	12.09	1.21	0.96	0.15		64.77	20.85	11.76	1.17	1.27	0.17
	7.5	65.27	21.22	11.64	0.78	0.94	0.16		64.49	20.47	12.25	1.35	1.27	0.17
	9	66.15	20.21	11.71	0.93	0.83	0.18		64.32	21.35	12.13	0.99	1.03	0.17
	10.5	65.90	19.67	12.44	1.06	0.75	0.18		66.00	20.71	11.20	1.14	0.78	0.18
	12	66.88	18.34	13.33	0.64	0.58	0.22		65.04	20.11	12.96	0.90	0.84	0.16
	13.5	49.37	10.30	38.88	0.49	0.49	0.48		63.93	19.34	15.32	0.48	0.72	0.21
	15	51.55	7.98	39.38	0.36	0.46	0.27		46.16	10.61	41.57	0.41	0.61	0.65
	16.5	61.24	8.64	28.95	0.47	0.48	0.22		47.45	8.22	43.14	0.40	0.48	0.32
	18	62.68	8.51	27.80	0.35	0.40	0.25		51.01	7.61	40.23	0.33	0.57	0.26
	19.5	63.83	8.59	26.47	0.44	0.46	0.21		56.37	7.96	34.54	0.40	0.48	0.26
	21	65.47	8.54	24.75	0.53	0.48	0.23		60.53	8.42	29.82	0.46	0.51	0.28
	22.5	70.82	9.79	18.22	0.42	0.54	0.21		66.57	9.43	22.67	0.58	0.52	0.23
	24	73.90	11.03	13.67	0.63	0.58	0.20		69.96	10.23	18.57	0.42	0.54	0.28
	25.5	72.84	12.88	12.70	0.73	0.62	0.24		72.02	12.65	14.12	0.31	0.66	0.24
	27	72.70	13.07	12.56	0.75	0.71	0.20		72.68	13.37	12.51	0.60	0.61	0.22
	28.5	72.98	13.99	11.54	0.57	0.68	0.24		71.67	14.50	12.45	0.54	0.59	0.25
	30	71.86	15.10	11.42	0.65	0.72	0.25		70.23	15.79	12.27	0.64	0.82	0.25

HiHf, 500C, 1 dpa

Meas.	Pos. (nm)	Fe	Cr	Ni	Mn	Mo	Si	Meas.	Fe	Cr	Ni	Mn	Mo	Si
1	0	65.78	18.96	12.79	0.97	1.32	0.19	2	64.77	19.30	13.20	1.14	1.36	0.23
	1.5	65.01	19.13	13.51	0.88	1.29	0.19		64.66	18.54	14.08	1.13	1.42	0.18
	3	66.31	17.96	13.14	1.23	1.15	0.20		65.99	18.10	12.91	1.47	1.33	0.20
	4.5	66.25	18.16	13.22	0.99	1.17	0.21		66.67	17.59	12.89	1.54	1.15	0.16
	6	68.56	17.01	12.16	0.90	1.19	0.17		66.96	17.64	12.94	1.08	1.16	0.21
	7.5	67.08	16.59	14.15	0.90	1.09	0.20		66.53	17.92	13.11	1.13	1.12	0.20
	9	67.34	15.55	14.99	0.87	1.01	0.25		67.42	17.55	12.98	0.61	1.24	0.20
	10.5	63.88	14.68	19.03	1.14	1.06	0.22		68.95	15.26	13.67	0.92	0.99	0.22
	12	60.86	14.90	22.01	0.80	1.13	0.30		65.54	15.06	17.42	0.77	0.98	0.23
	13.5	62.54	14.15	20.98	0.94	1.15	0.23		61.01	13.85	22.80	0.93	1.09	0.32
	15	63.23	14.57	19.70	1.24	1.02	0.24		61.59	13.49	22.52	0.87	1.26	0.27
	16.5	65.09	14.57	18.42	0.71	0.98	0.23		62.55	14.39	20.93	0.86	1.03	0.24
	18	65.14	15.54	17.22	0.84	1.06	0.20		64.24	14.86	18.82	0.79	1.05	0.24
	19.5	66.09	14.99	16.71	0.95	1.03	0.23		64.57	15.75	17.84	0.74	0.88	0.22
	21	65.42	15.97	16.16	1.09	1.17	0.18		66.16	15.42	16.28	0.77	1.18	0.19
	22.5	66.72	16.26	14.95	0.77	1.09	0.21		66.73	15.82	15.11	1.02	1.13	0.19
	24	66.51	16.47	14.67	1.07	1.06	0.22		66.04	16.61	14.98	1.14	1.03	0.19
	25.5	66.82	15.91	14.90	1.06	1.07	0.24		65.56	16.27	15.85	0.88	1.22	0.22
	27	66.93	16.93	13.81	0.96	1.15	0.23		66.94	16.64	14.24	0.92	1.06	0.20
	28.5	66.79	17.68	13.03	1.19	1.13	0.19		66.98	16.28	14.43	0.98	1.12	0.20
	30	66.82	17.44	13.15	1.11	1.27	0.21		66.99	16.46	14.06	0.86	1.40	0.23
3	0	64.62	19.08	13.95	0.83	1.30	0.22	4	65.50	18.69	13.27	1.03	1.32	0.19
	1.5	65.62	18.29	13.65	0.94	1.34	0.18		64.60	19.71	13.11	1.18	1.21	0.20
	3	65.97	18.07	13.41	1.05	1.31	0.19		66.30	18.25	12.89	0.96	1.38	0.22
	4.5	65.81	17.81	13.79	1.08	1.31	0.19		66.36	18.63	12.65	0.92	1.25	0.19
	6	66.69	17.39	13.53	0.95	1.24	0.21		66.63	17.41	13.58	1.18	1.02	0.18
	7.5	67.29	16.39	13.94	0.92	1.24	0.23		66.72	17.36	13.39	1.08	1.21	0.23
	9	67.15	16.16	14.96	0.57	0.93	0.22		67.45	15.91	14.31	0.97	1.15	0.21
	10.5	63.21	14.62	19.75	0.99	1.13	0.29		67.50	14.55	15.76	0.86	1.14	0.19
	12	60.37	14.75	22.92	0.65	1.03	0.28		63.01	14.26	20.38	0.78	1.28	0.29
	13.5	61.51	13.87	22.55	0.74	1.05	0.29		60.85	13.84	22.82	0.85	1.33	0.31
	15	63.02	14.70	20.19	0.88	1.00	0.22		61.34	13.69	22.84	0.79	1.08	0.26
	16.5	63.76	15.14	19.16	0.85	0.85	0.24		62.73	14.55	20.56	0.81	1.06	0.28
	18	64.30	15.13	18.68	0.70	1.00	0.20		65.06	15.25	17.82	0.81	0.83	0.24
	19.5	65.18	15.49	17.18	0.81	1.12	0.23		65.14	15.72	17.34	0.65	0.92	0.22
	21	65.23	15.80	16.84	0.97	0.96	0.20		66.25	15.27	16.40	0.89	0.96	0.23
	22.5	66.07	15.93	15.77	0.91	1.13	0.19		66.12	15.37	16.28	0.88	1.17	0.18
	24	66.87	15.65	15.21	0.93	1.12	0.22		66.17	15.82	15.60	1.06	1.14	0.20
	25.5	65.85	16.36	15.22	1.21	1.15	0.21		66.34	16.34	15.10	0.96	1.08	0.19
	27	66.31	16.31	15.16	0.84	1.20	0.18		66.50	17.77	13.16	1.11	1.26	0.20
	28.5	66.49	17.10	13.81	1.20	1.18	0.22		66.65	16.85	14.35	0.86	1.09	0.20
	30	66.75	16.26	14.44	1.11	1.21	0.22		67.29	16.50	13.65	1.15	1.21	0.19
5	0	65.54	19.21	12.81	0.77	1.43	0.24	6	64.83	18.84	13.38	1.36	1.37	0.23
	1.5	65.54	18.22	13.48	1.30	1.25	0.21		66.12	18.04	12.98	1.40	1.26	0.19
	3	65.87	18.67	13.05	0.96	1.24	0.21		65.28	18.81	13.18	1.11	1.42	0.20
	4.5	67.78	17.42	12.37	0.92	1.28	0.23		66.06	18.50	13.16	0.88	1.21	0.20

Meas.	Pos. (nm)	Fe	Cr	Ni	Mn	Mo	Si	Meas.	Fe	Cr	Ni	Mn	Mo	Si
5	6	68.19	17.66	12.12	0.74	1.09	0.20	6	66.88	17.78	12.64	1.25	1.27	0.18
	7.5	67.23	16.58	13.71	1.02	1.28	0.18		66.83	17.56	13.40	0.91	1.08	0.21
	9	66.76	14.72	16.24	0.96	1.10	0.23		67.49	17.05	13.01	1.03	1.21	0.22
	10.5	62.55	14.05	21.12	0.85	1.13	0.30		67.04	15.87	14.85	0.87	1.15	0.21
	12	59.88	14.25	23.59	0.84	1.16	0.29		64.79	15.71	17.52	0.67	1.04	0.27
	13.5	62.27	13.78	21.80	0.95	0.91	0.29		62.27	14.92	20.40	0.90	1.22	0.29
	15	62.82	14.43	20.50	0.92	1.10	0.24		60.63	14.51	22.53	0.67	1.35	0.30
	16.5	64.57	14.49	18.80	0.92	0.98	0.23		61.26	13.92	22.62	0.78	1.12	0.31
	18	63.93	15.13	19.06	0.69	0.97	0.23		62.56	14.55	20.84	0.77	1.05	0.22
	19.5	65.19	14.63	17.87	1.00	1.07	0.24		63.85	14.88	19.16	0.83	1.06	0.22
	21	65.22	15.76	16.97	0.76	1.05	0.23		65.28	14.72	17.79	0.96	1.05	0.20
	22.5	65.11	16.79	15.88	0.90	1.10	0.21		67.21	15.10	15.57	0.78	1.15	0.19
	24	66.70	15.93	15.26	0.79	1.10	0.22		66.78	15.62	15.22	1.09	1.09	0.19
	25.5	65.93	16.75	15.03	0.90	1.15	0.24		65.56	16.81	15.22	1.02	1.17	0.22
	27	65.87	16.92	15.12	0.84	1.12	0.14		66.29	16.54	14.83	0.89	1.24	0.21
	28.5	66.70	15.82	14.91	1.15	1.23	0.19		66.16	16.51	14.61	1.03	1.49	0.20
	30	66.78	16.52	14.19	1.08	1.23	0.20		65.95	17.62	14.15	0.78	1.31	0.19

HiHf, 500C, 3 dpa

Meas.	Pos. (nm)	Fe	Cr	Ni	Mn	Mo	Si	Meas.	Fe	Cr	Ni	Mn	Mo	Si
1	0	65.78	18.96	12.79	0.97	1.32	0.19	2	64.77	19.30	13.20	1.14	1.36	0.23
	1.5	65.01	19.13	13.51	0.88	1.29	0.19		64.66	18.54	14.08	1.13	1.42	0.18
	3	66.31	17.96	13.14	1.23	1.15	0.20		65.99	18.10	12.91	1.47	1.33	0.20
	4.5	66.25	18.16	13.22	0.99	1.17	0.21		66.67	17.59	12.89	1.54	1.15	0.16
	6	68.56	17.01	12.16	0.90	1.19	0.17		66.96	17.64	12.94	1.08	1.16	0.21
	7.5	67.08	16.59	14.15	0.90	1.09	0.20		66.53	17.92	13.11	1.13	1.12	0.20
	9	67.34	15.55	14.99	0.87	1.01	0.25		67.42	17.55	12.98	0.61	1.24	0.20
	10.5	63.88	14.68	19.03	1.14	1.06	0.22		68.95	15.26	13.67	0.92	0.99	0.22
	12	60.86	14.90	22.01	0.80	1.13	0.30		65.54	15.06	17.42	0.77	0.98	0.23
	13.5	62.54	14.15	20.98	0.94	1.15	0.23		61.01	13.85	22.80	0.93	1.09	0.32
	15	63.23	14.57	19.70	1.24	1.02	0.24		61.59	13.49	22.52	0.87	1.26	0.27
	16.5	65.09	14.57	18.42	0.71	0.98	0.23		62.55	14.39	20.93	0.86	1.03	0.24
	18	65.14	15.54	17.22	0.84	1.06	0.20		64.24	14.86	18.82	0.79	1.05	0.24
	19.5	66.09	14.99	16.71	0.95	1.03	0.23		64.57	15.75	17.84	0.74	0.88	0.22
	21	65.42	15.97	16.16	1.09	1.17	0.18		66.16	15.42	16.28	0.77	1.18	0.19
	22.5	66.72	16.26	14.95	0.77	1.09	0.21		66.73	15.82	15.11	1.02	1.13	0.19
	24	66.51	16.47	14.67	1.07	1.06	0.22		66.04	16.61	14.98	1.14	1.03	0.19
	25.5	66.82	15.91	14.90	1.06	1.07	0.24		65.56	16.27	15.85	0.88	1.22	0.22
	27	66.93	16.93	13.81	0.96	1.15	0.23		66.94	16.64	14.24	0.92	1.06	0.20
	28.5	66.79	17.68	13.03	1.19	1.13	0.19		66.98	16.28	14.43	0.98	1.12	0.20
	30	66.82	17.44	13.15	1.11	1.27	0.21		66.99	16.46	14.06	0.86	1.40	0.23
3	0	64.62	19.08	13.95	0.83	1.30	0.22	4	65.50	18.69	13.27	1.03	1.32	0.19
	1.5	65.62	18.29	13.65	0.94	1.34	0.18		64.60	19.71	13.11	1.18	1.21	0.20
	3	65.97	18.07	13.41	1.05	1.31	0.19		66.30	18.25	12.89	0.96	1.38	0.22
	4.5	65.81	17.81	13.79	1.08	1.31	0.19		66.36	18.63	12.65	0.92	1.25	0.19
	6	66.69	17.39	13.53	0.95	1.24	0.21		66.63	17.41	13.58	1.18	1.02	0.18
	7.5	67.29	16.39	13.94	0.92	1.24	0.23		66.72	17.36	13.39	1.08	1.21	0.23
	9	67.15	16.16	14.96	0.57	0.93	0.22		67.45	15.91	14.31	0.97	1.15	0.21
	10.5	63.21	14.62	19.75	0.99	1.13	0.29		67.50	14.55	15.76	0.86	1.14	0.19
	12	60.37	14.75	22.92	0.65	1.03	0.28		63.01	14.26	20.38	0.78	1.28	0.29
	13.5	61.51	13.87	22.55	0.74	1.05	0.29		60.85	13.84	22.82	0.85	1.33	0.31
	15	63.02	14.70	20.19	0.88	1.00	0.22		61.34	13.69	22.84	0.79	1.08	0.26
	16.5	63.76	15.14	19.16	0.85	0.85	0.24		62.73	14.55	20.56	0.81	1.06	0.28
	18	64.30	15.13	18.68	0.70	1.00	0.20		65.06	15.25	17.82	0.81	0.83	0.24
	19.5	65.18	15.49	17.18	0.81	1.12	0.23		65.14	15.72	17.34	0.65	0.92	0.22
	21	65.23	15.80	16.84	0.97	0.96	0.20		66.25	15.27	16.40	0.89	0.96	0.23
	22.5	66.07	15.93	15.77	0.91	1.13	0.19		66.12	15.37	16.28	0.88	1.17	0.18
	24	66.87	15.65	15.21	0.93	1.12	0.22		66.17	15.82	15.60	1.06	1.14	0.20
	25.5	65.85	16.36	15.22	1.21	1.15	0.21		66.34	16.34	15.10	0.96	1.08	0.19
	27	66.31	16.31	15.16	0.84	1.20	0.18		66.50	17.77	13.16	1.11	1.26	0.20
	28.5	66.49	17.10	13.81	1.20	1.18	0.22		66.65	16.85	14.35	0.86	1.09	0.20
	30	66.75	16.26	14.44	1.11	1.21	0.22		67.29	16.50	13.65	1.15	1.21	0.19
5	0	65.54	19.21	12.81	0.77	1.43	0.24	6	64.83	18.84	13.38	1.36	1.37	0.23
	1.5	65.54	18.22	13.48	1.30	1.25	0.21		66.12	18.04	12.98	1.40	1.26	0.19
	3	65.87	18.67	13.05	0.96	1.24	0.21		65.28	18.81	13.18	1.11	1.42	0.20
	4.5	67.78	17.42	12.37	0.92	1.28	0.23		66.06	18.50	13.16	0.88	1.21	0.20

Meas.	Pos. (nm)	Fe	Cr	Ni	Mn	Mo	Si	Meas.	Fe	Cr	Ni	Mn	Mo	Si
5	6	68.19	17.66	12.12	0.74	1.09	0.20	6	66.88	17.78	12.64	1.25	1.27	0.18
	7.5	67.23	16.58	13.71	1.02	1.28	0.18		66.83	17.56	13.40	0.91	1.08	0.21
	9	66.76	14.72	16.24	0.96	1.10	0.23		67.49	17.05	13.01	1.03	1.21	0.22
	10.5	62.55	14.05	21.12	0.85	1.13	0.30		67.04	15.87	14.85	0.87	1.15	0.21
	12	59.88	14.25	23.59	0.84	1.16	0.29		64.79	15.71	17.52	0.67	1.04	0.27
	13.5	62.27	13.78	21.80	0.95	0.91	0.29		62.27	14.92	20.40	0.90	1.22	0.29
	15	62.82	14.43	20.50	0.92	1.10	0.24		60.63	14.51	22.53	0.67	1.35	0.30
	16.5	64.57	14.49	18.80	0.92	0.98	0.23		61.26	13.92	22.62	0.78	1.12	0.31
	18	63.93	15.13	19.06	0.69	0.97	0.23		62.56	14.55	20.84	0.77	1.05	0.22
	19.5	65.19	14.63	17.87	1.00	1.07	0.24		63.85	14.88	19.16	0.83	1.06	0.22
	21	65.22	15.76	16.97	0.76	1.05	0.23		65.28	14.72	17.79	0.96	1.05	0.20
	22.5	65.11	16.79	15.88	0.90	1.10	0.21		67.21	15.10	15.57	0.78	1.15	0.19
	24	66.70	15.93	15.26	0.79	1.10	0.22		66.78	15.62	15.22	1.09	1.09	0.19
	25.5	65.93	16.75	15.03	0.90	1.15	0.24		65.56	16.81	15.22	1.02	1.17	0.22
	27	65.87	16.92	15.12	0.84	1.12	0.14		66.29	16.54	14.83	0.89	1.24	0.21
	28.5	66.70	15.82	14.91	1.15	1.23	0.19		66.16	16.51	14.61	1.03	1.49	0.20
	30	66.78	16.52	14.19	1.08	1.23	0.20		65.95	17.62	14.15	0.78	1.31	0.19

BIBLIOGRAPHY

BIBLIOGRAPHY

[1] E. E. Thum, "The book of stainless steels: corrosion resisting and heat resisting chromium alloys", Ed(s). E. E. Thum, The American Society for Metals, Cleveland, 1935,

[2] A. J. Sedriks, "Corrosion of Stainless Steels", Wiley, New York, 1996,

[3] E. A. Kenik, *Journal of Nuclear Materials*, **187** (1992) 239-246

[4] H. M. Chung, W. E. Ruther, J. E. Sanecki, A. Hins, N. J. Zaluzec, and T. F. Kassner, *Journal of Nuclear Materials*, **239** (1996) 61-79

[5] J. T. Busby, G. S. Was, and E. A. Kenik, *Journal of Nuclear Materials*, **302** (2002) 20

[6] L. K. Mansur, and M. H. Yoo, *Journal of Nuclear Materials*, **74** (1978) 228

[7] G. S. Was, and P. L. Andresen, *Journal of Materials*, **44** (1992) 8

[8] G. S. Was, and S. M. Bruemmer, *Journal of Nuclear Materials*, **216** (1994) 326

[9] K. Fukuya, M. Nakano, K. Fujii, T. Torimaru, and Y. Kitsunai, *Journal of Nuclear Science and Technology*, **41** (2004) 1218-1227

[10] G. S. Was, "Recent Developments in Understanding Irradiation Assisted Stress Corrosion Cracking", *Proceedings of the 11th International Conference on Environmental Degradation of Materials in Nuclear Power Systems - Water Reactors*, (American Nuclear Society, Stevenson, Washington, 2003), p. 965

[11] Gary S. Was, "Fundamentals of Radiation Materials Science", Springer, 2007,

[12] G. S. Was, and T. R. Allen, *Materials Characterization*, **32** (1994) 239

[13] H. W. King, *Journal of Materials Science*, **1** (1966) 79

[14] L. Kornblit, and A. Ignatiev, *Journal of Nuclear Materials*, **126** (1984) 77-78

[15] A. Janotti, M. Krčmar, C. L. Fu, and R. C. Reed, *Physical Review Letters*, **92** (2004) 085901

[16] M. Krčmar, C. L. Fu, A. Janotti, and R. C. Reed, *Acta Materiallia*, **53** (2005) 2369

[17] J. T. Busby, "Isolation of the Role of Radiation-Induced Segregation in Irradiation-Assisted Stress Corrosion Cracking in Proton-Irradiated Austenitic Stainless Steels", (University of Michigan, 2001)

[18] J. T. Busby, and G. S. Was, "Irradiation-Assisted Stress Corrosion Cracking in Model Austenitic Alloys with Solute Additions", *Proceedings of the 11th International Conference on Environmental Degradation of Materials in Nuclear Power Systems - Water Reactors*, (American Nuclear Society, Stevenson, WA, 2003), p. 995-1014

[19] A. Jenssen, L. Ljungberg, J. Walmsley, and S. Fisher, *Corrosion 96*, (NACE, 1996), p. paper 101

[20] N. Shigenaka, S. Ono, Y. Isobe, T. Hashimoto, H. Fujimori, and S. Uchida, *Journal of Nuclear Science and Technology*, **33** (1996) 577

[21] N. Sakaguchi, S. Watanabe, and H. Takahashi, *Nuclear Instruments and Methods in Physics Research B*, **153** (1999) 142

[22] H. Kinoshita, S. Watanabe, S. Mochizuki, N. Sakaguchi, and H. Takahashi, *Journal of Nuclear Materials*, (1996) 205

[23] T. Kato, H. Takahashi, and M. Izumiya, *Journal of Nuclear Materials*, **189** (1992) 167

[24] S. Kasahara, K. Nakata, and H. Takahashi, *Journal of Nuclear Materials*, **239** (1996) 194

[25] L. Fournier, B. H. Sencer, G. S. Was, E. P. Simonen, and S. M. Bruemmer, *Journal of Nuclear Materials*, **321** (2003) 192

[26] D. L. Damcott, T. R. Allen, and G. S. Was, *Journal of Nuclear Materials*, **225** (1995) 97-107

[27] J. T. Busby, "The use of proton irradiation to determine IASCC mechanisms in light water reactrs: solute addition alloys", (RP-P3038/C1434, Electric Power Research Institute, 2002)

[28] T. R. Allen, J. I. Cole, J. Gan, G. S. Was, R. Dropek, and E. A. Kenik, *Journal of Nuclear Materials*, **342** (2005) 90

[29] T. R. Allen, "Modeling of Radiation-Induced Segregation in Austenitic Fe-Cr-Ni Alloys", (University of Michigan, 1998)

[30] D. L. Damcott, "The use of proton irradiation in the examination of radiation-induced segregation in multicomponent alloys", (University of Michigan, 1998)

[31] D. L. Damcott, J. M. Cookson, R. D. Carter Jr., J. R. Martin, M. Atzmon, and G. S. Was, *Radiation Effects and Defects in Solids*, **118** (1991) 383

[32] T. R. Allen, J. T. Busby, G. S. Was, and E. A. Kenik, *Journal of Nuclear Materials*, **255** (1998) 44

[33] T. R. Allen, and G. S. Was, *Acta Materiallia*, **46** (1998) 3679

[34] M. Nastasi, J. W. Mayer, and J. K. Hirvonen, "Ion-Solid Interactions", Cambridge University Press, 1996,

[35] L. E. Rehn, *Journal of Nuclear Materials*, **174** (1990) 144 - 150

[36] D. J. Edwards, E. P. Simonen, and S. M. Bruemmer, *Journal of Nuclear Materials*, **317** (2003) 13

[37] N. Sakaguchi, S. Watanabe, and H. Takahashi, *Journal of Nuclear Materials*, **239** (1996) 176

[38] R. E. Stoller, and G. R. Odette, "Radiation-Induced Changes in Microstructure", *Effects of Radiation on Materials*, (ASTM, Phildelphia, PA, 1982), p. 1051

[39] F. A. Garner, and W. G. Wolfer, *Effects of Radiation on Materials*, (ASTM, Philadephia, PA, 1982), p. 1073

[40] N. Sakaguchi, S. Watanabe, and H. Takahashi, *Acta Materialia*, **49** (2001) 1129

[41] S. Watanabe, Y. Takamatsu, N. Sakaguchi, and H. Takahashi, *Journal of Nuclear Materials*, **283-287** (2000) 152-156

[42] G. S. Was, T. R. Allen, J. T. Busby, J. Gan, D. Damcott, D. Carter, M. Atzmon, and E. A. Kenik, *Journal of Nuclear Materials*, **270** (1998) 96-270

[43] J. Gan, and G. S. Was, *Journal of Nuclear Materials*, **297** (2001) 161-175

[44] J. Gan, E. P. Simonen, S. M. Bruemmer, L. Fournier, B. H. Sencer, and G. S. Was, *Journal of Nuclear Materials*, **325** (2004) 94

[45] G. S. Was, T. R. Allen, J. T. Busby, J. Gan, D. Damcott, D. Carter, M. Atzmon, and E. A. Kenik, *Journal of Nuclear Materials*, **270** (1999) 96-114

[46] R. A. Johnson, and N. Q. Lam, *Physical Review B*, **15** (1977) 1794-1800

[47] R. A. Johnson, and N. Q. Lam, *Physical Review B*, **13** (1976) 4364 - 4375

[48] H. Weidersich, P. R. Okamoto, and N. Q. Lam, *Journal of Nuclear Materials*, **83** (1979) 98-108

[49] P. J. Maziasz, *Journal of Nuclear Materials*, **205** (1993) 118

[50] C. M. Shepherd, *Journal of Nuclear Materials*, **175** (1990) 170

[51] A. D. Brailsford, *Journal of Nuclear Materials*, **56** (1975) 7

[52] L. K. Mansur, *Nuclear Technology*, **40** (1978) 5-34

[53] H. Takahashi, and N. Hashimoto, *Materials Transactions of the Japanese Institute of Metals*, **34** (1993) 1027

[54] N. Sakaguchi, S. Watanabe, H. Takahashi, and R. G. Faulkner, *Journal of Nuclear Materials*, **329-333** (2004) 1166-1169

[55] T. R. Anthony, "Atomic Transport in Solids and Liquids", Ed(s). A. Lodding and T. Lagerwall, Verlag Z Naturforch, Tubingen, Germany, 1971,

[56] T. R. Anthony, "Radiation-Induced Voids in Metals and Alloys", *AEC Symp. Series, Conf. 701601*, Ed(s). J.W. Corbett and L.C. Ianniello, (USAEC Technical Information Center, Oak Ridge, TN, 1972), p. 630

[57] P. R. Okamoto, and L. E. Rehn, *Journal of Nuclear Materials*, **83** (1979) 2-23

[58] N. Q. Lam, A. Kumar, and H. Wiedersich, "Kinetics of Radiation-induced Segregation in Ternary Alloys", *Effects of Radiation on Materias: 11th Conf.*, Ed(s). and J.S. Perrin H.R. Brager (ASTM, 1982), p. 985-1007

[59] J. M. Perks, and S. M. Murphy, "Materials for Nuclear Reactor Core Applications", BNES, London, 1987,

[60] J. M. Perks, A. D. Marwick, and C. A. English, AERE R, 12121, June, 1986)

[61] A. D. Markwick, R. C. Piller, and M. E. Horton, "Dimensional Stability and Mechanical Behavior in Irradiated Metals and Alloys", BNES, London, 1984,

[62] J. R. Manning, *Physical Review B*, **4** (1971) 1111-1121

[63] S. J. Rothman, L. J. Nowicki, and G. E. Murch, *Journal of Physics, F: Metall. Physics*, **10** (1980) 383-398

[64] B. Million, J. Ruzikova, and J. Verstal, *Materials Science and Engineering*, **72** (1985) 85

[65] S. Watanabe, N. Sakaguchi, N. Hashimoto, and H. Takahashi, *Journal of Nuclear Materials*, **224** (1995) 158 - 168

[66] H. Watanabe, T. Muroga, and N. Yoshida, *Journal of Nuclear Materials*, **239** (1996) 95

[67] M. J. Hackett, G. S. Was, and E. P. Simonen, *Journal of ASTM International*, **2** (2005) 1-13

[68] D. I. R. Norris, C. Baker, C. Taylor, and J. M. Titchmarsh, "Radiation-Induced Segregation in 20Cr/25Ni/Nb Stainless Steel", *Effects of Radiation on Materials: 15th International Symposium, ASTM STP 1125*, Ed(s). R. E. Stoller, A. S. Kumar and D. S. Gelles, (ASTM, Philadelphia, PA, 1992), p. 603-620

[69] S. Watanabe, and H. Takahashi, *Journal of Nuclear Materials*, **208** (1994) 191

[70] Y. Grandjean, P. Bellon, and G. Martin, *Physical Review B*, **50** (1994) 4228

[71] J. R. Manning, *Metallurgical Transactions*, **1** (1970) 499-505

[72] L. Kaufman, and H. Nesor, *CALPHAD*, **4** (1978) 295

[73] T. R. Allen, E. A. Kenik, and G. S. Was, *Journal of Nuclear Materials*, **278** (2000) 149

[74] T. R. Allen, G. S. Was, and E. A. Kenik, *Journal of Nuclear Materials*, **244** (1997) 278

[75] R. G. Faulkner, *Journal of Nuclear Materials*, **251** (1997) 369-275

[76] R. G. Faulkner, S. Song, and P. E. J. Flewitt, *Journal of Nuclear Materials*, **283-287** (2000) 147-151

[77] R. G. Faulkner, S. Song, P. E. J. Flewitt, M. Victoria, and P. Marmy, *Journal of Nuclear Materials*, **255** (1998) 189-209

[78] R. G. Faulkner, N. C. Waite, E. A. Little, and T. S. Morgan, *Materials Science and Engineering*, **A171** (1993) 241-248

[79] J. D. Tucker, J. Liu, D. Morgan, T. Allen, and R. Najafabadi, "Ab Initio Defect Properties for Modeling Radiation-Induced Segreagion in Fe-Ni-Cr Alloys", *Proceedings of the 13th International Symposium on Environmental Degradation of Materials in Nuclear Power Systems - Water Reactors*, (Canadian Nuclear Society, Whistler, British Columbia, Canada, 2007), p.

[80] L. K. Mansur, *Journal of Nuclear Materials*, **83** (1979) 109

[81] G. R. Gessel, and A. F. Rowcliffe, "Radiation Effects in Breeder Reactor Structural Materials", Ed(s). M. L. Bleiberg and J. W. Bennett, Metallurgical Society of AIME, 1977, p. 431

[82] S. Dumbill, and M. Hanks, *Sixth International Conference on Environmental Degradation of Materials in Nuclear Power Systems - Water Reactors*, Ed(s). R. E. Gould and E. P. Simonen, (Minerals, Metals and Materials Society, Warrendale, PA, 1993), p. 521

[83] T. Allen, G. Was, S. Bruemmer, J. Gian, and S. Ukai, "Design of Radiation-Tolerant Structural Alloys for Gen IV Nuclear Energy Systems", (Grant No. DE-FG07-03ID14542, Project No. 02-110, DOE, 2006)

[84] K. Asano, K. Fukuya, K. Nakata, and M. Kodoma, *Proceedings of the Fifth International Symposium on Environmental Degradation of Materials in Nuclear Power Systems - Water Reactors*, Ed(s). D. Cubicciotti (American Nuclear Society, Monterey, CA, 1992), p. 838

[85] J. Gan, J. I. Cole, T. R. Allen, R. B. Dropek, and G. S. Was, *To Be Published*,

[86] S. Ohnuki, S. Yamashita, H. Takahashi, and T. Kato, "Effect of IVa and Va Elements on Void Formation in Neutron-Irradiated 316 Stainless Steel", *Effects of Radiation on Materials: 19th International Symposium, ASTM STP 1366*, (ASTM, West Conshochoken, PA, 2000), p. 756

[87] J. Weertman, and D. M. Parkin, *Journal of Nuclear Materials*, **99** (1981) 66

[88] N. Q. Lam, P. R. Okamoto, and H. Weidersich, *Journal of Nuclear Materials*, **74** (1978) 101-113

[89] M. Nastar, P. Bellon, G. Martin, and J. Ruste, "Role of Interstitial and Interstitial-Impurity Interaction on Irradiation-Induced Segregation in Austenitic Steels", *Materials Research Society Symposium Proceedings*, (1998), p. 383-388

[90] S. M. Bruemmer, E. P. Simonen, P. M. Scott, P. L. Andresen, G. S. Was, and J. L. Nelson, *Journal of Nuclear Materials*, **274** (1999) 299

[91] G. S. Was, J. T. Busby, T. R. Allen, E. A. Kenik, A. Jenssen, S. M. Bruemmer, J. Gan, A. D. Edwards, P. M. Scott, and P. L. Anderson, *Journal of Nuclear Materials*, **300** (2002) 198

[92] G. S. Was, and J. T. Busby, "Use of Proton Irradiation to Determine IASCC Mechanisms in Light Water Reactors: Solute Addition Alloys", (EP-P3038/C1434, Electric Power Research Institute, 2002)

[93] The Stopping and Range of Ions in Matter (SRIM), James F. Ziegler, SRIM-2006.02, 2006

[94] "Standard Practice for Neutron Radiation Damage Simulation by Charged-Particle Irradiation", (E 521 – 96, ASTM International, 2003)

[95] G. Cliff, and G. W. Lorimer, *Journal of Microscopy*, **103** (1975) 203

[96] http://www.materialsdata.com/jd.htm, Inc. Materials Data, 12/04/2007

[97] Scion Image for Windows, Wayne Rasband, Scion Corporation, Beta 4.0.2, 2000

[98] National Bureau of Standards, Monograph 25, v21, p135 (1985)

[99] W. Wong-Ng, H. McMurdie, B. Paretzkin, C. Hubbard, and A. Dragoo, *Powder Diffraction*, **3** (1988) 117

[100] http://www.icdd.com, The International Centre for Diffraction Data, 02/06/2008

[101] F. Perez-Willard, D. Wolde-Giorgis, T. Al-Kassab, G. A. Lopez, E. J. Mittemeijer, R. Kirchheim, and D. Gerthsen, *Micron*, (2007) In Press

[102] A. C. Hindmarsh, "Construction of Mathematical Software, Part III: The Control fo Error in the GEAR Package for Ordinary Differential Equations", (UCID-30050 Part 3, Lawrence Livermore Laboratory, Aug., 1972)

[103] A. C. Hindmarsh, "Ordinary Differential Equation System Solver", (UCID-30001 Rev. 3, Lawrence Livermore Laboratory, Dec., 1974)

[104] A. C. Hindmarsh, "Linear Multistep Methods for Ordinary Differential Equations: Method Formulations, Stability, and the Methods of Nordsieck and GEAR", (UCRL-51186 Rev. 1, Lawrence Livermore Laboratory, March, 1972)

[105] N. Q. Lam, T. Nguyen, G. K. Leaf, and S. Yip, *Nuclear Instruments and Methods in Physics Research*, **B31** (1988) 415-424

[106] W. Kohn, and L. Sham, *Physical Review*, **140** (1965) A1133

[107] C. Domain, and C. S. Becquart, *Physical Review B*, **65** (2002) 024103

[108] A. Van der Ven, G. Ceder, M. Asta, and P. D. Tepesch, *Physical Review B*, **64** (2001)

[109] D. E. Jiang, and E. A. Carter, *Physical Review B*, **67** (2003) 214103

[110] G. Kresse, and J. Furthmüller, *Computational Materials Science*, **6** (1996) 15

[111] G. Kresse, and J. Furthmüller, *Physical Review B*, **54** (1996) 11169

[112] G. Kresse, and J. Hafner, *Physical Review B*, **49** (1994)

[113] G. Kresse, and J. Hafner, *Physical Review B*, **47** (1993) 558

[114] P. E. Blöchl, *Physical Review B*, **50** (1994) 17953

[115] J. P. Perdew, and Y. Wang, *Physical Review B*, **45** (1992) 13244

[116] H. J. Monkhorst, and J. D. Pack, *Physical Review B*, **13** (1976) 5188

[117] J. M. Perks, A. D. Marwick, and C. A. English, "Proceedings of the Symposium on Radiation-inducd Sensitization of Stainless Steels", (CEGB, Berkeley Nuclear Laboratories, 1987), p.

[118] R. W. Seigel, "Point Defects and Interactions in Metals", Ed(s). Takamura, North-Holland Publ. Co., p. 533

[119] P. Ehrhart, "Atomic Defects in Metals", New Series, Group 3, Vol 25, Ed(s). H. Ullmain, Landolt-Bornstein, Springer-Verlag, Berlin, 1991,

[120] E. P. Simonen, and S. M. Bruemmer, *Proceedings of the MRS Fall Meeting Symposium Y: Microstructure of Irradiated Materials*, Ed(s). I. M. Roberston, L. E. Rehn, S. J. Zinkle and W. J. Phythian, (1995), p. 95

[121] C. Dimitrov, and O. Dimitrov, *Journal of Physics, F*, **14** (1984) 793

[122] R. D. Carter, D. L. Damcott, M. Atzmon, G. S. Was, and E. A. Kenik, *Journal of Nuclear Materials*, **205** (1993) 361

[123] A. J. Jacobs, G. P. Wozadlo, K. Nakata, S. Kasahara, T. Okada, S. Kawano, and S. Suzuki, *Proceedings of the Sixth International Symposium on Environmental Degradation of Materials in Nuclear Power Systems - Water Reactors*, Ed(s). R. E. Gold and E. P. Simonen, (National Association of Corrosion Engineers, Houston, TX, 1993), p. 14

[124] L. K. Mansur, *Journal of Nuclear Materials*, **206** (1993) 306-323

[125] E. A. Kenik, *Scripta Metallurgica*, **10** (1976) 733

[126] S. Teysseyre, Z. Jiao, E. West, and G. S. Was, *Journal of Nuclear Materials*, **371** (2007) 107-117

[127] Z. Jiao, J. T. Busby, and G. S. Was, *Journal of Nuclear Materials*, **361** (2007) 218

[128] J. Cookson, R. Carter, D. Damcott, G. S. Was, and M. Atzmon, *Journal of Nuclear Materials*, **202** (1993) 104

[129] D. J. Edwards, E. P. Simonen, F. A. Garner, L. R. Greenwood, B. M. Oliver, and S. M. Bruemmer, *Journal of Nuclear Materials*, **317** (2003) 32

[130] P. J. Maziasz, *Journal of Nuclear Materials*, **191-194** (1992) 701

[131] D. Edwards, E. Simonen, S. Bruemmer, and P. Efsing, "Microstructural Evolution in Neutron-Irradiated Stainless Steels: Comparison of LWR and Fast-Reactor Irradiations", *12th International Conference on Environmental Degradation of Materials in Nuclear Power Systems - Water Reactors*, (TMS, Salt Lake City, UT, 2005), p. 419

[132] N. Shigenaka, T. Hashimoto, and M. Fuse, *Journal of Nuclear Materials*, **207** (1993) 46

[133] T. L. Choy, and Y. Y. Yeung, *Journal of Physics and Chemistry of Solids*, **54** (1993) 553

[134] D. P. Abraham, J. W. Richardson, and S. M. McDeavitt, *Scripta Materialia*, **37** (1997) 239-244

[135] F. Stein, G. Sauthoff, and M. Palm, *Journal of Phase Equilibria*, **23** (2002) 480-494

[136] M. Suzuki, S. Hamada, P. J. Maziasz, S. Jitsukawa, and A. Hishinuma, *Journal of Nuclear Materials*, **191-194** (1992) 1351-1355

[137] Paul G. Shewmon, "Diffusion in Solids", J. Williams Book Company, 1983,

[138] F. S. Ham, *Journal of Physics and Chemistry of Solids*, **6** (1958) 335-351

[139] D. P. Abraham, S. M. McDeavitt, and J. Park, *Metallurgical and Materials Transactions A*, **27** (1996) 2151-2159

[140] FactSage, Thermfact and GTT-Technologies, 5.5, 2007

[141] http://www.nndc.bnl.gov/exfor7/exfor00.htm, Brookhaven National Laboratory, 12/07/07

[142] D. B. Williams, and C. B. Carter, "Transmission Electron Microscopy", Plenum Press, New York, NY, 1996,

[143] J. Wiley, "Table of Isotopes", 8th Ed., Ed(s). R. B. Firestone and V. S. Shirley, Wiley-Interscience, New York, 1996,